A conceptual design diagram of a synchrotron upgrade. It features a complex network of yellow and orange lines representing particle paths, overlaid on a blue background with faint white circular and linear patterns. A prominent red dashed line traces a curved path through the center of the diagram. In the bottom left corner, there is a yellow rectangular graphic with a white sun-like symbol.

# Conceptual Design Report

SYNCHROTRON SOLEIL UPGRADE

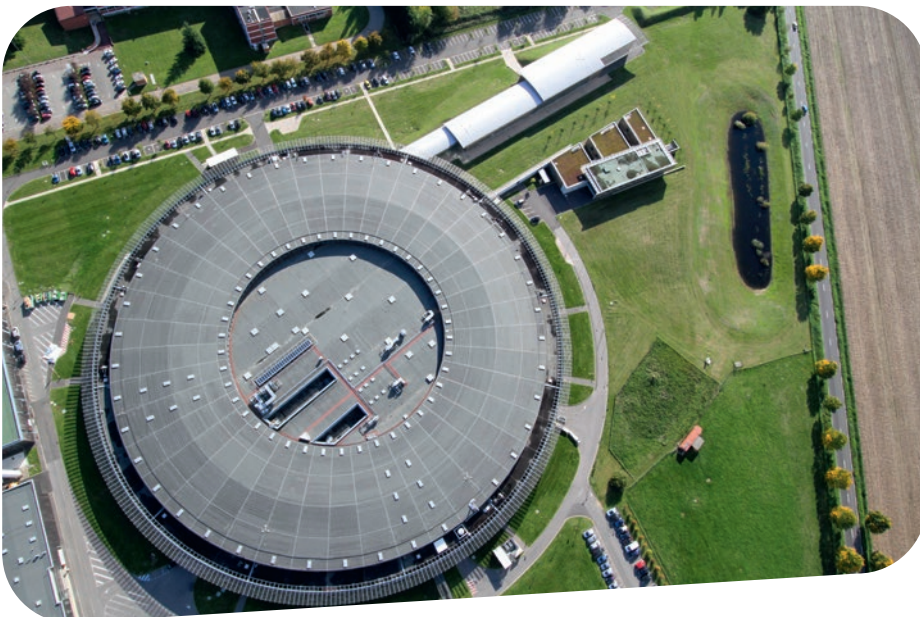


# Table of contents

<b>EXECUTIVE SUMMARY</b>	<b>5</b>	<b>4. BEAMLINES INSTRUMENTATION</b>	<b>113</b>
<b>1. INTRODUCTION</b>	<b>7</b>	<b>Introduction</b>	<b>114</b>
SOLEIL specific features and strengths	9	<b>Instrumentation and methods</b>	<b>116</b>
Our concept and approach	10	Introduction	116
<b>2. SCIENCE CASE</b>	<b>11</b>	Advanced materials	123
<b>Introduction</b>	<b>12</b>	Sustainable energy	125
<b>Advanced materials for novel technologies</b>	<b>16</b>	Biology and health	126
<b>Quantum materials</b>	<b>18</b>	Environment	128
Overview	18	Transverse instrumentation and approaches	130
Multiferroics	19	<b>Optics</b>	<b>132</b>
Skymions and chiral objects	20	Beamline optics	132
Emerging superconductivity at extreme conditions	20	Optical metrology and diagnostics	133
<b>Materials engineering</b>	<b>21</b>	<b>Detectors</b>	<b>136</b>
Overview	21	Simulation of the signal response of semiconductor detectors to photon beam through matter	136
2D Materials	23	Development of a multi-element germanium detector for XAS experiments	137
MOFs	23	Fast hybrid photon counting detector for time resolved experiments	137
<b>Sustainable energy: from production, conversion, storage and climate action</b>	<b>27</b>	Ultra-fast energy resolved imager for hard X-ray crystallography experiments with multi pink beams	138
<b>Overview</b>	<b>27</b>	Large and fast pixelated detector for soft X-ray experiments	139
Catalysis: a pivotal science for energy production	28	<b>Data reduction and analysis</b>	<b>141</b>
Conversion of solar energy: photovoltaic devices	31	Introduction	141
Electrochemical energy storage materials: solving the cost, energy density and safety issues	32	Remote data treatment	141
<b>Health and well being</b>	<b>36</b>	Automatic data processing	141
<b>Overview</b>	<b>36</b>	Material and beamline modelling	142
(Re)Emerging pathogens in their environment	38	Traceability and data analytics	142
Synchrotron methods for pathologists	39	<b>Scenario for beamlines implementation</b>	<b>143</b>
Plants for a changing world	41	Impact of new lattice on beamline implantation	143
<b>Environmental sciences</b>	<b>44</b>	Phasing of beamline (re)construction	143
<b>Overview</b>	<b>44</b>	<b>5. INFORMATION SYSTEM AND DATA</b>	<b>145</b>
Atmospheric chemistry & aerosols: fighting global warming	46	<b>Introduction</b>	<b>146</b>
The impact of nanoplastics on the health of our environment	47	Fundamentals of the Information System Strategy	147
Environmental behavior of trace elements	48	<b>Requirements of the information systems users</b>	<b>148</b>
Dynamic & transfer of contaminants	49	Multibeamline and multitechnical experimental projects	148
Waste recycling: reducing pollution & preserving resources	50	Simulation, prototyping, testing	148
<b>3. ACCELERATORS AND SOURCES UPGRADE</b>	<b>53</b>	Processes and data	148
<b>Introduction</b>	<b>54</b>	Optimizing accelerators and beamlines operation	149
Lattice design	58	Systems openness	149
Injection scheme	71	Communication	149
Magnets	76	<b>Strategic topics</b>	<b>149</b>
Alignment strategy	81	Traceability	149
Mechanical engineering	82	Smart processes and systems	150
Power supplies	85	Support for transversal activities	151
Vacuum systems	88	Agility and flexibility	152
Radio-frequency systems	94	Refactoring and modernization	153
Diagnostics and timing system	98	Security	154
Beam stability	102	Open science	155
Photon sources	105	Teams training and support, technical culture	155
Infrared extraction	111		

# Table of contents (continued)

<b>6. INFRASTRUCTURE</b>	<b>157</b>
Storage ring and beamlines implementation.....	158
Support buildings and logistics.....	162
Utilities adaptation.....	165
Disassembly, pre-staging and installation.....	167
<b>7. RISK MANAGEMENT</b>	<b>171</b>
<b>8. RADIATION PROTECTION</b>	<b>175</b>
Radiation protection issues in the storage ring upgrade.....	176
Preliminary studies.....	176
Storage ring tunnel shielding.....	176
Brief considerations about beamlines shielding.....	178
<b>9. SOCIO-ECONOMIC IMPACT</b>	<b>179</b>
Introduction.....	180
Multiple impact studies by the bureau of theoretical and applied economy (BETA – Bureau d'économie théorique et appliquée, Strasbourg).....	181
The impact of SOLEIL's expenditure on the local, regional and international economy: a study by VERTIGO LAB.....	183
<b>10. INNOVATION STRATEGY</b>	<b>185</b>
<b>11. PLANNING, PURCHASING, HUMAN RESOURCES</b>	<b>187</b>
Planning.....	188
Purchasing.....	188
Human resources.....	190



# **Executive summary**



**T**his document presents the conceptual design of an upgrade of synchrotron SOLEIL accelerators, beamlines and infrastructure. The project is planned in two phases of 5 years each, “construction” and “towards full performance”.

Twenty years after SOLEIL was established, science, and the role and breadth of a large scale infrastructure in scientific exploration have considerably evolved and widened. New scientific fields have emerged to which the facility needs to adapt. This sets the scientific case for this upgrade in the four areas which have been identified as key to meet the challenges our society is facing (advanced materials, sustainable energy, biology and health, earth and the environment): discovery of new quantum materials, use of Artificial Intelligence in materials or drug design, fight against new pathogens or dealing with new kinds of pollutants like nanoplastics are challenges where the upgraded SOLEIL has the ambition to have a decisive impact.

Addressing these challenges requires exploring heterogeneous and complex systems at the nanometer scale using complementary methods in order to understand their organization, properties and function. This will be made possible by reconstructing SOLEIL's storage ring as a Diffraction Limited Storage Ring (DLSR). The original and ambitious design proposed here will produce round electron beams with a record low emittance of less than 50 pm.rad x 50 pm.rad, hence photon beams with an exceptional brilliance exceeding by two orders of magnitude those of the present facility. At the new facility, nanometric resolution will become the rule for most of the beamlines, the increase in brilliance, coherence and flux will allow one to follow biological processes or the functioning of devices *operando* at ms or sub-ms timescales, the detection limit of trace elements will be decreased by three orders of magnitude, with an extraordinary impact expected in environmental science.

The development of new, revolutionary methods like structured UV imaging, use of streak cameras to study ultrafast dynamics, *in vivo* crystallography or soft X-ray interferometry, is an integral part of the project.

Together with the accelerators upgrade, these developments will keep the competitiveness of SOLEIL and extend its lifetime by at least 15 years as most of the European facilities are undergoing similar upgrades. SOLEIL will be unique owing to the broad range of beam energies from THz to hard X-rays it delivers, which will be even further extended. Its domain of

excellence continues to lie in the soft to tender X-ray range making it complementary of the ESRF-EBS. Thanks to this upgrade, an exceptionally broad range of techniques will be made available to the academic and industrial user communities, enabling truly integrative research opportunities which are at the heart of the upgrade vision.

Access modes will evolve in order to make the most efficient use of the upgraded facility in an open data perspective. This will be accompanied by an upgrade of information system which will be a data orientated transformative change benefiting all SOLEIL activities.

This upgrade will also represent a fantastic opportunity to develop the human capital of SOLEIL and its stakeholders along all the lines already exemplified in the socio-economic study attached to this Conceptual Design Report.

The upgraded facility will use the present storage ring tunnel and most of the present infrastructure in order to optimize the cost of the project. Replacement of the aging infrastructure after almost two decades of operation will allow a dramatic reduction in the facility environmental footprint, and the systematic use of permanent magnet for the storage ring will allow a reduction by one half of its electric power consumption, also significantly reducing operation cost.

The ambitious design which is proposed is accompanied by extensive prototyping in accelerator technology, insertions devices, vacuum system, optics, detectors, development of new experimental methods... Importantly, this development of innovative instrumentation will be leveraged from our partners of the League of European Accelerator-based Photon Sources (LEAPS), therefore reducing overall investment and its potential for technology transfer is already being explored.

# 1 – Introduction



**T**wenty years after the decision to build the facility was made in 2000, SOLEIL has considerably exceeded initial expectations in terms of beamline performance, service to academic and industrial user communities, productivity and results, as amply documented by the socio-economic impact study attached to this CDR. With more than 12,000 scientists from all disciplines having used the infrastructure, it plays an irreplaceable role for a number of scientific communities, both National and European.

Scientific interest, hence the role of a multidisciplinary analytic facility like SOLEIL has, however, considerably changed since the specification of the scientific case and initial technical design of SOLEIL were defined at the end of last century. New challenges have appeared during the last twenty years to which SOLEIL and its staff have successfully adapted, and we only start to see the future challenges we will face.

Quantum materials, use of Artificial Intelligence in materials or drug design, emergence of new pathogens, concerns about new kinds of pollutants like nanoplastics, need for unprecedented capacity in energy storage, were barely discussed 20 years ago and are now center stage. These major challenges pertaining to advanced materials,

sustainable energy, biology and health, earth and the environment and identified as pivotal in the scientific case, all imply understanding intrinsically complex systems. Indeed, the functioning of the natural systems and the properties and response of the advanced materials that will shape the future of our societies involve organization and response in a broad range of length- and time-scales. Their full understanding is beyond the present capabilities of SOLEIL but within reach with a storage ring using the new Multi-Bend Achromat technology (MBA), as already pioneered in Europe by the MAX-IV and ESRF-EBS facilities. Similarly, ELETTRA (Italy), the Swiss Light Source, the Diamond Light Source (UK) or PETRA and BESSY (Germany) have already engaged in upgrading to an MBA source, some of the projects being already funded (Table 1).

The very ambitious design proposed here, with parameters surpassing those of all existing or planned sources in Europe but PETRA-IV (6 GeV, 2.3 km in circumference), will ensure the competitiveness of SOLEIL for the next 30 years. It goes beyond the present state of the art of MBA machines, while preserving one of the most precious assets of SOLEIL, namely the very broad range of radiation it covers from TeraHertz (THz) and InfraRed (IR) to X-rays with a natural domain of excellence in the soft-tender X-ray range.

Combination of this upgraded SOLEIL with the already upgraded ESRF whose domain of excellence is in the hard and very hard X-ray range will offer the national scientific community an unrivaled suite of beamlines for matter characterization.

Among the many new possibilities which will be opened by an upgraded SOLEIL,

- Nanometric resolution will become the rule for most of the beamlines, allowing imaging organelles in living systems or determining chemical composition and electronic or magnetic properties in complex materials at such an exquisite resolution.
- The increase in brilliance, coherence and flux will allow the characterization of the dynamics of systems at much shorter times. For X-ray Photon Correlation Spectroscopy (XPCS), which allows the determination of fluctuation dynamics, the upgrade will give access to time scales five orders of magnitude shorter than presently possible. The functioning of devices will be followed *operando* using coherent diffraction imaging at ms or sub-ms timescales.
- The detection limit of trace elements, which is critical in particular in environmental sciences will be decreased by three orders of magnitude, which might lead to the discovery of fully unexpected effects.

## SOLEIL specific features and strengths

### Broad range of techniques and integrative research

SOLEIL is by far the synchrotron facility offering with its 29 beamlines the widest energy range (9 orders of magnitude!) and suite of techniques to its users in Europe. For the French users, it is complementary of the ESRF (French has a 27.5% share of its 33 public beamlines) and its five French Collaborative Research Group (CRG) beamlines (Figure 1).

Its intermediate energy of 2.75 GeV<sup>1</sup> and optimized beamlines allow an integrative approach of scientific problems using complementary spectroscopic and structural techniques at different length- and time-scales. The combination of complementary structural and electronic, optical or vibrational spectroscopies that SOLEIL offers indeed allows deciphering the dependence of chemical, electronic or magnetic properties of materials and processes on their structure, very often with imaging capabilities. A major goal of the proposed upgrade is to reinforce this unique capability.

### Stability and reliability

The storage ring has also proven to be among the most stable and reliable synchrotron sources in the world, reaching 99% scheduled beam delivery for users. It has a very low level of beam fluctuations and vibrations, which has to be preserved with the upgrade, all the more as the beam sizes will be drastically reduced.

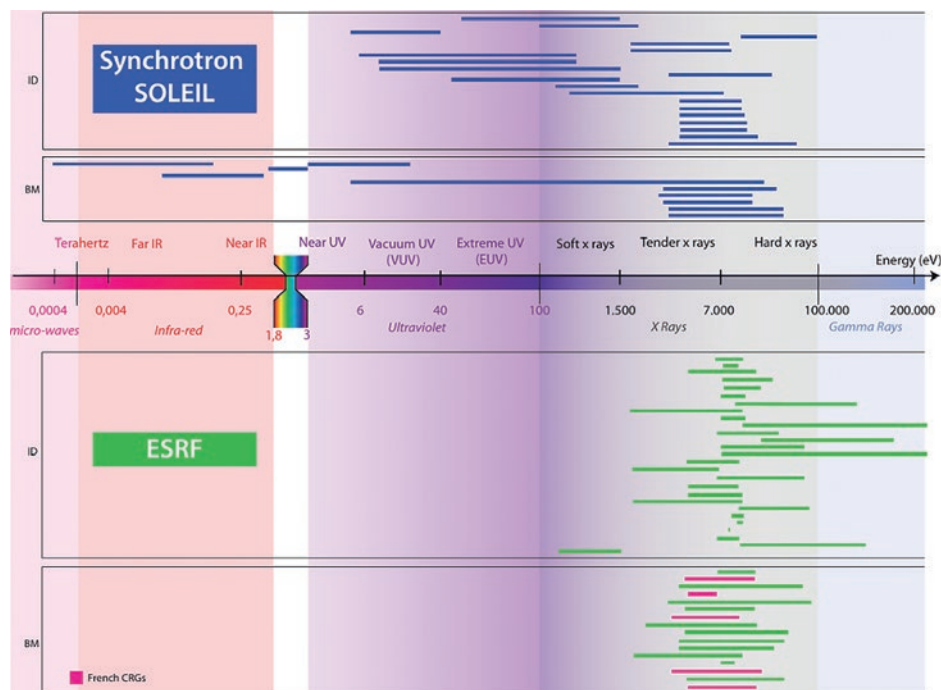


Figure 1: complementarity between SOLEIL (in blue) and ESRF (in green). French CRGs at the ESRF are marked in red.

### Quality of user support

User satisfaction surveys demonstrate the excellent level of user support, with 94% of the users rating the beamline staff support as excellent (and 5% very good!). Beyond user support, expertise and dedication of staff is a clear asset of SOLEIL.

Owing to its outstanding performance, the new SOLEIL will be flexible enough to adapt to different user community's needs, achieving for example an efficient complementarity between high throughput

measurements and highly sophisticated experiments, supported by new access modes and an upgraded information system. This upgrade of information system is a transformative change that will be beneficial to all SOLEIL activities, including administration.

### Strategic partnerships and high impact research

Last but not least, our strategy has been to establish close partnerships with key academic or industrial players. This both guarantees that the research conducted at SOLEIL makes the highest impact in a broad range of scientific domains, and that the most relevant instrumentation is developed in a timely fashion. High level input from those partners has nourished the scientific case presented below. The proposed upgrade will both build on and reinforce these strengths which make the strategic positioning of SOLEIL unique in Europe and a great opportunity for French Research.

Storage Ring	E in GeV (circumference in m)	Emittance (pm.rad)	Lattice	Status
ESRF-EBS (France)	6 (844)	140	7BA	Operation
ALS-U (USA)	2 (197)	109	9BA	TDR
APS-U (USA)	6 (1104)	42	7BA	Construction
Diamond-II (UK)	3.5 (562)	150	7BA	TDR (CD1)
ELETTRA 2.0 (Italy)	2 (259)	250	6BA	TDR (funded)
PETRA-IV (Germany)	6 (2304)	10 - 30	7BA	TDR
SLS-II (Switzerland)	2.7 (290)	160	7BA	TDR
SOLEIL-U (France)	2.75 (354)	80	7BA-4BA	CDR
SPring-8-II (Japan)	6 (1435)	140	5BA	Study & RD
SSRF-U (China)	3 (432)	203	7BA	Study

Table 1: MBA-based upgrade projects in the world.

<sup>1</sup>Complementary of the high energy ESRF and PETRA-III (6 GeV) and lower energy BESSY-II (1.7 GeV), ELETTRA (2 - 2.4 GeV) and SLS (2.4 GeV). SOLEIL also has many more soft X-ray beamlines than the 3 GeV machines (Diamond, MAX-IV, ALBA). This original positioning will be further reinforced with the Diamond upgrade were the energy will be raised to 3.5 GeV.

## Our concept and approach

With the development of Free Electron Lasers producing extremely intense femto-second pulses, the overarching figure of merit of storage rings is their brilliance and coherence allowing one to tailor beams almost at will. Targeting the lowest possible horizontal beam emittance will ensure a long term bright future for SOLEIL.

The new SOLEIL will build on the strengths of the present SOLEIL. Since the start of the project it was decided to keep a storage ring energy of 2.75 GeV as the best compromise for complementary soft and hard X-ray beamlines.

Another constraint we set was to reconstruct the storage inside the present ring tunnel and to keep the beamlines with heaviest infrastructure where they are in order to minimize capital investment.

Our concept is therefore an MBA (Multi Bend Achromat, see table 1) based storage ring of lowest possible emittance with twenty straight sections built in the present tunnel, with optimized beamlines covering a wide range of techniques from THz to hard X-rays.

The approach we have adopted consisting in first fixing the lowest possible horizontal emittance as unique goal and then progressively introducing constraints with frequent feedback between accelerator groups and Experimental Division, revealed remarkably successful. For example, electron beam characteristics were optimized to dramatically improve photon emission. Displacement of source points and number of beamlines to move were drastically reduced between the first version of the project and the "V0313" presented here and called now on "CDR reference lattice", while keeping the record horizontal emittance of 80 pm.rad.

Our project has the ambition to be a green one. It will be the first to make the use of permanent magnets the rule, only using electromagnets when strictly necessary, therefore reducing the storage ring electric consumption by about two thirds, hence operation cost and risk of failure. Similarly, infrastructure is aging and will be modernized so as to reduce our environmental footprint. Development of new concepts and instrumentation is an integral part of this upgrade project.

This implies prototyping critical equipment which does not presently exist and is necessary in order to guarantee the feasibility and success of the project. In order to establish the current CDR, it has been necessary to demonstrate the proof of concept of several critical technologies. This is the case for example for the magnets already mentioned, but also the vacuum system with vacuum chambers as small as 10 mm in diameter, power supplies or injection system. The latter strongly benefits from the developments made within the framework of the Swedish-French collaboration with the MAX-IV synchrotron in Lund. Small period insertion devices will benefit from the LEAPS<sup>2</sup> collaboration.

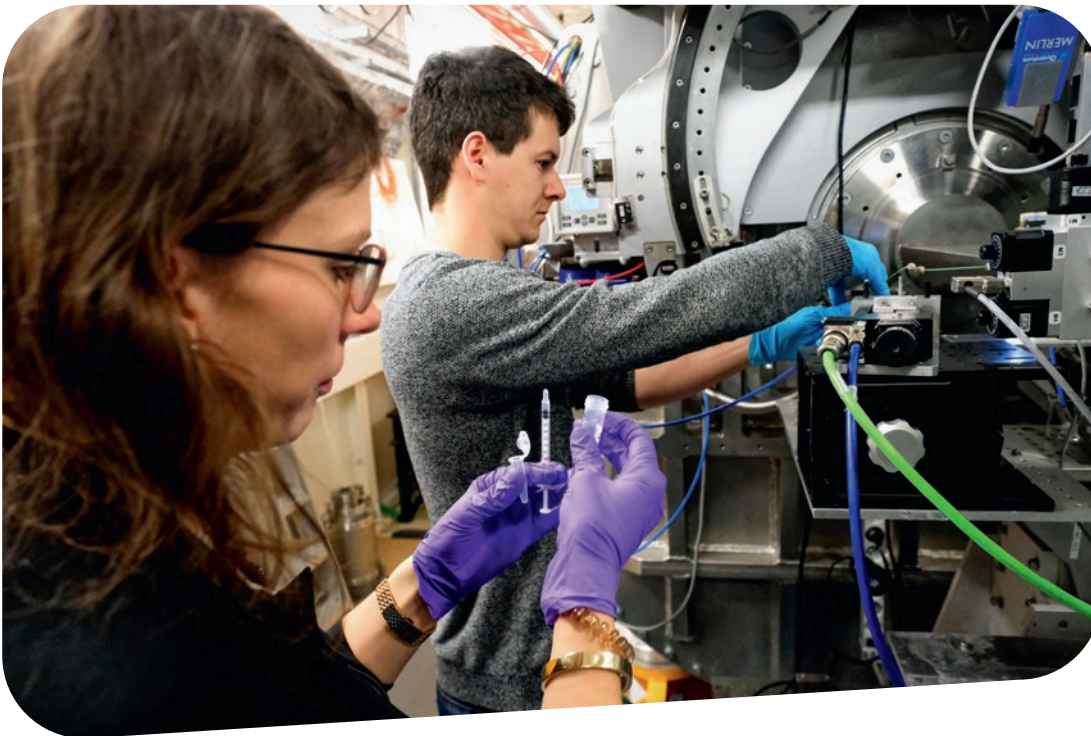
On the beamline side, we have started to develop experimental methods which will only reach their full potential with the upgraded machine and beamlines. This is the case for optics (LEAPS collaboration) and detectors, also benefiting from a bilateral collaboration with the Diamond Light Source. A number of beamlines have firmly engaged in innovative projects: 3D tomographic ptychography (again initiated within the MAX-IV collaboration), structured UV imaging, use of streak cameras to study ultrafast dynamics, spectroscopic ptychography, *in vivo* crystallography or soft X-ray interferometry, just to name a few.

Such instrumentation development will lead to great opportunities for technology transfer which is an integral part of our strategy. Identification of innovative developments has been initiated since the beginning of the CDR phase in order to take industry constraints into account. A patent has already been filed as we are writing this report.

<sup>2</sup> League of European Accelerator-based Photon Sources: ALBA (Spain), DESY Germany), DIAMOND (UK), ELETTRA (Italy), ESRF (France), EUROPEAN XFEL (Germany), FELIX (The Netherlands), HZB (Germany), HZDR (Germany), INFN (Italy), ISA (Denmark), MAX-IV (Sweden), PSI (Switzerland), PTB (Germany), SOLARIS (Poland), SOLEIL (France).



2 - **Science**  
**case**



## INTRODUCTION

Curiosity driven research is at the heart of science, and has proven to be crucial for identifying solutions to the wide range of societal and technical challenges that face the world: new discoveries enable us to respond to emerging concerns and requirements. The upgrade project, described in this Conceptual Design Report (CDR), will enable SOLEIL to continue to provide world-leading capabilities and cutting-edge tools in support of scientific endeavors. This CDR has been developed through workshops and round table discussions with national and international parties, involved in fundamental and applied research across all disciplines (round table discussion reports are available on demand. Contact: [webcom@synchrotron-soleil.fr](mailto:webcom@synchrotron-soleil.fr)). In particular, the upgrade project is strongly driven by the requirements of the CNRS and CEA, and by the context of the proximity of the rapidly-expanding University Paris-Saclay.

Science has always benefited society by providing answers to basic questions about the nature of our world and existence, as well as to develop knowledge that can be used to improve our lives such as the development of vaccines to avoid diseases, nitrogen-fixation to make fertilizers, the discovery of penicillin to cure infections and the development of lasers which are ubiquitous in modern technology. An upgraded SOLEIL will continue our tradition of developing tools and creating knowledge that will help to address many of the problems currently facing our society.

- On a planet with nearly eight billion people, threats to human, animal and plant health are emerging due to our methods of cultivation and consumption and increased mobility due to globalisation. No-one needs to be reminded of the effects of the current Covid-19 epidemic, which has had dramatic effects on both health and wealth, and which is a direct result of

poor environmental practices and lack of understanding of our interaction with the animal world. Several synchrotrons, including SOLEIL, have demonstrated their reactivity and influence in leading a science-based response when confronted with such a situation.

- > In addition to supporting urgent access for Covid-19 research, scientists from SOLEIL have joined forces with INRAE and Sanofi in a joint ANR-Flash research project referred to as AcceS-Ge CoViD-19, which aims to determine the crystallographic structures of all the viral proteins in complex with members of a fragment library.
- Global climate change is affecting weather patterns leading to permafrost melting, increasingly frequent cyclones or hurricanes, increased drought or flooding, according to geographical location. Changed rainfall patterns have increased the impact of wildfires in recent years, particularly in 2020, with severe consequences for the population and atmosphere.
  - > To understand the impact of drought on trees and identify species more resistant to drought conditions, users came to SOLEIL to detect air bubbles within the vessels transporting water in saplings. Tomography measurements have shown that the synchrotron allows us to see inside a tree as we read a book.
- Consumption of the Earth's finite resources proceeds at an ever-increasing rate, with extraction tripling in the period 1970 – 1997 <sup>[1]</sup>, motivating the EU to develop action plans to deliver a European Green Deal, including a Circular Economy Action Plan. For instance, feeding a growing world population whilst

preserving rich and unpolluted soil stocks or exhausting the planet's finite fresh water supplies presents a huge challenge, with agriculture already the main contributor (85%) to global water stress.

- > SOLEIL has joined an initiative to form a center for molecular water science (CMWS-DESY) aiming to achieve a detailed molecular understanding of water. This includes the dynamic processes in water and at water interfaces which are highly relevant for chemistry, biology, Earth and the environment as well as for technology.
- Society's increased appetite for energy, data storage and sharing, and the desire to be permanently and rapidly connected via the internet needs to be addressed by developing more energy efficient devices, by providing more efficient information storage. Developing improved methods of energy storage (battery technology), reduced energy consumption (with improved industrial processes via the reduction of friction or wear based energy losses or improved catalysis) and production of renewable and more efficient energy. Efficient and sustainable energy management is a key concept towards delivering tomorrow's smart cities.
  - > The efficient conversion of intermittent solar energy to storable H<sub>2</sub>, via photo-conversion in the presence of lignocellulose degradation products and a novel catalyst, has been studied at SOLEIL using *operando* spectroscopy, and shown to produce useful feed stock.
- Novel materials fabricated from nanoscale components to exhibit unique properties that can be tailored to meet electronic device manufacturers' needs. Detailed studies of nanomaterials and device design, synthesis, and fabrication with the most advanced characterization tools supports new technological advances.
  - > The combination of tools offered by an upgraded SOLEIL facility together with the nanofabrication and nano-characterization capabilities of the national platforms such as C2N<sup>1</sup>, METSA<sup>2</sup>, IR-RMN<sup>3</sup>, and international initiatives like NFFA<sup>4</sup>, will play a key role in the design and functionalization of new materials.
- The challenges ahead for clean and safe nuclear energy involve viable solutions for exploiting and reprocessing radioactive materials through their entire life-cycle, requiring detailed physical-chemical investigations.
  - > A dedicated facility, at SOLEIL, for radioactive materials, operated in collaboration with CEA, offers unique opportunities for needed studies.

More than ever, scientific progress cannot be equated solely with ever more complex technological solutions and an economical model based on increasing consumption. One of science's greatest emerging challenges is to provide the basic knowledge and concepts, enabling new technologies and leading to a less environmentally detrimental lifestyle and providing sustainable solutions that will help to save the planet. Progress towards a circular economy model where limited resources are recovered at the end of product lifetimes and used to make new products that are "made to be made again".

To identify the key scientific challenges resulting from the questions outlined above and define the parameters for an optimized upgrade of SOLEIL to address them, a series of Round Table discussions (covering areas where SOLEIL has developed a strong user community and impact), and seminars and workshops (involving academic and industrial proactive partners), have been organized over the last four years. Four main thematic areas have been identified and are outlined in this document. A survey of the instrumentation and methods that need to be adapted in order to deliver responses to these challenges is also given. The approach adopted in developing this Conceptual Design Report can be summarized as "*Addressing scientific needs through specific experimental techniques defining the requirements for the ideal source capabilities and beamline portfolio of the SOLEIL upgrade project*".

The key scientific challenges identified through this process, which we will address through the upgrade of the SOLEIL synchrotron light source, are:

**Advanced materials for future technologies:** Knowledge of the fundamental processes in manufacturing materials and understanding their behavior under real operating conditions will lead to the discovery of disruptive new materials for the future: materials for flexible electronics, nano-sensors, quantum computing materials, materials for energy conversion, nano-alloys, nano-composites, and new materials for smart clothing, construction, transport, automotive industry, aeronautics, and security. To have a societal impact these novel materials must be transferred from the lab into the real world. This is evaluated in this document in the light of two perspectives: Quantum materials and optimized materials for engineering.

**Sustainable energy:** Identifying and optimizing reliable and sustainable energy sources including nuclear energy, as well as the efficient long-term storage of this energy, is an urgent need that will be addressed through improved scientific capabilities. Along with the primary requirement of energy sources, new approaches are also needed to find ways to remediate prior environmental damage caused by energy generation, mining, industrial activities and treating the associated chemical and radioactive wastes. To aid the transition towards a carbon-free energy world, research is needed to develop cleaner and more efficient fuel combustion processes to realize the full potential of existing fuel stocks. The field is diverse and many materials are concerned such as heterogeneous catalysts, photovoltaic devices and ion-batteries.

**Health and well-being:** Exploring the causative agents of disease (human, animal and plant) and the development of innovative and effective methods to improve the health of the population (research on antibiotic resistance, viral infections, cancer, food supply etc...) by exploiting multiscale imaging techniques and extending *in vivo* studies. In particular transient complexes or variable composition molecular machines are key to understanding the detailed function of cells in response to different stimuli or stresses. Provide reactivity in the case of (re) emerging pathogens which, in the context of globalized trade or climatic change, can spread more freely. Responding to needs of health care professionals for new diagnostic tools using multi-modal synchrotron techniques for the rapid evaluation of biopsies.

<sup>1</sup> C2N: Centre for Nanoscience and Nanotechnologies.

<sup>2</sup> METSA: Transmission Electron Microscopy and Atom Probe is a French distributed infrastructure.

<sup>3</sup> IR-RMN: Research Infrastructure for Nuclear Magnetic Resonance is a French distributed infrastructure.

<sup>4</sup> NFFA: Nanoscience Foundries and Fine Analysis is an H2020 project.



**Environmental sciences:** An interdisciplinary topic that merges ecology, geology, climatology, biology, chemistry, engineering and physics in studying our environment and ensuring its preservation, remediation and protection. At its core lies a quest to develop a better understanding of the Earth and the interplay between its different compartments such as studies of the atmosphere and its rich chemistry (release and fate of natural aerosols such as sea spray or volcanic emissions, and artificial pollutants from industrial activities), studies of the effects of human actions on the terrestrial and aquatic environment (impact of toxic waste such as micro-plastics, pollution from mining or landfill activities), understanding and modeling of climate change.

The focus of this document on these key societal challenges does not imply a neglect of the fundamental scientific questions on the nature of matter, its elementary atomic and molecular building blocks and their interaction in chemical bonds and reactions. Scientific progress includes new and creative approaches to basic science, via a bottom-up building approach from atoms and molecules to complex matter. Synchrotron radiation facilities in general, and SOLEIL in particular, are well suited to provide precise information on these building blocks for the understanding of complex systems (solids, ices, biopolymers, ...) and materials with adaptive properties. Optimizing the light source and our experimental methods and techniques, to probe the electronic and structural nature of matter, will help to identify new chemical reactions, electronic transitions, biological processes, molecular and magnetic structures, at best only predicted by theory up until now. The acquisition of fundamental scientific knowledge plays a key role in understanding the natural world, and also facilitates the investigation of ancient materials that represent our patrimony (such as paintings, scrolls, artifacts, etc.). Fundamental science also provides answers to questions that have occupied philosophers since the dawn of civilization, such as the origins of life on Earth and the evolution of the universe at all scales, from galaxies to interstellar medium and star-forming regions to planets.

SOLEIL provides an extraordinarily wide range of photon energies enabling diverse scientific methods in a multidisciplinary environment, and consequently occupies a pivotal position in facilitating science in Europe.

This pluridisciplinarity yields huge volumes of data using a variety of techniques in characterizing different forms of matter over a large range of length scales. Making this data available in an Open Science approach is a huge challenge but also a huge opportunity. Machine learning and artificial intelligence-based approaches can help leverage this data to identify subtle correlations and identify rare events, enabling discovery and novel material developments. The Battery2030 EC initiative (to which SOLEIL is a partner via the Big MAP project) is an example of this strategy, aiming to optimize energy storage media via an objective based cycle of production, characterization, and machine learning based prediction, offering perspectives of the industrial development of new generations of batteries.

To better address these scientific challenges and prepare for future challenges yet to be identified, the upgrade of SOLEIL proposes a diffraction limited storage ring (DLSR), achieved by constructing a new multi-bend achromat (MBA) lattice, to produce brighter beams of synchrotron radiation with vastly increased coherence. The improved beam properties offered by an upgraded SOLEIL synchrotron source will open new avenues for studying matter in exquisite detail, including:



- Heterogeneously and / or hierarchically organized structures, disordered or aperiodic structures and amorphous materials. The increased coherence and brilliance will permit multi-length scale investigations using different imaging modalities, and unlock the opportunity to improve the temporal resolution of the dynamics of these systems. Applications exist throughout science, for example in the physics and chemistry of hard and soft matter, in biological systems, in environmental and Earth sciences.
- Nanomaterials for energy applications, catalysis, micro-electronics, drug delivery, surfaces and interfaces, quantum materials, magnetic structures etc. The efficiency and functionality of these materials are a direct consequence of the size and organization of the components of the material. The improved source properties will enable their characterization at improved spatial and spectral resolution helping to unveil emergent properties.
- Samples in their natural environment can be studied with the extremely brilliant beams from the upgraded SOLEIL coupled to improved methods of sample handling (such as microfluidic cells). Measurements on realistic complex systems (for example cells or tissues *in vivo*, batteries, fuel cells or catalysts under *operando* conditions, surface components of electronic systems *in situ*) can even permit exploration of their dynamics. When coupled to very-low temperatures, high magnetic fields, or high-pressure environments, studies of condensed matter structures such as topological superconducting phases, magnetic skyrmions and Majorana fermion quasiparticles will become accessible.

- Fragile or radiation sensitive samples will benefit from the increased brilliance from an upgraded SOLEIL source through faster and more localized measurements. With modern specialized sample delivery systems and careful dosimetry, it will be possible to limit the degradation of the signal due to radiation damage processes (such as free radical diffusion, sample heating, etc.).
- Low density systems, diluted targets and buried interfaces will become amenable to study due to the brilliance of the upgraded SOLEIL source. Improved sensitivity, spatial resolution and measurement time will enable experiments in, for example atomic, molecular and astrophysics, X-ray imaging of unmarked single cells, in-depth measurements of solids and buried interfaces.
- Measurements will become faster with the increased beam brilliance, coupled with detector and acquisition scanning developments, hugely decreasing acquisition times enabling the study of larger cohorts of samples, improving the statistical quality of extracted data and permitting a wider coverage of sample space. Enhanced celerity, together with the integration of novel computational methods, will allow high-throughput measurements for combinatorial chemistry type studies. High-speed data collection will be particularly beneficial for industrial applications.

New scientific opportunities will encourage the evolution of new technical solutions, in some cases stimulating high-tech industries. Progress in optical design and fabrication will be essential in order to preserve the coherence, spectral and focal properties, from source to detector. Complementary techniques applied simultaneously to the same sample will enable the study of complex systems at different length scales using the wide range of photon energies provided by the upgraded SOLEIL. The idea of a single technique synchrotron beamline will become increasingly rare, with various imaging modalities routinely combined with spectroscopic measurements to permit full characterization of a sample in both space and time. The gain in brilliance and coherence will enable the development of new techniques (structured imaging, Fourier transform spectroscopy at shorter wavelengths, spectroscopic ptychography...) which will expand the capabilities. New methods for visualizing the data from multimodal approaches will be needed to allow users to evaluate the progress of the experiments "online".

Synchrotron radiation studies often provide only part of the information required to understand the sample. Combining results from different techniques and correlating them to the properties of the sample with a meta-data approach will form an essential aspect of a successful experimental approach. Strategic partnerships with academic partners in a "super-platform", both *intra-* and *extra-muros*, would be extremely attractive. A broad community, including industrial companies that may have specific scientific or technical questions but lack the resources to develop research in order to address them, would benefit from such a range of capabilities.

The following opportunities for the upgraded SOLEIL, capitalizing on its increased brightness and coherence, were developed considering the complementarity with the ESRF (the other synchrotron radiation source present on French soil and whose principle excellence and scientific opportunity derives from the much higher storage ring energy).

The scientific opportunities discussed below represent our best analysis today and are unlikely to represent the "state of the art" at the time that an upgraded SOLEIL will come into operation, (2028). Moreover, technical developments will inspire new scientific ideas, opening up new and unforeseen opportunities. SOLEIL has adopted an iterative approach to the upgrade process and flexibility for future evolution of the project is included to accommodate new ideas. A phased approach to beamline and method development, in conjunction with the storage ring upgrade, has been adopted, with beamline construction, renewal and development planned over a 10-year period. The detail of the first phase (2023 – 2028) of a 3 phases upgrade plan is currently being developed, and will form a critical objective of a Technical Design Report, which we expect to complete in the 2 years following the approval of this CDR.



# Advanced Materials for Novel Technologies

## Introduction

- > Materials are ubiquitous in novel technology. Their extraordinary diversity in terms of structure or morphology, the rich interplay at the fundamental level of the different degrees of freedom and their broad range of dynamical responses offer an outstanding variety of properties and functionalities, which in turn have spawned numerous technological advances strongly impacting our everyday life. New materials have been elaborated to face societal, industrial and economic needs. The challenge now and in the future is changing towards products that are more respectful of the environment, the nature, the human health and wellbeing. They should ensure a more secure, clean and efficient energy, smart, green and integrated transport, innovative, reflective and secure societies (cf. EU H2020 challenges<sup>1</sup>). To ensure the success of novel technologies in this direction, more advanced materials are needed. The critical factors for these materials are their intrinsic properties. This is where fundamental science plays its role.

A vivid illustration of the major importance of advanced materials from fundamental science to industry are the recent Nobel prizes of Physics and Chemistry awarded for the discoveries of topological phase transitions and topological phases of matter (2016) and for the elaboration of Li-ion batteries (2019).

The development of new materials is the key to several of the major scientific challenges which have been recognized in the international scientific community. **We can identify four questions of special priority for which the SOLEIL Upgrade will have a strong impact**, though not with the same thrust:

**1. Advanced Energy Storage and Production:** The steep rise of energy consumption calls for renewable and sustainable energy storage and production. Recent technological developments have brought up major improvements in perovskites, light absorbing dyes, nanocomposites, inorganics, polymer - based materials in solar cells, Li-ion batteries, catalysts for fossil fuel production, thermoelectrical materials for new sources of heat,

rare Earth for hybrid electric vehicles, energy efficient concrete, carbon-free and high quality metals for green metallurgy, bio-inspired materials for green chemistry alternatives and new energy devices, but new materials are required to further enhance their performances. This challenge covers a wide research field from solid state physics, to materials engineering and chemistry. It will be more amply treated in the science driver “Sustainable Energy”.

**2. Quantum Information Revolution:** Quantum computing appears as a revolutionary way to overcome the current slowing down of Moore’s law as limits of miniaturization in Si-based technology are approaching. By relying on exotic quantum effects such as entanglement or superposition, it is possible to renew computing and communication technology. New classes of materials hold strong promises for realization of solid-state qubits protected from decoherence. Among these: 2D materials, NV centers, single molecular magnets, Majorana-type superconductors are all considered as potential, long-term candidates for quantum computation.

**3. Faster and Sustainable Computing:** Big data and AI technology require ever faster computing performances and increased data storage, leading to a steep increase of the energy consumption. According to recent studies, the total data storage capacity today is in the 10–50 zettabyte ( $10^{21}$ ) range, a value which could double every two years<sup>[1]</sup>. High performance computing will rely more and more on nanomaterials (magnetic nanoparticles, nanoparticle thin films) which offer higher density data storage and lower electrical consumption. To that aim, materials where electronic and magnetic degrees of freedom are strongly coupled, as best exemplified in multiferroics, could help reducing the writing energy cost per bit by several orders of magnitude. At the same time, new magnetic objects with nm dimension such as single molecular magnets, domain walls or skyrmions could offer new routes of designing storage media with high information density.

<sup>1</sup><https://ec.europa.eu/programmes/horizon2020/en/h2020-section/societal-challenges>

**4. Artificial Intelligence Hardware:** AI is progressively entering in many aspects of everyday life and technological processes. Besides the development of new methods and algorithms for improving AI and machine learning, new AI systems could rely on the hardware fabrication of artificial neuron networks with the benefits of easier scaling and enhanced robustness. Hardware based AI will tremendously increase the processing power while decreasing energy consumption<sup>2</sup>. Memristors based on transition metal oxides are specially considered for AI hardware owing to their capacity to exhibit neuromorphic properties and to be assembled in dense stacks. Although of minor caliber today, this topic will undoubtedly gain importance in the future as AI progressively spreads in the labs and society.

In spite of their diversity, all these new materials share similar issues in terms of growth, defects control, interfacial interactions, time response or unconventional electronic properties. **Synchrotron-based techniques can effectively contribute to these questions** by offering new sophisticated, non-invasive methods of characterization which would provide a complete view of the materials properties along different perspectives: in **space domain**, to characterize the structure from the mm to the nm scale, **energy domain** to reveal the underlying excitations or interactions with meV resolution and **time domain** to follow the materials changes *in situ* during real time operations down to 10 ps.

The development of advanced materials can be summarized by a virtuous cycle illustrated here by a Möbius “strip” (Figure 1). The figure schematically illustrates the back-and-forth interactions needed between materials structure or morphology, their properties, control by external parameters and applications. The validity of the whole process is judged by confronting expectations to physical measurements and theoretical modeling. In other words, if the materials development forms the backbone of the process, the driving mechanism is powered by our capacity to provide an accurate characterization as close as possible to the real-life conditions, possibly guided by artificial intelligence and at each step of the process.

The extreme brilliance of the synchrotron light, its tunability and pulsed structure offers plethora of information. Among other synchrotron sources, SOLEIL singles out by its large portfolio of beamlines covering a broad range of wavelength, experimental techniques and focusing capacities. Thanks to this richness, SOLEIL can provide a multiscale, multimodal

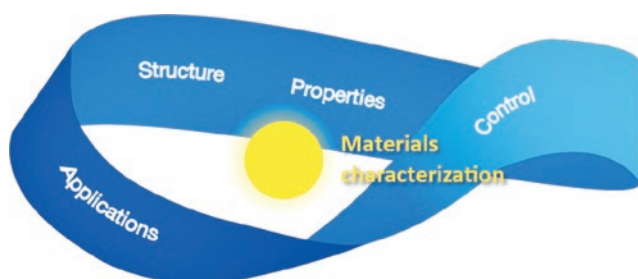


Figure 1: Materials process “strip”

characterization of the materials complexity in terms of structure, interactions, dynamics along three directions of study: space, using diffraction, scattering or imaging techniques with ultimately atomic resolution; energy, using high resolution spectroscopy and inelastic scattering, and time down to ultrafast regime, thanks to time resolved / pump probe studies.

Yet, the current, 3<sup>rd</sup> generation design of the SOLEIL machine with a large beam size, broad divergence in the horizontal direction and low coherent flux imposes severe limitations when it comes to in-depth characterization of advanced materials. For instance, structural reconstruction at the nm scale, though possible today, suffers from the poor efficiency of the focusing optics, thus lengthy acquisition time.

To become effective, advanced materials demand to be translated into the “real world”. In the working on this challenge, we evaluate this issue in the light of **two perspectives: Quantum materials and Materials Engineering** which are very relevant to nanoscience innovation and transverse to the different questions. This dual view further illustrates the need to control both the microscopic interactions at the fundamental level (quantum view) and the macroscopic properties such as growth, defects control, or rheology (engineering view). Each part is illustrated by a selection of meaningful examples **with an emphasis on materials of fundamental interest**, which stress the benefits of the SOLEIL Upgrade.

In the quantum materials section, an overview of the interest and challenges of quantum materials research is given highlighting 3 examples on **multiferroics, skyrmions and superconductors at extreme conditions**. The second part on materials for engineering includes an overview of these materials with 2 examples on **2D materials and MOFs**.

Table 1 summarizes how these different topics relate to the relevant questions in advanced materials from both perspectives.

Perspective	Quantum Materials	Material Engineering
Quantum Information	Extreme conditions	2D materials
A.I. Hardware	Multiferroics	2D materials
Faster Sustainable Computing	Skyrmions Multiferroics	2D materials
Advanced Energy Storage	Multiferroics	MOF

Impact



Table 1 summarizes how these different topics relate to the relevant questions in advanced materials from both perspectives.

<sup>2</sup> <https://www.research.ibm.com/artificial-intelligence/hardware/>



# QUANTUM MATERIALS

## Overview

The research in “Quantum Materials” merges various fields of research including correlated materials, oxides, topology, multiferroicity, or nanomagnetism. It follows the initial research work in the 80’s on high-Tc superconductors and quantum Hall physics that seeded the seminal ideas on strong electrons correlations (Mott physics) and topology. In all these examples, quantum effects determine the materials properties. The “Quantum Materials” terminology, albeit fuzzy, has gained importance recently with the surge of new materials at the frontiers of physics, materials science and engineering and has been adopted by academic institutions and major scientific editors (e.g. the Quantum Materials collection of Nature). An illustration of this diversity is shown in Figure 2. In essence, the extraordinary properties of Quantum Materials arise from the coupling between **quantized degrees of freedom** involving spin, charge, orbital, lattice (e.g. phonons) and topology (e.g. Chern number). Mastering these interactions to design new materials is the ultimate goal of Quantum Materials research. This effort has led to the development of materials of high recent interest including **superconductors, 2D materials, topological insulators, heterostructures, Weyl semimetals, quantum spin liquids, and spin ices**, opening up new branches of materials science such as topological electronics, spin-tronics or Mott-tronics (based

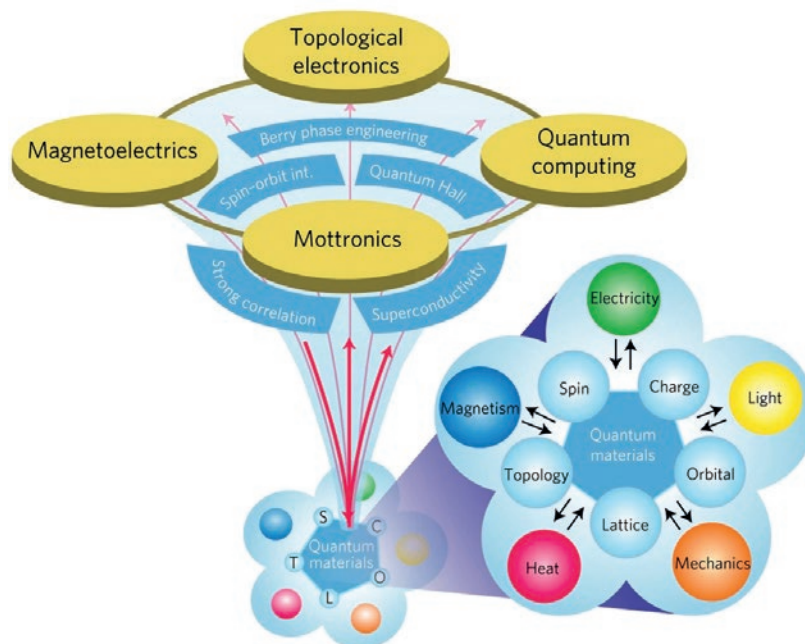


Figure 2: Overview of Quantum Materials<sup>[2]</sup>

on forming and disrupting the Mott insulating state). A key feature of quantum materials for future applications is their extreme sensitivity to external stimuli. In these systems, the fundamental interactions strength competes with the electronic kinetic energy. A rather fragile balance between coexisting ground states can be readily shifted via external stimuli, leading to a series of quantum phases and transitions, possibly on ultrafast timescales. Thanks to these competing orders, it is feasible to attain, in a predictable fashion, “properties on

demand”<sup>[3]</sup> by steering a quantum material towards a desirable ground, metastable or transient state, making quantum materials ideal candidates for advanced devices. These competing states may also lead to very complex phase diagrams and heterogeneous phases at the nm level.

## Challenges

The potential impact of quantum materials is tremendous with expected technological breakthroughs for instance for enhancing data storage and computing performances with low consumption, designing new quantum computer architecture or improving energy transport. More fundamentally, topological materials which can host new type of particles with exotic behavior (anyons) are envisaged as candidates for quantum computers<sup>[4]</sup>. Quantum effects also prevail in batteries cathodes, thermoelectric materials or memristors, thus having implication for low energy consumption device and hardware neuron network.

A first challenge is to characterize the intricate properties of the complex quantum materials at the relevant scales:

- Controlling the materials structure and morphology is crucial for mastering their functionality. As shown in Figure 3 in the case of ferroics and nanomagnetic materials, the structural hierarchy is multiscale ranging from the microscopic level to the mesoscopic scale with possible cooperative orders.

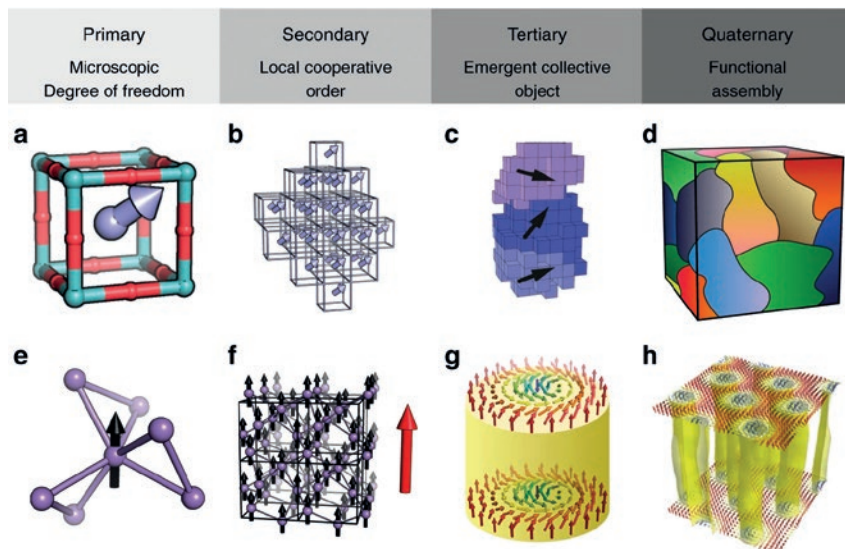


Figure 3: Hierarchical structure of complex materials: Ferroics (top row) and skyrmions (bottom row)<sup>[5]</sup>

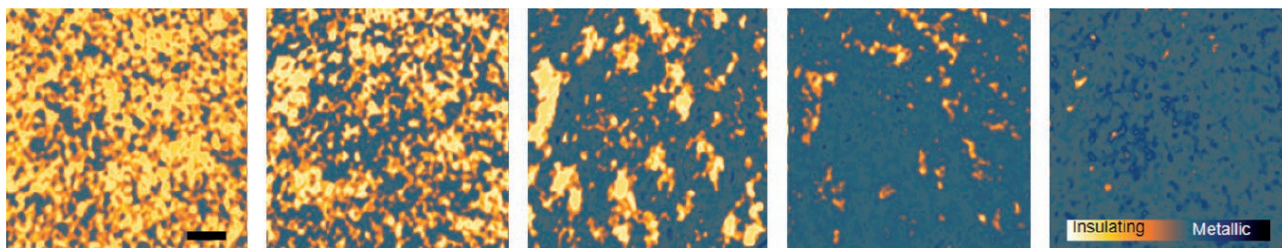


Figure 4: Observation of metallic domains in NdNiO<sub>3</sub> thick film by XPEEM through the T-induced metal-insulator transition. The scale bar represents 400 nm<sup>[6]</sup>

- On top of this structural complexity, another type of heterogeneity may arise due to the competing orders existing at the fundamental level. An enlightening example of such heterogeneous state is the electron correlation driven formation of metallic patch inside an insulating matrix at the nm scale as shown in Figure 4.
- The quantum behavior is often dynamic (up to the ps timescale) as the result of either the materials response to external stimuli or the propagation of well-defined quantized excitations (e.g. plasmons, magnons). Investigating this temporal response is primordial to understand their dynamical behavior, and eventually to devise novel strategies for designing fast responding materials.
- At the microscopic level, quantum materials are governed by competing interactions. The description of the materials in terms of interaction (and symmetry) rather than atomic structure can be an efficient way to reduce their apparent complexity. A skyrmion (Figure 3) for instance can be simply described by a handful of ingredients: ferromagnetism, lattice chirality and antisymmetric exchange. This calls for probes of the materials interactions and excitations.

### SOLEIL upgrade benefits

A complete characterization of quantum materials has to rely on complementary, multi modal approaches with spatial resolution from meso down to nm scale, a wide spectral range to the THz, and a temporal resolution up to ultrafast regime (10 ps). This calls for broad portfolio of advanced spectroscopic and 3D vector imaging techniques associating fast acquisition time, high spatial resolution (10 nm), high energy resolution (few meV for XPS, 10 meV for RIXS), aided by the coherence, the control of polarization or novel effects related to the orbital angular momentum of the light<sup>[7]</sup>. As explained through the examples hereafter, SOLEIL Upgrade will significantly improve the

performances in terms of coherent flux and focusing, making novel research possible in the field of quantum materials. SOLEIL Upgrade will also strongly benefit from the rich panoply of sample environments that have been developed over the years for exploring quantum materials under various conditions such as very low temperatures ( $\leq 200$  mK) or high pressure (up to several 100 GPa). New methodologies for enhancing spectral resolution, in the meV regime, are also under scrutiny, e.g. using interferometric methods for soft X-ray RIXS so far only used in the VUV.

## Multiferroics

### Interest

Multiferroics form a broad class of materials exhibiting more than one ferroic orderings including ferro (or antiferro) magnetism, ferroelectricity or ferroelasticity. Intensive research in this field over the last 20 years has led recently to a Renaissance of multiferroics materials<sup>[8]</sup>. Multiferroics appear the ideal material playground for applications (cf. the recent multiferroics portal on Nature Materials) owing to the possibility to manipulate one ferroic property with the conjugate field of the other (cf. Figure 5, left panel). One promising application is the low consumption (attojoules) switching of the

magnetization with an electric field in line with challenge 3.

The coupling between different interactions make multiferroics a paradigmatic example of complex quantum materials as described in Figure 3. Multiferroics come in a wide variety of different structures including crystalline phases in d-electron or f-electron materials or composite, artificially-built architectures (cf. Figure 5, right panel). The discovery of functional multiferroics domain walls are perhaps the most exciting outcome lately<sup>[9]</sup>. These atomic thin structures have been shown to present metallic conductivity or magnetoresistivity, opening new prospects for spin and charge transport through these nanoscale channels. More fundamentally, the coupling between spin, charge and lattice in multiferroics give rise to new, hybrid elementary excitations (e.g. electromagnon) which could be used as a novel way to carry and process information.

### Challenges

The multiferroics heterogeneity and manifold orders requires a tremendous effort of characterization to access their local structure, their electronic / magnetic properties and excitations while following their temporal evolution as the material is operated. Multiferroic materials often display additional functionality when reduced to nm scale, which is dominated by interfacial and confinement effects. Understanding multiferroics at the nanoscale level still poses a significant experimental challenge.

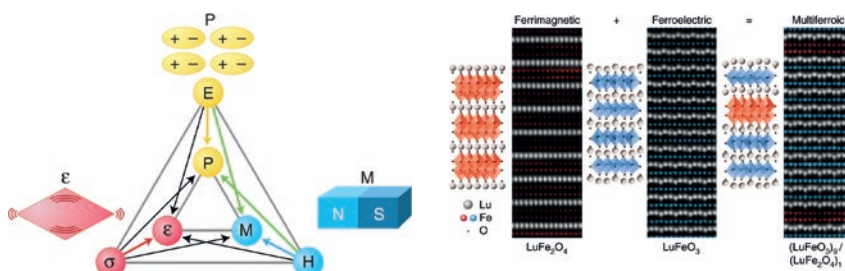


Figure 5: (left) phase control in multiferroics; (right) composite multiferroics structure (from<sup>[8,9]</sup>)

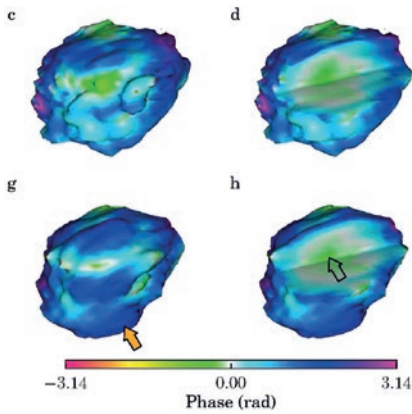


Figure 6: Scattered phase change due to tensile strain in BiFeO<sub>3</sub> nanocrystals (adapted from [10])

### SOLEIL upgrade benefits

As demonstrated in a recent study<sup>[10]</sup>, stress and deformation of crystalline samples can be efficiently investigated by Bragg-CDI (Figure 6) and Bragg ptychography at the nm scale. These methods will amply gain from the increase of coherent flux ( $\times 200$  or more at 8.5 keV expected with SOLEIL upgrade). Furthermore, a spatial resolution of a few nm could be achieved (vs. 10 nm today) and smaller samples (down to 100 nm) investigated. At the same time, the gain of coherence will entail faster acquisition time and better data quality, thus largely improving the success rate in the data reconstruction from ptychographic measurements, making possible **studies on thin films relevant for electronic devices and access to 100 ps timescales (pump-probe) or operando (real-time) conditions.**

## Skyrmions and chiral objects

### Interest

Skyrmions appear as promising candidates for creating nm-scale magnetic bits owing to their small size (10 nm), topologically protected magnetic structure and absence of stray field<sup>[11]</sup>. Skyrmions have been mainly studied so far in ferromagnetic materials. But using antiferromagnetic (AFM) structures instead would bring up several advantages including the reduced damping of skyrmions motion and faster responses. The dreamed objective will be to combine the gain on electrical consumption and the speed increase for storing information on small AFM-based devices, moving from ferromagnetic devices in the GHz regime

to antiferromagnetic-based technologies running in the THz regime. This could lead to new generations of fast, low consumption high density storage devices.

### Challenges

The observation of the domain walls and their dynamics – possibly in *operando* condition – still remains a formidable task. These have been investigated by near field microscopy MFM<sup>[12]</sup>, NV center magnetometry<sup>[13]</sup> or PEEM<sup>[14]</sup> in the past. Coherent scattering techniques offers alternative solutions of special interest for imaging magnetic texture materials because of the flexible sample environments for *operando* studies while keeping high spatial resolution (10 nm) and fast acquisition time. Recent examples of such studies include applications of XPCS<sup>[15]</sup> or coherence soft X-ray resonant scattering (REXS)<sup>[16]</sup>. The latter can access all spin, charge and orbital orders with element selectivity and high spatial resolution only limited by the X-ray wavelength, whereas XPCS gives the information on the dynamics of the domain walls.

### SOLEIL upgrade benefits

These approaches will strongly benefit from SOLEIL Upgrade. In the soft X-ray region for instance, the gain in coherence flux, focusing efficiency combined with a broad band monochromator will boost the scattering intensity by 5 orders of magnitude. The real space imaging of magnetic texture or other types of ordering will become possible by coherent scattering in reflection (ptychography) with a resolution of few nm. In spite of longer acquisition time, this geometry is more flexible than holography in transmission providing a novel view on chiral phases such as domains wall in multiferroics (Figure 7) or skyrmions. Coherent scattering will be complementary to other methods such as XMCD, XPEEM or STXM, all available at SOLEIL Upgrade.

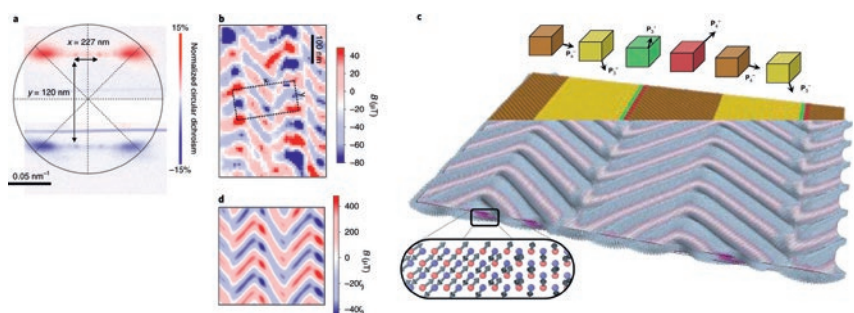


Figure 7: Magnetic texture of domain walls in BiFeO<sub>3</sub> (c) observed by RXES (a) and NV magnetometry (b) compared to micromagnetic simulations (d) (From [16])

## Emerging superconductivity at extreme conditions

### Interest

Materials are profoundly altered when submitted to external parameters such as high or low temperatures, high magnetic field, light pulses, electrical bias, pressure or strain. These can lead to drastic changes of the materials structure and modifications of their intrinsic properties. Novel orders (e.g metal-insulator transition, onset of ferromagnetism) can appear along with other emerging phenomena such as quantum critical phases or superconductivity (Figure 8). In turn, this opens up new possibilities to produce or manipulate these exotic phases.

Extreme conditions usually refer to this range of parameters which by far exceeds ambient conditions. Among these, pressure is arguably one of the most extreme with values possibly ramping up to several 100 GPa (1 million of atmospheres). The application pressure is of especially broad interest with strong impacts in condensed matter physics to stabilize novel phases, in materials design via the synthesis of ultra-hard compounds and in mineralogy and planetology. An emblematic example of extreme conditions study is the discovery of metallic hydrogen above 400 GPa at SOLEIL as illustrated in Figure 9 or the stunning recent finding of superconductivity at ambient temperature in carbonaceous sulfur hydride above 140 GPa<sup>[18]</sup>. Besides pressure, strain-induced phases can be more easily manipulated and fine-tuned, offering an exciting platform to stabilize or control novel states.

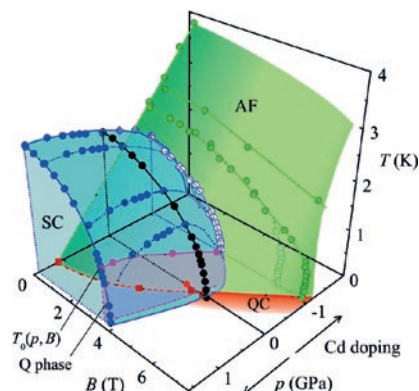


Figure 8: B, T, P phase diagram of CeInCo<sub>5</sub> showing superconducting (SC), antiferromagnetic (AF) and quantum critical (QC) phases (from<sup>[17]</sup>)

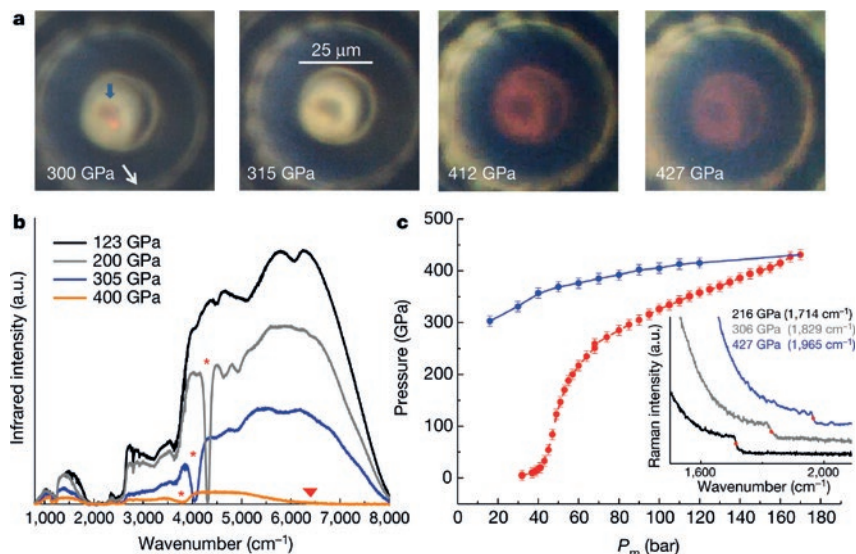


Figure 9: Metallization of hydrogen observed by optical microscopy (a) and infrared spectroscopy (b); the closing of the band gap is indicated by the red triangle in (b). The internal pressure (c) was estimated from diamond Raman (inset) (from<sup>[18]</sup>)

### Challenges

Experiment at extreme pressures or strain requires very intense, stable and highly focused beam to match the small size of samples in pressure cells with typical diameters ranging from 5 to 100  $\mu\text{m}$ . Pressure often generates cascades of events implying structural transitions, magnetic instabilities or changes of the transport properties. This calls for a multimodal approach on the same sample capable of tracing these multiple effects. Furthermore, the sample changes are not uniform but may occur from nm-scale patches which progressively expand under the external parameter. Following these multidimensional changes in real time on a small sample and in a constrained environment remains to be achieved.

### SOLEIL upgrade benefits

With the expected strong increase of brightness and coherent flux, SOLEIL upgrade will provide a formidable

machinery to attack these challenges while boosting the performances of existing setups. The increase in brilliance will enable an enhancement of the energy resolution whilst maintaining high flux. Micro-spectroscopy will significantly gain in efficiency and spatial resolution as more photons will be focused onto the sample. Imaging techniques compatible with extreme conditions such as ptychography will also benefit from the improved performances of the sources, leading to acquisitions at higher speed and better spatial resolution. Hard X-ray diffraction with a brighter source will allow the structural determination that is not possible today. Finally, the bright source will further help enlarging the parameters ranges – to the TPa regime for instance – and speeding up acquisition for real time measurements.

## MATERIALS ENGINEERING

### Overview

Materials have been continuously used, transformed and tailored to answer our various needs. Starting from stone tools to metallurgy and now nanoscience, the aim has remained to target specific properties with growing sophistication.

### Challenges

The advent e.g. of artificial building of materials from a stacking of functionalized blocks holds strong promise for engineering materials properties on demands. A recent example of such Lego-like approach is illustrated in Figure 10 showing the synthesis of field-effect transistors using heterogeneously stacked of atomic-thin 2D materials. Albeit quantum by nature, 2D materials pose severe

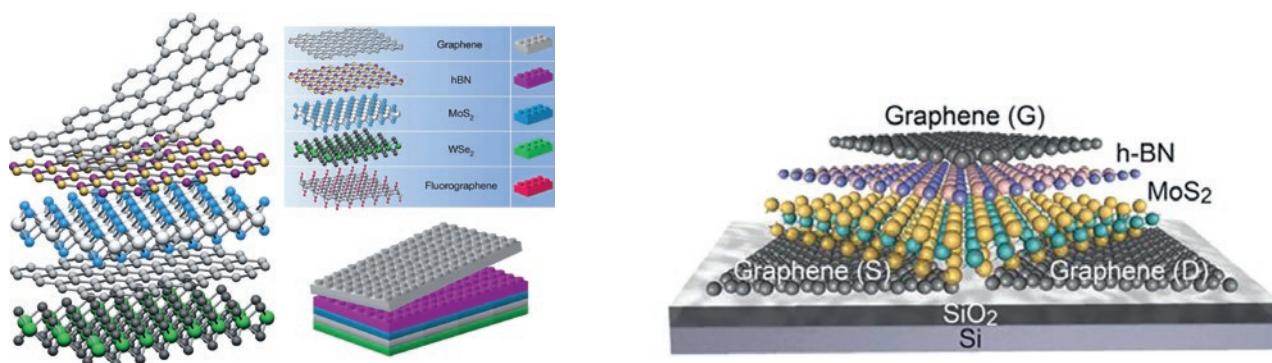


Figure 10: Building functionalized materials from artificial stacks (from<sup>[20,21]</sup>)

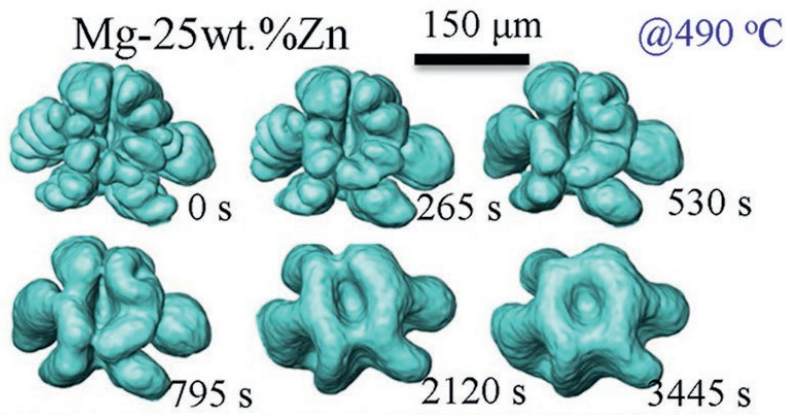


Figure 11: Dendritic evolution of Mg-Zn alloys during isothermal coarsening from X-ray tomography (from<sup>[22]</sup>)

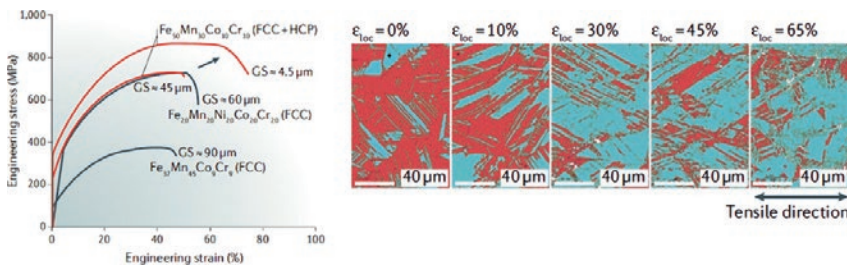


Figure 12: (left) Mechanical properties of the dual-phase, high-entropy, transformation-induced plasticity alloy; (right) Domains formation with increase local strain (from<sup>[25]</sup>)

engineering issues (growth / defects) and will be purposely treated in this section.

At the microscopic level, another example of structural complexity is revealed in the process of solidification of alloys that often results in the formation of dendritic patterns<sup>[22]</sup>. The growth of dendrites from the liquid melt is usually accompanied by coarsening, a change in shape driven by variations in interfacial curvature to decrease the total interfacial area, hence free energy (Figure 11). Understanding this process is of technological importance: the mechanical properties of alloys are directly determined by this microstructure. Beside metallurgy, dendrites growth has gained further importance as key determinant to the safety and performances of high-density lithium-metal batteries<sup>[23]</sup>.

Metallurgy has long been based on pure metals and alloys doped with minor quantities of other elements: e.g. stainless steel contains 10% of Cr and 1% of C, common bronze alloys are made of Cu and a 5% of Sn. However, the very partial knowledge of the phase diagram has made the search for new phase a tedious and random process. The recent development

of multi-principal element alloys<sup>[24]</sup> has permitted the discovery of so-far unexplored portions of phase diagrams in a much efficient way. This method can lead to materials with new properties far from the pure elements, much stronger, fault tolerant alloys as those used by demanding applications as jet turbines (Figure 12). For instance, Cantor alloy is a highly fracture tough material demonstrating crack resistance up to 200 MPam<sup>1/2</sup>;

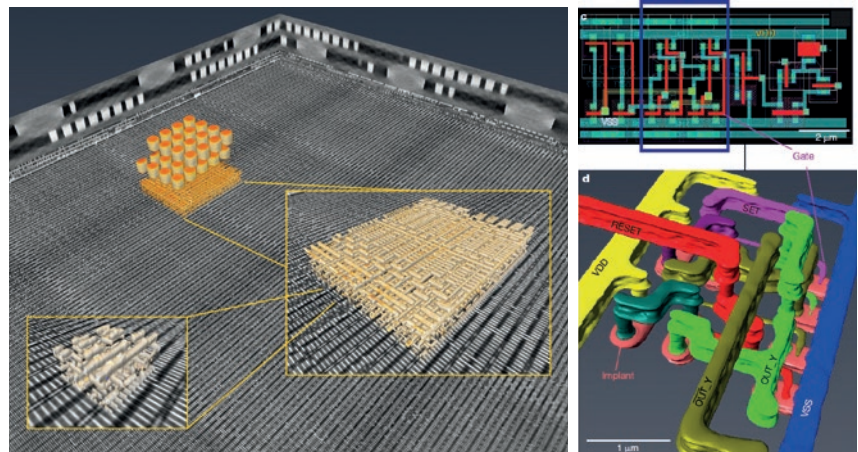


Figure 13: Reconstruction of a nanodevices from X-ray laminography (from<sup>[28]</sup>)

CrCoNi alloy ranks as one of the most fault tolerant material<sup>[25]</sup>. Moreover, multi-scale modelling will be possible by coupling this experimental approach with artificial intelligence and theoretical simulations to accelerate materials design. In particular, additive manufacturing which consist in 3D building of objects by adding layer-upon-layer of material (metal, polymer, concrete, biomaterial...) will strongly benefit from this approach.

### SOLEIL upgrade benefits

Synchrotron based techniques are well suited for addressing these issues. They offer an extended view from mm and the nm scales, sensitive to the chemical composition and to the presence of trace elements. These approaches will be considerably improved by SOLEIL Upgrade owing to the renewed performances in terms of coherence and focusing capability. The novel performances will help investigating materials processing, growth or ageing under *operando* conditions. Tomographic measurements will provide a direct access to these processes as shown in Figure 11, where 4D (space and time) tomography has been used to unravel the coarsening of Mg-Zn alloys at the μm level. Such studies will immediately benefit from focusing optics or phase contrast in order to delve into the dendrites morphology at sub μm scale. The faster measurements will allow the exploration of vast compositional space or help identifying phase segregations, domains and crack propagation e.g. by coherent diffraction or nano-tomography. Artificial intelligence and new predictive algorithms will accelerate the discoveries. On the other hand, SOLEIL upgrade will advantageously turn current scattering or spectroscopic approaches (ARPES,

IR/THz, RIXS) into local probe at scales ranging from  $\mu\text{m}$  to nm. Thanks to the smaller source, micro or nanospectroscopic techniques will provide the band structure and excitations spectrum of a single domain in real working components<sup>[26]</sup> while coherent diffraction will determine the strain changes induced by current and voltage even for their buried parts<sup>[27]</sup>. A striking example of these novel capabilities is the application of ptychographic X-ray laminography to nanodevices. Components inside an actual micro circuit can be observed *in situ* combining a large analysis area ( $300 \times 300 \mu\text{m}^2$ ) and local sub  $\mu\text{m}$  resolution (Figure 13).

## 2D materials

### Interest

As illustrated in Figure 2, the functionality of novel complex materials derives from the competition between the various internal degrees of freedom and phases. In his Nobel Prize speech in 2000, H. Kroemer promoted the idea that “the Interface is the device”, then referring to the physics observed at semiconductor interfaces. These emerging phenomena have led to the fast development of electronic devices such as transistor, laser or diodes. Following the discovery of graphene and emerging physics in oxides, the interest has more recently shifted to van der Waals exfoliable 2D materials stack, oxide interfaces, oxides heterostructures and so-called hybrid interfaces opening a whole new world of materials design, properties and functionalities. This includes the discovery of 2D electron gas at the LAO/STO interface<sup>[28]</sup>; the use of oxides heterostructures for voltage-controlled metal-insulator transition<sup>[30]</sup> or magnetism<sup>[31]</sup>; the enhancement of superconductivity in the hybrid FeSe/STO interface<sup>[32]</sup>; the manipulation of domain walls in ferroelectrics and ferromagnetic perovskites<sup>[33]</sup>. These examples all come down to the creation of “artificial materials by design” by a control at the atomic and molecular levels of the materials growth. Additional control knobs can be brought by the modification of the nanomechanical structure and its relation with the dynamics in the material or defects manipulation and their relation to structure and magnetism. By their polymorphism and tunable, extraordinary properties, 2D materials and heterostructures can boost devices performances. They are also considered for quantum computing.

### Challenges

The development of 2D materials relies on our ability to control their growth and presence of defects at the atomic level and follow their electronic properties while operated. The role of phase mixing at the nanoscale range and of low-concentration defects in the bulk of oxide materials are critical to understanding their properties once integrated in actual devices. This calls for probes of the structural and electronic properties down to the nm scale and compatible with *in situ*, *operando* conditions.

### SOLEIL upgrade benefits

The progress in coherence and lateral dimensions of SOLEIL Upgrade will help answering such questions. Surface scattering will benefit from the high brilliance and micro-beam to follow *in situ* growth (Figure 14) with possible access to mesoscopic scale structures at lower  $q$  values. XPCS could be used for addressing the kinetics of materials growth and structural displacement. On the other hand, the electronic structure can be addressed by ARPES (Figure 14) and other spectroscopic techniques such as RIXS or IR with  $\mu\text{m}$  down to nm focusing. Note that a microbeam spot (ca.  $1 \mu\text{m}$ ) can be easily obtained with the new machine thanks to the reduced source size, making micro-ARPES measurements as efficient as classical ARPES and opening the way to *operando* conditions. Furthermore, **acquisitions are expected to be faster by a factor 10** due to the brighter source and more efficient thanks to energy independent focusing optics.

## MOFs

### Interest

Nanoporous solids include zeolites, metal-organic and covalent organic frameworks (MOFs and COFs) and porous polymers. MOFs and COFs can be designed as the linking of building blocks into (infinite) 2D or 3D structures by reticular chemistry. In these compounds, both organic and inorganic units are linked by metal-ligand bonds (MOFs) or organic units are covalently bonded (COFs) via reversible bonds (e.g. imine). The interest of these compounds relies in our capability of finely tuning several of their properties by choosing their building blocks and by post growth modifications. The most evident property that can be tuned is the porosity that can be expressed in specific surface

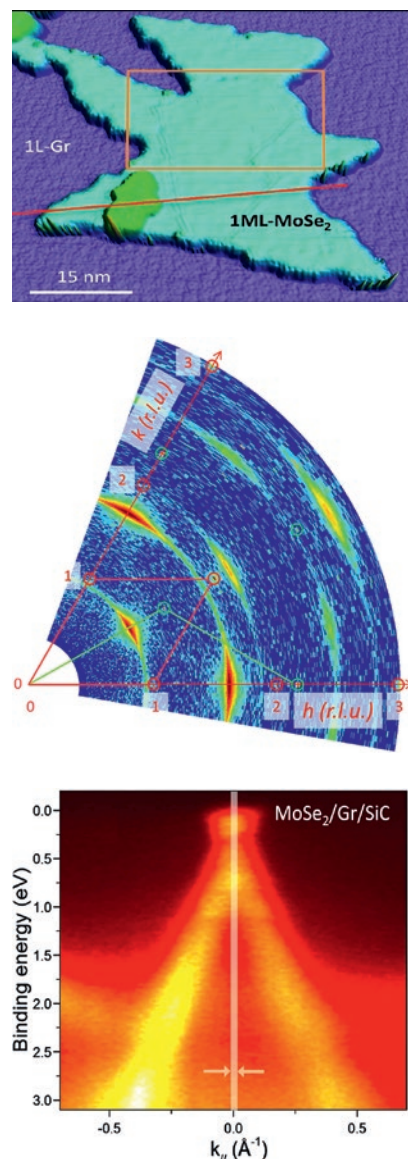


Figure 14: Characterization of a 1 ML flake of MoSe<sub>2</sub> deposited on graphene (up) by surface scattering (middle) and nano ARPES (down) (from<sup>[34]</sup>)

area terms, but not only. For instance, the MOF-5 series (Figure 15) exhibits pores and channels of different sizes and specific functions can be targeted by modifying the chemical functions on the organic building blocks. This outstanding flexibility makes MOFs excellent materials for gas separation or storage, thus well suited to cleaner, more sustainable energy production. Using MOFs in a gas propelled vehicles for instance, can significantly extend the travel range without increasing the tank pressure<sup>[35,36]</sup>. Gas separation can be performed thanks to the differential affinity of the MOFs for absorbing one or another molecule, e.g. highly selective absorption can be used to separate ethylene from its dangerous sub product acetylene<sup>[37]</sup>, which not only

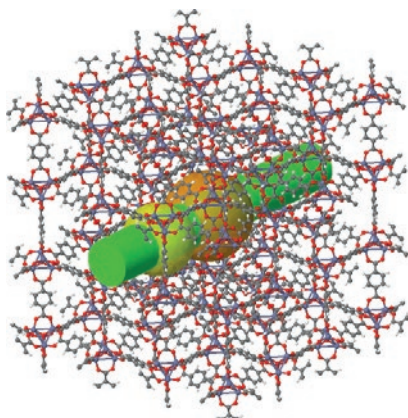


Figure 15: MOF-5 structure showing the different pores size (spheres) and channel (tube) (from<sup>[39]</sup>)

poisons polymerization catalysts, but it's also highly explosive.

### Challenges

In spite of their robustness and versatility, MOFs/COFs have not yet deployed their full capabilities: MOFs could be more efficiently used as heterogeneous catalysts, photocatalysts, electrocatalysts or improve catalytic/functional sites at the metal or organic centers<sup>[39]</sup>. But applying MOFs in catalysis and generally speaking rationalizing their behavior require a detailed knowledge of their structures. MOFs and COFs can also modify their

host structure by gate opening or breathing (*i.e.* opening and closing the access to pores or pores themselves) when in contact with a solvent or gas molecule, the structure can even react to light as recently demonstrated<sup>[40]</sup> and open new perspectives for its functionalization.

Characterization of MOFs/COFs has been performed by chemical probes, solid state NMR and electron microscopy, EXAFS and especially XRD. Single crystal diffraction provides location of atoms of the host and the guest molecules and, as EXAFS, does not suffer from limitations regarding the sample environment. However MOFs usually comes in micron size<sup>[41]</sup>, making structural determination difficult and leading to a bottleneck for future research.

### SOLEIL upgrade benefits

SOLEIL Upgrade will provide a more brilliant and smaller source making micron sized beams routine on undulator beamlines. **Simulations indicate a gain in brilliance from hard X-ray undulators** (up to two order of magnitude at  $E > 20$  keV with smaller gap and an increase of the number of periods). Another factor 100 can be obtained by exploiting the pink beam and fully using a finer undulator harmonics bypassing the monochromator. This will reduce data

collection from several hours to minutes or possibly seconds. In particular, **pink beam serial crystallography** appears as an appropriate solution for the rapid structural determination of micron sized crystals<sup>[42]</sup> avoiding beam damage. The pink beam approach will help increasing completeness of the datasets and reduce timescale down to 100 ps resolution, well below the characteristic time of an entire MOFs crystal rearrangement or crystal growth kinetics. Thus, it will be possible to quickly determine the structure of batches of  $\mu\text{m}$  scale MOFs and follow their growth in *operando* conditions by developing suitable cells or microfluidic supplies as already developed for macromolecular crystallography<sup>[43]</sup>. Here again, coupling experimentation to artificial intelligence and simulations will optimize multi-scale characterization which will advance material design. THz spectroscopy will also benefit from SOLEIL Upgrade. THz modes have been shown to be intrinsically linked to gate-opening and pore-breathing mechanisms, shear-induced phase transitions and the onset of structural instability<sup>[44]</sup>. THz spectroscopy will provide signature of gate openings or amorphization as a function of pressure that is a technologically relevant aspect for gas storage and selective absorption.

## REFERENCES

- [1] International Data Corporation "Data Age 2025" whitepaper.
- [2] Tokura, Y., Kawasaki, M., Nagaosa, N. "Emergent functions of quantum materials" *Nature Physics*, 13: art. n° 1056 (2017).
- [3] Basov, D.N., Averitt, R.D., Hsieh, D. "Towards properties on demand in quantum materials" *Nature Materials*, 16: art. n°1077 (2017).
- [4] Lee, S.R., Sharma, P.A., Lima-Sharma, A.L., Pan, W., Nenoff, T.M. "Topological quantum materials for realizing Majorana quasiparticles" *Chemistry of Materials*, 31: art. n° 26 (2019).
- [5] Goodwin, A.L. "Opportunities and challenges in understanding complex functional materials" *Nature Communications*, 10: art. n° 4461 (2019).
- [6] Preziosi, D., Lopez-Mir, L., Li, X., Cornelissen, T., Lee, J. H., Trier, F., Bouzehouane, K., Valencia, S., Gloter, A., Barthélémy, A., Bibes, M. "Direct mapping of phase separation across the metal-insulator transition of NdNiO<sub>3</sub>" *Nano Letters*, 18: art. n° 2226 (2018).
- [7] Lee, J.C.T., Alexander, S.J., Kevan, S.D., Roy, S., McMorran, B.J. "Laguerre-Gauss and Hermite-Gauss soft X-ray states generated using diffractive optics" *Nature Photonics*, 13: art. n° 205 (2019).
- [8] Spaldin, N.A., Fiebig, M. "The renaissance of magnetoelectric multiferroics" *Science*, 309 art. n° 391 (2005).
- [9] Spaldin, N.A., Ramesh, R. "Advances in magnetoelectric multiferroics" *Nature Materials*, 18:art. n° 203 (2019).
- [10] Newton, M.C., Parsons, A., Wagner, U., Rau, C. "Coherent X-ray diffraction imaging of photo induced structural changes in BiFeO<sub>3</sub> nanocrystals" *New Journal of Physics*, 18:art n° 093003 (2016).
- [11] Fert, A., Reyren, N., Cros, V. "Magnetic skyrmions: advances in physics and potential applications" *Nature Reviews Materials*, 2: art. n° 17031 (2017).
- [12] Geng, Y., Das, H., Wysocki, A.L., Wang, X., Cheong, S.-W., Mostovoy, M., Fennie, C. J., Wu, W. "Direct visualization of magnetoelectric domains" *Nature Materials*, 13: art. n° 163 (2014).
- [13] Gross, I., Akhtar, W., Garcia, V., Martinez, L.J., Chouaieb, S., Garcia, K., Carrétéro, C., Barthélémy, A., Appel, P., Maletinsky, P., Kim, J.V., Chauleau, .Y., Jaouen, N., Viret, M., Bibes, M., Fusil, S., Jacques, V. "Real-space imaging of non-collinear antiferromagnetic order with a single-spin magnetometer" *Nature*, 549: art. n° 252 (2017).
- [14] Moubah, R., Elzo, M., El Moussaoui, S., Colson, D., Jaouen, N., Belkhou, R., Viret, M. "Direct imaging of both ferroelectric and antiferromagnetic domains in multiferroic BiFeO<sub>3</sub> single crystal using X-ray photoemission electron microscopy" *Applied Physics Letters*, 100: art. n° 042406 (2012)
- [15] Gorfman, S., Bokov, A.A., Davtyan, A., Reiser, M., Xie, Y., Ye, Z.-G., Zozulya, A.V., Sprung, M., Pietsch, U., Gutt, C. "Ferroelectric domain wall dynamics characterized with X-ray photon correlation spectroscopy" *Proceedings of the National Academy of Sciences*, 115: art. n° E6680 (2018).
- [16] Chauleau, J.Y., Chirac, T., Fusil, S., Garcia, V., Akhtar, W., Tranchida, J., Thibault, P., Gross, I., Blouzon, C., Finco, A., Bibes, M., Dkhil, B., Khalyavin, D.D., Manuel, P., Jacques, V., Jaouen, N., Viret, M. "Electric and antiferromagnetic chiral textures at multiferroic domain walls" *Nature Materials*, 19: art. n° 386 (2019).
- [17] Zaum, S., Grube, K., Schäfer, R., Bauer, E. D., Thompson, J. D., v. Löhneysen, H. "Towards the identification of a quantum critical line in the (p, b) phase diagram of CeCoIn<sub>5</sub> with thermal-expansion measurements". *Phys. Rev. Lett.*, 106: art. n° 087003 (2011).
- [18] Snider, E., Dasenbrock-Gammon, N., McBride, R., Debessai, M., Vindana, H., Ven- catasamy, K., Lawler, K.V., Salamat, A., Dias, R.P. "Room-temperature superconductivity in a carbonaceous sulfur hydride" *Nature*, 586: art. n° 373 (2020).
- [19] Loubeyre, P., Occelli, F., Dumas, P. "Synchrotron infrared spectroscopic evidence of the probable transition to metal hydrogen" *Nature*, 577: art. n° 631 (2020).
- [20] Geim, A. K., Grigorieva, I. V. "Van der waals heterostructures". *Nature*, 499: art. n° 419 (2013).
- [21] Roy, T., Tosun, M., Kang, J. S., Sachid, A. B., Desai, S. B., Hettick, M., Hu, C. C., Javey, A. "Field-effect transistors built from all two-dimensional material components". *ACS Nano*, 8(6):6259–6264 (2014).
- [22] Guo, E., Phillion, A.B., Cai, B., Shuai, S., Kazantsev, D., Jing, T., Lee, P.D. "Dendritic evolution during coarsening of Mg-Zn alloys via 4D synchrotron tomography" *Acta Materialia*, 123: art. n° 373 (2017).
- [23] Zachman, M.J., Tu, Z., Choudhury, S., Archer, L.A., Kourkoutis, L.F. "Cryo-stem mapping of solid-liquid interfaces and dendrites in lithium-metal batteries" *Nature*, 560: art. n° 345 (2018)
- [24] Yeh, J.-W., Chen, S.-K., Lin, S.-J., Gan, J.-Y., Chin, T.-S., Shun, T.-T., Tsau, C.-H., Chang, S.-Y. "Nanostructured high-entropy alloys with multiple principal elements: Novel alloy design concepts and outcomes" *Advanced Engineering Materials*, 6: art. n° 299 (2004).
- [25] George, E.P., Raabe, D., Ritchie, R.O. "High-entropy alloys" *Nature Reviews Materials*, 4: art. n° 515 (2019).
- [26] Bostwick, A., Rotenberg, E., Avila, J., Asensio, M.C. "Zooming in on electronic structure: NanoARPES at SOLEIL and ALS" *Synchrotron Radiation News*, 25: art. n° 19 (2012).
- [27] Robinson, I., Harder, R. "Coherent X-ray diffraction imaging of strain at the nanoscale" *Nature Materials*, 8: art. n° 291 (2009).
- [28] Holler, M., Odstrcil, M., Guizar-Sicairos, M., Lebugle, M., Müller, E., Finizio, S., Tinti, G., David, C., Zusman, J., Unglaub, W., Bunk, O., Raabe, J., Levi, A. F. J., Aeppli, G. "Three-dimensional imaging of integrated circuits with macro- to nanoscale zoom" *Nature Electronics*, 2: art. n°464 (2019).
- [29] Ohtomo, A. Hwang, H.Y. "A high-mobility electron gas at the LaAlO<sub>3</sub>/SrTiO<sub>3</sub> heterointerface" *Nature*, 427: art. n° 423 (2004).
- [30] Hwang, H.Y., Iwasa, Y., Kawasaki, M., Keimer, B., Nagaosa, N., Tokura, Y. "Emergent phenomena at oxide interfaces" *Nature Materials*, 11: art n° 03 (2012).
- [31] Yin, Y.W., Burton, J.D., Kim, Y.-M., Borisevich, A. Y., Pennycook, S.J., Yang, S.M., Noh, T.W., Gruverman, A., Li, X.G., Tsymbal, E.Y., Li, Q. "Enhanced tunnelling electroresistance effect due to a ferroelectrically induced phase transition at a magnetic complex oxide interface" *Nature Materials*, 12: art. n° 397 (2013).
- [32] Ge, J.-F., Liu, Z.-L., Liu, C., Gao, C.-L., Qian, D., Xue, Q.-K., Liu, Y., Jia, J.-F. "Superconductivity above 100 K in single-layer FeSe films on doped SrTiO<sub>3</sub>" *Nature Materials*, 14: art. n° 285 (2015).
- [33] Tokunaga, Y., Furukawa, N., Sakai, H., Taguchi, Y., Arima, T.-h., Tokura, Y. "Composite domain walls in a multiferroic perovskite ferrite" *Nature Materials*, 8: art. n° 558 (2009).



- [34] Dau, M.T., Gay, M., Di Felice, D., Vergnaud, C., Marty, A., Beigné, C., Renaud, G., Renault, O., Mallet, P., Le Quang, T., Veuillen, J.-Y., Huder, L., Renard, V. T., Chapelier, C., Zamborlini, G., Jugovac, M., Feyer, V., Dappe, Y. J., Pochet, P., Jamet, M. "Beyond van der Waals interaction: The case of MoSe<sub>2</sub> epitaxially grown on few-layer graphene" *ACS Nano*, 12: art. n° 2319 (2018).
- [35] "BASF metal organic frameworks (MOFs): Innovative fuel systems for natural gas vehicles (NGVs)" *Chemical Society Review*, 43: art. n° 6173 (2014).
- [36] He, Y., Zhou, W., Qian, G., Chen, B. "Methane storage in metal-organic frameworks" *Chemical Society Review*, 43: art. n° 5657 (2014).
- [37] Lin, R.-B., Xiang, S., Xing, H., Zhou, W., Chen, B. "Exploration of porous metal-organic frameworks for gas separation and purification" *Coordination Chemistry Reviews*, 378: art. n° 87 (2019).
- [38] Yaghi, O. M. "Reticular chemistry: Molecular precision in infinite 2D and 3D" *Molecular Frontiers Journal*, 03: art. n° 66 (2019)
- [39] Li, H., Li, L., Lin, R.-B., Zhou, W., Zhang, Z., Xiang, S., Chen, B. "Porous metal-organic frameworks for gas storage and separation: Status and challenges" *EnergyChem*, 1: art. n° 100006 (2019).
- [40] Song, W.-C., Cui, X.-Z., Liu, Z.-Y., Yang, E.-C., Zhao, X.-J. "Light-triggered supramolecular isomerism in a self-catenated Zn(II)-organic framework: Dynamic photo-switching CO<sub>2</sub> uptake and detection of nitroaromatics" *Scientific Reports*, 6: art. n° 34870 (2016)
- [41] Zheng, W., Tsang, C.-S., Lee, L.Y.S., Wong, K.-Y. "Two-dimensional metal-organic framework and covalent-organic framework: synthesis and their energy-related applications" *Materials Today Chemistry*, 12: art n° 34 (2019).
- [42] Meents, A., Wiedorn, M.O., Srajer, V., Henning, R., Sarrou, I., Bergtholdt, J., Barthelmess, M., Reinke, P.Y.A., Dierksmeyer, D., Tolstikova, A., Schaible, S., Messerschmidt, M., Ogata, C. M., Kissick, D.J., Taft, M.H., Manstein, D.J., Lieske, J., Oberthuer, D., Fischetti, R.F., Chapman, H.N. "Pink-beam serial crystallography" *Nature Communications*, 8: art. n° 1281 (2017).
- [43] Heymann, M., Opathalage, A., Wierman, J.L., Akella, S., Szebenyi, D.M.E., Gruner, S.M., Fraden, S. "Room-temperature serial crystallography using a kinetically optimized microfluidic device for protein crystallization and on-chip X-ray diffraction" *IUCrJ* 1: art. n° 349 (2015).
- [44] Ryder, M.R., Civalleri, B., Bennett, T.D., Henke, S., Rudic, S., Cinque, G., Fernandez-Alonso, F., Tan, J.-C. "Identifying the role of terahertz vibrations in metal-organic frameworks: From gate-opening phenomenon to shear-driven structural destabilization" *Physical Review Letters*, 113: art. n° 215502 (2014).

# Sustainable Energy: from production, conversion, storage and climate action

## — Overview

Energy drives our modern society and its sustainability is a main concern leading the United Nations to decide at the Rio+20 Conference a set of Sustainable Development Goals (SDGs) (Figure 1)<sup>[1]</sup>. The 2030 Agenda for SDGs encourages our society to stimulate research to afford reliable, sustainable and modern energy for all in a future and healthy world with environmentally sound technologies, reducing pollution of water and terrestrial ecosystems, integrating climate change measures and favouring recycling and remediation.



Figure 1: List of the 17 goals established by the United Nations in 2015 to achieve a better and more sustainable future. Each goal having to be achieved by 2030<sup>[1]</sup>

Scientists then have to respond to new challenges to support the sustainability of energy resources with science and technology roadmaps, including on the one hand reduction of the use of fossil feedstocks and mitigation of greenhouse gases and pollutants related to fossil fuel combustion, and on the other hand considering a more efficient production, conversion and storage of intermittent energy sources such as sun or wind. The progress in the technology development in those fields must be integrated into a global strategy which takes into account the three dimensions of sustainable development, *i.e.* economic, societal and environmental. In particular the concept of a circular economy, in which waste and pollution are eliminated by design, products and materials are kept in use, natural systems are regenerated and the sought transition towards a green energy, are not only promising levers for the implementation of the 2030 Agenda but also drivers of industrial opportunities for new technology. Indeed, discovery of new “green” energy-related materials, performance optimization and durability are of paramount importance to achieve a mature level for commercial solutions against global warming and sustainable resources. Bottlenecks, limiting such progress today, have been identified during discussions of the Round Table related to the sustainable development of energy-related materials. A large class of materials for energy production, conversion and storage has been

addressed by the users scientific community of SOLEIL including homogeneous and heterogeneous catalysts, electro-catalysts, photocatalysts, electrode and electrolyte materials for Li or Na-ion batteries and for solid state batteries, advanced materials for supercapacitors and metal-air batteries, organic, inorganic and hybrid materials for solar photovoltaics, thermoelectric or piezoelectric materials, high temperature and environmental degradation resistant materials for low carbon energy (fuel cells, concentrated solar energy) and nuclear energy technology applications. In parallel, climate actions with focus on CO<sub>2</sub> conversion and sequestration could be achieved with bio-inspired materials, hierarchically porous materials such as metal organic frameworks and bio-based hybrid foams with applications for instance in steel industry or modern concrete technology... Only some of these, centred on heterogeneous catalysis, photovoltaic devices or ion-batteries, are presented in this section, aiming to illustrate the impact of the SOLEIL upgrade in the field and how these challenges can be addressed using techniques which will become possible due to a substantial decrease of the beam size and increase of coherence with specific techniques and methods over a broad photon energy range. Then again, today’s emerging techniques, which will fully flourish with the upgrade and the development of new infrastructures favoured by the upgrade, will benefit many other energy-related materials such as electro-catalysts used in fuel cells as developed in the document gathering the conclusions of the “Energy” Round Table, appended to this report (annex available on demand. Contact: [webcom@synchrotron-soleil.fr](mailto:webcom@synchrotron-soleil.fr)). The “Energy” Round Table report details extensive discussions on many aspects of the study of materials for the deployment of renewable and sustainable energy. The case of nuclear materials and energy has been developed in a different round table on “Radioactive Materials” which can also be found in the annex.

It is not the aim of the present chapter to cover the large field of materials for energy but rather illustrate the potential offered by the upgrade of SOLEIL in three domains:

- Catalysis as a pivotal science for energy production and conversion
- Conversion of solar energy and photovoltaic devices
- Electrochemical energy storage materials.

Those materials share as specificity to have applications governed by chemical reactions or physical interactions at the interfaces of different media. The techniques pushed ahead in one of the three domains can benefit obviously to the other fields.



## Catalysis: a pivotal science for energy production

On the global challenge of a sustainable society based on the development of new energy sources, interdisciplinary research is carried out to tackle the major issues related to the production or conversion of sustainable energy. Heterogeneous catalysis is a crucial discipline for making cleaner, more efficient and economically viable chemicals or fuels from sustainable resources such as biomass and derivative products or for reducing greenhouse gas emissions released from vehicles. Electro-catalysis is the driving force for converting CO<sub>2</sub> in a wide range of C1 products (CO, HCOOH, CH<sub>3</sub>OH, CH<sub>4</sub>) and H<sub>2</sub> into electricity in fuel cell technology developed for stationary power applications or transportation. Photo-catalysis is at the heart of self-cleaning applications and reduction of air pollutants with mitigation of important non-CO<sub>2</sub> greenhouse gases such as NO<sub>x</sub> or CH<sub>4</sub>. The success of the energetic transition is strongly related to gaining fundamental understanding of catalytic processes, requiring the study of real systems under process conditions (*operando* characterization), at different length scales (from the macroscopic level to the nanometric or atomic ones), and at different time scales (picoseconds to seconds). Considerations on the long term ageing of catalytic materials and devices are also of paramount importance to understand their durability and stability, and are mandatory for bringing them to a commercial scale for the benefit of our planet.

### Reinventing catalysts with emerging 4D or 5D hyperspectral data collection

#### Interest

Rather to focus on specific reactions, this section emphasizes common characteristics shared by catalysts encountered in heterogeneous catalysis, electro- or photo-catalysis which will require the complementarity of different techniques available at a Synchrotron Radiation facility to fully depict their complexity. The discovery of efficient catalytic systems for energy production involving biomass conversion, the hydrogen oxidation reaction and the kinetically-sluggish oxygen reduction reaction in fuel cells, for mitigation strategies of greenhouse gases, requires a better understanding and control of the nature and evolution of the catalytic sites under working conditions. Irrespective of the applications, the activity of the catalyst is

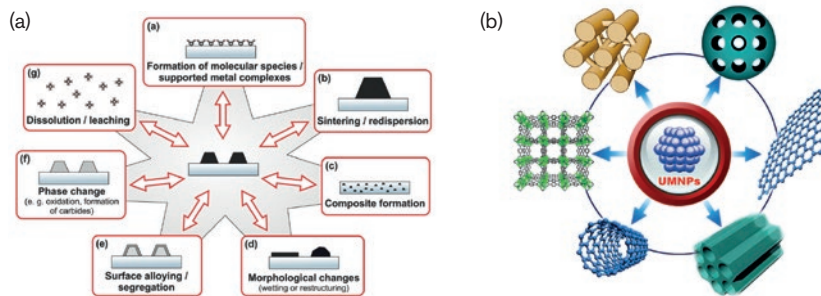


Figure 2: (a) Structural changes of supported metal nanoparticles upon reaction<sup>[2]</sup>. (b) Desired composition must be produced and immobilized into various high surface area materials<sup>[3]</sup>

provided by multicomponent (metallic) active nanoparticles (typically in the range 3-7 nm, (Figure 2a) dispersed on a porous support, embedded in a membrane electrode assembly or associated with a semiconductor light harvesting antenna, which can suffer from manifold reorganisation under reaction conditions at different time scales ranging from microseconds to minutes, hours or months depending on activation, reaction and deactivation related processes. The control of the (metallic) nanoparticle (NP) morphology and composition, with a narrow size distribution, is required for providing a high density of active sites and then enhancing catalytic efficiency (which is often synonymous with cost reduction at the industrial level). The understanding of parameters influencing the accessibility of the active site by the feedstock molecules is also of prime importance for an improved rational design of long-term stable heterogeneous catalysts.

In heterogeneous catalysis for instance, integrative chemistry, which allows nanoparticle immobilization in high-surface area materials (Figure 2b) with hierarchical porosity and 2D-nanolayer structures, is a promising research avenue to avoid aggregation promoted by the spatial confinement around the particles, but also to favour mass transfer of

reactants and products to and from the active sites using the support channels, respectively. These considerations explain why, today, catalysts are hierarchically structured materials encompassing many length scales, passing from the active sites (Å to nm) to catalyst grains (nm to μm) characterized by a porosity passing from macro pores (size > 50 nm), meso (2 nm < size < 50 nm) to micropores (size < 2 nm) and catalyst bodies (μm to mm) loaded in the reactor.

#### Challenges

The characterization of nanoparticle size, porous morphology, chemical composition and speciation of the as-prepared catalysts at different length scales is mandatory to improve design strategy towards catalysts with higher performance and excellent stability. The length scale of information must cover several orders of magnitude: from mm size to sub-nm scale.

**Tomography Imaging techniques** will be essential at the SOLEIL's DLSR to cover the multi-length scale characterization of the porosity inside a catalyst at the μm and sub-μm spatial resolution with field of view encompassing catalyst grains and catalyst bodies<sup>[4]</sup> whereas **Scanning Transmission X-ray Microscopy (STXM)** using both hard and soft X-rays will be of prime importance for accessing to the chemical composition of nanoparticles<sup>[5]</sup> as illustrated in Figure 3.

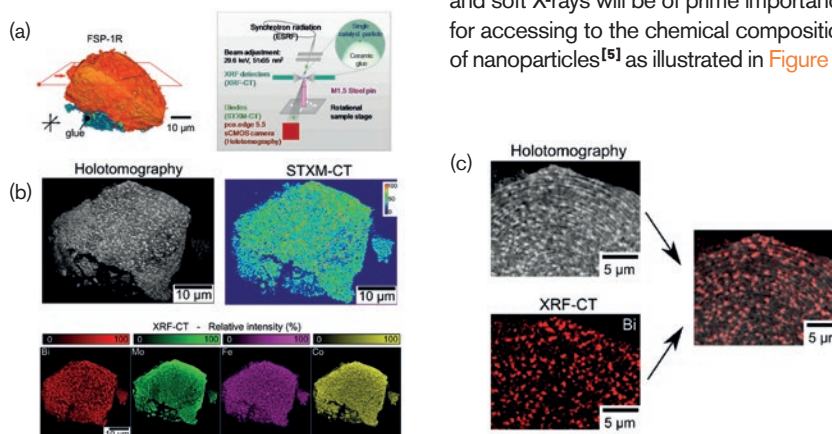


Figure 3: Full field phase tomography of ca. 50 μm multicomponent Bi-Mo-Fe-Co oxide spent catalyst particle which reveals particle morphology combined with STXM of the same particle which displays the elemental compositions. The spatial resolution for both techniques was ca. 100 nm and (c) zoom in a common area and overlay of phase tomography (50% transparency) with Bi X-Ray Fluorescence-Computed Tomography (Bi XRF-CT) showing a very good match of the Bi distribution to the heterogeneous features revealed by the multimodal approach<sup>[6]</sup>

### SOLEIL upgrade Benefits

The increase in beam coherence provided by the SOLEIL's upgraded source will be useful for phase sensitive 2D imaging and 3D tomography providing higher image contrast than those available today. With a brighter source, the acquisition time of images will become significantly shorter (down to 50 ms or less for a full volume) making possible large surface characterization with  $\mu\text{m}$  or nm spatial resolution giving access to **statistical evaluation of the structure and composition of the catalysts at the various length scales** but also to **conditions for *operando* time-resolved measurements of the catalysts**. The spatial resolution of scanning X-ray nano-imaging techniques, which necessitate highly coherent X-ray beam to obtain diffraction-limited focusing, is limited by the quality of the nano-focusing optics and by the energy of the beam. Diffraction-limited focused beam could be achieved at a few nm in the soft X-ray range and around 10 nm in the hard X-ray range which is not so far from today's performances but taking advantage of the **increased source brilliance** after upgrading SOLEIL, **significantly increased coherent flux** (up to 2 orders of magnitude at hard X-rays) will be available whereas an increase of spatial resolution performances (a few nm for soft X-rays) using *e.g.* ptychography imaging could be achieved allowing to tackle the tinier NP ( $\sim 5$  nm) composition. **The upgrade of SOLEIL** will then provide **invaluable information to understand the evolution of NP dispersion (particle and aggregate nanometer-sized dispersions) on the support, sub-micron and micron-sized catalyst grain composition and hierarchical porosity**

**evolution during each unitary step of the catalyst life: genesis, activation, reaction and deactivation, through the opportunity of emerging time-resolved characterizations of those complex systems at beamlines devoted to 2D and 3D imaging coupling to chemical speciation.** The in-depth description of the complexity of those processes happening at multiple length scales will strongly benefit from the possibility to carry out all these measurements in a correlative approach using several beamlines<sup>[4]</sup>. **The 4D or 5D hyperspectral imaging** (2 or 3D for the spatial resolution, 1D for the energy-dependent chemical information and 1D for the time, temperature or pressure evolution) so obtained will **tremendously shake up the dynamic description** of those evolving complex materials putting in front metastable intermediate species playing a key role for the kinetic descriptions of the system at the various relevant length scales of the studied objects. Sub-second time resolution for 4D or 5D hyperspectral imaging will be currently offered matching perfectly the time scale for the study of catalytic processes involving a mass transport.

### What and where is the active site?

#### Interest

The identification of the active sites is crucial for mastering efficient catalysts as well the understanding of the role of promoter and of the choice of the support. If the NP dispersing role of the support on the catalytic activity and selectivity has long been recognized, less is known on the sites at which reaction takes place (Figure 4a). Some supports can participate in the catalytic reaction itself for instance by

supplying oxygen via molecularly adsorbed oxygen or via the so-called Mars-van Krevelen mechanism<sup>[7]</sup>.

The question **“where is the active site?”** is crucial: Is the active site localized only on a specific metallic NP facet? Are specific sites involved at the metal-oxide support boundary? Do electronic transitions (charge transfer, ligand effects...) or structural effects (leading to strain, relaxation...) between the NP and support play a role in the activity by influencing the adsorption of reactants?<sup>[9]</sup>

The active role of some oxide supports ( $\text{CeO}_2$ ,  $\text{ZrO}_2$ ,  $\text{TiO}_2$ ) and the tailoring of their interactions with the active NPs are so important that new preparation routes emerged in the last decade where a close contact between NP and active oxide support (Figure 4b) is provided with the concept of NP encapsulation inside a thin layer of support<sup>[10]</sup> or formation of Janus particles<sup>[8]</sup>. Those strategies generally lead to an improvement of the catalytic activity compared to dispersion on flat support<sup>[8,11]</sup> however, the case of support coating active NP remains an intriguing concept regarding the access of reactants to the active sites, which must be studied in more details.

#### Challenges

In the last decade, **Bragg Coherent X-ray Diffraction Imaging (Bragg CDI)** has emerged as a powerful technique to gain knowledge on the internal structures of micro and nano crystalline particles with today at the best sub-10nm spatial resolution by measuring strains and atom displacements inside crystals with pm sensitivity. Hard X-rays represent a unique probe to perform ***in situ* measurements in temperature and pressure of catalysts** using

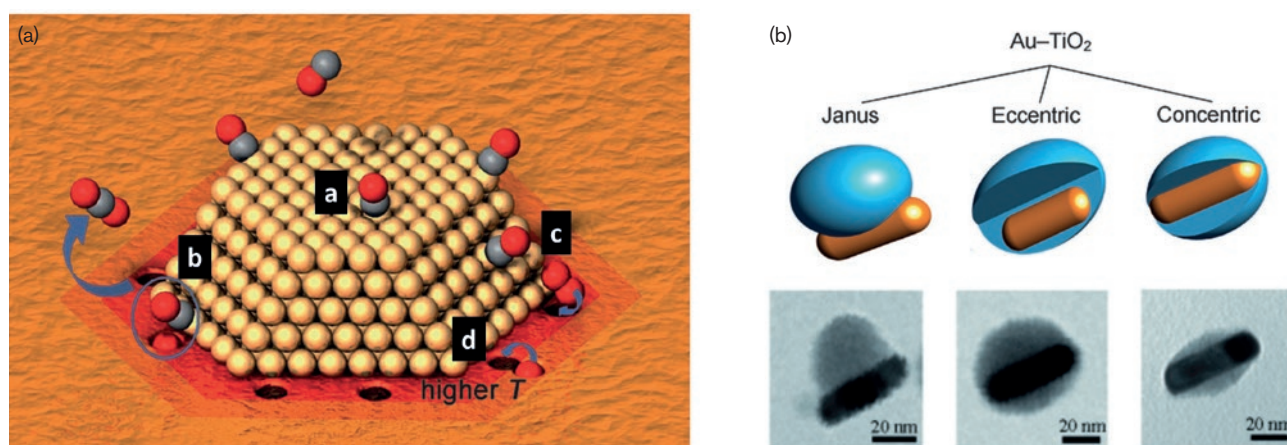


Figure 4: (a) Where are the active catalytic sites? Illustration for CO oxidation reaction<sup>[7]</sup> a. location: CO adsorption on NP sites, b. and c. locations: interface sites between the support and the NP. (b) Schematic representations of catalytic systems where  $\text{TiO}_2$  coated-Au nanorods with Janus, eccentric and concentric geometries were prepared from<sup>[8]</sup>

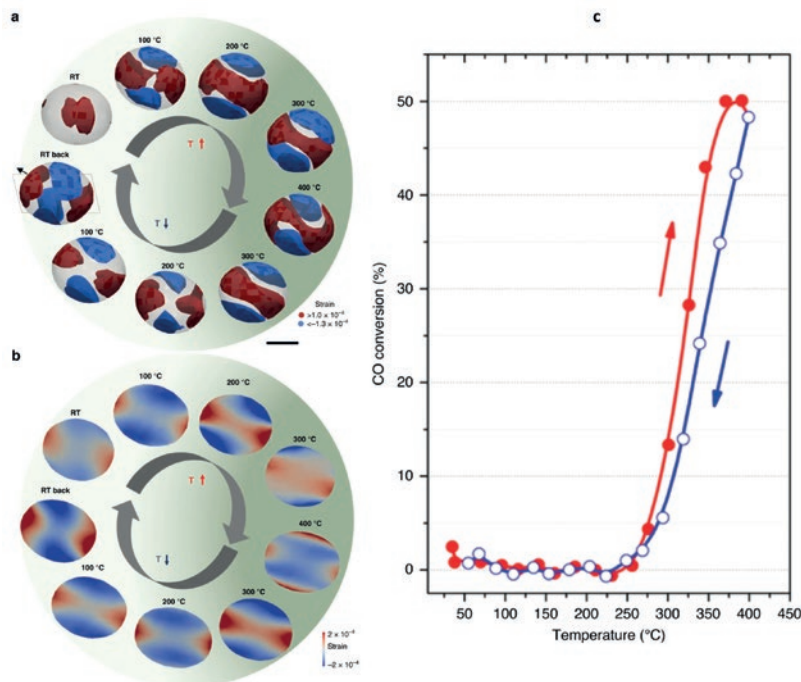


Figure 5: (a) Bragg CDI measurements of the distribution of the strain field projected along (111) of the same Au/TiO<sub>2</sub> NP upon exposure to CO/O<sub>2</sub> atmosphere at RT, 100, 200, 300 and 400°C and (b) corresponding particle cross section views of the internal strain field at the dashed line box in a. Scale bar, 30 nm, NP size = 68 nm, Spatial resolution = 15 nm, time for collection of Bragg CDI for one temperature condition = 35 min. The green gradient in a and b illustrates the increase/decrease of catalytic activity with temperature as measured by mass spectrometry. (c) CO conversion as a function of temperature for the same batch of Au/TiO<sub>2</sub> NPs. The red symbols were measured upon heating while the blue ones upon cooling [13]

dedicated reactors as shown in Figure 5 for Au NP supported on TiO<sub>2</sub> under CO/O<sub>2</sub> atmosphere for CO oxidation reaction [12, 13]. The Bragg CDI monitoring of the changes of compressive (blue) and tensile (red) strain distribution in the NP (Figure 5a and b) measured simultaneously to the catalytic activity by mass spectrometry correlates the catalytic performances and the propagation of tensile-strained areas from the NP surface to inside the nanocrystal upon heating. During cooling, the release of the tensile strain occurs with a temperature offset compared to the heating which is coincident with the light-off hysteresis loop typically measured for the catalytic activity (Figure 5c) of CO oxidation reaction. This study reveals that the lattice reorganisation to accommodate the tensile strains in the NP is the driving force for building the active sites at 400°C and elucidates the origin of the catalytic performance hysteresis.

### SOLEIL upgrade benefits

This proof of concept performed on large model NPs (68 nm or 400 nm today at SOLEIL on nickel NP used for CO<sub>2</sub> hydrogenation) illustrates how Bragg CDI will develop. 2 orders of magnitude of coherence increase in the upgraded source will lead to better time resolution, moving from *in situ* characterization with time frame of 1 hour to *operando* characterization with

collection time in the sub-min or sec range, together with a few nm spatial resolution for imaging the smaller particles found in the most efficient catalysts. The short penetration depth of electrons is still a restriction for environmental high resolution electron microscopy, which provides nm or atomic resolution information, limiting its usefulness for *operando* characterisations of important industrial processes requiring pressure (such as hydrotreating and hydrocracking processes, Fischer-Tropsch reaction, Haber ammonia synthesis). This restriction is overcome by the use of hard X-rays with

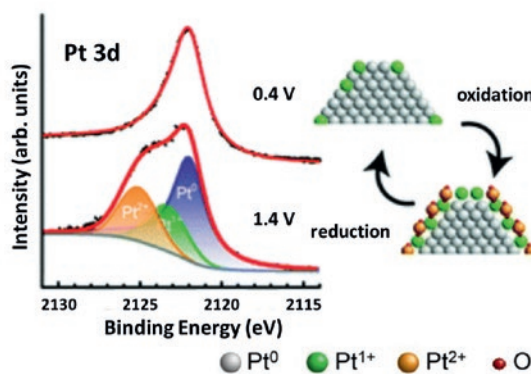


Figure 6: *in situ* NAP-HAXPES(8keV) Pt 3d<sub>5/2</sub> spectra of Pt/C cathode catalyst coated onto a Membrane Exchange Assembly containing Nafion membrane for 0.4 and 1.4 V, with 40 mbar water atmosphere provided at the cathode whereas H<sub>2</sub> was supplied to the anode. Quantitative peak-fitting analysis showed that the fraction of Pt<sup>1+</sup> and Pt<sup>2+</sup> species matched the ratio of the surface to total Pt atoms in 2.3 nm nanoparticles which suggests that Pt oxidation only takes place at the surface of Pt NP on the fuel cell cathode and the inner Pt atoms do not participate in the reaction. [16]

Bragg CDI. The imaging of the strain suffered by the particle under real working conditions will offer valuable answers to questions about the role of the support in catalytic activity and provide important levers for the design of efficient catalysts involving a more rational and less empirical selection of oxide supports. One should also emphasize the importance of the stability of the beam at SOLEIL (an important feature of SOLEIL today) which will be maintained or improved post upgrade and which participate to the precision of the measurements. The results gained by Bragg CDI in these conditions will also provide important structural/electronic inputs for evaluation of catalyst performance by state of the art computational analysis (e.g. DFT) [14].

The complementary use of X-ray Absorption Spectroscopy (XAS), X-ray Photoelectron Spectroscopy (XPS), Surface Ray Diffraction (SXR) and Resonant Inelastic Scattering (RIXS) carried out in *operando* conditions could provide a complete description of the nature and evolution of the active sites during the life span of catalysts. It will allow differentiation between the core and surface signals and inform about the charge transfer occurring upon atmosphere exposure as well as probing in depth interface activity. Major breakthroughs are also expected in the field of electro-catalysis which is known to be more complex than heterogeneous catalysis with the presence of water and the applied electrochemical potential. On the one hand, the use of NAP-XPS in the hard X-rays which permits to pass through the thick catalyst layers of fuel cells will strongly benefit of a small focused bright beam for *operando* measurements (Figure 6) by pushing at higher pressure the today pressure limit by reducing pre-lens aperture and working distance between the aperture

and sample<sup>[15]</sup>. On the other hand, XAS and its combination with imaging techniques for 3D, 4D or 5D hyperspectral studies will be unique for the development of efficient single atom catalysts for hydrogen oxidation and oxygen reduction reactions taking place at the fuel cell electrodes<sup>[16]</sup>.

## Conversion of solar energy: photovoltaic devices

The amount of solar energy our planet receives in 1 hour is more than the total energy consumed by the world's population per year. This would enable solar energy to meet our energy demand and definitely stabilize the atmospheric CO<sub>2</sub> concentration. Without calling for 100 percent solar energy which would have a detrimental impact on the environment by the requirements of large land area better used for agriculture and forestry, it is nevertheless agreed that the conversion of solar energy to electricity through the **solar photovoltaic technology** could impact significantly the global carbon emissions provided its expansion at a terawatt scale. However to reach such a TW market, several bottlenecks must be overcome as the scalability, cost and efficiency of the cell technology (Figure 7).

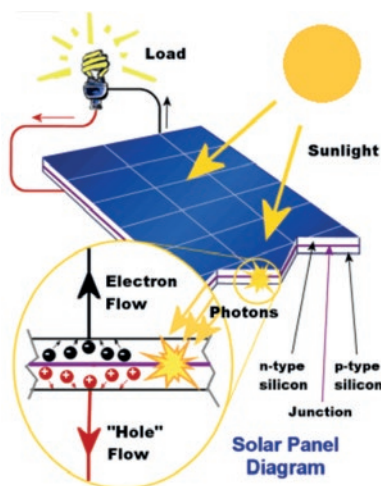


Figure 7: Principle of solar photovoltaic cell (above; from Wikipedia: Silicon\_solar\_cell.gif) where semiconductor layers absorb photons coming from the sunlight, generating electrons and positive charge carriers (holes). Solar cell field in a farm (below; from doi.org/10.1073/pnas.1820406116).

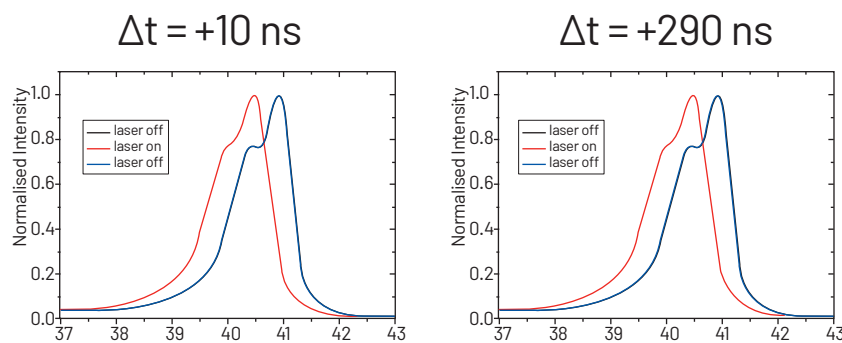


Figure 8: Laser pump-probe photoexcitation of a n-type Si(111) 7x7 allows the measure of Surface PhotoVoltage (SPV) changes. The SPV induces an energy shift of Si 2p photo-emission lines due to promotion of electrons from the valence into the conduction band. Herein, the measurements at different delay times  $\Delta t$  after laser illumination show the long lasting carrier lifetime. Courtesy of W. Flavell, D. Graham, B. Spencer.

## New generations of solar cells: beyond silicon market

### Interest

Although today silicon shares 90% of the market, this technology is not really viable to provide the required scalability for TW needs due to resource limitations. Furthermore, the Shockley-Queisser limitation associated with the use of narrow bandgap semiconductor (1.1 eV for Si) to generate carriers from a broad spectrum of sunlight restricts the theoretical efficiency for Si to 32% meaning that the 26% today lab scale performance is close to this limit. Combinations of materials must be sought to boost solar cell conversion efficiency by a better use of the solar irradiance spectrum. For instance in tandem solar cells, based on perovskite technology and silicon, the perovskite can be engineered to have a bandgap of 1.7 eV complementing the silicon's 1.1 eV, to achieve a theoretical efficiency limit around 43%<sup>[17]</sup>. Intense interdisciplinary efforts in Material Science Engineering support the quest for new materials with better energy efficiency to provide commercial devices to be hosted in solar cell fields (Figure 7).

### Challenges

The development of **new photovoltaic materials** calls for a direct experimental assessment of **electronic structure at functional interfaces** with a full description of the band structure and the position of the Fermi level in the bandgap by **photoemission techniques** with depth-profiling data according to the excitation energy<sup>[18]</sup>. Combination of **high resolution (HRPES) and time resolved pump-probe photoemission (TRPES)** is also

powerful in studying charge separation in photo-devices with chemical specificity by following the time evolution of excitons and the charge dynamics. Laser pulses can inject charge into the system on ultrafast time scales. The slower recombination and transport processes can then be studied with a time delayed synchrotron radiation pulse, with the site specificity provided by the chemical sensitivity of photoemission<sup>[19]</sup> as shown in Figure 8 and of core-level absorption spectroscopies<sup>[20]</sup>. Combination of HRPES and TRPES has already provided its unique potential in revealing the chemical composition of complex structures as core shell Quantum Dots (QDs)<sup>[18]</sup> but also the band energy diagram of QDs after ligand exchange procedure permitting to tune the doping of the QDs. Using pump probe (Laser/photoemission) experiment it is possible to unambiguously determine the nature of the majority charge carriers and measure the minority charge carrier lifetime which is directly related to the photovoltaic device efficiency.

### SOLEIL upgrade benefits

Increased brightness will be key in offering new opportunities to study electronic structure of photovoltaic devices involving QDs by offering a better S/N for the HRPES data which is today limited by the size and low element loading of the dots, but also to probe selectively the lifetime of photoexcited charge carriers in buried active solar cell layers giving detailed insight into the wave functions of occupied and unoccupied electronic states with discrimination between atomic species in different chemical environments. An extended time scale, ranging from a

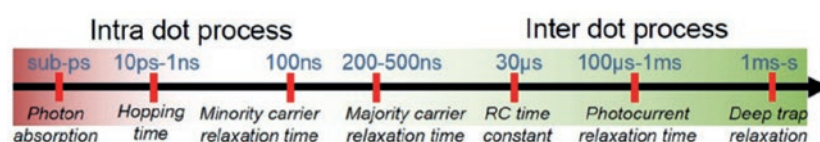


Figure 9: Multiple time scales in the photoexcitation and relaxation of quantum dots. Courtesy of W. Flavell.



few ps to s, has also to be investigated as exemplified in Figure 9 for tackling the large dynamics of charge carrier lifetime in QDs based photovoltaic materials. In that context the temporal modes of the upgraded SOLEIL source will provide a significant flux increase at the shortest time resolution (*i.e.* 10 ps) improving the data collection statistics without leading, as for the brighter pulsed X-ray Free Electrons Laser sources, to the well-known generation of vacuum space-charge transfer effects which induce spectral shift and broadening of the photoelectron kinetic energy distribution.

## Understanding the formation of defects

### Interest

Besides the engineering of multicomponent semiconductors, used to overcome the efficiency limitation of single junction solar cell associated with the Shockley-Queisser limit, an in-depth understanding of defects physics (such as composition inhomogeneity, dislocation and grain boundaries, or surface instabilities) is necessary to control solar cell efficiency. The study of defects in semiconducting materials is of paramount importance due to their ambivalence role in the performances by sometimes favouring the band alignment at the solar cell heterojunction or at the opposite by strongly limiting the mobility of photo-generated electrons and holes which do not have lifetimes sufficient for collection to the p-n junction. Correlative X-ray microscopy has been widely used in the field of photovoltaics after the demonstration in 2000, that the X-ray beam permits the

mapping of charge recombination efficiency using the so-called X-ray Beam Induced Current (XBIC) measurements<sup>[21]</sup>.

### Challenges

Combining **XBIC** (for local electrical performance of the device) with **nanoscale synchrotron-based hard X-ray fluorescence microscopy** offers new opportunities to study compositional aspects of nano-defects in semiconductors with imaging of full devices, and buried structures due to the high penetration depth of X-rays. Using the high sensitivity of X-ray fluorescence (XRF) as a probe, in-depth information with spatial resolution well adapted to the length scales of the defects of interest in solar cells ( $\approx 100$  nm) can be provided. Combined with **X-ray absorption**<sup>[22]</sup> or with **X-ray topography**<sup>[23]</sup>, **scanning XRF nanomicroscopy** reveals the phase speciation taking place during defect formation or the lattice structure with information on compressive/tensile strain at the defect sites as illustrated in Figure 10.

### SOLEIL upgrade benefits

The capabilities offered by a SR source perfectly match the needs of the community not only for *ex situ* defect characterizations, but also for the investigation of dynamics of defect formation/annihilation studied *in situ* during growth of active absorber materials<sup>[24]</sup>. With the increase of brightness with the SOLEIL upgrade, the time frame for image acquisition will be dramatically shortened leading to high-throughput mapping over more extended sample areas (*e.g.* for instance, a factor 90 can be expected to

acquire the same 2D map with field of view of  $450 \times 450 \mu\text{m}^2$  using STXM). This drastic shortening of time collection is essential to yield statistically meaningful knowledge on complex solar cells (such as the tandem perovskite-Si cells) by increasing the field of view in which data are collected. Furthermore coherence based imaging will benefit from the coherent flux increase inherent to the improved emittance, offering new opportunities to improve not only the spatial resolution (to a few nm) but allow coherent diffraction imaging at higher energies, well adapted for buried structures. Using lens-less imaging techniques will also relax the space around the sample offering new opportunities for the installation of complex sample environment able to study defect kinetics in solar cell under realistic industrial processing conditions including gaseous atmospheres and temperature<sup>[25]</sup>, critical for establishing local structure/property relationships necessary to improve processing.

## Electrochemical energy storage materials: solving the cost, energy density and safety issues

Improved means of energy storage are needed in developing a sustainable carbon-neutral energy economy. Regardless the origin of electric energy, from intermittent renewable sources, traditional fossil or nuclear plants, lithium-ion batteries (LIB) offer high storage capacity to weight ratio compared to competing technologies of the same size, especially for portable storage and its viability for smart grid applications. A battery operates in a “rocking chair” mode between the cathode and the anode that can insert  $\text{Li}^+$  at different potentials. During the discharge, the movement of  $\text{Li}^+$  from anode to cathode (supported by electrolyte carrier) creates free electrons in the anode flowing from the positive current collector to the negative one through a device which must be electrified. The reverse phenomenon occurs during the charge providing an electric current to the battery to oblige  $\text{Li}^+$  to migrate from the cathode towards the anode. During this process the so-called Solid Electrolyte Interface (SEI) forms during the first cycles of the batteries. Its formation arises from the decomposition of the Li-based electrolyte at the electrode surface and gives rise to the  $\text{Li}^+$  trapping through the formation of various Li-based phases (Figure 11) causing the decrease of cell capacity. Despite this

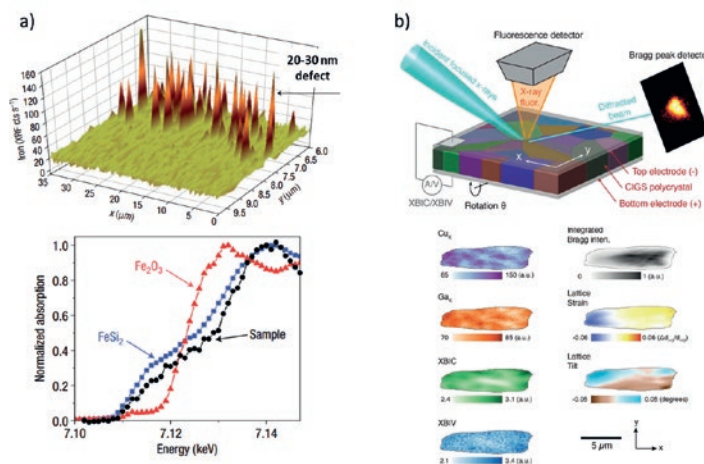


Figure 10: (a) 2D XRF-mapping of metal defect in commercial silicon solar cell material identified by Fe K edge XANES as  $\text{FeSi}_2$  nanoprecipitates<sup>[22]</sup> and (b) Multimodal X-ray imaging of defects in a commercially produced thin-film solar cell with a  $\text{Cu}(\text{In,Ga})\text{Se}_2$  absorber involving XRF for mapping Cu and Ga composition and X-ray topography for mapping compressive/tensile lattice strain correlated to XBIC measurements for mapping the low minority carrier diffusion length<sup>[23]</sup>. Correlation analysis of structural, electronic and compositional maps of individual micrometre-scale grains allowed concluding that near grain boundaries collection efficiency is increased, and that in these regions the lattice parameter of the material is expanded.

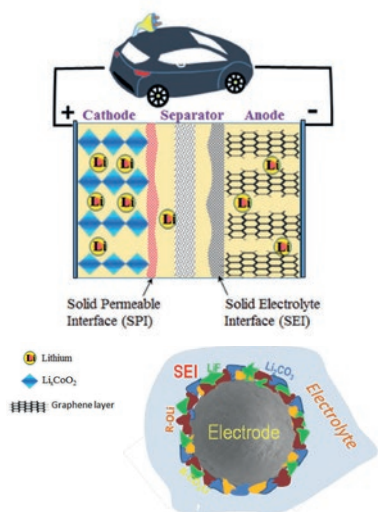


Figure 11: Schematic representation of a Li ion battery from [27] and of the Solid Electrolyte Interface (SEI) according to the Peled's model [28]

apparent drawback, the role of the SEI is crucial since this interface acts as an insulating layer to prevent electron transfer and as a good ionic conductor to provide the back and forth of  $\text{Li}^+$  ions between both electrodes. The understanding of SEI formation and of its stabilization is of prime importance for battery makers for the rationalization of very time demanding and costly formation protocols they carried out before commercialization to avoid unexpected failure at early calendar life [28].

## New electrode materials for high energy density and beyond Li technology

### Interest

Aggressive research programs are today stimulated by government policy, in the United States, China and recently with the France-Germany EUBatteryAlliance consortium to increase the market of electric

vehicles based on LIB technology. All these programs drive fundamental research in the materials design paradigm, in which fundamental understanding, obtained by materials advanced characterization, theory, artificial intelligence and data mining using a machine learning framework, guides materials synthesis and interfaces optimization to solve concrete economic and technological challenges [28] (e.g lower cost, longer cycle, higher energy density for increasing driving range of electric vehicles and better safety [29]). The quest of new materials with improved energy density must also take into account the sustainability of the elements currently used in LIBs. As the availability of lithium or cobalt is a major concern, major research efforts attempt to replace them by more abundant ions ( $\text{Na}^+$ ,  $\text{Mg}^{2+}$  or  $\text{Ca}^{2+}$ ) in Earth's crust [30], or to recycle them by chemical separation processes encouraging a circular economy in materials.

### Challenges

The impact of **Synchrotron Radiation imaging techniques**, to allow significant breakthroughs in elaboration of sustainable materials, has been recently exemplified with the development of **emerging intercalation of  $\text{Mg}^{2+}$  into a layered vanadium oxide** (Figure 12). This experiment was a proof of concept to validate new preparation routes leading to the efficient Mg intercalation: by conducting first cycling at  $110^\circ\text{C}$ , the limitation of Mg intercalation due to electrostatic repulsion has been overcome. Further long lasting room temperature cycling on pre-treated materials was observed and ascribed to the breaking of  $\text{V}_2\text{O}_5$  nanoparticles upon heating enabling more surface area for Mg to diffuse inside the electrode. The today limitation of this straightforward experiment is the long acquisition time necessary for this large field of view mapping (10h for a 2D

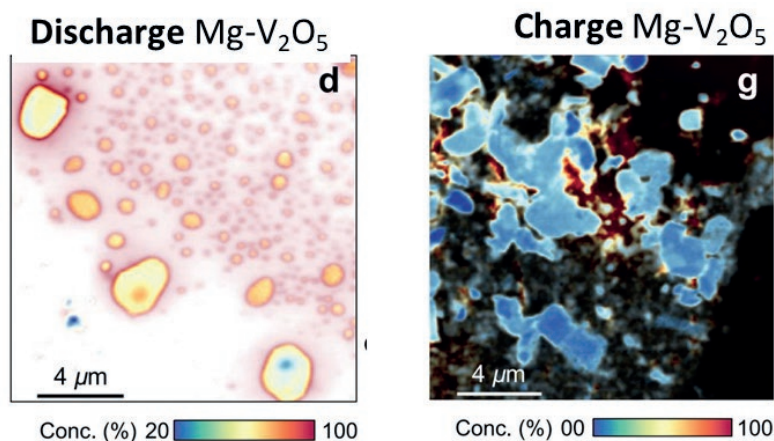


Figure 12: STXM maps of Mg distribution for discharged and charged particles deduced from oxidation state of Vanadium measured at the V L edge with a spatial resolution of 35 nm. The large field of view ( $13 \times 13 \mu\text{m}^2$ ) used in the experiments allows to map tens of those particles providing a statistical evaluation of the chemical state of particles in charge and discharge state [31] (time per map = 10 hours).

map) which is detrimental for the mandatory rapid throughput/screening approaches for optimizing new preparation or recycling methods of materials.

### SOLEIL upgrade benefits

A step forward could be achieved with the direct location of Mg (or Na) by emergent **soft X-ray ptychographic spectro-tomography** imaging method promoted by the coherence of the incoming beam. Recently soft X-ray ptychographic imaging and computed spectro-tomography have been applied to determine the 3D morphology and valence of iron in agglomerated cathode nanoparticles of lithium phosphate at 11 nm 3D spatial resolution (Figure 13) [32]. The increase in flux will reduce to a few second exposures for collecting 2D map in the ptychography mode (cf. 800 s necessary today). The significant improvement of time collection will open new opportunities for the development of high-performance battery materials, making the Synchrotron Radiation at the heart of a high-throughput optimization platform. The dreamed scenario would be to screen first

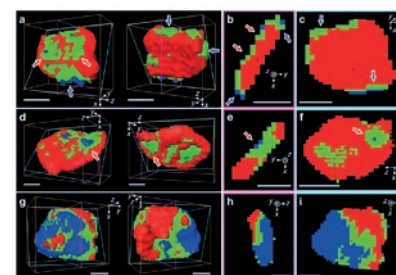
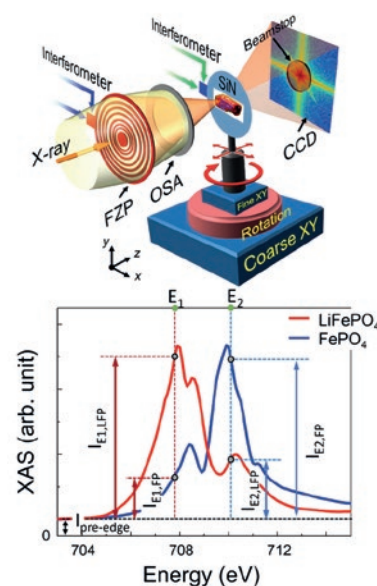


Figure 13: Representative 3D chemical phase distribution of individual  $\text{LiFePO}_4$  particle extracted from a battery electrode at 50% of charge by soft X-ray ptychography. The red, green and blue indicate  $\text{LiFePO}_4$ , rich, mixed and  $\text{FePO}_4$ -rich voxels, respectively. All scale bars equal 50 nm [32]. Spatial resolution 11 nm

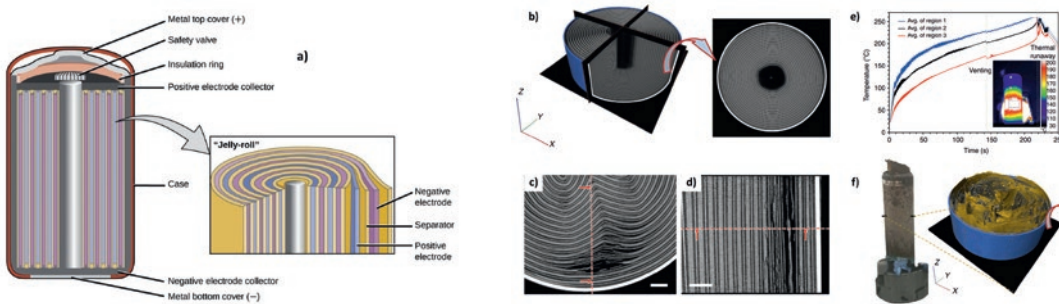


Figure 14: (a) schematic view of internal structure of commercial 18650 NMC cell. Electrodes and separators are prepared from long strips of foil to increase electrode surface areas and are rolled them into a spiral (from courses.lumenlearning.com/frostburg-chemistryformajorsxmaster, chapter "Batteries & Fuel Cells"). (b) 3D reconstruction with orthoslices in the XY, YZ and XZ planes of the cell before thermal runaway with the isolated XY slice. (c) and (d) Same cell as before thermal runaway where a collapse of the internal structure starts to be observed. Scale bar = 1 mm. (e) Mean surface temperature profiles and (f) Post-mortem tomography after thermal runaway, in the 3D reconstruction copper phase (yellow) is shown mostly intact in its laminar form<sup>[36]</sup>. Field of view = 10.5x7.6 mm<sup>2</sup>, pixel size=10.87 μm

the better candidate materials from computer simulations validated by electrochemical performances, and further, to characterize them at different length scales with required spatial resolutions using the upgraded synchrotron radiation hyperspectral imaging techniques for delivering structure-property relationship outcomes to the high-throughput computational screening in an ideal integrated workflow.

### Towards smart batteries able to detect failures and to generate self-healing actions

#### Interest

The increase of LIB technology into the large volume transportation markets leads battery makers to address its sustainability and durability. It is established that the life time of the battery must be higher than 400 charge-discharge cycles in order to have a positive energy balance in relation to the energetic production cost<sup>[33]</sup>. Battery makers then need to minimise undesirable battery failures before reaching the 400<sup>th</sup> cycle.

#### Challenges

Smart sensors, located within commercial battery packs to monitor in real time important parameters such as temperature, strain and state of charge can reveal the health state of the battery and give rise after real time analysis to self-healing processes to keep the cell integrity for longer time. The development of such passive diagnostics and self-healing integration devices<sup>[34]</sup> could highly benefit from the understanding of how the various materials embedded inside the complexity of the cell pack work cooperatively, and moreover, allow the selection of relevant observables to detect weaknesses and failures. SR imaging techniques at a few tens or hundreds of nanometer spatial resolution will be of prime importance for understanding short and long term cell failures. **Nano and micro-X-ray**

**tomography imaging** operating with hard X-rays could provide the bridge between the parameters measured by the smart sensors loaded inside the commercial battery pack and the degradation modes from which the battery is suffering. Hard X-rays can penetrate the metallic and plastic cell casing of commercial batteries providing a non-destructive *in situ* inspection of macroscopic defects in LIBs including anode, cathode, separator thickness and their packing<sup>[35]</sup>.

**At the micrometer scale**, the progression of internal structural deformation leading up to thermal runaway of a commercial LIB in external thermal abuse conditions has been already studied *in situ* by high speed SR X-ray computed tomography, as shown in Figure 14<sup>[36]</sup>.

#### SOLEIL upgrade benefits

The increase of coherence provided by the upgrade will be useful for phase sensitive imaging and phase contrast tomography, providing higher image contrast than those available today, at acquisition times that could go down to 50ms or less for a full volume reducing at the minimum X-ray dose absorbed by the sample to mitigate

the beam-induced sample degradation. The availability of speciation from XRD, XAS or XRF combined with imaging in a multimodal approach would be also of paramount importance to unravel the degradation mechanism. Furthermore, the possibility of combining imaging, spectroscopic and diffraction techniques over a broad energy range is a great asset for the study of these systems.

The spatially resolved investigations **at the nm scale** of inhomogeneity of particle packing, electrode and separator during induced mechanical, electrical, thermal stresses or electrochemical phenomena such as the SEI formation and lithium plating or stripping taking place with lithium metal battery family (Figure 15) will be of pivotal importance to better understand the mechanisms underpinning battery operation for establishing design strategies for systematic performance improvement. The dynamical information provided by SR imaging are highly required to decide what kind of analytical devices for health monitoring should be implanted inside the battery and to better inform safety focused computational models developed at the academic<sup>[37]</sup> and industrial scales.

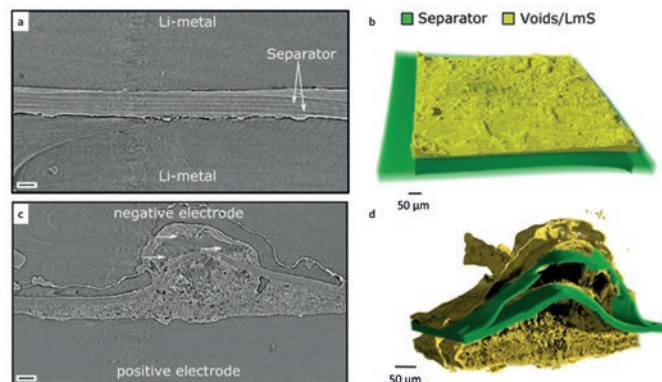


Figure 15: Monitoring of nucleation of Li microstructure and growth of porous Li interface on the Li metal electrode by in line phase contrast X-ray tomography. Cleavage of the separator (green) caused by growing Lithium microstructure (yellow) was visualized in 3D. Scale bar = 50 μm. Field of view = 1.7x1.2 mm<sup>2</sup>, pixel size = 438 nm<sup>[38]</sup>

## REFERENCES

- [1] A/CONF.216/16: Report of the United Nations Conference on Sustainable Development, Rio de Janeiro, Brazil, 20-22 June 2012.
- [2] Kalz, K. F., Kraehnert, R., Dvoyashkin, M., Dittmeyer, R., Gläser, R., Krewer, U., Reuter, K., Grunwaldt, J. D. "Future Challenges in Heterogeneous Catalysis: Understanding Catalysts under Dynamic Reaction Conditions" *ChemCatChem*, 9: 17. (2017).
- [3] Zhu, Q. L., Xu, Q. "Immobilization of Ultrafine Metal Nanoparticles to High-Surface-Area Materials and Their Catalytic Applications" *Chem*, 1: 220. (2016).
- [4] Liu, Y., Meirer, F., Krest, C., M., Webb, S., Weckhuysen, B. M. "Relating structure and composition with accessibility of a single catalyst particle using correlative 3-dimensional micro-spectroscopy" *Nature Communications*, 7: 12634. (2016).
- [5] de Smit, E., Swart, I., Creemer, J. F., Hoveling, G. H., Gilles, M. K., Tylliszczak, T., Kooyman, P. J., Zandbergen, H. W., Morin, C., Weckhuysen, B. M. de Groot, F. M. "Nanoscale chemical imaging of a working catalyst by scanning transmission X-ray microscopy" *Nature Letters*, 456: 222. (2008).
- [6] Sprenger, P., Sheppard, T. L., Suuronen, J.-P., Gaur, A., Benzi, F., Grunwaldt, J. D. "Structural Evolution of Highly Active Multicomponent Catalysts for Selective Propylene Oxidation", *Catalysts*, 8: 356. (2018).
- [7] Widmann, D., Jürgen Behm, R. "Active Oxygen on a Au/TiO<sub>2</sub> Catalyst: Formation, Stability, and CO Oxidation Activity" *Angewandte Chemie International Edition*, 50: 10241. (2011).
- [8] Seh, Z. W., Liu, S., Zhang, S.-Y., Bharathi, M. S., Ramanarayan, H., Low, M. Shah, K. W., Zhang, Y.-W., Han, M.-Y. "Anisotropic Growth of Titania onto Various Gold Nanostructures: Synthesis, Theoretical Understanding, and Optimization for Catalysis" *Angewandte Chemie International Edition*, 50: 10140 (2011).
- [9] Campbell, C. T. "Catalyst\_Support Interactions. Electronic Perturbations" *Nature Chemistry*, 4: 597. (2012).
- [10] Cargnello, M., Delgado Jaén, J. J., Hernandez Garrido, J. C., Bakhmutsky, K., Montini, T., Calvino Gamez, J. J., Gorte, R. J., "Exceptional Activity for Methane Combustion over Modular Pd/CeO<sub>2</sub> Subunits on Functionalized Al<sub>2</sub>O<sub>3</sub>" *Science*, 337: 712. (2012).
- [11] Varandili, S. B., Huang, J., Oveisi, E., De Gregorio, G. L., Mensi, M., Strach, M., Vavra, J., Gadiyar, C., Bhowmik, A., Buonsanti, R. "Synthesis of Cu/CeO<sub>2-x</sub> Nanocrystalline Heterodimers with Interfacial Active Sites To Promote CO<sub>2</sub> Electroreduction" *ACS Catalysis*, 9: 5035. (2019).
- [12] Suzana, A. F., Rochet, A., Passos, A. R., Castro Zerba, J. P., Polo, C. C., Santilli, C. V., Pulcinelli, S. H., Berenguer, F., Harder, R., Maxey, E., Meneau, F. "In situ three-dimensional imaging of strain in gold nanocrystals during catalytic oxidation" *Nanoscale Advances*, 1: 3009. (2019).
- [13] Passos, A. R., Rochet, A., Manente, L. M., Suzana, A.F., Harder, R., Cha, W., Meneau, F. "Three-dimensional strain dynamics govern the hysteresis in heterogeneous catalysis" *Nature Communications*, 11: 4733. (2020).
- [14] Jenness, G. R., Schmidt, J. R. "Unraveling the Role of Metal-Support Interactions in Heterogeneous Catalysis: Oxygenate Selectivity in Fischer-Tropsch Synthesis" *ACS Catalysis*, 3: 2881. (2013).
- [15] Takagi, T., Uruga, T., Tada, M., Iwasawa, Y., Yokoyama, T. "Ambient Pressure Hard X-ray Photoelectron Spectroscopy for Functional Material Systems as Fuel Cells under Working Conditions" *Accounts of Chemical Research*, 51: 719. (2018).
- [16] Zitolo, A., Ranjbar-Sahraie, N., Minerva, T., Li, J., Jia, Q., Stamatini, S., Harrington G. F., Lyth, S. M., Krtil, P., Mukerjee, S., Fonda, E., Jaouen, F. "Identification of catalytic sites in cobalt-nitrogen-carbon materials for the oxygen reduction reaction" *Nature Communications*, 8: 957. (2017).
- [17] Battersby, S. "The Solar Cell of the Future" *PNAS*, 116: 7. (2019).
- [18] Clark, P. C. J., Flavell, W. R. "Surface and Interface Chemistry in Colloidal Quantum Dots for Solar Applications Studied by X-Ray Photoelectron Spectroscopy" *The Chemical Record*, 18: 1. (2018).
- [19] Spencer, B. F., Leontiadou, M. A., Clark, P. C. J., Williamson, A. I., Sully, M. G., Sirotti, F., Fairclough, S. M., Tsang, S. C. E., Neo, D. C. J., Assender, H. E., Watt, A. A. R., Favell, W. R. "Charge dynamics at heterojunctions for PbS/ZnO colloidal quantum dot solar cells probed with time-resolved surface photovoltage spectroscopy" *Applied Physics Letters*, 108: 091603. (2016).
- [20] Penfold, T. J., Sziachetko, J., Santomauro, F. G., Britz, A., Gawelda, W., Doumy, G., March, A. M., Southworth, S. H., Rittman, J., Abela, R., Chergui, M., Milne, C. J. "Revealing hole trapping in zinc oxide nanoparticles by time-resolved X-ray spectroscopy" *Nature Communications*, 9: 478. (2018).
- [21] Stuckelberger, M., West, B., Nietzold, T., Lai, B., Maser, J. M., Rose, V., Bertoni, M. I. "Engineering solar cells based on correlative X-ray microscopy" *Journal Materials Research*, 32: 18251 (2017).
- [22] Buonassisi, T., Istratev, A. A., Marcus, M. A., Lai, B., Cai, Z., Heald, S. M., Weber, E. R. "Engineering metal-impurity nanodefects for low-cost solar cells" *Nature Materials*, 4: 676. (2005).
- [23] Ulvestad, A., Hruszkewycz, O., Holt, M. V., Hill, M. O., Calvo-Almazan, I., Maddali, Z., Huang, X., Yan, H., Nazaretski, E., Chu, Y. S., Lauhon, L. J., Rodkey, N., Bertoni, M. I., Stuckelberger, M. E. "Multimodal X-ray imaging of grain-level properties and performance in a polycrystalline solar cell" *Journal of Synchrotron Radiation*, 26: 1316. (2019).
- [24] Alsari, M., Bikondoa, O., Bishop, J., Abdi-Jalebi, M., Ozer, L. Y., Hampton, M., Thompson, P., Hörantner, M., T., Mahesh, S., Greenland, C., Macdonald, J. Emyr, Palmisano, G., Snaith H. J., Lidzey, D. G., Stranks, S. D., Friend, R. H. Lilliu, S. "In situ simultaneous photovoltaic and structural evolution of perovskite solar cells during film formation" *Energy Environmental Science*, 11: 383. (2018).
- [25] Chakraborty, R., Serdy, J., West, B., Stuckelberger, M., Lai, B., Maser, J., Bertoni, M. I., Culpepper, M. L., Buonassisi, T. "Development of an *in situ* temperature stage for synchrotron X-ray spectromicroscopy" *Review of Scientific Instruments*, 86: 113705. (2015).
- [26] Peled, A., Menkin, S. "SEI: Past, Present and Future" *Journal of the Electrochemical Society*, 164: A1703. (2017).
- [27] Tripathi, A. M., Su, W.-N., Hwang, B. J. "In situ analytical techniques for battery interface analysis" *Chemical Society Reviews*, 47: 736. (2018).
- [28] Bhowmik, A. Castelli, I. E., Garcia-Lastra, J. M., Jorgensen, P. B., Winther, O., Vegge, T. "A perspective on inverse design of battery interphases using multi-scale modelling, experiments and generative deep learning" *Energy Storage Materials*, 21: 446. (2019).
- [29] Lin, F., Liu, Y., Yu, X., Cheng, L., Singer, A., Shpyrko, O. G., Xin, H. L., Tamura, N., Tian, C., Weng, T.-C., Yang, X.-O., Meng, Y. S., Nordlund, D., Yang, W., Doeff, M. M. "Synchrotron X-ray Analytical Techniques for Studying Materials Electrochemistry in Rechargeable Batteries" *Chemical Reviews*, 117: 13123. (2017).
- [30] Larcher, D., Tarascon, J.-M. "Towards greener and more sustainable batteries for electrical energy storage" *Nature Chemistry*, 7: 19. (2015).
- [31] Yoo, H. D., Jokisaari, J. R., Yu, Y.-S., Kwon, B. J., Hu, L., Kim S., Han, S.-D., Lopez, M., Lapidus, S. H., Nolis, G. M., Ingram, B. J., Bolotin, I., Ahmed, S., Klie, R. F., Vaughey, J. T., Fister, T. T., Cabana, J. "Intercalation of Magnesium into a Layered Vanadium Oxide with High Capacity", *ACS Energy Letters*, 4: 1528. (2019).
- [32] Yu, Y. S., Farmand, M., Kim, C., Liu, Y., Grey, C. P., Strobridge, F. C., Tylliszczak, Celestre, R., Denes, P., Joseph, J., Krishnan, H., Maia, F. R. N. C., Kilcoyne, A. L. D., Marchesini, S., Costa Leite, T. P., Warwick, T., Padmore, H., Cabana, J., Shapiro, D. A. "Three-dimensional localization of nanoscale battery reactions using soft X-ray tomography" *Nature Communications*, 9: 921. (2018).
- [33] Peters, J. F., Baumann, M., Zimmermann, B., Braun, J., Weil, M. "The environmental impact of Li-Ion batteries and the role of key parameters – A review", *Renewable and Sustainable Energy Reviews*, 67: 491. (2017).
- [34] Grey, C. P., Tarascon, J. M. "Sustainability and in situ monitoring in battery development" *Nature Materials*, 16: 45. (2017).
- [35] Wood, V. "X-ray tomography for battery research and development", *Nature Reviews: Materials*, 3: 293. (2018).
- [36] Finegan, D. P., Scheel, M., Robinson, J. B., Tjaden, B., Hunt, I., Mason, T. J., Millichamp, J., Di Michiel, M., Offer, G. J., Hinds, G., Brett, D. J. L., Shearing, P. R. "In-operando high-speed tomography of lithium-ion batteries during thermal runaway" *Nature Communications*, 6: 6924. (2015).
- [37] Finegan, D. P., Darst, J., Walker, W., Li, Q., Yang, C., Jervis, R., Heenan, T. M. M., Hack, J., Thomas, J. C., Rack, A., Brett, D. J. L., Shearing, P. R., Keyser, M., Darcy, E. "Modelling and experiments to identify high-risk failure scenarios for testing the safety of lithium-ion cells" *Journal of Power Sources*, 417: 29. (2019).
- [38] Sun, F., Zielke, L., Markötter, H., Hilger, A., Zhou, D., Moroni, R., Zengerle, R., Thiele, S., Banhart, J., Manke, I. "Morphological Evolution of Electrochemically Plated/Stripped Lithium Microstructures Investigated by Synchrotron X-ray Phase Contrast Tomography" *ACS Nano*, 10: 7990. (2016).



# Health and well-being

## — Overview

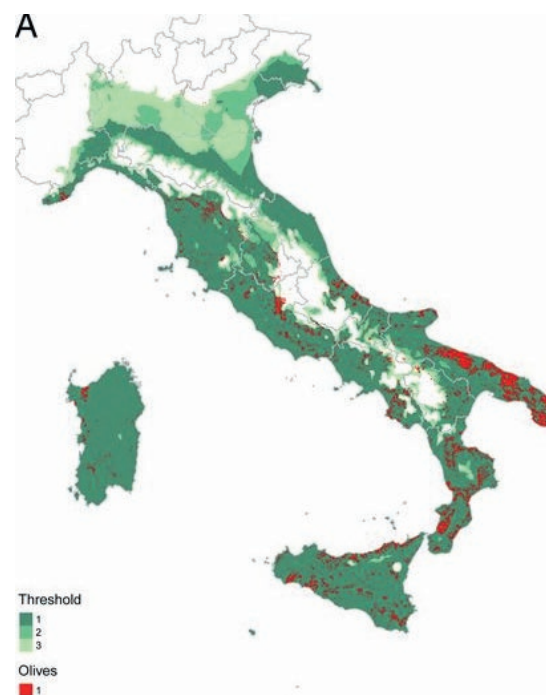
Life science research at synchrotron radiation sources has been remarkably productive since their inception over 40 years ago, and synchrotron X-ray crystallography alone has contributed to work resulting in the award of 6 Nobel prizes for Chemistry over the period (1982, 1997, 2003, 2006, 2009 and 2012). In particular, close to 1700 structures, derived from data collected at the SOLEIL structural biology beamlines, have been deposited in the Protein Data Bank since 2007.

The Covid-19 pandemic provides a clear example of the need to develop a rapid, structure-based response to emerging diseases : in 2019, the world health organisation's list of the top 10 threats to human health included a number of viral threats including influenza pandemic, Dengue, Ebola, Nipah, Zika, SARS and HIV, structural details of many of which have been studied at SOLEIL. The range of these tropical viruses has widened, both due to increased travel between countries and resulting from climatic change promoting a wider geographical range for disease carrying vectors (such as the tiger mosquito). Prior to 1970, severe Dengue viral outbreaks had been recorded in just 9 countries, whereas today the infection is endemic in over 100 countries (including the recent outbreak in Honduras that has killed over 400) and has reached Europe. It has also been suggested that climatic factors, provoking permafrost melting, may lead to the re-emergence of forgotten microbial threats.

Plant life on the planet is impacted by pathogens which, in the context of globalized trade, spread more easily. The *Xylella fastidiosa* bacteria, considered to be one of the most dangerous plant pathogens known, is an emerging threat in France. A new strain, detected in Italy in 2013 and in Corsica in 2015, is a pathogen for some thirty French plant species, in particular having a devastating effect on olive tree growth being the causative agent of Olive Quick Decline Syndrome. The potential major impact to three Mediterranean countries (Greece, Italy and Spain, who produce 95% of European olive oil), has been evaluated by Schneider et al.<sup>[1]</sup>, Figure 1. Their modelling predicts a potential production loss of 2 – 5 billion Euro to the European economy. Synchrotron radiations capabilities, for example to study plant vascularization and identify drought resistant strains of grape vines<sup>[2]</sup>, and, via structural biology,

reveal the structures and mechanisms of the different molecular machines<sup>[3]</sup> (secretion systems) responsible for exporting bacterial virulence factors, provide a rapid response mechanism to understand and mitigate such emerging threats.

The Life Sciences group at SOLEIL has been very active in adopting a multidisciplinary (integrated) approach, accounting for 15% of all SOLEIL publications citing the use of multiple beamline facilities. The success of a multidisciplinary approach depends critically on the strength of partnerships with other laboratories and the level to which common objectives can be defined. SOLEIL is particularly strong in this respect, having long standing collaborations with INRAE, the Pasteur Institute, FRISBI (the French Infrastructure for Structural Biology), the Aix-Marseille University, and the companies SERVIER and



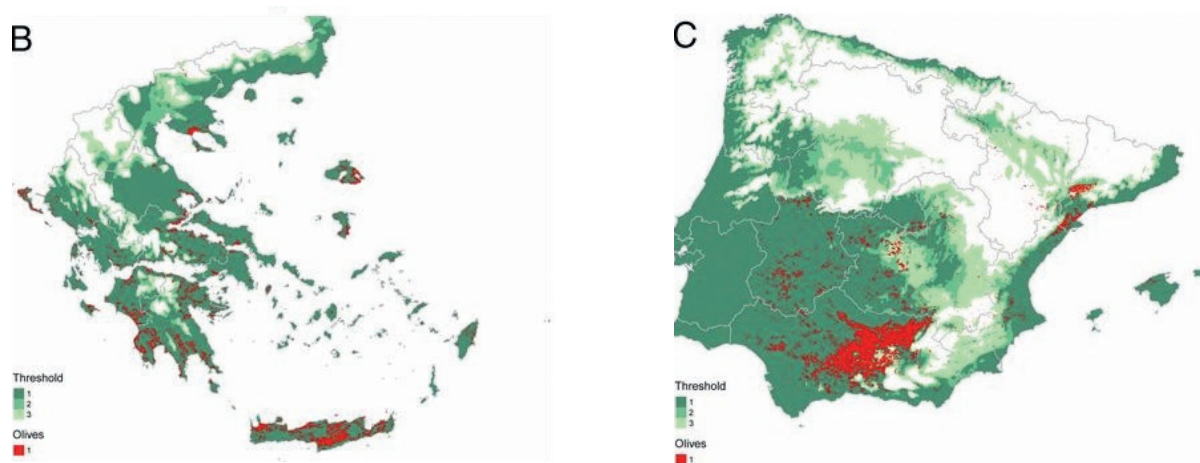


Figure 1: Climatic suitability to the propagation of *Xylella fastidiosa* (used to model future spread) and olive growth regions in Italy, Greece and Spain; reproduced from<sup>[3]</sup>.

SANOI. Several examples of interdisciplinary research at SOLEIL can be found in two recent impact studies: “What’s on our plates<sup>1</sup>” and “Medical Diagnosis and Prognosis<sup>2</sup>”, the latter providing the impetus for strengthening the use of SOLEIL for establishing protocols for medical diagnostic testing.

An upgrade of SOLEIL will encourage the emergence of methods to study biological molecules at high spatial and temporal resolution and at physiological temperatures permitting the transient mechanisms of protein-ligand interactions to be elucidated to a level of detail that is impossible today. This new technology will be particularly beneficial for the development of inhibitors, as described by Kotschy et al.<sup>[4]</sup>, who pioneered the development of a family of drugs aimed at controlling apoptosis in cancerous cells.

The following scientific case comprises three parts, each being derived from work undertaken at SOLEIL and illustrated by a selection of examples of clear societal and scientific interest and the future benefits of an upgrade.

The (re)emerging pathogens section draws attention to the role of SOLEIL in design and optimisation of medicaments or associated treatments and their efficiency, on both a molecular and cellular level. The second part outlines a novel role for synchrotron science as both a tool for medical diagnostics and an innovation driver for the development of hospital based diagnostic tools. The third part discusses the need of a multimodal approach to understand processes in natural living systems in order to better adapt to environmental pressures. A Technical Design Report, currently in preparation, will outline a beamline instrumentation and development plan to address these questions.

<sup>1</sup> <https://www.synchrotron-soleil.fr/contributions/WhatsOnOurPlates/>

<sup>2</sup> <https://www.synchrotron-soleil.fr/contributions/DiagnosticsAndPronostics/>



## (Re)Emerging pathogens in their environment

The recent apparition of new, and the re-emergence of old, diseases continues to be a serious threat to the human community. Many viruses and bacteria evolve quickly to spread and kill. Global warming has exacerbated this situation by spreading the vectors of these diseases, which can have dramatic consequences on our environment and health. The world has recently witnessed the emergence of a new coronavirus threat (SARS-Cov2), the full extent of the current pandemic will not be known for some years. Taking a different example, according to the World Health Organization (WHO), the impact of the influenza A virus is estimated to cause 3-5 million cases of severe illness and up to half a million deaths worldwide each year.

The overuse and misuse of antibiotic treatments in both humans and livestock, as well as the extensive quantities of drugs released in city wastes, are a major inducing factor in the appearance of multidrug-resistant bacteria, more commonly known as superbugs. In particular, the discovery, and development, of novel antibiotics are urgently needed to face the dangers arising with the emergence and spread of multidrug resistant bacteria, especially those Gram-negative pathogens belonging to the ESKAPE group. Our poor knowledge of their complex outer membrane structure and their internal organisation remains a serious breach that needs to be filled before understanding the mechanisms behind antibiotic resistance and their uptake into living bacteria. A better understanding of how pathogens interact with their host and propagate in the environment – and how they can be tackled – is crucial.

All (re)emerging diseases have, in common, strong links between the structural adaptation of the microbe's molecules and their specific virulence or resistance. As a support to national collaborative work among scientists of specialised research entities (CNRS, CEA, IRBA, Pasteur Institute, INSERM, INRAE...), SOLEIL will enhance its existing combination of state-of-the-art structural techniques for deciphering the molecular basis underlying the mechanisms of virulence and resistance. New and revolutionary imaging methods will be developed

i) at the cellular level where drugs and proteins may be followed in living cells or in delayed time-lapses for cryo-conditions on fully hydrated, vitrified samples, and ii) at the tissular level, where innovative imaging modalities will permit to better understand the effects induced by those diseases in animals and patients. It is only through the coordination of the broad spectrum of the expertise, provided by SOLEIL and independent research groups that long lasting solutions will emerge.

By assimilating Cryo Soft X-ray Tomography (Cryo-SXT) into the spectrum of techniques available at SOLEIL, the size scale covered for biology studies will widen, filling the missing gap between the structural investigations of protein function and the living cellular studies on phenotypic switches caused by structural changes in proteins. The method offers new perspectives, based on the improved coherence of future synchrotron beams, to couple full field tomography with local ptychography measurements to zoom into regions of interest in larger samples (such as entire cells or even tissues). In addition, full field imaging is a rapid technique, permitting the measurement of a statistically significant number of samples and, consequently, their classification in order to identify rare cellular events or prepare time sequences of different stages of cellular processes. In complement to the beamlines, the rapprochement of various techniques (e.g. CryoEM, Cryo super-resolution fluorescent microscopy) dedicated to biology, in a “complementary methods laboratory”, will not only facilitate sample

sharing between approaches, but also gather the scientific biology staff to further integrated methods. Opening end-stations to research at an L3 biohazard level, essential for rapid reaction studies of pathogens and given added value in an integrated context, will be facilitated when fully incorporating the shared expertise on sample preparation and pioneering microfluidic sample handling. Hence the upgrade will enable users to follow pathogen routes inside infected cells from molecular to tissular levels, accelerating drug developments. In this scheme, the perspective of *in vivo* macromolecular crystallography will become an ideal tool for studying virulence factors in cellulo at atomic resolutions. Such a facility, installed in a national synchrotron laboratory, would be a key security asset.

## Neutralising antibodies against Dengue and Zika

### Interest

Structural biology has proved to be a powerful tool for understanding viral entry in host cells<sup>[5]</sup>, as well as the rapid identification of potential inhibitors or neutralizing antibody targets against emerging viral threats. The epidemic of Zika fever in Brazil (2015-2016) was spread by mosquitoes carrying a flavivirus of the same name, and declared by the World Health Organisation as a “Public Health Emergency of International Concern”. As described in Figure 2, an international network of researchers, led by a team from the Institut Pasteur, used SOLEIL to understand the structural detail of recognition by the virus envelope protein of a cross neutralising antibody

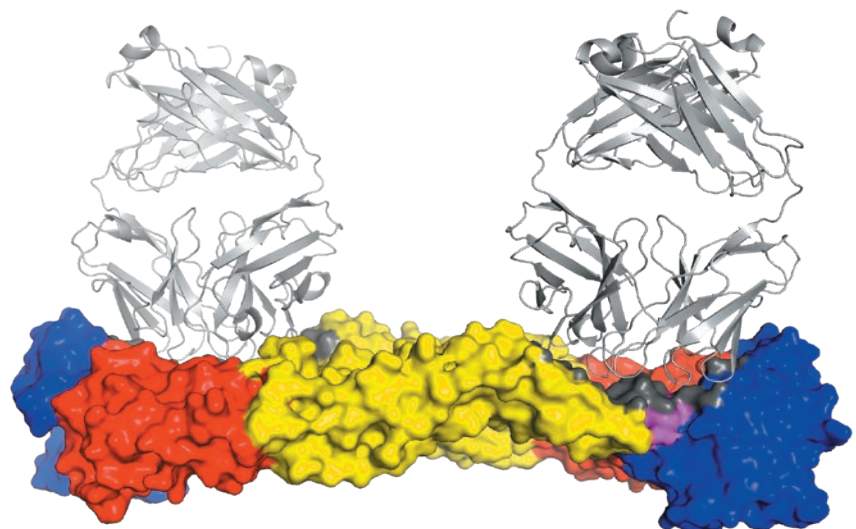


Figure 2: Crystal structure of the Zika virus envelope protein in complex with a cross neutralizing antibody (binding equally to the 4 identified serotypes of the Dengue virus). The structure was elucidated following rapid access experiments performed on the PROXIMA-1 and PROXIMA-2A beamlines, and reported, by Rouvinski et al., in Nature<sup>[7]</sup>.

(identified in previous work on Dengue). This information is essential for future rational design of a vaccine that can provide resistance against both Dengue and Zika viruses<sup>[6-7]</sup>. SOLEIL is currently working, in collaboration with SANOFI and INRAE, on identifying targets against the SARS-Cov2 virus via *in vivo* crystallization and rapid screening against a fragment library, demonstrating the capacity for rapid reaction to emerging threats.

#### SOLEIL Upgrade Benefits

Source brilliance driven improvements to structural biology beamlines will allow improved rapid screening of weakly bound fragments or ligands via fixed target serial crystallography, from tiny crystals (down to 1  $\mu\text{m}$  on edge), and at room temperature. When coupled with rapid detection systems, suitably rapid data reduction and micro-fluidic environments (permitting rapid substrate screening), investigation of the dynamics of drug binding will become possible with large potential impact in the development of antiviral drugs.

#### Mechanisms of antibiotic resistance and bacterial population specificity

##### Interest

The uptake and efflux, by bacteria, of labelled or unlabelled antibiotics can already be studied using DUV imaging<sup>[8]</sup>, as shown by the example in Figure 3. The enormous advantage of these methods is the characterization of required dose (the overuse of antibiotics being one of the reasons for the evolution of resistance) and the ability to look at individual bacteria in a large population.

##### SOLEIL Upgrade Benefits

The upgrade will permit a re-optimisation of methods and optics for DUV imaging,

unlocking the route to improved spatial resolution, provided by structured illumination, and hence allowing the study of the periplasmic sub-localisation (and hence efflux) of antibiotic in gram-negative bacteria. Coupling with structural methods (via serial crystallography or Cryo-EM, both methods being particularly well adapted to the study membrane proteins in operation) will allow detailed understanding of the molecular mechanisms of efflux, giving further information on how to modify existing drugs or administer them as a cocktail adapted to overcome a particular resistance mechanism.

#### Synchrotron methods for pathologists

Medical practitioners, who are at the frontline of handling diseases and trauma, are always searching for new diagnostic tools. Therapeutic technologies and biomedical imaging have greatly benefitted from synchrotron radiation methods for faster and more reliable diagnosis. These include, but are not limited to, X-ray micro-beam irradiation and photon activation therapies, computed tomography, coronary angiography, bronchography and mammography. The integration of complementary synchrotron techniques continuously participates in enriching the reliability of databases used by surgeons during tumour removal for the better definition of the malignant tissue boundaries. The imaging tools available in hospitals can be complemented in specific cases (such as the occurrence of false positives in radiolabelling) by access to state-of-the-art imaging technologies available only at synchrotrons. To be effective, access mechanisms must be

facilitated for pathologists. Hospitals, through biomedical applications, need better access to synchrotron radiation centers in order to accelerate their diagnoses or to provide data to help build technical and computing tools, hence favoring an improved response to diseases. Emerging from consultations with specialised institutions (INSERM, APHP...), diagnoses on a case-by-case basis do not present any legal issue, since they are under the responsibility of the practitioner. SOLEIL has already contributed to such diagnoses, with several medical cases reported that have been resolved, notably for a patient suffering from di-hydroxy adenine crystals. Such biomedical studies are expected to require spatial resolutions of typically 0.5 to 10 micrometers, seldom below 50 nanometers. The modalities for accessing the instrumentation must follow the bioethics and great care must be given to return biopsy samples to the hospital after analysis. Similarly, caution should be applied when analysing the samples as no degradation (such as radiation damage caused by excess doses from Visible, UV or X-ray beams) can be tolerated: the development of a sample passport (see section 4) is an important enabling technology. Additionally, improving diagnosis by characterising mutation-induced diseases at the molecular level becomes mandatory.

Establishing new beamtime access modes is a pre-requisite to bringing medical diagnosis to synchrotrons. Dedicated weekly access for hospital units, INSERM, and IRBA, will permit fast turnaround of diagnostic measurements, based on synchrotron techniques, with rapid access modalities that may require a major update program of the logistic infrastructure. New opportunities linked to the SOLEIL upgrade will give access to faster detection of elemental composition in human biopsies, and an improved (phase) contrast in full field tomography of large anatomical pieces, tissues and cells. Importantly, French medicine has pioneered the development of artificial organs, where SOLEIL will play a role in assisting breakthrough discoveries, with several projects just beginning. Inspired from remote access already implemented in biocrystallography (and being extended to other beamlines), automated sample mounting and analysis, combining the technologies for semi-automated sample exchange with

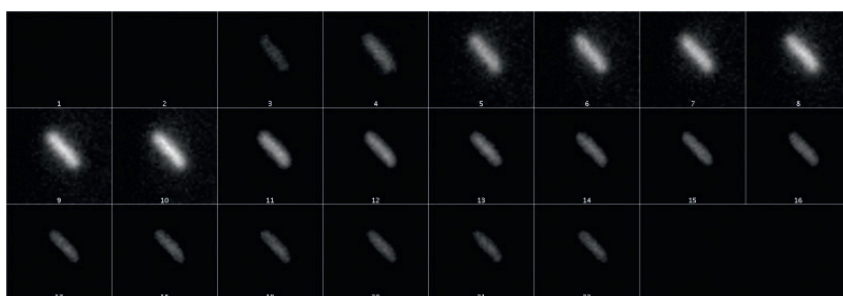


Figure 3: Time sequence of images, obtained at DISCO beamline, demonstrating the uptake of a fluorescent quinolone based antibiotic (with a protocol of washing excess antibiotic accumulating outside the cell) in a single gram negative bacterial cell. Methods have been developed to correct intensity for autofluorescence due to metabolic changes in the cell after antibiotic treatment. Individual cell lines can now be examined for the efficient uptake of antibiotic and perhaps come closer to understanding the mechanisms of persistence. See<sup>[9]</sup>.



## Steatotic liver tissue section

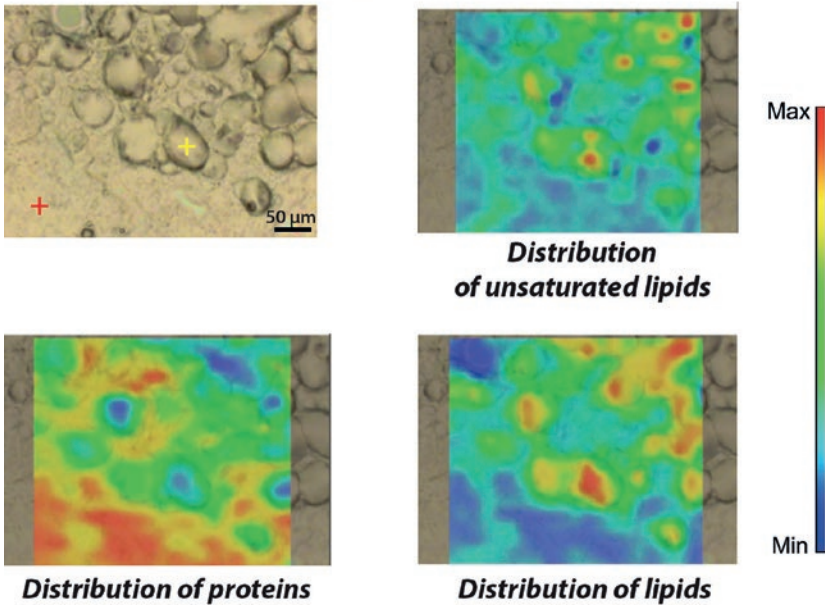


Figure 4: Cross section of a steatotic liver containing vesicles rich in lipids (optical image, top left). Each point of the section is analysed by Infrared spectroscopy to determine its chemical composition, allowing the reconstruction of the various components of the tissue shown in the other 3 images. The steatotic zone is marked by a yellow cross. See<sup>[10]</sup>.

the virtual slide microscopy available at hospitals, would become a real asset. A realizable objective is that the samples, and not the pathologists, would go to the synchrotron. Synchrotron diagnostic based data will also become a primary asset for artificial intelligence based diagnostic programs. The parallel development of collection, analysis and advanced synchrotron based diagnostic methods (exploiting the new source brilliance and coherence), offers a unique opportunity for advancing medical science.

## Liver steatosis

### Interest

The early diagnosis of liver-based disease is critical for a successful outcome. The example in Figure 4 illustrates how polyvalent synchrotron techniques can be developed and refined in order to produce a tool that can be used in the operating theatre. This result is based on combining two synchrotron characterization methods, DUV and IR hyperspectral imaging, where sample transfer compatibility has already been developed.

### SOLEIL Upgrade Benefits

Extending measurement capability to a larger variety of techniques by developing a multi-environment “slide changer” for biopsy samples, and coupling the result with the methodological expertise in sample analysis available at SOLEIL, offers the prospect of rapid, automatic machine learning based diagnostic methods. In particular, the use of scanning SAXS / WAXS and / or micro-diffraction, combined with a coherent beam and rapid scanning nano-positioning stages (currently being developed for scanning SAXS at SOLEIL), will allow the examination of micro calcifications (for example in collagen) using both imaging and structural methods on the same sample.

## Meningioma

Meningioma are very frequently occurring cancerous tumours of the central nervous system. Unfortunately, existing diagnostic tools (such as MRI scans) do not give sufficient sensitivity or resolution to make early diagnosis possible. The only available treatment is via brain surgery, an invasive technique where the delineation of the margins of the tumorous tissue (allowing its removal without that of undamaged brain tissue) is crucial for surgeons. Augmented visualization of the tumor, via multimodal (TPFE, SHG, FLIM and DUV) endomicroscopy (Figure 5 and see<sup>[11]</sup>), offers one way to improve on this situation.

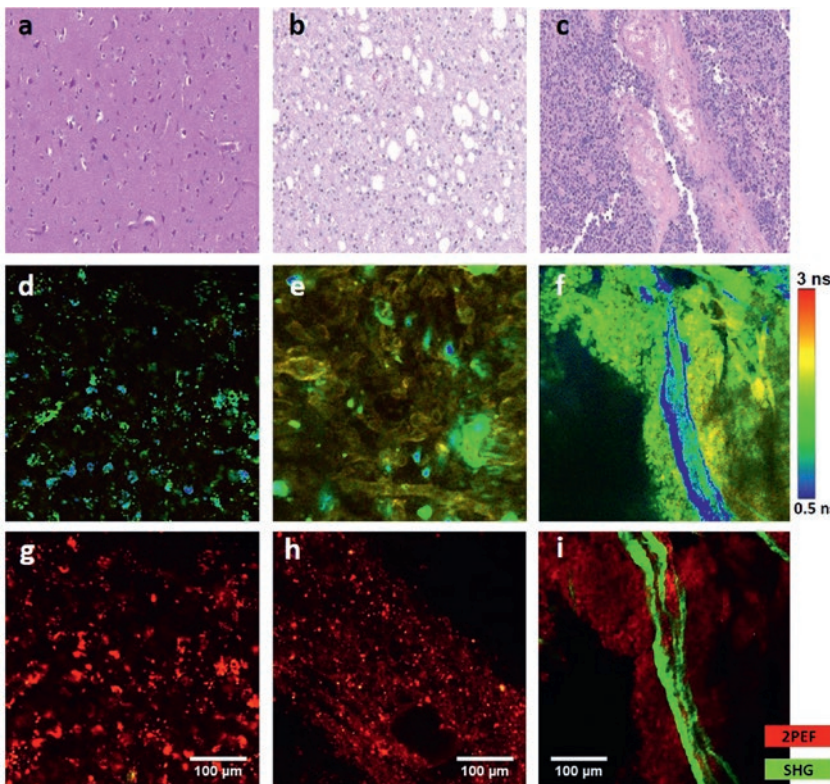


Figure 5: The optical signature of biopsy tissue observed using DUV, near Infrared and two photon imaging has been used at SOLEIL to investigate glioma tumours. The figure shows different grade tumours with (a, b, c) histological staining viewed by light microscopy, (d, e, f) FLIM imaging at 810 nm and two photon imaging at 890 nm (g, h, i). Compiling a database of patient cases demonstrated the possibility to give image assisted grading with a high level of confidence. Taken from<sup>[12]</sup>.

### SOLEIL Upgrade Benefits

Improved methods of phase contrast micro/nano-tomography scans, coupled with other synchrotron imaging modalities (such as improved DUV fluorescent imaging), can be associated to artificial intelligence based diagnostic algorithms. Full diagnostic cycle (measurement, diagnosis, prediction and clinical outcome), in concertation with hospital partners, will allow the refinement of both algorithms and the choice of the most sensitive measurement conditions for different tumour types.

### Plants for a changing world

- Food:** With a growing population, global food intake must be adapted to limit the human impact on global warming. Numerous reports recommend decreasing the consumption of animal-based proteins. New sources of proteins are needed, and vegetal-based proteins arise as promising targets. Practically, plant proteins are difficult to digest by omnivores due to their low solubility, sulphur content and cellular accessibility - pushing towards the need for their prior enzymatic processing for better metabolization by human enzymes. Maintaining the quality level of soils free from pollutants and preventing such pollutants from entering the food chain is addressed in the CDR chapter on "Environment".
- Drought:** In response to changing rainfall patterns due to climatic change, it is urgent to study the drought resilience of trees and plants and the adaptation of agriculture towards new, more resilient crops. Trees and crops, and their adaptation to drought need to be studied from tissular to molecular scales. Structural and chemical imaging, at the highest possible resolution of living and fixed samples, would provide understanding of the molecular and cellular basis of their resilience.
- Biosourced materials:** The looming challenges from our ever-changing world are numerous and the solutions to tomorrow's problems will emanate from various fields of research and development. Facing a post-petroleum era may become one of the most laborious issues to tackle, notably in terms of polymer chemistry, applicable to all the objects employed in our consumer society. In this respect,

the synthons (structural unit within a molecule) needed to produce our favourite gadgets can also be found in (organic/soft) wastes, either by valorising city and industrial waste, or vegetal waste from sustainable agricultural production. Enzymes to catalyse the production of these synthons are still to be fully characterised and optimised. The full life cycle of materials, in particular the processing and exploitation of waste to produce a "circular (bio-) economy", is discussed in the CDR chapter on "Environment".

- Plant Health and Disease:** Plants are susceptible to the effects of global warming and intensive agricultural techniques. A consequence of this environmental pressure is the vulnerability of plants to the fast spread of pathogens that can destroy crops and lead to significant loss of economic income.

The upgrade at SOLEIL will bring new imaging capabilities in terms of resolution, contrast and dynamics in fluorescence and tomography methods, which are especially amenable to plant tissue and will enable scientists to follow the processes of infection. Furthermore, plant research would benefit from state-of-the-art sample preparation techniques supported by the integrated biology initiatives in place at SOLEIL. For example, the bio-engineering studies of dynamic root systems could take advantage of devices designed by the microfluidic lab to simultaneously monitor pathogen localisation and the biomechanical adaptation of tissues *operando*. At the atomic and molecular level, unravelling the specificities and complexities in plant-pathogen interactions, which are poorly understood simply because they have not been subject to the same attention as human health problems, would be facilitated by methodologies already employed in structural biology (SAXS & MX). SAXS is particularly amenable to the study of plant cell wall components (celluloses, complex carbohydrates, pectins, etc.). The study of pesticide action and design is akin to the drug discovery efforts spearheaded by the pharmaceutical industry, whereby interactions between ligands or fragments of ligands can be studied with structural methods opening the way to true molecular design. Indeed, the same structure based tools could, after bio-informatic informed targets have

been identified, allow design to take into account of, for example, potential unwanted side effects, in pesticides, to human health. All of these techniques combined with the improvements in imaging techniques offered by the upgrade, would help answer questions on how to assess and improve the durability of plant resistance. Crop health has a huge impact on yields in agriculture and agronomy – a major income provider for the French economy – motivating the creation of dedicated, world-leading, research institutes, such as INRAE. Plants also play their part in emerging methods of waste and pollution management, for example in heavy metal pollution remediation. Further details are discussed in the section on "Environment". Data and knowledge acquired from synchrotron plant based research can be expected to provide opportunities for an emerging "green economy".

Further insights in the carbon cycle and to decipher the properties behind plant mechanisms related to human enzymes' function, require fully integrated approach towards all size and resolution scales. New enzymes will be tailored to deconstruct and reconstruct biological materials without the needs for extensive and unnecessary energy. Detailed structural studies at atomic scales of enzymes in action, are mandatory. The addition of cryo-Electron Microscopy tools to the current portfolio of high-resolution techniques, and the further development of full-field tomography to look at large scale systems in a variety of conditions, will provide with a set of instruments to characterize enzymes in action in natural systems.

New access modes adapted to long term follow up of plants should help getting more specific answers in the studies of the evolution of new crops that shall emerge in Europe, sorghum notably. Studying crop adaptation to a changing world may also assist in understanding how to decrease the use of herbicides and pesticides, which plague modern cultures. The study of digestion and/or plant deconstruction processes in controlled conditions will benefit from faster dynamic imaging. In particular, new avenues of research shall emerge from the implementation and improvements of full-field tomography at the upgraded SOLEIL source. The tight coupling of techniques and the possibilities to investigate one single mechanism

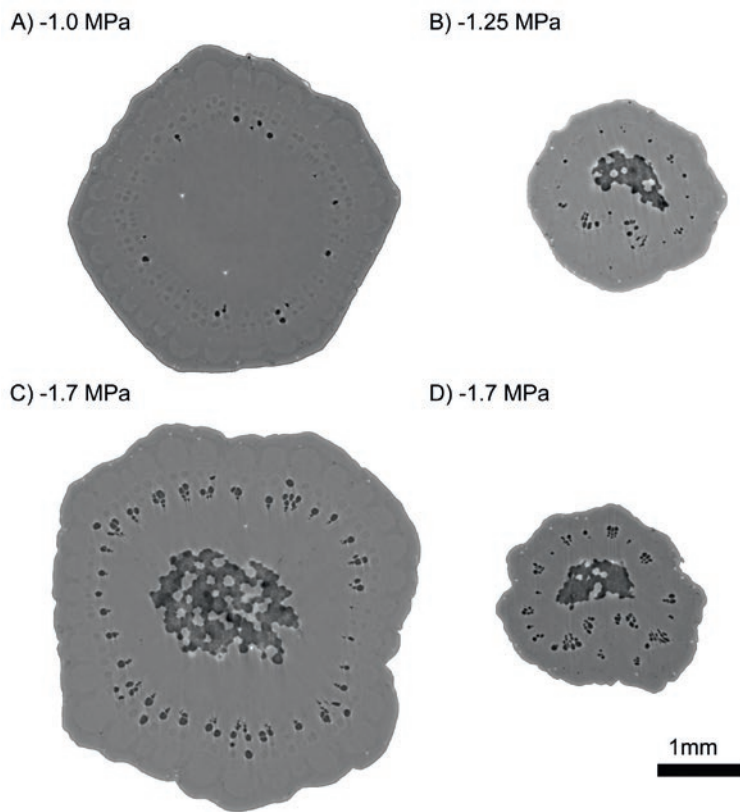


Figure 6: Scientists from the national institute for agricultural research, INRAE, are conducting, at SOLEIL, a research program designed to understand the impact of drought on trees and plants, by investigating the formation of embolism in conducting vessels via X-ray tomography. The image shows the tomographic reconstructions of sap filled and air filled vessels in grape vines at different water potentials (see<sup>[18]</sup>)

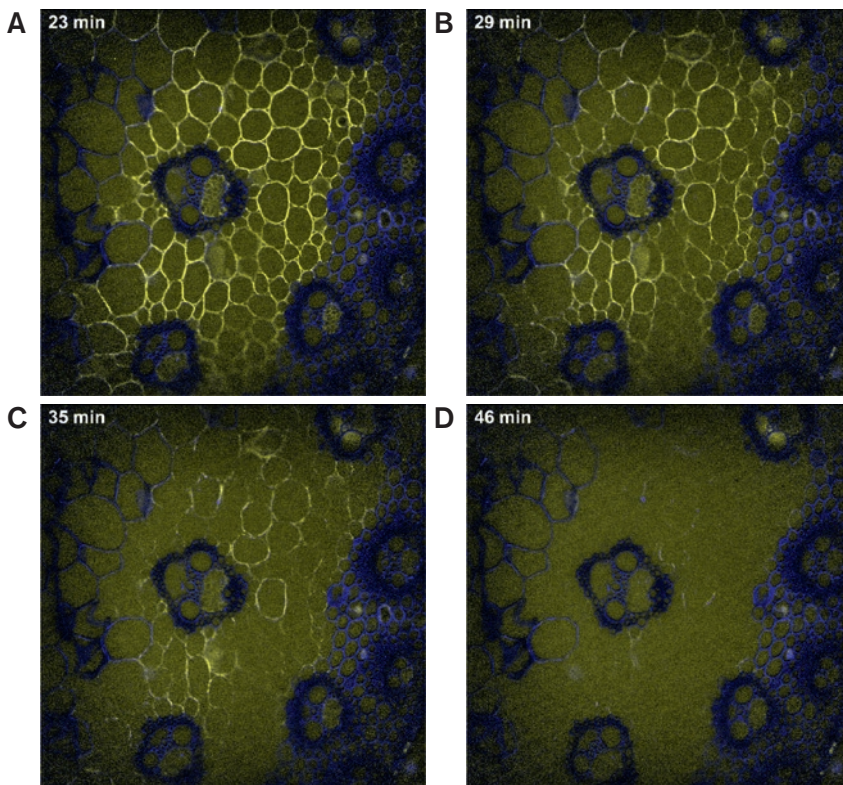


Figure 7: Time lapse sequence of a section of maize stem treated with a commercial cellulase, produced by DUV imaging. The sequence of degradation at different parts of the cell are demonstrated, as is the recalcitrance of lignified cell walls. In blue, cell wall; in yellow, enzymes; in white, co-localization of enzymes and cell walls<sup>[19]</sup>.

or sample on various independent instruments will be achievable with new developments for handling samples and mimicking the biological systems under study, e.g. microroots. The creation of an integrated laboratory (i-Lab) will favour the exchange of the various expertises, accelerating the research in the field. Most of the objects of this theme appear as high-quality drivers for the developments of new techniques / and illuminations schemes (i.e. light sheet and structured illumination), in order to improve spatial resolution and produce different forms of contrast.

## Drought resistance of trees and plants

### Interest

Drought resistance of different species of grape vine has been examined as a function of diurnal and seasonal rhythm in both normal and drought conditions. The onset of embolism, which decreases the vines' vascular capacity, has been investigated using the capacity of synchrotron-based tomography to investigate large volume, living samples at  $\mu\text{m}$  spatial resolution (Figure 6).

### SOLEIL Upgrade Benefits

Current measurements are limited to short measurement campaigns at the synchrotron, leaving the worry that an insufficiently representative statistical sample has been considered. Additionally, improved Zernicke phase contrast and magnification (offered by nano-tomography using the upgraded source beam properties and long imaging distances) offer the possibility to investigate connections in plant vasculature, whose presence is deduced but unseen by existing methods.

## Biomass degradation

### Interest

Many microorganisms gain nutrients by "eating" plant or bacterial matter around them. The family of organisms that degrade biomass can be used for industrial processes, for example to produce fuel precursors. The cellulosome, found in a number of micro-organisms, is a multi-enzyme complex comprising a scaffold, which via its cohesin domains promotes the assembly of a toolkit of enzymes (cellulases, xylanases) adapted to the degradation of different components of cell walls and have particular strategies for dealing with recalcitrant substrates. The degradation of "wasted" biomass (for example certain seaweeds which for "green" and "red" tides are proliferate close to the coast as a

result of pollution and human activity) must be addressed when attempting to develop a circular bio-economy.

### SOLEIL Upgrade Benefits

The elucidation of the spatial organisation of complexes that degrade plant matter, their specificity in relation to a particular substrate, and the dynamics of their interactions, are all questions susceptible to the development of new and improved imaging, diffraction and scattering methods at an upgraded SOLEIL. Enzymes and their interactions can be

further explored using room temperature serial X-ray crystallography, and methods are already being developed to examine, by DUV imaging (as shown in [Figure 7](#)) and under close to physiological conditions, the order in which cell components are degraded.

Improved imaging modalities (for example soft X-ray microscopy and tomography, DUV imaging incorporating light sheet methods, in-line X-ray holography) will improve spatial resolution and facilitate the coupling of high resolution and low

resolution data. Moreover, the improved source brilliance will enable improved throughput of measurements, allowing a wider variety of systems to be studied rapidly. With the acquired structural knowledge (for example important sequence motifs), bioinformatic signatures and tools will be improved to more closely examine the specificities of genetic loci responsible for the enzymes comprising the “tool kit”, hence pointing the way to modified enzyme cocktails for different substrates.

### REFERENCES

- [1] K. Schneider, W. van der Werf, M. Cendoya, M. Mourits, A. Navas-Cortes, A. Vicent, A. Oude Lansink. “Impact of *Xylella fastidiosa* subspecies pauca in European olives”. *PNAS* 117 (17) 9250-9259 (2020).
- [2] Charrier, G., Torres-Ruiz, J.M., Badel, E., Burlett, R., Choat, B., Cochard, H., Delmas, C.E.L., Domec, J.C., Jansen, S., King, A., Lenoir, N., Martin-StPaul, N., Gambetta, G.A., Delzon, S. “Evidence for hydraulic vulnerability segmentation and lack of xylem refilling under tension.” *Plant Physiology*, 172(3): 1657-1668. (2016).
- [3] Chandran, V., Fronzes, R., Duquerroy, S., Cronin, N., Navaza, J., Waksman, G. “Structure of the outer membrane complex of a type IV secretion system” *Nature*, 462(7276): 1011-1015. (2009).
- [4] Kotschy, A., Szlavik, Z., Murray, J. et al. “The MCL1 inhibitor S63845 is tolerable and effective in diverse cancer models” *Nature*, 538(7626): 477–482. (2016).
- [5] Voss, J.E., Vaney, M.C., Duquerroy, S., Vornrhein, C., Girard-Blanc, C., Crublet, E., Thompson, A., Bricogne, G., Rey, F.A. “Glycoprotein organization of Chikungunya virus particles revealed by X-ray crystallography” *Nature*, 468(7324): 709–712. (2010).
- [6] Barba-Spaeth, G., Dejnirattisai, W., Rouvinski, A., Vaney, M.C., Medits, I., Sharma, A., Simon-Loriere, E., Sakuntabhai, A., Cao-Lormeau, V.M., Haouz, A., England, P., Stiasny, K., Mongkolsapaya, J., Heinz, F.X., Screaton, G.R., Rey, F.A. “Structural basis of potent Zika-dengue virus antibody cross-neutralization” *Nature*, 536(7614): 48–53. (2016).
- [7] Rouvinski, A., Guardado-Calvo, P., Barba-Spaeth, G., Duquerroy, S. et al. “Recognition determinants of broadly neutralizing human antibodies against dengue viruses” *Nature*, 520(7545): 109–113. (2015).
- [8] Dumont, E., Vergalli, J., Conraux, L., Taillier, C., Vassort, A., Pajovi, J., Réfrégiers, M., Mourez, M., Pagès, J.M. “Antibiotics and efflux: combined spectrofluorimetry and mass spectrometry to evaluate the involvement of concentration and efflux activity in antibiotic intracellular accumulation” *Journal of Antimicrobial Chemotherapy*, 74(1): 58-65. (2019).
- [9] Vergalli, J., Dumont, E., Pajovic, J., Cinquin, B., Maigre, L., Masi, M., Réfrégiers, M., Pagès, J.M. “Spectrofluorimetric quantification of antibiotic drug concentration in bacterial cells for the characterization of translocation across bacterial membranes” *Nature Protocols*, 13(6): 1348–1361. (2018).
- [10] Peng, C., Chiappini, F., Kašćáková, S., Danulot, M., Sandt, C., Samuel, D., Dumas, P., Guettier, C., Le Naour, F. “Vibrational signatures to discriminate liver steatosis grades” *Analyst*, 140(4): 1107-1118. (2015).
- [11] Poulon, F., Chalumeau, A., Jamme, F., Pallud, J., Varlet, P., Mehidine, H., Juchaux, M., Devaux, B., Refregiers, M., Abi Haidar, D. “Multimodal Analysis of Central Nervous System Tumor Tissue Endogenous Fluorescence With Multiscale Excitation” *Frontiers in Physics*, 6: art.n° 109. (2018).
- [12] Mehidine, H., Jamme, F., Chalumeau, A., Poulon, F., Varlet, P., Devaux, B., Refregiers, M., Abi Haidar, D. “Discrimination between primary low and high grade tumor and secondary metastasis tumor from deep-UV to NIR” *Proceedings of SPIE*, 10871: art.n° 1087109. (2019).
- [13] Charrier, G., Torres-Ruiz, J.M., Badel, E., Burlett, R., Choat, B., Cochard, H., Delmas, C.E.L., Domec, J.C., Jansen, S., King, A., Lenoir, N., Martin-StPaul, N., Gambetta, G.A., Delzon, S. “Evidence for hydraulic vulnerability segmentation and lack of xylem refilling under tension.” *Plant Physiology*, 172(3): 1657-1668. (2016).
- [14] Devaux, M.F., Jamme, F., André, W., Bouchet, B., Alvarado, C., Durand, S., Robert, P., Saulnier, L., Bonnin, E., Guillon, F. “Synchrotron Time-Lapse Imaging of Lignocellulosic Biomass Hydrolysis: Tracking Enzyme Localization by Protein Autofluorescence and Biochemical Modification of Cell Walls by Microfringed Infrared Microspectroscopy” *Frontiers in Plant Science*, 9: art.n° 200. (2018).



# Environmental Sciences

## — Overview

Over the last decades, it has become clear that a full understanding of the Earth, and the complex interplay between its different components, is critical to developing a sustainable approach to fulfilling the needs of the Earth's growing population. The atmosphere, which is menaced by particulate and gaseous emissions resulting from human activity, protects us from harmful UV solar irradiation whilst permitting useful heat to penetrate through to the surface, being a key element defining climate<sup>[1]</sup>. The atmosphere is also responsible for the circulation of both (natural and anthropogenic) gaseous and particulate matter, including microbes, nanoparticles and nanoplastics, having a major role in the propagation of pollutants. Indeed, the World Health Organisation estimates that 7 million deaths per year are caused by air pollution<sup>1</sup>. Respiratory problems result from particulate pollution, underlining the need to understand atmospheric chemistry and the resulting propagation of allergens, natural and unnatural nanoparticles and volatile chemicals.

The oceans and surface water network harbor an immense diversity of life, increasingly exploited by humankind as an energy and food source as well as inspiring the development of medicines, providing useful enzymes for industrial processes etc. At the same time ocean life is a major contributor to the production of atmospheric oxygen via algal photosynthesis. The role of the ocean as a reservoir for non-exploited carbon is only becoming evident as chemical and temperature driven changes modify oceanic conditions<sup>[2]</sup>. The interplay between ocean currents and atmosphere has major impact on both weather and climate.

Interactions with the natural world can be the root cause of major human health issues. The passage of the SARS-Cov2 virus, from its likely origin in bats to the human population, was caused by non-regulated interaction between man and animal, giving rise to what may be the worst pandemic in living

memory. In addition global warming has the potential, through melting of permafrost, to release previously frozen or trapped microbes, ice-nucleating particles and greenhouse gases into the environment<sup>[3]</sup>.

The subtle exchanges between the different compartments of the Earth, and the evolution of the life it supports, culminated, over geological time, in an ecological equilibrium between "supply and demand" where nothing is wasted. Soils support microbial and plant life, playing a similar role to the oceans as the medium supporting food sources upon which surface life depends.

Microbial, plant or animal life evolve to fill unexploited niches, sometimes in harsh environments, to recover and reuse energy and raw materials. Human resource consumption, on the other hand, is highly inefficient, with resources used without replenishment and waste products of consumption liberally spread across the environment. Our current use of planetary resources is unsustainable. Indeed, in 2009 Steffen developed the concept of "planetary boundaries"<sup>[4]</sup>, setting broad limits to nine categories of resource, and the amount of 9 categories of resource that we can consume without seriously endangering planetary equilibrium. In two of these categories (biochemical flows and biosphere integrity) we have already ventured into uncharted territory.

Whereas many subjects of environmental interest are already (and will continue to be) treated at SOLEIL, we base this CDR on challenges underpinning a number of **emerging areas of pollution and its remediation**. This choice of challenges is made to underline how science has changed over the last 20 years and how the proposed evolution of SOLEIL can make a major contribution towards responses directed to them. In doing so, we ignore a number of equally important environmental issues (for example gaseous emissions of CO,

<sup>1</sup>[https://www.who.int/health-topics/air-pollution#tab=tab\\_1](https://www.who.int/health-topics/air-pollution#tab=tab_1)

CO<sub>2</sub> and NO<sub>x</sub>, the carbon cycle and its relationship to deep earth and oceanic processes). That such questions are indeed critical is demonstrated by the very recently published findings of<sup>[5]</sup>, reported in the journal PNAS, which indicate that today's CO<sub>2</sub> emissions are currently far outstripping those that caused the Paleocene Eocene Thermal Maximum. Issues such as the impact of climate change to available fresh water supply (via investigations of drought resistant species or species which require less water to grow), and the retention of water in porous media, critical to avoiding dry and dead forest areas susceptible to fire, continue to be investigated at SOLEIL (The resistance of plants to water shortage, and the use of bio sourced materials as a primary resource are discussed elsewhere in this report, since many environmental challenges are multi-disciplinary in nature).

In this chapter, we have chosen to focus on emerging challenges related to anthropogenic pollution. In part 1 we discuss **atmospheric pollution** and its impact on **global warming. Pollution of the Critical Zone<sup>2</sup> by anthropogenic nanoparticles and trace elements dissemination**, and, more generally, the **dynamics of pollutants in the land-sea**

**continuum**. Part 2 discusses **plastics, and in particular micro- and nanoplastics, as emerging contaminants**, now found in all compartments of the Critical Zone, and whose impact on the environment and the health of ecosystems is still in question. Synchrotron radiation will help address their **prevalence**, their **interaction with natural matter** and their role as a **vector of pollution**. Subsequently, we address the issue of the **bioeconomy and recycling, in the context of circular economy** and the desire to **preserve resources**. Recovery or reuse of waste can contribute to establishing a circular economy, whereby humankind ensures that the use and production of resources remains in equilibrium and nothing is wasted. Significant commercial opportunities will emerge from in depth study of these phenomena. Many of these applications will benefit from essentially similar opportunities afforded by the proposed upgrade to SOLEIL, notably increased flux density leading to improved spatial resolution for both imaging and spectroscopic techniques, the exploitation of coherence based imaging techniques at ultra-high resolution, and coupled with a decrease in the concentration of trace metals that can be measured.



<sup>2</sup> "heterogeneous, near surface environment in which complex interactions involving rock, soil, water, air, and living organisms regulate the natural habitat and determine the availability of life-sustaining resources" ([https://en.wikipedia.org/wiki/Earth%27s\\_critical\\_zone](https://en.wikipedia.org/wiki/Earth%27s_critical_zone); National Research Council. 2001. Basic Research Opportunities in Earth Science. Washington, DC: The National Academies Press. <https://doi.org/10.17226/9981>)



## Atmospheric chemistry & aerosols: fighting global warming

### Interest

In the current context of global warming, there is a crucial need to develop models which can accurately predict climate change, estimating the impacts of anthropogenic activities and helping identify mitigation strategies. One of the key steps in this approach relies on better predicting the distribution, reactions, lifetimes, and the quantify of emission of gases and particles in a changing atmospheric system, based on a detailed understanding of the sources and atmospheric processes controlling the presence of the species. Climate change is expected to increase the frequency of wildfires, such as those occurring in California, as well as the release of aerosolized pathogenic microbes and greenhouse gases related to melting permafrost, underlining the importance of understanding the impact of these emissions on atmospheric chemical equilibria and the carbon cycle.

### Challenges

Atmospheric aerosols can have a natural (sea spray, dust, volcanoes) or anthropogenic (pollution, combustion) origin, or can be produced by oxidation process of volatile organic compounds (secondary organic aerosols) exhibiting a wide range of size (from a few nm up to 1  $\mu\text{m}$ ), time-evolving chemical composition and reactivity as described in Figure 1. An already complex picture is further impacted by the discovery of emerging aerosols (such as nanoplastics released from tyre or brake liner wear<sup>[7]</sup>, or aerosolized pathogenic microbes arising from permafrost melting). Atmospheric aerosol effects vary according to particle size, structure and color (with a direct impact on atmospheric radiation scattering and consequently the surface and cloud albedo). The overall impact of natural, emerging and anthropogenic aerosols on the atmosphere is very difficult to estimate. This is further compounded by our lack of understanding of the interactions between aerosols and clouds, by the wide variability and rapid evolution of aerosol size and chemical composition (notably caused by their short lifetime), and by their capacity to transport pollutants<sup>[7]</sup>. To develop robust, physically-based, models of climate change as well as to understand impact of aerosols on health and the environment and carbon and

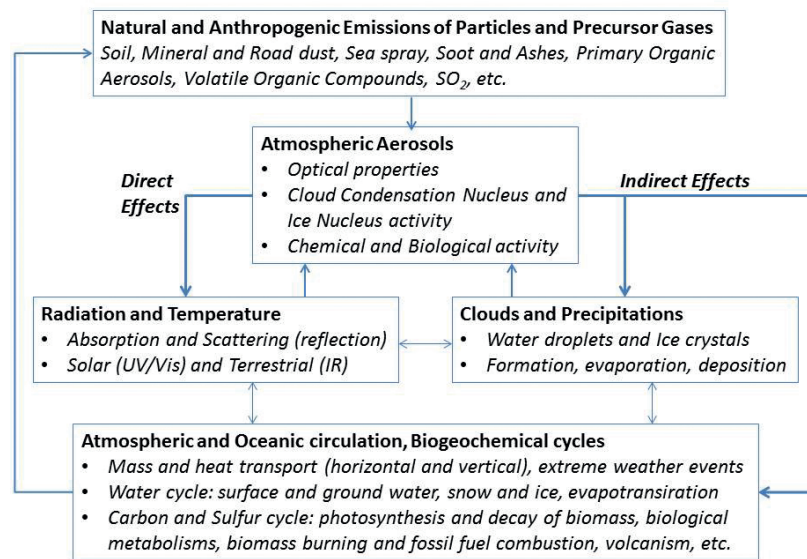


Figure 1: Aerosol effects and major feedback loops in the climate system (from<sup>[6]</sup>)

water cycles, a detailed understanding of aerosols composition (Figure 2), and their modification in the atmosphere, is necessary.

### SOLEIL upgrade benefits

The energy range of SOLEIL, which is preserved in the proposed upgrade, is well adapted for building powerful low energy beamlines for analyzing gas composition and aerosols processes of transformation. Structure and reactivity of radicals which are key intermediates in atmospheric chemistry as well as the reactivity, and therefore lifetime, of atmospheric aerosols, and isomer-specific picture of the chemical composition of the secondary organic aerosols, can be efficiently probed, in direct connection to the chemical process driving their formation. The

mid-IR region is sensitive to many gases including greenhouse molecules ( $\text{CO}$ ,  $\text{CO}_2$ ,  $\text{CH}_4$ , etc.) as well as common smokestack pollutants ( $\text{SO}_2$ ,  $\text{N}_2\text{O}$ , etc.). The use of mid IR to terahertz radiation for detection and identification of gases is complementary to well established laboratory techniques and provides rotationally resolved cross sections of vibration bands, needed as inputs in modeling the greenhouse effect<sup>[8]</sup>. Synchrotron-based XPS measurements, combined with liquid jet instrumentation, allows studying free standing aerosols composition (avoiding artefacts from sample – substrate interactions). For example, sea spray aerosols have complex and size-dependent chemical composition since they contain both inorganic salts and organic species in varying proportions. They play a

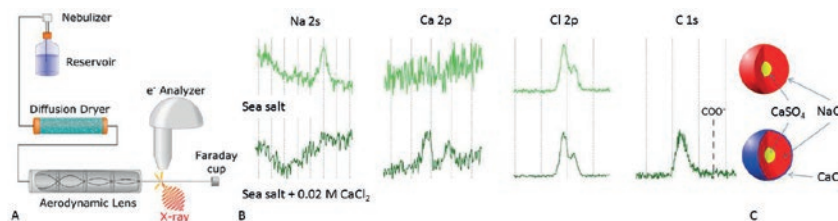


Figure 2: Sea spray aerosols have complex and size-dependent chemical composition. They play a significant role in the earth's radiation budget as they scatter solar radiation and act as cloud condensation nuclei, for which their efficiency depends on their size and surface composition. The investigation on the chemical composition of such nanoparticle surfaces necessitates chemical and surface sensitive probes offering nanometric resolution. Synchrotron-based XPS experiments using aerodynamic lenses offer additionally the possibility to study free standing particles (avoiding sample – substrate interactions artefacts). Unger *et al.* (2020)<sup>[9]</sup> used this method to determine that the formation of a core-shell structure governs the surface composition of the aerosol, whose structure varies according to conditions of formation.

- A. XPS measurements of sea spray aerosols focused by an aerodynamic lens.
- B. Na 2s, Ca 2p, Cl 2p and C 1s photoelectron spectra obtained from different aerosol particles.
- C. Representation of the corresponding sea spray aerosols forming core-shell structures.

significant role in the earth's radiation budget as they scatter solar radiation and act as cloud condensation nuclei, for which their efficiency depends on their size and surface composition. The investigation on the chemical composition of such nanoparticle surfaces with **a new XPS chemical and surface sensitive probe offering currently inaccessible nanometric resolution** could thus unravel that the formation of a core-shell structure governs the surface composition of the aerosol, which structure varies according to conditions of formation (Figure 2)<sup>[9]</sup>. **A reduction of the detection limit will result from improvements to the source properties, which will in turn offer opportunities to further optimize detection and experimental arrangements of XPS, VUV and IR beamline instrumentation, providing increasing sensitivity** to make valuable progress in atmospheric processes knowledge. Furthermore, SOLEIL's upgrade will provide powerful complementary tools for a dynamical structural and chemical characterization of aerosols, accessing processes of formation and impact on health and climate. **Hyperspectral tools, coupling 2D or 3D imaging techniques to chemical speciation, will benefit from an increase in source brightness, enabling operando characterization. Probing complex nano-systems, that may be mixtures of solid, liquid and gas, with spatial resolution down to a few nm, will become possible.** Interface interactions play a key role in the complete understanding of aerosols chemistry. **The ability to access spatially resolved chemical state with element sensitive techniques will benefit from brightness driven increases in acquisition speed, by up to a factor of 10, to follow composition variations with time and physicochemical conditions.** Furthermore, **combining these improved techniques with microfluidic chips** (see the "dynamic and transfers" part of this section) will provide promising tools for these dynamical studies (such as characterizing, *in vitro*, emissions due to permafrost melt). **This combination of techniques will shed light on the physicochemical transformation mechanisms of aerosols and overall effects on global radiative forcing and thus on the impact of changing emission profiles to atmospheric equilibria and the consequent effects on the water and carbon cycles.**

## The impact of nanoplastics on the health of our environment

### Interest

Plastic emissions, and their effects, represent an urgent issue for the planet. Annual emissions of plastic may reach 53 million metric tons by 2030, whereas, after making reasonable assumptions, even with major improvements in waste management capacity it is currently inconceivable to attain a 10% reduction in annual emissions<sup>[10]</sup>. A 40% reduction will be required to reduce emissions to the target scenario of 8 Mt per year<sup>[10]</sup>. Clearly, new, disruptive, technologies must be developed to reduce plastic emission and subsequent impact on natural ecosystems.

Europe has integrated the reduction of environmental plastic pollution as a key objective of its European Strategy for Plastics in a Circular Economy (2018), and is affirming a strong "zero pollution" ambition for the environment (including plastics) in the European Green Deal (2019). Although recycling plastic waste is hindered by the difficulty of separating materials which exhibit a wide range of composition, spectroscopic separation methods, in conjunction with pattern recognition machine learning methods, show promise for separating different species. However, when plastics reach environmental systems, fragmentation from macro to nanoplastics occurs in all compartments with the result that nanoplastics can impact

environmental health in the same way as nanoparticles. Ecotoxicological studies have demonstrated that nanoplastics, by crossing biological barriers, may menace flora and fauna<sup>[11]</sup>. Furthermore, nanoplastics can accumulate in soil, combining with pathogens, persistent organic pollutants, antibiotics, heavy metals and other toxic chemicals, with potential for changing propagation modes and dynamics (Figure 3). The fate of nanoplastics, their implications for the soil environment and their contribution to the transfer and availability/toxicity of associated pollutants are currently largely unknown, especially since they are hard to detect. Little is known about plastic degradation processes and the subsequent release of toxic metals (which must be different if they are included in, or sorbed to, the plastic structure). Moreover, the role of biofilms in the sorption processes has to be further investigated. This question is crucial knowing that nanoplastics have been described as exhibiting colloidal properties in aqueous systems and migrate in soil<sup>[12]</sup>. More research is needed to fully understand the risk of exposure to nanoplastics, and their role as contaminant vectors.

### Challenges

Research has focused on plastic pollution in marine waters (notably oceanic gyres), highlighting the dramatic impact of plastics on marine ecosystems. In contrast, the impact of plastics on freshwater and soils has been less studied. While photo-oxidation is considered the main process of plastic fragmentation in oceans and seas, the mechanisms involved in soils,

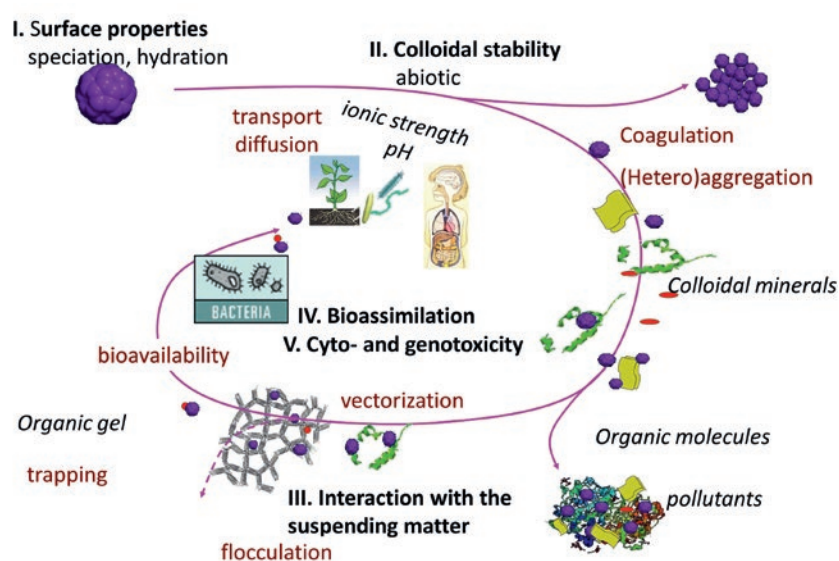


Figure 3: Possible interactions of nanoplastics as nanoparticles in the environment (case of an aquatic system)(© Jérôme Rose : rose@cerege.fr)



fresh waters and sediments are largely unknown, and biota is expected to play an important role in fragmentation. Nanoplastics are difficult to observe, in both the soil matrix and living organisms, because of their size and light elemental composition. Characterizing their fate (transfer and degradation) in soils and ecosystems is of primary importance to assess their ecological impact, but extremely challenging. Recently, accumulation of fluorescent polystyrene nanoplastics (PNP) in the brain region of zebrafish embryos could be followed using laser scanning microscopy and TEM images<sup>[15]</sup>. Along with other analyses, these observations could demonstrate the oxidative DNA damage in the brain regions where PNP accumulates, leading to an increase of mortality and prevailing abnormalities, perhaps resulting from the buildup of reactive oxygen species leading to apoptosis, especially in the brain. Degradation processes are implicated in the release of associated toxic substances and generation of reactive O-containing sites, hence modifying plastics surface reactivity. Such modifications are expected to allow not only the coating and precipitation of new minerals, but also the formation of biofilms and the binding of many other contaminants such as metal or organic pollutants. Investigations into these processes will lead to the understanding of the wide-ranging implications of plastic pollution on environment and ecosystem health, and suggest modification to production and recycling methods in order to mitigate them.

#### SOLEIL upgrade benefits

Amongst the methods currently used to characterize plastics, Fourier transform infrared spectroscopy shows promise to single out nanoplastics from particulate matrix<sup>[16]</sup> and hence follow the modifications of surface sites due to plastics degradation. In addition, pioneer experiments show the potential of STXM to follow the alteration of polystyrene and polymethylmethacrylate (PMMA) under UV irradiation by collecting NEXAFS data at the carbon and oxygen edges<sup>[15]</sup>. Assessing nanoplastics-metals interactions in soils, plants or animals by a combination of spectroscopic and imaging techniques, spanning IR to X-ray, driven to higher spatial resolution by the upgrade beam properties, will allow chemical discrimination of nanoplastics within a heterogeneous system and subsequent correlation with local metal speciation. As proof of principle, Deng *et al.* (2015)<sup>[16]</sup> have demonstrated the feasibility of

ptychographic transmission and XRF imaging at low contrast in cryogenically preserved algal cells. Techniques such as high energy nano-XRF imaging can probe a volume large enough to be representative of the entire complex system, and do not require the destructive manipulation of the 3D structure. The spatial resolution can be adjusted from low (*i.e.* 10th of a  $\mu\text{m}$ ) to very high (*i.e.* up to few nm thanks to the upgrade) to detect nanomaterials even those smaller than 10 nm to unravel their scale-dependency. Furthermore, focusing on interactions of toxic heavy metals with nano-plastics, spectrally resolved XAS HERFD-XANES, will be able to differentiate between multiple metal organic ligands<sup>[17]</sup> and will be developed at 100 nm spatial resolution at the upgraded source.

**The increased beam brightness of the upgraded source will lead to an order of magnitude increase in concentration sensitivity for X-ray fluorescence and in spatial resolution across the whole energy range (even in the IR domain where increased brightness will facilitate optical arrangements and allow improved illumination of, for example, SNOM probes). By correlating chemically sensitive high spatial resolution nano-IR imaging and spatially resolved XAS with nano-X-ray imaging methods (*i.e.* combining ptychography with X-ray microscopy), the speciation of tiny concentrations of metallic pollutants associated with nanoplastic vectors, their binding modes, chemistry and structure, correlated with their spatial localization within a heterogeneous environment becomes accessible. These enhanced capabilities of SOLEIL beamlines will provide an unprecedented set of tools to enable in situ characterization of the fate of plastics (*e.g.* transfers, degradation processes and products, etc.) in the various ecosystem components, providing essential information for understanding of the global ecodynamics of plastics and its impact on the environment and**

**ecosystems health.** As nanoplastics can be considered as colloidal vectors for pollutants, one can expect this approach to be rapidly extended to the study of the behavior and impact of nanoparticles and colloids in natural systems.

## Environmental behavior of trace elements

### Interest

Trace metals are naturally present, at very low concentration, in the earth's crust. As an example, cadmium (Cd) occurs at  $\sim 0.1$  ppm (mg/kg) and molybdenum (Mo) at  $\sim 1.4$  ppm. Although some trace metals, so-called oligo-elements, are indispensable to biological processes (*i.e.* Zn, Cu, Cr, Mo, Se), they are all potentially polluting (depending on their concentration and chemical form). Releases from anthropogenic activity (*i.e.* industrial emission and waste, motor traffic, spreading of manure, sewage sludge or fertilizers, etc.) may modify their chemical form and increase their concentration to high levels with respect to background, but still too low for accurate chemical identification by bulk synchrotron techniques (Figure 4).

These analytical limitations partly explain why some pollutants, despite being toxic at very low concentrations, (Cd and Mo lethal doses are lower than 20 mg / corporal kg) have been less studied in natural systems than other more concentrated elements. However, they exhibit a potential risk for environmental and human health, according to their speciation, and they are expected to be able to migrate to the groundwater table or trickle down to cropland. Furthermore, an emerging issue is the augmented toxicity arising from interactions between several substances (pesticides, pollutants, drugs etc.) which individually occur at concentrations which lead to dose levels that are accepted as being harmless. It is currently technically challenging to evaluate potential impact

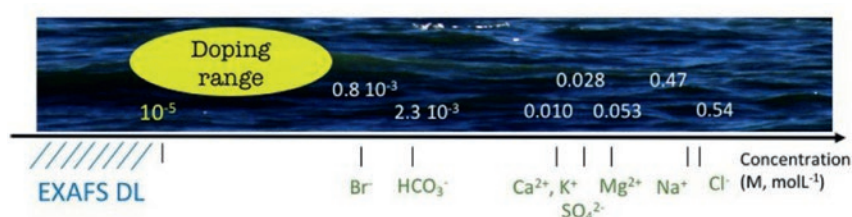


Figure 4: Schematic representation of the average concentrations of major inorganic constituents of seawater compared to EXAFS detection limit (DL)(from<sup>[18]</sup>)

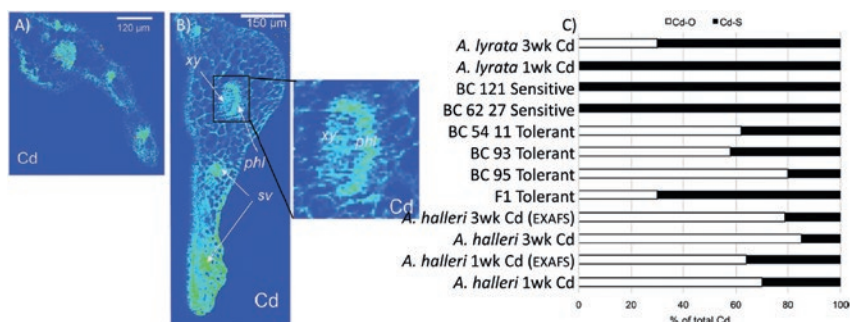


Figure 5: Elemental  $\mu$ XRF maps of cryo cross-sections of (A) *Arabidopsis lyrata* (Cd non-tolerant, [Cd]=250 ppm) and (B) *A. halleri* (Cd hyperaccumulator, [Cd]=820 ppm). For both plants Cd is distributed in the vascular system. The non-tolerant plant contains also Cd in the epidermis while the hyperaccumulator also contains Cd in the mesophyll. (C) Proportion of Cd species (in % mole fraction) obtained by linear combination fits of XAS data showing the different Cd species in different plants (from [19] studies at ESRF and SOLEIL).

due to the low concentrations, but such “cocktail” effects are known in the case of medicines.

### Challenges

Considering the toxicity of trace metals, the accepted maximum permissible Cd concentration fixed by the EC in sludge amended soils (directive 86/278/EEC) is 3 ppm. These concentrations are one order of magnitude beyond the current detection limit of conventional EXAFS analyses (which are usually combined with XANES to determine metal speciation). However, Cd is highly toxic. Anthropogenic inputs of Cd (in connection with industrial activities, phosphate fertilizers and waste spreading) to soils are significant compared to other trace elements. In soils, Cd is potentially more mobile than other divalent metals and more readily bioavailable. Understanding its interactions with soil components and plants, even at such low concentration is essential to prevent Cd poisoning. Figure 5 illustrates the different concentration, location and phases of Cd that can be observed in different highly enriched plants (although lower than 1000 ppm) according to their Cd tolerance.

### SOLEIL upgrade benefits

Currently bulk EXAFS analysis is limited in sensitivity to few 10th of ppm. For example, EXAFS spectra from a rice sample containing 1 ppm of Cd with the current SOLEIL source, remain noisy even after 9h acquisition times. **Both EXAFS and photon hungry HERFD-XANES facilities (with high energy resolution for the characterization of heavy metals speciation) would experience a drastically improved detection limit by at least one order of magnitude from the proposed source upgrade.**

The improved brilliance of the upgraded storage ring will particularly **benefit nano-XRF imaging by improving the signal-to-noise ratio by a factor of 10. It will be then possible to map sample areas 10 times larger, collect maps 10 times more rapidly, or increase the detection limit by a factor of 10<sup>[20]</sup>**, enabling efficient and accurate imaging of heterogeneous naturally occurring samples where pollutants are present at trace levels. **This will reinforce the complementarity between synchrotron-based nano-imaging (capacity to image large samples) and electron microscopy (very high spatial resolution).**

The combination of far higher beam brilliance with a new generation of detectors offering improved sensitivity (see section on detectors), presents the opportunity to overcome concentration limitations whatever the probed spatial scale, and, hence, to evaluate the dangers to health and environment of the presence, accumulation, cocktail effect, transport and bioavailability of (ultra) trace elements.

## Dynamic & transfer of contaminants

### Interest

Natural environments undergo continual change (e.g. due to tides or water flow, day/night alternation, etc.). Assessing the ecotoxicological impact of contaminants in soils and identifying remediation solutions require the complete description of the evolution of these systems, and consequently the study of the life cycle and dynamics of contaminants must take into account spatial and temporal

variability. To improve reactive transport models<sup>[21]</sup>, kinetic and thermodynamic parameters (rate parameters, diffusion coefficients, surface areas) measured in situ are needed, taking into account the transport of the contaminant, its interactions with soil components in the connected pore network, and at appropriate length and time scales.

### Challenges

Integrating the temporal dimension into analyses requires reducing counting times to match system kinetics. This approach is more or less easy to implement depending on the studied system: contamination levels may be low and matrixes are always complex. Furthermore, regardless of the spatial scale studied, the issue of extreme events (storms, floods, etc.), which are of primary importance and are expected to increase in frequency and violence in the context of global warming, appears to be challenging to address.

Organo-metallic colloids, a key vector controlling the transfer and speciation of micropollutants (such as metals or metalloids) in the different compartments of the Critical Zone (soil to river, lake or aquifer transfers), are extremely complex systems. Variations in physico-chemical environment (pH, ionic strength etc.) modify aggregate arrangements and, consequently, their capacity for adsorption of pollutants with dramatic implications for metallic pollutants' mobility and (bio) availability. Understanding the complexity of colloid structural modifications, structural information has to be collected in situ, when modifications of physicochemical conditions occur<sup>[22]</sup>, and combined with modelling methods or the search for trends and correlations in data (for example via machine learning). The complexity of such a study arises from the reaction itself, which may involve several steps proceeding at different rates (for example oxidation occurs in milliseconds, whereas aging may take hours).

### SOLEIL upgrade benefits

The use of micro-fluidic reactors that allow transposing the reaction time onto spatial coordinates<sup>[23]</sup> is a promising technology to explore the impact under extreme flood or storm conditions. Indeed, developments in micro-fluidic tools represent a real opportunity, in the field of environmental sciences, to develop model reactors capable of testing precise mechanistic hypotheses. For example, microfluidic cells have been coupled with X-ray tomography and spectroscopy for investigating acid erosion of fracture

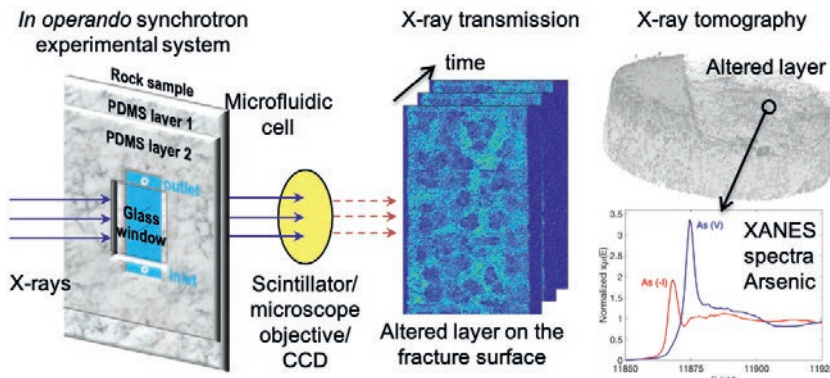


Figure 6: A microfluidic cell, coupled with full-field X-ray tomography applied to calcite, evidenced calcite alteration. Parallel XAS demonstrated a modified As oxidation state, evolving from arsenopyrite As(-I) into As(V) associated with ferrihydrite (from [24])

surfaces in calcite rocks (Figure 6). Carbonate geological settings play a crucial role in oil and gas extraction, waste injection, aquifer recharge or geologic carbon sequestration. Carbonates are dissolved when acids are introduced or formed from injected fluids, their dissolution substantially altering subsurface geologic media, leading to the release of heavy metals or metalloids and causing freshwater and soil contamination. Pioneering in situ under pressure investigations, under microfluidic conditions, have provided necessary data for constructing a detailed 3D reactive transport model and the detailed characterizations of the subsequent arsenic abundance and oxidation state that can be used to predict its mobilization [24].

**Brightness driven improvement in signal to noise ratio for structural characterization techniques such as SAXS and XAS will lead to improved detection limit and temporal resolution, by one order of magnitude, for the dynamical characterization of evolving natural systems at physically meaningful time scales. Micro or nano-focused beamlines will benefit directly from improvements of beam size and brightness.** Phase-contrast tomography will also benefit, offering improved discrimination between low and very-low absorbing matter, such as liquid and gas inside pores hence permitting in situ and real-time studies of the transport of the soil solution inside the pore network. **Coupling time-resolved imaging with chemical speciation will be the next step, allowing the dynamical description of evolving complex systems highlighting intermediate metastable species playing a key role in the evolution processes.**

Then, with the development of these synchrotron-based characterization techniques and operando capabilities, **microfluidic systems are expected to provide in situ observations that are otherwise impossible.** Indeed, on the model shown in Figure 6, **one can consider devices capable of better replicating the complexity of surface processes and developing "Ecosystem in a box" or "Soil-on-chip"** [25]. A dedicated micro-fluidics laboratory has been created for chips conception and fabrication and user support (discussed in Chapter 4). **Microfluidic experiments coupled with SOLEIL techniques capabilities will thus play an increasing role in advancing our fundamental understanding of soils and ecosystems dynamic. In this context, the demand of studying the evolution of natural systems as a whole, combining temporal and spatial resolution, is projected to dramatically increase.**

## Waste recycling: reducing pollution & preserving resources

### Interest

The best practice to prevent pollution is to produce no pollutant. Developing new sustainable materials that consume less energy to produce, have a long operational lifetime and can be recycled into useful products at the end of their life, are challenging yet urgent questions (see sections on Advanced Materials and Sustainable Energy). However, to clean-up previous pollution and prior to the development of more efficient products, we need to recycle or eliminate waste from product life cycles. In this context,

recycling chains are developing more and more, including techniques dedicated to emerging pollutants such as plastics. For example, it has been shown that postconsumer PET can be enzymatically by certain bacterial hydrolases [26]. This result is currently leading to commercial applications for PET using optimized enzymes. In a circular plastics economy, the resulting monomers can be recovered and re-used to manufacture PET products or other chemicals without depleting fossil feedstocks and damaging the environment. On the other hand, waste materials contain precious resources such as metals or rare earth elements: extraction techniques offer the possibility of recovering elements of economical or industrial interest that can then be reused. All recycling techniques will help sustain our limited resources. In addition, ecological stabilization or even more ecological rehabilitation of highly polluted sites (such as old mine or disused industrial sites) is necessary as their intensive exploitation over a long period has generated severe environmental damage (*i.e.* the release and dissemination of metallic pollutants, erosion or soil depletion leading to the loss of potential agricultural land). The rehabilitation of these sites requires depollution or stabilization of their soil, which in many cases can be successfully achieved by phyto-stabilization or remediation. Phytoremediation may even represent an even more sustainable approach as shown by the pioneering work on the (re) introduction of metal hyper-accumulating plants on polluted sites for their subsequent transformation into biosourced eco-catalysts for the synthesis of bio-sourced organic molecules [27]. All of these approaches are entering into four out of the seven pillars of a circular economy (*i.e.* sustainable sourcing, eco-design, extension of usage life, recycling) as outlined in the EC Circular Economy Action Plan 2020.

### Challenges

Plants are a key element in this unavoidable challenge of preserving natural resources. But a lot of knowledge is still to be obtained on their interaction mechanisms to be able to fully exploit their potential.

Due to global warming and anthropogenic activity, marine seaweeds increasingly grow into extensive algal blooms, which are detrimental to coastal ecosystems. However, algal biomass is also emerging as a sustainable raw material for the

bioeconomy. The potential exploitation of algae is hindered by our limited knowledge of the microbial pathways (and hence the distinct biochemical functions of the enzymes involved) that convert algal polysaccharides into simplest molecules. Understanding these complex processes is essential, however, for a complete degradation of algal biomass into bioethanol and other value-added compounds which will turn algae into a valuable and ecologically sustainable bio-resource<sup>[28]</sup>.

Developing phytoremediation applications to stabilize or extract soil metallic pollution needs to fully understand the whole involved mechanisms during metal uptake by plant roots in the soil rhizosphere as well as subsequent metal transport and storage in the plant tissues, in order to develop new strategies to optimize the phytoremediation technique. To avoid any artefact in the diagnosis, these mechanisms have to be observed *in situ* while plant roots are still in the ground to preserve physico-chemical conditions, interfaces integrity, metal speciation and plant structure<sup>[29]</sup>. This is analytically challenging, given the small scales at which these mechanisms occur, and the heterogeneous nature of the systems.

An example that perfectly illustrates the need to consider all mechanisms is the realization of biosourced metal-rich catalysts that have demonstrated competitive catalytic activity in green organic synthesis<sup>[27, 30]</sup>. These new catalysts have polymetallic and original compositions which can permit synergetic catalysis leading to novel synthesis of complex biomolecules (Figure 7). This concept then allows the conversion of

wastes derived from phytoextraction into a mineral and sustainable resource for an eco-friendly and innovative organic synthesis. It is expected that other novel developments of ecological catalysis will emerge in the future. To efficiently expand the use of these bio-sources eco-catalysts in organic chemistry, their catalytic activity has to be correlated with their structure and properties (including composition, crystalline structure and chemical environment around active catalytic center), from the plant inside to the catalyst, following the entire chain of processes from the metal extraction from the soil by the plant to the transformation of the plant into the catalyst.

#### SOLEIL upgrade benefits

To develop new technologies for waste recycling and pollution remediation, it is crucial to understand the mechanisms involved over the entire process (from the waste or the pollutant to the final product) in which interface interactions play a great role. There is thus an increasing need for analytical tools that can characterize the chemical forms of elements (such as rare earth elements or metal pollutants) present in inorganic or organic waste materials, soils or plants. Since these systems are heterogeneous, the characterization of the mechanisms involving the contaminants in the various waste, soil or plant components must be scale-dependent. Therefore, the volume of sample probed should be sufficiently large to be representative of the average physicochemical properties of the sample and the probe must be small enough to probe processes occurring in specific locations or at interfaces. Furthermore, analytical tools that allow characterization whilst avoiding artefacts due to sample

manipulation (*i.e.* sampling, sample preparation for analysis, sample environment, etc.) are of particular value. This point is further developed in the “beamline instrumentation” section. As an example, metal speciation in plant aerial parts, plant roots, and soil, root – soil interface, has to be ideally determined without uprooting plant from soil and with sufficient sensitivity to measure tiny metallic concentrations. **As mentioned in the section “Nanoplastics”, SOLEIL will offer facilities that allow the coupling of chemical speciation from small sample volumes and imaging, via a factor of 10 in chemical sensitivity and spatial resolution and even the possibility to perform routine 3D imaging via the increase in beam brightness and coherent flux. Additionally, an increase in beam coherence will allow improving phase-contrast mapping and employing ptychography-based techniques to enhance the resolution of the images whilst maintaining elemental specificity, hence unambiguously revealing the local distribution of contaminants in the waste, plant, soil components or at interfaces.**

Note that these applications will generate very large volumes of data, amenable to analysis using machine learning methods. New tools are being developed for fast acquisitions and high-throughput data treatment procedures (see sections on data acquisition and data analysis).

Improvements of the SOLEIL capabilities, especially for speciation coupled with imaging, associated with a reinforcement of the instrumentation for the environment of specific samples and laboratory support, will benefit to the researches on waste recycling and pollution mitigation. **This research includes both fundamental and industrial research as the understanding of the mechanisms of pollutants uptake and subsequent potential transformation is a fundamental in the elaboration of sustainable technologies for both waste management and recycling.**

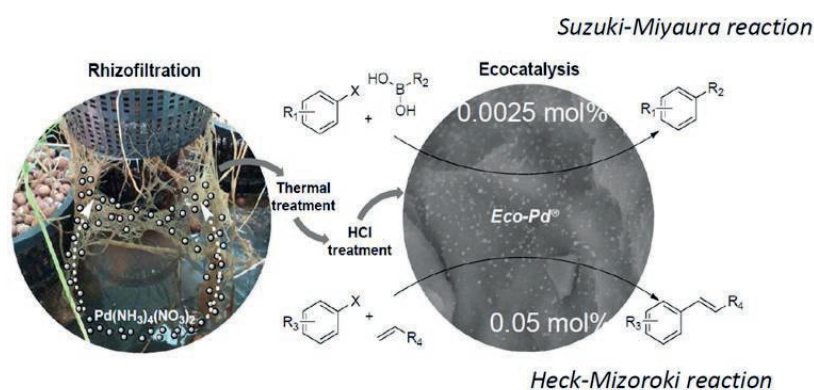


Figure 7: Palladium is efficiently accumulated by rhizofiltration inside the plant *Brassica juncea*. The plant is then treated to synthesize a Pd-rich eco-catalyst able to catalyze numerous reactions. To efficiently expand the use of these bio-sourced eco-catalysts, their catalytic activity has to be correlated with their structural composition and active catalytic metal chemical environment from plant to eco-catalyst. (from<sup>[30]</sup> © Claude Grison)



## REFERENCES

- [1] McNeill, V.F. "Atmospheric aerosols Clouds, Chemistry and Climate". Annual Review of Chemical and Biomolecular Engineering., 8, 427-444. (2017).
- [2] Suarez, C. A., Edmonds, M., Jones, A. P. "Earth catastrophes and their impact on the carbon cycle." Elements., 15, 301-306. (2019).
- [3] Waits, A., Emelyanova, A., Oksanen, A., Abass, K., Rautio, A., "Human infectious diseases and the changing climate in the arctic" Environment International., 121, 1, 703-713. (2018).
- [4] Steffen, W., Richardson, K., Rockstrom, J., Cornell, S.E., Fetzer, I., Bennett, E.M., Biggs, R., Carpenter, S.R., de Vries, W., de Wit, C.A., Folke, C., Gerten, D., Heinke, J., Mace, G.M., Persson, L.M., Ramanathan, V., Rayers, B., Sorlin, S. "Planetary Boundaries: Guiding human development on a changing planet" Science., 347, 6226, art.n° 1259855. (2015)
- [5] Haynes, L., Honish, B. "The seawater carbon inventory at the PaleoceneEocene Thermal Maximum". PNAS. 117, 39, 24088-24095. (2020).
- [6] Poschl, U. "Atmospheric Aerosols, Composition, Transformation, Climate and Health Effects" Angewandte Chemie., 44, 7520-7540. (2005).
- [7] Evangeliou, N., Grythe, H., Klimont, Z., Heyes, C., Eckhardt, S, Lopez-Aparicio, S., Stohl, A. "Atmospheric transport is a major pathway of microplastics to remote regions". Nature Communications., 11: art.n° 3381. (2020).
- [8] Tran, H., Turbet M., Hanoufa, S., Landsheere, X., Chelin, P., Ma, Q., Hartmann, J.-M. "The CO<sub>2</sub> -broadened H<sub>2</sub>O continuum in the 100–1500 cm<sup>-1</sup> region: Measurements, predictions and empirical model" Journal of Quantitative Spectroscopy & Radiative Transfer., 230, 75–80. (2019).
- [9] Unger, I., Saak, C.-M., Salter, M., Zieger, P., Patanen, M., Björneholm, O. "Influence of Organic Acids on the Surface Composition of Sea Spray Aerosol" Journal of Physical Chemistry A., 124, 422-429. (2020).
- [10] Borrelle, S.B., Ringma, J., Law, K.L., Monnahan, C.C., Lebreton, L., McGivern, A., Murphy, E., Jambeck, J., Leonard, G.H., Hilleary, M.A., Eriksen, M., Possingham, H.P., De Frond, H., Gerber, L.R., Polidoro, B., Tahir, A., Bernard, M., Mallos, N., Barnes, M., Rochman, C.M. "Predicted growth in plastic waste exceeds efforts to mitigate plastic pollution". Science., 369, 6510, 1515-1518. (2020).
- [11] Shen, M., Zhang, Y., Zhu, Y., Song, B., Zeng, G., Hu, D., Wen, X., Ren, X. "Recent advances in toxicological research of nanoplastics in the environment: A review" Environmental Pollution., 252, 511-521. (2019).
- [12] Gigault, J., ter Halle, A., Baudrimont, M., Pascal, P.-Y., Gauffre, F., Phi T.-L., El Hadri, H., Grassl, B., Reynaud, S. "Current opinion: What is a nanoplastic?" Environmental Pollution., 235, 1030-1034. (2018).
- [13] Sökmen, T. O., Sulukan, E., Türkoglu, M., Baran, A., Özkaraca, M., Ceyhan, S.B. "Polystyrene nanoplastics (20 nm) are able to bioaccumulate and cause oxidative DNA damages in the brain tissue of zebrafish embryo (Danio rerio) "Neurotoxicology., 77, 51–59. (2020).
- [14] Möller, J., Löder, M., Laforsch, C. "Finding Microplastics in Soils: A Review of Analytical Methods" Environmental Science & Technology., 54, 2078-2090. (2020).
- [15] Melo, L., Hitchcock, A., Susac, D., Stumper, J., Berejnov, V. "Effect of UV radiation damage in air on polymer film thickness, studied by soft X-ray spectroscopy" Physical Chemistry Chemical Physics., 20, 16625-16640. (2018).
- [16] Deng, J., Vine, D., Chen, S., Nashed, Y., Jin, Q., Phillips, N., Peterka, T., Ross, R., Vogt, S., Jacobsen, C. "Simultaneous cryo- X-ray ptychographic and fluorescence microscopy of green algae". PNAS., 112, 8, 2314-2319. (2015).
- [17] Manceau, A., Lemouchi, C., Rovezzi, M., Lanson, M., Glatzel, P., Nagy, K., Gautier-Luneau, I., Joly, Y., Enescu, M. "Structure, Bonding, and Stability of Mercury Complexes with Thiolate and Thioether Ligands from High-Resolution XANES Spectroscopy and First-Principles Calculations" Inorganic Chemistry., 54, 11776- 11791. (2015).
- [18] Beccia, M.R., Solari, P.L., Monfort, M., Moulin, C., Den Auwer, C. "Focus on speciation assessment in marine radiochemistry with X-ray absorption spectroscopy" New journal of Chemistry., 42, 7582-7591. (2018).
- [19] Isaure, M.-P., Huguet, S., Meyer, C.-L., Castillo-Michel, H., Testemale, D., Vantelon, D., Saumitou-Laprade, P., Verbruggen, N., Sarret, G. "Evidence of various mechanisms of Cd sequestration in the hyperaccumulator Arabidopsis halleri, the non-accumulator Arabidopsis lyrata, and their progenies by combined synchrotronbased techniques" Journal of Experimental Botany., 66, 11, 3201-3214. (2015).
- [20] Somogyi, A., Baranton, G., Medjoubi, K. "Estimated Performance of Nanoscopy at an Upgraded Synchrotron Soleil" Microscopy and Microanalysis., 24 (Suppl 2), 256-257. (2018).
- [21] Tourmassat, C., Steefel, C. "Reactive transport modeling of coupled processes in nanoporous media" Review in Mineralogy and Geochemistry., 85, 75-109. (2019).
- [22] Vantelon, D., Davranche, M., Marsac, R., La Fontaine, C., Guénet, H., Jestin, J., Campaore, G., Beauvois, A., Briois, V. "Iron speciation in iron–organic matter nanoaggregates: a kinetic approach coupling Quick-EXAFS and MCR-ALS chemometrics » Environmental Science: Nano., 6, 2641-2651. (2019).
- [23] Chan, E. M., Marcus, M. Fakra, S., El Nagggar, M., Mathies, R. Alivisatos, A.P. "Millisecond Kinetics of Nanocrystal Cation Exchange Using Microfluidic X-ray Absorption Spectroscopy" Journal of Physical Chemistry A., 111, 12210-12215. (2007).
- [24] Deng, H., Fitts, J., Tappero, R., Kim, J., Peters, C. "Acid erosion of carbonate fractures and accessibility of Arsenic bearing minerals: in operando synchrotronbased microfluidic experiment" Environmental Science & technology., 54, 19, 12502-12510. (2020).
- [25] Stanley, C., Grossmann, G., Casadevall I Solvas, X., de Mello A. "Soil-on-aChip: microfluidic platforms for environmental organismal studies" Lab on a Chip., 16, 228-241. (2016).
- [26] Zimmermann W. "Biocatalytic recycling of polyethylene terephthalate plastic" Philosophical Transactions A., 378: art.n° 20190273. (2020).
- [27] Garel, C., Fonda, E., Michalowicz, A., Diliberto, S., Boulanger, C., Petit, E., Legrand, Y.M., Poullain, C., Grison, C. "Structure and composition of the first bio-sources Mn-rich catalysts with a unique vegetal footprint". Materials Today Sustainability., 5: art.n° 10020. (2019).
- [28] Reisky, L., Préchoux, A., Zuhlke, M.K., Baumgen, M., Robb, C., Gerlach, N., Roret, T., Stanetty, C., Larocque, R., Michel, G., Song, T., Markert, S., Unfried, F., Mihovilovic, M., Trautwein-Schult, A., Becher, D., Schweder, T., Bornscheuer, U., Hehemann, J.-H. "A marine bacterial enzymatic cascade degrades the algal polysaccharide ulvan" Nature chemical biology., 15, 803-812. (2019).
- [29] Lamarque, L., Corso, D., Torres-Ruiz, J., Badel, E., Brodrribb, T., Burrell, R., Charrier, G., Choat, B., Cochard, H., Gambetta, G., Jansen, S., King, A., Lenoir, N., Martin-StPaul, N., Steppe, K., Van den Bulcke, J., Zhang, Y., Delzon, S. "An inconvenient truth about xylem resistance to embolism in the model species for refilling Laurus nobilis L." Annals of Forest science., 75: art.n°88. (2018).
- [30] Garel, C., Renard, B.-L., Escande, V., Galtayries, A., Hesemann, P., Grison, C. "CC bond formation strategy through ecocatalysis: Insights from structural studies and synthetic potential" Applied Catalysis A: General., 504, 272-286. (2015).



### 3 - **Accelerators and sources upgrade**



## INTRODUCTION

Over the last few years, storage-ring based light sources have been experiencing a revolution with the advent of ultra-low emittance Storage Rings (SR) based on Multi-Bend Achromat (MBA) lattices aiming to achieve much higher average spectral brilliance, coherent flux and nano-focused flux than previously obtained<sup>[1]</sup>. The MAX-IV facility in Sweden, in operation since 2016, has pioneered the field<sup>[2]</sup>, followed by the SIRIUS facility in Brazil, whose commissioning is in progress<sup>[3]</sup> and the HEPS facility which is under construction in China<sup>[4]</sup>. In addition to these green-field projects, many 3<sup>rd</sup> generation SR upgrades exist at various stages of completion and planning

worldwide. Among them, the ESRF-EBS facility, whose commissioning is now completed and where users have been working since August 25<sup>th</sup>, 2020<sup>[5]</sup>, the APS-U which is under construction<sup>[6]</sup>, ALS-U<sup>[7]</sup>, SLS-2<sup>[8]</sup> and ELETTRA-2<sup>[9]</sup> which are approved and whose start of construction is imminent. The Diamond-II project is in the Technical Design Report (TDR) phase<sup>[10]</sup> which should end at the end of 2021. The TDR of the SOLEIL upgrade project is expected to start early 2021 immediately after the completion of the CDR phase. **Figure 1** compares the new projects (green field and upgrade) with respect to the existing facilities in terms of equilibrium natural emittance.

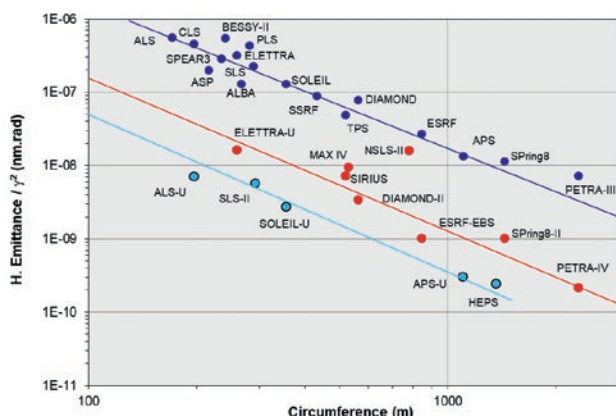


Figure 1: Horizontal equilibrium emittance comparison for storage rings: 3<sup>rd</sup> generation (in blue) and MBA generation (in red and cyan)

### Objectives and constraints

While maintaining the broad spectrum of photons ranging from the far infrared (IR) to hard X-rays, the SOLEIL upgrade project aims at maximizing the intensity of coherent photon flux (the highest possible brilliance and transverse coherence) especially for the beamlines working in the soft to tender X-ray photon energy domain. To achieve this goal, the electron beam emittances in both horizontal and vertical planes must be close to the single-electron photon beam emittance in this energy range. As the diffraction limited emittance for a single-electron photon beam emitted by an undulator at the wavelength  $\lambda$  is approximately  $\lambda/2\pi$ <sup>[11]</sup>, an electron beam emittance of at most 50 pm.rad in both planes is needed for X-ray energies up to 4 keV. Our strategy is based on the objective to obtain a natural horizontal emittance of less than 100 pm.rad which provides the target of 50 pm.rad in each plane after equal sharing. Together with equal  $\beta$ -functions in the two planes,

this will produce at Insertion Device (ID) source points round electron beams that are more suited for imaging or diffraction techniques and will allow reducing scattering effects on the electron beam performance such as Touschek and Intra-Beam Scattering (IBS). With such ultra-low emittances, it is also necessary to match properly the electron and photon phase spaces to maximize the coherent flux. Horizontal and vertical  $\beta$ -functions close to the matching value of  $L_u/\pi$  [m], where  $L_u$  is the length of the ID, are set as a goal at each ID source point. To further mitigate the IBS effects and achieve higher beam lifetime, the bunch length will be increased by a factor of three to four with the use of a harmonic Radio-Frequency (RF) system. An upper limit of 100 ps FWHM bunch length still allows cutting edge time-resolved experiments. These objectives should be reached while maintaining the stability and reliability presently achieved at SOLEIL (see section Beam Stability) and without increasing the total radiated power as well as the electric power needed for operation.

In addition, the project must take into account a large number of constraints and fulfill several requirements:

- Reuse the existing accelerator tunnels and its radiation shielding walls.
- Reuse much of the existing technical infrastructure.
- Limit downtime between the last user photon beams and the first new user photon beams to a maximum of two years.
- Minimize the impact on the existing ID source point positions.
- Preserve infrared (IR) beamlines.
- Provide alternative radiation sources to the existing bending magnet-based beamlines.
- Keep the storage ring energy commensurate with a very broad photon energy range.
- Preserve the beam current of 500 mA in uniform filling pattern operation.
- Study the possibility of operation modes suitable with the time structure and time resolved experiments.
- Minimize operation costs, in particular the wall-plug-power.

While maintaining the same circumference, the geometry of the new lattice must allow:

- Keeping the dipole source point of the MARS beamline unchanged (heavy hutches for radioactive samples).
- The two long NANOSCOPIUM and ANATOMIX (~200 m) beamlines to fit with their current experimental hutches by using canted in-vacuum IDs.

**Highlights**

**Storage ring lattice.** The CDR reference lattice, detailed in section Lattice Design, is based on 20 non-standard alternating 7BA and 4BA Higher-Order Achromat (HOA) cells reaching a horizontal natural emittance of about 80 pm.rad at the energy of 2.75 GeV and equal horizontal and vertical  $\beta$ -functions between 1.5 to 1.0 m at the center of all ID straight sections. Figure 2 compares the arrangement of the magnets in Double Bend Achromat (DBA) cell of the present SR (top) and in the 7BA cell of this new lattice (bottom). A striking feature is the rather short length of the new cell (~16 m), due to the more modest storage ring circumference and large number of straight sections, as compared to those of other projects (between 23 to 30 m) which increases the problem of compactness. The choice of the lattice emerged from considerations and constraints which are developed in section Lattice Design and in particular a great

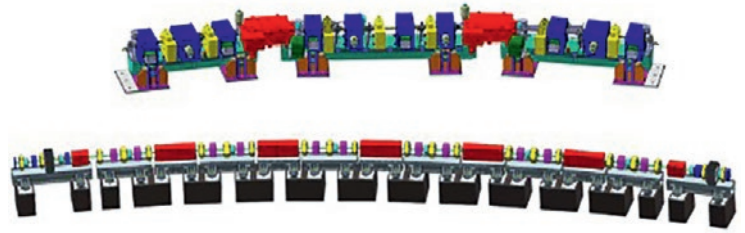


Figure 2: Engineering layout of a present SOLEIL DBA arc (top) and of a typical arc for a 7BA cell of the upgrade (bottom)

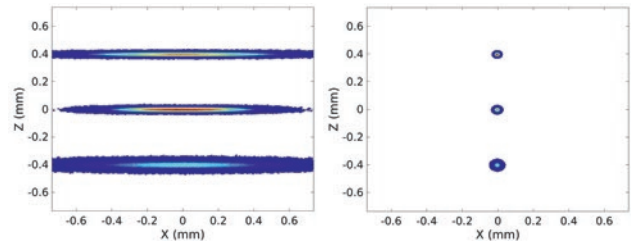


Figure 3: Comparison of the transverse beam profiles (x: horizontal, z: vertical plane) of the present SOLEIL (left) for 3 types of straight sections (short, medium and long / plots shifted for convenience) with 1% coupling and SOLEIL upgrade CDR reference lattice (right) with 50 pm.rad emittance

effort was invested to minimize the impact on the beamline photon source points and to preserve the radiation shielding walls. The lattice presents a workable solution but can be further improved. The achieved natural horizontal emittance is about 50 times smaller than that of the present SOLEIL SR (4000 pm.rad) and the effective emittance calculated in the straight section source points would be about 100 times smaller than the average value calculated in those of the current SR. By operating on a linear coupling resonance, round beam sizes in ID straight sections of less than 10  $\mu\text{m}$  RMS in both planes can be produced. Figure 3 shows a beam size comparison between the current and the upgraded SRs and Figure 4 shows the optimal convolution reached between the electron and photon ellipses in both planes calculated for the photon energy of 4 keV. The performance of this lattice in terms of on and off-momentum dynamic apertures seems compatible with the implementation of a betatron off-axis injection scheme. However

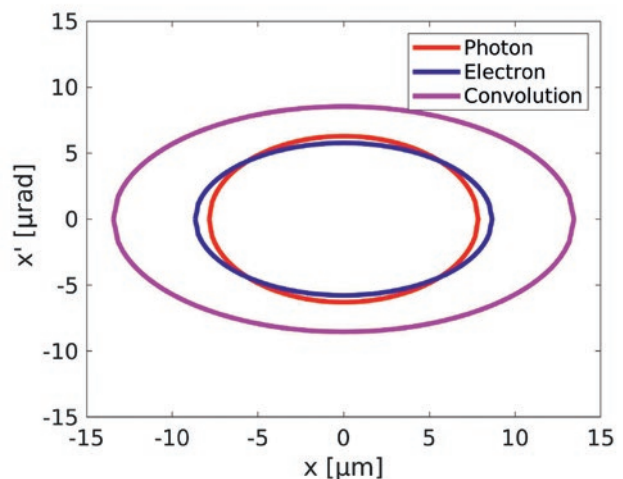


Figure 4: Horizontal phase space (x, x') in the center of a medium straight section of the electron beam (blue), diffraction limited photon beam at 4 keV (red) and their convolution (purple). Calculation made with a 4 m-long undulator



as off-axis injection with full coupling is complex and needs careful investigations to validate all aspects, another scheme based on synchrotron on-axis injection is also being studied in the CDR phase together with first general considerations on the swap-out injection, see section Injection Scheme.

The main parameters of the SOLEIL upgrade SR and the existing SOLEIL SR are compared in Table 1.

	Present lattice	CDR reference lattice
Lattice type	modified DBA	MBA (7BA-4BA)
Circumference (m)	354.10	353.74
Electron beam energy (GeV)	2.75	2.75
Maximum electron beam current (mA)	500	500
Natural emittance (pm.rad)	4000	80
Energy spread (%)	1.16	0.9
Energy loss per turn w/o IDs (keV)	917	490

Table 1: Main parameters of the present and CDR reference lattice

The new lattice will provide 20 straight sections (SS): 4 long straight sections (2 of 7.66 m and 2 of 7.36 m), 8 medium straight sections (4.15 m) and 8 short straight sections (2.73 m). One long straight section will be dedicated to the injection system, two long straight sections will host two canted undulators each and the fourth one will be shared for an ID and for the harmonic RF system. Except one medium straight section which will host the fundamental RF cavities, all medium as well as short straight sections are available for ID based beamlines. This corresponds to a total of 20 possible beamlines from IDs. Figure 5 shows schematically the current proposal for the implantation of 20 insertion devices, the two RF systems and the injection system. Since the dipole fields become weaker, the sources for the bending magnet beamlines will be replaced by new 1.7 T bending magnets or 3 T superbends.

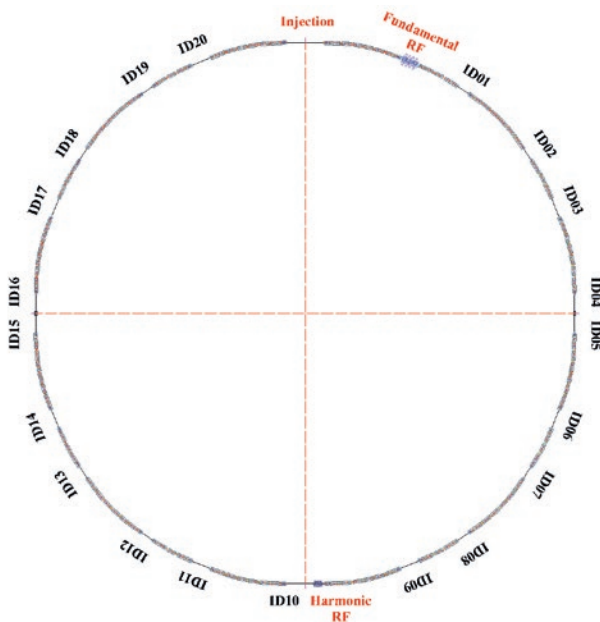


Figure 5: Implantation of the IDs, injection system and RF cavities

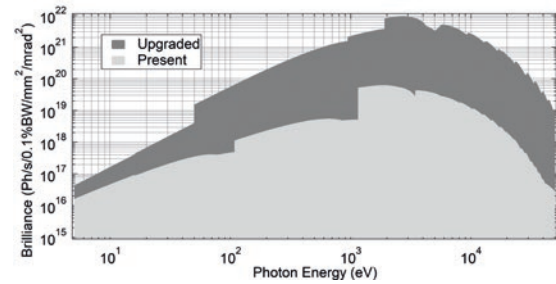


Figure 6: Comparison of undulator photon brilliance between upgraded (100% coupling) and present SOLEIL storage ring (1% coupling)

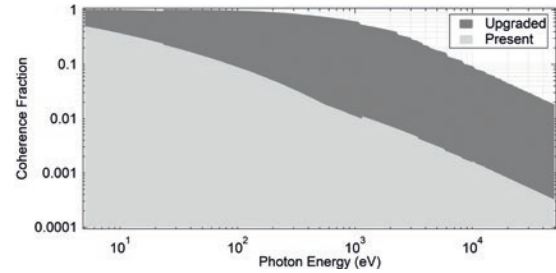


Figure 7: Comparison of coherent fraction between upgraded (100% coupling) and present SOLEIL storage ring (1% coupling)

Using several candidate IDs, Figure 6 and Figure 7 show respectively the dramatic increase in photon brilliance and coherent fraction, mainly due to the lower emittance but also to the possibility of using IDs with lower magnetic gaps and shorter periods. Figure 8 exhibits the corresponding increase in the coherent flux. One can notice that the brilliance and coherent flux will be improved by up to more than two orders of magnitude. Over a wide range of photon energies (100 eV to 30 keV) the brilliance exceeds  $10^{20}$  photons/s/mm<sup>2</sup>/mrad<sup>2</sup>/0.1%b.w and reaches a maximum of  $10^{22}$  photons/s/mm<sup>2</sup>/mrad<sup>2</sup>/0.1%b.w around 3 keV. Figure 9 compares the spectral photon flux density at 10 m from the source for a 2 m long in-vacuum IVU20 undulator for the present and new lattices. It shows the improvement of purity of the undulators harmonics obtained by decreasing the emittance.

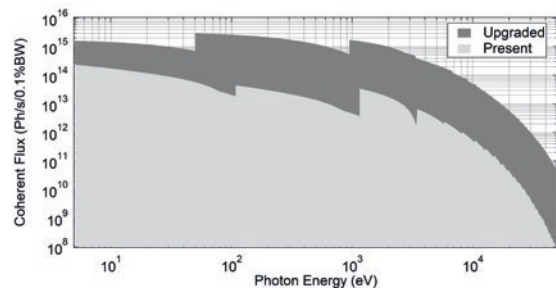


Figure 8: Comparison of coherent flux between upgraded (100% coupling) and present SOLEIL storage ring (1% coupling)

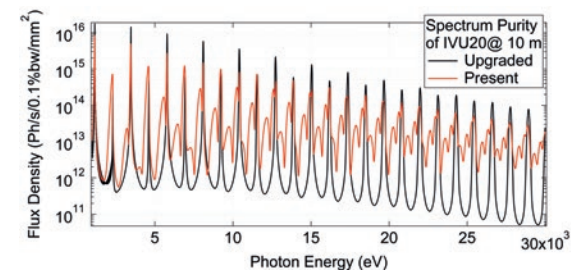


Figure 9: Spectral photon flux density at 10 m from the source for a 2 m-long in-vacuum undulator (gap = 4 mm) for the present (1% coupling) and the upgraded (100% coupling) storage ring

**Storage ring lattice engineering.** These features describing the performance are based on ambitious and challenging technical choices. Strong quadrupole gradients (max.  $\sim 140 \text{ T.m}^{-1}$ ), sextupole (max  $\sim 8000 \text{ T.m}^2$ ) and octupole strengths (max  $\sim 250000 \text{ T.m}^3$ ) are necessary to reach such low emittance, low  $\beta$ -functions and a dynamic aperture large enough to allow betatron off-axis injection and acceptable beam lifetime. The maximum quadrupole gradient is 7 times higher than the maximum used in the present SR while the sextupole strength is 25 times higher. In order to reach these values the SOLEIL upgrade SR must rely on a 10 mm inner diameter circular copper vacuum chamber with NEG-coating. To the best of our knowledge, this would be the smallest diameter used or proposed in the arcs of synchrotron radiation machines (half of the values used for MAX-IV, SIRIUS or ESRF-EBS). This allows for a small magnet bore diameter (16 mm) and a very dense magnetic lattice. The other key technology to guarantee the feasibility of the lattice and in particular efficient injection of the electrons, is the need to develop a new high performance nonlinear multipole injection kicker (MIK) allowing the electrons to be injected at a very short horizontal distance (3.5 mm) from the SR beam axis, in top-up transparent mode (see section Injection Scheme). In addition to the “standard” photon extraction for IDs and bending magnet beamlines, specific extraction has to be considered for Infrared and VUV energy range. The low photon energy extractions require large horizontal and vertical solid angles which are hardly reached because of the compactness of the proposed lattice. As for the infrared photon source which is already being evaluated (See section Infrared extraction), the VUV photon extraction will need a specific configuration which will be studied later on in the TDR phase.

As all these technical challenges are pushing the engineering technology to the limits, they are being investigated through an intensive R&D program based on extensive numerical simulations, prototyping and measurement with beam as it will be explained in section Vacuum Systems for the vacuum system and in section Magnets for the magnets. We are considering an extensive use of the pure permanent magnet technology in the new SR lattice beyond what has been done so far. All combined bending magnets, all reverse bends and 70% of the quadrupoles will be based on the pure permanent magnet technology. The sextupoles and octupoles will be electromagnetic and will integrate respectively dipolar and quadrupolar (normal and skew) correction coils. In addition to the considerable reduction in operation costs due to the decreased RF electric consumption (the energy loss without IDs dropping from 0.944 MeV to 0.490 MeV) and the substantial use of permanent magnets, the global electrical consumption for the SR power supplies is expected to be reduced by about two thirds as compared to the existing machine. Moreover, to fully explore the potential of this new source, it is necessary to

optimize other variables such as the possibility of using new kinds of IDs (see section Photon Sources). The use of very small beams and very small vacuum chambers will require state of the art diagnostic systems which will be presented in section Diagnostics. Other main design decisions are discussed in the respective sections such as the choice for the fundamental RF system technology, normal conducting cavities powered by solid state-amplifiers and the technical options for the harmonic RF system (see section Radio-Frequency Systems), the choice between ex-situ and in-situ bake-out and first solutions for the extraction of the photons from such small vacuum chambers (see section Vacuum Systems), the strategy to define the optimal number of girders (see section Mechanical Engineering) and for the power supplies (see section Photon Sources). A new booster ring is required to have a beam with smaller emittance and shorter bunch length to allow efficient injection rate into the new storage ring (see section Injection Scheme).

A further major challenge that is common to this type of SR upgrade is the need to shorten to a minimum the period without beam for the users. This requires careful preparation and anticipation, which will be addressed in the other sections of this part of the document.

**Modes of operation.** The main operational mode or filling pattern of the SOLEIL upgrade will be fully optimized to maximize soft to tender X-ray brilliance and increase transverse coherence together with good conditions of stability and lifetime. It will use a round electron beam with equal emittance in both planes, a total beam current of 500 mA where all the 416 bunches are uniformly filled and lengthened up to about 100 ps FWHM using the harmonic RF system. The voltage of the harmonic cavities can also be set at the opposite phase to increase the slope of the overall voltage, in order to provide an operational mode with relatively short bunches; of about 10 ps FWHM, with lower beam current ( $\sim 100 \text{ mA}$ ) and relaxed emittance ( $< 1 \text{ nm.rad}$ ), obtained by applying white noise in both planes. The hybrid filling pattern remains very challenging; it should be possible only if a solution is found to mitigate the transient beam loading effects that decrease the average bunch lengthening (see sections Lattice Design and Radio-Frequency Systems). It will still be possible to deliver time resolved modes (single bunch and 8 bunches), even though impedance effects will be higher, and IBS and Touschek lifetime will set more stringent limits on possible bunch charges.

The targeted performances in the soft to tender region will be well beyond those at any storage-ring based light source operating, under construction or planned at the time of writing the CDR. The sections that follow will give insights into the viability of proposed technical solutions while waiting to demonstrate their feasibility under the TDR phase.

## REFERENCES

- [1] Hettel, R., “DLSR Design and Plans: an International Overview”, *Journal of Synchrotron Radiation*, 21, 843-855 (2014).
- [2] Tavares, P. F., et al., “Status of the MAX-IV Accelerators”, IPAC 2019 proceedings, TUYPLM3, 1185-1190 (2019).
- [3] Liu, L., “SIRIUS Commissioning Results”, IPAC 2020 (2020).
- [4] Jiao Y., “The HEPES Project”, *Journal of Synchrotron Radiation*, 25, 1611-1618 (2018).
- [5] [www.esrf.eu](http://www.esrf.eu)
- [6] Borland, M. et al., “The Upgrade of the Advanced Photon Source”, IPAC 2018 proceedings, THXGBD1, 2872-2877 (2018).
- [7] Steier, C. et al., “Design Progress of ALS-U, the Soft X-Ray Diffraction Limited Upgrade of the Advanced Light Source”, IPAC 2019 proceedings, 1639-1641 (2019).
- [8] Streun, A., et al., “SLS-2: the Upgrade of the Swiss Light Source”, *Journal of Synchrotron Radiation*, 25, 631-641 (2018).
- [9] Karantzoulis, E. et al., “Status of Elettra and Future Upgrades”, IPAC 2018 proceedings, 4054-4056 (2018).
- [10] <https://www.diamond.ac.uk/Home/About/Vision/Diamond-II.html>
- [11] Onuki, H., Elleaume, P., “Undulators, wigglers and their applications”, Taylor and Francis Editions, Part. I, Chap. 3 (2003).



## Lattice design

### Lattice layout

The current lattice of the SOLEIL storage ring is composed of 16 two-bend achromat cells, 8 of which have introduced short straight sections in between the dipoles, altogether providing 24 straight sections. There are three types of straight sections with the lengths of 12, 7 and 3.8 m covering up to 46% of the total length. With a circumference of 354.1 m, this lattice provides a natural horizontal emittance of 4 nm.rad at an energy of 2.75 GeV (Figure 10).

In the scope of a storage ring upgrade having a natural horizontal emittance below 100 pm.rad (*i.e.* 40 to 50 times lower), the use of Multi-Bend Achromat (MBA)<sup>[1]</sup> lattice has been investigated. A first attempt was made by alternating the hybrid 7BA ESRF-EBS<sup>[2]</sup> cell type with another hybrid consisting of a 6BA with a split in the middle similar to that proposed and developed for Diamond-II<sup>[3]</sup>, allowing lattice geometry very close to the current one. But still with only 16 cells, the emittance reduction was limited at the level of 220 pm.rad<sup>[4]</sup>. Furthermore, no good matching of the electron beam phase space ellipses was attained with those of the photon beam over the photon energy range of interest. To further reduce the emittance value, the best way out was to increase the number of cells from 16 to 20. During the last few years, two solutions with 20 identical cells: 7BA ESRF hybrid and 7BA HOA (Higher-Order Achromat) types giving about 75 pm.rad have been investigated<sup>[5,6,7]</sup>. Despite being competitive, their geometry ends up producing major changes to beamline source points and requires reconstruction of up to 8 ratchet walls.

To keep the beamlines parallel to existing ones, the lattice geometry has to include 22.5° deflection and half deflection cells (11.25°). Alternating 7BA and 4BA cells was then identified as the natural solution to best adapt the current beamline positioning and leave the tunnel shielding wall unchanged. The HOA type cell, being

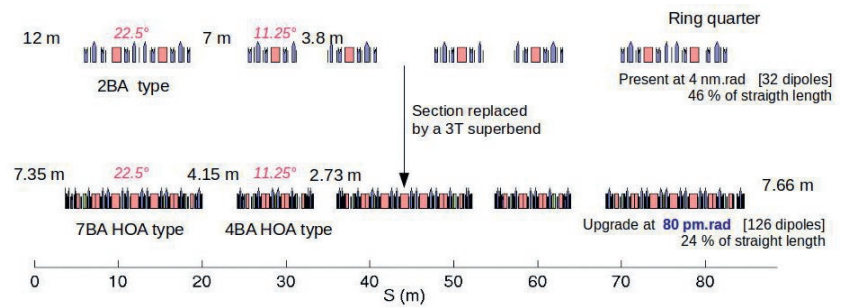


Figure 10: Present (top) and CDR upgrade lattice (bottom) layout comparison along one quarter of the circumference (s)

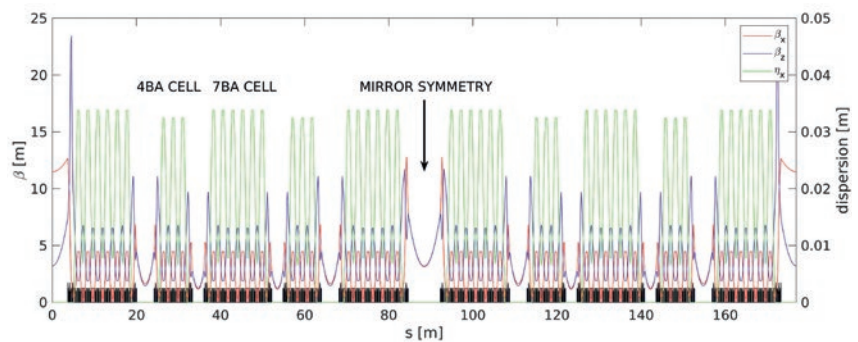


Figure 11: CDR upgrade lattice optical functions for the horizontal (x) and vertical transverse plane (z) along half of the circumference (s)

more modular and exhibiting possibly larger momentum acceptance, has therefore been chosen. The CDR upgrade reference lattice is then composed of 20 HOA cells alternating 7BA and 4BA (Figure 10), giving a natural horizontal emittance of 80 pm.rad at an energy of 2.75 GeV. In addition, to perfectly align the two existing long canted beamlines, as well as to minimize the radial offset<sup>1</sup> for the others, the lattice has two-fold symmetry (Figure 11) with four different straight section lengths listed in Table 2 (see section Storage Ring and Beamline Implementation, page 158).

### Cell layout

To achieve an emittance below 100 pm. rad, the use of reverse-bends<sup>[8]</sup> in the

unit cell arcs is necessary. The main focusing quadrupoles in the arcs are converted into reverse-bends and their negative deflections are scanned within the range that the momentum compaction factor stays greater than  $10^{-4}$  and the horizontal damping partition number remains smaller than 2 (Figure 12). With a negative deflection of -4.6 mrad per reverse-bend, the natural horizontal emittance reaches about 80 pm.rad, which gives 50 pm.rad in both planes at full coupling at the energy of 2.75 GeV. The total deflection angle of the storage ring is then of 460°. The required, yet still modest, negative deflection is simply provided by shifting the focusing quadrupoles by 3.8 mm in the horizontal plane. The arc unit cell and matching cell are depicted in Figure 13. The arc unit cell is composed of one long bend with a transverse defocusing gradient and two reverse bends with a focusing gradient. They are both based on the permanent magnet technology without any additional correction coils. Three sextupoles and one octupole which are electromagnetic complete the magnet list.

To match the optics of the four different straight sections, all the matching sections contain a quadruplet of quadrupoles of which only one is an electromagnet and two octupoles and two sextupoles which are both electromagnets. At this stage of the development, the dipolar correctors,

<sup>1</sup>Unless otherwise stated, x, z and s represent respectively the horizontal, vertical and longitudinal coordinates of the beam.

Section	Long	Long (Injection type)	Medium	Short
Length (m)	7.66	7.36	4.15	2.73
Radial offset (mm)	0	+256	+33 / -107	+33 / -38
Number	2	2	8	8
$\beta$ functions (H/V) (m)	3 / 3	11.5 / 3.2	1.5 / 1.5	1.1 / 1.1

Table 2: Available straight sections in the CDR reference lattice and their characteristics

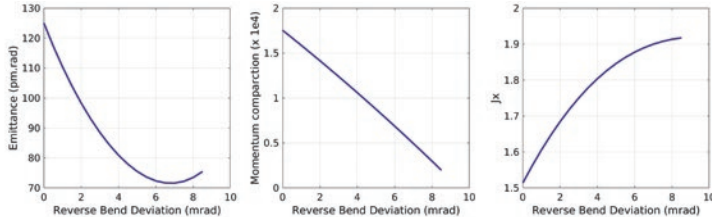


Figure 12: Emittance (left), momentum compaction factor (center) and horizontal partition number (right) versus reverse bend deviation strength. The black dot is the working point.

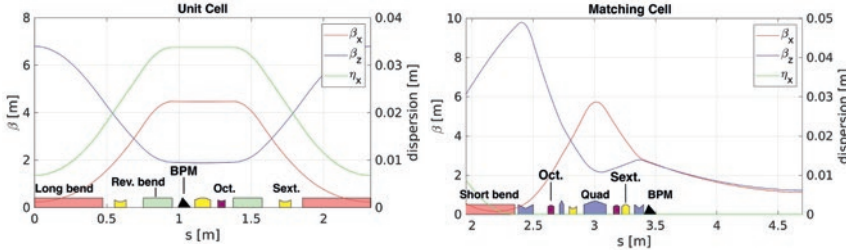


Figure 13: Arc unit cell (left) and matching cell (right) layouts.

horizontal and vertical, are all combined in sextupole magnets while normal and skew quadrupole correctors are all combined in octupole magnets. One of the distinguishing features of this CDR lattice design is the widespread use of permanent magnets from combined bends and reverse bends to quadrupole magnets. In term of diagnostics, one Beam Position Monitor (BPM) is accommodated in the center of every unit HOA cells (nearby the focusing sextupoles and octupoles) and two in the matching sections leading to 176 BPMs in total.

### Lattice working point

In order to reduce the number of different magnet families we opt to keep the same unit arc cell in both 7BA and 4BA cells. When alternating different HOA cells, the best phase advances of ( $\Delta\nu_x=3/7=0.427$   $\Delta\nu_z=1/7=0.143$ ) for 7BA<sup>[7]</sup> is not valid anymore to obtain good beam dynamics performance. At present time, we found an optimum with a bit lower phase advances of ( $\Delta\nu_x=0.408$   $\Delta\nu_z=0.118$ ). They still are in the lower emittance regime. With a medium electron energy of 2.75 GeV, the photon energy of interest where the brilliance gain has to be maximized, is in the soft X-ray range (*i.e.* up to a few keVs). At full betatron coupling, attained emittances are about 50 pm.rad in both planes. These are very comparable to diffraction limited photon emittance ( $\epsilon_{ph}=\lambda/2\pi=50$  pm.rad at 4 keV) emitted from an undulator. It is then worthwhile matching electron beam to photon beam phase space ellipses optimizing the emitted flux density, brilliance and transverse coherence. With small  $\beta$  functions at the center of the medium

and short straight sections of the order of 1.5 and 1.1 m, the CDR reference upgrade lattice is then close to fulfilling the typical matched beta functions ( $\beta_{xz} \sim L_v/\pi \sim 1$  m) for 2 to 4 m long Insertion Devices (ID).

Although horizontal off-axis injection is foreseen for accumulation, we also opt to operate the storage ring on full coupling in order to relax the high electron density per bunch. It will then provide larger Touschek beam lifetime and less emittance and energy spread increase from the Intra-Beam Scattering (IBS) effect. For both effects, there is a non-negligible beneficial gain of the order of 2 to 3, as compared to a 10% coupling case with only 8 pm.rad in the vertical plane. Among different techniques, we opt for the most natural and simplest one sitting the tune working point on a difference coupling resonance.

Altogether, the storage ring working point has been chosen to be: ( $\nu_x=54.2$ ,  $\nu_z=18.2$ ) which then has also the advantage of exhibiting the largest region free of systematic resonances equal to or below the order 5 (Figure 14) in the limited lattice fold symmetry of two.

## Beam dynamics optimization

### Targets

The main proposed scheme for injection is based on on-momentum horizontal off-axis injection. The kick is provided by a dedicated Multipole Injection Kicker (MIK) (see section Injection Scheme) having a flat top deflection at 3.5 mm from the central axis. To enlarge the horizontal Dynamic Aperture (DA), larger  $\beta$  functions ( $\beta_x=11.5$  m,  $\beta_z=3.2$  m) are provided in the injection section. We also plan to use a harmonic cavity (harmonic 4 or 3) in order to lengthen (by a factor of 3 to 4) the bunch and further relax the Touschek beam lifetime, as well as to reduce the IBS effect. Obtaining 10 hours beam lifetime in the high brilliance operation mode of 500 mA (or 1.2 mA per bunch over 416) seems a reasonable target. We then need to respectively obtain an on momentum DA of at least of 5 to 6 mm at injection location as well as at least 3 hours of Touschek beam lifetime without any harmonic cavity lengthening. These target values are imposed including all possible errors (lattice systematic and random, insertion devices, injection jitter, etc.).

### Methods

The first steps of the optimization have been done only targeting the DA together with limiting the off-momentum tune expansion by means of simple sextupoles and octupoles scans. It allows to reach a DA of about 6 mm in horizontal and 2 mm

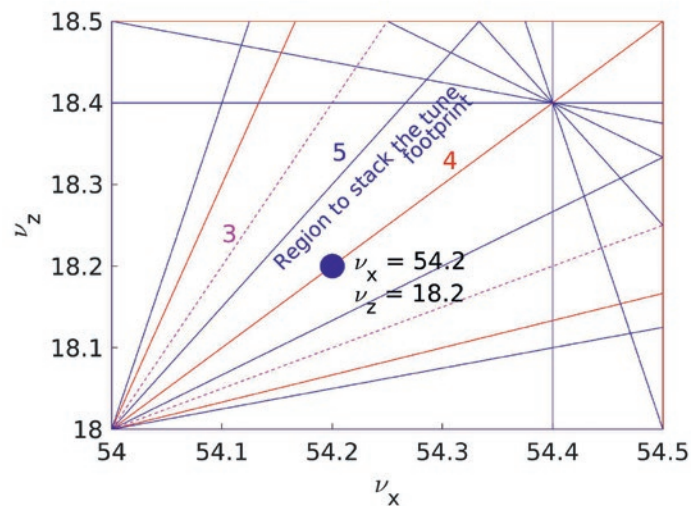


Figure 14: Tunes working point

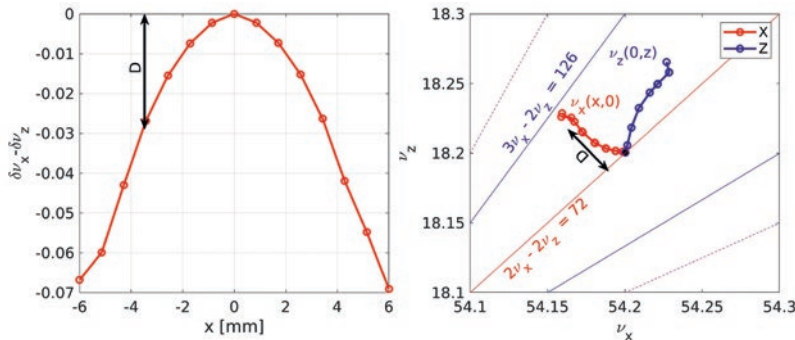


Figure 15: Left: dissonance versus horizontal betatron amplitude. Right: on-momentum horizontal and vertical tune excursions

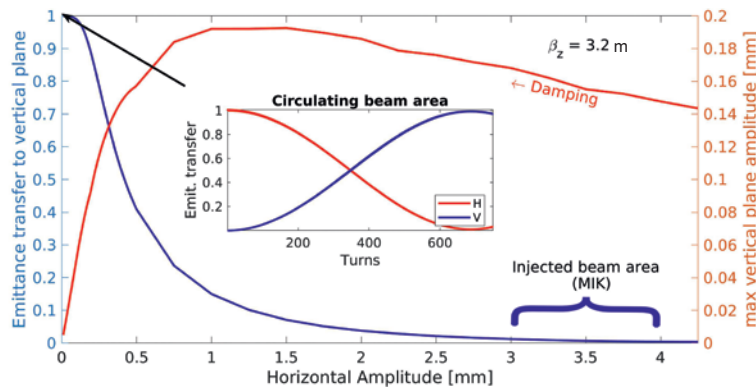


Figure 16: Coupling and vertical transfer versus horizontal initial amplitude at the injection point (MIK position)

in vertical but too limited Touschek beam lifetimes (here, the Energy Acceptance (EA) was not controlled).

The next step involves a MOGA (Multi Objective Genetic Algorithm)<sup>[9]</sup> process to be able to control both DA and EA at some locations along the lattice to enlarge the Touschek beam lifetime. The number of objectives was limited to 2 by minimizing the maximum difference between DA to an ellipse and the maximum difference between the EA and a given energy acceptance. Some pre-constraints on first to third-order energy tune shifts, by means of numerical matrix responses (on chromatic sextupoles and octupoles), are applied to control linear chromaticities and tunes expansion. All tracking are performed using the Accelerator Toolbox (AT)<sup>[10]</sup>.

With a two-fold symmetry lattice of which a superperiod additionally possessing mirror symmetry, the maximum independent variables (sextupoles and octupoles) is large: 136, we limit here to 28 (16 harmonic in the straight sections and 12 chromatic ones in the arcs). Typical optimization runs with 22-32 processors in the parallel computation mode last over 1 to 3 days.

### Dynamics

At this level of optimization, the on-momentum non-linear tune shifts with amplitude are not yet under control.

To prevent or minimize the transfer of the injected beam amplitude from the horizontal to vertical plane, with a low clearance gap, one still needs to reshape the horizontal Amplitude-Dependent Tune Shift (ADTS). The dissonance  $D$ , the distance from the coupling resonance  $D(x) = \nu_x(x) - \nu_z(x)$  which is null at the

origin  $x=0$ , has to be large enough for the injected beam amplitude to avoid this transfer. The re-tuning is simply done manually with small variations of harmonic sextupoles and octupoles.

The results of the on-momentum tune variations are plotted in Figure 15 showing that the maximum tune excursions are still within the target area as well as a dissonance of about  $3 \cdot 10^{-3}$  at  $x \sim -3.5$  mm from the axis (Figure 15). The coupling resonance is easily activated by turning on some skew quadrupoles located in the dispersion-free matching section. Weak gradients of the order of 0.01 to 0.05 T/m are enough. Based on a simple single particle tracking, the coupling ratio and the vertical transfer amplitude are depicted in Figure 16. At low horizontal amplitudes, up to 100  $\mu\text{m}$ , the coupling is very close to 100% and drops down to 5% in the injected beam area. At the center of injection straight, the vertical amplitude of the injected beam is kept below 200  $\mu\text{m}$  during the damping process. A complete injection simulation investigated in section Injection Scheme confirms that the vertical transfer in the presence of skew quadrupole components is effectively almost negligible.

In the optimization process, only the DA envelopes are used as a guideline to save large computing times. A deeper analysis of the resulting DA is provided by Frequency Map Analysis (FMA)<sup>[11]</sup>. The diffusion maps, for both on- and off-momentum motions taken at the center of the injection section are plotted

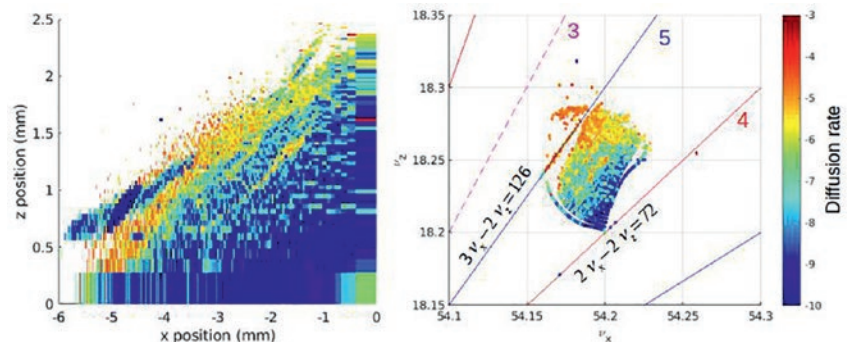


Figure 17: On momentum Frequency Map Analysis at the injection point

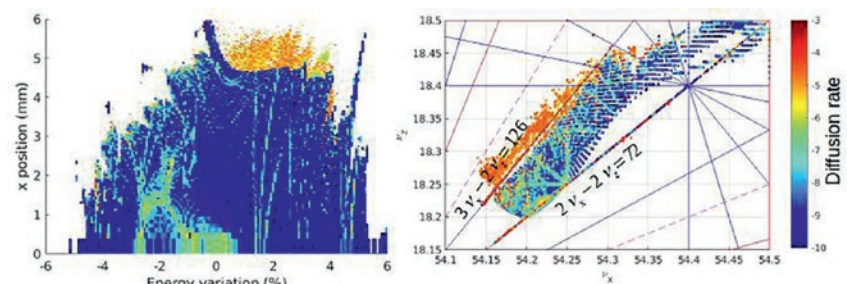


Figure 18: Off momentum Frequency Map Analysis at the injection point

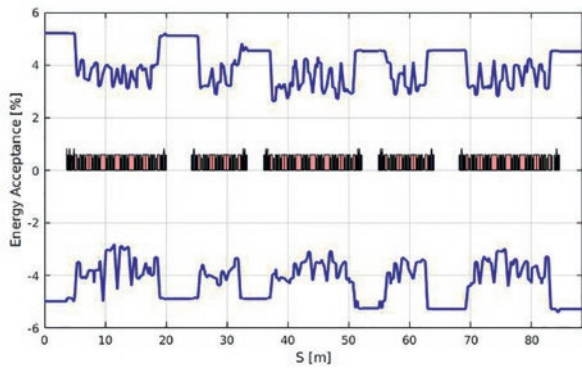


Figure 19: Energy acceptance along a quarter of the lattice

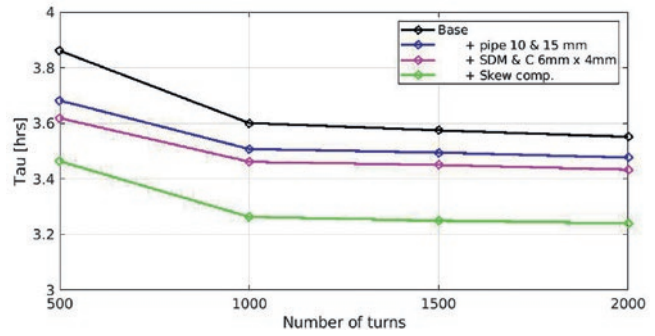


Figure 20: Touschek beam lifetime in different pipe limit configurations

respectively in Figures 17 and 18. They clearly show that the tune is well stacked in the target area, in between the systematic resonances of order 4 in the lower part:  $2\nu_x - 2\nu_z = 72$  and of order 5 in the upper part:  $3\nu_x - 2\nu_z = 126$ . The maximum horizontal amplitude of about 5 to 6 mm is mainly limited by the latter 5 order resonance. In general, these acceptances are weakly affected when tracking with or without the synchrotron motion (6D) as well as with or without the presence of weak skew quadrupoles. The second quantity of interest is the energy acceptance along the lattice driving the Touschek beam lifetime. Thanks to the MOGA optimization, the energy acceptance has been enlarged (Figure 19) and ranges typically from -4% to +3.5%. Based on the Piwinski model, the Touschek beam lifetime without any bunch lengthening (at zero current bunch length) and with emittances of 50 pm.rad in both planes is a little bit above 3 hours in the high brilliance operation mode of 500 mA (or 1.2 mA per bunch over 416). The Figure 20 exhibits the Touschek beam lifetimes in different configurations of the vacuum chambers. The reduced standard pipe of 10 mm diameter as well as the use of the possible stringent horizontal ID gap of 6 mm has already an effect. They will typically limit the Touschek

beam lifetime to 3.5 hrs. It drops down to 1.4 hours with only 10% of coupling (80 pm.rad in horizontal and 8 pm.rad in vertical). In parallel, the vacuum lifetime is larger with about 40 hours at 500 mA and  $10^{-9}$  mbar (100% nitrogen) dynamic mean pressure. The longitudinal dynamics is weakly affected by higher-order momentum compaction factors. With  $\alpha_2 = 3 \cdot 10^{-4}$  the upper and lower energy deviation limits are of +15 and -30%, far beyond the 6D dynamics exhibiting from +5 to -5.6% maximum energy deviation acceptance (Figure 21).

**Magnet and beam pipe specifications**

The magnets are listed in Table 3. Based on the HOA type cell, the number of magnets is large (close to a thousand for a machine of only 354 m circumference).

In addition, the choice of using permanent magnets, with a fixed gradient of 110 T/m for most of the quadrupoles, also tends to enlarge the number of different types in terms of their length. The relatively high magnet density naturally tends to increase the strength of the quadrupoles, sextupoles and octupoles. For instance, with the sextupole gradient up to 8000 T/m<sup>2</sup>, it is then preferable to limit the bore diameter to 16 mm. Including a clearance for the *in situ* vacuum chamber baking of 2 mm and a pipe thickness of 1 mm leads to a standard inner pipe diameter of 10 mm all along the lattice except for the long injection type straight matching section (with weaker magnet strengths), where it has to be increased to 15 mm (Figure 22). In the *ex situ* vacuum baking option (see section Vacuum

Table 3: Magnetic length and strength specifications of the Magnets. Numbers with asterisks represent maximum values

	L (mm)	B (T)	G (T/m)	No.	Tot	Location
Short bend 7BA cell	400	0.998	-8.013	24	40	Arcs dispersion suppressor
4BA cell	400	0.957	-8.013	16		
Long bend 7BA cell	947	0.696	-15.88	60	76	In the arcs
4BA cell	947	0.668	-15.88	16		
Rev bend 1 7BA cell	200	-0.210	56.34	120	152	In the arcs
4BA cell	200	-0.201	56.34	32		
Rev bend 2 7BA cell	200	-0.178	57.79	24	40	Arcs dispersion suppressor
4BA cell	200	-0.171	57.79	16		
Quadrupoles [B']	Various	-	120	144	144	Quadruplet in the straights
Sextupoles [1/2 B'']						Both arcs and straights
H&V correctors	60/80/110	-	8,000 T/m <sup>2*</sup>	368	368	Combined magnet
Octupoles [1/6 B''']						Both arcs and straights
Q correctors	60	-	25 10 <sup>6</sup> T/m <sup>3*</sup>	176	176	Combined magnet
<b>Total</b>					<b>996</b>	

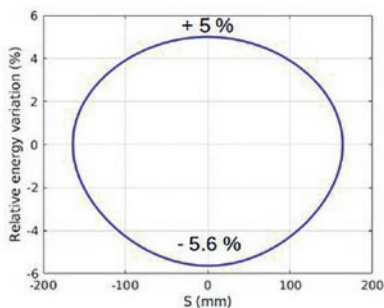


Figure 21: Longitudinal phase-space trajectory and maximum energy acceptance at the center of the injection straight section

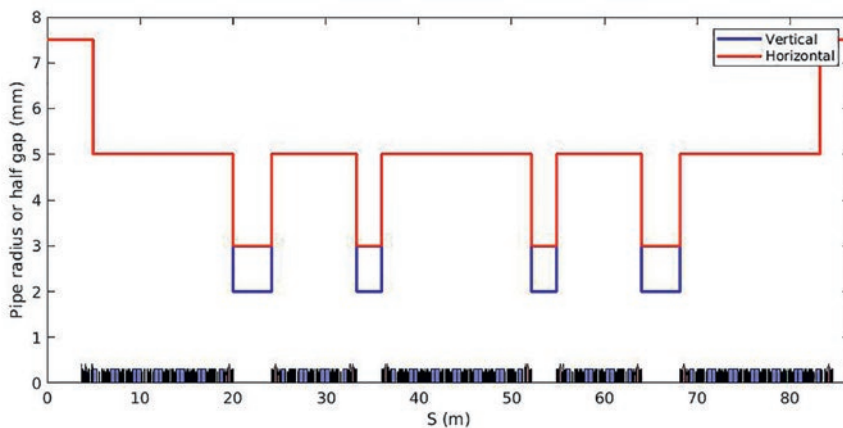


Figure 22: Pipe radius and in-vacuum undulator half gap profiles along 1/4 of the circumference

Systems), the standard pipe diameter would naturally be raised to 12 mm keeping a clearance of 1 mm to the magnet bore. The pipe will be made of copper to limit the resistive-wall effect and preferably round to also limit some other undesirable collective effects. Based on the first systematic multipole estimates (see section Magnets), the large 18-pole component (~2% relative to the main field at 5 mm radius) of the sextupoles located just after the short dipoles having a larger vertical gap for ID light port extraction, has a very marginal impact on the beam dynamics. On the contrary, the 8 and 12-poles (~0.6% relative to the main field at 5 mm radius), which are the systematic components of the permanent magnet quadrupoles not yet optimized, have a strong impact and should be reduced by a factor of at least four in their field contributions.

## Extended lattice options

### Superbends

As part of the CDR lattice upgrade proposed, four of the current twelve medium sections would be replaced by superbends located in the central long bend of the central 7BA cell of each quarter (Figure 10). The two-fold symmetry of the lattice is preserved. The long dipole is divided into three regions having the peak field of 3 T in the central one. The peak field width is typically of 60 mm to half maximum. In order to contain an emittance increase and restore the optical functions, the four reverse-bend magnets flanking the superbend are slightly re-tuned in terms of deviation angles and gradients. The impact of four superbends on the emittance and the energy spread increase is then limited to less than 3%.

The energy loss per turn is also slightly increased, from 490 to 503 keV with the four superbends. With the two-fold lattice symmetry being preserved, along with a limited local re-tuning, the beam dynamics acceptance is marginally affected by the presence of these four additional superbend magnets.

### Impact of insertion devices

On the same theme, the impact on synchrotron equilibrium from high field insertion devices is not at all negligible. Table 4 lists these effects on the basis of possible in-vacuum undulators such as CPMU15, CPMU18 and CPMUE (Cryogenic Permanent Magnet Elliptic Undulator) (see section Photon sources). For instance, with all ID gaps closed, the natural horizontal emittance drops from 80 down to 62 pm.rad together with a significant increase in the energy loss per turn from 490 (without superbends) up to 770 keV/turn for the IDs of phase 1.

### Canted beamlines

As part of the current SOLEIL storage ring, two long canted beamlines including an additional triplet of quadrupoles providing low vertical beta functions are to be naturally included in the SOLEIL lattice upgrade. As the new long straight section of 7.66 m is perfectly aligned with the current one, accommodating a chicane alone to cant

the two beamlines does not present any difficulty. Re-tuning the optics while preserving the non-linear dynamics, including a triplet of quadrupoles alone (without any chicane), has been investigated as well, but at this stage of the CDR lattice, implementing both the chicane and the triplet has not yet been completed.

## Operating modes

The current operating modes of SOLEIL facility are: the uniform filling pattern at 500 mA, the hybrid filling pattern at 450 mA and, to a lesser extent in terms of beam time, the 8 bunches (100 mA), the single bunch (16 mA) and the low alpha operating modes. In the frame of the upgrade, the main mode will be the uniform filling mode at 500 mA but studies are in progress to assess the possibility of operational modes suitable for the time structure and time resolved experiments.

### Intra-beam scattering

Operating a low-emittance storage ring at a medium energy of 2.75 GeV opens the risk of strong intra-beam scattering effects blowing up the latter, hence deteriorating the performance of the machine. Investigation and cross-check using different codes exhibit effectively a large effect in high current per bunch operation modes<sup>[12]</sup>. Nevertheless, mitigation effects, by means of full coupling operation and bunch lengthening with harmonic RF cavities, moderate the emittance blow up. For instance, in the high brilliance operation mode of 500 mA, with only 1.2 mA per bunch, the increase in emittance is contained within 10%, from 52 to 56 pm.rad.

### Lattice parameter list

The major machine and beam parameters of the CDR lattice are listed in Table 5 in comparison with those of the present SOLEIL ring. The free straight section lengths, beta and dispersion values as well as the transverse RMS beam sizes and divergences at the source points are given in Table 6.

Configuration	Emittance (pm.rad)	Emittance (K=100%)	E-spread (‰)	E-loss/turn (keV)
Lattice w / o IDs	80	52	0.90	490 (503**)
Lattice w / IDs of phase 1**	62	38	0.89	770
Lattice w / IDs of phase 2**	60	36	0.88	850

\*\* including 4 superbends of 3 T.

Table 4: Impact of insertion devices on synchrotron equilibrium. The two ID phases correspond to the insertion device configuration expected at the end of construction phase and of the full performance phase

Lattice	Unit	CDR lattice upgrade	Current lattice
Symmetry		2	1
Energy	(GeV)	2.75	2.75
Circumference	(m)	353.74	354.10
Straight ratio	(%)	24	46
Number of straight sections		20	24
RMS Natural H. emittance	(pm.rad)	81	4000
RMS Coupled H&V Emittance	(pm.rad)	53	
RMS Energy spread	(%)	0.09	0.10
RMS Natural Bunch length	(ps) (mm)	9.18 2.7	15.17 4.6
Harmonic number		416	416
Main RF frequency	(MHz)	352.56	352.20
Energy loss per turn W/o ID	(keV)	490	917
RF Voltage	(MV)	1.38	2.9
Momentum compaction factor		$9.1 \cdot 10^{-5}$	$4.4 \cdot 10^{-4}$
Synchrotron frequency	(kHz) (turns)	1.4 600	4.5 190
Damping times (H/V/L)	(ms) (turns)	7.3 / 13.1 / 11.7 6000 / 11000 / 10000	6.9 / 6.9 / 3.5 5800 / 5800 / 2900
Nominal tunes (H/V/L)		54.2 / 18.2	18.16 / 10.22
Natural chromaticities (H/V)		-108 / -65	-53 / -19
Corrected chromaticities (H/V)		+1.6 / +1.6	+1.3 / +2.2

Table 5: Main CDR upgrade lattice parameters in comparison with the current SOLEIL ring

Source point	Long SS	Injection SS	Medium SS	Short SS	Superbend
Length (m)	7.66	7.35	4.15	2.73	-
$\beta$ function (H/V) (m)	3.1 / 3.2	11.5 / 3.2	1.6 / 1.4	1.1 / 1.2	0.2 / 6.8
Dispersion function (m)	0	0	0	0	$6.8 \cdot 10^{-3}$
RMS size (H/V) ( $\mu\text{m}$ )	13 / 13	25 / 13	9.3 / 8.8	7.7 / 8.1	7.1 / 19.1
RMS div. (H/V) ( $\mu\text{rad}$ )	4.1 / 4.1	2.1 / 4.1	5.7 / 6.1	6.9 / 6.6	15.1 / 2.8

Table 6: Main machine and beam parameters related to the source points for 50 pm.rad in both planes

### First turn steering and lattice robustness

Because of the significantly stronger magnetic fields and much smaller beam pipes required for the CDR upgrade lattice as compared to 3<sup>rd</sup>-generation machines, the beam sensitivity to errors of magnet alignment, magnetic field calibration and of diagnostics elements are accordingly amplified. These errors must be compensated using dedicated corrector magnets implemented along the ring. Due to strong sextupoles in the CDR reference lattice, the residual orbit errors in sextupoles are expected to be the dominant quadrupolar errors, indicating the need for a highly performant closed-orbit correction system to minimize them. Moreover operation with full betatron

coupling is required for the mitigation of IBS effects. An efficient coupling correction shall therefore be required before introducing betatron coupling in a controlled way.

As to the restoration of linear optics, a complication arises from the fact that a majority of magnets with quadrupolar

gradients (combined-function dipoles and reverse-bends) shall be permanent magnets, signifying that they cannot take part in the correction procedure. To reach the performance goal of the CDR reference lattice described earlier, it is thus highly important to carefully optimize the number, locations and strengths of all types of correctors (dipolar, normal and skew quadrupolar) that must be introduced in the ring.

A first BPM configuration in the lattice was chosen. Two BPMs are placed at the entrance and exit of the matching section of each cell. In the arcs one BPM is placed next to the focusing sextupole in each HOA unit. Figure 23 shows the BPM arrangement in the 4BA cell. That in the 7BA cell follows analogously. Under this configuration, the total number of BPMs in the entire ring is 176.

Dipolar correctors for the orbit correction are located in the two sextupoles of each matching section, and every other defocusing sextupoles in the HOA unit. The total number of dipolar correctors in this configuration is 176 for each transverse plane. Their maximum strength is tentatively limited to 250  $\mu\text{rad}$ . Figure 23 shows also the dipolar corrector locations in the 4BA cell. Figure 24 shows the horizontal and vertical phase advances for the first two cells of the lattice, and highlights phases at the BPM and dipolar corrector locations in those cells.

Because most of the magnets with quadrupolar gradients shall be permanent-magnet based, quadrupole correction coils are introduced in the 176 octupoles distributed in the ring. Moreover one quadrupole in each matching section will be electromagnetic, adding 40 more quadrupolar correctors. Skew quadrupole corrector coils are also assumed to be integrated in the 176 octupoles around the ring. Magnets and BPMs are installed on girders whose positioning errors must be accounted for. A scheme with 172 girders is currently considered. The girder composition for the 7BA cell is shown in Figure 25. A 212 girders reference layout is also being investigated

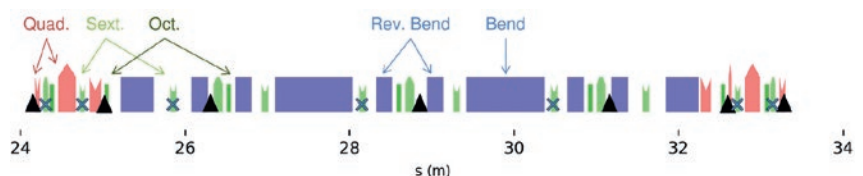


Figure 23: BPM (black triangles) and combined horizontal/vertical correctors (blue crosses) location in 4BA. Their implantation in a 7BA cell follows the same pattern

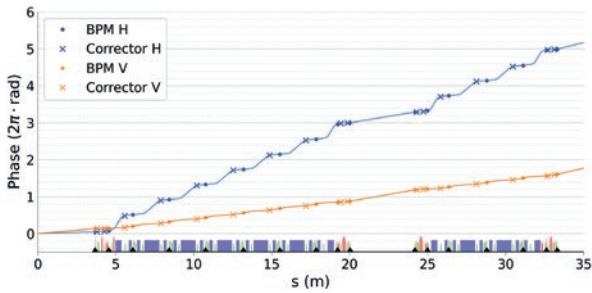


Figure 24: Horizontal (blue) and vertical (orange) phase advance in the first two 7BA and 4BA cells of the lattice. The phase advances at the BPMs and the dipolar correctors are indicated with dots and crosses respectively

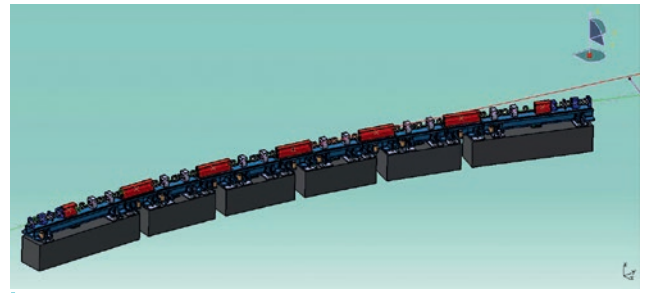


Figure 25: Girder composition for a 7BA cell used in the simulations. Courtesy of J.-L. Giorgetta (SOLEIL)

in the studies. The plinths on which girders are installed are not simulated. A simple aperture model is added for the beam pipe: a 5 mm square aperture is assumed all along the lattice. The Accelerator Toolbox (AT) code<sup>[10]</sup> is used, along with the Simulated Commissioning (SC) toolbox<sup>[13, 14]</sup> to integrate the assumed error model and simulate the correction procedure.

Several effects are currently included in the model:

- BPM transverse misalignment and roll errors as well as calibration and noise errors from the electronics
- Magnets transverse misalignment and roll errors, as well as the main magnetic field component calibration error
- Dipolar corrector calibration errors
- Girders misalignment and roll errors. A girder-to-girder misalignment amplitude limit is also included in the model.
- Injection errors: for one simulated machine, a random error for all injections can be applied to account for kicker magnets systematic errors. Then for each injection simulated with the toolbox, a random error can

be generated. Figure 26 schematizes the injection error generation.

- RF cavity frequency and voltage errors

The generated errors follow a Gaussian distribution truncated at  $\pm 2\sigma_{RMS}$ , except for the girder-to-girder misalignment limit which is an absolute value. Tables 7 to 11 detail the  $\sigma_{RMS}$  values used for the simulations, defined in collaboration with the diagnostics and alignment groups.

Type	$\sigma_{RMS}$ level
Misalignment x/z, before BBA*	500 $\mu\text{m}$
Misalignment x/z, after BBA w.r.t sextupoles	10 $\mu\text{m}$
Roll	100 $\mu\text{rad}$
Calibration	10%
Turn by Turn Noise	50 $\mu\text{m}$
Closed Orbit Noise	1 $\mu\text{m}$

\*Beam-Based Alignment

Table 7: RMS errors used for the BPM

Type	$\sigma_{RMS}$ level	Type	$\sigma_{RMS}$ level
Misalignment x/z	30 $\mu\text{m}$	Misalignment x/z	100/100 $\mu\text{m}$ (50/30 $\mu\text{m}$ )*
Roll	50 $\mu\text{rad}$	Roll	50 $\mu\text{rad}$
Calibration	0.1%		
Dipolar correctors calibration	5%		

Table 9: RMS error used for the girders. (\* girder-to-girder maximum misalignment limit)

Table 8: RMS error used for the magnets on their girders.

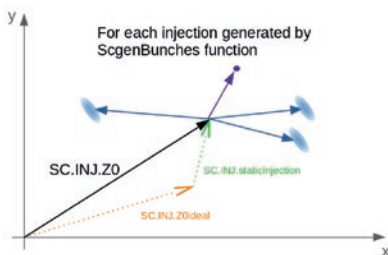


Figure 26: Principle of the injection error generation. Z0ideal (orange arrow) is the ideal injection position in the 6D phase, static injection (green arrow) is the injection error generated for one simulated machine. Their sum Z0 represents the injection point for a machine. Then for each injection simulated in a machine, a random error is generated, defining the beam injection location (blue ellipses)

Type	x	x'	z	z'	Energy	Phase
Static injection error	50 $\mu\text{m}$	100 $\mu\text{rad}$	500 $\mu\text{m}$	100 $\mu\text{rad}$	0.5%	10°
Random injection error	0	17 $\mu\text{rad}$	0	0	0.01%	0.1°

Table 10: RMS error used for the beam injection.

Type	$\sigma_{RMS}$ level
Frequency	100 Hz
Voltage	5 kV

Table 11: RMS error used for RF cavity.

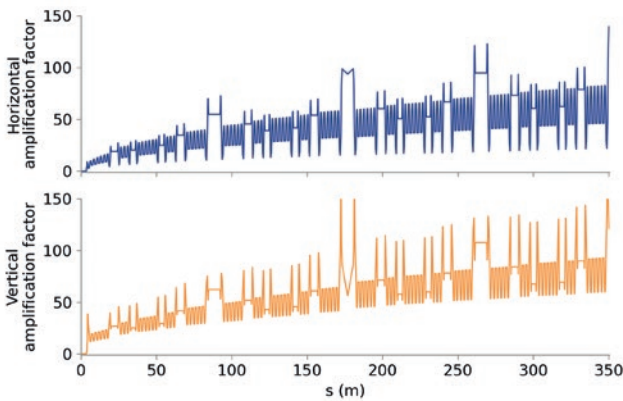


Figure 27: Beam trajectory amplification factor as a function of position along the ring. Top plot shows the horizontal plane, bottom plot shows the vertical plane

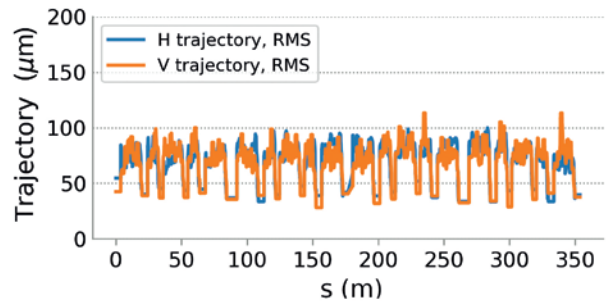


Figure 28: Horizontal (blue) and Vertical (orange) RMS orbit in all elements of the lattice obtained after convergence of the orbit correction procedure

Again, the combination of strong magnetic fields and small aperture shall make the first beam injection into the new accelerator particularly challenging as compared to 3<sup>rd</sup>-generation light sources. Therefore full commissioning simulations using SC are being made. The tool allows simulation of a series of corrections considered necessary, consisting of:

- First turn beam stitching with sextupole magnets off
- Multi-turn beam transmission and ramping of sextupole currents
- RF correction and beam capture
- Iterative Closed Orbit Correction
- Beam Based Alignment, with respect to quadrupoles or sextupoles to minimize orbit
- Beta beat and linear coupling corrections using LOCO

A set of 50 machines were simulated for statistics. Each machine simulated 10 injections of 100 particles. The injected beam was assumed to have a 5 nm.rad transverse emittance in both planes and was injected on-axis.

The strong focusing in the ring creates large amplification factors in both horizontal and vertical planes as pictured in Figure 27. Because of the large error amplification, only 6% of the simulated machines led to an injected beam making its first turn around the ring prior to steering correction. The trajectory correction over the first and second turns proved to be efficient: the beam could be transmitted in all simulated cases. The rest of the procedure (sextupole ramp, beam capture and orbit correction) was successful in every case as well.

Figure 28 shows the RMS orbit achieved in the ring for both planes. It is plotted for every element present in the lattice. The RMS level is below 100 μm in most elements for both planes. Figure 29 shows the orbit as read by the BPM, therefore including reading and calibration errors. In this case the RMS orbit level read at the BPM is below 50 μm with respect to the vacuum chamber center. Removing the reading and calibration errors of the BPMs, it was verified that the orbit can be corrected to zero at BPMs.

The absolute strength distribution of the dipolar correctors obtained with the 50 simulations is shown in Figure 30. The median corrector strength is 50 μrad for the horizontal and 45 μrad for the vertical plane, both being well below the 250 μrad limitation specified for these correctors. Some correctors however reach the limiting values.

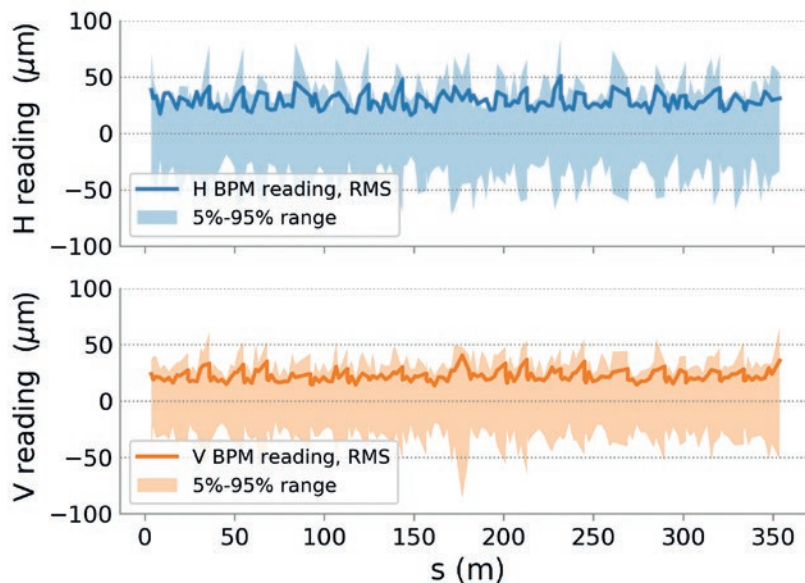


Figure 29: Horizontal (blue) and Vertical (orange) RMS orbit in all elements of the lattice obtained after convergence of the orbit correction procedure

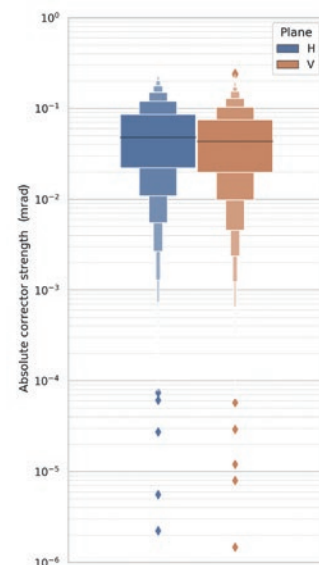


Figure 30: Distribution of the absolute strength of the dipolar correctors after the closed orbit correction procedure. In blue the horizontal corrector values, in orange the vertical correctors. For each distribution the black line shows the median value and the diamonds show extreme values



Element	Number	Remarks
BPM	200	only 176 BPMs are currently identified
Keyhole profile chamber	12	
Bellow	125	"comb" type [33, 34]
Flange	250	"impedance free" type [33, 35]
Taper for main RF cavity (per pair)	1	L = 250 mm ↔ 10.2°
Taper for harmonic RF cavity (per pair)	1	L = 100 mm ↔ 8.5°
Taper for dipoles (per pair)	116	L = 43 mm ↔ 8°
Taper for in vacuum IDs (per pair)	9	L = 100 mm ↔ 2° (vertical plane only)
Resistive wall (elliptic shape beam pipe, 12 mm x 10 mm*, copper)	Over 336 m	
Resistive wall in IDs (elliptic shape beam pipe, 3 mm x 80 mm, copper)	Over 18 m	
NEG coating resistivity	Over 336 m	$\rho_{\text{NEG}} \approx 2.5 \cdot 10^{-5} \Omega \cdot \text{m}$
NEG coating thickness	Over 336 m	$h_{\text{NEG}} \approx 1 \mu\text{m}$

Table 12: Impedance model considered for simulations

\* The assumption made for these calculations is different from the rest of the document which assumes a circular beam tube with a radius of 5 mm.

Although the studies of beta beat and coupling corrections have not yet been accomplished for the CDR reference lattice, similar investigations were made on an earlier CDR lattice, even though the numbers of BPMs and correctors assumed along with their locations were somewhat different from those of the reference lattice. There, the residual beta-beating could be corrected below a 1% RMS level. For the coupling correction, less than 2% residual coupling could be achieved in 95% of the simulated machines<sup>[16]</sup>.

On the whole, the commissioning procedure appears to be robust enough to obtain a stored beam and provide a sound basis for lattice symmetrization. However the feasibility of the BBA with sextupole magnets or quadrupolar correctors should be further investigated. A lattice symmetrization procedure is being developed to recover the lattice properties, by following realistic steps. Alternative combinations for the numbers of BPMs and correctors and their locations in the lattice, the girder arrangement, as well as the error levels reachable for the different kind of magnets shall be studied from the lattice robustness point of view. Corrector magnet properties shall also be evaluated in view of the correction speed and precision, to ensure correct compensation of the insertion device effects on the linear optics.

### Collective effects

In this section, we discuss the collective effects, which can be defined as the interactions of beam particles with each other and with their environment.

The collective effects determine the beam intensity-dependent machine performance, especially on the single and multi-bunch current.

Compared to SOLEIL storage ring, the upgraded storage ring design includes many new features of 4<sup>th</sup> generation light sources that will impact collective effects, such as reduced beam pipe apertures, a smaller momentum compaction factor and presence of harmonic cavities (HC)... To mitigate them, we rely on several damping mechanisms provided by the synchrotron radiation, the transverse feedback system and the HC (Landau damping and bunch lengthening).

We estimate the impact of the collective effects by summing up the different machine element contributions in an impedance model which is then used to establish the current thresholds corresponding to the various single and multi-bunch instabilities. The collective effects induced by RF cavities (main and harmonic) are discussed in the section Radio-Frequency Systems.

### Impedance model

#### Impedance budget

For every element of the storage ring, the geometric impedance is computed from 3D drawings made by the SOLEIL design office using CST<sup>[16]</sup>. The Resistive-Wall (RW) impedance for the beam pipes and NEG (Non-Evaporable Getter) coating have been computed using IW2D<sup>[17]</sup>. The components included in the model and their respective numbers are described in Table 12.

The contributors for the geometric impedance include BPMs, keyhole-shaped chambers, bellows, flanges and various tapers transitions. For the resistive-wall part, the beam pipe is assumed to be elliptic with radii respectively 5 mm vertically and 6 mm horizontally. The in-vacuum insertion devices are also assumed to have an elliptic cross section with radii respectively 1.5 mm vertically (3 mm gap) and 40 mm horizontally. The standard beam pipes are coated with 1 μm thick NEG, where the NEG resistivity is assumed to be  $\rho_{\text{NEG}} \approx 2.5 \cdot 10^{-5} \Omega \cdot \text{m}$  (conservative value compared to measured ones<sup>[18]</sup>).

### Effective impedance

The spectrum for the longitudinal impedance is shown in Figure 31 for the real part and in Figure 32 for the imaginary part. The longitudinal effective impedance  $\Re(Z/n)_{\text{eff}}$  computed from the model is about 0.14 Ω for the natural bunch length of 9.2 ps (so without the HC), part of which the NEG coating is the major contributor. In comparison, the longitudinal effective impedance of the SOLEIL storage ring was estimated to be about 0.2 Ω from the model<sup>[19]</sup> and 0.45 Ω was measured<sup>[20]</sup>.

The reduced longitudinal effective impedance and power loss as compared to the present ring are due to two factors:

- The increase of the characteristic frequencies of the impedance from 1.8 to 12.5 GHz (cutoff frequency, in the rectangular waveguide approximation) thanks to the reduced beam pipe dimensions.
- The reduction of the frequency range of the bunch spectrum in high current modes thanks to the harmonic cavity (HC).

For the transverse planes, the sum of the transverse impedance weighted by the betatron functions at the impedance location is shown in Figures 33 to 36. The transverse effective impedances are  $\sum \beta_z \times (Z_z^{Dip})_{\text{eff}}^{[0]} = 1019 + j2458 \text{ k}\Omega$  and  $\sum \beta_x \times (Z_x^{Dip})_{\text{eff}}^{[0]} = 638 + j1448 \text{ k}\Omega$ , compared to  $\sum \beta_z \times (Z_z^{Dip})_{\text{eff}}^{[0]} = 328 + j1369 \text{ k}\Omega$  and  $\sum \beta_x \times (Z_x^{Dip})_{\text{eff}}^{[0]} = 94 + j695 \text{ k}\Omega$  in the SOLEIL model<sup>[19]</sup>.

The increase of the effective transverse impedance in both horizontal and vertical planes is the consequence of the reduced beam pipe apertures. The transverse impedance is dominated by the resistive-wall contribution which increases as  $1/(r^3\sqrt{\sigma})$ , where r and σ denote respectively the beam pipe radius and the wall electric conductivity, meaning that it increases

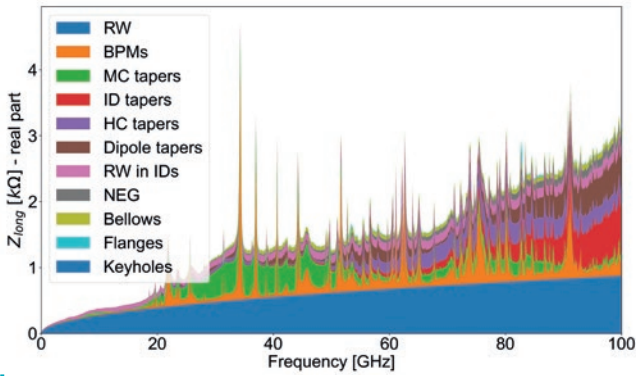


Figure 31: Real part of the longitudinal impedance

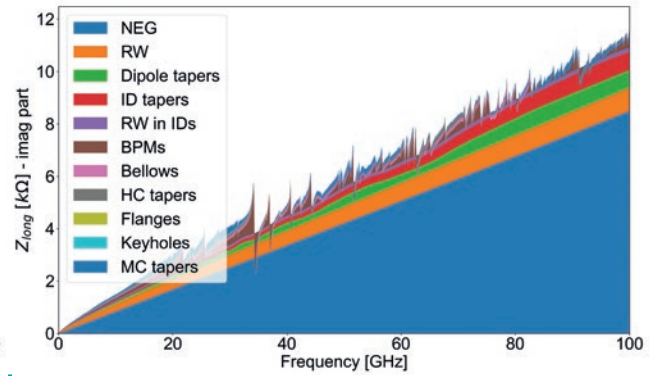


Figure 32: Imaginary part of the longitudinal impedance

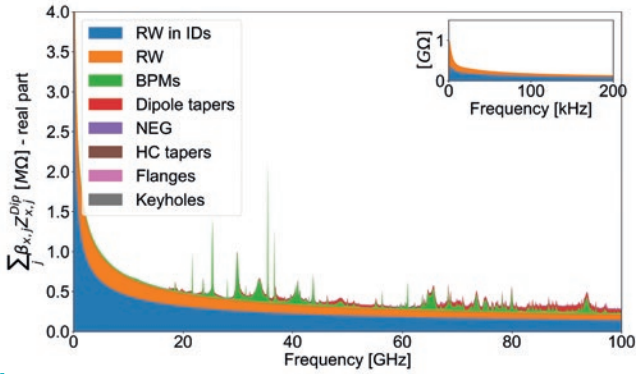


Figure 33: Real part of the horizontal dipolar impedance weighted by the horizontal  $\beta$  function

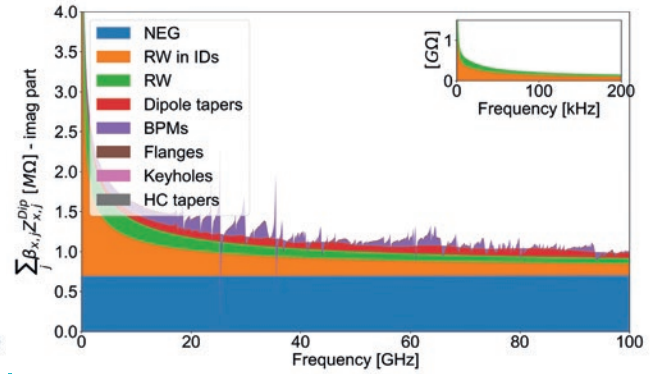


Figure 34: Imaginary part of the horizontal dipolar impedance weighted by the horizontal  $\beta$  function

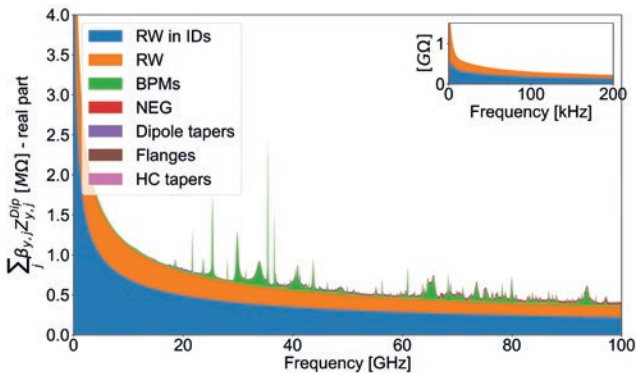


Figure 35: Real part of the vertical dipolar impedance weighted by the vertical  $\beta$  function

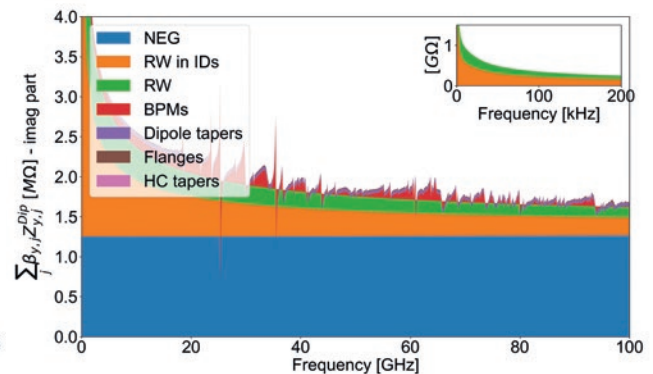


Figure 36: Imaginary part of the vertical dipolar impedance weighted by the vertical  $\beta$  function

by a factor of 12 in the vertical direction compared to SOLEIL (a factor 15 in going from  $r=12.5$  mm to 5 mm and a factor 0.77 in switching to copper beam pipe instead of aluminum). Thankfully, there are other effects which decrease the impact of the transverse impedance such as:

- Reduced mean betatron functions from  $\beta_x=8.0$  m and  $\beta_z=9.5$  m to  $\beta_x=3.5$  m and  $\beta_z=4.4$  m in the upgraded ring.
- An increase of chromatic frequency shift  $f_\xi$  from 2 GHz to 9.3 GHz per unit of chromaticity because of the reduced momentum compaction

factor  $\alpha_c$ . For a nominal chromaticity of  $\xi_x=\xi_z=1.6$  the chromatic frequency shift is 14.9 GHz compared to the 2.8 GHz and 4.6 GHz shifts for  $\xi_x=1.4$  and  $\xi_z=2.3$  in the present lattice of SOLEIL.

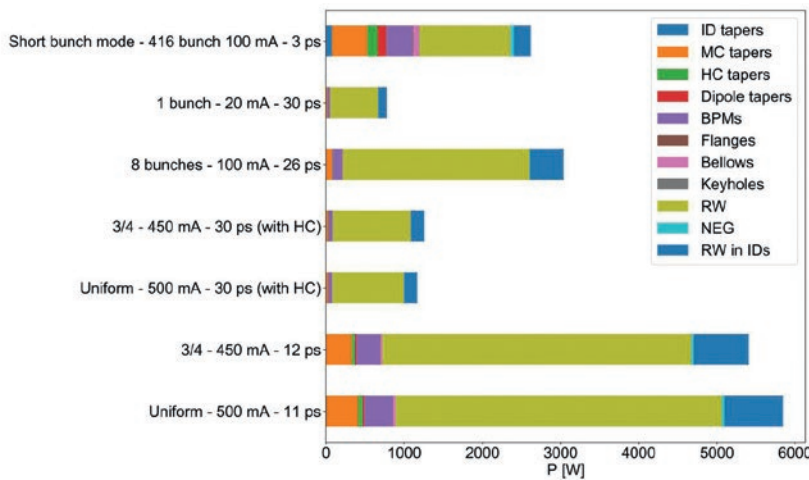


Figure 37: Power dissipated for different filling patterns and RMS bunch lengths

### Power dissipated

The power dissipated due to the real part of the longitudinal impedance, and the resulting heating of the components, is shown for the different modes of operation in Figure 37. The power dissipated depends on the RMS bunch length, the bunch current and on the filling pattern. The use of harmonic cavities to elongate bunches in high current modes allows decreasing significantly the beam-induced heating.

For comparison, the power dissipated at 500 mA in uniform filling of the SOLEIL ring is estimated to be 9.5 kW, whereas for the upgraded ring it is estimated to be less than 6 kW without the HC and about 1 kW with the HC under the same conditions.

The heat load of individual component has also to be monitored. For now, only two devices are on the power dissipated watch list: the BPMs and the main cavity tapers. About 1.8 W is dissipated in each BPM in uniform filling (500 mA) without the HC, compared to 4.6 W in the present SR and 0.2 W in uniform filling (500 mA) with the HC. The current design of the main cavity tapers produces a too high impedance, inducing 405 W of power dissipated in uniform filling without the HC, and will have to be optimized. In both cases, dedicated thermal simulations are ongoing to check that the device temperatures stay under control.

### Single bunch instabilities

In this section, we estimate the single bunch instability threshold which could prevent us from reaching the design performance in the different operation modes. In particular, for a total current of 500 mA in uniform

filling, the current per bunch is 1.2 mA. For the 3/4 filling pattern with 450 mA, it is 1.45 mA. For the 8 bunch and single bunch modes, the current per bunch is respectively 13.75 mA and 20 mA as a maximum value.

### Microwave instability

The Micro Wave Instability (MWI) is responsible for the emergence of density modulations within an electron bunch which results in the increase of the bunch energy spread. The MWI threshold given by the modified Boussard criterion<sup>[21]</sup> for the effective impedance  $\Re(Z/n)_{\text{eff}} \approx 0.14 \Omega$  (without HC) gives the current threshold of  $I_{th} \approx 0.8$  mA.

This value is, in fact, quite pessimistic as the Boussard criterion uses the effective longitudinal impedance, which only takes into consideration the imaginary part of the longitudinal impedance, and assume that the resistive part is of the same magnitude to estimate the MWI threshold. In the upgrade case, the imaginary part of the longitudinal impedance is significantly increased by the NEG coating, whereas it has no impact on the real part of the impedance which is responsible for the MWI threshold so the Boussard criterion threshold value is artificially lowered. The MWI threshold has also been estimated using the mbtrack tracking code<sup>[22]</sup>, using the longitudinal impedance model and  $10^6$  macro-particles:

- $I_{th} \approx 2.5$  mA  $\pm$  1 mA without the HC.
- $I_{th} \approx 6.5$  mA  $\pm$  1 mA with the HC.

### Coherent synchrotron radiation instability

The Coherent Synchrotron Radiation (CSR) instability corresponds to the same physical phenomenon as the MWI

but at higher frequencies. The CSR is partially shielded by the beam pipes up to a characteristic frequency  $f_{sh} \approx 430$  GHz for the upgrade, where  $f_{sh} \approx 80$  GHz for SOLEIL<sup>[23]</sup>.

The CSR instability threshold, considering the steady state parallel plate model<sup>[24]</sup> and a single dipole type, gives using an analytic formula<sup>[25]</sup>:

- Between  $I_{th} \approx 1.6$  mA and  $I_{th} \approx 1.9$  mA without the HC depending on the dipole radius.
- Between  $I_{th} \approx 9$  mA and  $I_{th} \approx 11.4$  mA with the HC depending on the dipole radius.
- $I_{th} \approx 6.5$  mA for the present lattice, for a measured threshold of 8 mA.

The CSR instability threshold also has been estimated using a Vlasov-Fokker-Planck solver<sup>[26]</sup> considering the same steady state parallel plate model but taking into account the different kind of magnets used in the upgrade. The results agree with the analytic formula:

- $I_{th} \approx 2.5$  mA without the HC.
- $I_{th} \approx 12.5$  mA with the HC.

### Transverse mode coupling and headtail instabilities

The Transverse Mode-Coupling Instability (TMCI) and the head-tail instability are transverse single bunch instabilities relevant respectively at zero and non-zero chromaticities. Both instabilities are estimated by tracking using mbtrack, taking into account both longitudinal and transverse impedances and using  $10^6$  macro-particles. For a nominal chromaticity of  $\xi_x = \xi_z = 1.6$ , the threshold currents for the head-tail instability are:

- $I_{th,z} = 2.5$  mA and  $I_{th,x} = 10$  mA without the HC.
- $I_{th,z} = 5$  mA and  $I_{th,x} = 16$  mA with the HC.

At SOLEIL, the measured thresholds for a nominal chromaticity of  $\xi_x = 1.4$  and  $\xi_z = 2.3$  are 8 mA in vertical and 13 mA in horizontal (all IDs open). The transverse bunch-by-bunch feedback then allows reaching 20 mA in single bunch<sup>[27]</sup>, and the same kind of feedback will be used in the upgrade which should also allow reaching 20 mA.

The evolution of the instability threshold versus chromaticity is shown in Figure 38. Recent studies using the Vlasov formalism<sup>[28]</sup> have shown that HC can decrease the TMCI threshold current and our simulations seem to confirm this prediction. For non-zero chromaticity, however, the HC increases the head-tail threshold.

**Short bunch mode**

This specific operation mode aims at producing a beam with bunch length in the range between 10 and 15 ps FWHM in uniform filling using the HC in “bunch shortening” mode. Tracking using mbtrack indicates that it should be possible to store 100 mA, corresponding to 0.24 mA per bunch, without single bunch instabilities nor excessive bunch lengthening due to longitudinal impedance (<15 ps FWHM).

The two main limitations for this mode are the CSR instability and the beam-induced power dissipated. The CSR instability, estimated using the analytic formula<sup>[25]</sup>, is expected to start from 0.63 mA/bunch, but it is very sensitive to the vertical aperture in dipoles. This mode is expected to be one of the most demanding in term of beam-induced power. For example, a power of 0.9 W is expected to be dissipated in each BPM for this mode at 100 mA compared to 0.2 W per BPM for the uniform filling at 500 mA with HCs in the bunch lengthening mode.

**Multibunch instabilities**

**Resistive-wall induced coupled-bunch instability**

Coupled-bunch transverse instabilities occur when certain frequencies of the beam (coherent modes) are excited by their interaction with impedances having neighboring frequencies. It is the case for the RW transverse impedance which presents a large narrow peak at the lowest beam frequency to which the beam strongly responds ( $f_{RW} = 0.2f_0 \approx 170$  kHz).

The RW instability has been estimated both by tracking with mbtrack, using 416 bunches with  $10^6$  macro-particles in each bunch, and by the Vlasov solver rwmibi<sup>[29]</sup>. The rwmibi code is used to benchmark the mbtrack code in the pure RW case (respectively blue and red dots in Figures 39 and 40), and then results including the full impedance model are obtained using mbtrack (green dots in Figures 41 and 42). At nominal chromaticity,  $\xi_x = \xi_z = 1.6$ , the multi-bunch current threshold is about 7 mA in vertical and 62 mA in horizontal.

At SOLEIL, the measured vertical threshold is 29 mA at zero chromaticity and the transverse feedback enables reaching 500 mA. We expect that the transverse feedback will also allow us to reach 500 mA in the upgraded ring at nominal chromaticity. The obtained tracking results indicate that if the HC is used, at 500 mA the instability is Landau damped by the synchrotron tune spread generated by the HC as far as the

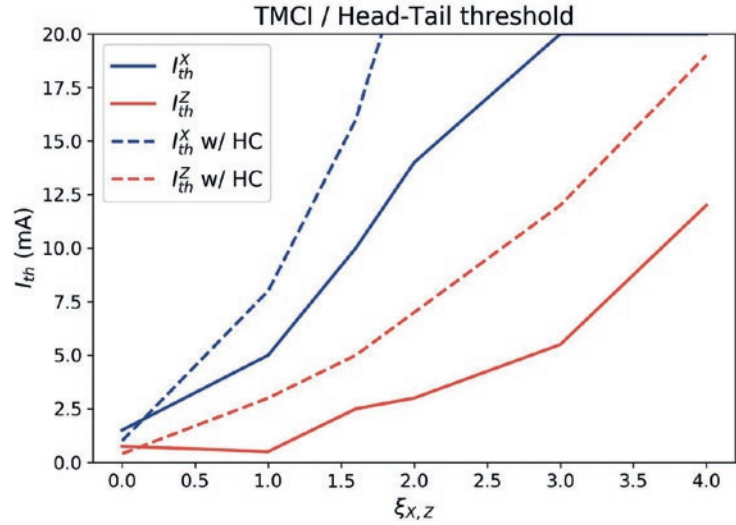


Figure 38: Transverse single bunch instability threshold versus chromaticity, with and without the harmonic cavity.

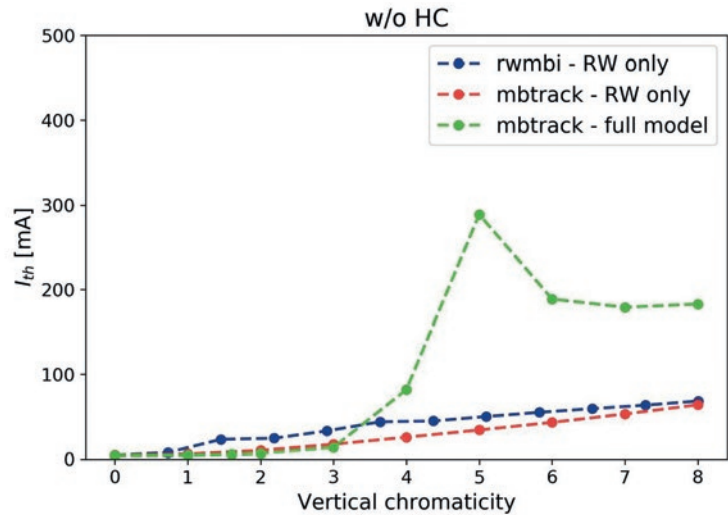


Figure 39: Vertical resistive wall coupled bunch instability threshold versus vertical chromaticity, in the absence of the harmonic cavity

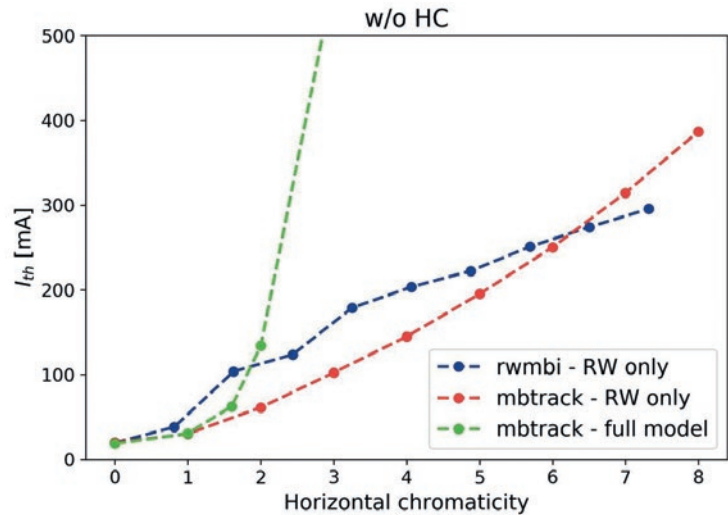


Figure 40: Horizontal resistive wall coupled bunch instability threshold versus horizontal chromaticity, in the absence of the harmonic cavity



chromaticity is superior to 2 in the vertical plane and superior to 1 in the horizontal plane. So, a slight increase of the vertical chromaticity from the nominal one in order to benefit from Landau damping can also be a cure for this instability.

### Ion-induced instabilities

There are two possible instabilities linked to ions produced by residual gas ionized by the electron beam or the synchrotron radiation. The first one is the Classic Ion

Trapping (CIT)<sup>[30]</sup>, where the ions are trapped by the electron beam over several turns. The second one is the Fast Beam Ion Instability (FBII)<sup>[31, 32]</sup>, where the fast ion production can lead to an unstable beam over a single turn of less, with or without ion trapping.

Under normal vacuum conditions, neither instability is expected to be a problem, and in any case, the transverse feedback is sufficiently effective against these instabilities.

## REFERENCES

- [1] Einfeld, D., Plesko, M., "Design of a Diffraction-Limited Light Source", Proc. SPIE, 2013, 201–212, (1993).
- [2] Farvacque, L., et al., "A Low-Emittance Lattice for the ESRF", Proceedings of IPAC (2013).
- [3] Alekou, A. et al., "Study of Double Triple Achromat Lattice for a 3 GeV Light source", Proceedings of IPAC (2016).
- [4] Loulergue, A., et al., "Linear and Nonlinear Optimizations of Combined 7BA-6BA Lattices for the Future Upgrade of SOLEIL", Proceedings of IPAC (2017).
- [5] Loulergue, A., et al., "Baseline Lattice for the Upgrade of SOLEIL", Proceedings of IPAC (2018).
- [6] "SLS-2 Conceptual Design Report", released December 2017, available at <http://www.lib4ri.ch/institutional/bibliography/psi/psi-berichte.html>.
- [7] Nagaoka, R., et al., "Study of Higher-Order Achromat Lattice as an Alternative Option for the SOLEIL Storage Ring Upgrade", Proceedings of IPAC (2019).
- [8] Streun, A., "The Anti-Bend Cell for Ultralow Emittance Storage Ring Lattices", NIMA, 737 (2014).
- [9] Martinez, M., et al., "Applied Pareto multi-objective optimization by stochastic solvers", Engineering Applications of Artificial Intelligence, 22, 455 – 465, (2009)
- [10] Accelerator Toolbox: a collaborative Matlab Toolbox for single particle dynamics, Github repository, <https://github.com/atcollab/at>.
- [11] Laskar, J., "Frequency Analysis for Multi-Dimensional Systems. Global Dynamics and Diffusion", Physica (Amsterdam) 67D, 257 (1993).
- [12] Vivoli, A., et al., "Intra-Beam Scattering effect in the SOLEIL Storage Ring Upgrade", Proceedings of IPAC (2019).
- [13] Hellert, T., et al., "Toolkit for simulated commissioning of storage-ring light sources and application to the advanced light source upgrade accumulator", Physical Review Accelerators and Beams 22(10), art. 100702. (2019).
- [14] Hellert, T., "Toolkit for Simulated Commissioning (SC)", <https://sc.lbl.gov/>, accessed 2020-09-18.
- [15] Vivoli, A., et al., "SOLEIL Storage Ring Upgrade Performance in Presence of Lattice Imperfections", Proceedings of IPAC (2019).
- [16] "CST Particle Studio", <https://www.cst.com/> (version 2019).
- [17] Mounet, N., "ImpedanceWake2D", <https://twiki.cern.ch/twiki/bin/view/ABPCComputing/ImpedanceWake2D>, CERN (2011).
- [18] Koukovini-Platia, et al., "High Frequency Electromagnetic Characterization of NEG Properties for the CLIC Damping Rings", Proceedings of the 5<sup>th</sup> International Particle Accelerator Conference (2014).
- [19] Nagaoka, R., "Numerical evaluation of geometric impedance for SOLEIL." Proc. EPAC2004. Vol. 2038. (2004).
- [20] Nagaoka, R., et al., "Beam instability observations and analysis at SOLEIL." 2007 IEEE Particle Accelerator Conference (PAC). IEEE, (2007).
- [21] NSLS-II Conceptual Design Report, BNL-77977-2006-V1-V2 (2006).
- [22] Nagaoka, R., et al., "Studies of Collective Effects in SOLEIL and DIAMOND Using the Multiparticle Tracking Codes sbtrack and mbtrack." Proceedings of PAC'09, Vancouver, BC, Canada (2009).
- [23] Murphy, J. B., et al., "Longitudinal Wake Field for an Electron Moving on a Circular Orbit", Part. Accel. 57, BNL-63090 (1996).
- [24] Faltens, A., Laslett, L. J., "Longitudinal Coupling Impedance of a Stationary Electron Ring in a Cylindrical Geometry." Part. Accel. 4 (1973).
- [25] Cai, Y., "Theory of Microwave Instability and Coherent Synchrotron Radiation in Electron Storage Rings." No. SLAC-PUB-15243. SLAC National Accelerator Laboratory (2012).
- [26] Evain, C. et al., "Spatio-Temporal Dynamics of Electron-Bunches in low Emittance Storage-Rings during the Microbunching Instability", To be published (2021).
- [27] Nagaoka, R., et al., "Operational Status of the Transverse Bunch by Bunch Feedback System at SOLEIL", Proceedings of IPAC 10 (2010).
- [28] Venturini, M., "Harmonic Cavities and the Transverse Mode-Coupling Instability Driven by a Resistive Wall", Physical Review Accelerators and Beams 21, no 2 (2018).
- [29] Nagaoka, R., "rwmbi: A Frequency Domain Solution of Transverse Coupled-Bunch Instability Driven by Resistive-Wall and Broad-Band Impedance", unpublished.
- [30] Sakanaka, S., et al., "Differences in the Ion Trapping between Uniform and Partial Bunch Gillings", Nuclear Instruments and Methods in Physics Research Section A: Accelerators, Spectrometers, Detectors and Associated Equipment 256, no 1 (1987).
- [31] Raubenheimer, T.O., Zimmermann, F., "Fast Beam-Ion Instability. I. Linear Theory and Simulations", Physical Review E52, 5 (1995).
- [32] Stupakov, G. V., et al., "Fast Beam-Ion Instability. II. Effect of Ion Decoherence", Physical Review E52, 5 (1995).
- [33] Seraphim, R. M. et al., "Vacuum System Design for the SIRIUS Storage Ring", 6th International Particle Accelerator Conference (2015).
- [34] Duarte, H. O. C., et al., "Analysis and Countermeasures of Wakefield Heat Losses for SIRIUS", 8th International Particle Accelerator Conference (2017).
- [35] Duarte, H. O. C., et al., "Evaluation and Attenuation of SIRIUS Components Impedance", 8<sup>th</sup> International Particle Accelerator Conference (2017).

## Injection scheme

### Introduction

Injection into the proposed SOLEIL upgrade storage ring is much more challenging compared to the case of the current ring, mainly due to the drastic reduction of the horizontal dynamic aperture from  $\pm 15$  mm to  $\pm 5$  mm (see section Lattice Design) with almost the same local betatron function. In addition, the Injection Straight Section (injection SS) length is reduced from 12 m to 7.35 m in the upgrade lattice. The use of the current injection system, composed of 4 dipole kickers and occupying the entire straight section, does not therefore appear to be an optimal solution, as it might be useful to have space for the installation of other necessary devices (diagnostics, scrapers...).

On the other hand, the feedback from using an injection system based on a single Multipole Injection Kicker (MIK) on MAX-IV storage ring has been very positive<sup>[1]</sup>. Indeed, based on a BESSY design<sup>[2, 3]</sup>, SOLEIL team has conceived, built and installed on the MAX-IV 3 GeV storage ring an in-air MIK that is successfully and routinely used in operation for top-up injection since 2017. Together with a good injection rate, the transparency of the injection process in terms of the stored beam position stability proved to be well below the requirement of 10% of the RMS beam size. Following these excellent results, it has been decided to install a similar device on the present SOLEIL storage ring in 2021, to prototype and experiment foreseen top-up injection schemes for the upgrade of SOLEIL. However, re-using this MAX-IV MIK magnet in the upgrade storage ring would generate a magnetic field plateau for the injected beam too far from the stored beam axis, typically 10 mm. And under these conditions, injection in the strong field gradient part of the MIK ( $50 \text{ T}\cdot\text{m}^{-1}$ ) would make it difficult to use a beam coming from a booster, regardless of the efforts made to reduce its emittance, because it would be too much sensitive to any injection jitter. For this reason, new developments have been carried out on the MIK by the SOLEIL team, leading to several different topologies for the distribution of conductors. For each topology, the peak field is obtained at  $x = 3.5$  mm with a sextupole-shaped plateau, while a sextupole or octupole-shaped zero field is proposed for the stored beam. Efforts have been made to preserve the full vertical aperture of these new MIKs, which should be greater than 7 mm, and to improve their kick efficiency with up to

Parameters	Units	Present booster	Upgraded booster
Circumference	m	156.6	~ 156.6 m
Natural H. emittance	nm.rad	140	8-10
RMS bunch length	ps	50	25-35
Maximum RF voltage	MV	4	4

Table 13: Parameters of the upgraded booster, in case of a top-up injection scheme

2.5 mrad/kA per meter of magnet (see MIK Design, page 74).

Based on these performances, two top-up injection schemes were studied in the frame of the CDR phase of the project: a betatron off-axis injection (see First top-up injection scheme on this page) and a synchrotron on-axis injection, both using the MIK associated with a thick and a thin septum (see Alternative scheme for a top-up injection, page 72). However, the technical risk on the new version of MIK cannot be ignored, as well as the reduction in top-up injection efficiency that could be revealed during the upcoming analyses of dynamics robustness. This is why the first considerations for a swap-out on axis injection are given in First considerations for a swap-out injection, page 74. For completeness, and if necessary, the interesting injection scheme proposed for the SLS-2 project with 3 kickers and an anti-septum<sup>[4]</sup> could also be considered, in parallel with countermeasures to compensate for the residual disturbance on the stored beam position<sup>[5, 6]</sup>.

Whatever the injection scheme, the horizontal emittance of the injected beam needs to be significantly reduced compared to the present value of 140 nm. rad. In case of top-up injection, we plan to replace the current booster with a new one having a typical natural emittance in the range of 10 nm.rad, and an RMS bunch length limited to 25 – 35 ps (Table 13), which should be reasonably achievable in the current 157 m circumference. It should take into account the relative

change in RF frequency induced by the storage ring upgrade. The design of such a lattice is foreseen to be achieved in the first six months of the TDR phase, while the completion of the whole booster system should then be handled as a turnkey system.

### First top-up injection scheme: betatron off-axis injection

The betatron off-axis injection is the first straightforward proposed one, optimized by increasing to 12 m the local horizontal  $\beta$ -function at the MIK position (Figure 41a) and by introducing the “dissonance”: the amplitude-dependent tune shifts are indeed such, that the working point is on the coupling resonance, but for the large amplitudes of the injected beam, tunes stay away from the resonance in order to avoid large induced vertical oscillations (see section Lattice Design). Figure 42a shows the implementation of the pulsed magnets in the injection SS, which leaves the necessary Beam Stay Clear (BSC) at septum (5 mm) and places the injected beam on a horizontal offset of  $x = -3.3$  mm at the MIK exit. Pulsed magnet parameters are described in Pulsed magnet development below. First turns in the horizontal phase space are shown in Figure 43a. The injection efficiency is 100% without any error, considering an injected beam of 512 particles distributed at  $\pm 3 \sigma$  on a 6D hyper-contour and with an equally shared emittance of 5 nm.rad in each transverse plane.

Taking into account a first series of errors, the robustness of this scheme is

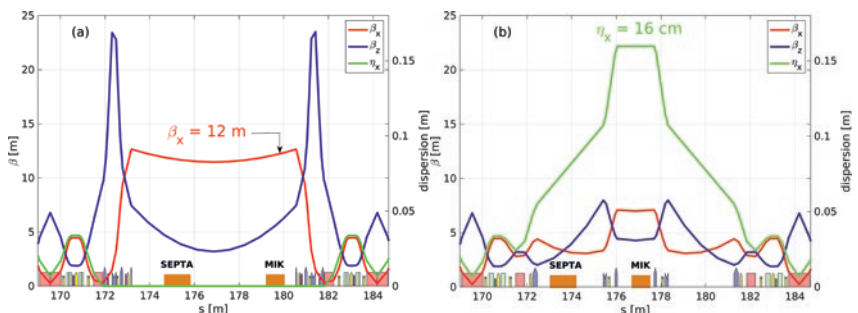


Figure 41: Bumps performed at injection section (a) Horizontal  $\beta$ -function bump for betatron off-axis injection - Horizontal and vertical tunes are  $\nu_x = 54.20$  and  $\nu_z = 18.20$ . (b) Horizontal dispersion function bump for synchrotron on-axis injection -  $\nu_x = 54.16$  and  $\nu_z = 18.16$



tested. First the impact of a horizontal angular jitter due to a pulse to pulse RMS repeatability  $\Delta B/B = 10^{-4}$  of the pulsed magnet field at booster extraction and storage ring injection is evaluated. The 100% injection rate is slightly affected for the extreme value  $+3\sigma$  ( $+50\ \mu\text{rad}$ ), due to the transverse angular acceptance, as well as the sextupolar component of the MIK field. The use of new pulsers for the septa magnets will soon be considered in order to possibly limit the field reproducibility  $\Delta B/B$  to a few  $10^{-5}$ . Second, the application of a typical set of systematic harmonic components to quadrupoles, sextupoles and reverse bends (see section Magnets) shows the relative sensitivity of the injection process to multipolar errors (Figure 44a).

Finally, the envelopes during injection are compared to the specific gap limitation imposed by in-vacuum undulators in short straights sections ( $\pm 2\ \text{mm}$  in vertical for planar insertion devices) and possibly in medium straight sections ( $\pm 3\ \text{mm}$  in horizontal and vertical for CPMUE type undulators). We do not observe any transfer of the horizontal betatron oscillation into the vertical plane, even with the storage ring working point set at full coupling ( $K=100\%$ ). Nevertheless, Table 14 shows that envelopes are close to physical apertures, which reduces the margin for an angular jitter error at injection.

### Alternative scheme for a top-up injection: synchrotron on-axis injection

An alternative scheme is studied to provide an injection that requires small dynamic apertures and would then be less sensitive to storage ring errors. The principle consists in injecting an off-momentum beam on a selected chromatic orbit and taking advantage from the zero dispersion in the straight sections to suppress horizontal amplitudes at undulator locations. The MIK is thus placed in a non-zero dispersion section to

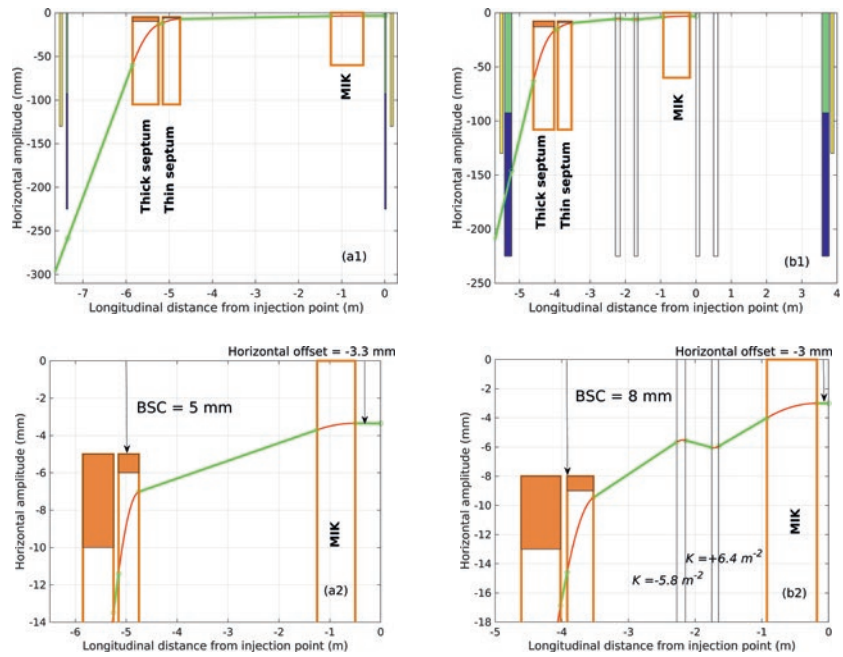


Figure 42: Implementation of pulsed magnets for both top-up injection schemes (a1) Betatron injection in the 7.35 m long injection section and (a2) zoom on beam stay clear (BSC) at septum. (b1) Synchrotron injection in the 8.8 m long injection section and (b2) zoom on BSC at septum and trajectory inside the additional quadrupole doublets. Distinct transverse dimensions are shown for permanent magnet quadrupole (green) and electromagnetic quadrupole (blue)

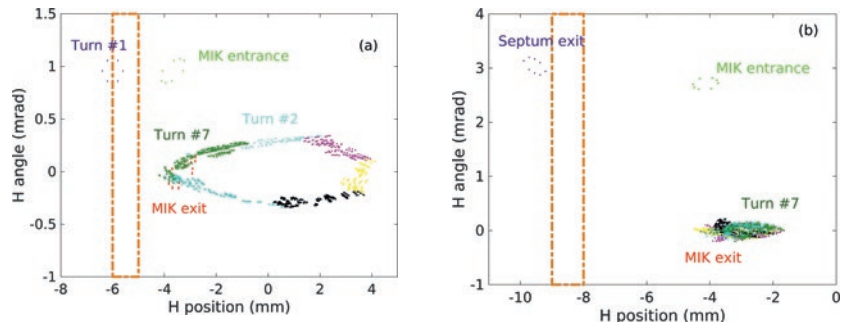


Figure 43: Horizontal position and angle of the injected beam at the middle of injection section for the 7 first turns w/o any error (a) Betatron injection (b) Synchrotron injection. Septum blade, MIK entrance and exit, and middle of injection section locations have been superimposed for convenience. Beam is distributed on a  $\pm 3\sigma$  6D hyper-contour with an equally shared booster emittance of  $5\ \text{nm}\cdot\text{rad}$  in each transverse plane

steer the off-momentum injected beam on its chromatic orbit, and Figure 45 shows how the horizontal trajectory amplitude in the lattice arcs is significantly reduced compared to the betatron injection scheme.

### Lattice adaptation

As the dispersion function in lattice arcs is very small (see section Lattice Design), it is necessary to create a dedicated dispersion bump at the MIK location in the injection section, breaking a priori

Max radius	CDR reference lattice Betatron off-axis injection				Adapted lattice Synchrotron on-axis injection			
	Short SS over 2.7 m	Medium SS over 4.15 m	Long SS over 7.35 m	Long SS over 7.66 m	Short SS over 2.7 m	Medium SS over 4.15 m	Long SS over 7.14 m	Long SS over 7.66 m
H (mm)	3.2 2.5*	3.6 3.1*	6.4 5*	5.2 4.2*	2 1.3*	2.6 1.6*	2.2 1.6*	3.9 2.7
V (mm)	2.3 1.6*	2.5 2.0*	2.9 2.3*	3.1 2.3*	1.5 1.2*	1.9 1.5*	1.9 1.5*	2.3 1.8*

Table 14: Envelopes during injection at straight sections w/  $+3\sigma$  horizontal angular jitter ( $+50\ \mu\text{rad}$ ) and w/o (\*) for both top-up injection schemes. Storage ring working point is set at full coupling. Horizontal and vertical emittances of the injected beam are  $5\ \text{nm}\cdot\text{rad}$ , RMS bunch length is 25 ps for betatron injection, 35 ps for synchrotron injection

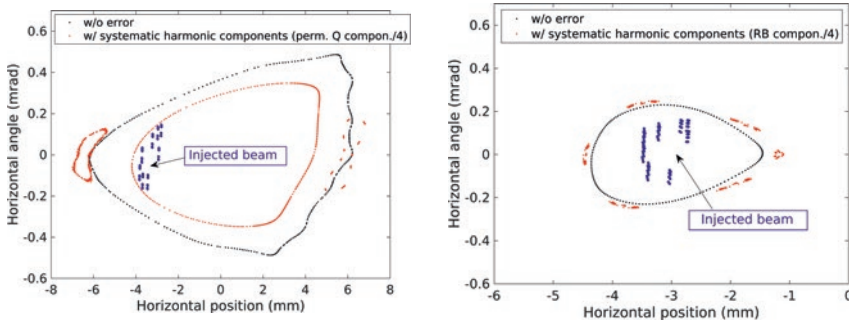


Figure 44: Impact of systematic harmonic components in Quad., Sext. and Reverse Bends on transverse acceptances at MIK exit (a) Betatron injection ( $\beta_x = 12$  m) (b) Synchrotron injection ( $\beta_x (\delta = -2\%) = 6$  m). Other kinds of errors applied at injection or in the storage ring are not considered here

the lattice symmetry 2 into symmetry 1. A trade-off is made between dispersion value (16 cm) and energy offset (-2%) so that the beam reaches a 3 mm horizontal off-energy orbit at the MIK exit. To achieve this, the injection SS should be modified such as two doublets of quadrupoles and two sextupoles are added, while in order to maintain sufficient lever arm between the septum and the MIK, the original quadrupole triplets are removed at both entry and exit of the injection SS and replaced by only one focusing quadrupole (Figure 41b). As a result, the natural horizontal emittance is increased from 80 to 90 pm.rad because the dispersion function in the dipole located at entry and exit of the injection SS is no longer going to zero. To recover the same tunes as the reference lattice ones, the horizontal and vertical  $\beta$ -functions are set respectively to 2.0 m and 3.7 m in the other 3 long

straight sections to accommodate for insertion devices. The MOGA-Bmad code<sup>[7]</sup> was used to optimize nonlinear dynamics, using the same sextupole and octupole implementation as the CDR reference lattice. The objectives were defined as the on and off ( $\pm 2\%$ ) momentum dynamic apertures, respecting zero total chromaticities and containing the energy-dependent tune shift in the half integer around the working point. Figure 46 shows an example of dynamic aperture obtained for the -2% energy deviation. The resulting Touschek lifetime, calculated under the same conditions as the CDR reference lattice, is 0.7 hour without bunch lengthening. Other tools are currently being used to improve off-momentum horizontal dynamic aperture and energy acceptance to achieve a Touschek lifetime beyond 2 hours without bunch lengthening. The option

of returning to a machine of symmetry 2 (i.e. with an additional dispersion bump in the opposite long straight section) is also being considered and a natural horizontal emittance smaller than 100 pm.rad should be recovered by modifying the upstream and downstream dipoles of the two modified straight sections.

### Injection performance

For this scheme, the MIK field is stronger (Table 15) due to a larger BSC required at the septum, and the implementation of the pulsed magnets is globally more constrained compared to the previous injection scheme (Figure 42b). The position at each turn of the injected beam in the injection SS will follow the slow damping of the chromatic orbit as shown in Figure 43b. The injection rate into the storage ring is 100% at full coupling, without any errors. We observe the same limitation of horizontal acceptance as the previous scheme, towards a horizontal jitter of  $+50 \mu\text{rad}$ , which leads to the same willingness to consider new pulsers. But the goals are reached, first of all regarding the sensitivity of the scheme to systematic harmonic components in magnets: Figure 44b shows the robustness of the horizontal aperture. Secondly, the envelopes during injection are significantly reduced in both planes over the whole ring (Figure 47): Table 14 shows that in the presence of horizontal jitter at injection envelopes are kept well below the undulator gap apertures.

### Comparison of the top-up injection schemes

In conclusion, the betatron scheme has the advantage of allowing straightforward implementation in the injection SS, and the pulsed magnet specifications are more relaxed. Disadvantages are sensitivity to lattice errors and the need for a large dynamic aperture, as well as the envelopes during injection that offer a limited margin to the insertion device gaps.

Conversely, the synchrotron scheme has the advantage of relaxed dynamic aperture requirements, and with it, less sensitivity to lattice errors. The envelopes during injection meet the demand well. However, it requires a lattice modification, an optimization of off-momentum dynamic aperture, and the MIK specifications are more demanding.

The respective studies of each of these injections will continue during the first six months of the TDR phase, since the choice of the top-up injection is not considered urgent until then.

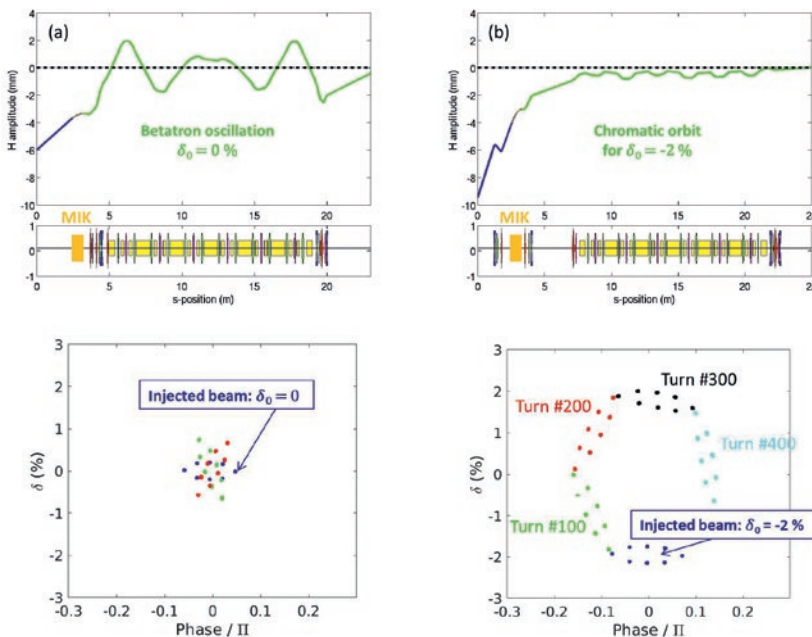


Figure 45: Comparison of injected beam horizontal orbit in the first arc after injection section and synchrotron oscillation in the longitudinal plane for (a) betatron injection, (b) synchrotron injection

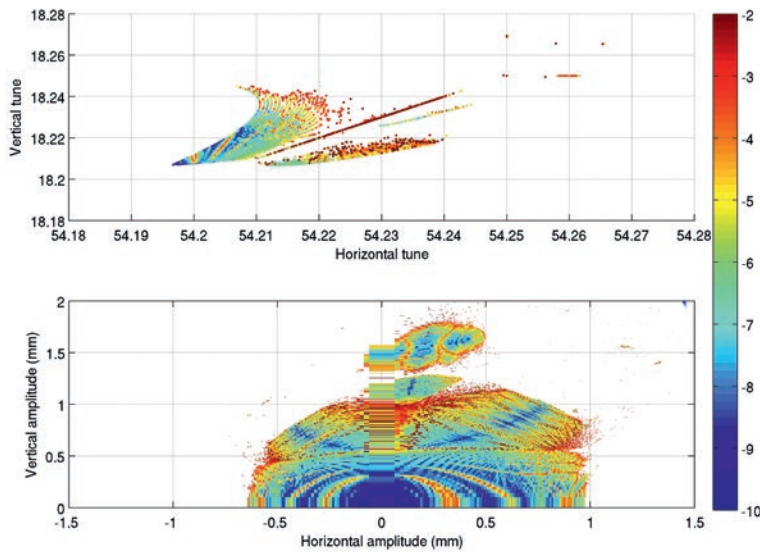


Figure 46: Frequency map and off-momentum dynamic aperture of the adapted lattice, calculated for -2% energy deviation at the centre of a long free dispersion straight section where  $\beta_x = 2.0$  m and  $\beta_z = 3.7$  m

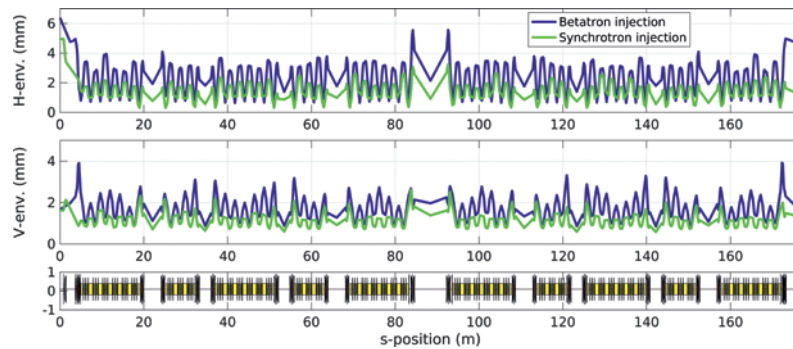


Figure 47: Comparison of horizontal and vertical envelopes over 900 turns, for half the circumference, after injection for both top-up injection schemes, w/o error at injection nor in storage ring. Storage ring working point is set at full coupling. Horizontal and vertical emittances of the injected beam are 5 nm.rad, RMS bunch length is 25 ps for betatron injection, 35 ps for synchrotron injection

## First considerations for a swap-out injection

To prevent any risk on MIK technology or on top-up injection schemes, we have anticipated the need for a very fast kicker to achieve on-axis injection, within the frame of a swap-out scheme (see Swap-Out Fast Striplines Kickers and Pulser on next page). But the first general considerations on this scheme do not make it attractive in the case of

SOLEIL. Firstly, it will not be a promising route to further reduce the natural emittance of the lattice because among many reasons, our will is to maintain the momentum compaction factor not lower than  $10^{-4}$ . Secondly, we aim to maintain two present filling patterns: uniform and time resolved (see Introduction of this Chapter). For the latter, a charge value per bunch as high as the current value of 19 nC in Single Bunch mode

would be unprecedented for a swap-out scheme, and even more challenging for a medium energy storage ring. Finally, the current booster and storage ring tunnels appear to be particularly narrow, which would result in a very constraining arrangement of additional transfer lines and an accumulator.

## Pulsed magnet development

### Pulsed magnet philosophy

The pulsed magnets for the SOLEIL upgrade storage ring need to complete three primary objectives. Firstly, the pulsed magnets must allow the schemes presented in the previous sections to work efficiently, *i.e.* to be able to accumulate beam in the storage ring with minimal losses. Secondly, the pulsed magnets must allow transparent injection in the storage ring, meaning that the stored beam is not perturbed during the injection process. Finally, the pulsed magnets and associated components (pulsers, vacuum chambers, control systems, etc.) must be designed with a high level of reliability and ease of maintenance and manufacture.

### MIK design

The pulsed magnet team has been working since 2018 on the development of new MIK topologies that place the peak magnetic field as close as 3.5 mm from the stored beam axis without compromising on the aperture of the vacuum chamber. The main parameters, constraints and specifications are given in Table 15.

At present, two new MIK topologies fulfill the basic requirements for the injection schemes. An in-air MIK magnet prototype has already been made and has been magnetically measured in-house with excellent results, as a step towards proving the feasibility of these new MIK. Some difficulties still need to be overcome such as final mechanical integration, with great care on the conductor position tolerance or the voltage withstand of such new compact magnets. These difficulties should be resolved during the TDR phase with the early design of the final in-vacuum magnet starting in 2021. The process of filing a patent for these new MIK topologies is on-going.

### Septa design

The 130 mrad deflection from the transfer line is split between a thick septum (110 mrad) and a thin septum (20 mrad). The main difficulties anticipated in the magnetic design are the RMS pulse to pulse field reproducibility ( $\Delta B/B < 10^{-4}$ ) for the thick septum (in case a pulsed thick

Parameters	Units	Betatron off-axis injection	Synchrotron on-axis injection
MIK current	A	500	1400
MIK deflection	mrad	1	2.7
Minimum chamber aperture	mm <sup>2</sup>	7 (vert.) x 20 (hor.)	
Foreseen electrical characteristics of magnets		Inductance of 1.5 $\mu$ H/magnet 2 kA peak current / 5 kV peak on magnet 2.4 $\mu$ s pulse width $\sim 10^{-4}$ pulse-to-pulse field reproducibility	
Defect fields on stored beam		< 1 $\mu$ T and < 0.1 Tm <sup>-1</sup> in both planes	

Table 15: MIK main specifications and constraints

Parameters	Units	Thick septum	Thin septum
Nominal deflection	mrاد	110	20
Septum thickness	mm	5	< 1
RMS pulse-to-pulse field reproducibility	-	< 10 <sup>-4</sup>	~10 <sup>-4</sup>
Beam Stay Clear at thin septum	mm	-	5 to 8 depending on injection scheme
Defect fields on stored beam		< 1 μT and < 0.1 Tm <sup>-1</sup> in both planes	

Table 16: Septa main specifications and constraints

septum is chosen) and the low leakage field for the thin septum for which a septum blade width should be less than a millimetre (see Table 16 for the main parameters). For the thin septum, many options have been analysed such as a classic eddy-current septum, a permanent magnet thin septum, a mass-less septum or even a pulsed octupole magnet. Further

studies in the TDR phase will narrow down the choices to fulfil the injection physics and transparency requirements.

#### Swap-out fast stripline kicker and pulsers

In case the final scenario for injection is swap-out, the pulsed magnet team has assessed the feasibility of ultra-short

pulsers, *i.e.* capable of generating nanosecond high voltage pulsers. A prototype of 2.5 ns – 2.8 kV was ordered from Sydor Kentech. In-house tests are extremely encouraging and tests on beam are foreseen in 2021 at SOLEIL. A preliminary design of the stripline kickers has also been done to determine the total length of stripline kickers needed for efficient injection with such scheme.

#### First day injection kicker

For first day injection, a classic dipole kicker is foreseen to inject beam in the storage ring, powered with a square current pulse to inject up to a quarter of the ring. The aim is to easily inject in the storage ring to be able to start correcting all the various sources of errors, before attempting to use the previously described schemes that require a well understood and tuned machine.

#### REFERENCES

- [1] Alexandre, P. et al. "Transparent Top-Up Injection into Fourth-Generation Storage Ring", Nuclear Instruments and Methods in Physics Research., section A, 986, art. n°164739. (2021).
- [2] Atkinson, T. et al, "Development of a Non-Linear Kicker System", Proceedings of the IPAC 2011 conference (2011).
- [3] Alexandre, P., "NLK at SOLEIL", TWISS workshop, Berlin, (2017).
- [4] "SLS-2 Conceptual Design Report", December 21, 2017.
- [5] Mitsuda, C., "The Fast Kicker Correction System for Transparent Top-Up Injection at SPring-8" Topical Workshop on Injection and Injection Systems, Berlin, Germany, 2017.
- [6] White, S., et al. "Damping of Injection Perturbations at the ESRF", Phys. Rev. Accel. Beams., 22, art. n°032803. (2019).
- [7] Ehrlichman, M. <https://arxiv.org/abs/1603.02459v2>, <https://www.classe.cornell.edu/bmad/> (2016).



## Magnets

### Introduction

The new storage ring, to be installed in the existing tunnel, is characterized by a high level of compactness, associated with a very strong focusing (with high gradient and combined dipole) and very high sextupole and octupole strengths. To lower the emittance value below 100 pm.rad, the CDR reference lattice includes some reverse-bends. Consequently, the layout of the magnetic structure of the upgrade machine requires a total of about 1000 magnets with demanding specifications and a compact structure (Figure 48).

The magnets should be compact, provide strong strength and operate at low cost. In consequence, permanent magnet (PM) technology is preferred over electromagnet (EM) technology, when it is possible.

All the sextupoles and the octupoles are standard electromagnets, as well as some of the quadrupoles, to ensure good flexibility and efficient correction of linear and non-linear field errors. Table 17 shows the main parameters (same parameters can be seen in Table 2 page 56) and the technology chosen for the magnets of the CDR reference lattice. This table does not include any injection section magnets as the requirements of these magnets are not completely defined. All the permanent magnets presented hereafter use Samarium-Cobalt ( $\text{Sm}_2\text{Co}_{17}$ ) magnets with a conservative strength (coercive field of 850 kA/m and remnant field of 1.12 T) as it exhibits strong resistance to radiation damage and a small temperature coefficient (below  $-0.04\% \cdot \text{K}^{-1}$ ). The dipolar correctors are located in the sextupoles while the quadrupolar (normal and skew) correctors are located in the octupoles. The Good Field Region (GFR) given by the beam dynamics specifications is defined as a circle with a 5 mm radius centred on the electron beam.

We present in this section the magnetic numerical models of those magnets. The

	Technology	Strength	Magnetic length	Quantity	GFR
Dipole	PM	1 T; $-8 \text{ T}\cdot\text{m}^{-1}$	400 mm	40	5 mm
	PM	0.7 T; $-16 \text{ T}\cdot\text{m}^{-1}$	947 mm	76	5 mm
Reverse-Bend	PM	$-0.2 \text{ T}$ ; $58 \text{ T}\cdot\text{m}^{-1}$	200 mm	192	8.75 mm
Quadrupole	PM	$120 \text{ T}\cdot\text{m}^{-1}$	40 → 200 mm	104	5 mm
	EM	$140 \text{ T}\cdot\text{m}^{-1}$	175 mm	40	5 mm
Sextupole	EM	$8000 \text{ T}\cdot\text{m}^{-2}$	60/80/110 mm	368	5 mm
Octupole	EM	$250000 \text{ T}\cdot\text{m}^{-3}$	60 mm	176	5 mm
Dipolar Correctors (H/V)	EM	0.5 mrad	-	176	5 mm
Quadrupolar Correctors (Normal/Skew)	EM	0.25 T	60 mm	176	5 mm

Table 17: Magnetic design parameters for the CDR lattice

	Short Dipole 1	Short Dipole 2	Long Dipole 1	Long Dipole 2
Yoke length (mm)	376	376	925	925
Angle (mrad)	41.75	43.5	68.9	71.8
$B_0$ (T)	0.957	0.997	0.667	0.695
$G_0$ (T/m)	-8	-8	-16	-16
Integrated Gradient (T)	-3.2	-3.2	-15	-15
PM block size ( $\text{mm}^3$ )	39x19x47	39x19x47	42x9x25	42x9x25
Bore radius (mm)	8	8	8	8
Weight (kg)	240	240	490	490
Overall dimension (Width x Height x Length) ( $\text{mm}^3$ )	235 x 266 x 400	235 x 266 x 400	215 x 308 x 925	215 x 308 x 925

Table 18: Dipole design values of the CDR lattice reference

simulations are carried out using DS Simulia Opera suite<sup>[1]</sup> and Radia software packages<sup>[2]</sup>.

The magnetic field in an accelerator magnet can be written as<sup>[3]</sup>:

$$B = \sum_{n=1}^{+\infty} (B_n + i A_n) \left( \frac{r}{\rho_0} \right)^{n-1}$$

where  $\rho_0$  is the reference radius and  $n$  the number of pole pairs. The circle with a radius  $\rho_0$  is usually identified as the GFR region. The  $B_n$  ( $A_n$ ) the normal (skew) multipole coefficients are used to

transcribe the beam dynamics requirements into magnetic requirements. The coefficients  $B_1$ ,  $B_2$  and  $B_3$  respectively correspond to the dipole, quadrupole and sextupole components of the field. The gradient  $G$  and the sextupole strength  $S$  of a magnet relates to the normal coefficients  $B_2$  and  $B_3$  as follows:  $G = B_2/\rho_0$ ,  $S = B_3/\rho_0^2$

The associated normalized coefficients of the field are defined for the quadrupole as:  $b_n = 10000 \times B_n/B_2$  and for the sextupole as  $b_n = 10000 \times B_n/B_3$

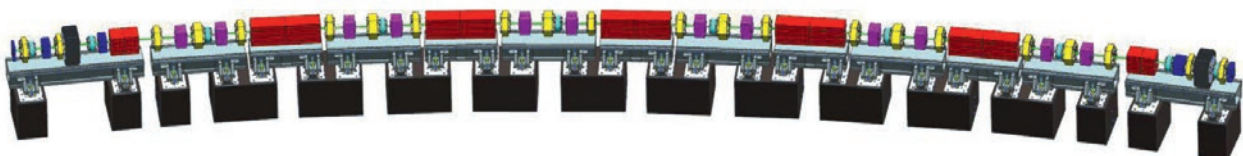


Figure 48: Part of the 7BA lattice with PM dipole in red, PM reverse bend in pink, PM and EM quadrupole in blue, EM sextupoles in yellow, octupoles in light blue

SHARED USER

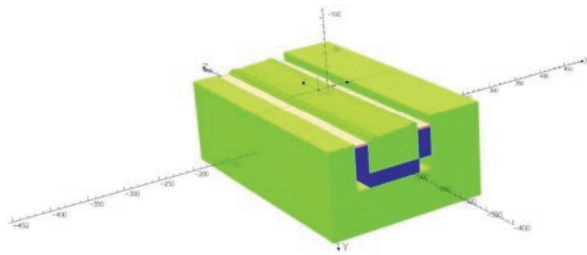


Figure 49: Half short dipole: permanent magnets (dark blue), yoke and poles (green) and thermal shims (yellow)

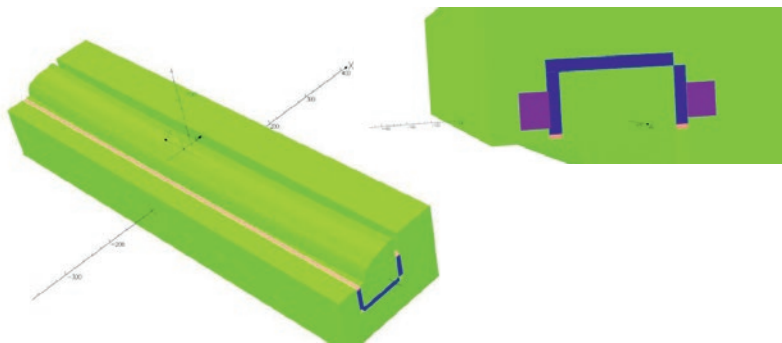


Figure 50: Half long dipole: permanent magnets (dark blue); yoke and poles (green) and thermal shims (yellow). Insert: detail view of the magnetic shunt (purple)

## Dipoles

### Dipole specifications

The CDR reference lattice needs 116 dipoles which are combined-function dipoles with both a dipole and a quadrupole field component. The main parameters are shown in Table 18.  $\text{Sm}_2\text{Co}_{17}$  magnets generate the magnetic field and in order to compensate for possible variation of the magnetic field with the  $\text{Sm}_2\text{Co}_{17}$  magnet temperature, we add some thick thermosensitive shims of magnetic material (known as Ni-Fe Thermoflux) next to the permanent magnet in yellow in Figure 49. The fine tuning of the field integral is done by some magnetic shunts at the entrance and exit of the dipole (shown in Figure 50). Those shunts can also modify the integrated gradient in the dipoles when they are moved asymmetrically in the horizontal direction.

For the standardization of the mass production, only two types of dipoles are designed and built: the short dipole and the long dipole. The adjustment of the deviation angle of the electron beam is done by radial displacement of the dipole on the girder after the results of magnetic measurements.

### Short dipoles

The CDR reference lattice needs 40 short combined-function dipoles which bend

the electron beam by either 41.75 mrad or 43.5 mrad according to their location in the lattice. The dipole provides a defocusing gradient in horizontal plane. The integrated gradient in the dipole is -3.2 T for both deviations. Dipoles have a C-shape where the yoke is straight and the pole follows the curved electron trajectory.

### Long dipoles

The CDR reference lattice needs 76 long combined-function dipoles which bend

the electron beam either by 68.9 mrad or 71.8 mrad according to their position. As the short dipole, long ones have also a defocusing gradient. The integrated gradient in the dipole is -15 T for both dipoles. Dipoles have a C-shape where the yoke is straight and the pole follows the trajectory.

## Quadrupoles and reverse-bends

### Quadrupoles

As for the dipoles, the compactness of the CDR reference lattice requires the use of permanent magnet quadrupoles. To facilitate their design and optimize their performance, PM quadrupoles provide a fixed integrated gradient, while the optics tuning and correction, which are conventionally devoted to electromagnetic quadrupoles, are left to quadrupolar correctors included in the EM octupoles.

### Permanent magnet quadrupole

The magnetic design of all of the permanent magnet quadrupole types is based on the hybrid design proposed by the European Synchrotron Radiation Facility (ESRF)<sup>[4]</sup>. This simple design shown in Figure 51 provides space for an off-axis vacuum chamber dedicated to the light extraction.

All of the PM quadrupoles share the same cross section but the length of each type of PM quadrupole is adjusted to reach the required integrated gradient. At similar integrated gradient, the proposed magnetic structure with a 8 mm bore radius produces a stronger gradient than the one used in the CDR reference lattice

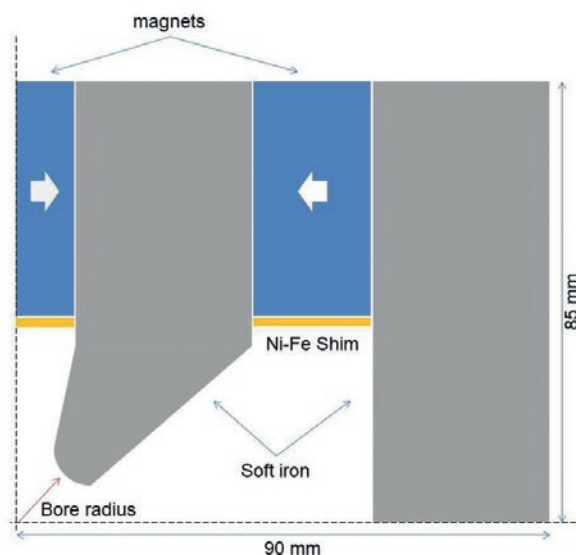


Figure 51: Cross section of the PM quadrupole design. The iron is in grey, the magnets in blue. The white arrow in the magnets indicates the magnetization direction. The Ni-Fe shims are in saffron



Yoke Length [mm]	Overall Length [mm]	Bore radius [mm]	Integrated Gradient [T]	Weight [kg]	Quantity	Normalized harmonic content at 5 mm			
						b <sub>2</sub>	b <sub>4</sub>	b <sub>6</sub>	b <sub>10</sub>
43.5	73.5	8	5.831	9	4	10000	-10.7	-65.4	-4.7
47.9	77.9		6.472	10	16		-10.5	-64.6	-4.7
58.4	88.4		8.001	12	16		-10.1	-63.3	-4.9
82.2	112.2		11.457	17	16		-9.5	-61.3	-5.1
96.9	126.9		13.599	20	16		-9.2	-60.4	-5.2
112.1	142.1		15.813	23	16		-8.9	-59.7	-5.3

Table 19: Main design values of the PM quadrupole for the CDR reference lattice

simulation. As a result, the magnetic and the yoke length of each PM quadrupole is shorter than the one defined in the CDR reference lattice. In addition, similarly to dipole magnet, nickel-iron shims are used to stabilize the quadrupole magnetic field against temperature fluctuation. Finally, the integrated gradient is tuned to the required value by means of flux shunt schemes similar to the ones described in the dipoles (shown in Figure 51).

Table 19 presents the main parameters of the PM quadrupoles and the harmonics content achieved with a non-optimized pure hyperbolic pole tip profile. A reduction of 4<sup>th</sup> and 6<sup>th</sup> harmonic by a factor 4 is necessary for robust electron beam dynamics. It is anticipated that the pole tip shape optimization will reduce by one order of magnitude the harmonic content.

A prototype PM quadrupole is currently being built in order to check the following points:

- Mechanical tolerances (machining and assembly)
- Tools for permanent magnet assembly
- Magnetic measurements and comparison with magnetic simulations
- Test of the temperature stabilization with the Ni-Fe shims.

### Electromagnetic quadrupole

Not all quadrupoles will be in permanent magnets. To guarantee the optimal flexibility some of them (to be defined during the TDR studies) could be electromagnets. The magnetic design of the EM quadrupole for the CDR reference lattice is shown in Figure 52. The main parameters of the

EM quadrupole are listed in Table 20. Similarly to PM quadrupoles, pole tip shape optimization of EM quadrupoles has yet to be performed.

The EM quadrupole integrated gradient ranges from 19 T to 24 T, depending on

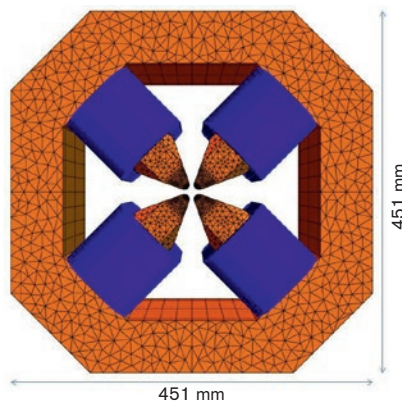


Figure 52: Magnetic design of the EM quadrupole. The yoke is in orange, the coils in blue

the EM quadrupole position in the CDR reference lattice. The excitation curve is given in Figure 53. The variation of the integrated gradient with the current is linear up to 3000 Ampere-Turn. Above this threshold the variation becomes non-linear as the yoke is close to saturation. There is no EM quadrupole prototype planned.

### Reverse bend

Owing the small dipole and the moderate gradient value of the reverse bends (RB), their magnetic design naturally leans towards offset quadrupole. As the dipole field and gradient of the RB are fixed, their magnetic design is also based on permanent magnet technology using the hybrid design shown in Figure 51.

The main parameters of the reverse bend are listed in Table 21. The dipole and the gradient values of the two RB families included in the CDR reference lattice

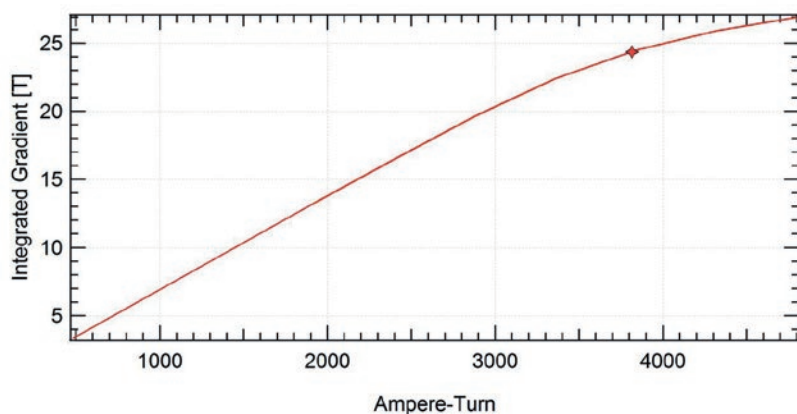


Figure 53: Excitation curve of the EM quadrupole. The red marker indicates the nominal working point

Yoke Length [mm]	Overall Length [mm]	Bore radius [mm]	Weight [kg]	Maximum Integrated Gradient [T]	Coils parameters	Normalized harmonic content at 5 mm		Quantity
						b <sub>2</sub>	b <sub>6</sub>	
175	217	8	216	24	48 turns x 80 A	10000	-43	40

Table 20: Main design values of the EM quadrupoles for the CDR reference lattice

are close enough to allow for sharing the same design for both families. The vertical adjustment of the permanent magnet slightly differs, by almost 2 mm, between RB families. Compared to quadrupoles, RB bore radii are enlarged to 10.5 mm

in order to accommodate the vacuum chamber which is horizontally offset from the magnet axis by almost 3.8 mm. The RB is a straight magnet as the curvature of the electron beam trajectory within its magnetic field is small; the sag in the

RB is less than 0.1 mm. The magnetic design being similar to the one of PM quadrupole, there is no RB prototype planned. Similarly to quadrupoles, RB pole tip shape optimization has yet to be performed. The same temperature stabilization and tuning schemes as dipoles and quadrupoles is implemented.

Reverse bend type		RB1		RB2	
Integrated Gradient (T)		11.558		11.269	
Integrated Dipole (T.mm)		35.69	34.24	41.94	40.24
Yoke Length (mm)		120.1			
Overall Length (mm)		150.1			
Bore radius (mm)		10.5			
Quantity		192			
Horizontal Offset (mm)		3.09	2.96	3.73	3.57
Magnet Vertical Offset (mm)		0		~2	
Normalized harmonic content at 8.75 mm.	b <sub>2</sub>	10000			
	b <sub>4</sub>	-4			
	b <sub>6</sub>	-23			
	b <sub>10</sub>	-2			

Table 21: Main design values of the reverse bend for the CDR lattice

Sextupole type	S60	S80	SN80 notched	S110
Yoke length (mm)	60	80	80	110
Maximum Sextupolar Strength (T/m <sup>2</sup> )	8000	8000	8000	8000
Integrated Sextupole (T/m)	472	685	685	924
Bore radius (mm)	8	8	8	8
Overall cross section (Width x Height; mm <sup>2</sup> )	340 x 300	340 x 300	340 x 300	340 x 300
Nominal Current (A)	47.5	52	52	51
Number of turns	24	24	24	24
Voltage (V)	1.2	1.7	1.7	1.8
Vertical corrector current (A)	12	12	12	12
Number of turns	16	16	16	16
Horizontal corrector current (A)	11	11	11	11
Number of turns	32	32	32	32

Table 22: Main design values of the sextupoles for the CDR lattice

### Sextupoles

The CDR reference lattice needs 368 sextupoles having a nominal strength ranging from 2200 T/m<sup>2</sup> to 8000 T/m<sup>2</sup>. The main parameters are shown in Table 22.

The vertical and horizontal dipolar correctors are included in the sextupole by means of additional coils around the poles. The presence of the dipolar correction in the sextupole introduces some dipolar harmonics content such as a decapole component (7% of the dipolar strength) whose effects on the beam dynamics are being studied. The orbit feedback will drive the correctors. The feedback cut-off frequency will be decisive for the sextupole design, in particular for the thickness of the lamination and the corrector coil turns. The bore radius is 8 mm and the pole to pole gap is 4 mm. The sextupoles are split in four types:

Three types where only the yoke lengths are different (60 mm, 80 mm and 110 mm) as shown in Figure 55 (Left). A fourth type is dedicated to the sextupole installed just after the first short dipole of the arcs. This sextupole needs to have a notch in the middle plane in order to allow for the integration of the vacuum chamber for the photon beam (Figure 54).

Figure 55 (Right) shows the magnetic design of the fourth type of sextupole. It has a notch of 16 mm diameter which gives enough space to let a 14 mm diameter vacuum chamber pass. In order to avoid any odd harmonics, the notches are horizontally symmetrical but the magnetic field still contains some harmonics due to the up and down

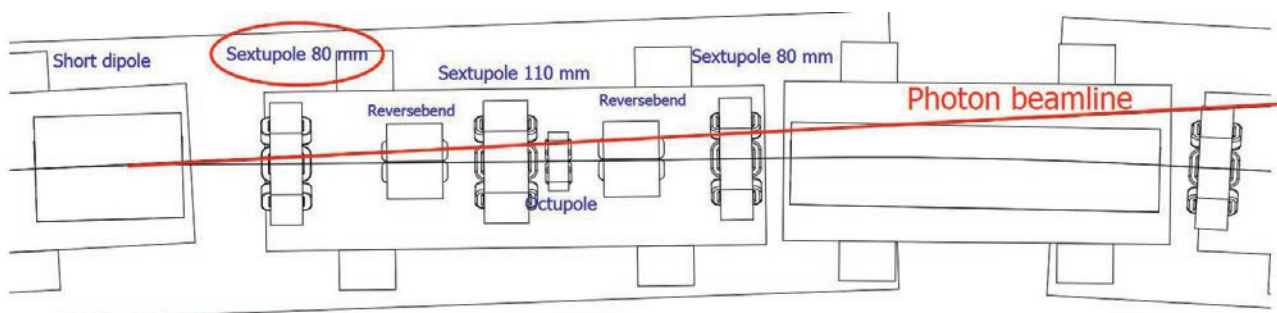


Figure 54: Layout of entrance of the 4BA cell

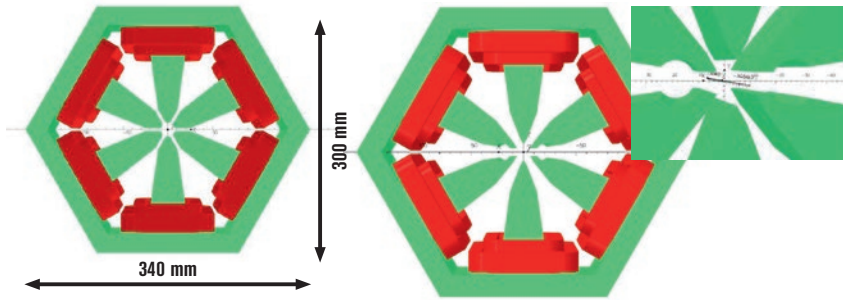


Figure 55: Left: Normal sextupole (60 mm, 80 mm and 110 mm); Right: Notched sextupole (80 mm). Insert: Detail of the notches

Harmonic number	60/80/110 mm	80 mm notched
n	$b_n$	$b_n$
1	0	-75
2	0	0
3	10000	10000
4	0	0
5	0	-18
6	0	0
7	0	-4
8	0	0
9	-10	-232
10	0	0
11	0	0
12	0	0
13	0	0
14	0	0
15	0	9

Table 23: Sextupole harmonic content measured at a radius of 5 mm

dipolar symmetry. Those harmonics can be cancelled with current in the vertical corrector coils or shims on the central poles. The magnetic content harmonics are computed with the DS Simulia Opera suite as shown in Table 23.

A prototype of EM notched sextupole is currently being studied and will be built in order to check the ability to reach

the performances such as harmonics contents, cross talk between sextupolar field and correction fields.

### Octupoles

The octupoles have a nominal strength ranging from 22000 T/m<sup>3</sup> to 250000 T/m<sup>3</sup>. The main parameters are shown in Table 24. The skew quadrupole and normal quadrupole correctors are included in the octupole by means of additional coils around the poles. Figure 56 shows the coil configuration to obtain the desired fields. Each pole is equipped by three windings. The bore radius is 8 mm and the pole to pole gap is 4 mm.

A prototype of EM octupole is currently being studied and will be built in order to check the ability to reach the performances such as harmonics contents, cross talk between octupolar field and quadrupolar correction fields.

Parameter	Value
Yoke Length (mm)	60
Maximal Octupolar Strength (T/m <sup>3</sup> )	250000
Integrated Octupole (T/m <sup>2</sup> )	15000
Integrated Normal quadrupole (T)	0.25
Integrated Skew quadrupole (T)	0.25
Bore radius (mm)	8
Outer radius (mm)	105
Octupole Current (A)	20
Normal Quad. Current (A)	30
Skew Quad. Current (A)	20
Number of turns per coil	12

Table 24: Main design values of the octupole for the CDR reference lattice

### Conclusion

Studies conducted to date have shown that the specifications required for the beam dynamics are attainable and that the solutions adopted fulfill the requirements. Studies on sensitivity to mechanical tolerances to the field quality requirements will be carried out in the future. Magnet measurements (Hall probe bench and stretched wire) will be also investigated further in particular with prototypes. The power supply/coils couples will be also optimized in order to reduce the energy consumption of the EM elements.

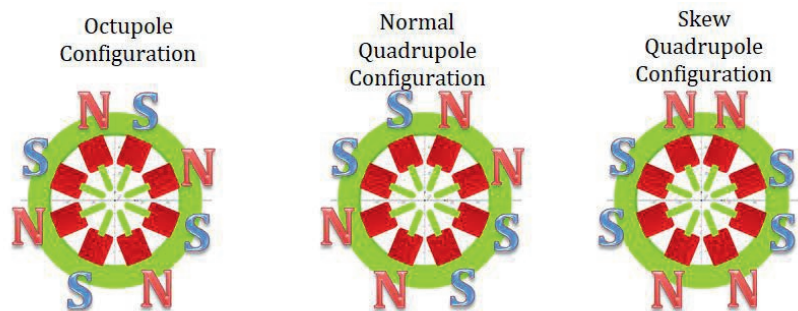


Figure 56: Octupole sketch and coil polarity configuration (N: North, S: South)

### REFERENCES

[1] <https://www.3ds.com/fr/produits-et-services/simulia/produits/opera/>  
 [2] Chubar, O., et al., "A Three-Dimensional Magnetostatics Computer Code for Insertion Devices", Journal of Synchrotron Radiation, 5, 481 (1998).

[3] Bottura, L. "Standard Analysis Procedures for Field Quality Measurement of the LHC Magnets—part I: Harmonics", LHC/MTA, Technical Report LHCMTA-IN-97-007 (2001).  
 [4] N'gotta, P., et al., "Hybrid High Gradient Permanent Magnet Quadrupole", Phys. Rev. Accel. Beams, 19, 122401 (2016).

## Alignment strategy

### Definition of the nominal orbit

The CDR storage ring reference lattice implementation in the tunnel has consequences on the beamline photon source positions. Several beamline positions will stay unchanged, such as the two long beamlines. The orbit of the new storage ring must then be aligned with respect to the position and direction of these two long beamlines, requiring measurement, with respect to wall reference positions, of the current photon source points and beam angles. The position of these references will be measured by means of laser tracker compared to the quadrupoles defining the beamline photon source points. The same procedure could be applied for all the other beamlines, so as to know precisely the offsets to be applied on realignment.

Magnetic imperfections on dipoles generate an error on their deflection angle, affecting the definition of the nominal orbit. Precise magnetic measurement (0.1% of their nominal value) of their real deflection angles would allow aligning the magnetic centers of the multipole magnets on the true outputs of the dipoles and not on the theoretical definition of the nominal orbit.

### Amplification factor

A campaign of numerical simulations dedicated to Alignment is necessary to explore the lattice in terms of:

- Amplification factor.
- Tolerances of magnets and girder positioning.
- Alignment accuracy sensitivity to Machine length (longer wavelength tolerances). Such a study was carried out for the ESRF-EBS<sup>1</sup>.
- Making the choice of the instrumentation (laser tracker, ecartometry, Hydrostatic Leveling System).
- Utility of measuring dipole angles.
- Realignment frequency.

These preliminary studies are planned for the TDR phase. They will help us defining the necessary and appropriate specifications in order to minimize errors and extra costs in the alignment mission.

Table 25 lists relevant alignment tolerances extracted from SOLEIL upgrade's accelerator physics requirements.

Magnets on their girders	$\sigma_{RMS}$
Misalignment x/y	30 $\mu\text{m}$
Roll	50 $\mu\text{rad}$
Girders	$\sigma_{RMS}$
Misalignment x/y	100 $\mu\text{m}$
Roll	50 $\mu\text{rad}$
Girder-to-girder misalignment	limit
Horizontal	$\Delta x_{girder,i+1} - \Delta x_{girder,i} < 50 \mu\text{m}$
Vertical	$\Delta y_{girder,i+1} - \Delta y_{girder,i} < 30 \mu\text{m}$

Table 25: Relevant magnets and girders alignment specifications

### Mechanical and magnetic designs

The mechanical and magnetic designs of all multipole components, as well as the magnetic measurement benches, will include a study of metrology loops defining alignment tolerances on the storage ring. Equipment tolerances are then included in the overall positioning error budget, from machining to final alignment.

### Instrumentation

The instrumentation of the Alignment-Metrology group mainly includes laser tracker and ecartometer for planimetry, and laser tracker, inclinometer, optical level and Hydrostatic Levelling System (HLS) for altimetry. The HLS system has the advantage of having the same accuracy regardless of the distance from the measurement point.

An estimate of the laser tracker accuracy is given as it will be the main instrument used. Typical maximum measurement distances are  $D=1.50\text{m}$  for the alignment of the girders and  $4\text{m}$  for the girders on either side of a long straight section. The estimated accuracy of the laser tracker in horizontal (X) and vertical (Y) directions are the following:

$\sigma_x = 10 \mu\text{m}$ ,  $\sigma_y = 13 \mu\text{m}$  on an achromat and  $\sigma_x = 20 \mu\text{m}$ ,  $\sigma_y = 30 \mu\text{m}$  on the long straight section.

In comparison, accuracy with ecartometry is  $\sigma_x = 5 \mu\text{m}$  for a distance of about  $15\text{m}$  including the two girders defining a long straight section, and with the HLS system is of  $\sigma_y = 5 \mu\text{m}$  whatever the distance between girders.

HLS is foreseen for the initial storage ring vertical alignment. In this case, few sensors are necessary because it is possible to move them from one cell to another. The system can also be used for permanent monitoring, in which case all girders must be equipped

with sensors. Nevertheless, the small size of the girders and the compactness of the upgrade storage ring requires smaller sensors than those currently in use.

### Magnet fiducialization

The fiducialization of magnets connects the magnetic center to external mechanical references. This step is necessary in order to align the magnetic centers on the orbit of the upgrade storage ring, even if the magnets are individually positioned on their girder by purely mechanical means. All fiducials on quadrupoles, reverse bends and dipole magnets must be installed at the same height in order to maintain their full visibility all along the tunnel. The idea of lateral offset of fiducials as on the present storage ring is retained only on girders located at either side of the straight sections in order to be able to use ecartometry and to ensure their visibility from beamline alignment windows and beamline front end.

Many of the magnets used in the CDR reference lattice will be based on permanent magnet technology, leading to compact designs which improve the quality of alignment by reducing the angular lever arms.

The fiducialization technique, used for the present machine, is based on a mixture of mechanical and magnetic measurements. This approach will be reused for the SOLEIL upgrade since the results in terms of accuracy and reliability were very good. It consists of a portable and lightweight mechanical structure to be centered on the magnet's fiducials and equipped with displacement sensors at its ends. These sensors detect the position of the magnetic measurement bench stretched wire in position on the center of the magnet.

However, it will be necessary to study a different detection technique than that used for the current machine, since the magnetic measurements will be carried out by stretched wire and not by a coil.

### Magnets alignment on girder

The configuration of the SOLEIL storage ring tunnel imposes a smaller girder dimension compared to the present machine. The longest girder of the proposed implementation measures  $1.80\text{m}$ . Such small dimensions objects are favorable to alignment operations because they are easier to adjust. One can use SOLEIL mechanical know-how at this stage by reusing the adjustment techniques of the previous machine: the magnets are purely aligned by the centering mechanics of the girder (via precisely machined surfaces and straightness references).

<sup>1</sup>Alignment of the ESRF Extremely Brilliant Source (EBS), p.10, IWAA2018 Fermilab Chicago, David Martin



136 girders, out of 212 of the proposed implementation, support multipolar magnets to be aligned precisely with respect to each other. In order to obtain the tight required alignment tolerances, it is also planned to study the capability of a pulsed wire technique to detect the zero positions of all the magnets directly on their common girder. The 76 other girders support a single long dipole, and consequently do not need the above approach for magnet inter-alignment.

### Alignment of vacuum chambers and BPM

The vacuum chambers of the cells have a typical internal diameter of 10 to 12 mm. In the case of *ex situ* vacuum bake-out, the distance between the magnet poles and the chamber is only 1 mm. The question of their positioning is therefore important, especially if a set of chambers per cell is baked as a whole. In this case, the assembly can suffer from angular imperfections of the flanges causing a deformation of the whole, which can be out of tolerance for inserting the chamber set into the magnet poles all along the cell. In the current study, some BPMs may be machined *in situ* on the chambers. Their positioning will be done mostly by mechanical centering on the girder. Detailed studies of these two topics are planned in the TDR phase.

### Global alignment of the storage ring

The large number of girders (212) implies a significant increase in alignment work compared to the present machine (56 girders).

It is proposed to align the girders by using only the quadrupole magnets to define the beam orbit of the storage ring. The basic instrument for planimetry is the laser tracker that can measure or adjust 2 or 3 girders from a station. The straight sections are too long to maintain the accuracy achievable on the cells. Ecartometry, regularly used on the current machine, makes it possible to compensate this weakness in the horizontal plane at a low cost. This is an opportunity to study a more compact and accurate ecartometer model based on capacitive sensors.

The altimetric adjustment of the storage ring can be mostly achieved with the HLS. The current SOLEIL storage ring has been successfully aligned with this method by equipping each girder with 3 sensors to adjust elevation and horizontality. Recent developments in the Alignment-Metrology group make it possible to achieve 10  $\mu\text{m}$

accuracy ( $1\sigma$ ) by linking the zeroes of HLS sensors to the magnetic centers of the quadrupole magnets.

Further simulations are needed to determine whether this instrumentation is to be retained or not. It is also possible to reduce the number of sensors in order to reduce the cost. In this case, HLS is used only for alignment and not for permanent alignment monitoring.

The laser tracker-based measurement network will be simulated to determine the absolute position errors of the quadrupole magnets and relative errors between them. This kind of simulation leads to the estimated alignment errors, given above in section Lattice Design, considering a laser tracker for the individual alignment of a girder.

### Realignment periodicity

HLS system and laser tracker planimetric surveys have enabled the monitoring of the settlement level of the current storage ring over a period of more than 10 years. It is not possible to separate the sources of disturbances (geophysical and/or mechanical). A first study reveals amplitudes of displacement between adjacent girders to  $\pm 200 \mu\text{m}$  in the vertical direction « Y » and  $\pm 250 \mu\text{m}$  in the horizontal direction « X ». These values can be extrapolated and applied to the proposed mechanical implementation for the upgrade by simulating the corresponding closed orbit distortion. It is therefore possible to estimate the frequency of realignment, if needed.

## Mechanical engineering

The mechanical engineering group is involved directly or indirectly in most studies, prototyping and R&D programs which are presented directly in the corresponding sections (vacuum

chambers, absorbers and RF bellows are detailed in the vacuum system section, BPM prototypes in Diagnostics, the new generation of undulators in Photon Sources etc.). The content of this section focuses on girder design and its consequences on the layout and alignment methods for the new storage ring.

### Girder design

The current girder set of SOLEIL consists of 4 girder types weighing from 1.85 t to 3 t, with a respective mass payload of 4.1 t to 8 t and lengths of 2.40 m to 4.80 m. The smaller size of magnets used for the SOLEIL upgrade allows a dramatic size and weight reduction of the magnet-girder assemblies (Figure 57). On the other hand, the number of magnets and girders has increased by a factor of 3, implying longer alignment and installation operations. Another constraint is due to the high compactness of the new lattice causing some limitations and access restrictions in the area between girders and tunnel wall.

### Design baseline

The design of the new magnet-girder assemblies considers experience gained from the existing installation, using concepts with proven efficiency and good performance in terms of stability. However, some other features are not optimized for the new storage ring and had to be adapted or totally redesigned. Indeed, the large number of girders and magnets in the new lattice, leading to a need to reduce unit cost and alignment time, are two main parameters to be considered.

The new design includes 4 girder types. The long (1.80 m), medium (1.5 m) and short (1.24 m) types are used for multipole sections whereas a fourth one (0.96 m) supports long dipoles. The construction of the girders uses welded steel plates

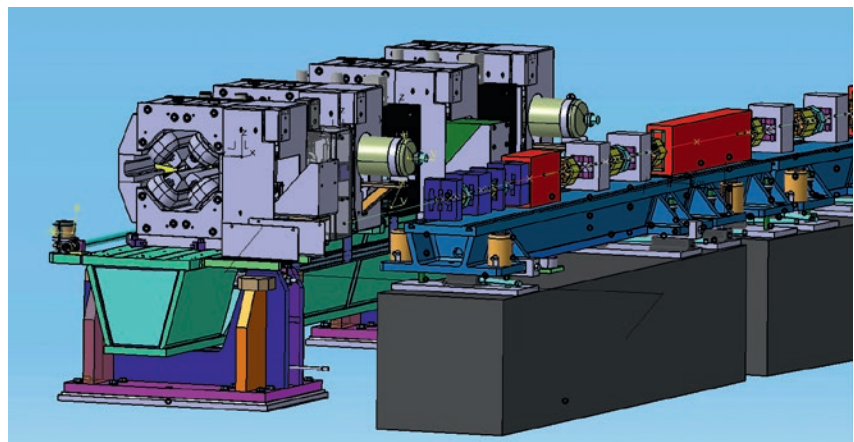


Figure 57: Comparison of the magnet girder assembly between SOLEIL (left) and the upgrade (right)

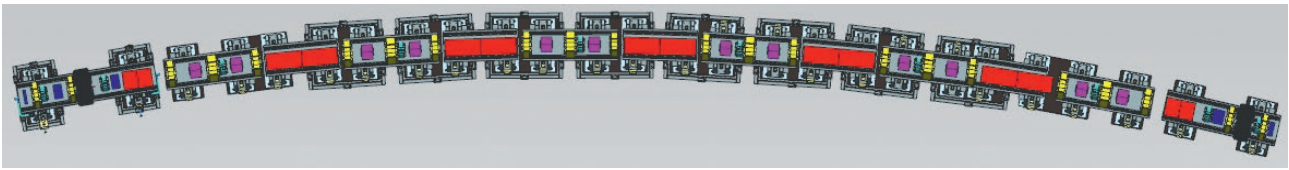


Figure 58: 7BA cell layout (dipoles in red)

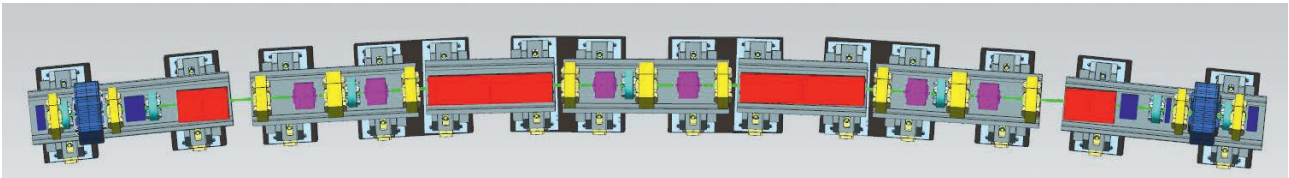


Figure 59: 4 BA cell layout (dipoles in red)

associated with cast steel parts common to the 4 types, allowing more complex shapes and reducing manufacturing cost (Figure 57). The small size of magnets makes it possible to reduce the distance between beam axis and the upper face of girders, improving overall stability. The girder position is then higher with respect to the ground, imposing increased stability requirements on the girder support structures. The new layout features granite plinths as girder supports, a technology that has been used with great success for supporting vibration and drift sensitive instruments on the beamlines. These blocs are aligned, in all directions, with an accuracy of  $\pm 1$  mm and grouted to the ground. Fine girder alignment is achieved using 3 wedges for vertical adjustment and 2 push-pull screws for horizontal position. Due to the high stability of the SOLEIL slab, very few alignment corrections were necessary during the 15-year operation of the machine. For this reason, motorization of the positioning system is not envisaged, particularly when considering its extra cost and increased tunnel heat budget. Considering the difficult access to the outer side of the machine, all the adjustment devices are accessible from

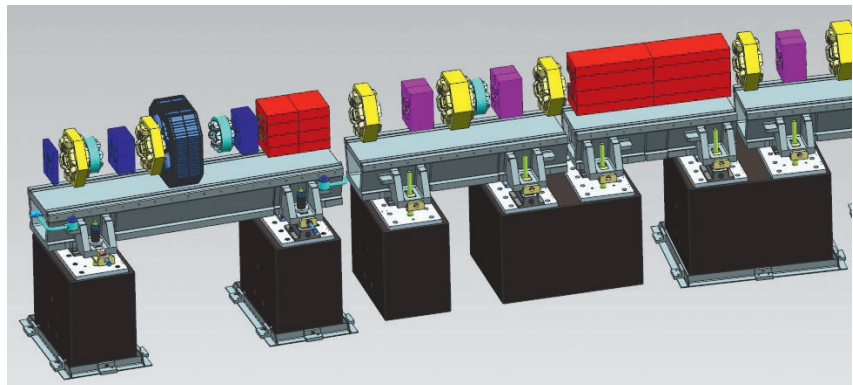


Figure 60: 3 girder types common to 4BA and 7BA cells

the inside face of girders. The current SOLEIL girder layout features 3 alignment points and 4 releasable manual clamping points. This design allows a kinematic positioning of the girder when the clamps are released, making alignment easier and improving linking stiffness after clamping (for example the 4.8 m girders feature a 47 Hz fundamental resonance frequency). Even if it would be possible to implement a similar system on the new girders, there is not a strong interest for using a complex releasable clamping in the case of the high stiffness/mass ratio of the new design.

Stiffness can simply be improved by applying a permanent vertical preload on wedges using compression springs.

SOLEIL storage ring is equipped with a HLS (Hydrostatic Levelling System), monitoring the vertical position of each girder and used as a survey system. The possibility to use the HLS system to align the girders is kept with some adaptations in the upgrade layout. The new design implements a tooling referenced on the girder side face to set magnets on the beam axis with the requested accuracy.

Girder type	Length	Width* x Height	Mass	Payload**	Number
Long	1800 mm	400 / 670 mm x 250 mm	712 kg	500 kg	8
Medium	1500 mm		650 kg	400 kg	32
Short	1240 mm		570 kg	300 kg	96
Dipole	960 mm		485 kg	490 kg	76

\* Top plate/fixation base

\*\* Estimated values

Table 26: Girder characteristics summary

Plinth type	Width x Height	Length	Mass	Number
Double	700 x 575 mm	850 mm	923 kg	168
Simple		400 mm	435 kg	64

Table 27: Plinth characteristics summary

### General layout

Effort was made to reduce the diversity of girders in order to reduce cost and simplify installation / production. The symmetry of the new lattice cells (see Figure 58 and Figure 59) allows the use of 2 main types only, provided that magnet positioning can be achieved in the same way on both ends of the cell. The 8 long girders are only used on both sides of long straight sections. The type common to long dipoles straddles 2 adjacent plinths. Using a girder as a dipole support allows for fine setting and avoids the low resonance frequency of dipoles encountered on the present SOLEIL setup. Figure 60 shows a typical layout common to 7BA and 4BA



segments where the 3 types of magnet-girder assemblies can be seen. [Table 26](#) and [Table 27](#) summarize dimensions and weights.

### Girder construction

In order to reduce manufacturing costs, the 4 girder bodies use only a total of 18 different elements. Each type uses 6 parts (see [Figure 61](#) and [Figure 62](#)): top, bottom, left and right plates welded with 2 cast steel end parts. Dipole girders use the same end parts in an inverted position (see [Figure 63](#) and [Figure 64](#)).

The end parts, made of cast steel, integrate functions as fixation, setting, HLS support and lifting points. In addition to cost

reduction, casting allows realization of continuous internal stiffeners and limits stress caused by welding. Functional surfaces of girders are machined after welding and stress relief treatment.

### Fastening and adjustments

The setting and fastening systems are located on steel plates screwed and glued on the top of plinths. Each girder is placed on 3 commercial NIVELL® DK3 jacks (featuring 7 mm setting range and a very high load capacity), one located on the upstream plate in the center ([Figure 65](#)) and two others placed symmetrically on the downstream plate ([Figure 66](#)). Despite the improved dynamic performances of a 4-tightening point configuration, the choice

of a 3-point configuration has been made to simplify the alignment operation (with 4 jacks it is difficult to control the twist of the girder). However, the high stiffness/mass ratio featured by the new machine gives a lower calculated resonance frequency near 100 Hz in the worst case (long girder) as detailed in “Dynamic simulations”, next page. Girder position along the beam axis is referenced by a spherical link in the center of the downstream plate ([Figure 67](#)). The sphere position is set by the alignment team before installing the girder.

Fastening is achieved using 4 sets of vertical rods and compression springs applying a 1 t preload at each point. It can be noticed that 2 t are applied on the central jack. This effort is permanently

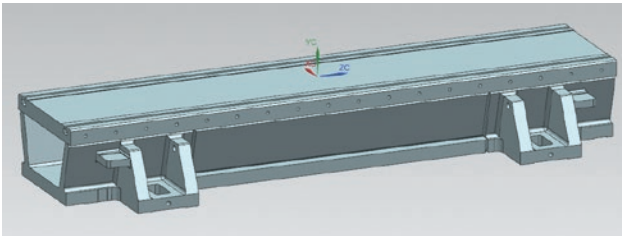


Figure 61: Long girder beam

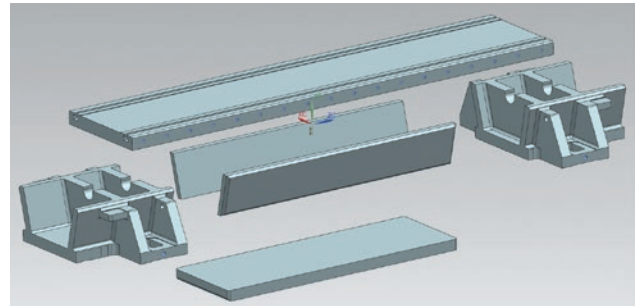


Figure 62: Long girder components

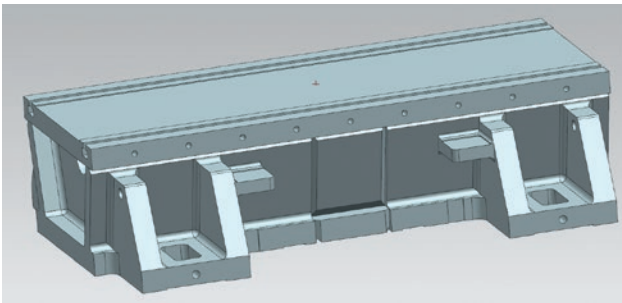


Figure 63: Dipole girder beam

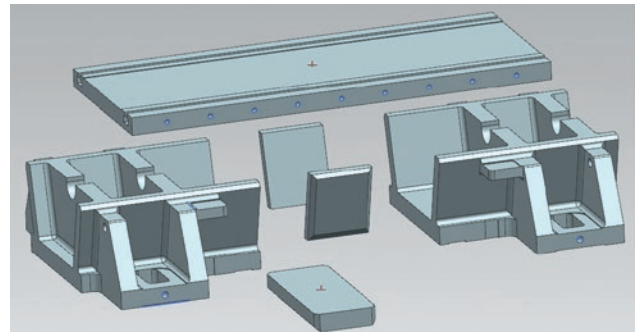


Figure 64: Dipole girder components

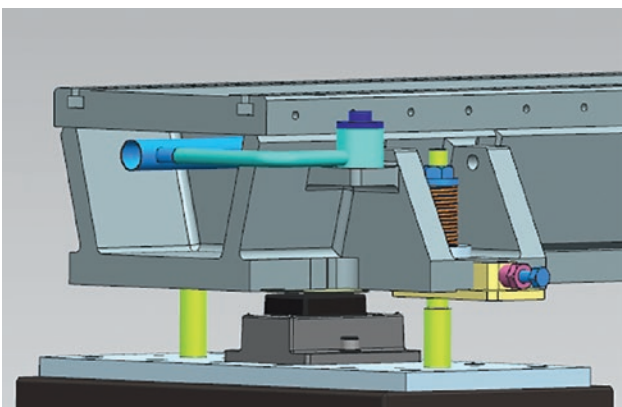


Figure 65: One point adjustment plate

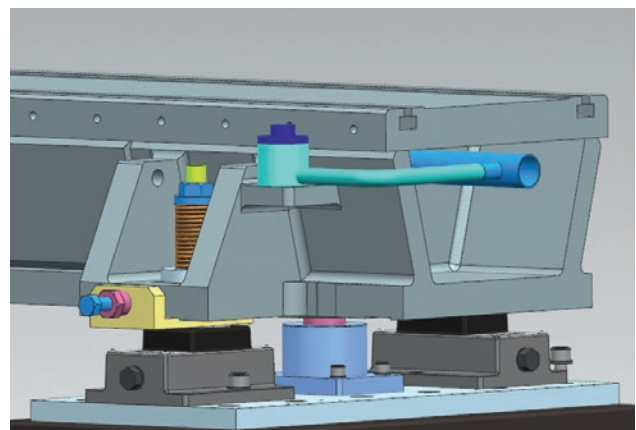


Figure 66: Two point adjustment plate

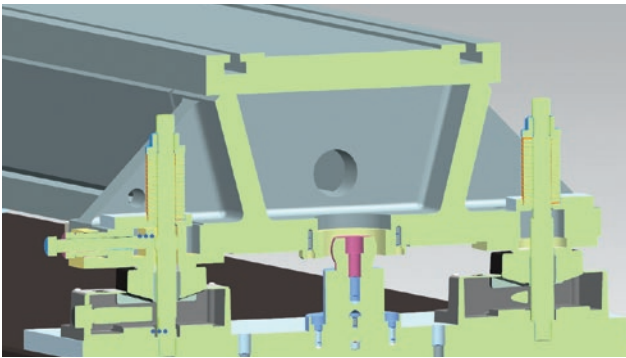


Figure 67: Spherical positioning point

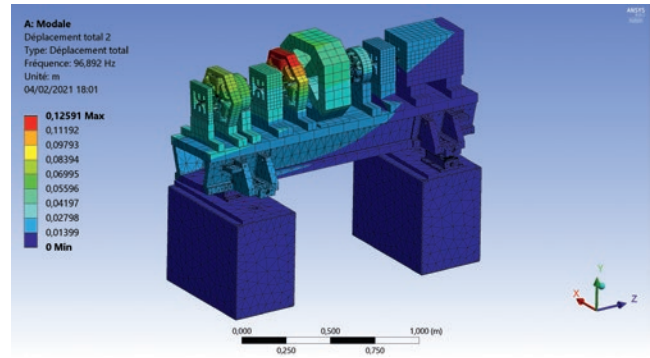


Figure 68: First resonance frequency simulation

applied, but allows sliding movements during the alignment operations (Table 28). Horizontal position adjustment is achieved using push-pull screws located on the inner side of girder, backlash is eliminated by tightening the opposite screws. A set of removable sensors monitor the position of the girder during alignment. Each girder can be equipped with 3 HLS sensors used as a reference to control long term motion.

**Magnet positioning and fastening**

Magnet position is referenced to the top face of the girder and the side surfaces of the plate. Both are machined with a ±15 µm max flatness tolerance. After alignment, magnets are fastened to the girder using the T-slots of the girder top plate. Further investigations are in progress in collaboration with Magnet and Alignment groups.

**Dynamic simulation**

Simulation by Finite Element Analysis (FEA) has been carried out for the 4 types of girders. Magnets are simulated by their 3D models, defined by a preliminary design. Jacks are modelled with their real

shape and materials in order to accurately estimate stiffness. However non-linear effects are not yet been considered. Thus, the effect of preload does not appear in the results. As an example, the lowest resonance frequency (twist mode) of the long girder is 97 Hz (Figure 68 and Table 29) which is much stiffer than the current SOLEIL girders (around 50 Hz).

**R&D program**

Several design features of the magnet-girders must be validated by the realization and test of a prototype. A long girder featuring all the characteristics of the planned model will be realized and loaded with dummy magnets in order to carry out vibration response tests. The aim of these tests is to check the validity of FEA calculation, in particular the influence of estimated characteristics leading to uncertainties such as jack stiffness or preload influence. If necessary, improvements will be made on the girder design. This prototype will also permit to validate alignment procedures for the girder itself and the magnets.

As design proceeds, this prototype will be equipped with all equipment (such as vacuum chamber, cables, and fluids), in order to validate and improve the mounting process.

In parallel, an R&D program is launched on the fabrication methods of the upgrade machine vacuum chambers. The main goal would be to verify the feasibility of 3D metal printing procedures to construct complex vacuum chambers in high purity copper or CuCr1Zr alloys.

**Power supplies**

This section describes the key aspects of the storage ring power supplies, along with the main characteristics, number and types of required power supplies, the main design choices considered for these systems, as well as the principal challenges to be faced.

**Key issues and challenges**

Notwithstanding the extensive use of permanent magnets for the storage ring, the new lattice requires a significant increase in the number of power supplies as compared to the existing lattice (from 390 to more than 1200), which brings challenges on the following aspects:

- Power supply availability: The objective, like for the existing machine, remains a user beam availability higher than 99% and a Mean Time Between Failures (MTBF) higher than 100 hours. To contribute to the achievement of this aim, a maximum number of 5 machine trips per year caused by the overall power supply system is targeted.
- Space required for the power supply racks: The storage ring power supplies will be installed in the technical service area, where additional rack space is limited.

Girder type	Y (vertical)	X (horizontal)	Ry (yaw)	Rx (pitch)	Rs (roll)
Long			± 0.47°	± 0.17°	
Medium	±3.5 mm	±10 mm	± 0.57°	± 0.20°	± 0.83°
Short			± 0.77°	± 0.27°	
Dipole			± 0.84°	± 0.29°	

Table 28: Adjustment range on the girder

Girder type	Mode 1	Mode 2	Mode 3	Mode 4
Long	97 Hz	213 Hz	244 Hz	247 Hz
Short	139 Hz	248 Hz	284 Hz	392 Hz
Dipole	143 Hz	266 Hz	286 Hz	411 Hz

Table 29: Summary of vibration modes for 3 types of girder



Magnet type	Type		No. per cell		Power Supply type	Power Supply No.
	Permanent magnet	Electromagnetic	7BA cell	4BA cell		
Bend	116		7	4		
Reverse bend	192		12	6		
Quadrupole	104		6	4		
		40	2	2	1Q 80A, 6V	40
Sextupole		368	22	13	1Q 50A, 6V	368
Octupole		176	10	7	1Q 20A, 10V	176
Quadrupolar corrector		176	10	7	4Q 40A, 10V	176
Skew Quad corrector		92	5	4	4Q 20A, 10V	92
Horizontal & Vertical corrector		352	22	13	4Q 20A, 10V	352
<b>Overall total</b>						<b>1204</b>

Table 30: Power supply needs for the new lattice

- Needed manpower: The design, construction and testing of all these power supplies will exceed the capacity of the Power Supply group. Substantial work will have to be performed externally.
- Operation of a high number of power supplies: To efficiently manage and operate such a large park of equipment, dedicated software tools are necessary. These tools should notably provide advanced online/offline measurements analysis and post-mortem functionalities (for effective fault diagnosis, breakdown prevention), auto-calibration, remote firmware updates.

Another important issue relates to the stability requirements for the low emittance beam (< 100 pm.rad), and to the fact that the cut-off frequency of the small size (with a diameter of 10 mm in arcs) vacuum chambers of the sextupole magnets, which also integrate the correctors for slow orbit correction, is much higher compared to the existing one (about 1 kHz, against 10 Hz for the present aluminum chamber). This translates into a higher precision requirement and a very

low current ripple specification for the orbit corrector power supplies, as it will be presented in Table 31.

### Main power supply characteristics

The storage ring lattice is divided into 20 cells, with an alternation of 7BA and 4BA cells. Table 30 summarizes the distribution of magnets over these different cells and the corresponding power supplies needs. All the electromagnets are intended to be individually energized. These parameters, which are not yet definitive at this stage, will have to be refined collaboratively with the Magnet group. The guiding principle is to standardize the equipment as far as possible, to reduce the output current ratings and hence lower the DC cables cross-sections as well as the overall power losses. For now, 4 different types of power supplies are necessary: 80A/6V unipolar power supplies (for the quadrupoles), 50A/6V unipolar power supplies (for the sextupoles), 40A/10V bipolar power supplies (for the quadrupolar correctors), and 20A/10V bipolar power supplies (for all the other magnets). It is worth noting that the global electrical consumption for the storage ring power

supplies (including low level electronics) is expected to be reduced by about two thirds as compared to the existing machine.

The performance requirements for the above listed power supplies are detailed in Table 31: Amongst these requirements, the ones for the slow orbit feedback corrector power supplies, in particular, are critical, and will request careful design both for power and control parts.

### Main design choices

The foreseen strategy for the control of all the needed power supplies is to use a universal control electronics platform. Having a single standardized controller is indeed a major advantage in terms of cost reduction, human resources / time required for system implementation, operation and maintenance, as well as obsolescence management. Amongst the solutions currently being studied, the CERN power converter control system<sup>[1]</sup> is notably being evaluated on the existing machine (within the TANGO framework). This control platform, now available through licensing, is the standard at CERN in the medium to long term (2035 at least). It can manage all sorts of

Magnet type	PS Bandwidth	Current resolution	Current ripple/noise	Stability 8 hours	Stability 7 days	Absolute precision
Quadrupole	10 Hz	15 ppm	10 ppm RMS	±10 ppm	±100 ppm	500 ppm
Sextupole	10 Hz	15 ppm	10 ppm RMS	±10 ppm	±100 ppm	500 ppm
Octupole	10 Hz	15 ppm	10 ppm RMS	±10 ppm	±100 ppm	1000 ppm
Quadrupolar corrector	100 Hz	15 ppm	100 ppm RMS	±10 ppm	±40 ppm	500 ppm
Skew Quad corrector	100 Hz	15 ppm	100 ppm RMS	±10 ppm	±40 ppm	500 ppm
Horizontal & Vertical corrector	100 Hz	5 ppm	5 ppm RMS	±10 ppm	±40 ppm	1000 ppm

Table 31: Performance requirements for the storage ring power supplies

power converters, including commercial off-the-shelf products. The advantages of this solution include an extensive set of expert tools to efficiently manage a large park of equipment, and the guarantee that it will not be obsolete in the next couple of decades.

For the power part of the unipolar (1Q) power supplies, it is planned to supply commercial off-the-shelf voltage sources, with low output ripple and large input voltage range (to provide sufficient immunity against mains voltage dips). These voltage sources will be embedded with precision current transducers and the adopted standardized control electronics (where the current loop is implemented) to build high precision current sources.

For the input stage of the 4-quadrant (4Q) power supplies, the use of commercial off-the-shelf n+1 redundant power supplies is considered. This choice will notably ensure a better overall system availability, and minimization of the space and volume needed for the 4Q power supplies. In addition, by choosing large voltage input range supplies, the new system will be insensitive to most network disturbances. The resulting low voltage DC link will be distributed to the standardized 4Q output power converters, which are planned to be designed in house. Studies are currently being carried out to introduce redundancy at this output stage level in order to further increase the availability. Besides, other studies aim at determining

whether the power supplies (notably those for the slow orbit feedback system, which require a high current stability) have to be installed in water-cooled cabinets. It has to be noted that the horizontal / vertical trim power supplies needed for the newly installed insertion devices will use the same standardized output power modules.

**Physical space requirements**

The estimates of required space for the storage ring power supplies are outlined in the Table 32, below: The total number of cabinets amounts to 52, as compared to the 55 existing ones, which confirms that the storage ring power supplies can be accommodated within the technical service area, as foreseen.

Cell	Power supply type	Subsystem	No. per cell	No. per 19-inch sub-rack	Sub-rack height (U)	Total rack units (U)	No. of 47U cabinets per cell
7BA cell	1Q 80A, 6V	Voltage source	2	1	2	4	3
		Controller	2	2	3	3	
	1Q 50A, 6V	Voltage source	22	2	2	22	
		Controller	22	4	3	15	
	4Q 40/20A, 10V	Output power module	47	4	3	36	
		Controller	47	4	3	36	
DC link supply		2	1	1	2		
4BA cell	1Q 80A, 6V	Voltage source	2	1	2	4	2
		Controller	2	2	3	3	
	1Q 50A, 6V	Voltage source	13	2	2	13	
		Controller	13	4	3	9	
	4Q 40/20A, 10V	Output power module	31	4	3	24	
		Controller	31	4	3	24	
		DC link supply	2	1	1	2	

Table 32: Space requirements for the storage ring power supplies

**REFERENCE**

[1] Page, S., Afonso, J., Ghabrous Larrea, C., Herttuainen, J., King, Q., Todd, B. "Adaptation of CERN Power Converter Controls for Integration into Other

Laboratories using EPICS and TANGO", Proceedings of ICALEPCS2019, MOPHA105, New York, NY, USA (2019).



## Vacuum systems

### Introduction

The vacuum system of the SOLEIL upgrade has to fulfill a number of performance requirements to enable an optimized operation of the new Storage Ring (SR). Among them, vacuum performance, heat load management and impedance budget of the overall machine have to be specifically addressed:

- **Vacuum performance:** the vacuum system shall provide and maintain an average pressure of below  $10^{-9}$  mbar all around the SR at the maximum current of 500 mA after an integrated beam dose of 100 A.h.
- **Heat load management:** vacuum vessel walls and absorbers shall be designed to provide the correct power handling and heat dissipation of synchrotron radiation from bending magnets and insertion devices.
- **Low Impedance budget design:** geometric effects on the machine impedance can be minimized by lowering the gaps and steps between flanges, reducing and softening the transitions along the electron beam path and by using shielded RF bellows. The chambers' surface characteristics, like roughness or resistivity, shall be estimated to control the Resistive Wall effects.

However, the SOLEIL upgrade project pushes the vacuum system conception to a new limit: the high gradient quadrupoles of the 7BA-4BA achromat (over 110 T/m) and the large strength of the sextupoles ( $8000 \text{ T/m}^2$ ) require the minimum size of the vacuum chamber inner diameter to be as low as 10 mm.

The SOLEIL facility followed by the new synchrotron light sources, like MAX-IV and SIRIUS, opened up the way [1]: they demonstrated that Non-Evaporable Getter (NEG) can be extensively used such that the required vacuum level can be achieved in a conductance limited system by partly compensating the standard "lumped pumps scheme" with NEG coating (MAX-IV and SIRIUS have a minimum vacuum chamber size of 22 mm and 24 mm inner diameter, respectively).

For the SOLEIL upgrade, with a characteristic size of the vacuum chambers as low as 10 mm with commensurate conductance reduction, the level and quality of the vacuum will depend mostly on the NEG pumping performances and

only partially on discrete standard pumping (mainly to pump methane and noble gases or in specific location with extra Photon Stimulated Desorption (PSD) gas load). As a consequence, preliminary calculation of the vacuum pressure profile along the lattice is meaningless without a fine study of the NEG pumping properties in small tubes and under synchrotron radiation. Parameters such as initial pumping speed (sticking factors), saturation threshold (sorption capacity), balance between pumping and photodesorption and photodesorption evolution with the beam dose must be carefully considered [2,3,4].

The strong strength lattice magnets also result in an extreme compactness and in very narrow drift spaces to insert the vacuum elements (pumps, flanges, absorbers, valves). Especially, extraction from the ring of the required photon fan for each beamline through the available aperture has to be considered.

### Vacuum system pre-conception strategy

The main features of the SOLEIL upgrade vacuum system are:

- Full distributed pumping provided by TiZrV NEG coating of an average thickness of 1  $\mu\text{m}$  and discrete Sputter Ion Pumps (SIP) as close as possible from extra PSD gas load like in photon extraction areas.
- *Ex situ* bakeout to facilitate the initial conception of the ultra-compact vacuum system and to avoid any risk of damaging the permanent magnet elements of the lattice. This well-considered decision is based on a clear positive feedback from the new generation SR with NEG coating pumping which are already in operation like MAX-IV or in the final conception phase like SLS-II. The choice of *ex situ* bakeout is also backed-up by the proven practice of "Neon venting" for vacuum interventions which preserves the NEG coating activation [5].
- Extensive use of OFS copper (Silver-Bearing Oxygen Free Copper, Ag-0.02/0.12%) for vacuum chambers and absorbers materials but also the likely use of copper alloy like CuCrZr as an alternative for absorbers and flanges.
- Distributed photons power absorption of the Dipole photons emission along the Cu-OFS vacuum vessels walls on the horizontal mid-plane.

The pre-conception strategy is based on:

- 1• Development and capacity building

of in-house NEG coating deposition and characterization

- One NEG coating magnetron sputtering facility already operational for the existing SOLEIL ring.
  - Two transmission factor test benches in the SOLEIL vacuum laboratory for pumping speed and sorption capacity measurements. Calibration of the benches parameters with MOLFLOW+ [6].
  - One PSD measurement beamline on the Dipole D08-1 photon exit of the present SR. Chamber lengths from 20 cm to 2 m and diameters from 6 mm to 63 mm can be tested.
- 2• Effective collaborations for a better understanding of the NEG behavior in small tubes
    - Collaboration agreement (CONV-19-014) between SOLEIL and SAES-Getter Spa to study with or without photon beam irradiation the downscaling properties of the NEG coating: sticking factors, sorption capacity and PSD measurements.
    - MTA & NDA agreement (CV-20-012) between SOLEIL and the Berkeley Lab (ALS) for PSD studies of 6 mm inner diameter tubes.
  - 3• A "photon extraction task force" to tackle the specific challenge of the photon beam delivery to beamlines in the framework of the SOLEIL upgrade lattice. This implies regular meetings and feedback documents between accelerator physicists, magnets and undulators conception team, mechanic and vacuum people.
  - 4• Step by step consideration of the impact of the vacuum system conception on the Impedance budget of the machine to minimize impedance-driven beam instabilities: NEG coating type and thickness, type of absorbers and pumping ports, vacuum vessels material and shape are periodically reviewed.
  - 5• A first prototyping phase of the flanges type and RF bellows to evaluate their technical feasibility and added value to the project.

### Vacuum system general layout – Vacuum chambers pre-design

The basic layout of one fourth of the future ring is shown in Figure 69. The 7 bending achromats and the 4 bending achromats (7BA-4BA) are successively separated by upstream and downstream Straight Sections (SS) of different lengths. The new lattice has 4 types of SS: two types of Long SS (7.355 m and 7.661 m long), one type of Mid SS (4.151 m long) and

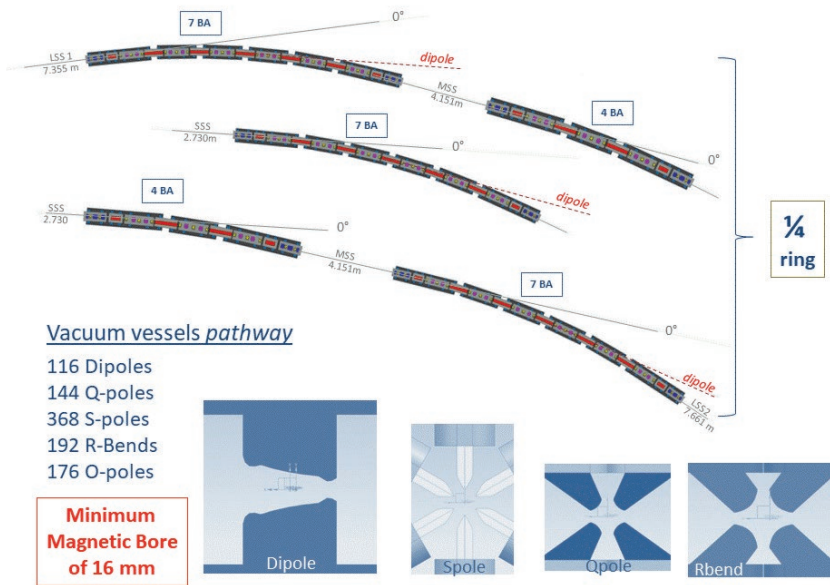


Figure 69: Basic layout of a quarter of the future ring. The 7BA and 4BA achromats are separated by long, medium and short straight sections (SS)

one type of Short SS (2.730 m long). This configuration allows to extract the photon beam for a maximum of 20 undulator beamlines (the distribution and total number of undulator beamlines along the ring will depend on the implantation scheme of the Injection and RF cavity elements). In addition, for each 7BA achromat, one photon beam extraction from a 1.7 T or 3 T superbend can be considered. Overall, this new lattice layout covered the need of about 32 beamlines and is compatible with the SOLEIL upgrade experimental strategy. The vacuum vessels pathway crosses 116 dipoles, 144 quadrupoles, 368 sextupoles, 176 octupoles and 192 reverse-bends. The minimum magnet bore diameter is 16 mm.

Figure 70 shows in more detail the compact magnetic lattice elements. The small size of the empty drift spaces limits a large-scale installation of lumped vacuum pumps and many of these spaces will be shared with BPM blocks (an installation of more than 176 BPM blocks are planned). This severely reduces the number of possible standard pumping locations (SIP types) to a maximum of about 10 in a 7BA cell and of about 5 in a 4BA cell. It leads to a worst case configuration for one third of the ring length with approximately one SIP pump every 1.4 m drift of 10 mm inner diameter pipe.

The pre-design of the SOLEIL upgrade SR vacuum chambers is based on two generic shapes presented in Figure 71: through the geometric pattern of the sextupoles, quadrupoles, reverse-bends, and octupoles, an inner ellipsoid profile

of 10 mm in vertical and 12.4 mm in horizontal could be considered (for conservative estimations a circular 10 mm inner diameter pipe will be used later on for vacuum simulations). For the dipole chambers a geometric ellipse of 10 mm in vertical and 24 mm in horizontal (inside dimension) could be conceived. For the pre-conception phase the chambers have a 1 mm wall thickness and a 2 mm clearance between the vessels and the magnet poles. This would give us the possibility in the next design stage to choose between a general increase of the chambers inner diameter (up to 12 mm), to relax the magnetic design by reducing the magnetic bore radius

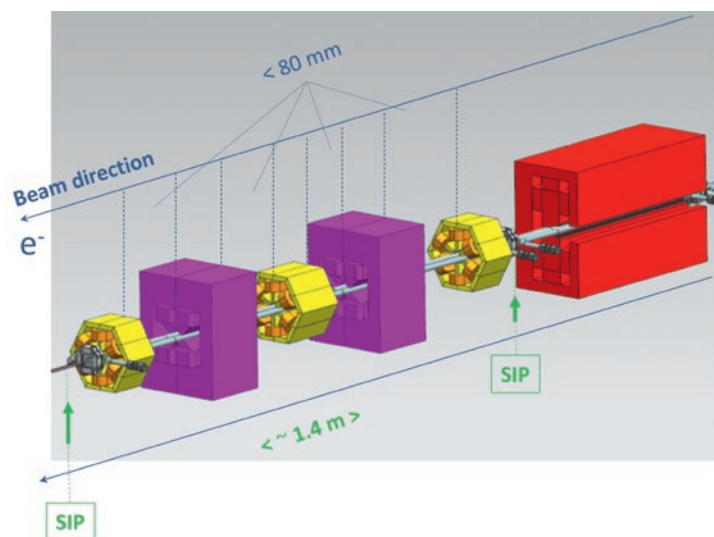


Figure 70: Detail of the compact magnetic lattice with one dipole, 3 sextupoles and 2 reverse-bend elements. In the worst case configuration of the SIP pumps implementation, pumps are separated by a 1.4 m drift of 10 mm inner diameter pipe

by 1 mm, or increase the chamber wall thickness. These generic profiles will be adapted to deal with the photon beam extraction issues or the geometric transition requirements to reduce the beam instabilities (see Photon extraction challenge). Vessel material will be mainly Silver bearing OFS copper alloy due to its appropriate combination of mechanical, magnetic, conductive and thermal properties.

Synchrotron radiation from bending magnets will be absorbed by longitudinal water cooling channels distributed along the vessel walls. Thanks to a large bending radius and a small angle of incidence the surface power densities in the vessels are significantly less than for the existing SOLEIL ring. At its maximum the synchrotron radiation power distribution will be less than 4 W/mm and the corresponding surface power density around 25 W/mm<sup>2</sup> which is easily handled with a plain copper material and an 8 mm diameter water channel outside of the vacuum vessel (Figure 71). At 500 mA in such a geometric and material configuration, a finite element simulation (ANSYS) shows a maximum temperature of the vessels skin of about 80 °C and an elevation of the cooling water temperature of 5 °C. In any case, the thermomechanical conditions are far below the OFS copper material yield strength.

As a transition between the two different chambers generic profile, a small pumping and absorption block of only 60 mm long could be designed. The transition slope is reduced to an 8° angle and is repeated on each side of every dipole chambers (dipole chambers with no photon beam extraction).

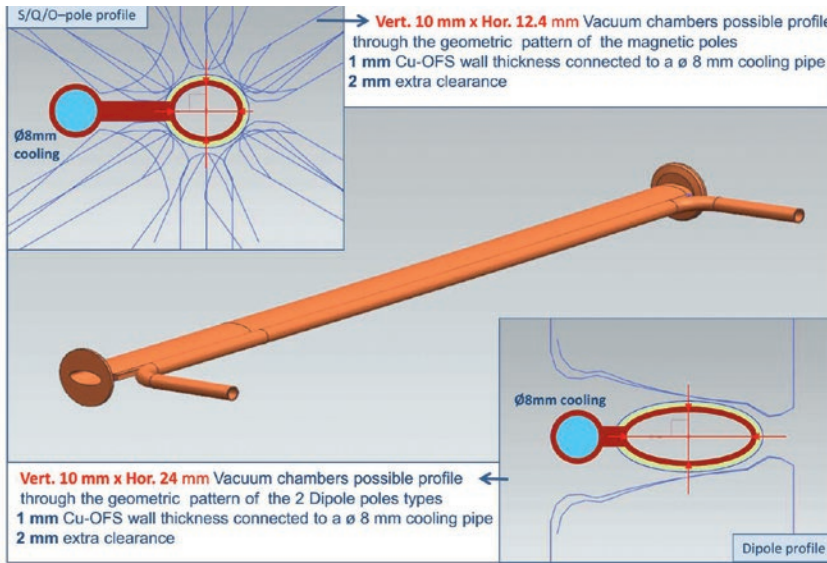


Figure 71: Detail of the vacuum chambers generic shapes of the SOLEIL upgrade ring

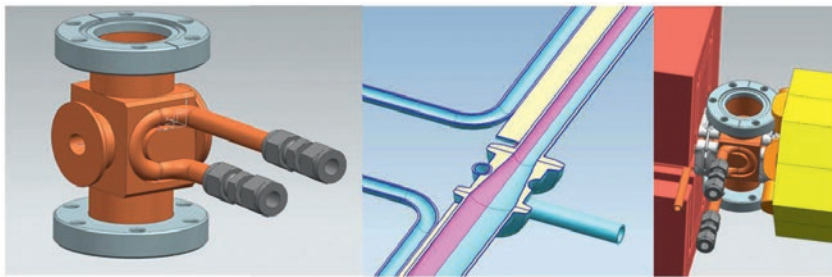


Figure 72: Example of a 60 mm long block for RF transition, pumping and synchrotron radiation power absorption

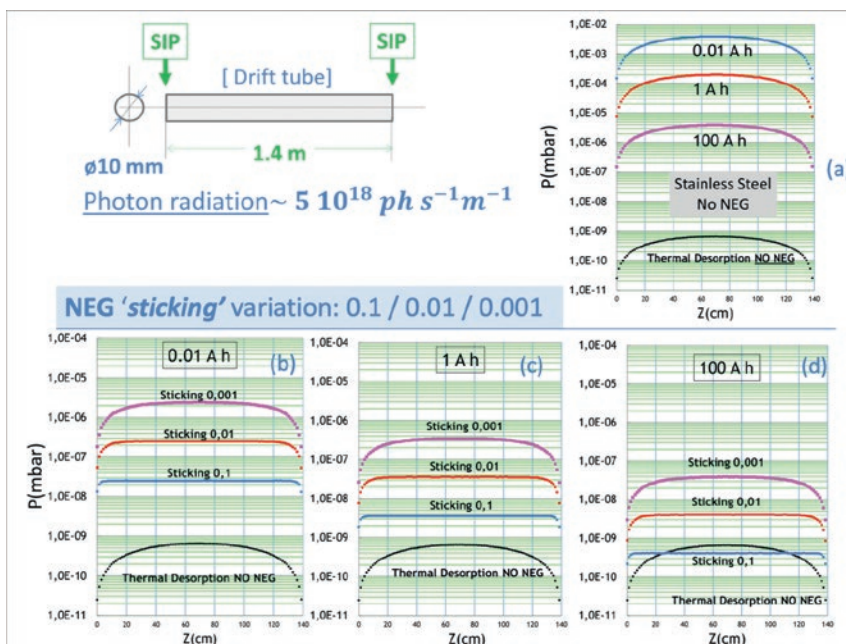


Figure 73: Simulations of pressure profiles in a 1.4 m drift tube with a  $5 \cdot 10^{18}$  ph/s/m beam irradiation for different cases:  
 (a) Stainless steel chamber without NEG  
 (b) NEG coated-chamber with a sticking probability of 0.1, 0.01(b) and 0.001(c)

A first estimation of the transition impact on the machine impedance budget is proposed in the Lattice design section but seems manageable from a beam dynamics point of view. An example of integration of these blocks between the chambers and inside the compact magnetic lattice is presented in Figure 72. Two DN40CF flanges could be used as pumping and vacuum measurement ports and a water cooled channel can be added.

### Preliminary vacuum simulations

We used a classical three step approach for preliminary vacuum simulations:

- conventional CAD-assisted ray tracing to calculate the photon flux per unit length in the lattice.
- photon to molecule yield data for different accumulated beam dose taken from existing literature
- synchrotron radiation-induced outgassing profile and gas loads which generate pressure profiles with MOLFLOW+.

This approach does not take into account the photon scattering process due to the probability of reflection of the low energy photons [7] (which could be addressed later on with SYNRAD+ [8]) but it gives a very useful overview of what is at stake with a 10 mm inner diameter chamber with or without a full distributed NEG coating pumping.

As a representative section of the future lattice we considered a straight 1.4 m drift tube of 10 mm inner diameter with one sputter ion pump on each side (a 10 mm opening reduces the maximum pumping speed to only  $\sim 9$  l/s). This represents approximately one third of the future SOLEIL upgrade ring and a worst case configuration from a vacuum point of view (see Vacuum System General Layout above).

Figure 73 shows the simulations carried out for 2 different chamber wall materials (stainless steel with no NEG coating in Figure 73a and an activated NEG-coated chamber in Figure 73b, 73c, 73d) with a constant and uniform photon beam irradiation of  $5 \cdot 10^{18}$  photons/s/m (actually the photon beam irradiation will geometrically decrease along the drift tube but we kept it constant as a conservative estimate). Each vacuum profile has been calculated for 3 different beam integrated doses (1 A.h, 10 A.h and 100 A.h) and compared to a standard thermal outgassing (no beam, no NEG with a gas load of  $10^{-12}$  mbar.l/s/cm<sup>2</sup>). For the NEG-coated chambers a sticking probability

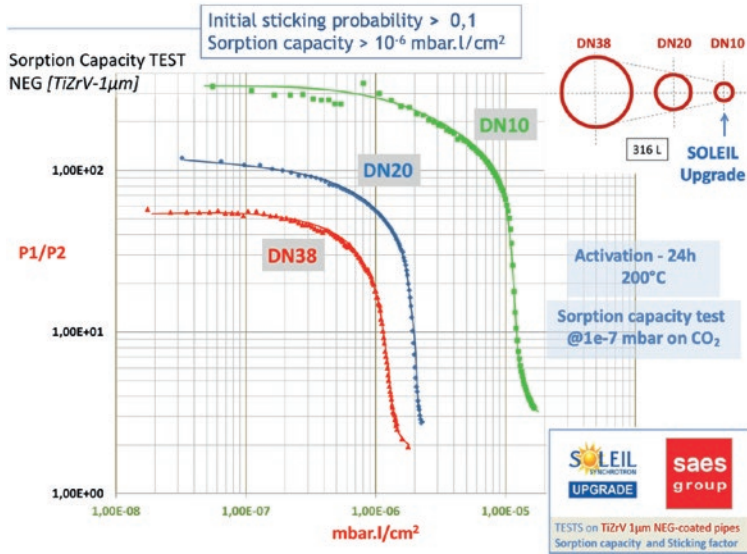


Figure 74: Sorption capacity tests for NEG-coated chambers of DN38/DN20/DN10 mm inner diameter. The 3 curves represent the evolution of the ratio between the upstream pressure P1 and the downstream pressure P2 with the number of injected molecules of CO<sub>2</sub>. Initial sticking probabilities come from a MOLFLOW+ calibration which gets very asymptotic for high aspect ratio chambers. Only an approaching minimum value of the sticking probability can be assessed in that case

range between 0.1 and 0.001 was used to depict a situation from a freshly activated NEG coating to a partly saturated one. According to the pressure profiles simulation the use of a stainless steel vacuum vessel with no NEG coating will not allow any reasonable beam commissioning scenario: after a beam dose of 100 A.h the vacuum inside of the 1.4 m drift tube would reach  $5 \cdot 10^{-6}$  mbar and the initial pressure peak will be prohibitive (the results would have been rather similar with a plain OFS copper chamber with no NEG coating). For the NEG-coated vessels the vacuum target pressure can be achieved with a sticking probability between 0.01 and 0.1: vacuum levels below  $5 \cdot 10^{-8}$  mbar at 1 A.h down to  $5 \cdot 10^{-10}$  mbar at 100 A.h can be reached. It clearly means that a substantial residual sticking probability of the NEG is necessary to fulfill the vacuum pressure requirement of the SR in its commissioning phase

### NEG coating characterization of small diameter chambers

NEG coating can be characterized by its sticking probability, its sorption capacity, the possible number of re-activation cycles and its PSD yield under photon irradiation<sup>[2][3][4]</sup>. The evolution of all these parameters with a reduction of the size of the vacuum chamber is of paramount importance for the SOLEIL upgrade<sup>[9]</sup>. We focused on standard 1 μm thickness TiZrV NEG coating (Ti 40%, Zr 30%, V 30%) for which we have the necessary know-how for a possible large scale deposition process. Also, encouraging

results based on resistive wall calculations show that a TiZrV film thickness of 1 μm ( $\rho_{NEG} = 2.5 \cdot 10^{-5} \Omega.m$ ) could be tolerated for the SOLEIL upgrade.

Figure 74 presents the pumping properties measurements on a 38 mm (DN38), 20 mm (DN20) and 10 mm (DN10) inner diameter NEG-coated chamber for CO<sub>2</sub> (in the framework of the collaboration agreement [CONV-19-014] between SOLEIL and SAES-Getter Spa). The same activation procedure and test protocol have been followed on all the chambers (activation with a 24h plateau at 200°C; evolution of the upstream and downstream pressure ratio for a gas injection pressure of  $10^{-7}$  mbar through a 1 l/s conductance). With an activated NEG coating, all the chambers show a similar behavior for the

evolution of the pressure ratio with an increasing number of injected molecules: for CO<sub>2</sub> the sorption capacity is over  $10^{-6}$  mbar.l/cm<sup>2</sup> and the initial sticking probability over 0.1 which demonstrate that the pumping properties of a NEG coating can be preserved even with DN10 chambers. In addition, few re-activation cycles do not show any significant evolution of the performance. A full characterization of the pumping properties with CO, H<sub>2</sub>, O<sub>2</sub> is now underway and shall back up these results obtained for with CO<sub>2</sub>.

PSD yield measurements on a dedicated beamline are also planned on the D08-1 photon exit of the SOLEIL ring. The measurements shall confirm that the balance between the photodesorption gas load and that the pumping capacity of the NEG is still favorable in DN10 tubes. Especially the evolution of the PSD yield with the photon beam dose shall describe a sharp decrease after a NEG coating activation (close to two orders of magnitude lower after activation) and assured the target pressure profile of the future ring<sup>[3,4]</sup>.

### Photon extraction challenges

The vacuum chambers diameters of the present SR are large enough to transmit any Insertion Device photons into the front-end absorbers without any interaction with the SR walls. For the SOLEIL upgrade it will not be the case anymore. In the tight photon extraction area of the 7BA-4BA lattice, the insertion device photon beams must go through a minimum magnetic pole clearance defined by the electron beam dynamics. At least, the entire range of the useful photon flux radiation shall be transmitted to the beamline users even for helical insertion devices in circular, horizontal or vertical polarization mode.

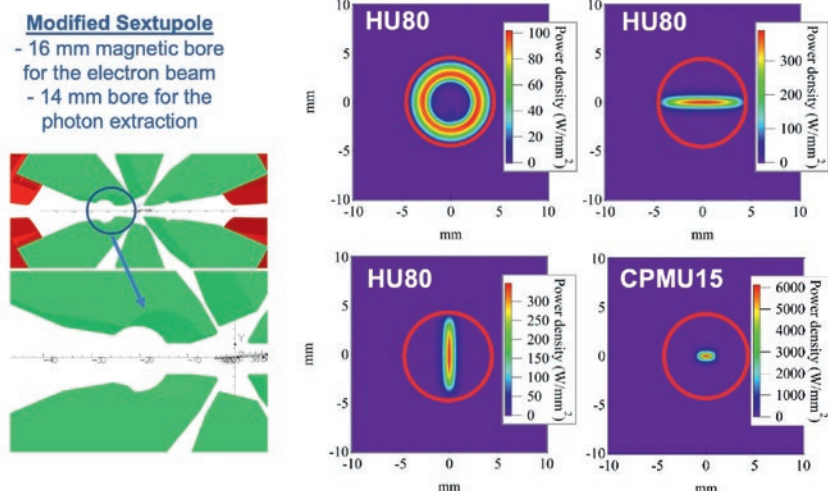


Figure 75: Modified Sextupole at the photon beam extraction location. An 8 mm inner diameter for the UHV photon chamber is compared to the power density map of 2 standard Insertion Devices emission: helical with vertical, horizontal and circular polarization (HU80) or linear (CPMU15)



To tackle this issue in the timeframe of the conceptual design of the SOLEIL upgrade an overall compromise has been found between the accelerator physicists, the magnetic and undulator conception teams and the mechanical and vacuum groups. The minimum clearance in the vertical plane between the poles of the sextupole in the extraction region has been modified (a standard sextupole has a minimum magnetic pole clearance of 7.5 mm) to allow the implementation of an 8 mm inner diameter vacuum chamber (for a minimum pole clearance of 16 mm). Figure 75 presents the proposition of a modified sextupole for the photon beam extraction and shows the power density map of 2 representative insertion device emission [11] at this location (helical APPLE-II type HU80, linear in-vacuum type CPMU15). The 8 mm inner diameter of the vacuum chamber is also represented as a comparison.

This configuration does not guarantee full transmission of the insertion device power to the front-end even with stringent values of the beam based interlock (BPM or XBPM interlock angles). As a consequence, a specific absorber shall be designed immediately upstream in the SR to secure the photon beam extraction. Extra pumping capacity shall be also added to deal with excess values of the PSD gas load.

The existing “crotch absorbers” developed at SOLEIL or in the new generation light sources like ESRF-EBS (see the full CuCr1Zr crotch design machined from one solid piece [10]) seem difficult to replicate for the SOLEIL upgrade in the configuration of the photon extraction area: the gap between the axis of the electron trajectory and the axis of the extracted photon beam is only a few millimeters.

In Figure 76 an early design of a pumping and power absorption block is proposed: it can absorb a total photon power of 3 kW with a power density over 25 W/mm<sup>2</sup> from the upstream dipole and the insertion device. Two vacuum ports for SIP pumping are added and a screening grid reduces its impedance contribution. NEG coating of the wall will be considered.

### Superbend radiation

At the center of each 7 BA a room temperature high field bending magnet can be installed (Figure 69) with a maximum peak field of 3 T. The radiation can be transmitted directly to the front-end through the compact magnetic lattice (and the 7.5 mm magnetic pole clearance

of the sextupole) via a ‘keyhole profile’ vacuum chamber with a vertical slot of 3 mm. Downstream, a window with an opening of 10 mrad in a standard “crotch absorber” could allow the beam to pass. Figure 77 represents the vacuum vessel specific profile at the extraction point, the power density map and horizontal power cross section at 2 m from the source point of the superbend [11].

### Vacuum chamber connections

The vacuum chamber connections (flanges, bellows) where the RF continuity is required need a particular attention to reduce their impedance budget contribution. We started two prototyping programs based on an adaptation to the SOLEIL upgrade needs of successful designs already used on different accelerators projects:

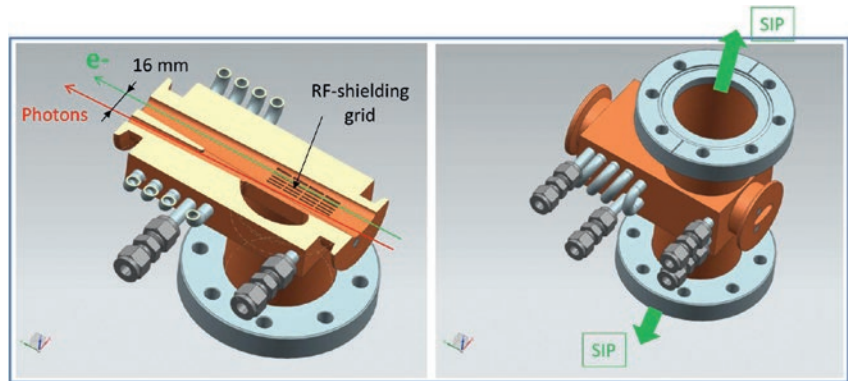


Figure 76: Early design of a pumping and absorber block for the photon beam extraction at 0° from the insertion device straight section

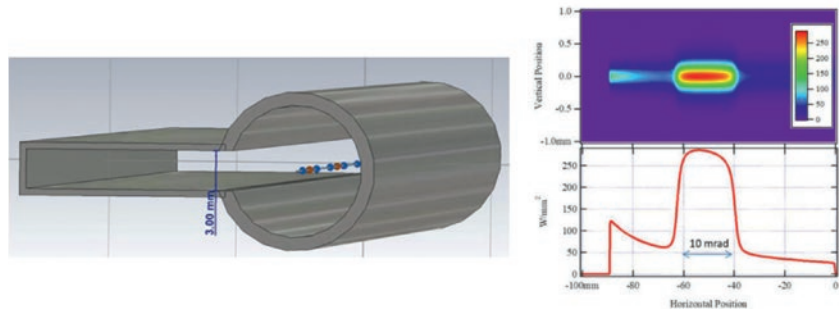


Figure 77: “Keyhole” profile chamber with a vertical slot of 3 mm. Power density map of the superbend at 2 m from the emission point. A window with a 10 mrad opening in a standard “crotch absorber” could be used to transfer the beam to the front-end

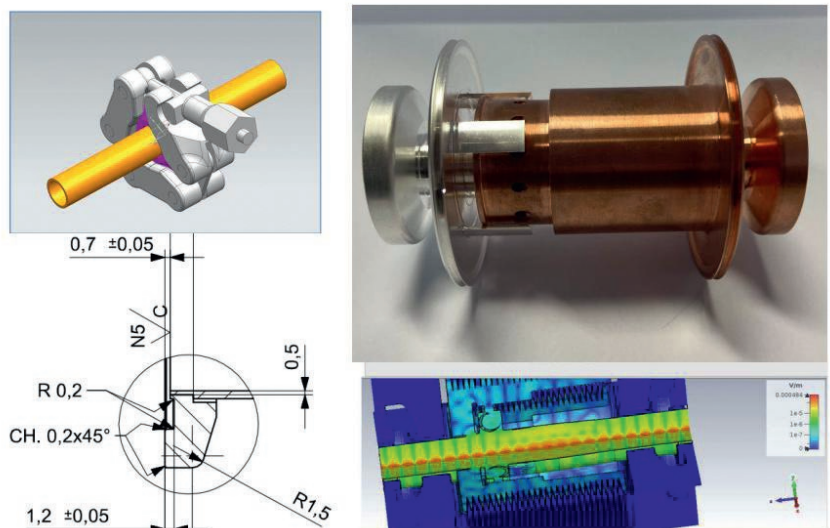


Figure 78: M0 seal flange with a standard KF chain clamps for tightening (left) RF shielded bellow mechanical prototype (without membranes) and wakefield simulation for impedance contribution estimation (right)

- for the RF shielded bellows, we adapt as a proof of concept 2 mechanical solutions already studied for the SIRIUS Synchrotron<sup>[12]</sup> (SIRIUS has a generic round vacuum chamber of 24 mm inner diameter).
- for the flanges, we focus on a solution where the RF continuity and the vacuum seal are made by the same gasket: the “MO type seal flange”<sup>[13]</sup>.

Figure 78 shows the early mechanical designs for the flanges and bellows of the SOLEIL upgrade. An example of wakefield losses in the “telescopic bellow” prototype is also presented. Mechanical feasibility, vacuum performances, thermal cycling and electrical contacts will be soon surveyed with respect to the total ring impedance budget.

### Vacuum system next steps

Preliminary vacuum simulations show the crucial importance of the NEG pumping characteristics for the SOLEIL upgrade vacuum system. Further investigation on 10 mm inner diameter NEG-coated chambers need to be carried out especially under photon beam irradiation for PSD measurements. The evolution of the PSD yield with the photon beam dose would give us a closer insight into the evolution of the vacuum profile in the lattice for the commissioning of the ring.

From now on, vacuum and thermomechanical calculations have to be detailed as the mechanical design progresses:

- full 3D simulation using Monte-Carlo molecular-flow approach of a 7BA-4BA achromat will be carried out. It should integrate a photon scattering model to take into account low intensity radiation from reflected photons which affect the beam commissioning behavior.
- dipole chambers, transitions and absorbers for the photon beam extraction to the front-end (insertion device or superbend) have to be mechanically refined with thorough Finite Element Analysis (FEA) studies.

### REFERENCES

[1] Al-Dmour, E., et al. “Diffraction-Limited Storage Ring Vacuum Technology”, *Journal Synchrotron Radiation*, 21, 878–883 (2014).

[2] Chiggiato, P., and Costa Pinto, P., “Ti-Zr-V Non-Evaporable Getter Films: From Development to Large Scale Production for the Large Hadron Collider”, *Thin Solid Films*, 515, 2, 382-388 (2006).

[3] Chiggiato, P., and Kersevan, R. “Synchrotron Radiation-Induced Desorption from a NEG-Coated Vacuum Chamber”, *Vacuum*, 60, 67-72 (2001).

[4] Tanimoto, Y. et al., “Vacuum Properties of NEG and Carbon Coatings Exposed to Synchrotron Radiation”, VSC Seminar, CERN, 25 September 2015.

[5] Al-Dmour, E., “MAX-IV: Experience with NEG Coated Chambers as Absorbers and Pumps” The 6th Diffraction Limited Storage Ring (DLSR) Workshop, 30th October 2018.

[6] Kersevan, R. and Pons, J.-L., “Introduction to MOLFLOW+: New graphical processing unit-based Monte-Carlo code for simulating molecular flows and for calculating angular coefficients in the compute unified device architecture environment”, *Journal of Vacuum Science & Technology, A* 27, p. 1017 (2009).

[7] Kersevan, R., “Integrated Monte-Carlo Simulation Environment for Light Source Design” IUVSTA Workshop, Ultra Low Emittance Light Source Vacuum System, NSRRC, Hsinchu (2016).

[8] Kersevan, R., “SYNRAD, a Monte-Carlo Synchrotron Radiation Ray-Tracing Program”, Proceedings of the 1993 IEEE Particle Accelerator Conference, Washington, DC (1993).

[9] Porcelli, T., et al. “NEG Coating Deposition and Characterisation of Narrow-Gap Insertion Devices and Small-Diameter Chambers for Light Sources and Particle Accelerators”, *Vacuum*, 138, 157-164 (2017).

[10] Thomas, F. et al., “X-Ray Absorber Design and Calculation for the EBS Storage Ring”, Proceedings of MEDSI2016, Barcelona, Spain (2016).

[11] Marcouillé, O., SOLEIL, private communication.

[12] Duarte, H. O. C., et al., “Design Review of Bellows RF-Shielding Types and New Concepts for SIRIUS”, IPAC2019, Melbourne, Australia (2019).

[13] Suetsugu, Y., Shirai, M., Ohtsuka, M., “Application of a Matsumoto-Ohtsuka type Vacuum Flange to Beam Ducts for Future Accelerators”, *Journal of Vacuum Science & Technology, A* 23, 1721 (2005).



## Radio-Frequency systems

### Introduction

The Storage Ring (SR) of the SOLEIL upgrade will essentially rely on two RF systems:

- a fundamental one at 352 MHz, which will provide the RF voltage and power necessary for an adequate electron beam energy acceptance and for compensation of its energy loss per turn;
- a harmonic one, at 3 or 4 times 352 MHz, aimed at lengthening the bunches up to about 100 ps FWHM in order to preserve the low emittance and insure a suitable beam lifetime. In addition, thanks to this harmonic system, it should be possible to produce relatively short bunches, around 10 ps FWHM, with relaxed beam current and emittance.

A feed-forward system into a dedicated very wide band cavity at 352 MHz could be also used in order to compensate the destructive effect, in terms of bunch

	SOLEIL	SOLEIL UPGRADE
$E_n$ (GeV)	2.75	2.75
$f_{RF}$ (MHz)	352	352
$I_b$ (mA)	500	500
$\delta U$ (keV*)	1150	770
$V_{RF}$ (MV)	2.8 - 4**	1.8
$P_b$ (kW)	560	385

\* Including 280 keV for the ID's

\*\* 2.8 MV in standard mode and 4 MV in low  $\alpha$  mode ( $\alpha_{nom}/100$ )

Table 33: Compared RF operating conditions using 1 SOLEIL CM or 4 ESRF-EBS cavities

	1 CM SOLEIL 2 SC cavities	4 NC cavities ESRF-EBS type
$P_b$ (kW)	385	385
$V_{RF}$ (kV)	1.8	1.8
$V_{cav}$ (kV)	900	450
$P_{dis}$ (kW)	$\approx 0$	20 x 4
$P_{cav}$ (kW)	194	117
Coupling	$Q_{ext} = 5 \cdot 10^4$	$\beta = 5$
$P_{RF}$ (kW)	385	470
Length (m)	$\sim 6$	$< 4.15$
$Z_{HOM}$	$\sim 0$	TBD

Table 34: SOLEIL and SOLEIL upgrade determining parameters for the RF system

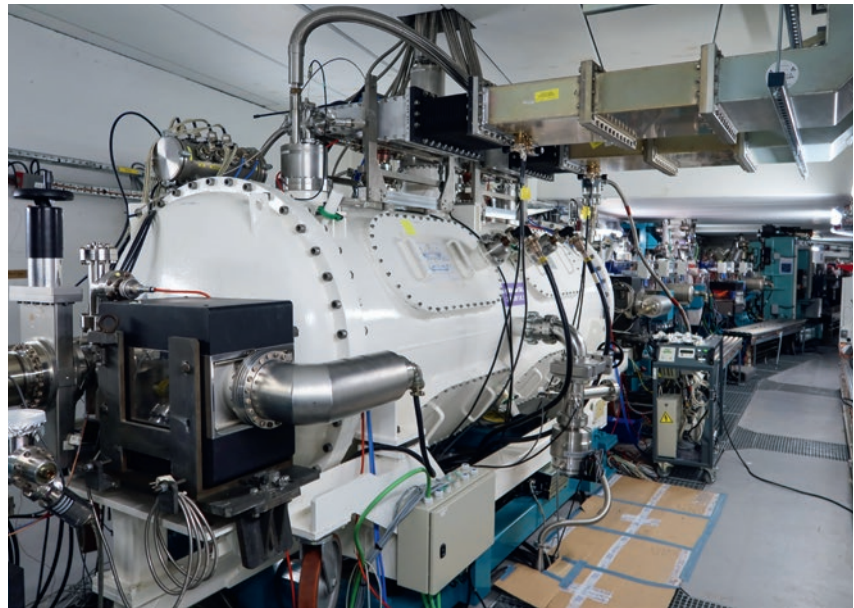


Figure 79: One of the two SOLEIL cryomodules inside the SR tunnel, hosting 2 SC cavities

lengthening, from the Transient Beam Loading (TBL), due to the gap of empty buckets in hybrid mode (3/4 filling).

### Fundamental RF system at 352 MHz

In Table 33 are listed the main parameters dictating the choice of the fundamental RF system for the SOLEIL upgrade SR, compared to the present SOLEIL ones, which are achieved using four "HOM damped" SuperConducting (SC) cavities, housed inside two Cryo-Modules (CM), each cavity being powered with its own Solid State Amplifier (SSA), capable of delivering up to 200 kW [1-4].

For the same energy ( $E_n$ ), RF frequency ( $f_{RF}$ ) and average beam current ( $I_b$ ), the SOLEIL upgrade is significantly less demanding in terms of RF voltage ( $V_{RF} = 1.8$  MV) and power delivered to the beam ( $P_b = 385$  kW), due to the lower energy loss per turn ( $\delta U = 770$  keV, including the insertion devices).

### Choice of the RF cavities

We have considered two cavity options, based on state of the art designs : reuse one of the present SOLEIL CM's (Figure 79) or use 4 Normal Conducting (NC) cavities of the ESRF-EBS type (Figure 80) with a fundamental shunt impedance,  $R_s \approx 5$  M $\Omega$  and unloaded quality factor,  $Q_0 \approx 35$  000 [5,6]. The operating conditions are compared in Table 34 and indicate that the NC option is more favorable on most aspects:

- required space: the 4 NC cavities fit in a 4.15 m medium straight section;
- redundancy: the SC system with a single CM and cryogenic station does not provide any redundancy while the nominal performance is still achievable when 3 out of the 4 NC cavities are in use, at the expense of about 6% additional RF power;
- operational cost: the NC system requires some more RF power ( $P_{RF}$ ) than the SC one, due to the cavity

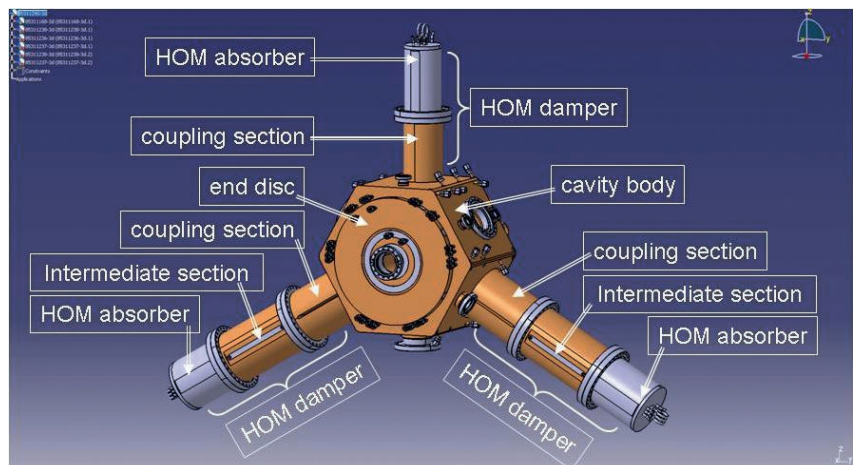


Figure 80: ESRF - EBS cavity



Figure 81: SOLEIL solid state amplifiers for the cavities 1 and 2

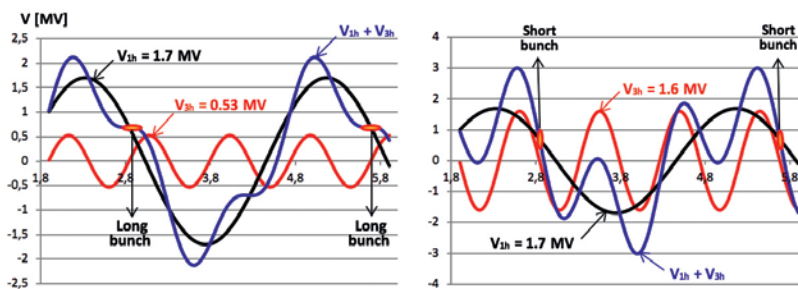


Figure 82: Bunch lengthening (left) and shortening (right) from a 3<sup>rd</sup> harmonic system

wall dissipation ( $P_{\text{dis}}$ ). However, taking into account the electrical consumption of the cryogenic station ( $\sim 300$  kW), it remains globally less power-consuming and it does not need any cryogenic coolant (Helium and Nitrogen);

- investment cost: the use of NC fundamental cavities makes the existing cryogenic station available for the harmonic RF system (see Harmonic RF System below) and the investment cost of the four NC cavities ( $\sim 2$  M€), is much less than the cost of a cryogenic station.

All the above reasons have led us to favor the NC option with 4 cavities of the ESRF-EBS type, each being powered with its own amplifier. However it remains to be demonstrated that it is relevant in terms of longitudinal HOM impedances. Although up to 200 mA have been already stored in the ESRF SR using 13 such cavities, without any occurrence of Coupled Bunch Instability (CBI<sup>[7]</sup>), this is not yet conclusive

for the SOLEIL upgrade case, which is more critical in this respect. Preliminary computations anticipate that only one longitudinal mode, whose frequency is around 1.7 MHz, might be slightly above the CBI threshold<sup>[8]</sup>.

Moreover, ESRF has agreed with the loan of its two spare cavities and their test in the SOLEIL SR by 2022 in order to remove any doubt as to the need for a bunch by bunch longitudinal feedback. In the transverse planes, for other reasons (see section Beam stability, page 102), it was planned to reuse the present bunch by bunch transverse feedback system<sup>[9]</sup>, which will also cope with the cavity transverse HOM impedances.

#### RF power sources, waveguide network and LLRF systems

SOLEIL is presently exploiting four 200 kW SSAs for the SR, each consisting in four 50 kW towers (Figure 81). Developed in house, they are based on the combination of elementary SSA modules of about 300 W (165 modules

per tower), each containing a LDMOS transistor and an integrated circulator and being supplied by its own 270/50 V DC-DC converter<sup>[4]</sup>.

After 15 years of operation, these have demonstrated an outstanding level of reliability and flexibility, thanks to their extreme modularity and redundancy. They have been upgraded recently by replacing the original transistors with new generation ones, more robust and better performing in terms of power, gain and efficiency. A replacement of their power supplies to use AC-DC converters, connected directly on the mains, is under investigation, hence solving obsolescence issues and further improving the efficiency and reliability.

Therefore, we intend to reuse the four SSAs in the SOLEIL upgrade SR, after a few possible adaptations (for instance connecting the 4 amplifier towers directly on the waveguide hence providing the possibility of easily operating with only 3 of them in order to optimize the efficiency). They will remain at their present location, adapting the waveguide network to reach the new cavity locations in the SR.

In the present SOLEIL Low Level RF (LLRF) systems, the frequency, amplitude and phase regulation loops as well as the direct RF feedback are fully based on analogue devices. A generic digital version, based on a  $\mu$ TCA platform, is being developed for the LUCRECE project at 1.3 GHz<sup>[10]</sup>, which will be easily adapted for the SOLEIL upgrade<sup>[11]</sup>.

### Harmonic RF system

#### Requirements

The harmonic RF system will have to fulfill two tasks:

- lengthen the bunches to about 100 ps FWHM, thus reducing their charge density so as to preserve the low emittance and insure a suitable beam lifetime;
- provide relatively short bunches, about 10 ps FWHM, with lower current and relaxed emittance.

The two conditions are represented in Figure 82 for the 3<sup>rd</sup> harmonic case. Bunch lengthening is achieved by adjusting the harmonic voltage amplitude ( $V_{3h} \approx V_{1h} / 3 \approx 0.5$  MV) and phase such that the overall voltage (fundamental + harmonic) is flat at the synchronous phase. On the other hand, bunch shortening is obtained when the harmonic voltage is set at the opposite phase so as to increase the slope of the overall voltage at the synchronous phase; bunch length down to 10 ps FWHM requires about 1.6 MV<sup>[12, 13]</sup>.

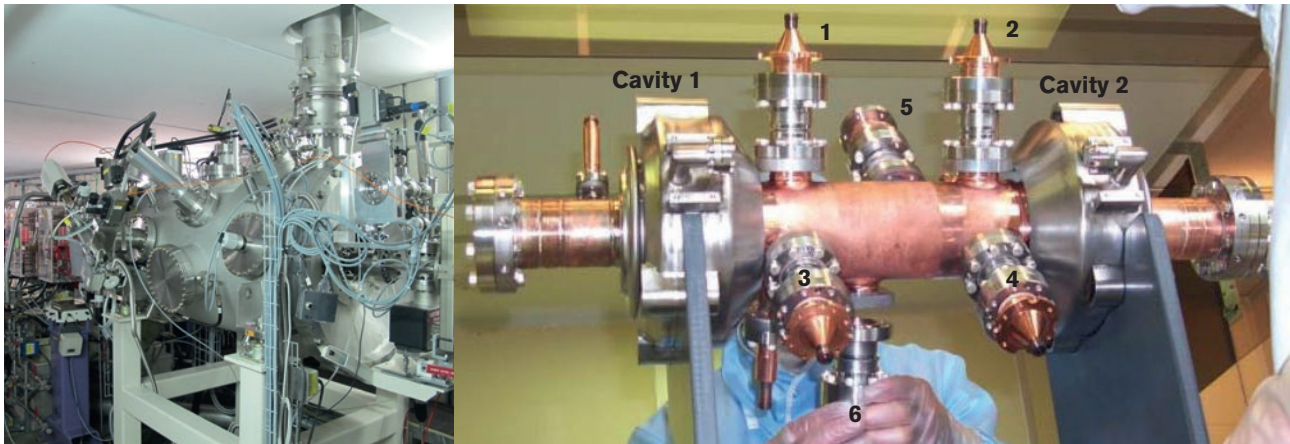


Figure 83: Super-3HC cryomodule (left) and cavities (right) with transverse HOM dampers (1-4) and longitudinal ones (5-6)

### Technological options

The above requirements could be achieved using several technological options: NC or SC, passive or powered, 3<sup>rd</sup> or 4<sup>th</sup> harmonic RF systems. These are all under investigation and compared in terms of stability, transient beam loading, compatibility with all modes of operation, etc. This study is conducted in the frame of a collaboration with ESRF, KEK, PSI and HZB, who encounter similar problems. Longitudinal beam dynamics simulations are performed using two particle tracking codes, mbtrack<sup>[14]</sup> and P-Elegant<sup>[15]</sup>, which will be crosschecked with the experimental results from tests in SLS (SC cavities)<sup>[1]</sup> and BESSY II (NC cavities)<sup>[16]</sup>.

Although all options remain open, a passive SC RF system of the Super-3HC type (Figure 83)<sup>[1, 17, 18]</sup>, scaled to 3 or 4 times 352 MHz, is regarded as the most suitable for the SOLEIL upgrade bunch lengthening and shortening needs. The Super-3HC CM, used in SLS and ELETTRA, is already a scaling to 1.5 GHz of the SOLEIL CM with two HOM free SC cavities, but without any power coupler. The passive SC cavities profit from the beam induced voltage and therefore require neither external harmonic power source nor additional power from the fundamental RF system. They are no longer seen by the beam as resonators and behave as pure (lossless) reactance components of the impedance, which makes their operation much easier, without need for phase control and fast feedbacks to ensure the stability (Robinson, microphonics...). At given current  $I_b$ , the induced voltage is simply inversely proportional to  $\delta f$ , the cavity detuning:  $V_{ind} = I_b R/Q f/\delta f$ , as long as  $\delta f \gg f/Q$  and for SC cavities with very narrow bandwidth, this condition will be met even at beam current as low as a few mA. A limitation could come from the AC Robinson instability in single bunch mode ( $I_b \approx 20$  mA), however mbtrack

simulations show stable conditions even at current as low as 10 mA<sup>[19]</sup>.

It turns out that the main issue may come from the TBL, produced by the gap of empty buckets in the hybrid mode (3/4 filling). The resulting phase spread along the bunch train strongly affects the bunch lengthening efficiency from the harmonic system. We have started to study the possibility of compensating this destructive effect by means of a feedforward into a dedicated very wide band 352 MHz cavity, as proposed by KEK<sup>[20]</sup>; mbtrack simulations show a beneficial, but insufficient, effect<sup>[18, 19]</sup>. The investigations are going on.

### Collaboration projects

In 2018, the RF Groups of SOLEIL and ESRF, which had common problematics within the frame work of their upgrades, proposed to collaborate on four workpackages (WP), as listed next and in a second stage, three other laboratories, KEK, PSI, HZB decided to join some of them; formal agreements are under writing:

- WP1: Test of a pair of 352 MHz ESRF-EBS cavities in the SOLEIL SR, in passive mode for their qualification in terms of HOM's (ESRF/SOLEIL)
- WP2: Beam dynamic studies in presence of harmonic RF systems; tracking code computations and experiments on existing machines (SOLEIL/ESRF/KEK/PSI/HZB)
- WP3: Design and implementation of a harmonic RF system with TBL compensation (ESRF/SOLEIL/KEK)
- Design of a generic  $\mu$ TCA-based DLLRF system adaptable to all the above systems, fundamental, harmonic and TBL compensation (SOLEIL/ESRF/HZB)

Two other tripartite collaborations are being set up:

- Design and realization of a Super-3HC type CM at 1.41 or 1.06 GHz (SOLEIL/CEA/CERN)
- Development of a 40 kW SSA at 1.41 GHz (SOLEIL/SigmaPhi-Electronics/ESRF).

### Conclusions

For the fundamental RF system of the SOLEIL upgrade SR, it is proposed to use four 352 MHz NC cavities of the ESRF-EBS type, each powered by one of the SSAs presently operating at SOLEIL. We still need to demonstrate that all cavity longitudinal HOMs are sufficiently damped without using any additional longitudinal feedback system. For the transverse planes, the bunch by bunch transverse feedback system, presently operating in SOLEIL, will be reused.

Although other options are still open and studied, the use of a Super-3HC type CM with two passive SC cavities, adapted to 3 or 4 times 352 MHz, is regarded as the most suitable solution for the bunch lengthening and shortening needs. The main issue may come from the destructive effect on the bunch lengthening, produced by the transient beam loading in the hybrid mode (3/4 filling). The possibility of compensating this effect by means of a feedforward system into a dedicated very wide band 352 MHz cavity is under investigations.

A generic digital low level RF system, based on  $\mu$ TCA, which can be adapted to all these RF systems, is being developed. Collaboration projects, aimed at conducting R&D in the above domains are being set up with other institutes (ESRF, HZB, KEK, PSI, CEA, CERN) and SigmaPhi Electronics.

## REFERENCES

- [1] Marchand, P., "Superconducting RF Cavities for Synchrotron Light Sources", Proceedings of EPAC2004, Lucerne, 21-25 (2004).
- [2] Marchand, P., et al, "Operational experience with the SOLEIL Superconducting RF System", Proceedings of SRF2013, Paris, 269-273 (2013).
- [3] Diop, M., et al, "Status of the SOLEIL Superconducting RF System", Proceedings of SRF2017, Lanzhou, 141-143 (2017).
- [4] Marchand, P., "Review and Prospects of RF Solid State Power Amplifiers for Particle Accelerators", Proceedings of IPAC2017, Copenhagen, 2537-2542 (2017).
- [5] Serrière, V., et al, "352.2 MHz HOM Damped Normal Conducting ESRF Cavity: Design and Fabrication", Proceedings of IPAC2011, San Sebastian, 68-70 (2011).
- [6] Revol, J.-L., et al, "ESRF Operation and Upgrade Status", Proceedings of IPAC2013, Shanghai, 82-84 (2013).
- [7] Jacob, J., (ESRF), private communication.
- [8] Marchand, P., "RF Systems for the SOLEIL Upgrade", Virtual 24<sup>th</sup> ESLS-RF workshop KIT, Karlsruhe (2020).
- [9] Sreedharan, R., et al, "SOLEIL Digital Transverse Bunch by Bunch Feedback System Upgrade, LLRF2017 workshop, Barcelona, 16-19 October 2017.
- [10] Sreedharan, R., et al, "LUCRECE DLLRF Status", Low Level Radio Frequency workshop, Fermilab-BNL, Chicago (2019).
- [11] Zhao, L. and Sreedharan, R., "Digital LLRF System for the SOLEIL Upgrade and LUCRECE projects", Virtual 24th ESLS-RF workshop KIT, Karlsruhe (2020).
- [12] Tordeux, M.-A. and Marchand, P., "Proposition pour la production d'impulsions de l'ordre de 10 ps FWHM dans le cadre de l'upgrade de SOLEIL", internal SOLEIL note AI-RF-PM-CR-I-0957 (2019).
- [13] Gamelin, A., "Estimation des effets collectifs pour le mode paquets courts de l'Upgrade de SOLEIL", internal SOLEIL note CDR-M1-NT-I-2021 (2021).
- [14] Yamamoto, N. et al., "Investigation of Longitudinal Beam Dynamics with Harmonic Cavities by Using the code mbtrack", Proceedings of IPAC2019, Melbourne (2019).
- [15] Wang, Y. and Borland, M. "Implementation and Performance of Parallelized Elegant", Proceedings of PAC2007, Albuquerque, New Mexico, 3444-3446 (2007).
- [16] Anders, W. and Kuske, P., "HOM Damped NC Passive Harmonic Cavities at BESSY", Proceedings of PAC2003, Portland, 1186-1188 (2003).
- [17] Marchand, P., "Possible upgrading of the SLS RF System for Improving the Beam Lifetime", Proceedings of PAC1999, New York, 989-991 (1999).
- [18] Pedrozzi, M. et al, "SLS Operational Experience with Third Harmonic Superconducting System", Proceedings of SRF2003, Lübeck, 91-94 (2003).
- [19] Gamelin, A., et al., "Longitudinal Beam Dynamics Studies for the SOLEIL Upgrade in Presence of a Harmonic RF System", Internal report (2020).
- [20] Yamamoto, N. et al., "Reduction and Compensation of the Transient Beam Loading Effect in a Double RF System of Synchrotron Light Sources", Physical Review Accelerators and Beams, 21, 012001 (2018).



## Diagnostics and timing system

### Diagnostics

The upgrade of the SOLEIL storage ring will require state of the art diagnostics systems in order to fully characterize the new electron and photon beam properties. Even though part of the existing diagnostics can be easily adapted to the new machine, other important ones require significant modifications, commensurate with the new beam parameters (horizontal emittance reduction by a factor  $\sim 50$ ) and the drastically reduced vacuum chamber dimensions, shown in Table 35.

### Emittance measurement

#### Specifications

The electron beam transverse emittance is expected to be close to 50 pm.rad in both planes in the full coupling mode, and could be reduced down to 1 pm.rad in the vertical plane for coupling correction (machine optimization). This corresponds to electron transverse beam sizes between 2 and 20  $\mu\text{m}$  RMS depending on the location around the storage ring. This small transverse emittance being one of the critical parameters of the future machine, it has to be accurately ( $< 1$  pm.rad resolution) as well as rapidly ( $\sim 100$  Hz repetition rate) measured.

#### Preliminary diagnostics studies

The measurement of electron beam transverse sizes of a few microns will be achieved using the synchrotron radiation emitted by the electron beam in the magnetic field of magnets such as dipoles, wigglers or undulators. A preliminary bibliography enabled the pre-selection of four different techniques: two using synchrotron radiation in the X-ray range and two using the visible range. A measurement in the X-ray is probably the most appropriate to fit our specifications in terms of resolution and flux. Two kinds of measurements are foreseen. Pinhole cameras, with their high reliability, will be used for the online measurement of the beam emittance in user operation at high repetition rate ( $> 100$  Hz). Because the pinhole cameras will not resolve the 1 pm.rad emittance expected for coupling correction, we propose to implement also Fresnel diffraction based measurement. The resolution should be significantly increased at the cost of a lower repetition rate. The system design will enable to swap from one technique to the other. To reach their

Diagnostic	SOLEIL	SOLEIL upgrade
Horizontal Emittance	4000 pm.rad	80 pm.rad
Vertical Emittance	40 pm.rad (at 1% coupling)	8 pm.rad (at 10% coupling)
BPM aperture H/V	84 mm / 25 mm	10 mm round
RMS Beam Size (minimum value at source point) H/V	50 $\mu\text{m}$ (dipole) / 8 $\mu\text{m}$	7.4 $\mu\text{m}$ (3 T) / 2.8 $\mu\text{m}$ (10% coupling in short SS)
Position and Angle Stability (with respect to beam size and divergence)	10%	2-3%
Orbit Feedback efficiency range	0.01-150 Hz	0.01- 1000 Hz

Table 35: Main beam and storage ring parameters

ultimate resolution, both pinhole cameras and Fresnel diffraction monitors will be operated in the 50-100 keV range. The generation of such high photon energies requires high field dipoles ( $> 1.7$  T as shown in Figure 1). To reach 100 Hz repetition rate, a field of 3 T might be mandatory. Such high fields could be obtained in the middle of the Long Bending Magnets (LBM) located in the middle of the 7 BA arcs. To guarantee a reliable emittance measurement, we suggest dedicating two high field LBMs for beam size measurement purposes. In the visible range, synchrotron radiation polarized imaging could be used as an alternative to monitor the electron beam stability and to measure its transverse sizes however with a low resolution. It is not expected indeed to resolve beam sizes smaller than 5  $\mu\text{m}$ -RMS. Another technique in the visible range, interferometry, could be used to try higher resolution measurements but at the detriment of flux and repetition rate of the measurements. Both visible range synchrotron radiation diagnostics

would be implemented on the same source dipole in parallel to other diagnostics such as filling pattern monitor and bunch length measurement. According to simulations, a low field dipole (0.5-1 T) is the most efficient to generate the required synchrotron radiation flux in the visible range (Figure 84). The dipole source could then be one of the Short Bending Magnets (SBM) of the ring lattice (1 T).

#### On-going simulation work and prototyping

Extensive simulations (based on SRW code<sup>[1]</sup>) already enabled to give the specifications on the source dipole for both visible and X-ray range diagnostics. On-going simulations are now targeting the optimization of the performances of each diagnostic in terms of resolution.

Regarding prototyping, one of the measurements in the visible range is being experimentally tested by implementing a prototype of interferometric measurements

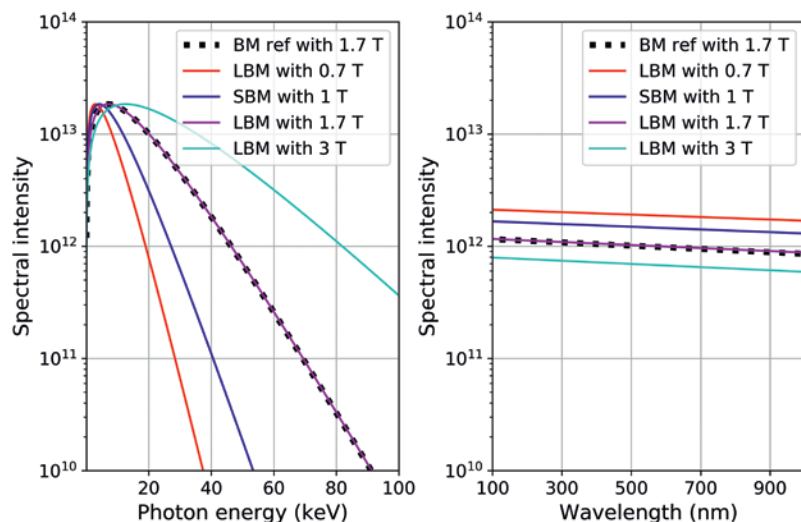


Figure 84: On-axis spectrum in the four different cases of sources studied for SOLEIL upgrade, and for recall in the present case for SOLEIL Bending Magnet (BM init of 1.7 T), in the X-ray range (left) and in the visible range (right). SRW simulations

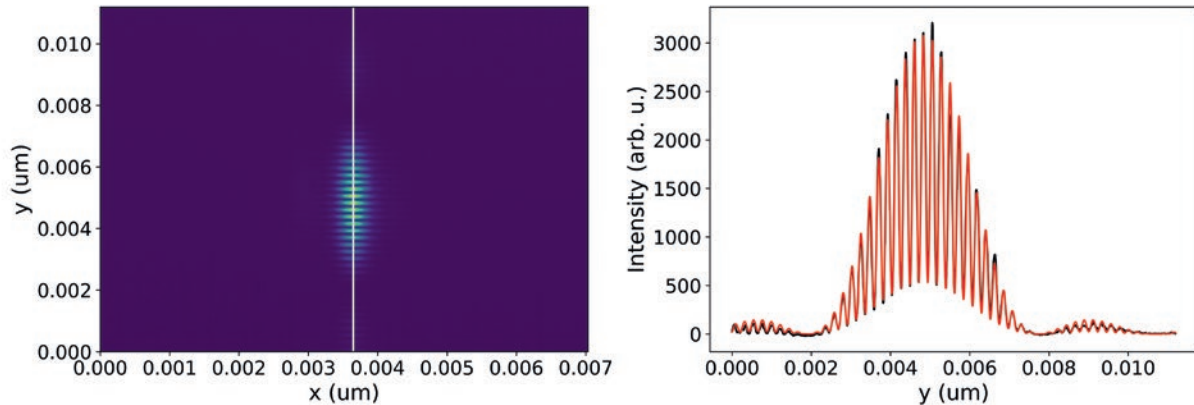


Figure 85: Double slit interference pattern (left) and profile (right) obtained in the image plane of SOLEIL MRSV beamline. Extraction mirror in full-insertion mode, lens focal length: 3.2 m, distance between double slits: 12.5 mm, double-slit width: 1 mm, synchrotron radiation wavelength: 400 nm (using band-pass filter), stored current: 2.5 mA. Interferogram recorded with a camera ace1920-50gm from Basler.

on the already existing visible light extraction port. Encouraging preliminary results have already been obtained (Figure 85), and an upgrade of the extraction mirror is planned which should enable to operate this diagnostic during users operation.

In the case of the X-ray range measurement (pinhole camera and Fresnel diffraction), in addition to extended simulations, we are also considering the possible techniques that could be implemented to ensure that the ultimate resolutions will be reached, which can be very challenging for low coupling measurements (coupling correction): high resolution crossed-slits systems, large bandwidth monochromating systems based on specular mirrors, etc. Small prototypes could be installed within a few years on an unused dipole beam exit port at SOLEIL.

#### Fast processing

The beam size stability at SOLEIL is already as important as the beam position stability and will become even more crucial with the beam size reduction on the future machine. With several insertion devices able to switch the configuration in a short time, we are considering having a hardware (FPGA/GPU) image acquisition and processing for the beam size measurement. This fast measurement will be used as input for a beam size

feedback system. A first prototype of such an image processing system is already under development.

#### Beam Position Monitors

The Beam Position Monitor (BPM) system is the largest (and one of the most critical) diagnostic systems for a synchrotron light source: 176 position measurement units are foreseen in the CDR reference lattice. The system should deliver beam position measurement with a resolution of less than 50 nm RMS in closed orbit measurement (used for feedback loops). The measurement stability is also very important with a drift below 1  $\mu\text{m}$  over 24 hours.

#### BPM sensors

The BPM sensors for the SOLEIL upgrade will be the usual RF button pickups installed at 45° on the vacuum chamber. If the technology is well known, it will be the first time the pickups are mounted on such a small vacuum chamber aperture (10 mm diameter). The challenge will be the manufacturing of a small dimension pickup (with a 3 mm diameter button) and its positioning on the BPM body with respect to tight tolerances in order to maintain an absolute position measurement error below 300  $\mu\text{m}$ .

A first (simplified version) prototype (Figure 86) has been realized in order to validate such a tight mechanical

integration and also to try new ideas for the button positioning during the welding process. Resulting metrology is promising and improvements on the dedicated mechanical tools are already foreseen.

Preliminary studies have also been carried out to design the future BPM pickups. With the usual delta over sum equation used to compute the position, the response is linear on a  $\pm 1$  mm range around the BPM center with an on-axis error below 3% (Figure 87). We can consider a polynomial response to enlarge the linear range if needed for machine physics studies at large amplitude.

Accurate electromagnetic simulations will be conducted in order to design the BPM feedthrough and possible mode trapping around the BPM button and reduce the BPM contribution on the overall impedance budget. Deposited power in the most stringent mode of operation has also to be evaluated to decide on the necessity of having a water cooling circuit around the BPM body. At the moment, in order to ensure the mechanical stability of the BPMs, we are considering to fix the BPM blocks to the girders with bellows close to the body part.

#### BPM electronics

The BPM electronics must perform low noise acquisition and processing of the signal with excellent long term stability. On the basis of the system currently in use at SOLEIL, the following characteristics should be improved in order to meet the new machine specifications:

- A turn by turn resolution lower than 100  $\mu\text{m}$  RMS for a current of 0.01 to 1 mA in 104 bunches (for the commissioning) and lower than 1  $\mu\text{m}$  RMS at 500 mA.
- A beam current dependence below 10  $\mu\text{m}$  on the 0.1 to 20 mA range in single bunch filling pattern.



Figure 86: BPM first prototype with 3 mm diameter buttons on a 10 mm diameter block (left), inside view (center), support (right)

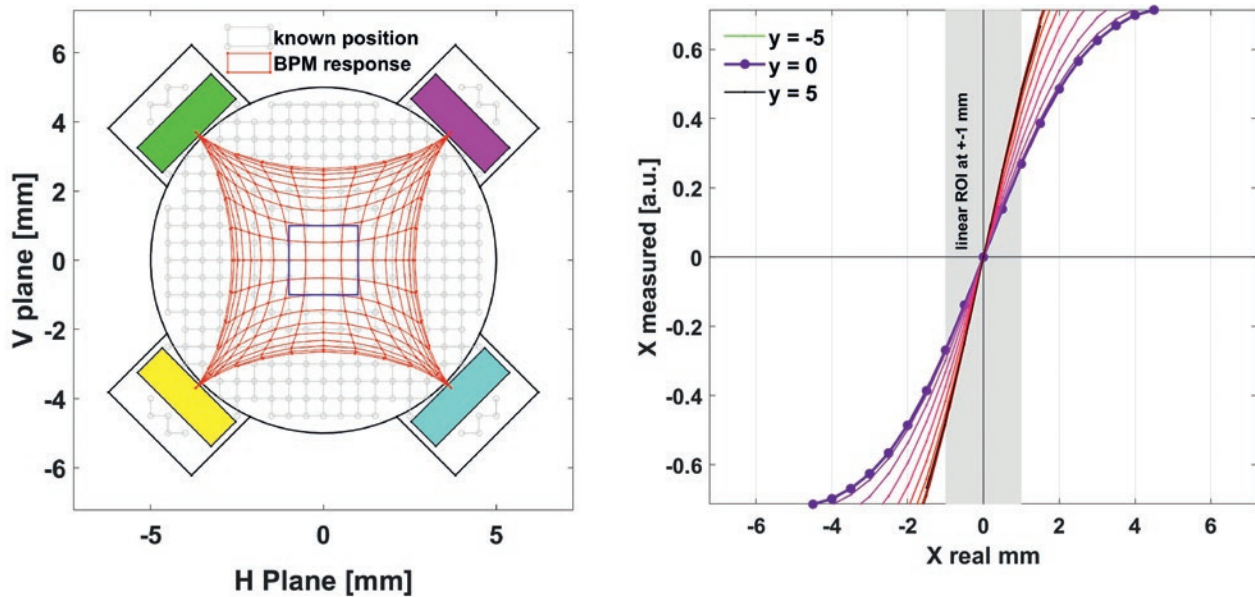


Figure 87: Delta over Sum mapping (left) and response (right). BPM Lab simulations<sup>[2]</sup>

- A closed orbit resolution better than 50 nm at the frequency of the fast orbit feedback (10 kHz) for the 500 mA nominal current in 416 bunches.
- A reduction of the latency to few tenths of  $\mu$ s for the data used by the fast orbit feedback in order to improve its bandwidth.

This kind of electronics has compensation mechanisms in order to damp the effects of thermal drifts and stabilize the measurement on the long term (minutes to hours). If the multiplexing mechanism is well known and generalized on this kind

of equipment, it has also some drawbacks (like the limited switching speed or the need for additional filtering) that may go against our intention to reduce the latency of the fast data. For that reason we are currently considering and testing a new scheme called 'pilot tone' that consists of injecting a reference signal very close to the RF frequency and compensating the drifts seen by this reference on the BPM position.

Commercial products are being characterized to see if it can fit our requirements. Nevertheless we are

also considering possible collaboration with other accelerator institutes for the development of this equipment.

### Beam Loss Monitors

The Beam Loss Monitor (BLM) system has recently been upgraded for scintillators/Photo Multiplier Tube (PMT) detectors associated to dedicated fast electronics<sup>[3]</sup>. Its data acquisition is synchronized with the revolution frequency and injection events. The system is able to measure short events (like partial sudden losses) and also slow losses due to stored beam lifetime. Thanks to a precise relative calibration, and systematic location around the future storage ring and injection system, those beam loss monitors will be a very useful tool to ease the commissioning. All 80 BLMs recently installed will be reused on the future machine.

### Other diagnostics

The other diagnostic systems that are foreseen for the new machine will be similar to those currently in operation at SOLEIL. For those, there is no need of improvement in their performance.

The storage ring beam **current** will be measured by two DC current transformers. The sensors will be renewed to fit the new machine geometry, whereas the acquisition electronics which is being upgraded can be reused.

The distribution of the electrons in the different buckets, or **filling pattern**, will be measured by high sampling rate ADCs acquiring either the signal of a visible

Diagnostic	Type	Quantity
Emittance Monitor	PHCs/Fresnel diffraction on X-rays	2
	Interferometry/Polarized imaging on visible light	1
Beam Position Monitor	RF-BPMs	176
	X-BPMs	30
Beam Current	DCCT	2
Filling Pattern	APD + fast acquisition	1
	BPM + fast acquisition	1
Bunch Purity	TCSPC	2
Bunch Length	Streak Camera	1
Beam Loss Monitor	Scintillators + PMT	80
Dose Monitor	RadFET	40
Tune Excitation	Shaker magnet	1
Tune Detection	BPM + FFT on Turn by Turn position data	1
Machine Protection	Scrapers H/V	2
	Collimators H/V	2

Table 36: Diagnostic systems for the upgraded storage ring

light avalanche photodiode (installed on a branch of the visible light synchrotron radiation monitor), either on a BPM signal. The **bunch purity** (determined by the electron quantity ratio between filled and empty bunches) will be based on Time Correlated Single Photon Counting (TCSPC) method, with an X-ray avalanche photodiode collecting the synchrotron radiation produced by a bending magnet (or photon induced by fluorescence of a target, like typically the pinhole camera copper attenuator) and a time to digital converter.

On low emittance rings, **collimators** are required in order to localize the beam losses. It is foreseen to install one or two collimators to protect the machine and in particular the permanent magnets.

The list of all the diagnostics foreseen for the upgrade is shown in [Table 36](#).

### Feedbacks

In order to assure the tight beam stability requirements (see section Beam Stability), feedback loops will be implemented with improved performances with respect to existing ones at SOLEIL.

The **orbit feedback** loop efficiency will be pushed up to 1 kHz (compared to ~150 Hz now). The main limitation for the closed loop bandwidth in SOLEIL architecture is the latency. This latency should not exceed 50  $\mu$ s for the upgrade. The processing will be centralized in order to keep flexibility in the controller implementation.

The **beam size/coupling feedback** will also be improved by speeding up the correction frequency. Firmware image acquisition and processing will provide faster and synchronous beam size measurement as input for this feedback.

### Timing system

The specifications of the timing system are not supposed to evolve drastically for the SOLEIL upgrade. This system is the 'heart' of the facility, delivering the trigger signals for all equipment on the accelerators or beamlines. The current system is based on master/slaves events architecture and has proven since 2006 its very high reliability. Nevertheless most of its electronic components are becoming obsolete and this system needs also to be upgraded.

Three different solutions are currently under study for the future timing system:

- The most obvious is to keep a system based on master/slaves architecture. Two very similar commercial products are available and already spread in the synchrotron community:
  - > Greenfield Technology solution: It is the system used at SOLEIL. It is well known and well mastered by our teams. Most of all, it has been so far very reliable and satisfactory.
  - > Microresearch system is the de-facto standard when it comes to timing system for synchrotrons. It is successfully used by many facilities around the world and it has a huge user community.

Another possibility is to use the White Rabbit solution. This system, undertaken by an open hardware collaboration initiated by the CERN, is based on time distribution architecture. It is well known among the collider accelerators and the radio-telescopes communities, and has been recently adapted to be used on synchrotrons by ESRF. This kind of architecture would require more work and in depth changes to be implemented at SOLEIL, but it has a fast growing community and a steep development rate. Moreover SOLEIL is about to become a partner of the REFIMEVE project that distribute a high precision absolute clock through the french territory from the LNE-SYRTE laboratory. Its network relies also on White Rabbit electronics, and SOLEIL would soon have in house some modules as receivers. This makes it an interesting alternative solution.

### REFERENCES

[1] Chubar, O. and Elleaume, P., "Accurate and Efficient Computation of Synchrotron Radiation in the Near Field Region", Proceedings of EPAC'98, Stockholm, Sweden, p. 1177 (1998).

[2] Nosych, A. A., et al. "Electrostatic Finite-element Code to Study Geometrical Nonlinear Effects of BPMs in 2D", proceedings of IBIC15, Melbourne, Australia. doi:10.18429/JACoW-IBIC2015-TUPB047 (2015).

[3] Torino, L., and Scheidt, K., "New Beam Loss Detector System for EBS-ESRF", Proceedings of IBIC'18, Shanghai, China, doi:10.18429/JACoW-IBIC2018-WE0B01 (2018).



## Beam stability

### Introduction

#### Stability as a guiding principle for high performance

Stability is essential to guarantee the best performance for both the electron and photon beams in terms of flux, brilliance, spectral purity and coherence fraction. Overall, the third and fourth generation synchrotron light sources aim at 99% beam availability and 100 h meantime between failures. Those stability criteria shall be expressed over short, medium and long-term periods and can be translated as stability requirements on the position and angle of beam size and divergence of the source points, stability of the current during top-up injection with its tolerable transient effects, magnetic reproducibility between two user weeks, between two shutdown periods, etc. Preservation of quantities such as the temporal structure of the beam, namely the bunch length, the bunch separation and bunch purity are also essential for time resolved experiments. The stability is therefore a very broad and transverse subject where special attention should be paid to the weak link of the stability chain. All sources of noise should then be carefully identified and alleviated as much as possible during the design for both accelerator and beamline components (thermal drifts, mechanical vibration of rotating machines, supports of magnets, mirrors, detectors of beamlines, frequency dependent electric noise of power supplies, etc.). On the top of that, the use of mechanical vibration dampers is mandatory for all systems. Active systems (feedbacks, feedforwards) shall be used at a last stage to ensure that stability will not jeopardize state-of-the-art science carried out by the BeamLines (BL).

#### Stability achievement for the present facility

Stability requirements have already deeply evolved since the early design of the present SOLEIL facility in line with new generations of detectors, new experimental techniques with a significant increase of the acquisition velocity, the use of nano-beams and coherence property of the photon beam to cite just a few of them. The stability requirements for orbit initially of 10% of the beam sizes was revised down to 2 to 5% for crystallography beamlines. NANOSCOPIUM and ANATOMIX request not only orbit and angle stability over an 8 h timespan but also for beam sizes and divergences. Today the storage

ring operates with 5 feedbacks (slow and fast orbit feedback, vertical beam size, tune and transverse bunch per bunch feedback, [See Table 37](#)). Thanks to a very stable slab with settlement lower than  $10 \mu\text{m}/\text{year}/10 \text{ m}$ , the storage ring was never realigned since the first beam. It is worth noting that a day-night impact is seen by the long beamlines and is due to the change of the solar illumination and temperature on the ratchet wall inducing to local variation of the slab supporting the BPM and XBPM of  $3.25 \mu\text{m}/^\circ\text{C}$  and  $0.65 \mu\text{rad}/^\circ\text{C}$ ; Overall, low thermal expansion terminations have been installed for all BPM electronics hosted in the cabinets of the technical gallery to guarantee long-term stability. Besides thermal drifts, the stability is currently limited by the power supply noise.

### New accelerator specificities and requirements

#### New challenges and target for a state-of-the-art stability

The upgrade of the SOLEIL accelerator complex is only possible thanks to the advancement of technologies and miniaturization of the devices allowing the use of extremely high magnetic fields defining the electron beam properties circulating within narrow vacuum vessels. Regarding stability, several requirements were not specified or necessary when SOLEIL was originally built; others are tighter and sometimes more stringent than those of other upgraded facilities like ESRF-EBS.

For the SOLEIL upgrade, a reduction by a factor 40 (30) is expected on the horizontal beam sizes for the short (medium) straight sections due to the reduction in emittance, beta functions and dispersion with respect to the present lattice; the vertical divergence is reduced by a factor 2 to 5 for 10% coupling operation (Table 2, page 58). This makes challenging the achievement of the required stability that scales with the transverse beam sizes: for user operation the working emittance ratio is assumed to be either 100% (Table 38, Table 39) or 10% (Table 40, Table 41) taking into account ID configurations. Moreover, for machine studies and preparing user operation, it will be necessary to work at minimum of coupling (0.1-1%).

#### Impact of technology choices on stability

The vacuum chambers act as a low-pass filter: whereas the cut-off frequency was around 10 Hz for the present arc chamber,

it increases to more than 850 Hz for a Cu chamber of 1 mm thickness because of the small diameter in the arcs (10 mm) and straight sections (6 mm). The direct consequence is that high frequency power supply (PS) noise, attenuated by the present chamber for the present lattice, will become unacceptable for the upgrade lattice, leading to a more complicated design of their electronics, expected to be the limiting factor of the stability.

Then, if the extensive use of permanent magnet-based dipoles and quadrupoles avoid cooling circuits, an inherent source of instability, it puts on stress the stability with temperature, where the use of thermo-shims becomes necessary and will require special calibration. Moreover, the absolute energy calibration of the magnets will be more difficult, and a nuclear magnetic resonant probe cannot be used anymore to guarantee over a long period of time an energy stability better than 0.01%. Finally, radiation damaged and magnet degradation should be carefully monitored.

#### Impact of round beam and IDs on stability

Working on the coupling resonance to equalize the transverse emittances is challenging in terms of daily operation; stabilizing betatron tunes will require further investigation. Due to the low natural emittance for a 2.75 GeV storage ring, the horizontal emittance will be tightly linked to the ID configurations (decreasing from 55 to 38 pm.rad for round beam): IDs represent more than 68% of the dipole-based energy loss per turn (<30% for the present lattice). Consequently, beam size and lifetime stability will vary over time: use of controlled white noise to excite the beam in both planes is being considered. Lower beam lifetime will put a strain on the injector complex which much larger solicitation for the time resolved filling patterns. Moreover, a new low emittance booster (< 10 nm.rad) is required to fulfill the injection requirement into the storage ring.

A list of foreseen FeedBack (FB) and FeedForWarD (FFWD) systems to ensure beam stability is given with stability levels in [Table 42](#). Assuming BL requirements with fast acquisition of 1 ms, the Fast Orbit FeedBack (FOFB) bandwidth shall be pushed up to 1 kHz (150 Hz today), targeting a 50 nm RMS beam stability (200 nm RMS for the present facility). From day one, the FB architecture should

Feedback	Application frequency	Beam stability	Remarks
SOFB	DC-0.2 Hz	Application frequency: 0.2 Hz	Smart communication between the two FB
FOFB	DC-150 Hz	500 (H)/250 (V) nm RMS over 1 kHz	
Tune FB	DC-0.2 Hz	$5 \cdot 10^{-4}$	Global compensation of ID induced focusing variations
V-beamsize FB	DC-2 Hz	0.7% with slow IDs < 2% with fast IDs	White noise excitation using TFB Only 2 points of measurement For NANOSCOPIUM BL, peak-to-peak requirement (no reached today)
TFB	176 MHz	Against resistive wall instability, Fast ion instabilities, etc.	SOLEIL/SPring8/TED Processor
FFWD	NA	15 A/100 ms (HU640)	For fast ID switching

Table 37: Performance of FB and FFWD systems for the present lattice: SOFB (Slow Orbit FeedBack), FOFB (Fast Orbit FeedBack), (FFWD FeedForWarD), TFB (bunch-by-bunch Transverse FeedBack)

Location	H-beam size (μm)	H-beam divergence (μrad)	V-beam size (μm)	V-beam divergence (μrad)
Injection SS	20.90	<b>1.82</b>	11.03	3.45
Long SS	11.03	3.45	11.03	3.45
Medium SS	7.80	3.45	7.29	5.21
Short SS	6.47	5.88	<b>6.75</b>	5.63
3T Superbend	<b>6.99</b>	12.58	16.07	<b>2.36</b>

Table 38: RMS Beam sizes and divergences for a 100% coupling beam, using an emittance of 38 pm.rad in both planes (reference lattice w/ IDs)

Location	H-beam size (μm)	H-beam divergence (μrad)	V-beam size (μm)	V-beam divergence (μrad)
Injection SS	26.70	<b>2.32</b>	4.53	1.41
Long SS	14.09	4.4	4.53	1.41
Medium SS	9.96	6.22	2.99	2.14
Short SS	8.26	7.51	<b>2.77</b>	2.31
3T Superbend	<b>7.39</b>	16.07	6.60	<b>0.97</b>

Table 39: RMS Beam sizes and divergences for a 10% coupling beam, using emittances of 62/6 pm.rad in H/V planes (reference lattice w/ IDs)

Location	H-position (nm)	H-beam angle (nrad)	V-position (nm)	V-beam angle (nrad)
Injection SS	418.1	<b>36.4</b>	220.5	68.9
Long SS	220.5	68.9	220.5	68.9
Medium SS	155.9	97.5	145.9	112.5
Short SS	<b>129.3</b>	117.6	<b>135.1</b>	112.5
3T Superbend	139.7	251.7	321.5	<b>47.3</b>

Table 40: Requirements for 2% stability of position and angle in the case of a 100% coupling beam, using natural 62 pm.rad (reference lattice w/ IDs)

Location	H-position (nm)	H-beam angle (nrad)	V-position (nm)	V-beam angle (nrad)
Injection SS	534.0	<b>46.4</b>	90.5	28.3
Long SS	281.1	88.0	90.5	28.3
Medium SS	199.2	124.5	59.9	42.8
Short SS	165.2	150.2	<b>55.4</b>	46.2
3T Superbend	<b>147.7</b>	321.5	131.9	<b>19.4</b>

Table 41: Requirements for 2% stability of position and angle in the case of a 10% coupling beam, using natural 62 pm.rad (reference lattice w/ IDs)



FB / FFWD system	Frequency bandwidth	Stability level	Remarks
FB: closed orbit	0.01- 1000 Hz	2-3%	A single or an interleave of two systems as today
FFWD: closed orbit	20-100 Hz	2-3%	Depending on the types of ID
Tune	1) 10 Hz 2) 20-100 Hz	10 <sup>-5</sup>	1) Global feedback working close the coupling resonance 2) Local feedforward system Dedicated ID FFWD systems when required
Vertical beam size	20-100 Hz	5-10%	Type 1: using with noise in the vertical plane from the minimum emittance Type 2: using skew quadrupoles to excite a vertical dispersion wave Type 3: dedicated ID FFWD systems when required
Horizontal beam size	20-100 Hz	5-10%	Use of the white noise to compensate the variation of emittance due to the configuration of insertion gaps. Same system used to blow-up the beam during short bunch operation.
Bunch by bunch charge feedback	DC - 3 Hz	<0.2% full current 5-10% per bunch	If an even filling pattern is mandatory by beamline request
Bunch by bunch transverse feedback	176 MHz	N/A	Same as today
Bunch by bunch longitudinal feedback	176 MHz	N/A	New system if required
Transient Beam position	10 μs	< 10% beamsize	Type 1: Gating signal on demand Type 2: FFWD table using the bunch by bunch feedback
Transient Beam size	10 μs	TBD	Gating signal on demand

Table 42: List of feedback and feedforward systems together with the stability level and the requested bandwidth.

be designed to incorporate XBPMs installed on beamline front-ends or on the beamline themselves. Benefit of XBPMs should be explored further, especially considering the challenge associated with the changing emission shape of EPU type undulators used for intermediate energy BLs.

Even with an intermediate energy of 2.75 GeV, the lattice could be even more sensitive than today to ID errors (first and second field integrals, pointing value, tunes, couplings, non-linearities); IDs will require new carefully optimization and faster analog feedforward compensation systems allowing efficient energy scans.

### Thermal and vibration stability requirements

Temperature regulation is critical for stability (better than  $\pm 0.05^\circ\text{C}$ ): extension of the air-conditioning systems to the injector complex, the new booster ring and special care for the electronics of the storage ring component whose electronics boards should be hosted in thermo-regulated cabinets.

To mitigate cooling water and mechanical induced vibration, all rotating equipment (fans, compressor, pumps, etc.) should

be located outside the tunnel or BL hutches, as far as possible and equipped with dedicated vibration dampers and isolated using viscoelastic dampers or attached to the ceiling away from the support guaranteeing the beam stability. Flow velocities of the cooling water should be below 2 m/s (to avoid vibration induced corrosion, cavitation, etc.). Mechanical vibration of supports and girders will need careful analysis to make the eigenfrequency preferably higher than 100 Hz. Analytical models double checked with dedicated measurements should be employed to ensure that the flow velocity and support do not jeopardize the stability requirements.

### Photon beam stability

Regarding beamlines, the photon beam stability also strongly depends on the stability of the optical components which are themselves entirely dependent on the stability of their support. Low frequency drifts originate mainly from thermal drift in the optical and experimental hutches. The temperature stability is expected to be at least of  $0.1^\circ\text{C}$ . Moreover, past experience has shown that the best way to obtain a stable set-up is to design it with a high intrinsic stability which can be, if possible, reinforced by

deploying active compensation systems such as the control of a high precision piezoelectric movement in closed loop with an interferometer. Depending on the BL configurations and the experimental techniques, a study shall be carried out on a case by case basis. When dealing with higher sources of vibrations, optomechanical devices are often the limiting factors due to the optics cooling system (coolant circulation but also cooling tubes acting as an antenna). The same systematic rules described for the electron beam stability should be carefully applied to reduce, from the design stage, the introduction of vibration to the photon beam up and the user sample.

### Conclusion

Finally, a stability work group will be set up across all divisions to ensure that stability is well taken into account from the design stage, call for tenders to the implementation and, from the electron sources to the photons shed on user samples.

## Photon sources

This section presents a first vision of photon sources from insertion devices and from bending magnets. The new lattice will enable the installation of insertion devices with magnetic material surrounding a circular vacuum chamber, with magnetic gap closed to smaller values than presently. Such insertion devices could not have been installed in the present ring. As a consequence, SOLEIL upgrade will benefit both from the emittance reduction and from the change of the insertion devices, delivering both larger flux and brilliance with respect to the present situation.

### Insertion device photon sources

#### The necessary evolution of the insertion devices portfolio due to new constraints

The present panoply of Insertion Devices (ID) at SOLEIL (Figure 88) covers four decades in photon energy. Different spectral domains can be distinguished. Variable polarization is provided in the low and intermediate energy range with Helical Undulators (HU): in the low energy part with a 10 m long HU640 electromagnetic undulator enabling fast switching of the polarization, in the intermediate soft X-ray range with one or two HU devices in series in the straight section (a 3.5 m long ID named HU256 with possible aperiodicity, 1.6 m long APPLE-II undulators with periods ranging from 36 to 80 mm, Electromagnetic Permanent Magnet Helical Undulator EMPHU65<sup>[1]</sup> enabling fast polarization switching for dichroism experiments). The hard X-ray spectral range is supplied thanks to In Vacuum Undulator (IVU) with SmCo and NdFeB magnets (periods 20 and 24 mm, 5.5 mm minimum gap), two Cryogenic Permanent Magnet Undulators (CPMU)<sup>[2,3]</sup> CPMU18 using PrFeB magnets period (5.5 mm minimum gap) for the two canted long beamlines, an In Vacuum Wiggler (IVW) that can be

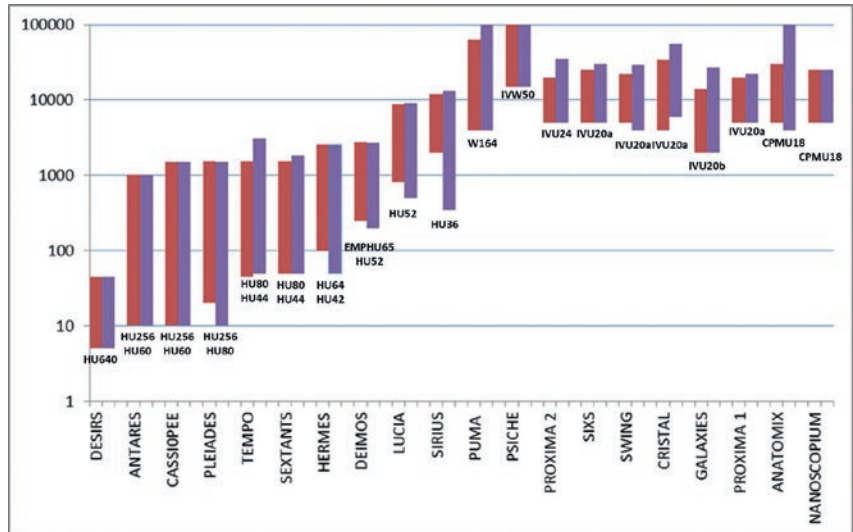


Figure 88: Evolution of the spectral range (Energy range in eV) for the SOLEIL beamlines: present (red) and upgraded (violet) SOLEIL. Insertion devices presently installed with associated horizontal /vertical deflection parameter  $K_u$  and period number  $N_u$ :  
 HU640,  $K_u = 5.4/9$ ,  $N_u = 14$ ; HU256,  $K_u = 7.9 / 10.6$ ,  $N_u = 12$ ; HU80,  $K_u = 5.7/6.4$ ,  $N_u = 19$ ; EMPHU65,  $K_u = 1.46/1.46$ ,  $N_u = 26$ ; HU64,  $K_u = 3.7/5.2$ ,  $N_u = 25$ ; HU60,  $K_u = 3.08/4.48$ ,  $N_u = 26$ ; HU52,  $K_u = 2.6/3.7$ ,  $N_u = 31$ ; HU44 :  $K_u = 1.7/2.6$ ,  $N_u = 36$ ; HU42,  $K_u = 1.4/2.2$ ,  $N_u = 38$ ; HU36,  $K_u = 1.8/2.5$ ,  $N_u = 44$ ; IVU24,  $K_u = 1.88$ ,  $N_u = 83$ ; IVU20a,  $K_u = 1.8$ ,  $N_u = 98$ ; IVU20b,  $K_u = 2.05$ ,  $N_u = 98$ ; CPMU18,  $K_u = 1.95$ ,  $N_u = 107$ ; W164,  $K_u = 27.6$ ,  $N_u = 20$ ; IVW50,  $K_u = 10.7$ ,  $N_u = 40$

closed down to 4.5 mm and an out of vacuum wiggler W164<sup>[4]</sup>.

#### Update of the beamlines specifications

Figure 88 shows the evolution, resulting from a survey of scientific needs, of the photon spectral range to be covered by the IDs for the upgrade. Whereas the soft X-ray region is barely modified in terms of range, one can notice an extension of spectral range towards harder X rays and an increased demand for lower energies. The survey also points out that the request in terms of polarization variation is similar and that both flux density and brilliance are of high necessity for a great part of experiments.

#### Constraints from the machine

Table 43 presents the geometrical constraints imposed by the CDR reference lattice V0313 considering the

beam stay clear for the stored beam and at injection, and the remaining available space resulting from the implementation of the different hardware. Because of the straight section reduced lengths, it is no longer possible to provide two HUs for one beamline or accommodate the very long HU. These devices should be replaced by new IDs.

Table 44 presents the geometrical constraints for the different IDs depending on the type of straight section where they will be implemented and the possible vacuum chamber requirement. Thanks to the possibility of closing the gap further, ID periods can be modified to properly fit the required photon spectral range. The 3 m length of the short straight section given in the table does not correspond to the one present in the CDR reference lattice (2.73 m). Indeed, it has been assumed that a revised version of the lattice, to be studied in the TDR phase, will enable an

Straight section	Length	ID length	Minimum Horizontal Aperture	Minimum Vertical Aperture
	m	m	mm	mm
Short Straight Section	2.73***	2	6	4
Medium Straight Section	4.15	3	6	4
Long Straight Section #1	7.35	5*	14	8
Long Straight Section #2	7.66	2**	6	6

\*one long straight section will host an insertion device of about 5 m and the harmonic cavity. \*\*: two canted in-vacuum undulators. \*\*\*: to be soon extended to 3 m

Table 43: Geometrical constraints for the beam stay clear and from the lattice compactness



Straight section	ID type	ID length	Minimum Horizontal gap	Minimum Vertical gap
		m	mm	mm
Short Straight Section	<i>In vacuum</i>	2	6	4
Medium Straight Section	<i>In vacuum</i>	3	6	4
Medium Straight Section	<i>Out of vacuum</i>	3	10	10
Long Straight Section #1	<i>Out of vacuum</i>	5	18	12
Long Straight Section #2	<i>In vacuum</i>	2	6	4
Long Straight Section #2	<i>Out of vacuum</i>	2	10	10

Table 44: ID geometrical constraints according to their type and straight section allocation

increase in length, allowing for the existing IVUs and CPMUs to be re-installed for the upgrade commissioning, with only the minor modifications required for the new mechanical interfaces.

### ID photon beam extraction and power deposition challenges

In the geometry of the new lattice, the electron angular deviation and the photon beam pipe diameter are much smaller than in the present ring, making critical the extraction of the photon beam for the ID. In some cases, unused power can be directly absorbed in the vacuum chamber. The power deposited on the first beamline optics has also to be handled.

### ID renewing strategy

In the current strategy, the machine would restart with 3 to 5 new IDs, with high photon energy beamlines using existing in-vacuum undulators at 5.5 mm gap, while the beamlines equipped with two EPUs will have to select one of the existing IDs. The 10 m long HU640 will be rebuilt. Over a longer period, the majority of the IDs have to be rebuilt (the exception being the two existing CPMU18s), to fit and be optimized for a 4 mm gap with the new geometrical constraints. A full scale prototype of each new type of ID will be built prior to the machine upgrade shutdown.

### Helical undulator for the low / intermediate energy adjustable polarisation beamlines

#### Helical Undulator for low photon energy beamline

The HU640 10 m long ID of the beamline for the 5-40 eV spectral range will be replaced by a 250 mm period and 5 m length crossed Adjusted Phase Undulator (APU) (Figure 89), either cancelling one of the fields producing horizontal and vertical polarization, or setting the phase to  $\pi/2$  and  $-\pi/2$  for the generation of vertical and horizontal magnetic fields (see calculated field in Figure 89 with

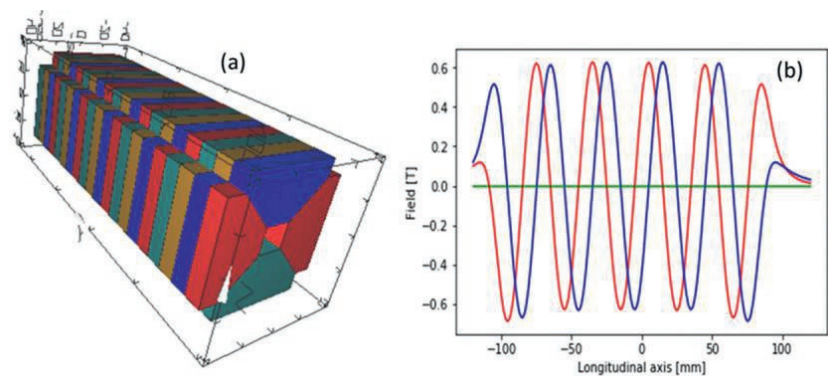


Figure 89: RADIA model of the APU250 for DESIRS beamline a) 3D magnet sketch b) Vertical and Horizontal magnetic fields calculated with RADIA software

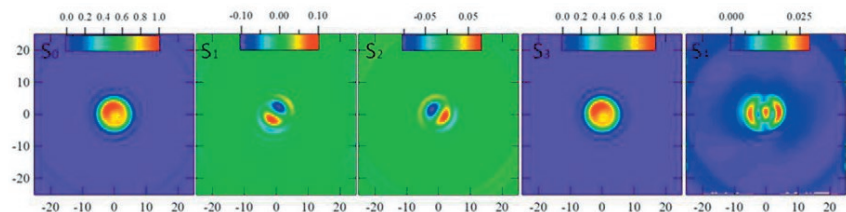


Figure 90: Stokes parameters (S0, S1, S2, S3, S4) spatial distribution normalized by the peak intensity ( $2.33 \cdot 10^{13}$  Ph/s/0.1%bw/mm<sup>2</sup>) for the helical undulator case at E = 5 eV

RADIA<sup>5</sup> software) and thus circular right and left polarization. The field is varied by independent longitudinal dephasing from 0 T to 0.46 T of each girder. The photon energy is adjusted by girder motion. Stokes parameters calculated with SRW software<sup>[6]</sup> are illustrated in Figure 90.

#### Solutions for the intermediate energy range with adjustable polarization

Three technical options are being explored to cover the intermediate energy range (10 eV-5 keV) with adjustable polarisation: dual EPU, bi-periodic undulator, cryogenic APPLE-III undulator. Contrary to the approach of present SOLEIL where two EPUs are installed one after the other in the medium straight section, only one ID will cover the whole spectral range in the upgraded ring.

#### Dual EPU

The dual EPU is equipped with a mechanical system enabling to switch from one undulator to another by means of lateral displacement (translation stage such as in CLS<sup>[7]</sup> and in Shanghai Light Source) or girders rotation with sufficient reproducibility. Figure 91 illustrates proposed mechanical solutions: two independent EPUs (a), simple for construction and measurement, but requiring sufficient lateral space; aligned magnet rows on a single carriage (b), very compact one, enabling lateral access as compared to the crossed magnet row case (c). The lateral movement is more adapted than the rotation (revolver type (d)) for the phase movement.

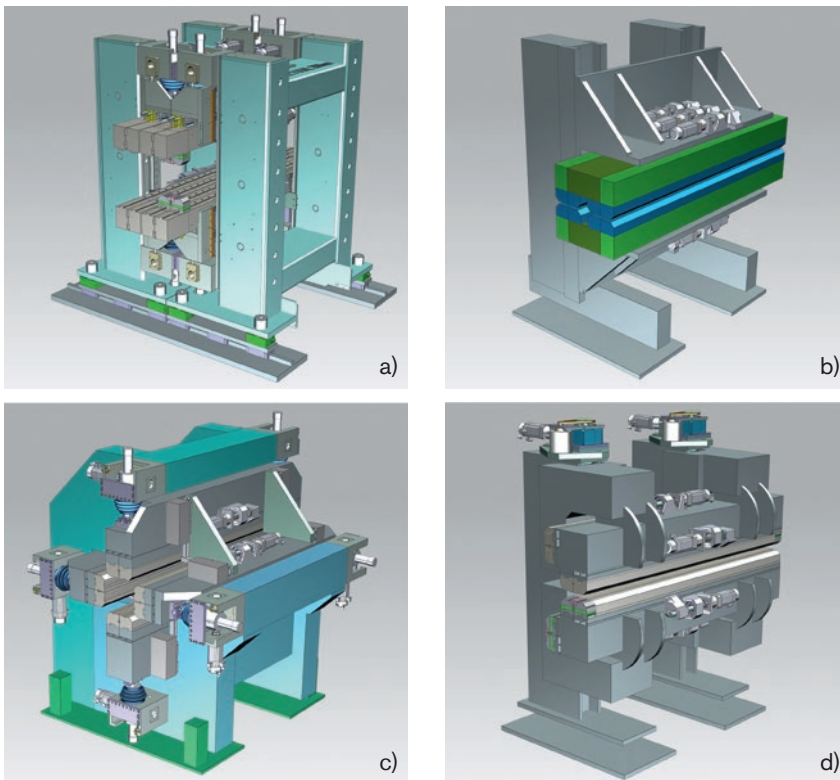


Figure 91: Mechanical solutions for dual EPU : a) two independent ID solution, b) single carriage aligned magnet rows, c) single carriage crossed magnet rows, d) revolver case

force compensation (additional magnet row), the liner holding (Figure 92).

#### Solutions for the hard photon Energy range

#### Evolution of the in-vacuum undulators (IVU) to CPMUs

Present IVUs will be replaced by CPMUs with adapted period length to provide the desired spectral range. The search for small period length with thin magnets and poles pushes the technique of pole-magnet-pole keeper to the mechanical limits. A prototype of few periods of 12 mm (Proto-CPMU12), installed on 8-period keepers, is under construction for checking in particular the mechanical tuning, the accuracy of positioning of magnets and poles and the rigidity of keepers (Figure 93).

In addition, a 3 m long CPMU15 is presently under construction at SOLEIL, with a specifically developed embedded magnetic measurement bench targeting measurements down to 3 mm gap, robotization tests for improving the efficiency in manufacturing (such as for the module magnetic measurements).

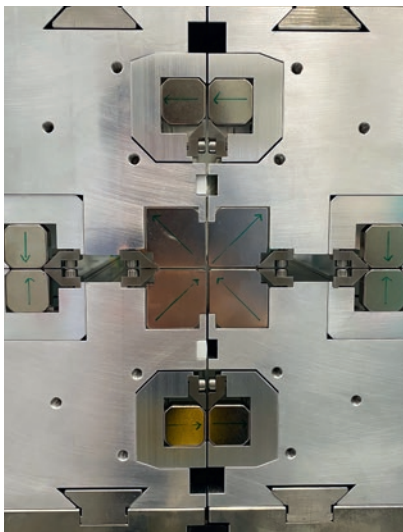


Figure 92: Picture of the CPMUE32 prototype

#### Bi-periodic undulator

The bi-periodic undulator is a new type of insertion device operating with 2 magnetic periods distinguishably.

#### Cryogenic Permanent Magnet Elliptical Undulator (CPMUE)

Reducing the gap by putting the magnet under vacuum enables an increase in magnetic field, hence deflection parameter, further extending the radiation towards the lower energy range compared to an out-of-vacuum device of identical period. A CPMUE41 has been designed, using the APPLE-III magnet configuration and PrFeB magnets for cryogenic use, with a 6 mm diameter aperture. A prototype of CPMUE32 is under construction, in order to validate the assembly of the magnets, the magnetic

#### Evolution of the wigglers

One Permanent Magnet (PM) in-vacuum wiggler of 2.3 T and one out-vacuum wiggler of 1.8 T are presently in operation at SOLEIL respectively at a gap of 4.5 mm and 14.5 mm. To increase the magnetic field and the critical energy, new PM in-vacuum wigglers are planned to operate with lower gap (4 mm) at room temperature such as with WSV50 and later at cryogenic temperature to increase the magnetic field.

#### ID performance

Figure 94 compares the ID brilliance between the present and the upgraded machine with typical IDs. The brilliance has been calculated using SPECTRA<sup>[8]</sup> in the Gaussian approximation.

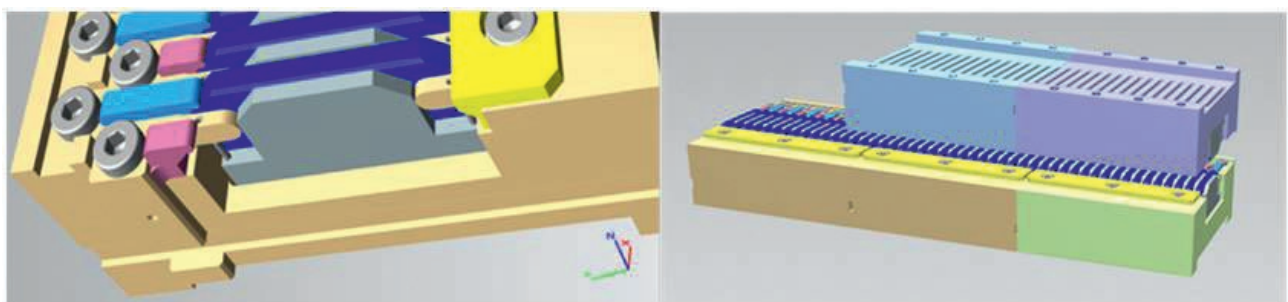


Figure 93: Mechanical design of the proto-CPMU12. Left: Magnets (dark blue) poles (Gray), clamps (Bright yellow, light blue and magenta) keeper (Light yellow). Right: Assembly of top and bottom keepers.

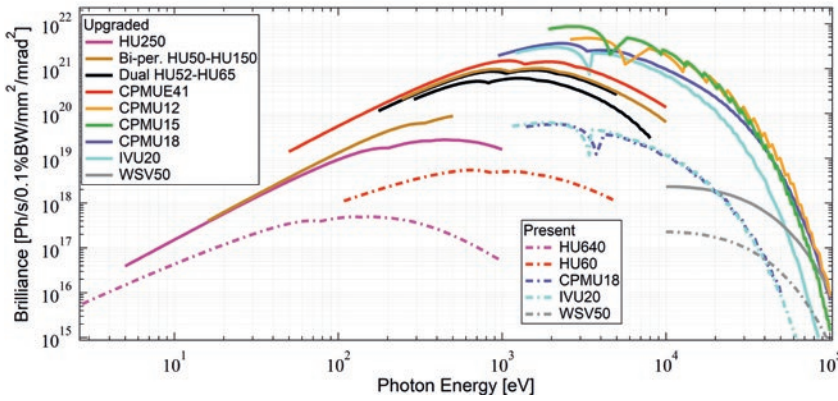


Figure 94: Evolution of the spectral brilliance with SOLEIL upgrade. Present (dashed line, 1% coupling) and upgrade (full line, 100% coupling). Calculations with SPECTRA considering the Gaussian approximation. ID parameters: for the present lattice IDs, see parameters in the caption of Figure 88; for the new lattice: HU250,  $K_u = 0.46/0.46$ ,  $N_u = 20$ ; Biperiodic HU50-HU150,  $K_u = 3.17/3.17 - 7.74/7.74$ ,  $N_u = 60-20$ ; Dual HU52-HU65,  $K_u = 2.52/3.74 - 1.46/2.43$ ,  $N_u = 57-46$ ; CPMUE41,  $K_u = 8.27/8.27$ ,  $N_u = 73$ ; 14; CPMU12 is operated down to 3.5 mm with  $K_u = 1.62$  and  $N_u = 125$ ; CPMU15 is operated down to 4 mm with  $K_u = 1.75$  and  $N_u = 200$ ; CPMU18 is operated down to 4 mm with  $K_u = 2.57$  and  $N_u = 111$ ; IVU20, same as present lattice, IVW50,  $K_u = 11.2$ ,  $N_u = 40$

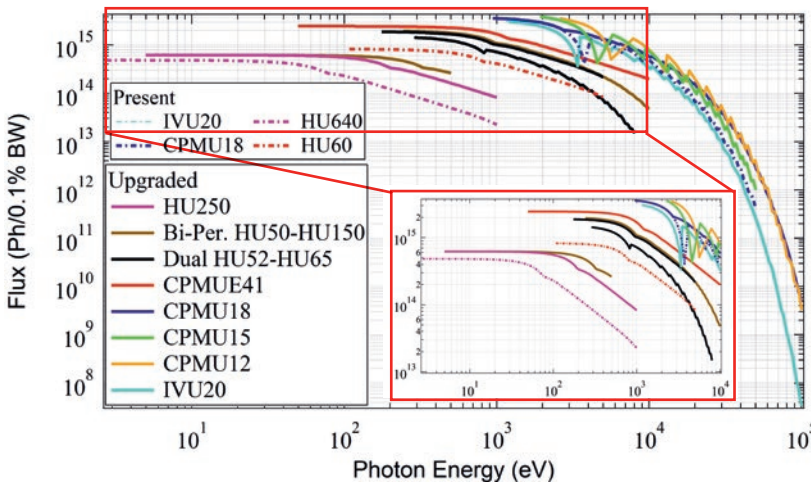


Figure 95: Evolution of the photon flux with SOLEIL upgrade. Present (dashed line) and upgrade (full line). Calculations with SPECTRA considering the Gaussian approximation. ID parameters: for the present lattice IDs, see parameters of Figure 88; for the new lattice: HU250,  $K_u = 0.46/0.46$ ,  $N_u = 20$ ; Biperiodic HU50-HU150,  $K_u = 3.17/3.17 - 7.74/7.74$ ,  $N_u = 60-20$ ; Dual HU52-HU65,  $K_u = 2.52/3.74 - 1.46/2.43$ ,  $N_u = 57-46$ ; CPMUE41,  $K_u = 8.27/8.27$ ,  $N_u = 73$ ; 14; CPMU15,  $K_u = 1.75$ ,  $N_u = 200$ ; CPMU18,  $K_u = 2.57$ ,  $N_u = 111$ ; IVU20, same as present lattice, IVW50,  $K_u = 11.2$ ,  $N_u = 40$

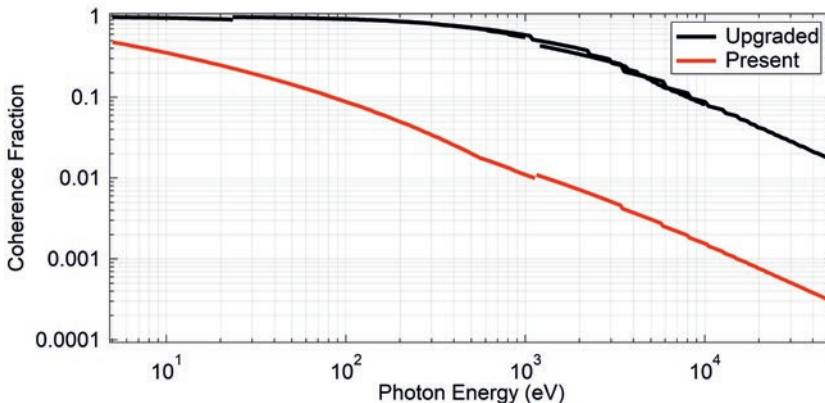


Figure 96: Evolution of the ID coherent fraction with SOLEIL upgrade: present (red, 1% coupling) and upgrade (black, 100% coupling). Calculations using SPECTRA using the Gaussian approximation. ID parameters of Figure 8

Additional calculations using the Wigner distributions<sup>[9, 10, 11]</sup> does not introduce significant changes in the result. *In vacuum* insertion devices and CPMUs are supposed to operate on present machine down to their nominal minimum gap (5.5 mm for IVU/CPMU and 4.5 mm for IVW50). Even if most of IVUs, CPMUs and IVW50 will be re-used during restart of operation, final performance on the new machine has been evaluated considering new CPMUs (CPMU12, CPMU15 or CPMU18) that take the place of the previous ones. The spectral range covered by the dual and bi-periodic undulator is modelled by two ID (two brown / black curves). The brilliance increases by one order of magnitude (in the low energy range) up to more than two orders of magnitude (in the high energy range), thanks to the combined effect of emittance reduction and ID period number increase.

The flux evolution of a selection of typical IDs, presented in Figure 95, results from a renewing of the ID. Despite the reduced length of the ID, the APU HU250 delivers a larger flux than the present HU640. For the EPU in the intermediate energy range, the adopted solutions (bi-periodic, dual, CPMUE) cover the requested spectral range with the total available 3 m long length, with a gain up to one order of magnitude in flux. The CPMUE keeps this flux increase over a broader spectral range. In the hard X-ray domain, whereas re-installing the present IVU20 undulator at the beginning will keep the flux constant, a progressive renewal of the IDs to CPMU devices of shorter periods benefiting from the smaller possible gap will lead to increased flux (typically by a factor of 4 at 10 keV and 14 at 50 keV).

The transverse coherent fraction, a figure of merit on how one approaches the diffraction limit, is shown in Figure 96. The behavior follows the brilliance evolution, and results from the emittance and ID changes. The increase with the SOLEIL upgrade ranges from a factor 2 at low energy to two orders of magnitude at high energy, where the emittance reduction enables to approach closer the diffraction limit at these photon energies with respect to the present SOLEIL.

### Evolution of the bending magnet photon sources

In SOLEIL upgrade, the number of bending magnets will be greatly increased in order to decrease the emittance. As a consequence, the magnetic field of

bending magnets drops from typically 1.7 T on the present machine to 1 T or even less (additional dipole of 0.7 T, Reverse Bend of -0.2 T). Beamlines operating in the UV or in the IR and THz domains are favoured as the critical energy is reduced. Studies of extraction of VUV and IR/THz light are in progress. Alternative solutions to reach high photon energies on non ID sources are planned. Some of the conventional bending magnets will be modified or replaced by magnetic systems with locally higher field to reach higher photon critical energy.

**Superbend sources**

The superbends present a low background field of 0.5 T and a local peak field of 3 T (Figure 97a) located at the center of the magnetic region. Figure 97 presents the magnetic field distribution of the superbend and the flux density at various photon energies.

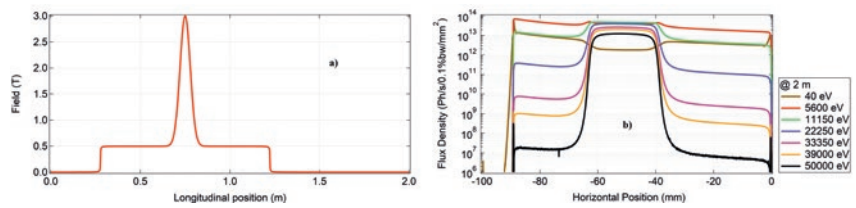


Figure 97 a): Longitudinal profile of the magnetic field of the superbend. b) Flux density between 40 eV and 50 keV

**Double superbend sources**

The number of superbends at 3 T is limited to 4 so as not to alter the emittance. The other beamlines will use bending magnet with 1.7 T peak field. In order to keep the new photon beam trajectory parallel with the present one, the position of the peak field has to be shifted. A solution with two peak fields of 1.7 T (Figure 98a) located symmetrically from the magnetic device center is proposed to keep unchanged the symmetry of the optics of the machine. Figure 98 presents the magnetic field distribution of the superbend and the flux density at various photon energies.

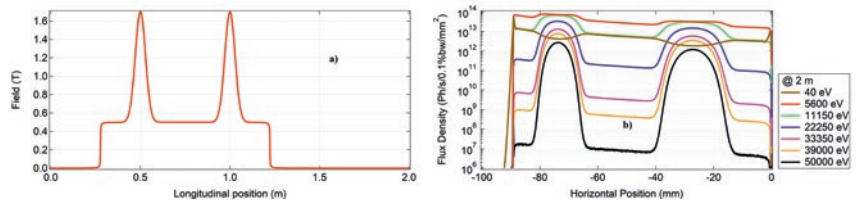


Figure 98 a): Longitudinal profile of the magnetic field of the double superbend. b) Flux density between 40 eV and 50 keV

**N-pole wiggler source**

A preliminary 3-pole wiggler (Figure 99), composed of permanent magnets and ferromagnetic poles is expected to reach 1.7 T. It can be installed on a straight section or between machine magnets thanks to its compactness (100 - 120 mm length).

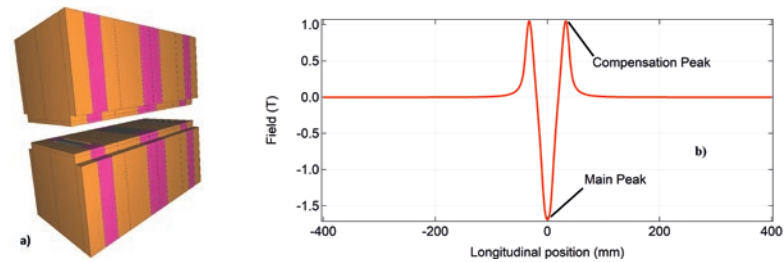


Figure 99 a): RADIA model of the 3-pole wiggler. b) Magnetic field distribution along the electron axis

However the compactness of the system leads to high compensation fields (of the same order of the main field). It results in multi-source effects (interference pattern) limiting the transverse flux homogeneity of typically 1 mrad (Figure 100) in particular at low photon energy (<10 keV).

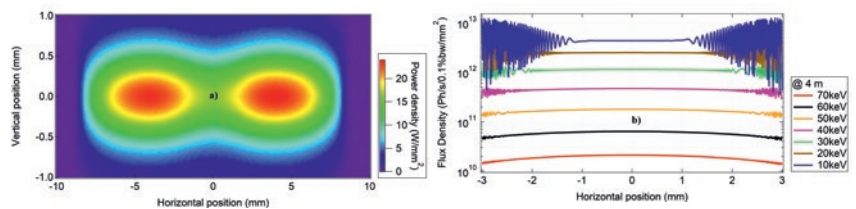


Figure 100 a): Spatial distribution of power observed at 4 m from the 3-pole wiggler center. b) Flux density between 10 keV and 70 keV

It is worthwhile reducing the compensation peak amplitude. A 2 m long alternative pre-design (Figure 101a) in which compensation peaks are strongly reduced from 1.1T to 0.042T (Figure 101b) is proposed. Of course, this solution needs the availability of a short straight section.

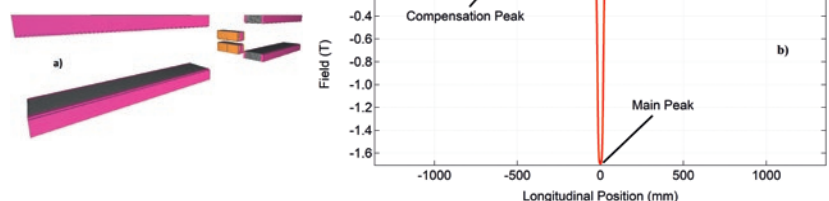


Figure 101 a): RADIA model of the alternative 3-pole wiggler. b) Magnetic field distribution along the electron axis

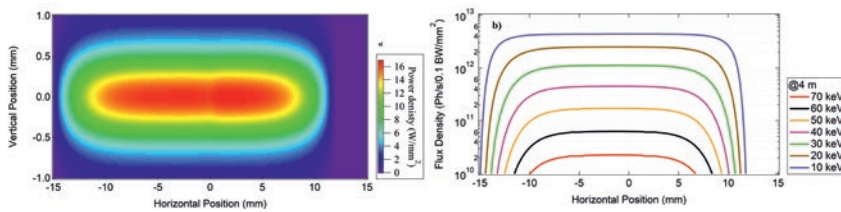


Figure 102 a): Spatial distribution of power observed at 4 m from the 3-pole wiggler center.  
b) Flux density between 10 keV and 70 keV

Compensation peaks still emit photons but their critical energy is much lower than the main peak one and interference are negligible. The power and the flux are much homogeneously spatially distributed (Figure 102).

Figure 103 summarizes the flux density delivered by the different sources.

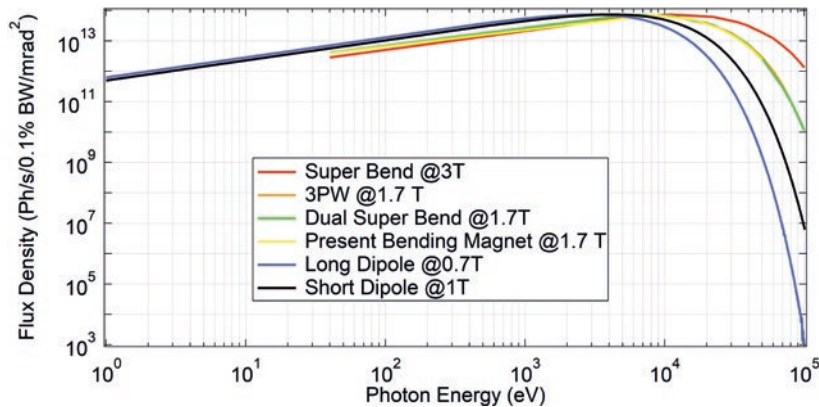


Figure 103: Flux of present bending magnet and alternative synchrotron radiation sources

## REFERENCES

- [1] Marteau, F., et al., "Description of an Electromagnetic/Permanent Magnet Helical Undulator for Fast Polarization Switching", IEEE Transactions on Applied Superconductivity, 22(3), 4102004-4102004 (2012).
- [2] Benabderrahmane, C., et al., "Development and Operation of a Pr2Fe14B Based Cryogenic Permanent Magnet Undulator for a High Spatial Resolution X-Ray Beam Line", Physical Review Accelerators and Beams, 20(3), 033201 (2017).
- [3] Valléau, M., et al., "Development of Cryogenic Permanent Magnet Undulators at SOLEIL", Synchrotron Radiation News, 31(3), 42-47 (2018).
- [4] Marcouillé, O., et al., "In Vacuum Permanent Magnet Wiggler Optimized for the Production of Hard X-Rays", Phys. Rev. Spec. Topics AB 16, 050702 (2013).
- [5] RADIA is a collaboration ESRF/SOLEIL and is freely available for download from <http://www-sources.synchrotron-soleil.fr:8002/mid/software/>. Details have been published in: Elleaume, P., Chubar, O., Chavanne, J., "A Three-Dimensional Magnetostatics Computer Code for Insertion Devices", Journal of Synchrotron Radiation, 5, 481 (1998).
- [6] Chubar, O. and Elleaume, P., "Accurate and Efficient Computation of Synchrotron Radiation in the Near Field Region", Proceedings of EPAC'98, Stockholm, Sweden, p. 1177 (1998).
- [7] Sigrist, M., et al. "Insertion Device Development at the Canadian Light Source, Simulated and Measured Magnetic Performance of a Double APPLE-II Undulator at the Canadian Light Source", Proceedings of IPAC2010, Kyoto, Japan, pp. 3090-3092 (2010); Baribeau, C., "Simulated and Measured Magnetic Performance of a Double APPLE-II Undulator at the Canadian Light Source", Proceedings of IPAC2016, Busan, Korea, 40254027 (2016); Chen, S. Y., et al. "Support Structure Design of Quantum Material Spectroscopy Center Beamline Insertion Devices", MEDSI, Diamond Light Source Proceedings, vol. 1, e52 doi:10.1017/S204482011000078X (2011).
- [8] <http://spectrax.org/spectra/>
- [9] Tanaka, T. and Kitamura, H., "General Methods for SR Calculation", Journal of Synchrotron Radiation 8, p. 1221 (2001).
- [10] Tanaka, T., "Numerical Methods for Characterization of Synchrotron Radiation Based on the Wigner Function Method", Physical Review Special Topics Accelerators and Beams 17, 060702 (2014).
- [11] Tanaka, T., "Coherent Mode Decomposition of Partially Coherent SR", Optics Letters 42, 1576 (2017).
- [12] Kim, K. J., "Angular Distribution of Undulator Power for an Arbitrary Deflection Parameter K", Nuclear Instruments and Methods in Physics Research Section A: Accelerators, Spectrometers, Detectors and Associated Equipment, 246(1-3), 67-70 (1986).
- [13] Bazarov, I. V., "Synchrotron Radiation Representation in Phase Space", Physical Review Special Topics-Accelerators and Beams, 15(5), 050703 (2012).
- [14] Walker, R. P., "Undulator Radiation Brightness and Coherence Near the Diffraction Limit", Physical Review Accelerators and Beams, 22(5), 050704 (2019).

## Infrared extraction

In order to dispose of a suitable flux in the InfraRed (IR) range, it is mandatory to extract a large solid angle of the emitted radiation. For this purpose, on third generation storage rings, a solid angle of typically  $20 \times 80 \text{ mrad}^2$  is collected on a plane mirror placed after the dipole<sup>[1]</sup>. The feasibility of extracting such large solid angles on the future source is challenging, the difficulty being related to the compactness of the proposed lattice and the significant reduction in the vacuum chamber diameter.

At present, two infrared beamlines (SMIS and AILES) are successfully exploited at SOLEIL. The objective is to develop a new design which will allow the extraction of at least the same photon flux as the present sources. The flux emitted for the upgraded lattice has been simulated in the near field approach using the SRW software<sup>[2]</sup>. These simulations show that among the two bending magnet sources: the 400 mm long dipole with  $B = 1 \text{ T}$  or the 943 mm long dipole with  $B = 0.7 \text{ T}$ , the latter will allow the extraction of  $35 \times 65 \text{ mrad}^2$  implying a photon flux meeting this criteria for the entire infrared range (Figure 104).

Various schemes for the extraction mirror have been considered: between the dipole and the sextupole magnets or inside the dipole magnetic gap. The best scenario is based on an extraction mirror placed inside the magnetic gap of the dipole magnet (Figure 105). The IR photons can then be carried to the outer side of the dipole vacuum chamber all the way to the spectroscopic stations. In this case, the design of the extraction set-up needs to take into account two adjustable parameters: - the distance of the mirror to the electron beam (i), - the dimensions of the mirror (ii).

The distance between the mirror and the electron beam impacts the impedance of the storage ring and the electron beam dynamics. Meanwhile, the dimensions of the mirror dictate the geometry of the dipole vacuum chamber and of the bending magnet. Clearly, these two elements will be specific for the IR extraction. Moreover, the mirror will need to present a slot in the orbit plane to let hard X-rays passing through. Further studies must be performed to confirm the feasibility of the vacuum chamber and of the magnet as well as to verify that the impact on the impedance budget remains acceptable.

Mechanical studies will also include an evaluation of the thermal stability

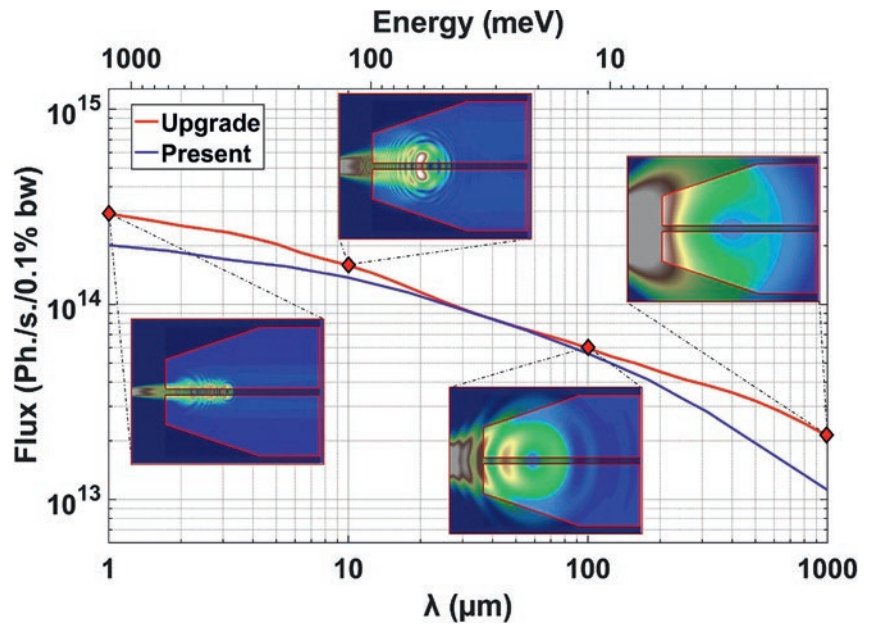


Figure 104: Characteristics of the infrared source of the upgrade.

red line: Flux collected at the level of the extraction mirror located downstream of the dipole magnet, for 500 mA current in number of photons per second and per 0.1% bandwidth as a function of the wavelength (bottom axis) and the energy (top axis); blue line: Flux collected on the extraction mirror on the present IR beamlines at SOLEIL (same units)<sup>[1]</sup>. The 4 inserts present the photon distribution for the SOLEIL upgrade at various wavelengths in the plane of the extraction mirror. The color scales from maximum flux in white to lower flux in blue. The contour of the mirror is indicated by the red line

of the mirror taking into account the power deposited on its surface (about 5 W for the specific solid angle and a 2.5 mm wide slot of the mirror). Vibration stability will be also studied. Note that the precise mechanical design of the extraction system could be based on the one developed for the MIRAS beamline at ALBA synchrotron light source<sup>[3]</sup>. With the extraction set-up described here, the infrared photon source is the combination of photons radiated in the considered dipole magnet and in the upstream long dipole magnet. The characteristics of the infrared sources on the upgraded accelerator shown in

Figure 104 can be summarized as follow: (i) The extracted flux will be equal or higher than what is available on the present AILES and SMIS beamlines in all the range extending from 10 to 10000  $\text{cm}^{-1}$ , (ii) the lowest energy available on the beamline should be extended toward the THz range, (iii) the brilliance of the source is expected to be significantly higher than the brilliance of the present IR beamlines at SOLEIL. These features combined with the high stability of the synchrotron source will allow unprecedented performances for both FTIR spectroscopy and spectro-microscopy including Scanning Near Field Optical Spectroscopy (SNOM).

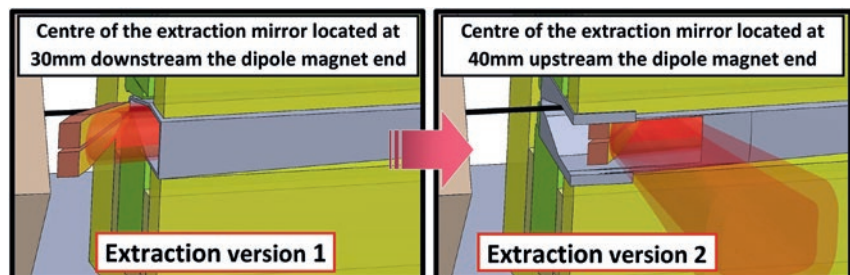


Figure 105: The two considered positions of the extraction mirror

Version 1: the mirror is located between the dipole magnet and the downstream sextupole magnet  
Version 2: The magnet is located inside the magnetic gap of the dipole magnet



## REFERENCES

[1] Roy, P. et al., "The AILES Infrared Beamline on the third generation Synchrotron Radiation Facility SOLEIL", *Infrared Physics & Technology*, 49, 139–146 (2006).

[2] Chubar, O. and Elleaume, P., "Accurate and Efficient Computation of Synchrotron Radiation in the Near Field Region", *Proceedings of EPAC'98*, Stockholm, Sweden, p. 1177 (1998).

[3] Llibert Ribó et al., "Mechanical Design of MIRAS, Infrared Microspectroscopy Beam Line at ALBA Synchrotron", 9<sup>th</sup> Edit. of the Mech. Eng. Des. of Synchrotron Radiat. Equip. and Instrum., Barcelona, Spain, doi:10.18429/JACoW-MEDSI2016-FRAA03 (2016).



## 4 – **Beamlines instrumentation**



## INTRODUCTION

In order to fully realize the promise of the upgrade, new approaches to beamline and laboratory equipment, new methods of working and new modes of access need to be conceived. In the following chapter, the directing principles of current and future choices of instrumental development are illustrated with examples. The underlying infrastructure and approaches to instrument control are discussed in "Instrumentation and Methods" part of this chapter.

The upgraded machine will be characterized by a strong reduction of the source size in the horizontal plane and up to two orders of magnitude increase in the brilliance, and available coherent flux, over the whole range of energies. In the following, we present our vision as today on the possible evolution of our instruments, starting from the experimental techniques, in order to tackle defined scientific challenges. Our future needs in **Instrumentation and Methods, Detectors, Optics, Data treatment, Sample Environment** developments, **Radiation Damage** mitigation, **Support Laboratories** requirements, as discussed in the scientific sections of SOLEIL as well as with the science community in the round Tables, have been evaluated according to the 4 science drivers described earlier. A general holistic approach for Beamline Simulation and a first scenario for Beamline Implementation is proposed.

SOLEIL offers a very wide range of methods in a multidisciplinary environment as summarized in [Table 1](#).

All these techniques will be available post SOLEIL upgrade, with renewed performances especially exploiting improved beam coherence, while keeping a broad energy coverage from THz to hard X-rays. This variety of techniques and wide energy range is a strong asset of SOLEIL, but imposes constraints on the design of possible magnet lattices of the upgraded source. [Table 2](#) (in "Instrumentation and Methods") presents a detailed view of all these approaches. A figure of merit is proposed for each technique, along with the potential gain after a source upgrade before and after further experimental optimization of individual beamlines. By experimental optimization, we refer to developing and adapting instrumentation (including nano-positioning), sample environments, new detectors with performance beyond the state-of-the-art, as discussed in the parts below. New possibilities, also presented in this table, can be offered thanks to the brightness and / or coherence, flux and smaller size of the new source which are displayed in the last column of the table among which are, structural imaging, Fourier transform spectroscopy at shorter wavelengths, ultra-fast imaging, fast spectroscopy, spectroscopic ptychography, possible novel capabilities that are currently being evaluated. The improved brilliance will also lead to an increased purity of undulator spectral lines, offering the opportunity of using pink beam methods and dispensing with the need for monochromatisation. However, in the presence of a monochromator the exploitation of these narrow spectral lines will require improved motor control and

synchronization, between undulator and beamline, to maintain the required level of tunability.

The smaller source size will facilitate nano-focusing and thus revolutionize the study of nano-or heterogeneous objects. The coherence increase will allow coherence based techniques, such as X-ray Photon Correlation Spectroscopy (XPCS, which does not exist today at SOLEIL). XPCS could be implemented after the upgrade enabling dynamics studies (down to ns to sub-ns scale) of various equilibrium and non-equilibrium processes. Moreover, the multimodal fast data acquisitions at high spatial resolution, which will be the signature of SOLEIL beamlines post upgrade, will represent a rich resource for data analysis and data mining, as further discussed in the introduction to the science case, and the chapter on data analysis.

Amongst the synchrotron sources in Europe, SOLEIL has been quick to realize the emerging importance of microfluidic sample environments. The further development of the microfluidic laboratory from a “self-service” in-house lab to an open-access user laboratory is a strategic objective in the medium term. This action will be accompanied by either expansion or specialization of existing laboratory facilities (for example to provide a laboratory environment for electrochemical characterization or test- battery preparation).

The upgraded SOLEIL will certainly increase the capabilities and productivity of our beamlines, but also offers the capacity for developing three more beamlines giving flexibility for adjusting the beamline portfolio without increasing the overall number of beamlines. A first proposal for beamlines layout around the V0313 reference machine is given here showing a possibility for accommodating existing beamlines (except those that will be re-purposed, for example to make way for a new high throughput beamline for absorption /PDF analysis). The extremely

large energy range of the SOLEIL source, a key asset, will be still further enhanced via work underway on the technological possibilities for IR and UV extraction (see part “optics”), and the design of shorter period insertion devices further opening the beam towards higher energies.

Key to the future of synchrotron radiation facilities is the link between modelling and measurement. To define and establish a close link will facilitate advances in a number of areas:

- a) Creating an ontology describing data and its meaning, will allow correct modelling of meta data and add value to post analysis (for example via data mining or machine learning). Such an approach will also help the determination of metrics that can be rapidly calculated during an experiment, to give a “real time” evaluation of success or failure.
- b) Developing methods to allow the simulation of beamline optics will lead to improvements in automated methods of beamline alignment and definition and follow up of performance metrics, as well as assisting the efficient specification of optical and diagnostic equipment.
- c) Full modelling of an experimental arrangement will allow an *a priori* prediction of the likely success of an experiment optimising efficient use of costly beamtime. It will also lead to informed specifications for state-of-the-art equipment (detection, alignment precision) allowing design effort to be focussed on the most important criteria.

To develop such a holistic approach implies developments in modelling methods and diagnostics, and providing an integrated formalism with which to describe experiments and beamlines. Initial approaches to the problem are discussed in the sections on Detection, Optics, Data analysis, and Data Acquisition sections.

Techniques	Sample environment
<b>Diffraction</b> <ul style="list-style-type: none"> <li>• Diffraction of biological sample</li> <li>• Single crystal diffraction</li> </ul>	<ul style="list-style-type: none"> <li>• Furnaces / high temperature</li> <li>• Low temperature cryostats</li> <li>• High pressure cells</li> <li>• Magnets for B fields/</li> <li>• Electric contacts for electric Fields</li> <li>• 4 points contacts for transport measurements</li> <li>• Pump probe / Laser excitation</li> <li>• <i>Operando / in situ</i> conditions</li> <li>• Electrochemical cells</li> <li>• Microfluidics</li> <li>• Molecular Beam Epitaxy</li> </ul>
Diffraction & Spectroscopy <ul style="list-style-type: none"> <li>• DAFS</li> </ul>	
<b>Spectroscopy</b> <ul style="list-style-type: none"> <li>• XAS, EXAFS</li> <li>• XMCD</li> <li>• XES</li> </ul>	
Spectroscopy & Imaging <ul style="list-style-type: none"> <li>• PEEM</li> </ul>	
<b>Imaging and Microscopy</b> <ul style="list-style-type: none"> <li>• CDI, Tomography</li> <li>• DUV imaging</li> <li>• TXM FTIR</li> </ul>	
Imaging & Reflectivity <ul style="list-style-type: none"> <li>• Ptychography</li> </ul>	
<b>Reflectivity</b> <ul style="list-style-type: none"> <li>• XRR</li> <li>• RXES</li> </ul>	

Table 1: Experimental techniques at SOLEIL



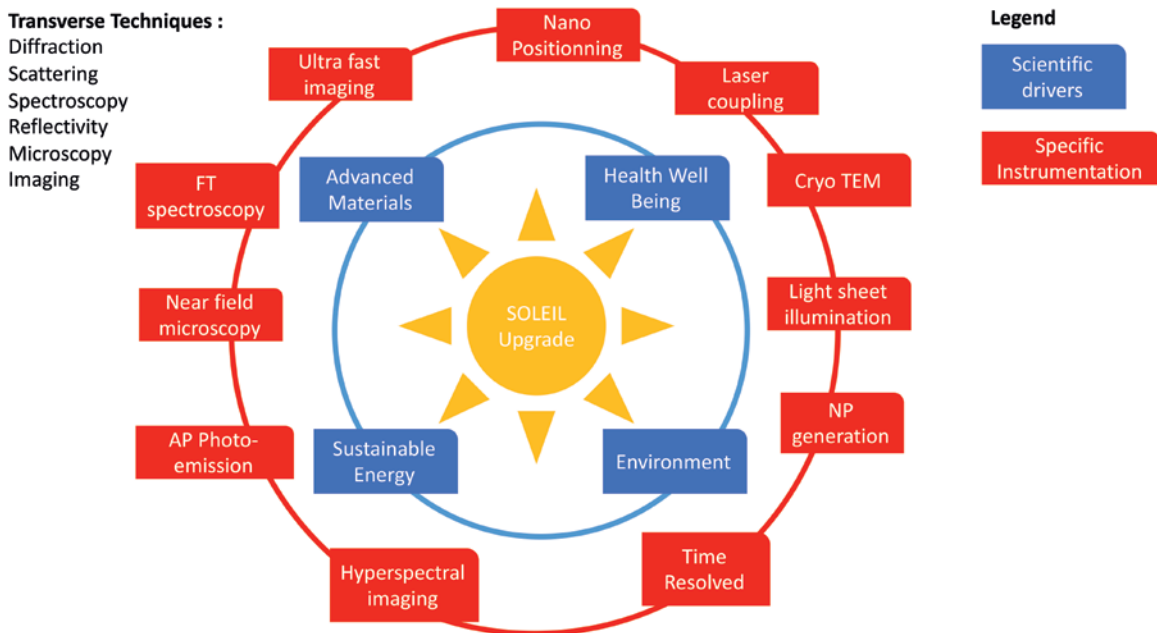
# INSTRUMENTATION AND METHODS

## Introduction

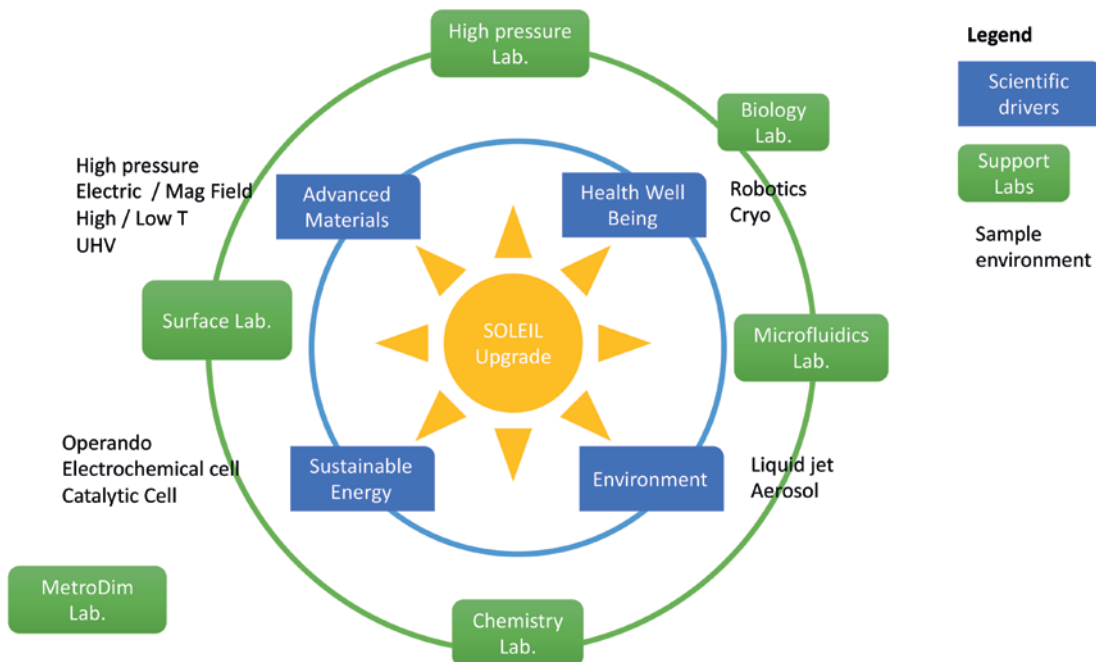
Prototyping essential equipment that doesn't exist, developing new methods, improving existing methods

and instrumentation, are necessary in order to respond to the scientific case of the SOLEIL upgrade project. Besides existing techniques and their evolutions summarized in Table 2 below, new instrumental developments responding to the scientific challenges and specially benefiting from the upgrade characteristics (increased brightness and coherence) are envisaged. A non-exhaustive selection of such developments is presented

in this chapter along with the sample environments and support Labs. The overall view highlighting the links between the scientific drivers, support labs, first ideas of upgrade driven instrumentation and methods developments, and sample environments is summarized in the following schemes.



Scientific Cases and First ideas of Instrumentation and Methods.



Scientific Cases and Support Lab Integration.

Techniques*	Figure of merit	Gain with the upgrade and current beamlines	Potential Gain with optimized beamlines (sources, optics, detector)	New possibilities to explore	Science opportunities	Main challenges**
<b>UV and IR spectroscopy and imaging</b>						
<b>UV imaging</b>	Spatial resolution / chemical selectivity / acquisition time		Possibility to increase flux using several (low field) magnets; check new methods based on structured illumination	Use of coherence (ptychography) to improve resolution while keeping chemical selectivity	Biochemistry, chemistry and cell biology. Cultural Heritage. Environmental science.	Materials Energy Health Environment
<b>Mass spectrometry</b>	Mass resolution		Ionic mobility+ Orbitrap	high resolution imaging coupled to microscopy	Isotopic measurements in gas phase. Composition of hydrophobic molecules. Proteomics and metabolomics.	Health Environment
<b>CD</b>	I Low limit Time resolution		Possibility to increase flux using several (low field) magnets	Time-resolved CD (T-jumps, pH-Jumps) Pump/probe experiments	Dynamics of protein folding and formation of complexes in liquid state. Molecular chirality. Static and dynamic molecular structures. Heterogeneous aerosol chemistry.	Health Environment
<b>FT</b>	Energy resolution Absolute calibration		Gain with coherent flux increase	Going to higher energies	High resolution gas phase atomic and molecular electronic structure..	Health Environment
<b>Photoionization</b>	Energy resolution Transmission Rapidity of CPL switch (PECD)		Gain with flux increase. (new source and adapted optics).	Low PECD signals. CD and mass spectro on NPs (large biopolymers)	Gas phase atomic and molecular electronic structure. Chemical processes. Astrophysics- Astrochemistry.	Materials Energy Health Environment
<b>IR THz Spectroscopy</b>	Sensitivity; Signal / noise ratio	Possible higher flux	Gain in flux expected up to THz (low field magnets) if integration possible; Stability important.		Molecular spectroscopy (roto-vibrational studies) and materials optical properties, gas, solid and liquid phase.	Materials Energy Health Environment
<b>IR Spectro-microscopy</b>	Spatial resolution; acquisition time	Possible higher flux	Adaptive optics to use full field method and FPA detector; better optics to increase signal/ noise	Possibility to increase flux using several (low field) magnets in the whole range of energy and in the Thz as well	Microscopic analysis of a variety of samples, plastics, polymer films and multilayers, minerals and other geological materials, biological and biomedical samples, to archaeology.	Materials Energy Health Environment
<b>SNOM: scanning near-field optical Microscopy</b>			Spatial resolution of a few 10 nm		Extension of IR methods to nanoscopic analysis.	Materials Energy Health Environment
<b>Soft X-ray spectroscopy and imaging</b>						
<b>XPS PEEM</b>	Spatial / time / energy resolution, (angular, spin) Surface sensitive Chemical contrast	Gain in spatial resolution (from 100 µm to few µm); beamlines with 2 undulators no longer possible	Gain in energy resolution with increase flux. Possibility of a « dual apple 2 » to extend the energy range.		Nanomaterials, nanomagnetism, quantum materials, Biomaterials. Functional materials.	Materials Energy Health Environment

\* See glossary of technique acronyms page 135

\*\* See page 13



Techniques*	Figure of merit	Gain with the upgrade and current beamlines	Potential Gain with optimized beamlines (sources, optics, detector)	New possibilities to explore	Science opportunities	Main challenges**
<b>ARPES/Nano-ARPES</b>	Energy and momentum of electronic bands Spatial resolution	Better focusing with coherence	Better efficiency: brightness and resolution increase	News focusing methods	Advanced Materials. Nanomaterials, quantum materials. Nanocatalysts, fuel cells. Biomaterials. <i>Operando</i> studies. Composite materials and devices.	Materials Energy Health Environment
<b>XPS NAP-XPS</b>	Maximum pressure / energy resolution	Possible higher flux.  Small beam spots allow the use of small apertures, facilitating small sample-to-aperture distances which reduces the electron scattering and an increase in the pressure limit.	Gain in flux / energy resolution with increased flux.	NAP-PEEM Higher energies Dynamics adding time resolved studies	Advanced functional materials / <i>operando</i> chemical reactivity.  Catalytic Nanoparticles. Electro and photo-catalysis. Photovoltaics, radiolysis.  Materials Kinetics and dynamics - Charge transfer.	Materials Energy Health
<b>RIXS</b>	Energy and momentum of valence states Spin excitations Element and orbital selective Spatial / time / energy resolution; acquisition time ( <i>operando</i> ) Bulk sensitive	sub- $\mu\text{m}$ spot size: gain for small / inhomogeneous sample. Possible higher flux	Gain in energy resolution with increased flux; possible change to in-vacuum undulator	Higher energy resolution: FT RIXS Nanoscale sensitivity : Nano-RIXS Spin resolution: RIXS-MCD	Electronic structure of solids, liquids, wet systems complex oxides, superconductors, metals, hybrid perovskites, organic materials... Applicable to all sample environments.	Materials Energy Environment
<b>XAS Hyperspectral XAS</b>	Limit of detection / acquisition time ( <i>operando</i> ) / spatial resolution	Gain in spatial resolution (sub- $\mu\text{m}$ spot). Possible higher flux. Tender X-rays will benefit the most from the new source	Gain in sensitivity (new source, new detection)	Hyperspectral XAS; <i>Operando</i> of heterogeneous samples; natural samples Nano-XAS	Chemical imaging of heterogeneous materials.  Materials for energy. Catalysis, batteries, solar cells, nanoparticles, environmental materials radioactive materials, materials for combustion ... Ancient materials. Biomaterials. Mineralogy. Geology.	Energy Health Environment
<b>XMCD</b>	Chemical and orbital selectivity Signal to noise ratio; sensitivity to weak signal		Gain in sensitivity (new source, better detector); beam stability	Dispersive approach Nano-XMCD -Tomographic reconstructions with full polarization	Physical and chemical properties of materials. Magnetism (nature and origin). Molecular magnetism. <i>Operando</i> studies. Magnetic nanostructures.	Materials Energy Environment

\* See glossary of technique acronyms page 135

\*\* See page 13

Techniques*	Figure of merit	Gain with the upgrade and current beamlines	Potential Gain with optimized beamlines (sources, optics, detector)	New possibilities to explore	Science opportunities	Main challenges**		
<b>Scattering / coherence</b>	Magnetic contrast; spatial / time resolution	Ptychography in reflection geometry: usable flux x 10 <sup>5</sup> (coherent flux x 100 (gain due to source and new undulator), usable spot size /100, new monochromator x 10 better matching the harmonic bandwidth)		New imaging methods: in-line holography  Holography and ptychography in reflection mode	Advanced materials: quantum materials – skyrmions, topological phases. Magnetic structures. Nanomagnetism. Nanomaterials in general, magnetic bits, catalytic nanoparticles, sub-cellular bio-structure...	Materials Energy		
		XPCS: gain by the brilliance squared	Gain in time resolution (towards ms dynamics) with new sCMOS detector				Magnetic domains dynamics. Fluctuations. Phase behavior. Spin flip. Catalytic correlations in space and time.	Materials Energy
		Holography and ptychography in transmission: gain x100 due to gain in transverse coherence	Need faster detector (e.g. sCMOS)				Exotic magnetic structures. Spin textures.	Materials Energy
<b>FT Interferometry</b>	Energy; energy resolution	Coherent wave fronts	New concept at 80 eV with grazing incidence; FT absorption with soft X-rays possible	FT RIXS	high resolution electronic structure in gas phase and condensed matter.	Materials Energy		
<b>STXM</b>	Spatial / time resolution ( <i>operando</i> )	Brilliance, coherence, better spatial resolution; Ptychography, spectro-ptychography	Better efficiency thanks to optimized beamline optics and detectors	High throughput measurements	Solid/Soft/organic/biological/geological/materials. Nanochemistry. Catalytic nanoparticles under operating conditions. Liquid media. solar cells. Microfossils, Interstellar particles. High throughput cellular tomography.	Materials Energy Health Environment		
<b>XPCS</b>	Spatial / time resolution	Gain in flux and coherence	Higher quantum efficiency with fast 2D detectors needed	New opportunity Do not exist today at SOLEIL Faster processes: sub-microsecond regime	Spontaneous processes. Magnetic domains dynamics. Fluctuations. Phase behavior. Catalytic correlations in space and time.	Materials Energy		
<b>Hard X-ray spectroscopy</b>								
<b>XAS HYPER SPECTRAL IMAGING</b>	spatial / time resolution; access to high energy edges	Better focusing; full field imaging possible using superbends divergence  Faster <i>operando</i>	Gain in flux with new sources, better optics, better detectors; superbends with 10 mrad divergence (vs 3-4 mrad); better focusing; use of crystal analyzers	Increase the limit of detection of trace elements by up to 2 order of magnitude. Higher spectral resolution with better monochromator.	Chemical imaging and catalytic kinetics. Materials for energy, catalysis, batteries, solar cells, nanoparticles, nanochemistry, environmental materials radioactive materials, materials for combustion... Biomaterials	Materials Energy Health Environment		
<b>XES</b>	Element /site Specific Energy / time resolution	Possible gain in flux	Faster / time resolved measurements (using dispersive optics);	diluted samples	Electronic structure of chemical and physical compounds	Materials Energy Environment		

\* See glossary of technique acronyms page 135

\*\* See page 13



Techniques*	Figure of merit	Gain with the upgrade and current beamlines	Potential Gain with optimized beamlines (sources, optics, detector)	New possibilities to explore	Science opportunities	Main challenges**
<b>HAXPES</b>	Energy and momentum of electronic nabds energy / spatial resolution; depth profiling; acquisition time; ( <i>operando</i> )	Better focusing ( $\mu\text{m}$ size); smaller and micro-structured samples; imaging	Gain in flux with new source, better optics.	Energy and k resolved microscopy with time of flight spectrometer	Advanced materials. Quantum materials. Nanocatalysts, batteries. Biomaterials. Interfaces. <i>Operando</i> studies. Composite materials and devices.	Materials Energy Environment
<b>AP-HAXPES</b>	Ambient pressure; acquisition time	Possible gain in flux  Small beam spots allow the use of small apertures, facilitating small sample-to-aperture distances which reduces the electron scattering and an increase in the pressure limit.	Gain in flux; higher pressure with increase brightness ( $P_{\text{max}}$ related to opening size in front of the analyzer); grazing geometry favored		Nanocatalysts, batteries. Biomaterials. Interfaces. <i>Operando</i> studies. Composite materials and devices.	Materials Energy Environment
<b>RIXS / XRS</b>	Energy / spatial resolution; acquisition time	Better resolution with increased brilliance	Gain in flux with new sources, optimized optics		Electronic structure of solids (complex oxides, superconductors, metals, hybrid perovskites, Carbon compounds...).	Materials Energy Environment
<b>Hard X-ray diffraction, scattering</b>						
<b>MX</b>		Sub- $\mu\text{m}$ focusing due to higher brilliance; Focusing et automatization for serial crystallography; ambient T to isolate dynamical effects; higher energies possible (optimum dose / data ratio around 25 keV) Room temperature serial crystallography can be used identify different structural states (by clustering solutions).		serial crystallography for structures determination at very low dose; lateral chains dynamics; drugs optimization, enzymology and complexes; <i>in vivo</i> crystallography without sample manipulation; multi-energy crystallography; $\mu\text{s}$ diffraction with flux $\times 10^3$ (molecular interaction)	Dynamics of ligand binding, Optimization of medicaments or to diminish ecological and health impact of bio-active agents such as insecticides or herbicides via high throughput crystallography and fragment based methods. Non-radiation damaged structures.	Health
<b>Single crystals</b>					Dynamics – mechanical constraints, lubrication, friction; medical diagnostics (micro calcifications).	Energy Health Environment
<b>Powder Diffraction</b>	q range	High flux at high energy			Solid state chemistry- inorganic or organic materials. Biology. Order/Disorder. Multidimensional disorder. Complex mixtures. Microstructure. Strain. Dynamics.	Materials Energy Health Environment
<b>PDF</b>	Access to high energies	Gain in flux with superbend		Fast analysis of disordered materials (requested by industry); possible high throughput beamline	Defective and non-crystalline materials or poorly crystalline materials. Confined water. Cultural heritage materials.	Energy Environment

\* See glossary of technique acronyms page 135

\*\* See page 13

Techniques*	Figure of merit	Gain with the upgrade and current beamlines	Potential Gain with optimized beamlines (sources, optics, detector)	New possibilities to explore	Science opportunities	Main challenges**
<b>SAXS</b>	Acquisition time / q-range / crossed correlation	BioSAXS will not particularly benefit from the upgrade. Scanning SAXS and ptychography; larger q range (divergence); crossed correlations for local order determination.	high flux with pink beam (expected x 40 at 10 keV)		Heterogeneous materials, dynamics of ligand binding.	Energy Health
<b>Surface Diffraction</b>	Surface size / background for buried surfaces.	Smaller sizes (50 nm spot vs 50 $\mu\text{m}$ ); smaller illuminated area leads to reduced background by 2 orders of magnitude for buried surfaces	Better efficiency	Better combination of methods (surface diffraction surface + XPS)	Surface and low dimensional systems. Advanced materials, quantum materials and functional materials. Materials for energy, catalytic nanoparticles, fuel cells. <i>Operando</i> studies. Buried soft interfaces. Biological systems.	Materials Energy Environment
<b>XPCS</b>	Time resolution	Gain with brilliance squared $\sim 10^4$ - $10^5$ .	Faster detector (e.g. UFX). Need photon arrival time	New opportunity Do not exist gtoday at SOLEIL Spatio - temporal measurements	Spontaneous processes. Magnetic domains dynamics. Fluctuations. Phase behavior. Catalytic correlations in space and time. Soft matter and biological systems dynamics.	Energy Health Environment
<b>Pink beam or multi pink beam</b>	Flux / acquisition time; ambient T to isolate dynamical effects	flux x 40 at 10 keV with pink beam		Faster measurement; systems dynamics	Dynamics – intermediate states by stopped flow soaking.	Energy Environment
<b>White beam</b>	High pressure; high temperature	Increase of energy range and flux; measurement in less than 1 ms		Coupling with full field tomography; measurement of the density of liquids and amorphous materials	<i>Operando</i> measurements of material formation or modification.	Energy
<b>Hard X-ray imaging</b>						
<b>Tomography</b>	Spatial resolution volume / acquisition time	Phase contrast, large distances / TXM with different focal lengths; full tomogram in ms; lower dose due to faster measurements	Higher flux (more brilliant source/better optics)		Earth science. Material Science. Energy Materials. Biology.	Energy Health Environment
<b>Diffraction Computed Tomography</b>	Micro resolution	5 $\mu\text{m}$ spatial resolution	1-2 $\mu\text{m}$ with optimized KB optics		Microstructures	Energy Health Environment

\* See glossary of technique acronyms page 135

\*\* See page 13



Techniques*	Figure of merit	Gain with the upgrade and current beamlines	Potential Gain with optimized beamlines (sources, optics, detector)	New possibilities to explore	Science opportunities	Main challenges**
<b>Scanning</b>	Spatial resolution / image size / detection limit / acquisition time	Smaller spot size for scanning; possibility to zoom from mm size to few nm; coherent flux x 100; 2D map in few min; 3D possible;	Higher flux (more brilliant source/better optics) Better efficiency (fast detectors)		Earth science and geobiology: biocalcification, micro-fossils, paleo-geochemistry, micro-organisms in rocks and soils. Environmental science: pollution, remediation, climate proxies, paleoclimatology. Biology-Health: metals in cells/tissues. Material science: microelectronics, energy storage materials, functional devices, nano-structures, dopants, buried structures. Cultural Heritage.	Energy Health Environment
<b>Hyperspectral imaging</b>	Spatial / energy / time resolution	Possible with XAS, IR, XPS, XRS, etc.; better spatial resolution; faster acquisition	More flexible sample environment (working distance increased)	Use of coherence?	Chemical imaging and catalytic kinetics. Materials for energy, catalysis, batteries, solar cells, nanoparticles, environmental materials Radioactive materials, materials for combustion... Biomaterials.	Energy Health Environment
<b>Coherence</b>	Spatial resolution / acquisition time	Bragg CDI, ptychography. Spectro-ptychography; multi-scale		CDI in 100 $\mu$ s – 1 ms / frame ; pink beam beam after reconstruction based on spectral intensity distribution normalization Temporal structure Possibility of a high throughput beamline	Structural studies of materials. Heterogeneous materials. Nanosystems. Advanced materials Energy. Biology. Environment. Catalytic nanoparticles, nanocatalysts, MOFs. Nanoscale mapping, strain and orientation, mapping in thin films and nanostructures. Correlation between structural, electronic and magnetic properties-charge and spin order and catalytic properties. High pressure induced structural transitions. Magnetostructural phase transitions. Interphases. Structural dynamics.	Materials Energy Health Environment

\* See glossary of technique acronyms page 135

\*\* See page 13

Table 2: Evolution of Experimental techniques (The techniques in **that color** correspond to the ongoing developments)

**Operation modes after upgrade:**

The main operational mode or filling pattern of the SOLEIL upgrade will be fully optimized to maximize soft to tender X-ray brilliance and increase transverse coherence together with good conditions of stability and lifetime. It will use a round electron beam with equal emittance in both planes, a total beam current of 500 mA where all the 416 bunches are uniformly filled and lengthened up to about 100 ps FWHM using the harmonic RF system.

**Temporal structure for time resolved studies:**

The voltage of the harmonic cavities can be set in order to provide an operational mode with relatively short bunches; of about 10 ps FWHM, with lower beam current (~100 mA) and relaxed emittance (<1 nm.rad), obtained by applying white noise in both planes. To suit the X-ray experimental requirements, the bunch length could also be varied between 10 to 30 ps FWHM (for instance) either by adjusting the current per bunch or by tuning the harmonic cavities. The hybrid filling pattern remains very challenging; it should be possible only if a solution is found to mitigate the transient beam loading effects that decrease the average bunch lengthening. It will still be possible to deliver time resolved modes (single bunch and 8 bunches), even though impedance effects will be higher (see Machine operations modes - page 62).

First ideas of upgrade driven instrumentation and methods developments are presented below, for each scientific challenge.

## Advanced materials

Advanced materials require multimodal approaches to investigate their properties in the spatial, energy and time domains along with optimized sample environments to explore their complex phase diagram or reach new quantum states. This requires instrumentation for a combination of spectroscopic, imaging and structural techniques over a broad energy range from THz to hard X-rays at the nm scale, down to sub-meV resolution, ultra-low temperatures ( $T < 200$  mK), high pressure up to several 100 GPa and temporal resolution down to 10 ps.

### Fourier Transform Spectroscopy for soft X-ray RIXS at ultra-high spectral resolution

A broad range of samples, including complex hetero-structures that could become important new materials for the design of advanced technologies, can be studied by RIXS. RIXS can probe material deep below the surface and thus allow the study of functioning devices, and as a fully photonic technique can be used in the presence of an electric and/or a magnetic field.

In the context of the upgrade project, a new compact instrument reflective Fourier Transform Spectrometer is under study to analyze the inelastic photons ultimately collected from the sample. A scanning wavefront division interferometer has already been successfully implemented in the VUV spectral range for ultra-high resolution absorption spectroscopy, with an ultimate resolving power of  $\sim 10^6$ <sup>[1]</sup>. The perspective of reducing the source size and divergence, as offered by the upgrade, should relax the required optical tolerances and improve the incident beam characteristics onto the sample, particularly in the horizontal plane. In addition, the useful flux on the sample should be enhanced by the implementation of new undulators, with more periods, making possible the use of the first harmonic over a broad energy range with a 10-fold increase in flux.

Fourier Transform Spectroscopy applied to RIXS should lead to a  $10^6$  resolving power, which is not feasible using more conventional techniques, together with

a full multiplex capability over a broad spectral range. For condensed material studies, the challenge is to reach the meV spectral resolution at 1 keV.

### High-resolution near-field microscopy in Terahertz extended range

For surfaces and nanomaterials characterization, e.g. to explore thin antiferromagnetic (AF) oxides nano-domains, spectroscopic capabilities at nanometer range with resolution in the MIR-THz range is required. Although a number of IR beamlines worldwide are already equipped with Scanning Near-field Optical Microscopes (SNOM), optimization of the method is required for operation with THz radiation. A project, in collaboration with different academic and industrial partners, is underway to develop a new SNOM coupled to a Fourier Transform InfraRed (FTIR) step scan spectrometer, advanced cryogenic THz bolometry, and new probes tips specifically optimized for THz with faster demodulation and low Noise Equivalent Power. The goal is to achieve resolution at the nanoscale (20-50 nm) with FTIR spectroscopy. By exploiting new oscillating tips compatible with cryogenic operation, proceeding toward controlled-temperature IR-THz spectroscopy of nano-entities with excellent signal to noise performances will be possible. This method will reach unprecedented performances with the high brilliance of the new source.

This new development is also of interest for experiments that need to couple techniques (XPS-SNOM, X-ray-SNOM).

### New ultra-fast imaging

For the study of inhomogeneous materials, the combination of time resolution (with an accuracy of 10 ps), and coherence with spatial resolutions of 10 nm under complex sample environments (temperature, magnetic field...) is required to explore dynamic phenomena in pump-probe experiments. The use of streak cameras, in the soft X-ray domain, is currently being studied at SOLEIL in collaboration with the manufacturer and other institutes. This development could benefit all time-resolved dynamics studies at the time scale of the electron bunch provided by the machine. Resolutions of 5 to 10 ps should be attainable, post upgrade, with a 2D streak camera and about 0.7 ps for a 1D streak camera, with spatial resolution of 10 nm.

Innovative design both of the streak cameras and on the coupling to the ultra-vacuum enclosure, including existing sample environments, will have to be

performed. Additional work on the kHz optical synchronization of the pump laser with the streak camera will be required, as well as on the vibrational and thermal stability of the entire experimental set-up. Improved signal to noise ratio by addition of a soft X-ray high-precision chopper, under UHV, is under discussion. Similarly, high-speed choppers for pump-probe experiments could be implemented for hard X-rays beamline, combined with the new fast detector being developed by the Detector group for pump-(multi)probe experiments.

### Extreme sample environments for exploring materials phases

To study new states of matter where quantum effects may become dominant, it is crucial to enlarge the parameters available phase space, towards lower temperature in the mK range, high pressure up to several 100 GPa or high magnetic field with full vector control. These extreme conditions will be possible at the upgrade project.

### Low temperature

Phase transformations can occur, as a function of the temperature, revealing new properties of the sample (magnetic states, electronic states or structural organization). To follow these phase transitions, it is necessary to perform experiments at controlled low, and variable temperatures, such as afforded by liquid N<sub>2</sub> or He cryostats. In addition, experiments at low temperature are often performed to offset free radical propagation induced by radiation damage. For Ultra Low Temperatures (ULT), **specific cryostats have to be developed and adapted to the beamlines, taking into account beam heating effects.**

Recently, X-ray Magnetic Circular Dichroism has been performed at SOLEIL at 200 mK (Figure 1)<sup>[2]</sup> using dilution refrigeration with a <sup>3</sup>He-<sup>4</sup>He mixture, and IR/THz spectroscopy at 100 mK<sup>[3]</sup> using the adiabatic demagnetization of paramagnetic salts. In both cases, the beam entrance is small, the sample fixed and detection does not require a large aperture, permitting efficient thermal shielding. In the context of the SOLEIL upgrade, the possibility to achieve still lower temperatures (50 mK) and extend ULT to other characterization techniques (like photoemission, diffraction or imaging) are being considered, opening up new perspectives in optimizing and characterizing advanced materials.

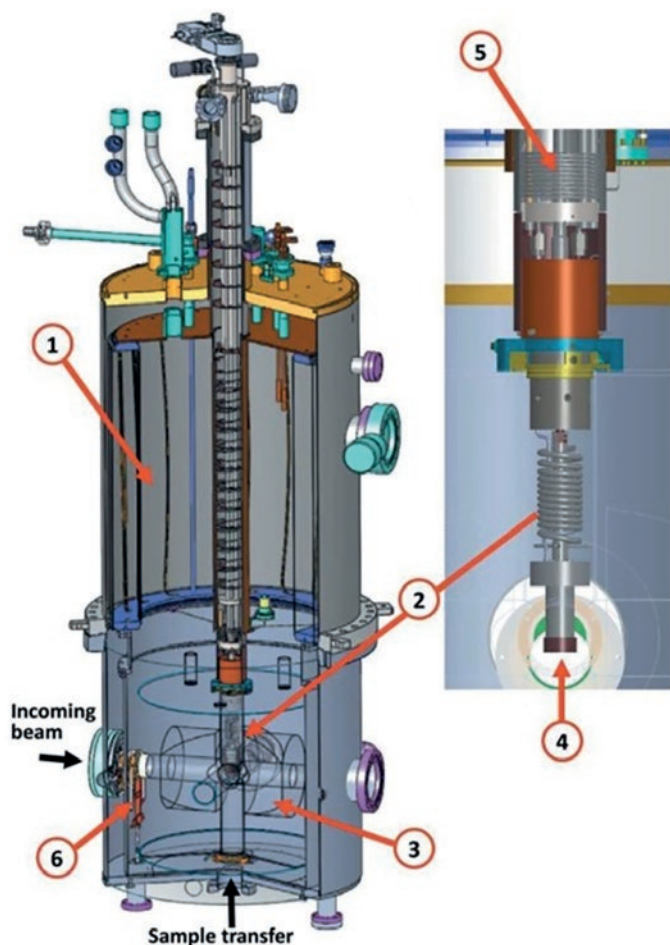


Figure 1: 3D drawing of the SOLEIL ULT dilution cryostat: (1) main He tank, (2)<sup>3</sup>He-<sup>4</sup>He dilution refrigerator, (3) cryomagnet, (4) sample, (5) pre-cooling tank, (6) thermal shield (from [2])

### High pressure

SOLEIL have developed a wide range of high pressure environments, ranging from the Diamond Anvil Cells (DAC) to the large volume Paris-Edinburgh (PE) or Multi-Anvil Presses (MAP). New developments using Focused Ion Beam (FIB) setup to shape toroidal anvils, a pressure > 400 GPa has been achieved<sup>[4]</sup>, opening the accessible pressure range. The improved brightness of the upgrade project and the small beam dimensions will be advantageous for such high pressure environments, finding applications in IR, UV, and X-ray spectroscopy (XAS, XES, RIXS), in X-ray diffraction and scattering and in 2D and 3D X-ray imaging (from 3 to 100 keV).

### Complex magnetic fields

Measurements of complex magnetic objects require a full control of the magnetic field direction in 3D. This is illustrated in Figure 2 for REXS experiments, which provide magnetic, electronic, structural and orbital orders relevant to condensed matter physics.

The current REXS magnetic setup will be extended from currently 2D to 3D magnetic assemblies allowing the application of an external magnetic field in all the symmetry axes of the studied samples. This setup will allow REXS to be performed in Fourier transform holography or ptychography modes using scattering geometry, offering sub 10 nm spatial resolution while keeping a complex sample environment. Although routinely attaining 20 K in both holography and REXS experiments, keeping the low/high temperature possibility in REXS-ptychography will be a real challenge because ideally the sample displacement has to be controlled within the expected spatial resolution (10 nm or below) when changing temperature by a few hundreds of Kelvin.

### Integration of laboratories

The support labs will provide efficient and integrative support for the preparation and analysis of materials and surfaces in complement to synchrotron methods.

### Surface Laboratory

The Surface Laboratory within the upgrade project will include spectral analysis performed *operando* and/or various sample environments as a standard. The envisaged upgrade will close the gap between sub-nanometric and mesoscopic sample conditioning and modification under UHV including integrated FIB and Scanning Electron Microscopy (SEM) and robotized sample transfer.

Portfolio analysis with existing international facilities has led to a new SOLEIL-specific concept for the mutualisation of UHV equipment. Standardized interconnectivity with the other internal and external laboratories will allow to trace and to control the samples path across all experiments (*i.e.* sample passport). This flexible approach maximises efficiency of operation implementing modular instrumentation, eco-green labelling, cutting-edge local probe analyses and a project-oriented manpower scheduling. Proven high innovation potential as well as closest industrial contacts worldwide assure the availability of timely solutions for outstanding scientific tasks.

### High Pressure laboratory

The high pressure laboratory (HP Lab) already offers all the necessary instrumentation to perform high pressure experiments including pressure cells (DAC and, large volume PE presses), pressure controller, microscopes, micro manipulators and spectrometers using the ruby fluorescence to measure *in situ* the pressure. In the future, a new laser-drilling setup will be accessible to drill micro-holes in the metallic gaskets or to cut micro-samples at the requested



Figure 2: SOLEIL prototype of a complex 5 coils magnetic system to apply 3D magnetic fields at the sample position while keeping the scattering space free

size and shape. The lab will also host a Raman spectrometer to test the vibrational properties of the samples under examination by diffraction or absorption. Raman spectroscopy will be possibly used to assess radiation damages depending on samples.

Access to electronic microscopy is foreseen in collaboration with nearby laboratories of the Paris-Saclay area for examination of samples recovered after a high pressure cycle with phase transformations. Similarly, an access to a FIB instrument would be possible to machine the shape of the anvils for the ultra-high pressure regime (> 200 GPa).

## Sustainable energy

The complexity of the energy-related materials requires instrumentation for multi length scale characterization, from macro to micro resolution, down to nm range, with a high time resolution for data collection and pushing the materials characterization towards realistic working conditions. This will allow the study of the chemical state and physical properties evolution *in situ* and *operando*.

### Towards ambient pressure X-ray photoelectron spectroscopy

Soft X-ray Near Ambient Pressure X-ray Photoemission Spectroscopy (NAP-XPS) has been widely used for studying surface reactions or liquid / solid interface in real time with strong interest for catalysis, electrochemistry or batteries. Novel, high-performance photoelectron analyzers using electrons of higher kinetic energy can now operate at even higher pressure, reaching several bars locally around the sample. These ambient pressure photoelectron analyzers operating in the tender to hard X-rays range (AP-HXPES) permit to reach realistic operation conditions e.g. for catalytic reactions.

The higher brilliance of the SOLEIL upgrade will push the performances of NAP-XPS / AP-HXPES to unprecedented level: (i) Higher photon density will boost the signal intensity, strongly reducing the acquisition time; (ii) smaller X-ray spot will strongly favor grazing incidence geometry which helps to enhance the electron yield; (iii) the new source will make NAP-XPS / AP-HXPES more efficient when applied to small or multi-domain samples or when the samples are contained in a cell with narrow membranes.

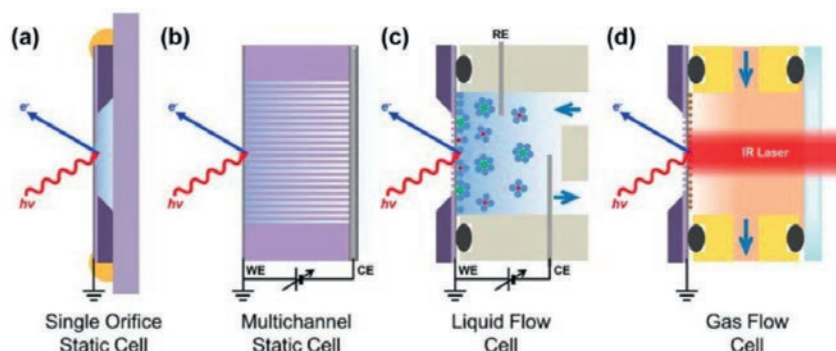


Figure 3: Membrane-based liquid cells adapted from [6]

In the context of the upgrade project, both NAP-XPS and AP-HXPES instruments are envisaged cumulating the advantages of soft X-rays (enhanced surface sensitivity, strong cross section, high resolution) and hard X-rays (high penetration depth, deeper core levels, high pressure environment). The extreme surface sensitivity of photoemission spectroscopy, however, imposes severe constraints in terms of sample environments mandatory for probing the chemistry of liquid-solid interfaces under realistic process conditions. Then in addition to the development of high pressure photoemission setups, where molecules in the vapor phase can be condensed onto a substrate, membrane-based liquid cells have been proposed for the study of heterogeneous catalysts or solid electrolyte interface in batteries (Figure 3). To withstand the differential pressure, thin membranes (such as single layer graphene or graphene-coated  $\text{Si}_3\text{N}_4$ ) require lateral dimensions of a few microns. Having a brighter beam would significantly enhance the signal intensity coming from such area.

This kind of set-ups for probing liquid-solid interfaces supports a wide range of devices interesting for sustainable energy studies including the use of gas or liquid flow, light illumination or electrochemical potential. Noteworthy it is possible to use the same cells for complementary or combined spectroscopic or scattering techniques such as XAS, RIXS, STXM and SXR. D.

### X-ray hyperspectral imaging at different length scales

The upgrade project will permit valuable new imaging techniques coupling to chemical or phase speciation, for which the brightness increase will transform the currently *in situ* characterization into *operando* ones by reducing the acquisition time of full area or volume from hours to

minutes or seconds. Collection of 4D or 5D hyperspectral data in which 2D or 3D imaging is combined with fluorescence or absorption at specific element threshold, or with time resolution, will be facilitated by faster read-out times for CCD cameras, reduced dead-times of acquisition electronics, as well as increasing speed of motions, acquisition and data processing with fast detectors (see section on Detectors). The decrease of acquisition time and improved sensitivity will be also of prime importance for minimizing the radiation damage which is recognized today as an important limiting factor in high resolution soft X-rays imaging.

New sample environment developments are required in order to combine this full field imaging technique with coherent X-ray imaging techniques (Bragg CDI, ptychography) offering new opportunities for *operando* studies based on optimized sample environments required for tracking synthesis, reactivity, deactivation/degradation or ageing of energy-related materials. New focusing devices, producing versatile beam sizes for imaging heterogeneous samples at different length scales will be developed taking into account to save room around the sample to accommodate cumbersome environments (catalytic reactors, electrochemical or photovoltaic cells) (Figure 4). Strong stability, accuracy and robustness of displacements for sample, optics and detection nanopositioning (e.g. diffractometers) are crucial to meet the need for rapid 2D/3D mapping, especially in case of heavy set-ups, weighing up to kilograms (Figure 4b).

*Operando* terminology means that experiments are performed under operational conditions close to those used in laboratory or industrial catalytic reactors, fuel cells or batteries with simultaneous monitoring of the materials performances permitting to derive structure-function

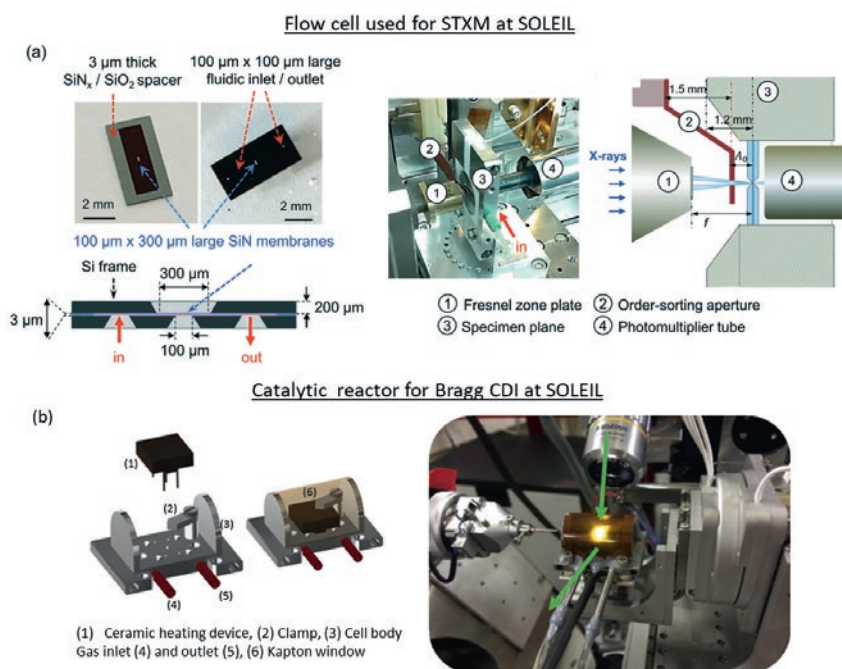


Figure 4: (a) Pressure actuated liquid flow cell installed for STXM [8]; (b) Catalytic cell for *in situ* Bragg CDI measurements [7]

relationships. Microfluidic technologies show great promise to sort and immobilize single particles down to the micron scale and possibly offer sample environment miniaturization requested by hyperspectral imaging with spatial resolution of a few nanometers. For heterogeneous catalysis *e.g.*, convection and diffusion processes can be addressed under *operando* conditions, both with a global (full flow-bed) and single particle (immobilized particle) approach [8]. It is noteworthy that no unique reactor for a given imaging technique can be used to fulfill the diversity of reaction conditions in temperature and/or pressure, whereas, depending on the X-ray interaction-matter channel used for the imaging technique, different sample environments have to be designed even used for the same application. The design of those sample environments will benefit from strong collaborations in the so-called integrative approach: using the SOLEIL know-how in the design of sample environments, possibly including microfluidic devices, combined with the expertise of the community, relevant cells can be proposed both for imaging techniques but also dedicated sample preparation and characterization laboratories.

It is noteworthy that the improvements of instrumentations for X-ray hyperspectral imaging will benefit also other science drivers.

## Integration of laboratories

### Chemistry laboratory

The success of those complex *operando* experiments requires preparation and test stages in the support chemistry laboratory or ideally in dedicated catalysis and electrochemistry “super-platforms”. New challenges in the dynamic monitoring of performances of energy-related materials (*i.e.* catalytic activity, electrochemical property, etc) will emerge by the use of micro- or nano-reactors or electrochemical cells requested for *operando* characterization by the coherent and/or hyperspectral imaging techniques. Before using those environments at the beamline, a set of analytical techniques already available at the chemistry lab (Mass Spectrometry,  $\mu$ -Gas Chromatography...) have to be used in order to assess the catalytic or electrochemical properties to guarantee the sample performances in comparison to the laboratory or industrial scale measurements. The chemistry lab is also well equipped in additional analytical techniques (XRD, UV-vis, FTIR and Raman spectroscopies, DTA-TG, DLS) to provide pre and post-characterizations of materials at the macro scale but also at the sub-micron scale with state-of-the-art Raman microscopy. This large offer of analytical techniques will be also of prime importance for multimodal experiments with the coupling, *in situ*, synchrotron and non-synchrotron techniques (UV-vis,

Raman spectroscopies) which, besides offering complementary information on the samples and/or processes, could be useful for monitoring possible radiation damage.

### Microfluidic laboratory

The microfluidic lab of SOLEIL has developed the tools and expertise to produce microfluidic chips to sort and immobilize biological cells. This technology could easily be transferred to materials in order to select and trap catalytic particles. Further addition of liquid inlets will allow modifying these particles *in situ* by modifying the pH, providing a substrate or any appropriate chemical. In order to match the experimental constraints of hyperspectral imaging or near-ambient pressure photoemission spectroscopies, specific cell design will be developed with a small footprint, low spectroscopic background and high mechanical reproducibility. The chips produced in the microfluidic laboratory are currently produced using soft lithography (PDMS) or hot embossing (PMMA) methods. To meet the requirements posed by high temperature ( $>600^\circ\text{C}$ ) and pressure (up to 200 bar) flow-bed catalytic microreactors (particularly in the gas phase), novel microfabrication methods will be proposed. Glass or silicon will be preferred over polymers, with the development of in-house fabrication facilities or collaboration with partner institutes (C2N, Paris-Saclay).

## Biology and health

The science case for Biology and Health implies instrumentation and methodological developments for measuring dynamic biological systems at high spatial resolution, whilst moving towards *in vivo* conditions. State of the art approaches are needed for sample handling under cryo-conditions and *in situ*, coupled to sample alignment methods in complex environments (applicable over the whole energy range provided by the upgraded source).

### High-resolution UV-fluorescence microscopy

High-resolution UV-fluorescence microscopy is needed to better localize and monitor the effects of antibiotics in bacteria or the behavior of the nucleus and cytoplasm in cells. To do this, improved resolution and image contrast are necessary in full-field fluorescence imaging of samples. Two instrumental developments are envisaged that use the generation of a phase matrix with

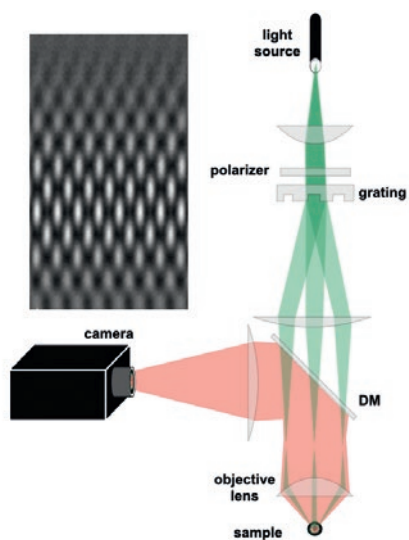


Figure 5: Principle of structured illumination microscopy, with the resulting pattern represented in the left inset. (adapted from [10])

micro-mirrors to make sheets of UV-light in different planes of the sample thickness. These techniques, called Structured Illumination Microscopy (SIM) and Lattice Light Sheet UV microscopy (LLSM) [9,10], are currently being developed at SOLEIL (Figure 5). A Matrix of Micro-mirror Device (DMD), coupled with a UV-adapted microscope, structures the illumination of the UV photon source following a phase map chosen in the focal plane. An image reconstruction algorithm extracts the sample area of interest.

With these methods, the diffraction limit inherent to optical microscopes can be overcome and a reduction of the spatial resolution by a factor of 2 can be achieved giving a value close to 60 nm at the 280 nm excitation wavelength. Simultaneously an improvement of the vertical contrast of fluorescence images, on 3D reconstruction of samples, will be obtained.

In addition, the LLSM enables reducing photo toxicity on the sample. During the rapid scan of the sample thickness, each plane sees the UV photon flux only once. This also allows high imaging speeds to study dynamic processes. Stable optical set-ups, good UV qualities with a collection lens very close to the illumination lens and sample, combined with a fast, spatially resolved color camera are required. The availability of coherent light at X-ray energies will open up new opportunities for extending the LLSM technology.

### Integrated biology concept

Developing and improving multimodal or integrated approaches is a strategic objective of the instrumentation program for the upgrade. In the Integrated Biology concept (Figure 6), *in vivo* crystallography, combined with the use of a bi-photonic microscope for precise detection of cells or crystals, is already in operation at SOLEIL. Protein diffraction data collection at room temperature, such as encountered for the *in vivo* crystallography, requires higher speed and spatial resolution in serial crystallography measurements. These will be achieved by improving the accuracy and robustness of goniometry, as well as developing monochromator free pink (or multi-pink, see section on Detectors) beam methods. New designs of highly precise sample handling, microfluidic chips and rapid automated *in situ* data collection are currently being developed at SOLEIL.

Similarly, reference sample holder adapters will be designed in order to combine X-ray, UV and IR imaging techniques and X-ray diffraction, passing samples from one analysis technique to another. The acquisition of a cryo-Electron Microscope, to be operated as part of a national network, offers the opportunity to extend medium-to-high resolution structures of large complexes with very high resolution MX studies of their components. Its use within the

proposed P3 biological sample beamline environment will provide tools to study hazardous biological systems. Contacts with French laboratories already equipped with P3 installations have been made for examining possible collaborations and infrastructure needs. This would be an equivalent in the biology domain of what has been successfully implemented at SOLEIL for radioactive materials or for MOT samples.

Moderate pressure microfluidic sample environments have been identified as an important instrumental development post upgrade. In particular, for food processing, pressure is used to inactivate all micro-organisms. This technique (called "pascalisation") requires pressures up to 5 kbar (500 MPa) and (non-denaturing) temperatures up to 60°C. Under these conditions micro-organisms are killed without breaking aromatic molecules, keeping vitamins and flavors of the food. Using IR or X-ray imaging with phase contrast, *operando* measurements will become possible with nanometric resolution and long working distances, allowing optimization of pascalisation conditions (pressure, temperature and time) leading to improvement in energy and cost efficiency of industrial processes.

Microfluidics will hold a central role in the development of tools for sample handling and integration in the beamline

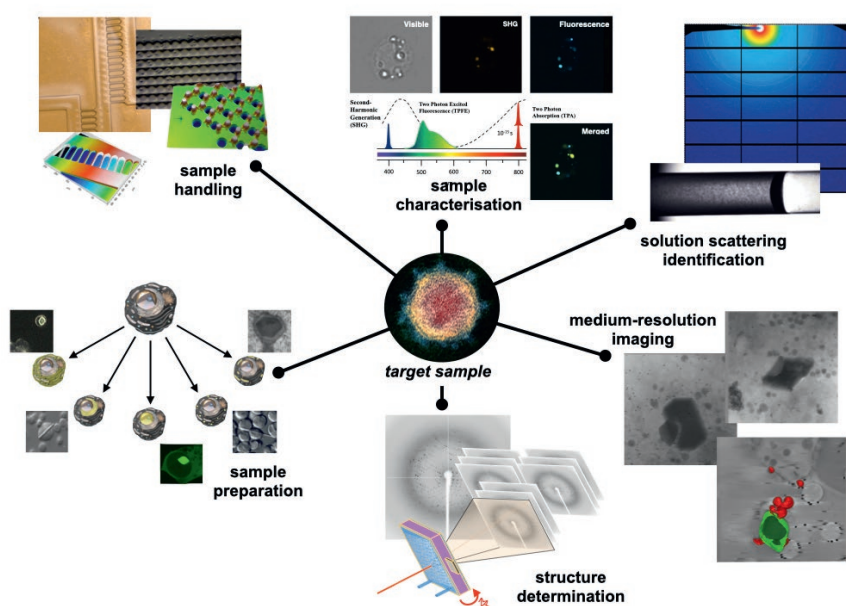


Figure 6: Integrated biology as implemented at SOLEIL. The represented example studies imply sample preparation within the Biology Laboratories, sample handling via microfluidic chips, sample characterization by Second Harmonic Generation-based microscopy, sample scattering identification through bio-SAXS, medium-resolution imaging by Cryo SXT, and atomic structure resolution by macromolecular crystallography



environment. Upgraded beamlines will allow imaging of biological objects at the micrometric and nanometric scales, with tunability giving atomic sensitivity in certain cases. Microfluidics allows manipulating tissues, cells, viruses or proteins, either as an ensemble or as unique subjects. Capitalizing on the current know-how available at SOLEIL, microfluidic chips will be designed to sort, select and store samples before they are positioned under a photon beam. Chips will also be designed to present the sample under the beam, where it will be studied under near-physiological conditions, observing *in situ* their response to a specific stimulus. The so-called organ-on-a-chip and roots-in-chip technologies will be implemented at SOLEIL, allowing studying the growth of organs or plants under *in vivo* conditions.

Dynamic MX and bio-SAXS experiments on photo-sensitive systems will benefit from the integration of a visible pulsed laser directly within the sample environment. Such experiments will be carried out in a pump-probe scheme, where the laser, synchronized to the storage ring will pump molecules into excited states. The time evolution of those excited states is probed with the synchrotron pulses after a variable time delay.

One main objective of the microfluidic lab, for the upgrade, will be to provide efficient technologies for flow cytometry. In combination with fluorescent or biphotonic microscopes, specific chips and procedures will be setup to spot specific cells with features of interest, sort and store them. These capabilities will be performed prior to online experiments and will be fully integrated in the research pipeline of in-house teams and external users.

The microfluidic lab has been engaged in the last years in the development of systems for the preparation of time-resolved samples for cryogenic electron microscopy. These developments will further automated, providing tools for in house and external users to prepare samples of proteins, fibers, viruses or other biological objects after an external stimulus (chemical or light). Such offline sample preparation methods will be critical for an optimized use of cryo-EM or a proposed cryogenic soft X-ray imaging beamline. This user-driven sample preparation will also benefit the environmental and sustainable energy scientific cases (time-resolved cryo-EM studies of nanoparticles and colloids).

## Biology laboratory

For life sciences experiments performed at synchrotron facilities, macromolecules in solution frequently require one last purification step (quick, reliable, analytical characterisation level) or other specific preparation (i.e. techniques or instruments) prior to beamtime. At a larger scale, for bacteria or cells, fast freezing preparation for imaging analysis approaches can be performed at SOLEIL (grid preparation and cryoplunge). The Biolabs will play a crucial role in sample preparation, pre-experiment screening and multimodal research. Specifically, authorisation has been granted to SOLEIL, from the 'ANSM' (National Agency for Medicines and Health Products Safety), for handling MOT samples (Micro-Organism and Toxin).

To provide a rapid structure-based response to re-emerging or new diseases, the Biolabs must prepare for the preparation, distribution and (complementary) measurement of samples of up to class 3 biohazard. Such an integrated L3 facility would be unique at synchrotrons in Europe, and would enable the manipulation and characterization of, for example, aerosol transmitted viruses particles. The use of this facility requires the development of new access modes (proposal planification, sample tracking and preparation), following the biosafety conditions, to allow safe transfer of sample between beamline and laboratory. These possibilities will be analyzed in a future Technical Design Report.

To optimize approaches for multi-technique research projects, the Biolabs have developed specific instruments (such as coupled SEC-MALLS-RI or LC-MS/CE-MS<sup>1</sup>), and will continue to develop specific complementary methods when appropriate. Such a new configuration will be even more efficient if the Biolabs are connected to related beamlines and if the sample preparation expertise covers all the panel of available synchrotron techniques at SOLEIL.

<sup>1</sup> SET-MALLS-RI: Combination of Size exclusion chromatography, Multi-angle laser light scattering and measurement of refractive index. LC-MS is a combination of liquid chromatography and mass spectrometry, CE-MS is a combination of capillary electrophoresis chromatography and mass spectrometry.

## Environment

The science case for environmental sciences highlights the multiscale heterogeneity, the complexity and the reactivity of environmental systems. To meet this challenge, instrumentation and methodological improvements and developments are needed for dynamical multi-scale *in situ* analysis of chemical speciation at high spatial resolution in systems ambitioning to reproduce the complexity of natural ones.

### Multimodal probing with nanometric spatial resolution

In terms of morphology, chemistry, crystallo-chemistry, the complexity of natural systems occurs on an extraordinarily large range of observation scales, from the (kilo)metric to the nanometric. The impact of this diversity and heterogeneity on elements (such as pollutant or nutrient) flow and cycle is critical. Probing this morphological and (crystallo-) chemical heterogeneity down to the nanometric scale is one of the challenges facing environmental scientists to understand and predict reactivity and transport of natural systems.

Understanding and predicting reactivity, transport and mechanical properties of such systems requires the use of a combination of various characterization tools and simulation methods. For example, monitoring the behaviour of heavy metals in the environment requires not only to assess their speciation but also to characterize the phases of the system that are able to trap them, together with their interaction modes. X-ray imaging combining spatially resolved chemical information and speciation in both the hard and soft X-ray ranges (nano, micro-XRF + XAS, STXM + NEXAFS) are particularly valuable. The increase in coherence provided by the upgraded SOLEIL will open new and unique opportunities in the field. X-ray imaging techniques (such as full-field microscopy, with millimetric field of view) to obtain a view of entire samples can be combined with ptychography or spectroscopic-ptychography to zoom in on specific regions of interest (<5 nm spatial resolution) by switching to a higher-resolution imaging mode. Furthermore, coupling these techniques with others providing additional spatially resolved chemical information on the systems is fundamental. Such coupling can be envisaged *in situ* with laboratory equipment (i.e. Raman) or moving the

sample to another equipment or beamline (*i.e.* tomography, nano-IR); the challenge being to probe exactly the same region.

The stability and repositioning of the sample will have to be optimized at the nm scale despite the weight and space requirements of the sample environments required for *in situ* experiments. Cooling will become essential to slow down beam damage (especially organic materials), but caution in design and careful characterization will be required to ensure sample stability under such conditions. Additionally, as samples will be measured in different experimental stations, referenced sample holders will be designed and adapted to different energy ranges in order to combine complementary techniques and ensure a perfect knowledge of the spatial location of the measured area.

Sample environment for simulating *in situ* conditions (redox cycles, pH adjustment, water controlled conditions, etc.) are currently cumbersome. Nano-positioning and fast displacement of such heavy material is difficult. Smaller beam sizes and more highly collimated beams will simplify miniaturization of samples environments. Miniaturization also has the advantage of freeing up space around the sample which will allow approaching detectors (that will also be more sensitive as described in the Detectors part) to improve signal acquisition, which will be crucial for trace elements characterization. Additionally, the design of specific setups (such as the VUV PEPICO end station) will be optimized to lower detection limits. Microfluidic cells, offer promising possibilities that are currently being explored.

### Advanced high throughput sample delivery

Environmental systems are dynamical by nature. The time-resolved description of these complex evolving systems, highlighting surface interactions and key intermediate metastable species, will be made possible by an upgraded SOLEIL. As an example, assessing the ecotoxicological impact of contaminants in a soil needs to take into account the spatial and temporal variability of the system, especially for the description of the soil components able to trap or transport the contaminants and their interactions. Additionally, understanding reaction processes and lifetime of gases and particles emitted to the atmosphere is key to predicting the evolution of global heating. High throughput approaches

(for example using electrospray) will be developed to provide, when coupled with more intense beams, an improved sampling rate to study the variability of such systems.

Moreover, the above techniques will allow studying molecules, aerosols, colloids, nanoparticles or aggregates and even soil systems during their formation or under reaction conditions. Using high throughput delivery, the intrinsic physico-chemical properties of molecules or nano-systems could be revealed with sufficient statistical multiplicity as to offset the effects of random sample preparation artefacts or diminish the effects of time dependent radiation damage. Sample delivery instrumentation will be developed towards a drastic diminution of required sample volume to work on size-selected nanoparticles (below 10 nm). The continuous circulation of a sample under the beam with the possibility to probe various locations into the delivered flow will offer the possibility to perform time-resolved studies down to the microsecond. Indeed, the micro- to nanometric size of the beam will allow probing a flowing liquid at short but variable distances (sub-micron) from the chemical reaction.

Three specific methods for *in situ* studies of nanoparticle formation and reaction, that are already developed at SOLEIL, will be further improved to exploit the smaller and more brilliant beams:

Electrospray based techniques will be developed as new aerosol generators to deliver gas phase samples from VUV to soft and hard X-ray beams for photoelectron spectroscopy measurements allowing the monitoring of aerosols formation and the study of surface interactions.

Liquid microjets will be further improved to carry environmentally relevant molecules and nanoparticles. Reducing the beam spot size, as expected on hard X-ray beamlines post upgrade, will allow focusing all available photons on the liquid sample. Together with the absence of any window between the sample and the detector, this will make it possible to study the formation and the surface interactions of low-concentration species (closer to natural conditions), by photoemission spectroscopy or X-ray absorption spectroscopy from soft to hard X-rays.

Microfluidic cells will be developed to provide a more complex pattern of liquid circulation than microjets and then propose model reactors capable

of reproducing the complexity of natural systems with controlled variations of physicochemical conditions ("Ecosystem in a box" or "Soil-on-chip" concepts<sup>[8,11]</sup>). Combined with micro to nano-focused probe, microfluidic systems make it possible to carry out *in situ* to *operando* investigations on soils and ecosystem dynamics, combining temporal and spatial resolution and will open up opportunities for a hyperspectral approach in the study of these systems. Then time resolved studies of morphological (SAXS, Tomography) and chemical (XRF, XAS, STXM) modifications will be accessible with the upgraded project.

## Integration of laboratories

### Biology laboratory

Advanced procedures for samples preparation are critical to ensure representativeness and integrity of the samples. It is even more crucial when they contain organic material or elements whose chemistry is highly sensitive to surrounding physico-chemical conditions. In addition to classical resin inclusion, cut and polishing, the preparation of thin films of soils or plants is realized using cryo-microtome technique. Furthermore, the fast freezing (cryo-plunge) preparation of samples deposited on grids is available at SOLEIL. These techniques require specific know-how, possessed by the staff of the Biolabs. The validation of the quality of sample preparation as well as the samples post-experiment integrity would strongly benefit of the use of a cryo-EM instrument that is planned to equip SOLEIL.

### Chemistry laboratory

The chemical composition of complex samples needs to be analyzed with complementary techniques, especially when very low concentration elements are present. The Chemistry laboratory will offer a platform of techniques with elemental analysis down to the ppb level in absolute (Inductively Coupled Plasma spectroscopy) and mapping with deep-submicron lateral resolution (Raman microscopy). Compact instruments for characterisation for determining phase (XRPD) and size (Dynamic Light Scattering) sensitive techniques are already available in the laboratory, together with vibrational (FTIR), electronic (UV-vis spectrophotometry) and coupled thermal and gravimetric (DTA-TG) analysis. Those instruments together with the know-how of the chemistry lab staff for the advanced analytics (Inductively Coupled Plasma



Mass Spectrometry, Raman) provide a support to the user experiments to prepare their beamtime, but also post-analysis for checking the outcome of *in situ* synthesis. Data from complementary methods will be collected and made available to users via a LIMS. A clean room will be required for environmental sample preparation, to avoid artefacts due to uncontrolled and external pollution, together with a glove box for working in controlled conditions ( $O_2$ ,  $H_2O$ ).

Both biology and chemistry laboratories will play a crucial role in the preparation of samples for environmental sciences and pre- and post-experiment screening.

### Microfluidics laboratory

High throughput sample delivery systems will be designed, fabricated and tested in the microfluidic laboratory. Pre-experiment, offline testing of microjets or microfluidic cells are a pre-requisite to ensure an efficient use of beamtime. The laboratory has the instruments and his staff has the expertise to design and test such samples environments. Importantly, the instrumentation is oriented towards a fast chip design and fabrication (maskless lithography, 3D printing), so as to quickly provide solutions to technical issues during on-line experiments. Additionally, the laboratory staff already collaborates with in house and external users to propose more complex specific chips able to reproduce the variations of physico-chemicals conditions of environmental systems (pH,  $H_2O$  and  $O_2$  saturation, etc..) and allowing measurements in the tender to soft X-ray domain (*i.e.* able to resist to the vacuum of the experimental vessel and allow low-energy X-rays to pass through it), as presented in Figure 7.

## Transverse instrumentation and approaches

### Nanopositioning

Building on previously developed nanoprobe projects, and on a prototyping project that is underway, 3D maps with a resolution of 40 nm have been attained on a first  $10 \times 10 \times 10 \mu m^3$  porous silica sample. This approach offers new scientific opportunities for the study of the nanostructures of extremely varied solid samples (cement formulation, tooth or bone mechanics, network structure of plant cell walls, micro-fossils, battery electrodes...). High resolution imaging based on 2D scans will be much faster with the upgrade, due to the increase in coherent flux and brilliance.

Work is now planned (led by SOLEIL and in the context of LEAPS) on different aspects of the instrumentation, to increase scan speed, incorporate cryogenics suitable for nano-positioning, and to demonstrate the use of positioners controlled by interferometry and actuated magnetic levitation positioners for large loads and samples:

(i) Performance of magnetic levitation on trajectory quality in the case of flyscan and fast stepscan will be tested. Magnetic technology can also be used to maintain optical components in position; in this case, the system must demonstrate its ability to reduce vibration and maintain position for a period of a few hours.

(ii) The SOLEIL MetroDim laboratory is working on the evaluation of heterodyne interferometry for closed loop control position and for absolute position. The former is essential *e.g.* for STXM scanning for which sample positioning with an accuracy of around 20 nm is required,

whereas the second is mandatory for 3D scan sample for ptychography imaging for which ultimate accuracy in absolute position (1 nm) is important. The compensation for low-frequency vibrations associated for instance to the cryogenic operations by closed loop system will be in-depth investigated.

### Robotics

Automation and the use of robots, to carry the detector or for sample handling, will become more widespread in the future. Building on previous experience, SOLEIL is in the process adapting robotics to new problems via development of new movements and robot trajectories, and designing new applications adapted to complex environments. To guarantee safe operational working conditions requires further development of collision mapping methods. Indeed, the need for putting instruments at distances close to the sample, in *operando* conditions, increases the risk of collisions. Improving flexible 3D collision simulating models will also assist the preparation of experiments and measurement protocols, leading to increasingly rapid acquisitions.

### Sample passport

The upgrade project will bring a unique range of techniques to unprecedented spatial and temporal resolution as requested by the four identified scientific challenges. In order to respond to these challenges and to complete the new capabilities offered by the future beamlines a rich panel of complementary tools is required. A full understanding of systems under study requires a multiplicity of analytical techniques (multimodal characterisation). Furthermore, a thorough sample characterisation prior to acquisition on a beamline is always required in order to optimise

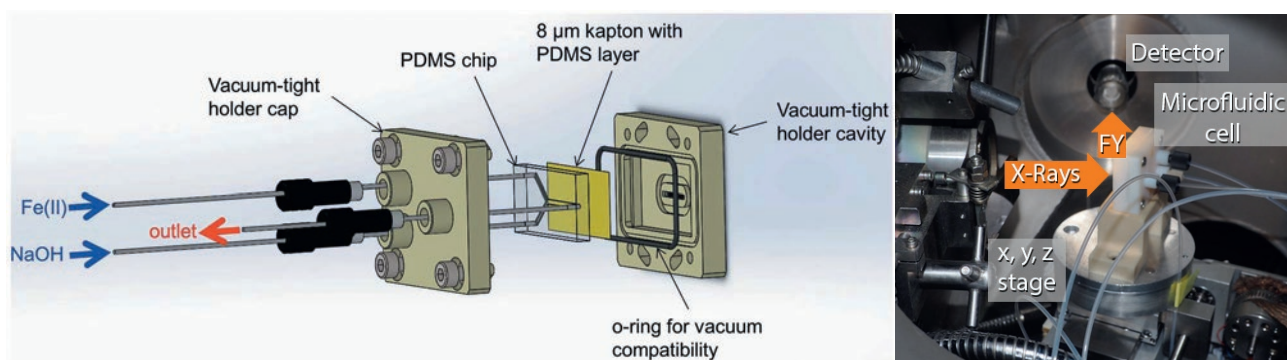


Figure 7: Left: Schematic representation of the vacuum-compatible microfluidic device used on the tender X-ray beamline. Right: Picture of the experimental setup inside the beamline experimental chamber. FY stands for fluorescence yield. (from [12])

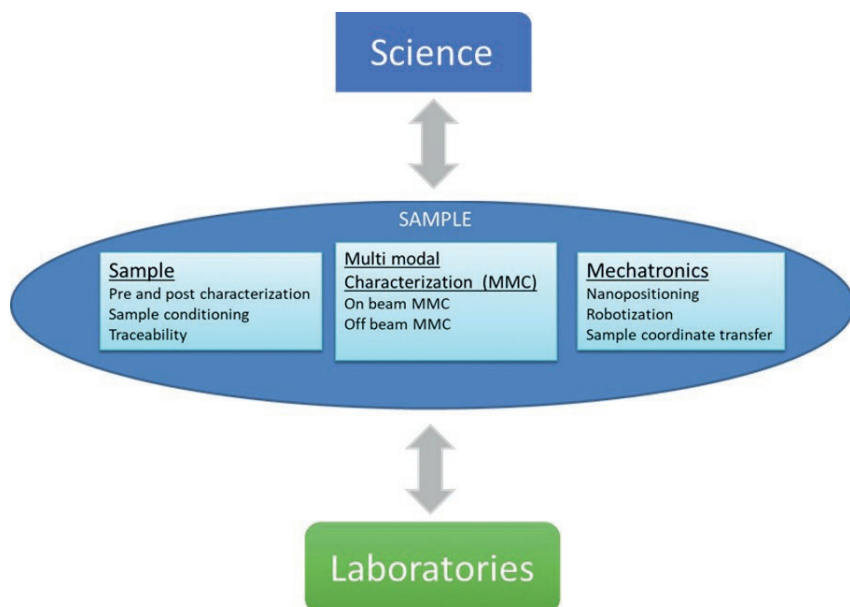


Figure 8: Sample passport gathering all the analysis information

beamtime and provide complementary data (Figure 8). This is of paramount importance considering that maintaining the integrity of a studied object is a central issue in obtaining representative results and face to the increased brilliance of the upgrade project.

A key-feature is to concatenate and structure all analytical and conditioning data on a sample, all along its life-cycle from synthesis to disposal. This includes all techniques, a generalised “passport” federating all knowledge acquired on the sample at the SOLEIL upgrade

or external laboratories; these data (meta-data) will ease successive data analysis and promote further research. Moreover, all science drivers stress on the increasing importance of mapping and space resolved measurements, thus coordinate-transfer from the laboratory characterization methods to the beamlines and from beamline to beamline must be available facilitating localization of regions of interest.

This will be the way to constitute a high throughput pipeline with a fluid transition between analytical techniques,

beamlines and (external) support laboratory-based instrumentation.

The upgrade project will leverage on the existing experience to cope with the increased demand of new needs. Chemistry, Biology, High Pressure, Microfluidic and Surface laboratories will be federated and strengthened by these needs. For instance, the traceability and monitoring of samples will be ensured by the introduction of a LIMS (Laboratory Information Management System) and ELN (Electronic Laboratory Notebook).

## REFERENCES

- [1] de Oliveira, N., Roudjane, M., Joyeux, D., Phalippou, D., Rodier, J. C., Nahon, L. "High-resolution broad-bandwidth Fourier-transform absorption spectroscopy in the VUV range down to 40 nm" *Nature Photonics*, 5: 149. (2011).
- [2] Kappler, J.P., Otero, E., Li, W., Joly, L., Schmerber, G., Muller, B., Scheurer, F., Leduc, F., Gobaut, B., Poggini, L., Serrano, G., Choueikani, F., Lhotel, E., Cornia, A., Sessoli, R., Mannini, M., Arrio, M.A., Saintavit, P., Ohresser, P. "Ultralow-temperature device dedicated to soft X-ray magnetic circular dichroism experiments" *Journal of Synchrotron Radiation*, 25 : 1727. (2018).
- [3] Langerome, B., Souske, T., Rader, K., Verseils, M., Tongtong, L., de Brion, S., Manceron, L., Brubach, J.B., Roy, P. "A new Setup for probing condensed matter in the Far IR to THz ranges at sub-Kelvin temperatures on the AILES beamline at SOLEIL" *Infrared Physics and Technology*, 107: art. n° 103223. (2020).
- [4] Loubeyre, P., Occelli, F., Dumas, P. "Synchrotron infrared spectroscopic evidence of the probable transition to metal hydrogen" *Nature*, 577: 631. (2020).
- [5] Weatherup, R. S. "2D materials membranes for operando atmospheric pressure photoelectron spectroscopy" *Topics in Catalysis*, 61: 2085. (2018).
- [6] Gosse, C., Stanesco, S., Frederick, J., Lefrançois, S., Vecchiola, A., Moskura, M., Swaraj, S., Belkhou, R., Watts, B., Haltebourg, P., Blot, C., Daillant, J., Guenoun, P., Chevallard, C. "A pressure-actuated flow cell for soft X-ray spectromicroscopy in liquid media" *Lab on a Chip*, 20: 3213. (2020).
- [7] Rochet, A., Suzana, A. F., Passos, A. R., Kalile, T., Berenguer, F., Santilli, C. V., Pulcinelli, S. H. Meneau, F. "In situ reactor to image catalysts at work in three-dimensions by Bragg coherent X-ray diffraction" *Catalysis Today*, 336: 169. (2019).
- [8] Solsona, M., Vollenbroek, J. C., Tregouet, C. B. M., Nieuwelink, A. E., Olthuis, W., van den Berg, A., Weckhuysen, B. M., Odijk, M. "Microfluidics and catalyst particles" *Lab on a Chip*, 21: 3575. (2019).
- [9] Chen, B.-C., Legat, W. R., Wang, K., et al. "Lattice light-sheet microscopy: Imaging molecules to embryos at high spatiotemporal resolution" *Science*, 346 (6208): 125799824. (2014).
- [10] Gustafsson, M. G. L., Shao, L., Carlton, P. M., Wang, C. J. R., Golubovskaya, I. N., Cande, W. Z., Agard, D. A., Sedat, J. W. "Three-Dimensional Resolution Doubling in Wide-Field Fluorescence Microscopy by Structured Illumination" *Biophys J*, 94(12): 4957–4970. (2008).
- [11] Stanley, C. E., Grossmann, G., Casadevall Solvas, X., deMello, A. J. "Soil-on-a-Chip: microfluidic platforms for environmental organismal studies" *Lab on a Chip*, 16(3):622. (2016).
- [12] Chaussavoine, I., Beauvois, A., Mateo, T., Vasireddi, R., Douri, N., Priam, J., Liatimi, Y., Lefrançois, S., Tabuteau, H., Davranche, M., Vantelon, D., Bizien, T., Chavas, L.M.G., Lassalle-Kaiser, B. "The microfluidic laboratory at Synchrotron SOLEIL" *Journal of Synchrotron Radiation*, 27(1): 230-237. (2020).



## OPTICS

From an optical design point of view, the upgraded machine will be mainly characterized by a strong reduction (by a factor between 30 and 50 times) of the horizontal photon source size, whereas the other parameters (vertical size and beam divergence) will remain almost the same. This will result in a significant brightness gain, but moreover improve the ability of focusing the beam into a smaller round beam without exceeding the optical collection capability with over large aperture angles. These small sources will exhibit coherence properties.

This diminution in source size will be achieved by decreasing the strength of the bending magnets and increasing the fraction of the ring circumference occupied by electron optics. In consequence, the straight sections, and some of the insertion devices (ID) they host, will need to be shorter. Preserving the energy range of beamlines will require an increase in magnetic field, and hence the emitted flux, but also the number of emitted harmonics and consequently the heat load on the optics.

The challenge faced by optical design is then to improve the optics quality to preserve the reduced source size, at the same time as adapting to even more severe conditions.

### Beamline optics

#### Optical surfaces

X ray beamline optics mainly rely on **grazing incidence mirrors**. Mirrors are ubiquitous components since, by simple change of the grazing angle, they can be used from visible to hard X-ray and they are achromatic. The focus quality at the end of a beamline is dependent on the optical surface manufacturing. As a rule, the spot widening is proportional to the average angular departure of the surface to its ideal shape, called slope error. Slope errors have a direct effect in the incidence direction but, due to the grazing incidence, their widening effect is strongly reduced in the transverse direction. Current SOLEIL optics have relied on this effect to orient the slope error widening in the horizontal direction, where the source size is intrinsically larger, and consequently relax the surface specifications (about 0.3  $\mu$ rad RMS). This will no longer be possible with a small round source: both axes will need state of the art surface accuracy (below

50 nrad RMS, corresponding to height errors around 1 nm RMS)

Procurement of top quality optical surfaces is seen as a potential issue, since the leading European manufacturers have been outclassed by a single supplier in Asia, who is presently the only source of nrad precise surfaces. This situation has been acknowledged by the League of European Accelerator-based Photon Sources (LEAPS), which has targeted the development of European nrad precise polishing technologies as its highest priority action. A project oriented to support the development of ultra-precise polishing techniques by the European manufacturers, via the common PCP (Pre Commercial Procurement) of an ultra-flat mirror, has been submitted by LEAPS to the EC (coordination ESRF and SOLEIL).

#### Reflective coatings

Good substrate materials, such as silica or silicon, have a low atomic number and therefore a low surface reflectivity. The polished substrate must be coated with some reflective layer. This coating can be either a single layer of a high Z material (Pt, Au) or a stack of alternate layer of low and high Z materials (e.g. Mo/B<sub>4</sub>C). A periodic multilayer (ML) acts as an interferential mirror and reflects a narrow wavelength range (a few %) around the tuning energy defined by its period and the grazing angle. Larger reflectivity profiles will be achieved by tuning the layer pair thickness according to their depth. Reflective layer deposition is often provided (or subcontracted) by the mirror manufacturer. However some components, such as the multilayer gratings developed by SOLEIL to extend the grating spectral domain to the tender X-ray range (1500 - 5000 eV), require an

accurate match of the layer thickness to the design parameters, namely the grating groove depth. For manufacturing this kind of component, SOLEIL has established a collaboration with Laboratoire Charles Fabry of Institut d'Optique (LCFIO, Palaiseau) to run a joint deposition facility named CeMox. This facility will give us more flexibility for producing the special coatings, with very thin layers (1nm), required by the upgraded optics<sup>[1]</sup>. See Figure 9 below.

#### Dispersive and active elements

A number of other components are used for specific needs, ranging from stacks of thin **refractive lenses** (CRL), **crystals** for energy selection, and various kinds of **gratings** made by holographic printing or e-beam writing, for dispersion, focusing purposes or production of light sheet beams. Their fabrication is, as a rule, technologically demanding and only mastered by a small number of actors. An active technology watch and market survey will ensure the supply of all these special elements which are not required in large numbers.

Variation of the focus size can be achieved by mechanical benders which change the curvature of the mirror. However the position of the focus also changes, which limits the applications. In the hard X-ray part of the spectrum, CRLs offer an alternative with so called transfocators. These devices allow a focal length change by inserting or removing individual lenses in the stack. A division in two groups should perform as a zoom lens.

When the quality of the focused beam on the sample is critical, it can be optimized with active mirrors in the last focusing stage, as customary for astronomic

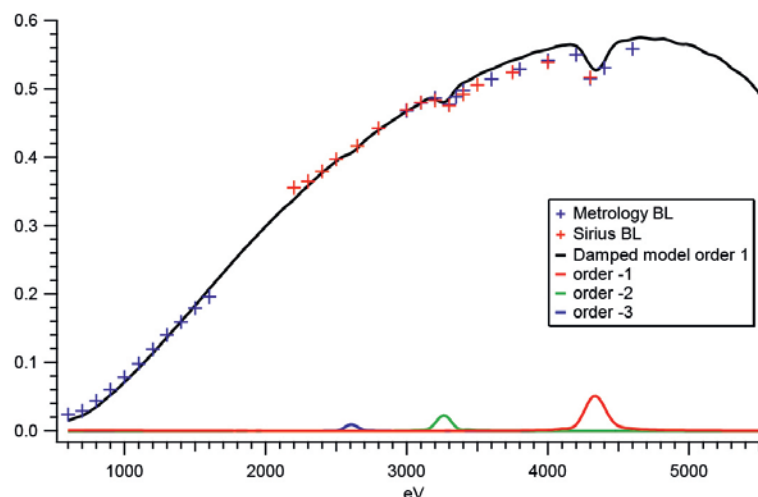


Figure 9: Measured diffraction efficiency of the Cr/B<sub>4</sub>C multilayer grating of SIRIUS beamline, versus CARPEM code model

telescopes. It is not easy to implement enough actuators on the focusing mirrors themselves, especially if the aperture angle is large. Currently 1 or 2 actuators only are used. A good level of correction can be achieved by adding an active compensating mirror behind the focusing one<sup>[2]</sup>. Being nearly flat, it can be thin and is set at a much more grazing angle in order to avoid reflectivity and bandpass losses and have length to accommodate enough actuators.

### Mechanical mounts and stability

Mechanical parts of an optical instrument are quite as critical as the optical surfaces. Their design is mainly subcontracted, making them more difficult to control. At the required level of accuracy, the utmost care must be taken not to constrain the element and distort its shape. The task is complex for the first mirrors of a beamline which are subjected to an important heat load from all radiations emitted by the source inside their collection aperture. SOLEIL first mirrors are currently able to withstand some 300 W, but they are often deviating the beam horizontally so that thermal bending is affecting the largest source dimension. Thermal bending will need to be actively controlled on the upgraded machine to preserve the manufactured surface quality level, at even higher thermal loads. SiC may be used, instead of Si, as the substrate material thanks to its better heat transfer properties. However, material quality is quite dependent on the manufacturing process. New suppliers are under evaluation. Other directions such as compensation schemes, where a controllable additional source maintains a constant heat load to the mirror, are being actively studied.

Maintaining the **stability** and rigidity of a 50 m long optical instrument, such as a beamline, is not a simple problem. Present vertical stability, with respect to the source, is already around 1  $\mu\text{m}$ . This will not need to be further improved for the new machine, but the same stability will be required in the horizontal direction. Stability issues are twofold: vibrations and long term thermal drifts. Drift sensitive elements should be placed in enclosures isolated from user activities. Thermal stabilization of hutches can be greatly improved from the present situation by collecting and evacuating the thermal output of electronic appliances. Mechanical designs must systematically include a vibration analysis study to track low frequency modes. However the contribution of vibrational sources such

as cooling pipes is difficult to evaluate, and can vary with time, particularly for centralized cooling systems serving many applications. Prototyping of new cooling schemes for monochromators and first mirrors has to be performed with selected suppliers.

The mechanics is also responsible for positioning and aligning the optical elements in a fast, precise and reproducible way. The required level of positioning accuracy has to respond to the slope accuracy of the optical surface, namely on the  $\mu\text{rad}$  scale or better, and be reliably referred to the laboratory frame. This is far from being achieved by "off the shelf" products of instrumentation manufacturers. Absolute encoding should be preferred whenever possible. All these efforts can be ruined by the failure of an encoder, especially in hutches where ionizing radiation levels are high. Shielding and duplicating the elements, as well as hardened electronic components, must be considered. Because they add much cost without visible improvement of performance, these issues are often badly underestimated in the mechanical procurement process.

### Optical design and computation

Due to their extreme grazing incidence, X-ray optics are badly handled by usual optical design codes. SOLEIL has been relying on its own **ray tracing** codes, SpotX<sup>[3]</sup> and Solemio<sup>[4]</sup>, the latter implementing **optimization** capabilities (a common feature of visible optics code, missing in most X-ray ones). These codes have been fully benchmarked against the reference code SHADOW. However their maintenance is problematic in the long term.

Several actions have been started to face this issue. First, the whole set of beamline configuration data has been moved to OASYS, a repackaging of SHADOW, which seems to become the main choice of the synchrotron community. A new source emission modeling library has been developed to be interfaced to the ray tracing codes. The next step will be exporting the ray tracers output toward other modeling codes. Export toward McXtrace (promoted by the Data Reduction and Analysis Group of SOLEIL for end to end simulations) can be achieved through a common interface (MCPL). Exporting ray traces as wavefront information for **simulating the diffraction** limited spot is also considered. Automatic **tolerancing** is a very useful tool found in all visible light codes. It is missing from the X-ray ones. Its development, which uses mechanisms close to optimization, is under way.

The internally developed CARPEM<sup>[5]</sup> code allows a precise modelling of **reflectivity of mirrors and gratings**, single or multilayer coated. New monochromator schemes using conical diffraction have been recently proposed. A new vector code, under development, allows coping with any grating line orientation. These codes are too heavy to be integrated in the ray tracing simulation codes. Interfacing them to the ray tracers by means of precomputed tables is considered.

These code evolutions are expected to simplify and speed-up the process of redesigning nearly 30 beamlines over a few years, by automating some of the most time-consuming tasks such as optimization, tolerancing and production of throughput tables and graphs.

### Optical metrology and diagnostics

Minimizing the beam shutdown period will require to setup rigorous procedures of **quality** control throughout all the phases of procurement, specification, selection of providers, acceptance, mounting, alignment and commissioning. Respect of specifications obviously cannot be expected if the purchaser does not have the means to control and produce indisputable records. This validation has always been the main axis of SOLEIL optical metrology policy, with a special attention to leaving no gaps in specification coverage.

Later on, during the alignment and commissioning phases, diagnostics are essential to ensure that the components, as they have been actually manufactured and measured, are used in the best possible way. These diagnostics must be anticipated and studied together and in the same process as the optical design.

### Metrology of beamline components

#### LMO (laboratoire de métrologie optique)

Measuring the physical parameters of all the beamline optical elements is, as already stated, a critical requirement in order to ensure the expected performances. The optics laboratory (LMO) has been part of the Optics group, since the first days of SOLEIL. It has progressively constituted a large panel of metrology instruments able to measure all the optical parameters of mirrors and gratings with the best available accuracy. A large part of the instrument development was done internally. It gives the



LMO a full control over the performances and a capacity of managing the evolutions in order to respond to new requirements – 2D maps of surface height errors, larger spatial frequency domain– and closely match the coherence management demand.

Figure 10 shows the evolution of the spatial frequency coverage of SOLEIL's LTP (Long Trace Profiler) over the last 20 years, together with the accuracy of the demanded, and achieved, slope error measurements. This instrument, which measures the local slope along a linear profile, has been continuously upgraded and is still the reference for long range shape distortions. LMO is upgrading to stitching interferometry<sup>[6]</sup>, first with a micro-interferometer (20  $\mu\text{m}$  resolution, 300 mm stitching length)<sup>[7]</sup>, now with a large pupil interferometer (80  $\mu\text{m}$  resolution, 1 m stitching length, under development). The Atomic Force Microscope (AFM) enables accurate measurement of grating profiles and micro-roughness<sup>[8]</sup>. The overlap of instrument capabilities is crucial for cross-checking result validity in various frequency ranges. See Figure 10 below.

Since 2018, LMO has undertaken many measures in order to conform to the ISO 17025 norm ("General requirements for the competence of testing and calibration laboratories.") in order to obtain the accreditation from COFRAC for a part of its activity (LTP, AFM). This is expected for 2021. Inter-comparisons with other metrology laboratories are one requirement of the norm. LMO is presently engaged in the project MoonPics (Metrology on One Nanometer Precise Optics), which is a part of the European program CALIPSOplus. Besides, LMO maintains long term relationship with metrology groups of other synchrotrons (ESRF, ALBA, NSLSII)

### Metrology beamline

The METROLOGY beamline complements the LMO for measurements such as mirror reflectivity, crystal or grating diffraction properties, which must be performed at the working energy, and are requested for beamline final alignment and fine tuning. With two branches, one located on a high field local bend, and the other located on a standard field dipole, it will be able to cover almost completely the available energy range of SOLEIL beamlines from 30 eV to 40 keV. Some overlap between the two branches will be given by a convenient multilayer pair. Access to white beam will also be provided. In addition to metrology of optical elements and detectors, the high energy branch configuration will make possible a wide

set of test experiments, from imagery to irradiation, including the development of beam and source point diagnostics for the upgraded beamlines. Bendable mirrors and KB will give the required flexibility of focusing.

The availability of the METROLOGY beamline is crucial to complete the optics and detector prototyping program, which in particular should include the development of wavefront sensors for beam characterization and fine tuning in front of coherence sensitive experiments.

### Mechanical metrology

Conformity of mechanical beamline elements to the fabrication specification has the same importance as to optical parts. Accuracy of positioning and indexing are critical for monochromator rotations, but keeping the parasitic movements inside very strict tolerances is not less important. These measurements, in particular angular ones, must be carried out upon receipt of all mechanical equipment. Systems with composite movements like hexapods, which are very sensitive to parameter definition, require specific control procedures.

The correct behavior in operation condition must be also ensured, hence checked, but it is made difficult since sensitive elements under ultra-high vacuum are not directly accessible. Vibrations of mirrors can now be monitored *in situ*, with high precision, with a recently acquired fast autocollimator, but mirror deformations under beam still cannot be tracked.

### Diagnostics and beam characterization

The alignment of a beamline is firstly done with survey instruments. But, though the precision of this alignment has progressed with the generalization of laser trackers, it is seldom sufficient to achieve the optimal performances. Final adjustment must be done under beam with the beamline diagnostics. Being mostly under vacuum, these diagnostics, and the associated alignment procedure, must be an integral part of the beamline design. Considerable experience has been gained on the present SOLEIL beamlines by the operating teams. It will be used for improving the diagnostic implantation at beamline reconstruction. Diagnostics should be robust, precise, complete and fast. The simple screen at focus position gives a fast diagnostic of spot size with limited lateral resolution ( $\sim 0.5\mu\text{m}$ ). It doesn't give information on residual aberration limiting the spot size and often doesn't withstand the beam intensity. More information can be extracted from the far-field of a known obstacle, which can be of different nature, knife-edge, gratings<sup>[9, 10]</sup>, diffuser<sup>[11, 12]</sup>, or a high resolution pattern<sup>[13]</sup> typically analyzed by ptychographic methods. These techniques are not yet capable of giving the real time response required for adaptive tuning, but they are actively considered for SOLEIL upgraded beamlines, together with holistic beamline simulation.

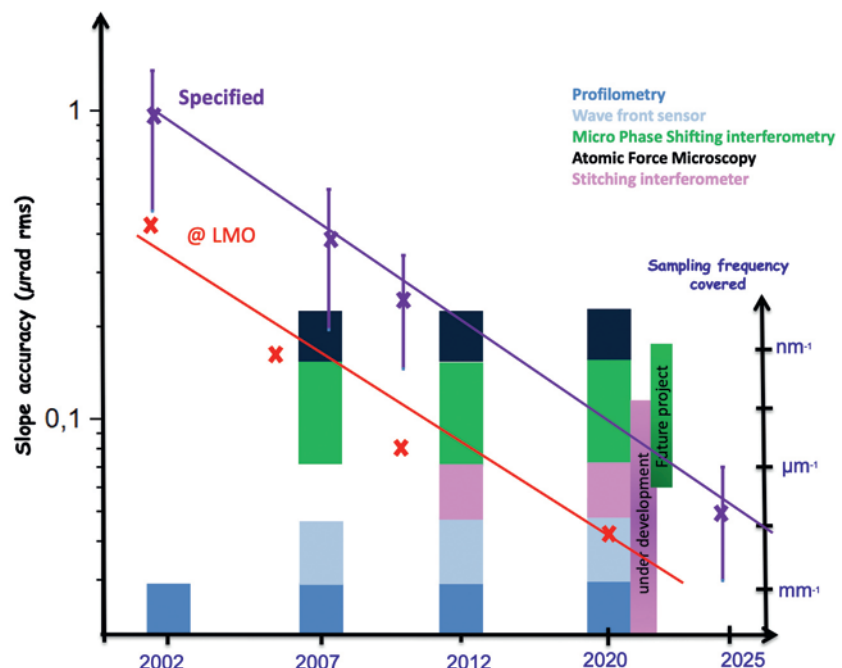


Figure 10: Evolution of the measurement demand and capabilities of LMO since SOLEIL beginning

## REFERENCES

- [1] C. Burcklen, R. Soufli, D. Denetiere, F. Polack, B. Capitanio, E. Gullikson, E. Meltchakov, M. Thomasset, A. Jérôme, S. de Rossi, F. Delmotte, "Cr/B4C multilayer mirrors: Study of interfaces and X-ray reflectance," *J. Appl. Physics*, 119 125307 . (2016).
- [2] H. Mimura, S. Handa, T. Kimura, H. Yumoto, D. Yamakawa, H. Yokoyama, S. Matsuyama, K. Inagaki, K. Yamamura, Y. Sano, K. Tamasaku, Y. Nishino, M. Yabashi, T. Ishikawa, and K. Yamauchi, "Breaking the 10 nm barrier in hard-X-ray focusing," *Nat. Phys.* 6(2), 122–125 (2010).
- [3] T. Moreno, et M. Idir, "SPOTX a ray tracing software for X-ray optics," *J. Phys. IV France*, 11, 527:531 (2001).
- [4] F. Bonnemason et al., "Etude et mise au point des éléments et des techniques optiques pour le développement de lignes de lumière adaptées aux sources synchrotron de nouvelle génération," Rapport final du contrat d'aide EUREKA n° 96 W 0112, Nov 1998.
- [5] A. Mirone, E. Delcamp, M. Idir, G. Cauchon, F. Polack, P. Dhez, and C. Bizeuil, "Numerical and experimental study of grating efficiency for synchrotron monochromators," *Appl. Opt.* 37, 5816-5822 (1998).
- [6] L. Huang, T. Wang, J. Nicolas, A. Vivo, F. Polack, M. Thomasset, C. Zuo, K. Tayabaly, D.W. Kim, M. Idir, "Multi-pitch self-calibration measurement using a nano-accuracy surface profiler for X-ray mirror metrology," *Optics Express*, 27(19): 26940-26956. (2019).
- [7] F. Polack, M. Thomasset, S. Brochet, D. Denetiere, "Surface shape determination with a stitching Michelson interferometer and accuracy evaluation," *Rev. Sci. Instrum.*, 90(2): art.n° 021708. (2019).
- [8] M. Thomasset, J. Dvorak, S. Brochet, D. Denetiere, F. Polack, "Grating metrology for X-ray and V-UV synchrotron beamlines at SOLEIL" *Rev. Sci. Instrum.*, 90(2): art.n° 021714. (2019).
- [9] S. Matsuyama, H. Yokoyama, R. Fukui, Y. Kohmura, K. Tamasaku, M. Yabashi, W. Yashiro, A. Momose, T. Ishikawa, and K. Yamauchi, "Wavefront measurement for a hard-X-ray nanobeam using single-grating interferometry," *Optics Express* 20, 24977-24986 (2012).
- [10] A. Montaux-Lambert., P. Mercère, J. Primot, "Interferogram conditioning for improved Fourier analysis and application to X-ray phase imaging by grating interferometry," *Optics Express*, 23(22): 28479-28490. (2015).
- [11] S. Berujon, H. Wang, S. Alcock, and K. Sawhney, "At-wavelength metrology of hard X-ray mirror using near field speckle," *Optics Express* 22, 6438-6446 (2014)
- [12] L. Xue, Z. Li, T. Zhou, X. Dong, H. Luo, H. Wang, K. Sawhney, and J. Wang, "Absolute metrology method of the X-ray mirror with speckle scanning technique," *Appl. Opt.* 58, 8658-8664 (2019)
- [13] E. Torbjørn B. Skjønsfjell, Y. Chushkin, F. Zontone, N. Patil, A. Gibaud, and D.W. Breiby, "Wavefront metrology for coherent hard X-rays by scanning a microsphere," *Optics Express* 24, 10710-10722 (2016).

## GLOSSARY OF TECHNIQUES

**ARPES:** Angle Resolved PhotoEmission Spectroscopy

**CD:** circular dichroism

**FT:** Fourier Transform

**HAXPES:** HArd X-ray PhotoElectron Spectroscopy / **AP-HAXPES:** Ambient Pressure HAXPES

**MX:** Molecular Crystallography

**PDF:** Pair Distribution Function

**PEEM:** PhotoEmission Electron Microscopy

**RIXS:** Resonant Inelastic X-ray Scattering

**SAXS:** Small Angle X-ray Scattering

**SNOM:** Scanning Near-field Optical Microscopy

**STXM:** Scanning Transmission X-ray Microscopy

**XAS:** X-ray Absorption Spectroscopy

**XES:** X-ray Emission Spectroscopy

**XMCD:** X-ray Magnetic Circular Dichroism

**XPCS:** X-ray Photon Correlation Spectroscopy

**XPS:** X-ray Photoelectron Spectroscopy / **NAP-XPS:** Near Ambient Pressure XPS

**XRS:** X-ray Raman Spectroscopy



## DETECTORS

The high brilliance and coherent beams resulting from the SOLEIL upgrade will open the way for a large range of experiments, where detectors will play a key role in the techniques and methods developed to fully exploit the upgraded synchrotron.

Main detector properties such as high dynamic range, extended spatial resolution, photon sensitivity, low noise and high frame rate capability are consequently of great importance. Dedicated fast data acquisition systems and fast data transfer to informatics servers, enabling on-line data reduction and/or in order to follow acquisition in real time, are also critical points to fully address scientific objectives. In particular, the ability to flag images, according to specific criteria of 'usefulness' before they are stored, represents a great challenge in the context of data volume storage.

Our detector development strategy, established following a careful review of activities in 2016, consists of both pursuing the acquisition of recent commercial detectors and, in parallel, launching an evolving R&D program on a few detector systems that are particularly innovative and important in order to respond to the scientific challenges presented in the Science cases chapter. The development of a new detector is a very long process (more than 5 years), and consequently only highly ambitious projects, unlikely to be pursued as a commercial venture, are chosen as the subject of R&D. The SOLEIL Detector group has already started, or contributed to, the prototyping phase of new hard- and soft- X-ray detector systems addressing critical upgrade requirements, a number of them in collaboration with other institutes. Important for the future is to further broaden the detector group

activities towards soft X-ray, UV and IR applications.

Finally, in addition to the detection for data acquisition, detection as a diagnostic tool remains an enabling technology for beamline automation (in alignment and performance) and to provide experimental meta-data in response to FAIR data criteria.

### Simulation of the signal response of semiconductor detectors to photon beam through matter

#### Challenges

Before starting the design of a new challenging detector, it is essential to assess its feasibility, performance and capacity to enable the resolution of scientific problems. As "big science" is expensive science, the need to minimise uncertainty in experimental results is both a societal and scientific objective.

The simulation of the signal response of a semiconductor detector to photon beam through matter is a powerful tool able to provide guide lines for designing, prototyping and improving detectors, as well as modelling experimental environments, reducing time and cost mainly in the instrument design phase. Full modelling of experimental performance represents an opportunity for successful data reduction, casting light on experimental reliability and enabling the user to identify, with confidence, rare events that may be critical for full understanding. Although currently unattainable, the full coupling of acquisition, modelling and results analysis (using machine learning) will revolutionise science in the foreseeable future, and the simulation of detector and experimental performance is a key step in the process.

#### Solution under development

Consequently, the SOLEIL Detector group has invested efforts in the implementation of such simulation tools. This work benefits from the development of validated well-known simulation codes and the reduction of computing time using dedicated informatics clusters. The simulation work is based in two codes: GEANT4 (a CERN C++ open-source code widely used, to cover the photon-matter interaction, in several domains), and COMSOL Multiphysics with the Semiconductor module (a licensed code to generate the 3D nonlinear electric field inside a complex semiconductor detector). The output data of these codes are integrated in the ALLPIX2 simulation framework<sup>[1]</sup>, originally developed for High Energy Physics experiments using pixelated silicon detectors. This data framework already includes a series of modules that simulate charge creation, propagation and diffusion, pulse induction at the pixels and electronics digitalization. However several features have been implemented to simulate a synchrotron beamline environment, including photon polarization<sup>[2]</sup>, sample dimensions and composition, Germanium properties for the detector and the associated electronics<sup>[3]</sup>.

The simulation tools have been first applied to the design of a new multi-element Germanium detector prototype for future XAS experiments (Figure 11). The whole simulation is being calibrated by the modelling of a XAS experiment (Figure 11 left), where a complex soil sample was studied. A comparison between real and simulated data is illustrated on Figure 11 right, showing good agreement for the main X-rays lines of the target elements (Cd, Fe, Sr, Zr). Other improvements of the simulation are still on-going to better reproduce the Compton scattering background.

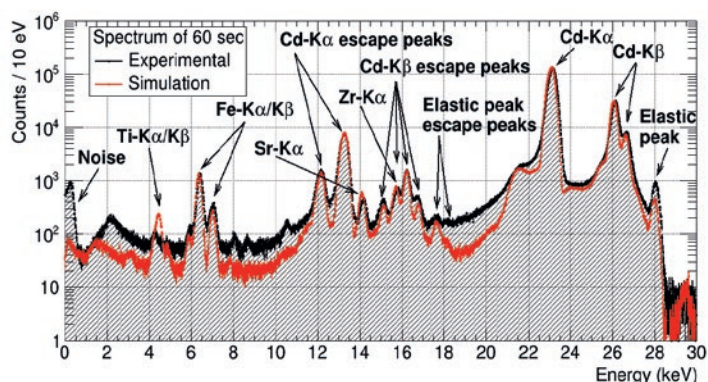
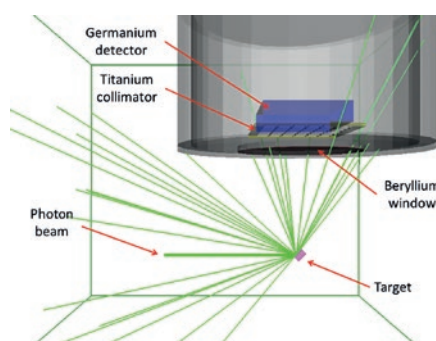


Figure 11: Modelling of an XAFS experiment (left) and first comparison between simulated and real data of the X-ray fluorescence energy spectrum emitted from a complex soil sample (right)

## Perspectives

This simulation framework will become a design tool of future detectors for the SOLEIL upgrade. In the short-term, it will be reused for any other beamline where a future multi-element Germanium detector will be tested, and will also be used within the future European project LEAPS. In the medium-term, it will be applied to an ultra-fast energy resolved detector based on pixelated Silicon chip, in the context of several experiments (see “Ultra-Fast Energy Resolved Imager for hard X-ray crystallography experiments with Multi Pink Beams”, on next page). The incorporation of the framework in experimental modelling approaches, such as McXtrace<sup>[4]</sup>, as well as its incorporation in automated data analysis as a service and machine learning methods to identify trends and signatures in data, is a long-term objective.

## Development of a multi-element germanium detector for XAS experiments

### Challenges

The importance of detecting and tracking ultra-low concentrations of trace elements in matter has been highlighted in Chapter 2. No currently available commercial detector allows optimized geometry with sufficient count rate and sensitivity in order to achieve this objective. The goal of this development is to design a new generation of Germanium detectors for X-ray spectroscopy applications in the energy range from 5 keV to 100 keV. The expected detection performance should consist in a high throughput per unit area (from 50 kcps/mm<sup>2</sup> to 250 kcps/mm<sup>2</sup>), high detection sensitivity (improved peak-to-background ratio) and an improved stability, overcoming limitations of current detectors available on the market.

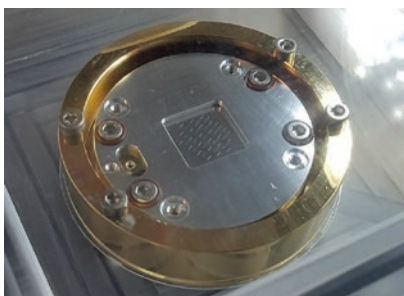


Figure 12: Ge crystal mounted on the holder viewed from pad side

## Technical solution and detector under development

To cope with this ambitious objective, a DIAMOND-SOLEIL joint project has been launched, the technology for the detection part being based on a pixelated Germanium crystal. The first prototype<sup>[5]</sup> (Figure 12) consists of a 4 mm thick Ge crystal, whose back-side has been segmented into 19 hexagonal pixels of 2 mm inner diameter. Pixels are connected to low noise preamplifiers, situated on a ceramic front-end board (under development). The Ge detector is located inside a cryostat and cooled to <90 K with LN<sub>2</sub>. Pre-amplifier output signals are transferred outside the cryostat and are digitized by the Xpress4 digital electronics<sup>[6]</sup>.

### Perspectives

A front-end board is being designed for the first prototype, and will be tested in the laboratory by the end of 2020. Meanwhile, SOLEIL simulation framework (see “Solution under development”, on previous page) has reproduced results in good agreement with previous measurements. Our framework will soon provide a first performance comparison between the reviewed prototype and existing Ge detectors in use at SOLEIL<sup>[7]</sup>. This comparison will help to improve the current design and to provide essential guidelines for the design of a 37-element prototype.

## Fast hybrid photon counting detector for time resolved experiments

### Challenges

Studies of fast phenomena (*in situ*, *operando*, dynamic) are a recurrent themes in all scientific challenges. For example,

pump-(multi) probe techniques rely on detectors able to isolate and sample signals from a single X-ray synchrotron pulse, with very challenging characteristics such as high linear count rate, energy selection, fast gated pixel architecture, fast readout and temporal resolution down to a few tens of ns. A wide range of hard X-ray experimental techniques would benefit from detectors with such performance, notably pump-(multi)probe X-ray diffraction, and time-resolved X-ray absorption spectroscopy. The X-ray Photon Correlation Spectroscopy (XPCS) technique would also benefit from this type of detector.

## Technical solution and detector under development

An R&D program was launched, in 2016, to develop small and medium scale detectors based on the UFXC32k readout chip<sup>[8]</sup>, which offers small pixel sizes, highly flexible acquisition modes and readout speeds in excess of those commercially available. A full 2-chip detector prototype has been designed internally<sup>[9]</sup>. The prototype consists of 256 × 257 square pixels with 75 μm pitch (19.2 × 19.3 mm<sup>2</sup>), fast readout of 20 kfps (and potentially more), linear count-rate up to 2.6 × 10<sup>6</sup> ph/s/pix, two thresholds and two 14-bit counters in every pixel and very short counting times with gates down to 50 ns for single X-ray pulse selection. The prototype performances have been demonstrated<sup>[10]</sup> by performing, for the first time, a benchmark pump-probe-diffraction experiment on the CRISTAL beamline (Figure 14 left), where two successive acquisitions were performed after each laser pump pulse. The first one aimed to study the excited state of the sample and the second one was used as a reference for normalizing the photo-induced relative changes and to remove possible drifts in the measurements (Figure 14 middle). The benchmark demonstrated

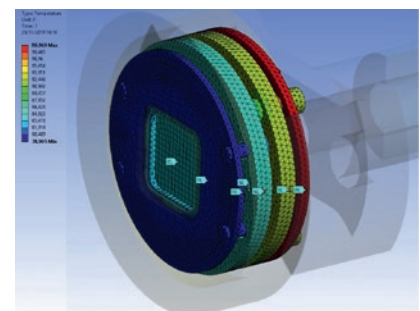
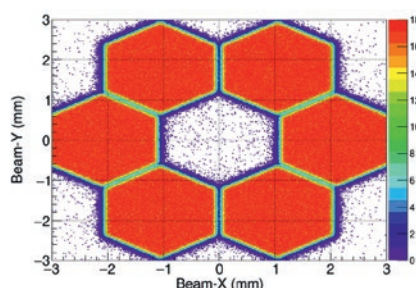


Figure 13: Simulation of charge sharing (left), temperature gradient in the prototype detector head (right)

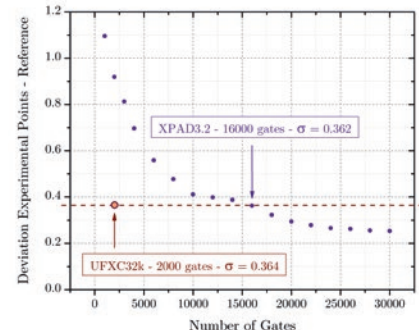
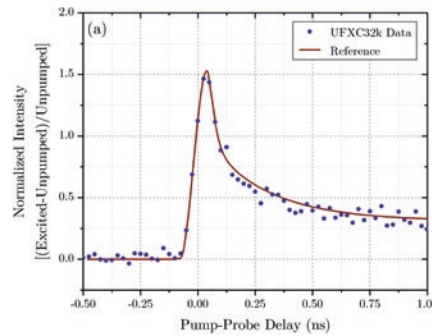
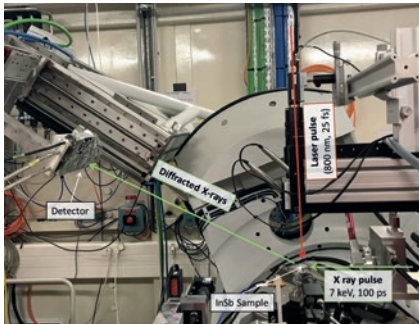


Figure 14: Experimental setup for the pump-probe measurements (left). Experimental curve compared to a reference model (middle). Deviation of the exp. data from the reference model for a standard detector (blue) and the 2-chips prototype (brown) (right).

better data quality, obtained 8 times faster than the XPAD detector previously used on the beamline (Figure 14 right).

### Perspectives

The small-scale prototype proved excellent performance for the time resolved pump-probe-probe experiments. Good detection efficiency below 6 keV has been also demonstrated. Use of this detector will be extended to other beamlines in the short-term, e.g. energy-dispersive and XES applications. A larger and more performant detector ( $4 \times 4 \text{ cm}^2$ ) is currently under development and should be ready for users before SOLEIL upgrade. A readout mode for XPCS applications is also under development.

## Ultra-fast energy resolved imager for hard X-ray crystallography experiments with multi pink beams

### Challenges

'Pseudo' Laue diffraction<sup>[11,12]</sup> (Figure 15 left), with multi pink beam, is being considered as an upgrade option for rapid time resolved crystallographic

applications. A factor of over 1000 in acquisition speed, compared to current performances, may be expected. The main advantage is the capability of simultaneous measurements of continuous photon fluxes at different energies, with integration of intensities using "pink" or "monochromatic" beam methods. No such detector exists or is planned at other facilities or suppliers, and the proposal is high-risk, high gain. Such a detector would address challenges in Advanced Materials and Health. Thematics under study are the serial synchrotron crystallography, *in situ* macromolecular crystallography, *in vivo* crystallography and high-pressure/temperature crystallography (quasi-crystal). Pump-probe techniques can also be considered.

### Technical solution and detector under development

A feasibility phase has been launched to assess the required performances needed for such a challenging imager, and for the design of future readout pixel ASICs. The energy range required is 5-30 keV. A very high counting rate for the detector is essential to be compatible with the photon flux expected on the detector surface (about  $10^{11} \text{ ph/s/mm}^2$ ), and also to record a maximum of images before the onset of radiation damage due to diffusion

products. Despite the fact that the charge integration detector concept seems preferable to deal with high counting rate, photon counting detectors are preferable where signal to noise ratio and extracting the best statistics from every input photon are critical issues (*i.e.* in the presence of radiation damage). Several thresholds are required per pixel to separate incoming photon energies without slowing down the readout speed (no embedded logic at the pixel level).

One of the main limitations for the detector feasibility is the charge sharing effect between pixels (depending of the photon energy) that will occur, affecting the hit assignment with the right energy level and consequently introducing fakes in the measurement that have to be assessed. This effect is currently under study. Figure 5-middle illustrates a simplified simulation of a Silicon n-in-p semiconductor of  $320 \mu\text{m}$  thick and pixels pitch of  $75 \mu\text{m}$ . The FWHM of the holes distribution is simulated versus incoming photon energy. Figure 5-right illustrates a real beam test results obtained on the same semiconductor sensor for  $E = 10 \text{ keV}$  and with a discriminator threshold of 7 keV. In this particular case, the size of the pixel affected by charge sharing is only less than  $10 \mu\text{m}$ , which means that 75% of the pixel surface is not affected by charge sharing.

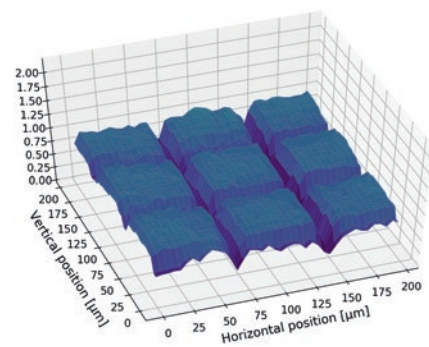
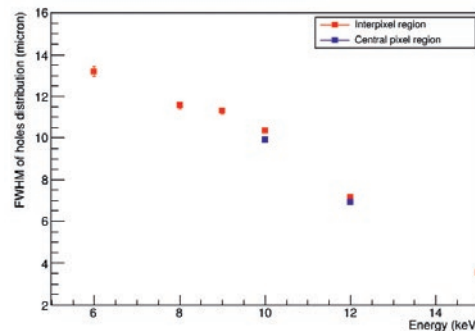
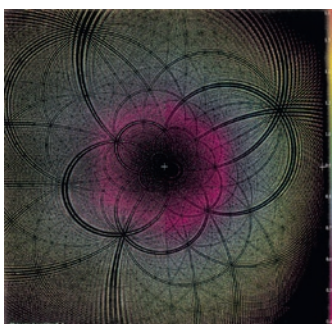


Figure 15: Simulated broadband Laue diffraction pattern from a virus crystal [1] (left); Charge sharing studies: simulated FWHM of holes cloud distribution drifted on a backplane of a semiconductor Si-sensor of  $320 \mu\text{m}$  thick versus incident photon energy (middle), 2D scan performed with a 10 keV pencil beam on a hybrid pixel detector (7 keV threshold is applied and the surface profile of pixels is normalized to 1) (right).

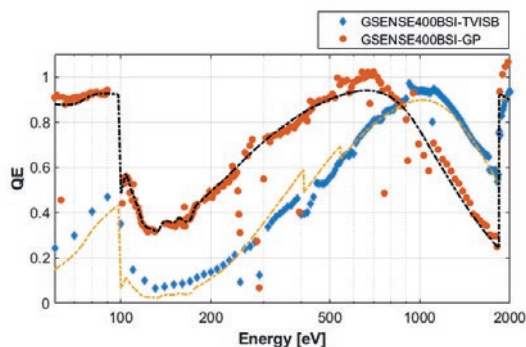


Figure 16: GSENSE400BSI 'Standard' and 'GP' Quantum Efficiency measured on a beamline at SOLEIL superposed with a theoretical model.

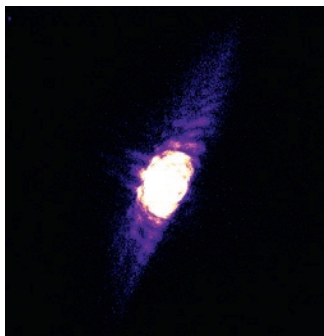


Figure 17: Diffraction pattern image of a part of the Siemens star obtained on the STXM at SOLEIL.

## Perspectives

Feasibility studies are on-going to determine both, by simulation and by experimental measurements with existing hybrid pixels detectors, the real limitations of such a challenging imager. This work will be pursued and, dependent on the results, we expect to launch the readout ASIC design phase in the coming months.

## Large and fast pixelated detector for soft X-ray experiments

### Challenges

For imaging in the soft X-ray domain (100-3000 eV), and particularly for the experiments in the water window, there is a lack of performing 2D detectors to respond to Advanced Material, Energy and Health scientific challenges. In addition to high performance needed in terms of frame rate, low noise and high dynamic range, a strong constraint comes from the very short absorption length of photons that imposes constraints on the detector entrance window. Monolithic Active Pixels Sensors (MAPS) technology, with dedicated pixel architecture, illuminated on the back-side with thin entrance window, is identified as the best available technical solution to fulfill these requirements.

Several developments are on-going around the world. SOLEIL Detector group works on two different options: on the short-term, a home-made adapted camera based on a performing commercial sCMOS sensor, and on the middle-term a fast CMOS monolithic imager, developed within a large collaboration of light sources (DESY, DLS, ELETTRA, PAL, SOLEIL) and STFC/RAL, and led by DESY.

### In-vacuum adaptation of a commercial sCMOS sensor

The detector proposed is based on the GPIXEL GSENSE400BSI sensor, a globally mass produced scientific sCMOS sensor, Back Side Illuminated (sCMOSBSI), of 4 Mpx (11  $\mu\text{m}$ ,  $20 \times 20 \text{ mm}^2$ ) and with an efficiency around 80%<sup>[13]</sup> over the large energy domain. With a very low readout noise ( $< 2 \text{ e}^- \text{ rms}$ ), relatively large full well capacity (up to 80 ke $^-$ ), and readout speed of 48 Hz (full frame), the detector provides X-ray single photon detection with a saturation better than 1000 ph/s/pixel.

First detector based on this sensor has been made at SOLEIL<sup>[14]</sup> to demonstrate the quantum efficiency (Figure 16), to evaluate the radiation hardness and to demonstrate X-ray ptychography capability. Figure 17 shows the diffraction pattern of a part of a Siemens star obtained by STXM.

From these promising first results, in-vacuum detectors based on the GSENSE400BSI sensor (now produced by the AXIS Company) will be implemented on the vacuum experiment station at SOLEIL. A technology survey on new sensors with smaller pixel size is on-going.

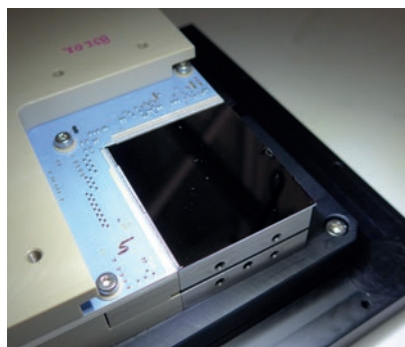


Figure 18: First wire bonded backside illuminated Percival P2M sensor

### Large CMOS monolithic imager - PERCIVAL

PERCIVAL is a CMOS monolithic imager (see Figure 18) combining a large detection area of  $4 \times 4 \text{ cm}^2$  area with over 2 million pixels, a fast readout of 300 frames/s, low noise ( $\sim 15 \text{ e}^-$ ), and a large dynamic range (linear full well capacity up to 4 Me $^-$ ), with a post-processed soft-X-ray-compatible entrance window<sup>[15]</sup>. The real time adaptive gain modulation, independent for each pixel, allows the detector to have simultaneously a high gain for pixels exposed to a low photon flux, and a coarser level of charge discrimination (increased dynamic range) for pixels exposed to a high photon flux. On-chip data processing capabilities eliminate reset and fixed pattern noise.

An important effort concerns the data acquisition and software systems to cope with the considerable data rate of  $\sim 20 \text{ Gbit/sec}$ . A data analysis framework<sup>[16]</sup> (developed by SOLEIL and DESY), geared in particular towards calibration and characterization needs, has been set up for PERCIVAL.

A first 2-Megapixel PERCIVAL P2M sensor processed for backside illumination is available and has been tested in the laboratory<sup>[17]</sup> as illustrated on Figure 19 and, more recently, using soft X-rays down to 250 eV at Petra III's P04 beamline.

Future work will include demonstrating the full sensor performance and operation at higher frame rates of the P2M imager. Backside processing for soft X-ray detection is also under optimization for better reliability. Software for the integration of the detector in the synchrotron and FELs control system (TANGO and EPICS) will be finalized.

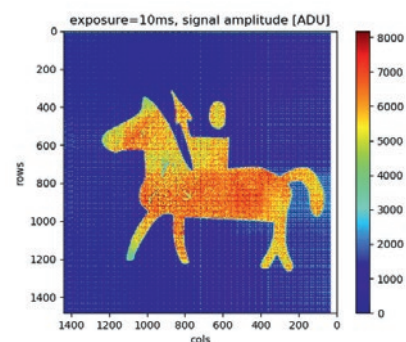


Figure 19: Image of a shadowgram recorded by the first operational P2M sensor



## REFERENCES

- [1] S. Spannagel et al., 'Allpix2: A modular simulation framework for silicon detectors', Nucl. Instr. Meth. A910 164-172 (2018).
- [2] M.R. Dimmock et al., 'Validation of a Geant4 model of the X-ray fluorescence microprobe at the Australian Synchrotron', J. Synchrotron. Rad. 22 354-365 (2015).
- [3] M. Bordessoule et al., 'Performance of spectroscopy detectors and associated electronics measured at SOLEIL synchrotron', AIP Conf. Proc. 2054 (2019) 060070, doi:10.1063/1.5084701.
- [4] E. Knudsen et al., 'McXtrace: a Monte Carlo software package for simulating X-ray optics, beamlines and experiments', Journal of Applied Crystallography, 46(3):679-696, (2013).
- [5] N. Tartoni et al., 'High channel density Germanium detector demonstrator for high throughput X-ray spectroscopy', IEEE NSC/MIC 1-3, (2017).
- [6] G. Dennis et al., 'First results using the new DLS Xspress4 digital pulse processor with monolithic segmented HPGe detectors on XAS beamlines', AIP Conf. Proc. 2054 060065 (2019).
- [7] T. Saleem et al., 'AllPix2 simulations of Pixelated Germanium Sensors for XAFS experiment at SOLEIL Synchrotron', presented at IEEE-NSS 2020 Conference and submitted for publication in 2020.
- [8] P. Grybos, et al., '32k Channel Readout IC for Single Photon Counting Pixel Detectors with 75  $\mu\text{m}$  Pitch, Dead Time of 85 ns, 9 e<sup>-</sup> rms Offset Spread and 2% rms Gain Spread', IEEE TNS 63.2: 1155-1161 (2016).
- [9] A. Dawiec, et al. 'Development of a new photon counting camera prototype for time resolved experiments at SOLEIL synchrotron', AIP Conference Proceedings. Vol. 2054. No. 1. (2019).
- [10] Bachiller et al. 'First pump-probe-probe hard X-ray diffraction experiments with a 2D hybrid pixel detector developed at the SOLEIL synchrotron', J. Synchrotron Radiation 27 (2020).
- [11] Z. Ren et al, 'Laue crystallography: coming of age', J. Synchrotron Radiation, vol 6, 891-917 (1999).
- [12] T. Cornelius et al, 'Progress of *in situ* synchrotron X-ray diffraction studies on the mechanical behavior of materials at small scales', Progress in Materials Science 94:384-434 (2018).
- [13] Harada 2020 et al., 'High-exposure-durability, high-quantum-efficiency (>90%) backside-illuminated soft-X-ray CMOS sensor', Applied Physics Express 13, 016502 (2020).
- [14] K. Desjardins et al., 'Characterization of a back-illuminated CMOS camera for soft X-ray coherent scattering', AIP Conference Proceedings 2054, 060066 (2019).
- [15] C.B. Wunderer et al, "The Percival 2-Megapixel monolithic active pixel imager," JINST 14 C01006 (2019).
- [16] B. Boitrelle et al., 'Software framework architecture for the high data rate soft X-rays PERCIVAL imager', Proc. 2018 Pisa Meeting, (2018).
- [17] A. Marras et al., 'Characterization of a back-illuminated CMOS camera for soft X-ray coherent scattering', AIP Conference Proceedings 2054, 060060 (2019).

## DATA REDUCTION AND ANALYSIS

### Introduction

In the following, we detail our vision to provide a coherent set of data treatment tools including remote services, automatic streaming for continuous processing and data quality assessment, modelling tools to help interpretation of acquired data, and enterprise-grade report generation items from data treatment steps to feed electronic log books.

The chosen software infrastructure will benefit from future deliverables from the LEAPS-IT, BIG-MAP, PaNOSC and ExPaNDS European projects. Our current rationale is to favour simple solutions in order to minimize the software maintenance and ensure a continuous service across EU project grants duration.

The building blocks will be gradually put into place before the Upgrade, opening up the opportunity to couple data, automatic data reduction and analysis, and model to Artificial Intelligence (AI) procedures for identifying hidden correlations and tendencies.

### Remote data treatment

The diffraction, tomography, ptychography and correlative imaging beamlines are amongst those producing massive data volumes. In addition, the data treatment requires heavy use of GPU with finely tuned software. It is estimated that such beamlines may produce over 10 TB/day at the time of the Upgrade, implying heavy duty computing resources. Hyperspectral analysis does not currently rely on GPU, but will most probably be improved in this respect in the years to come. Such data treatment requires specialised computing

resources (beyond the scope of a typical user laboratory) which must be made accessible, without moving data, to all users. Alternatively, a recurrent need on beam lines is to be able to mix data reduction and analysis, text, image and volume representations. We shall provide such a simple tool that can be shared among users. We shall provide a robust and scalable service (DAAA) to host scientific software used for synchrotron radiation data treatment. Our services will provide two distinct solutions gathering all required software running on powerful computers as well as easy access to the experimental data sets.

- The Remote Desktop<sup>[1]</sup> service allows distant users to login, specify the needs in computing power and data volume, and open a ready to use session with numerous pre-loaded software and libraries.
- The Notebook based solution provides a script-oriented data treatment service, which can advantageously mix commands, scientific text, images, volumes and simple user interfaces. Python-oriented software and libraries are pre-installed. Prepared template notebooks per experimental technique with associated documentation will be available, so that users can readily start processing their data.

Both services automatically attach a GPU for fast data reconstructions. No local installation is required on the user side, and currently data remains local at SOLEIL. The data treatment sessions can be shared between multiple users for collaborative data reduction and analysis. Users can also install their own software locally. Software will be tuned to handle SOLEIL experimental data sets, without duplicating data at the user side. Extensive documentation will be available, with tutorials and example data sets for every use case.

This service will gradually expand its software *portfolio* for data treatment, including segmentation, machine/deep learning classifiers, and super-resolution imaging.

Notebooks will be improved to include simple controls (e.g. sliders, menus, text boxes, plot and volume rendering) for better interactivity.

The services envisaged are all compatible with SOLEIL's future project in cloud based high performance computing and storage systems.

### Automatic data processing

In order to increase the scientific throughput of beam lines, fast and automatic data treatment procedures are required. As experiments are performed, an estimate of the quality of the acquired data in terms of scientific content is continuously assessed. In this way, it is possible to fine tune the acquisition strategy to optimise, for example, signal to noise ratio in the presence of radiation damage. In addition, data reduction processing may be made more efficient when applied as close as possible to the detection layer.

Simple scripts will be developed for experimental techniques to compute automatically a scientific quality metric, from raw experimental measurements. These scripts are to be executed after every acquisition sequence completion. They may also be shown as a web form for interactive use (Figure 20), and triggered as a web micro-service upon specified events. The development of these metrics imply close interaction with different user communities, such as that being put into place in the BIG-MAP H2020 project for applying artificial intelligence based optimisation to battery material fabrication and measured battery performance.

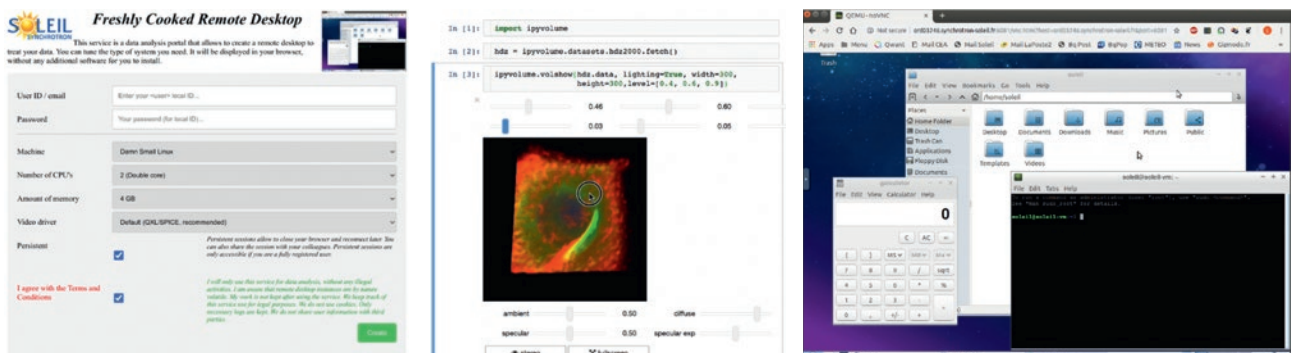
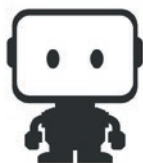


Figure 20: Screen shots of remote data treatment services, Jupyter Notebook and Remote Desktop.



Automatic scripts may also be triggered when experiment proposals are submitted to evaluate the feasibility of projects as well as beam time allocation estimate. Such feasibility assessments may involve material modelling (structure, electronic and vibrational dispersions...) running on high performance computing resources.



## DataRobot

### Material and beamline modelling

As part of data analysis, it is usual to compare measurements with computation results from a sample model. Material modelling is complex as it involves an extreme diversity of methods (*ab initio* and classical, coarse grain, bio-computing, chemical reactions, etc) and phases (liquid, solids, gases, compounds, surfaces, etc.). Materials are also involved in modelling sample environments.

Tools will be developed within our software suite to cover many of these needs.

In addition, integrated pipe-lines will gradually be set-up to assemble modelling tools in order to allow source-to-detector simulations, such as in the McXtrace<sup>[2]</sup> and SIMEX software.

Model parameters can further be optimised with *e.g.* genetic and swarm

algorithms in order to find the best configurations to provide *e.g.* highest signal to noise ratio, lowest radiation damage or cost. An approach to coupling modelling and experimental configuration has been developed, in the case of the I23 soft X-ray beamline at DIAMOND Light Source<sup>[3]</sup>. It is also possible, with the same underlying tools, to couple measurement and prediction to improve material optimisation.

### Traceability and data analytics

Most of the data acquired on synchrotron beamlines requires a high level of abstraction in order to be understood. A way to alleviate this complexity gap could be to seamlessly process the data as it comes in an “intelligent” way and report results in clear, concise yet precise reports. But in order to attract new users, including for instance from industry and medical research, the relevancy of such reports should be ensured with highest quality standards.

Every piece of information generated during all phases of an experiment – proposal submission, sample tracking, acquisition sequences, data treatment steps, storage – will be registered as events and made available into a global data lake, as described in the project PLUSS (PLatform for Urbanisation at Synchrotron SOLEIL, see Chapter 5). A set of micro-services (processing tasks) will then be triggered on events to execute automatic tasks and concatenate report entries with extensive metadata and

annotations. Data treatment operations will be recorded in order to provide traceability with automatic report generation. Additional records will include administrative, acquisition, reduction and analysis metadata information. Current ontology projects, such as planned as part of the BIG-MAP EU project, will help to categorise annotations into semantic groups for further data browser tools. The standardization of the e-logbook generation process will ensure a high level of traceability, and provide multi-modal analysis.

For this to come true, we shall rely on the IT infrastructure Upgrade plan (see Chapter 5, “Strategic topics”) involving major network and storage improvements together with optimized compression routines for different data types. In order to handle large data flows, processing methods will heavily make use of our computing resources (parallel processing, GPUs).

- Once data is standardized and certified, we can benefit from innovative data analytics and AI algorithms (*e.g.* machine learning, deep learning) for instance to assess the data quality, eliminate data with low or no information content, cross-correlate current results with similar past experiments, and obtain meta experiment results. In addition, the availability of coherent information streams allow an integration of the data generated at our beamlines within wider multi-modal analysis.

#### REFERENCES

- Wagner et al. “In vacuum long wavelength crystallography”. *Acta Crystallographica D* (2015) 72.
- Knudsen et al. “McXtrace: a Monte Carlo software package for simulating X-ray optics, beamlines and experiments”. *Journal of Applied Crystallography*, **46(3)**:679-696, 2013.
- Farhi, 2020, Remote Desktop <https://gitlab.com/soleil-data-treatment/soleil-software-projects/remote-desktop>

## SCENARIO FOR BEAMLINE IMPLEMENTATION

### Impact of new lattice on beamline implantation

The opportunities for beamline implantation, in relation to different storage ring lattices, were evaluated taking into account a number of criteria:

- Reaching a storage ring emittance of  $\sim 80$  pm.rad, hence increasing source brilliance.
- Keeping the diversity of the existing spectral range at SOLEIL, from far IR to soft and hard X-rays, via UV and VUV.
- Keeping, as far as possible, the existing infrastructure of the Synchrotron (tunnel and experimental hall dimensions).
- Keeping unchanged beam axes for critical lines (MARS, ANATOMIX, NANOSCOPIUM).
- Minimizing the displacement of radiation protection (RP) hutches or changes to equipment positions.
- Minimizing downtime for beamlines

The CDR reference lattice is the best compromise found which meets the above criteria. This lattice consists of 20 straight sections and 16 dipole extraction points, including a number of superbends and double superbends. The straight sections will be divided into 4 long sections, 8 medium sections and 8 short sections, with lengths significantly shortened from the current lattice.

Of the 20 straight sections, 18 will be available for beamlines and one is dedicated for injection, the other one will host the RF system. Of the 16 dipole extractions, 12 can be taken by beamlines, and 4 present extraction problems.

The dimensions and positions of the new sources in this lattice will lead to more or less significant changes to beamline alignment, depending on beamlines position around the storage ring.

The main changes, in terms of beamline implantation, between the CDR reference lattice and the existing SOLEIL lattice are:

- The geometry of the lattice results in 2 to 3 ID beamlines facing superbend sources (instead of an insertion) and hence which need to be relocated. Different scenarios are being considered and solutions are emerging. These solutions will lead to the displacement and complete reconstruction of 6 to 8 beamlines.
- Longitudinal displacements ( $\Delta s$ ) of source points, except for the 3 beamlines mentioned above, associated with lateral displacements ( $\Delta x$ , with different amplitudes depending on the proposed source) of beamlines.

In order to minimize these displacements for dipole beamlines, the solution chosen will be to use bicorns to adjust the beamlines axis as close as possible to the current axis.

Depending on the useful choice of source for each beamline, which will result from the selected scientific cases, we have identified 7 displacement classes. It should be noted that the larger displacements (classes 5 and 6) are associated with bending magnet or super bend beamlines, the lattice being optimised to minimize the impact for ID extraction.

- Class 1: very weak lateral displacements or at an angle ( $< 1^\circ$ ).  
o  $\Delta x \sim 2$  mm and  $\Delta s = 0$  will be for example the case for long beamlines enabling to avoid heavy reconstruction in the satellite building dedicated to these beamlines. Also, the MARS hot beamline will move less than  $0.6^\circ$  using a bicorn, which will allow only the first optics to be moved to coincide with the existing beamline axis at the experimental stations, retaining the specific infrastructure for radioactive samples.
- Class 2: lateral displacements ( $\Delta x \sim \pm 40$  mm), for which the optical supports inside the chambers can be moved.
- Class 3: lateral displacements ( $\Delta x \sim \pm 80$  mm) which will require support displacement of the optical chambers and partly of the experimental stations, but that remains possible in the space of the existing hutches.

- Class 4: lateral displacements ( $\Delta x \sim \pm 110$  mm) for which, reversal of the chicane of the first M1 mirrors is required, to coincide with the axis of the current beamline.
- Class 5: lateral displacements ( $\Delta x \sim \pm 285$  mm) requiring greater displacement of optical chambers and experimental stations but remaining compatible in the space of existing hutches.
- Class 6: lateral displacements ( $\Delta x \sim 609$  mm) for few beamlines on a superbend symmetrical axis of the lattice.  
More substantial modifications will have to be made with larger displacement of the optical chambers and experimental stations, but remaining possible with the existing hutches of the few beamlines concerned.
- Class 7: total beamline shift to a new location, concerning as previously mentioned about 6 to 8 beamlines.

In summary, the V0313 lattice can accommodate the 29 existing beamlines, with more or less significant modifications to their equipment according to the scientific needs and experimental techniques chosen, plus 3 new beamlines on dipole or superbend. Additional flexibility is offered by the potential for a soft X-ray and a hard X-ray beamline to share a second long straight section.

### Phasing of beamline (re)construction

The displacements previously indicated, associated with the new sources and characteristics of the new storage ring, will in many cases require modification of the beamline optics, and increased management of the thermal load and optics and experimental end-stations stability (see Optics part). Design studies for these modifications will start in the TDR phase, and be divided into 3 steps as shown in the master planning.

In the first step, we envisage the complete study, realization and reconstruction of 7 beamlines, so that they will be ready to start commissioning at the restart of the accelerators.



To do this, 6 of them will have to be stopped approximately 1 year before the shutdown of the accelerators, to be uninstalled prior to changing their location.

In the second step, we plan studies of optical modifications to 11 beamlines to adapt them to the parameters of the new storage ring, followed by optics fabrication, and installation of modified and/or displaced equipment. These beamlines could restart relatively quickly after the machine upgrade, in relation to the changes to be made.

In the third and final step, studies, fabrication and installation of 11 additional beamlines with more substantial modifications will follow, as well as improvements to the experimental stations of the beamlines that have previously started.

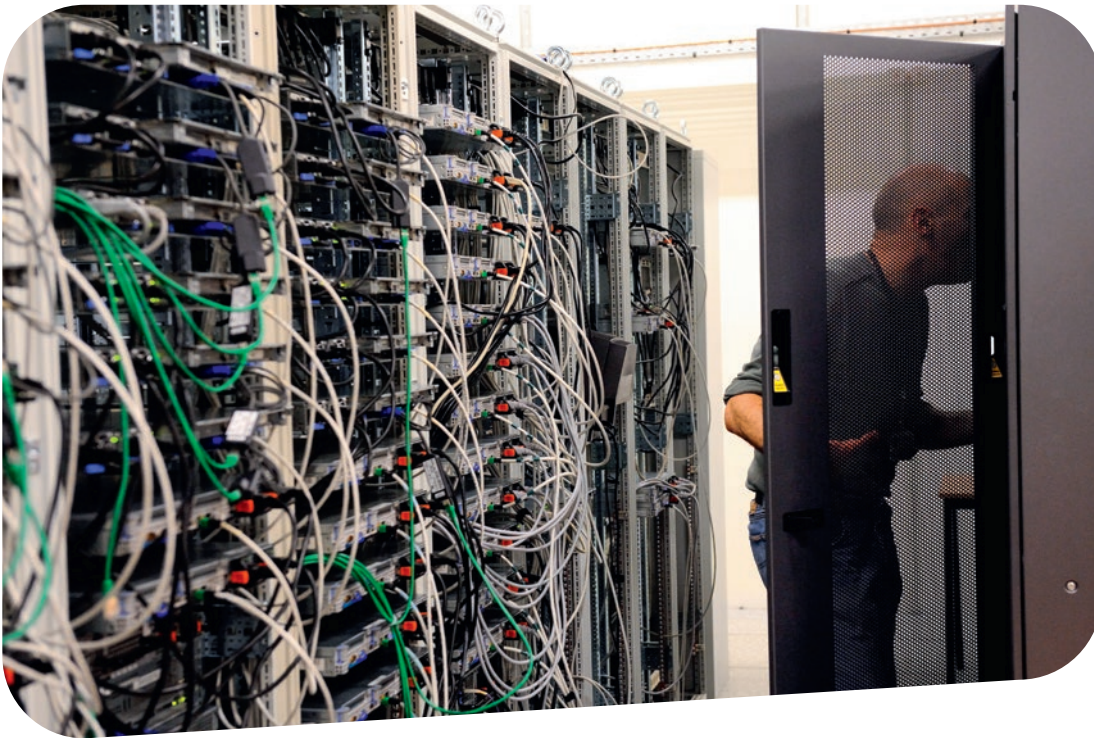
The lattice leaves space for the construction of up to 3 new beamlines, giving the possibility for future modifications to SOLEIL's 29 beamline portfolio. Their installation could be in step 1, 2 or 3.

The sequence envisaged in these steps is to install or modify first, the 7 beamlines in step 1, then 2 beamlines every 2 months later in step 2, and so on in step 3.

The time between installations may be longer in step 3 when the storage ring and a first beamline series will be in operation (between 2 and 6 months). However, the operating criteria of the accelerators and the beamlines (stability, current, operating time) will have to be adapted to facilitate the sequence of the beamline installation following the phasing indicated to remain for a reasonable upgrade time.



## 5 - Information System and Data



## INTRODUCTION

The attractiveness of a synchrotron radiation facility mainly relies on the services it delivers to its users. This includes the delivery of a photon beam with the expected characteristics from the accelerators, the production of high-quality experimental data on the beamlines and, finally, the extraction of knowledge from this data thanks to the provided data processing services. For SOLEIL, it is consequently crucial to ensure long-term competitiveness by aligning its technical and scientific offer with the future of synchrotron-based science. For the computing and controls teams, the SOLEIL upgrade can be seen as a **global enhancement of the user experience** in which the Information System<sup>1</sup> (IS), from the underlying control systems to high-level services, plays a strategic role.

Computer (or Digital) science will strongly contribute to fully exploit the potential of the new accelerators and beamlines and will act as the numerical foundations of the SOLEIL activity. Some strategic services, such as data processing (with algorithms coming from scientific expertise), will purely rely on computer science and information technologies. Computing is definitely a strategic component of the SOLEIL upgrade.

This chapter details the **Information Technologies (IT)** and **computer science** strategy defined by the SOLEIL teams to face the scientific and technical challenges of the next decades.

---

<sup>1</sup> The information system (IS) is an integrated set of hardware and software components covering all aspects of SOLEIL's activity: equipments controls, data collection, storage, and processing, information sharing, knowledge extraction, ... Organizations rely on information systems to carry out and manage their operations. In the present document, the terms information system (IS), information technologies (IT) and computing are considered synonyms and interchangeably used.

## Fundamentals of the Information System Strategy

### Leveraging the past

Contrary to the initial SOLEIL project, the Upgrade is not a blank page. Existing systems and technical culture must be considered when defining our information system strategy. Moreover, the continuity of operation during the first phases of the Upgrade project imposes an incremental innovation approach in order to smoothen the transition towards the targeted architecture.

SOLEIL benefits from 15 years of beam delivery to users and has acquired a solid expertise in computer science for synchrotron radiation experiments. Among the technologies currently deployed on both the accelerators and the beamlines, some have proven their ability to evolve and to fit in large scale enterprise architectures. Tango<sup>2</sup>, the SOLEIL control system framework – on which the controls of accelerators and all beamlines are currently based –, is one of the most representative of these technologies, whose evolution is continuously guided by the scientific and technical requirements. Such technologies are the foundations of the SOLEIL technical culture. They will continue to play a major role in the future as components of a global architecture operating at facility scale.

### Enterprise architecture and continuous transformation

Designing an Information System (IS) targeting the requirements of the synchrotron-based science for the next decades is a real challenge. In order to address this long-term adequacy of the IS with the technical and scientific needs, the chosen approach is to adopt a **continuous transformation** strategy. Instead of designing a system based on anticipated – and potentially over-dimensioned (or even undersized) – specifications, the idea is to implement an IS relying on a modular architecture whose hardware and/or software

components can be easily replaced to leverage technological opportunities in response to new needs and maintain the IS at the state of the art. Technically speaking, the idea is to generalize an **enterprise architecture** with native support of this continuous transformation paradigm.

Beyond the agility it provides in terms of continuous evolution of the information system, an enterprise architecture allows the support of SOLEIL activity as a whole and ensures an IS coherence at facility scale. At SOLEIL, the idea is to generalize this approach by enhancing communications and data exchanges at domains' boundaries. Most organizations – based on a vertical structure – tend to rely on an IS made of strongly isolated “functional silos” that tends to oppose the needs of transversal exchanges across domains, processes and teams. The adoption of an enterprise architecture aims at eliminating these cross-domain barriers and opens the system to feature-rich on- and off-premise services.

### Digital transformation and cloud integration

The IS strategy for the SOLEIL upgrade is also centered around a **digital transformation**<sup>3</sup> of the facility. In this approach, any valuable information, data or metadata<sup>4</sup>, is fully digitized in order to be appropriately stored, exposed and retrieved by smart processes creating technical, scientific or organizational added value. The digital transformation also aims at preparing the SOLEIL information systems to be integrated into large scale cloud infrastructures - such as the ones emerging from projects as European ones<sup>5,6</sup>, or from e-Infrastructures as national ones<sup>7,8</sup>.

For Users, beyond the new accelerators and beamlines capabilities, the added value of the SOLEIL upgrade will mainly rely on the quality of the experimental data and the provided data processing services. The latter tend to evolve towards complex cloud services mixing advanced algorithms, massive storage infrastructures, high-performance computing resources (HPC)

and modern information technologies (such as managed APIs<sup>9</sup>). SOLEIL will not be able to host and maintain the infrastructures that this will require – that's why a **cloud ready enterprise architecture** is mandatory in order to provide computing services at the expected level.

### Artificial intelligence for controls and maintenance

It is an established fact that **Artificial Intelligence** (AI) is playing an increasing role in experimental data processing. There is a very dynamic R&D activity to produce AI based algorithms and models to enhance knowledge extraction from scientific data. SOLEIL will directly benefit from these tools by integrating them into its data processing offer (see Data Reduction and Analysis in Chapter 4 – beamlines Instrumentation).

However, the application of AI to controls remains an emerging topic. In terms of controls, a 4<sup>th</sup> generation synchrotron generates new constraints. On some systems, the tuning range becomes narrower and optimum parameters are harder to determine. Fine-grained and close control of the beam characteristics – on both accelerators and beamlines side – will consequently require advanced computing technique - such as **Machine Learning** (ML) – to reach the ultimate performances. In a general manner, we expect AI technologies to play an increasing role in control systems. The same applies to the maintenance of the infrastructures where predictive tools will help enhance the availability of our systems. Our IS design must take into account the needs to collect massive data to continuously train ML models.

<sup>2</sup> Tango (<https://www.tango-controls.org>), a control system framework project initiated in 1999 at the ESRF and adopted by SOLEIL since 2002, now involves 11 large European facilities and continues to evolve with science needs and requirements.

<sup>3</sup> Digital Transformation is the adoption of digital technology to transform services, through replacing non-digital or manual processes with digital processes or replacing older digital technology with newer digital technology.

<sup>4</sup> Metadata aims at defining or describing another data. It generally helps manipulate, transform and interpret the data it refers to.

<sup>5</sup> PaNOSC (<https://panosc.eu>): The Photon and Neutron Open Science Cloud, a European project for making FAIR data a reality in 6 European Research Infrastructures (RIs), developing and providing services for scientific data and connecting these to the European Open Science Cloud (EOSC).

<sup>6</sup> ExPaNDS (<https://expands.eu>): the EOSC Photon and Neutron Data Service, a collaboration between 10 national Photon and Neutron RIs in partnership with the EGI e-Infrastructure to deliver standardized, interoperable and integrated data sources and data analysis services for Photon and Neutron facilities.

<sup>7</sup> GENCI, (<https://www.genci.fr/en>): national organization in charge of making available high-performance computing and processing data resources operated in 3 French computing centers (TGCC, IDRIS<sup>20</sup>, CINES).

<sup>8</sup> CC-IN2P3 (<https://cc.in2p3.fr/en/>): a CNRS (French National Centre for Scientific Research) computing center specialized in massive storage system and high-speed computing.

<sup>9</sup> An API or Application Programming Interface is a computing interface which defines interactions between multiple software intermediaries.



## REQUIREMENTS OF THE INFORMATION SYSTEM USERS

The requirements of IS users – collected during dedicated internal workshops in which a representative of SOLEIL Users Organization also attended – have been analyzed and organized into 6 functional themes. The present paragraph details each of them.

Following the internal workshops, in-depth work is underway to detail the requirements of IS users according to the 6 functional themes. The first detailed tables have just been produced, which will be very useful for the next steps.

Here, the idea is not to report specific needs or fine-grained details. We focus on fundamental requirements and topics that guide the SOLEIL upgrade in terms of IS infrastructure and computing resources from a functional and organizational point of view.

### Multibeamline and multitechnical experimental projects

As emphasized in Chapter 2 - Science Case, scientific investigations will increasingly rely on the combination of different experimental techniques (using different workflows, visualization methods, data analysis algorithms, etc.). Seen by the computing and controls teams, this concept of “multibeamline and multitechnical experimental projects” means a global enhancement of the services related to the management and traceability of users’ projects. It should cover the associated processes in an end-to-end manner - *i.e.* from the project proposal to the end of the data embargo period (as defined by the SOLEIL data policy).

Tools already exist at SOLEIL to address these topics, but they need to be extended in order to satisfy the **FAIR**<sup>10</sup> data paradigm (as defined by the **Open Science**<sup>11</sup> initiative) and to offer new advanced services to our users.

Functionally speaking, the main requirement is to generalize the **identification and traceability information of the samples** on which data acquisition are performed during the experimental sessions. The idea

would be using a Digital Object Identifier (DOI) that uniquely identify the sample in the associated lifecycle tools. The aim is to maintain detailed information at any stage of the sample lifecycle – *e.g.* characteristics, preparation, photon beam time exposure, storage, as required in Chapter 4 - beamlines Instrumentation (see Instrumentation and Method).

Beyond the sample lifecycle, the ambition is to enhance the overall level of traceability of an experimental project performed at the synchrotron. Such an experimental project can actually be seen as a sequential process made of events carrying information that can be summarized as follows: proposal → peers review → experimental sessions → data processing. These events (or facts) describe the lifecycle of the project. Both the adoption of an enterprise architecture and a digital transformation will allow to emit and dispatch these events in the information system in order to feed new services at facility scale:

- multi-view on the project information (users, sessions, samples, data<sup>12</sup>, processing),
- metrics of the SOLEIL activity (business intelligence applied to a synchrotron facility),
- smart link between technical facts (*e.g.* from accelerators) and data acquisition processes,
- storage or computing resources usage management.

The ultimate implementation of the “multibeamline and multitechnical experimental projects” feature would also provide users with tools allowing post-experiment comparison of results from different experimental techniques, or even data visualization and comparison in real time during the experiment.

### Simulation, prototyping, testing

Concerning the prototyping and testing aspects of the requirements, we need working environments in parallel to production systems in order to develop, integrate or validate new components (or component modifications) of the control systems. The aim is to increase our agility in the evolution of our systems and to provide autonomy to the SOLEIL teams.

**Agility and autonomy are the key words of the expressed requirements.**

Simulation is a real concern in the context of the SOLEIL upgrade. This is particularly true on the accelerators side where a simulator is required in order to prepare the accelerator commissioning. Such a simulator, made of an Accelerator model with a control system layer on top of it, can also act as a **digital twin** when bridged to the real world. This pairing of the virtual and physical worlds allows analysis of data and monitoring of systems to identify problems before they even occur, prevent downtime, develop new opportunities and even plan for the future by using simulations. When the digital twin is coupled to an AI-based **predictive maintenance** solution, it helps better control the life cycle of the systems and their availability.

On Beamline, simulations can also contribute to enhance development processes. Simulation is in fact already in use in SOLEIL’s robotics applications. A virtual environment – simulating the physical context – provides engineers with a way to develop the application in parallel with beamline activity (*i.e.* without requiring access to the beamlines). This drastically reduces time to production and enhance reactivity to new needs.

Our ambition is to increase the contribution of the simulation tools in the development phase of the systems in order to limit access to the physical infrastructure to actual validation tests.

### Processes and Data

This functional theme gathers the requirements associated with data production and data treatment processes. It also includes the ones related to data routing, data access and data storage infrastructure.

From a computing point of view, data management, data engineering and data processing are at the heart of the SOLEIL upgrade. In this vision, smart processes – based on the concepts of automation, sequencing and decision-making – consume the data to enhance users experience<sup>13</sup>. The increasing complexity of the systems must be hidden behind high-level and user-friendly interfaces. This is particularly critical for a synchrotron

<sup>10</sup> F(indable) A(ccessible) I(nteroperable) R(eusable) data as defined by the Open Science initiative.

<sup>11</sup> <https://ec.europa.eu/research/openscience/index.cfm>

<sup>12</sup> the concept of data catalog emerging from European projects should allow Users to search for data in a flexible and agile way thanks to well-defined metadata.

<sup>13</sup> User experience: user’s feeling and perception of a system (*e.g.* utility, efficiency, ease of use, stability).

facility with Users who are supposed to drive the experiments on their own. The idea would be to move towards a “beamline as a service” approach in which the user is assisted by decision-making tools. Artificial intelligence technologies will play a major role in the area.

This concept – which could be part of a wider concept of **computer-assisted experiment** – can be illustrated by smart feedbacks. Connecting the data processing services to the data acquisition platforms will allow to implement tools providing a way to validate the experimental context or even to reorient the user in his/her experimental session. Immediate online data processing (or preprocessing to qualify the experiment/data) would be a first step towards a smart beamline model and computer-assisted experiment.

From a more technical point of view, users express an expectation for a fast and reliable network and storage infrastructure. They identify the performance of the network and the storage solutions as the most critical and impacting components in terms of “user experience”. The extremely brilliant beams associated with high performance detectors will generate a data deluge that we will have to face (see Detectors in Chapter 4 – beamlines Instrumentation). Only based on beamlines scientists’ projection for the next years and regardless of the SOLEIL upgrade, we expect that the raw data production will be more than 6 petabytes per year (due to pixel detectors installations, use of the flyScan data acquisition techniques, ...). The Upgrade will lead to an even bigger explosion of data production.

## Optimizing accelerators and beamlines operation

This topic concentrates the requirements related to operational optimization. It mainly focuses on beam production, its usage on beamlines and its availability.

Artificial intelligence is frequently identified as a potential solution to complex problems. Here, it would be applied to the optimization of the operation parameters. Some recent publications tend to prove that machine learning – and more particularly, deep learning – techniques can significantly enhance the control of beam characteristics depending on a very large number of parameters (*i.e.* high dimensional problems)<sup>[1][2]</sup>. AI based solution is definitely the future of

accelerators and beamlines controls.

The tuning phases of the systems are described as time-consuming tasks. This is particularly true in transitions between operations modes. On beamlines, switching from one experimental setup to another – typically to welcome the next User – remains a time-consuming task. Such tasks could be assisted by automation in order to increase the effective beamtime (*i.e.* ratio between the allocated beam time and the actual data collection time).

Operational safety is also a major concern, including the automatic detection of incidents and corrective – or even predictive – measures to be taken. As raised above, **predictive maintenance** should help us optimize the availability of the infrastructures and ensure the expected safety level. Solutions emerging from the digital industry initiatives will help manage the lifecycle of our installations. The expected benefit is an improved availability of the systems and, consequently, a better quality of service to the users.

Finally, beyond the recovery mechanisms and procedures already in place for IS infrastructure and services, an IS business continuity plan will help ensure the operation of the accelerators and/or the beamlines in the event of a major disaster.

## Systems openness

Systems openness is a strong request from both the accelerators staff and the beamlines scientists. Here openness is related to **autonomy** and **flexibility**.

In our context, the notion of autonomy is linked to the idea of reducing the dependency level of the users with respect to the support groups – *i.e.* providing technical expertise for operation. Whatever is the user profile, autonomy is identified as a critical organizational need. For the computing team, it could be a key element of the targeted agility at upper (or users) levels of the information system (*e.g.* scripting, sequencing, GUI).

The flexibility extends the notion of autonomy to the ability to integrate hardware and software components into test and production environments. In this domain, the dependence on support teams remains very high. According to accelerators physicists and beamlines scientists, reducing this dependency could increase their productivity.

This is a challenging topic as systems openness must not compromise their security.

## Communication

Communication (and related tools) is a recurrent theme of the expressed requirements. It concerns internal as well as external exchanges and applies to any stage of the SOLEIL activity.

Today, some phases of the scientific projects – notably the feasibility and preparation ones -are not well covered by the communications tools we provide. Scientists expect an improvement of our offer on these topics. Requests for both advanced conversational and collaborative (*i.e.* virtual board) tools have been identified and intensified with the current Covid-19 pandemic. There is also a particular request for a **digital lab book** that fits with our digital transformation strategy.

Finally, it seems necessary to enhance our offer in terms of documentation, tutorials and knowledge base – in terms of both content and accessibility. This acts as a prerequisite for both user autonomy and smart beamlines – two notions we raised in the previous paragraphs.

## STRATEGIC TOPICS

Replying individually to every single requirement would lead to resources waste and potential technical silos. In order to ensure IS coherence at facility scale and mutualize our hardware and software solutions, we choose to adopt a transversal approach by identifying the **strategic topics** shared by users’ requirements. This methodology also aims to converge towards the **enterprise architecture** presented above in this Chapter (See Fundamentals of the Information System Strategy, page 147). In our approach, a strategic topic covers several requirements. The more a strategic topic covers the listed requirements, the better we mutualize the related design and development efforts. Strategic topics aim to share the technical fundamentals of our solutions at facility scale.

What follows give the details of the IS strategic topics identified for the SOLEIL upgrade. Without being exhaustive, some actions on going or to be carried out are indicated.

## Traceability

The notion of traceability emerges from many requirements: logistic of technical assets, life cycle of scientific instruments and experiment samples, data obtained



by users, ... It can be related to memory, history, traces or context. Traceability mainly relies on metadata produced by software and hardware at any point of the information system, including information enabling unambiguous identification of the component concerned (which technical asset, instrument, sample, user data, etc.). Metadata aims at enhancing accelerators and beamlines data processing and knowledge extraction from raw data.

For both internal and external needs, it appears necessary to maintain fine-grained information over a long-term period. More concretely, the aim is to produce, store and consume contextual information and metadata at any stage of the activity of SOLEIL. This contextual information is crucial to fully exploit the infrastructure and provide advanced services.

Traceability has a high potential in terms of use cases. The support of “multibeamline and multitechnical experimental projects” – as described above in this Chapter (see Multibeamline and multitechnical experimental projects, page 148) – will essentially rely on the metadata stored into repositories dedicated to traceability. On the accelerators side, the idea is to trace any technical fact (or event) that could impact the quality of the data acquired on beamlines. The IoT (Internet of Things) technologies will also contribute to traceability by producing contextual data from sensors placed on hardware systems. Generally speaking, a transversal traceability tool would allow to store any event of interest at facility scale in order to use it as contextual information in processes related to data processing, diagnostics or activity metrics. The foreseen services will provide a way to correlate the information (data, event or facts) at facility scale. The PLUS project – presented below in this Chapter (see Support for transversal activities, page 151) – provides the technical foundations of such a global traceability tool.

A traceability tool deployed at facility scale aims at consolidating and mutualizing information – *i.e.* contextual data and metadata – produced at any point of the information system into dedicated databases which content is exposed as dedicated micro-services to clients. Each micro-service (a.k.a. API) provides a specific view of the data for a specific need. Databases can still be accessed directly for more generic requirements. This schema will provide SOLEIL with a way to rationalize contextual data and metadata related to its activity in order to share them at facility scale. When attached to an event driven bus, such

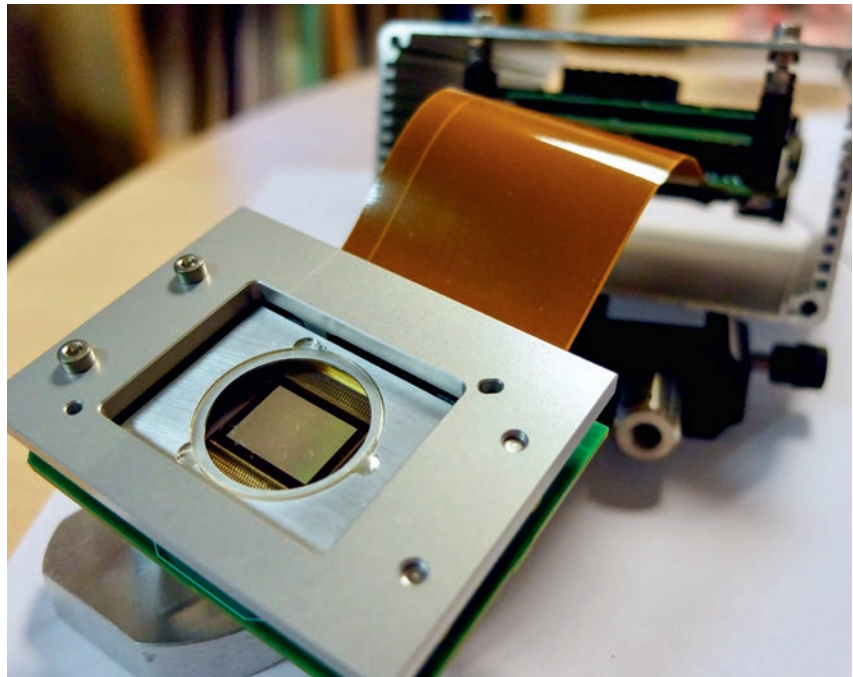


Figure 1: Use of MEMS for the development of Structured Illumination Microscopy at the DISCO Beamline.

data can also trigger processes acting as the clockwork cogs of the SOLEIL activity.

#### → Ongoing projects on Traceability

##### • IoT contribution

Emerging technologies coming from the IoT world are under investigation. It is expected that devices based on MEMS (*MicroElectroMechanical Systems*) will offer exciting opportunities in the near future: they are small, rugged, and lend themselves to the inclusion of additional circuit blocks in the same package for wired or wireless connectivity<sup>[3]</sup>. Wireless MEMS-based sensors, such as accelerometers or strain gauges, could be integrated in the mechatronic design – and perhaps bio-MEMS in the instrumental setup – to deliver data through an IoT Platform (see Smart Processes and Systems, below) and/or the transversal traceability tool. This will be very important, early in the upgrade, to track and optimize the multichannel logistic traffic of the new equipment for accelerators and beamlines, in order to save time. Later, the data delivered by these systems – *e.g.*, deformation or vibration measurements, radiation information – will feed numbers of services such as predictive maintenance (see Smart Processes and Systems, below), inventory databases, experimental metadata. Note that MEMS are already in use at SOLEIL – notably for the development of Structured Illumination Microscopy at the DISCO beamline, see Figure 1.

##### • Control Systems contribution

Keeping memory of data issued from accelerators and beamlines control systems, the archiving system is also an important element of traceability. It allows long-term monitoring of technical subsystems, statistics, parameters correlation or comparison of operating setups over time. Our current system must be upgraded to scale up with the sharply increasing volume of these data, to be able to archive at a high level of sampling, to improve and enrich functionalities (event-driven archiving, easier archived data access, visualization, comparison). SOLEIL will benefit of the active efforts of the TANGO community and continue to contribute to its development.

## Smart processes and systems

From the computing perspective, the idea of making processes and systems more intelligent is at the heart of the SOLEIL upgrade. For accelerators physicists and beamlines scientists the concept of “smart processes” is predominantly associated with artificial intelligence and applies to automation, decision-making, complex feedbacks and data processing. Machine learning – and deep learning, its neural declination – are already widely used for data processing. Their application to (accelerator) control is one of the most active part of the associated research and development activity.

AI is also recognized as the “de facto” solution for infrastructure maintenance. AI based predictive maintenance will definitely play a major role in the management of infrastructures lifecycle and will help enhance their availability for users.

On the hardware side, robotics is a potential source of improvement in assistance to users that could contribute to offering smarter systems. By reducing the human factor, robotics provides a way to increase systems reliability and beam time optimization. The increasing needs of “remote access” to systems – and particularly to beamlines (see Agility and flexibility, page 152) – will also guide us towards robotics deployment. AI and robotics are identified as critical topics in which SOLEIL is investing for its future.

#### → Ongoing projects towards Smart Systems

##### • Robotics contribution

Developing smart infrastructure to optimize daily beam time and simplify daily scientific life in a secure way is

already one of our main objectives. This is under development for smart mechatronic devices and more specific with first integrations of robots (from STAÜBLI, a range of which has been standardized) [4].

A first robot is in production, automating sample pick and positioning for powder diffraction experiments, see Figure 2. A second one, carrying a detector, is being integrated: here, the challenge consists in the precision and stability of the positioning which must not drift by more than 10 µm over 48 hours. A development platform is already available and allows to validate the robot integration into the control system.

Building on this first experience and on feedback from the use of robotics at other facilities and industry, an inventory of Upgrade needs is in progress: the approach targets the Upgrade construction phase with automation capabilities for disassembling, assembling, measuring, and sorting equipment, and the Upgrade operation phase with Accelerator safety inspection

and Beamline experiments automation (sample pick and positioning, smart instrument manipulating 2D Detectors).

##### • IoT and digital twin contribution

IoT and digital twin technologies can offer multi-level improvement for simulation, optimization or lifecycle management of a system.

In the early stages of a system, their use in a test bench allow the validation of information, communication and sensor technologies integration into a virtual environment, as the above platform used to validate the integration of a robot. Later, we would like to investigate connecting digital twins with the platform to improve optimization models, thanks to injection of real data in the model. At last, during the operation phase, a model-based system could allow smart monitoring and life cycle management, benefiting to teams operating the system as to those using it.

The introduction of robotics, AI and autonomous behavior in complex, safety- and time-critical systems will go along with beam improvement, faster multi-technique experiments and the upcoming data deluge.



Figure 2: Robotics for powder diffraction experiments

## Support for transversal activities

Advanced services require transversal exchange at facility scale. As mentioned in the previous paragraphs, the scientific and technical ambitions of SOLEIL must be supported by a digital model of its activity. The latter will take the form of a generalized enterprise architecture providing our facility with a way to consider its activity in an “end-to-end” manner.

Technically speaking, the idea is to break through the isolated silos on which the information system relies. The foreseen solution is to adopt an architecture made of micro-services producing and consuming data for both internal and external needs. Such an approach enhances the overall maintainability and scalability of the information system and provides a concrete implementation of the continuous transformation paradigm.

#### → PLUSS project

The PLUSS project – recently initiated at SOLEIL – aims at validating the concepts related to producing and using data at the facility scale. The underlying ecosystem – illustrated in Figure 3 – provides the



3 technical layers on which our global enterprise architecture could rely:

- a scalable, reliable and event-driven data bus (or broker) deployed at facility scale (Kafka),
- a document-oriented database acting as shared data repositories (mongoDB),
- a features-rich API manager of data retrieval through micro-services (WSO2 API manager).

At the lowest level of the architecture, the events broker allows to produce and consume data from any point of the information system. By decoupling producers and consumers – *i.e.* producers and consumers don't know each other – the broker contributes to improving both agility and flexibility. It consequently also provides support for the continuous transformation presented above in this Chapter (see Fundamentals of the Information System Strategy, page 147). The document-oriented database allows to efficiently store and retrieve information carried by events. At the upper level, micro-services (*i.e.* APIs) offer different views of the information stored into the database to other micro-services and client applications.

The proposed approach applies to support groups (or sub-systems) boundaries. It defines how technical silos exchange and retrieve information without requiring them to change their underlying technologies. This has a very positive impact on the organizational aspects of the facility by developing a common “digital culture”.

## Agility and flexibility

Agility and flexibility are key elements of both daily operation and evolution of the systems. They act as the foundation for our continuous transformation strategy. The standardization of the computing systems must be rethought in order to reduce the strength of dependency between systems components, and to increase our level of flexibility. Here, the ambition is to improve our ability to upgrade systems components to leverage technical opportunities without destabilizing the global activity.

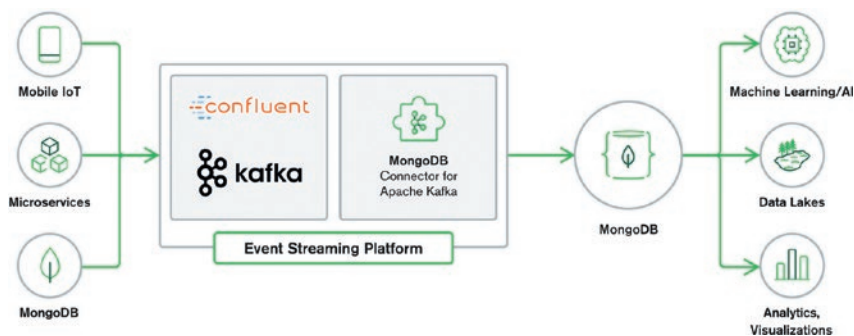


Figure 3: PLUSS platform architecture

Technical solutions exist to achieve our goal. Among them, virtualization<sup>14</sup> and containerization<sup>15</sup> techniques are certainly the most promising ones. On the hardware side, the *modularity-by-design* approach will also contribute to the expected flexibility. Finally, *DevOps*<sup>16</sup> technical and organizational tools will help keep software maintenance and deployment under control.

Agility and flexibility are permanent quests in systems design and deployment. These concepts are associated with systems maintainability – the most critical aspect of their life cycle. Both organizational and technical solutions have been provided to ensure long-term maintainability. Virtualization and containerization constitute the state of the art in terms of deployment and “on-demand” instantiation of the information system components (*i.e.* services). They contribute to agility and flexibility by running the services they host into isolated contexts. The main advantage of such an approach is to provide the ability to transparently change or inject new individual components without disrupting the global architecture. On-demand cloud services heavily rely on both virtualization and containerization.

Virtualization techniques are already widely used at SOLEIL. We are investigating containerization solutions for the deployment of data analysis services.

At IS users' level, it is essential to provide tools offering the expected flexibility to improve daily activity – whether for the operation of the facility, to carry out an experiment or to analyze data. Remote access services are typically such tools (beyond the fact that they are particularly useful in pandemic situations to ensure business continuity).

Remote Access is already fully available at two beamlines. It is being extended to many beamlines – not all of them being compatible with this operating mode – with four objectives:

- To allow SOLEIL Users and teams to operate SOLEIL beamlines and instruments from outside. We want to make it possible to perform a remote experience so that it is as close as possible to the experience performed in person on the Beamline,
- To allow users access to computing resources outside SOLEIL, as for data preprocessing,
- To provide a shared and secure experience notebook to facilitate the performance of experiments, commissioning and collaborative work between people on and off the site,
- To make it as simple and efficient as possible for users to transfer their experimental data to their laboratories, without forgetting that remote access will contribute to reducing the environmental footprint, as it limits travels for Users and allows staff to intervene remotely.

As a first step, a temporary solution allowing the continuity of the beamlines operation during the pandemic period has been deployed. This has been “application-driven” in close collaboration with the Experimental Division. In a second step, based on exchanges with other facilities and feedback from beamlines, solutions that meet the above objectives have been identified and are being implemented. The integration of robots will also extend remote access as it will facilitate the successive and automatic data acquisition of several samples for the same experimental project.

<sup>14</sup> Virtualization partitions a single physical computer or server into several virtual machines (VM), each VM running different operating systems or applications while sharing the resources of a single computer. It increases scalability and resiliency, reduces costs, carbon footprint, and downtime.

<sup>15</sup> Containers are smaller entities than VMs. They provide a way to execute an application (or a service) into an isolated environment on a traditional operating system on a traditional server or in a virtualized environment. It consequently becomes easier to replace this service without perturbing the global activity of the IS.

<sup>16</sup> DevOps involves a holistic strategy that includes people, processes and technology which aim is to ensure operation continuity while continuously updating systems (*e.g.* to fix bugs or inject new features).

In a longer term, coupling such services to a notification system would make it possible to intervene only when necessary rather than polling the progress of the experiment, the state of beamlines and instruments, ... further improving flexibility.

## Refactoring and modernization

Despite regular component upgrades, some systems have reached a legacy status – notably in terms of performances with respect to the scientific and technical needs. Such systems require to be redesigned and rescaled to face the upcoming challenges.

Efforts have already been initiated in some areas, such as the evolution of electronic systems<sup>17</sup> for which a multi-year roadmap is being carried out: electronic motorization systems have been redesigned with more advanced features, electronic fast control and data acquisition systems are in a redesign phase paying special attention to their modularity.

As raised above in this Chapter (see Leveraging the past, page 147), we are wholly satisfied with TANGO – our technology for both accelerators and beamlines controls. TANGO is a major component of our solutions and is a fundamental part of our local technical culture. Concerning the controls basics – *i.e.* the integration of small or large pieces of equipment through TANGO devices – SOLEIL benefits from its +18 years of expertise. There is consequently no plan to call the historical choice of TANGO into question. However, computing and controls teams are aware that they will have to face a peak workload to adapt components<sup>18</sup> to new accelerators and beamlines and to integrate new equipment. To cope with this is more a matter of human resources than technical challenges. From the computing and controls teams' point of view, the main technical challenges are centered on our ability to inject new technologies – such as AI and massive data processing – into the IS in order to fully exploit the new accelerators and beamlines.

On the client software side, the graphical user interface (GUI) strategy requires a thorough rethink to fit with the real-time data visualization needs expressed by Beamline scientists. The quest for new GUI tools also applies to the supervision of control systems, particularly on the accelerators side. This choice of tools must be guided by scalability (*i.e.* the ability to develop small as well as large applications), performances (*i.e.* the ability to deal with large control systems) and Users autonomy (*i.e.* the ability for Users to develop their own GUI applications).

The network and the (mutualized) storage infrastructure of SOLEIL are also identified as critical systems requiring to be upgraded. On beamlines, users identified both systems as a limitation in their scientific productivity that degrades the “user experience”. Besides, it is clear that a fast network will be a major component in the IS transformation: for accelerators and beamlines controls in particular because of the use of IoT technology (see Traceability, page 149), for Information System hybridization (see below in this paragraph), ... It appears that the performance and reliability of the network, storage and computing infrastructure are critical parts of the SOLEIL upgrade.

An iterative network<sup>19</sup> upgrade has been initiated. It mainly targets the enhancement of the overall performances in terms of data throughput and SOLEIL connectivity with external infrastructures. After the upgrade of our link to the Internet backbone, the internal network infrastructure is being updated. It includes:

- Uniform and systematic distribution of network in all racks of our 2 datacenters
- Change of network core switches.

The objective of this first step is to overcome the upcoming obsolescence of some equipment, to rationalize network distribution and to make a first performance increase, while considering the backbone architecture in perspective of SOLEIL upgrade. This will prepare our installation for a second iteration focused on performance improvement for the SOLEIL upgrade.

Concerning data storage and processing, it is announced that the volume of data managed or produced will increase by

several petabytes (or even tens of petabytes after the Upgrade) per year. This evolution should be measured over time as the figures announced are more or less accurate estimates. This requires relying on scalable resources that can easily adapt to changes in data production. The model used until now – purchases of equipment sized for the evolution of the estimated volume of data expected over a few years – will neither provide the required flexibility nor the guarantee to meet the need. Moreover, SOLEIL will not be able to deploy and maintain storage and computing resources at the required scale – this is out of the scope of its capabilities. It means that information system hybridization – *i.e.* a mix of on premises and off premises solutions - will even become mandatory and that cloud technologies must be in the DNA of our design.

### → Cloud and Information System hybridization

Technically speaking, our vision combines, see Figure 4:

- infrastructure located at SOLEIL to reduce and first analyze the “hot” raw data produced on beamlines, to evaluate their quality and make the relevant decisions during experiments.
- The transfer of “warm” data when experiments end to external computing and storage centers where Users can access and analyze them from their home laboratories, possibly by combination with data from other research facilities.
- The storage and the online access of “cold” data on external centers for up to 10 years. This storage can be based on slow access – low cost media.
- The offline archive at external centers, before removing data at the latest at the end of this 10 years period, in agreement with Users, and regularly as automated backup for disaster recovery.

To date, it appears that French national centers like the CC-IN2P3<sup>8</sup>, IDRIS<sup>20</sup> or CCRT<sup>21</sup> can provide solutions. Our vision is in line with the CNRS project for “Federated IT Services for Research Infrastructures”. Technical tests are in progress with

<sup>17</sup> By the end of 2020, more than 6,000 electronic systems are in production at the accelerators and beamlines.

<sup>18</sup> By the end of 2020, more than 10,000 software components (TANGO server devices) are deployed to control more than 20,000 devices at the beamlines and more than 15,000 at the accelerators.

<sup>19</sup> By the end of 2020, SOLEIL networks include more than 9,000 network endpoints distributed throughout the entire installation, and more than 200 physical servers (hosting more than 700 VMs).

<sup>20</sup> IDRIS (<http://www.idris.fr/eng/index.html>): Institute for Development and Resources in Intensive Scientific Computing, a CNRS (French National Centre for Scientific Research) Centre of very high performance intensive numerical computation.

<sup>21</sup> CCRT: Computing Centre for Research and Technology, <http://www-hpc.cea.fr/en/complex/ccrt.htm>, a CEA (French Alternative Energies and Atomic Energy Commission) Centre which has been set up to provide High Performance Computing resources for large scientific computations and to foster a real synergy between research organizations, universities and industry by promoting exchanges and scientific collaboration between S partners.



Figure 4: Architecture for experimental data

CC-IN2P3 and IDRIS centers (with the latter we have a direct fiber link), while we have set up a partnership with CCRT for simulation calculations.

In parallel, we must reconsider the current software solution for data migration between these different storage layers in order to have a more efficient solution better suited to future data production.

Calculation needs can be classified into two types:

- Numerical processing and analysis of experimental data (produced from sensors, detectors, etc.)
- Numerical simulations produced by supercomputers that process experimental data.

The democratization of computer use and the rise of free or Open Source software allow a wide range of processing methods and resources previously reserved for a few groups with access to very expensive computing resources. It is now common for the communities, to which the users and scientists of the SOLEIL synchrotron belong, to seek to combine access to the different computing architectures available, from the office workstation to the largest supercomputers. It is an established fact that external laboratories no longer have the required resources to store and process the data they produce during their synchrotron beam time. Storage and data processing must then be part of our offer to the SOLEIL Users. As raised above, the future of this type of resource necessarily involves the use of federating resource centers integrated seamlessly to SOLEIL's resources and

allowing users to benefit from their know-how through the implementation of:

- a distributed infrastructure for storage,
- the supply and processing of data,
- the dissemination and development of this data,

We also want to go further by making services as easy and transparent as possible. In addition to traditional methods of accessing resources, it will be essential to set up a web portal for accessing hosted data, also allowing the submission of workflows using supercomputers. This portal will also have to allow access to hosted data which will become open data after their embargo period, according to the corresponding Data Management Plans (see Open Science, page 155).

By relying on such resource centers, it will be possible to provide:

- an optimal hosting environment: secure and guarded access, controlled cooling environment, network connectivity, high availability, reliability;
- computing and data processing resources more easily adaptable to changing needs and combining high-performance computing and high-speed computing, supercomputers with graphic accelerators, containerization and cloud computing;
- the benefit of the high expertise of those operating the centers, including expertise about applications;
- the ability to use a variety of scientific computing technologies, including HPC and AI, MTC/HTC and Cloud, and secure management of large

volumes of data;

- a means of access to data and dissemination of open data.

### → Human Resources tools modernization

In the area of SOLEIL's administrative tools, Human Resources (HR) tools have been identified as critical components to be upgraded. An internal assessment shows that some of them are obsolete and that HR activities still managed manually could be digitized.

Human Resources digital transformation towards automated and data-driven processes is a hot topic for many facilities. Our goal is to implement an HRIS<sup>22</sup> in close discussion with all staff – from HR, IS and other employees to top management.

From an HR point of view, the Upgrade offers an opportunity to improve the SOLEIL HR management. It includes time saving, smart metrics and reporting, improved support, acculturation of employees to the digital world, attraction of new candidates thanks to social networking tools.

On the IS side, it would be relevant to set up HRIS as part of the global enterprise architecture, paying attention to its integration with existing applications without disruption or impact on the administrative management of the facility. HR is a typical topic for which off-the-shelf solutions can be found in off-premise offerings and the cloud market.

## Security

Since SOLEIL was built, IT services have changed significantly, and will continue to do so at an increasingly sustained rate in the future. Our IT architecture must be able to take these changes into account while guaranteeing an optimal level of security and confidentiality.

The PLUSS project, which has already been initiated, (see Support for transversal activities, page 151) requires networks and systems unification, simplifying access from both inside and outside SOLEIL, so new security issues will emerge.

- IT tools are now deeply interwoven within all activities of the Synchrotron, so every staff member should be able to acquire a certain level of autonomy in the management of systems and networks (code integration in control systems, network connection of equipment, etc.).

<sup>22</sup> Human Resources Management Information System.

- The need for experiments remote control, users support by internal or external experts, collaboration with other institutes means that we must make our systems open to the outside world, and network filtering rules management must be automated.

Systems and networks security constraints must remain hidden to the user, allowing for transparent access while ensuring actions logging and automated supervision and alerting. Our challenge will be to allow this delegation of responsibility by simplifying software applications and interfaces, at the same time as controlling the prerogatives of each and ensuring the security of the whole system.

This evolution, coupled with increased openness to the outside world, requires a complete rethinking of our identity and access management. Our current model of centralized directory-based authentication will move to identity federations and other distributed systems. Here too, complexity must remain transparent to users, via single authentication<sup>23</sup> mechanisms (SSO) or shared identity providers (GEANT, ORCID...). We will also consider multi-factor authentication mechanisms that can make life easier for the end user while strengthening the security access to SOLEIL IS.

## Open science

SOLEIL upgrade must consider the global movement towards open science. The underlying idea ruled by the European Commission for the funding of public research is that modern science must be based on interdisciplinary exchanges between scientists. With this in mind, SOLEIL has already adopted a scientific data management policy<sup>24</sup> to help researchers produce data according to the FAIR principles (Findable, Accessible, Interoperable, Reusable). This is reflected in particular by the effort to be made to generalize the use of standards for data recording format (NeXus / HDF5) and associated metadata. It will also be necessary to provide a tool to attribute unique persistent identifiers (so that each dataset will be uniquely attributable) and licenses, a more efficient Data catalogue, all the necessary help to Users to establish Data Management Plans (DMP) allowing them to manage the life cycle of data before, during and after their experiments in the spirit of open science... Several lines of work have thus been defined, see [Figure 5](#). This approach is part of the wider movement undertaken by the European Commission to build the future EOSC (European Open Science Cloud), a platform accessible via a single portal<sup>25</sup> providing remote access for all researchers to data and the computing means to process them.

SOLEIL is particularly involved in the European PaNOSC<sup>5</sup> and ExPaNDS<sup>6</sup> projects grouping together the Neutron and Photon sources. The two projects have already come up with a common FAIR enabling Data Policy framework. They are working on a way of federating their Data catalogs by providing a common research API and implementing a Data Analysis Service Platform connected to the data research API and accessible from the EOSC portal.

This approach is also in line with French National Plan for Open Science<sup>26</sup> published on 4 July 2018.

### → Ongoing Work lines for Data Management Policy implementation

The implementation of the data policy is already ongoing with a focus on development of a software service (DMS for Data Management Service) which will take care of DOI generation for the data sets produced at SOLEIL and their publication in DataCite. We are also planning to join the collaborative project of the SciCat<sup>27</sup> data catalog for its deployment at SOLEIL.

A prototype of a Data Analysis as a Service (DAaaS) has been developed (see Data Reduction and Analysis in Chapter 4 – beamlines Instrumentation). The final architecture of this service will benefit from the outcomes of ongoing collaborative projects on the topic, such as LEAPS-IT<sup>28</sup>, BIG-MAP<sup>29</sup>, PaNOSC<sup>5</sup> and ExPaNDS<sup>6</sup> European projects.

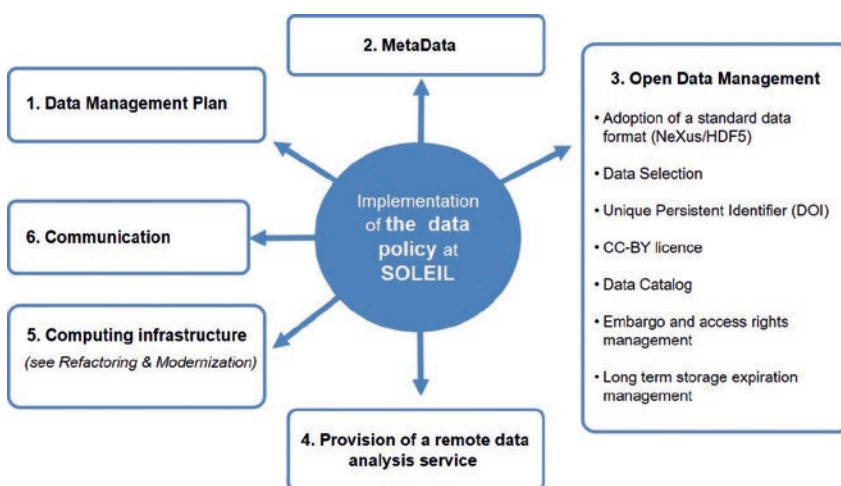


Figure 5: Ongoing worklines for data management policy implementation

## Teams training and support, technical culture

Beyond the technical considerations of the information system upgrade, staff training is critical to ensure the success of the SOLEIL upgrade on a long-term basis.

History tends to demonstrate that launching a new project involving new tools and technologies without being trained to the associated best practices often leads to performances, stability

<sup>23</sup> Multi-factor authentication allows to confirm the user identity by combining something the user knows (password), something the user has (e.g. phone, token) and/or something the user is (e.g. fingerprint, voice) and/or somewhere the user is (e.g. specific computing network).

<sup>24</sup> <https://www.synchrotron-soleil.fr/en/file/11308/download?token=9mSpYtJC>

<sup>25</sup> <https://www.eosc-portal.eu/>

<sup>26</sup> The ambition of French National Plan for Open Science, <https://www.enseignementsup-recherche.gouv.fr/pid39205/science-ouverte.html>, "is to ensure that data produced by government-funded research in France are gradually structured to comply with the FAIR Data Principles, and that they are preserved and, whenever possible, open to all".

<sup>27</sup> SciCAT (<https://scicatproject.github.io/>), a data catalog project developed by ESS, PSI, MAXIV to manage and annotate scientific data and publish as open data.

<sup>28</sup> LEAPS-IT is a working group of LEAPS initiative (the League of European Accelerator-based Photon Sources, <https://leaps-initiative.eu/>), a consortium of the Synchrotron Radiation and Free Electron Laser user facilities in Europe.

<sup>29</sup> BIG-MAP (Battery Interface Genome – Materials Acceleration Platform, <http://www.big-map.eu/>), a European project relying on the development of a unique R&D infrastructure and accelerated methodology that unites and integrates insights from leading experts, competences and data across the entire battery (discovery) value chain with AI, HPC and autonomous synthesis robotics.



or maintainability problems that finally required reimplementing to obtain the expected quality of service. The lack of training in new technologies – and self-information or even self-training if not accompanied by guidance – would be a risk for the Upgrade.

Daily operation and systems maintenance are time-consuming tasks preventing teams' members from upgrading their skills and leveraging new technologies. This leads to support legacy systems till they reach their maintainability limit.

Artificial intelligence, information system architecture, IoT and robotics have been identified as the main topics in which SOLEIL must invest and train its staff.

The foreseen digital transformation implies a transformation of our technical culture. It is also clear that many of SOLEIL's staff activities are or will be moving towards increased use of new digital technologies, due to the evolution of the techniques they have to implement or to work with. Training will consequently have to apply to any staff member whose activity requires advanced use of the information system. See *Human Resources* in Chapter 11. The SOLEIL staff must continuously acquire and maintain the required level of knowledge and skills to ensure that technologies fit the needs and are properly used. Technologies sharing at facility scale and mutualized tools would also contribute to the development of a local technical culture that crosses teams' boundaries. A shared technical culture – and a global enterprise architecture – can help maintain a coherent and effective interdisciplinary approach.

Another way to improve and share technical culture is through knowledge bases. Standardization of operational processes and documentation has been initiated a few years ago and is gradually being adopted by technical staff. Underlying IS tools (JIRA and Confluence from Atlassian) are in place to efficiently support these processes across SOLEIL organization<sup>[5]</sup>.

To date, special attention should be paid to the integration of engineering tools to improve efficiency from design to operation of scientific instrumentation on both the accelerators and the beamlines. In this area, the integration of new information and communication technologies can make it possible to better share knowledge between teams and to improve the dissemination of and access to information via micro-services.

Beyond training on new technologies and extending our technical culture, consulting (*i.e.* experts advisories) is also a way to optimize resources usage and to reduce time to production. We definitely need to get over the idea that we can do everything on our own.

As computer scientists, we must inject an “integrator” dimension into our “developer” role. This could mean focusing our development activity on the core components of our solutions (*e.g.* *Flyscan* and data recording ecosystems) and increasing our involvement in their deployment and tuning for new accelerators or beamlines. Assigning minor developments to fixed-term contracts (see *Human Resources* in Chapter 11) and subcontractors could enhance our ability to reply to new requirements and systems evolution. This could also make it easier to devote enough time to maintain the deployed systems in operational conditions.

The information system will definitely play a major role in the SOLEIL upgrade. Most of the SOLEIL scientific and technical ambitions rely heavily on computing technologies. In some cases, they will even act as critical components of success and will strongly contribute to the enhancement of the user experience.

Fully aware of the challenges related to the SOLEIL upgrade, the SOLEIL computing and controls teams adopted a strategy centered on an iterative digital transformation of the facility. This

strategy goes beyond the accelerators and beamlines upgrade and targets the global activity of SOLEIL around 2030. The aim is to generalize an enterprise architecture approach supporting the 3 components of the SOLEIL offer in a “end-to-end” manner: beam production and delivery (accelerators) → experimental processes and scientific data production (beamlines) → knowledge extraction from that data (data processing services).

Beyond the IS upgrade and modernization, for the computing and controls teams, the actual challenges of the SOLEIL upgrade mainly focus on the extraction of high added value from massive data produced by both the accelerators and the beamlines. From a computing point of view, it puts data management, engineering and processing at the heart of the Upgrade project. Technologies like artificial intelligence, cloud, IoT and robotics will act as the components of an enterprise architecture supporting the global activity of SOLEIL. In this context, staff training and external support (expert advices and minor developments) are critical keys of success and would help optimize resources usage and reduce time to production.

The foreseen digital transformation is not a pure technical journey. It will also have a critical organizational impact at the facility scale. The adoption of a global enterprise architecture will realign our activity on a transversal (or end-to-end) approach. This consequently requires the whole SOLEIL staff to also align with this new strategic vision and to also perceive our activity as a whole made of interdependent processes exchanging information. In the domain, change management<sup>30</sup> tools and technics should help us converge towards a clearly identified and shared Upgrade target – at individual, group and organization scale.

The presented IS strategy is now validated and appears in the roadmap of the IS teams.

## REFERENCES

[1] S.C. Leemann, S. Liu, A. Hexemer, M.A. Marcus, C.N. Melton, H. Nishimura, and C. Sun, “Demonstration of machine learning-based model-independent stabilization of source properties in synchrotron light sources,” *Phys. Rev. Lett.* 123, 194801 (2019)

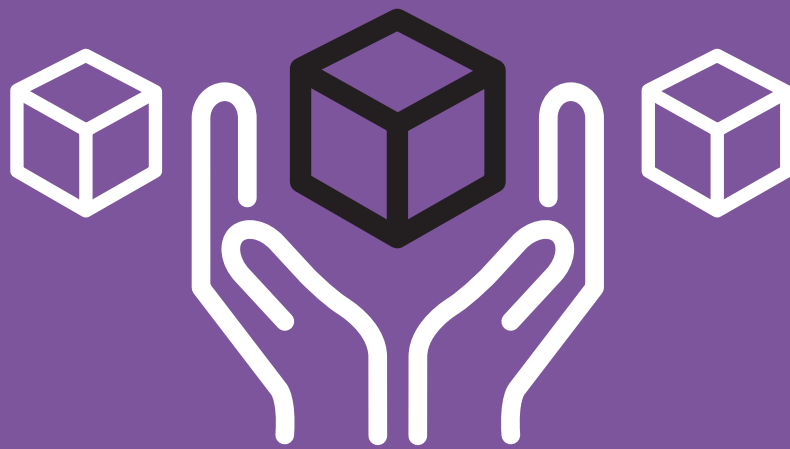
[2] Workshop on Artificial Intelligence applied to Photon and Neutron Science, 12-14 november 2019, ESRF-ILL-STFC

[3] M.A. Huff, “MEMS - An enabling technology for the Internet of Things (IoT)”, 23 december 2016, doi:10.1002/9781119173601.ch9

[4] Y.-M. Abiven, T. Bucaille, L. Chavas, E. Elkaim, P. Gourhant, Y. Liatimi, K. Medjoubi, S. Pierre-Joseph Zephir, V. Pinty, A. Somogyi, F. Thiam, S. Bouvet and B. Pilliaud, “Robotizing SOLEIL beamlines to improve experiments automation”, ICALEPCS 2019

[5] A. Buteau, G. Abeillé, X. Delétoille, J.-F. Lamarre, T. Marion and L. S. Nadolski, “Inception of a learning organization to improve SOLEIL's operation”, ICALEPCS 2019

<sup>30</sup> Change management ([https://en.wikipedia.org/wiki/Change\\_management](https://en.wikipedia.org/wiki/Change_management)).



## 6 - Infrastructure



## Storage ring and beamlines implementation

### Introduction

In contrast to new facilities, upgrades of existing storage rings are constrained not to exceed a maximum circumference. This constraint comes from the fact that the upgraded accelerator should stay in the existing tunnel. Minor modifications to the concrete are feasible but remain expensive and time consuming.

For SOLEIL upgrade, several iterations ended up with an optimized lattice fitting into the tunnel and offering minimal photon source point displacement compared to existing beamlines.

In addition to dimensional constraints, the new lattice needs to fulfil two other conditions:

- No (or very low) source point displacement for SOLEIL two long beamlines, which occupy a custom-made building which would be extremely difficult to modify. These two beamlines are currently situated on a canted long straight section (SDL13),
- The new lattice shall not modify the experimental hutch position of the MARS beamline because of its special radioactivity containment environment.

### Cell breakdown definition

The upgrade lattice is divided into 20 cells referenced from C01 to C20, as presented in Figure 1. Each cell starts from the beginning of a straight section and extends to the end of multipoles. The advantage of such a definition is to include the whole length of the straight sections in the cell. Consequently, the straight sections are named as SDXnn in which:

- SD: Straight section denomination in French (Section Droite)
- X: The type of the straight section.  
L: Long, M: Medium, S: Short
- nn: The cell number the straight section is attached to.

According to this definition SDM05 is a medium straight section attached to the cell C05. The beamline sources are referenced as X-Cnn in which:

- X: Source type. I: Beamline on Insertion Device, Dn: Beamline on dipole following by the dipole number in the lattice.

- Cnn: The cell number the beamline source point is attached to.

I-C02 would be a beamline on Insertion Device in C02 and D4-C16 is a dipole beamline coming from the 4<sup>th</sup> dipole of C16.

### Machine implementation inside existing tunnel

The CDR reference lattice (V0313) meets the challenge of providing record-low electron beam emittance and is optimized to meet the required performance within budget and size constraints. The overall layout of the storage ring and beamlines is shown in Figure 2 and in more detail in Figure 3.

In contrast to the existing SOLEIL, which is a symmetry 4 machine, the lattice V0313 offers only a symmetry 2. The accelerator is slightly oval shaped with two different lengths for long straight sections (7661 mm and 7355 mm), the medium and short straight section lengths are 4151 mm and 2730 mm respectively.

This is a major complication from the engineering point of view but helps

minimizing the photon source point displacements for insertion device beamlines, especially for the long ones where there is only a 2 mm offset. All other insertion device beamlines are shifted laterally by values between 33 mm to 107 mm (Table 1). The diameter of the hole on the front-end radiation shield is around 210 mm. This means that in most cases we do not need to make new holes in the concrete as far as the new beamline stays parallel to the old one.

The orientation of the new lattice implementation inside the tunnel is imposed by the actual SOLEIL's SDL13 canted straight section, which is the source of both long beamlines. In choosing this orientation, the upgrade injection straight section will also stay parallel to the existing injection straight.

The bending magnet beamlines are affected in any case, since the new lattice is closer to a circle than the present one due to the larger number of bends. Since the existing tunnel has been optimized for the SOLEIL lattice, the fact that the new lattice shape is closer to a circle creates some new difficulties. For example, at four

Straight Section	Source type	Lateral shift (mm)
SDL01 (L=7355mm)	Injection	256
SDM02	Fundamental RF	33
SDC03	Insertion	33
SDC04	Insertion	-36
SDM05	Insertion	-105
SDL06 (L=7661mm)	Insertion	-2
SDM07	Insertion	-107
SDC08	Insertion	-38
SDC09	Insertion	33
SDM10	Insertion	33
SDL11 (L=7355mm)	Harmonic RF + Insertion	256
SDM12	Insertion	33
SDC13	Insertion	33
SDC14	Insertion	-38
SDM15	Insertion	-107
SDL16 (L=7661mm)	Insertion	-2
SDM17	Insertion	-107
SDC18	Insertion	-38
SDC19	Insertion	33
SDM20	Insertion	33

Table 1: Source point offset for insertion device beamlines

places around the lattice, the beam axis passes within 372 mm from the concrete wall. Given that the construction tolerances on the concrete are  $\pm 10$  mm, installation of girders may be problematic. One of the solutions would be to make a  $\sim 100$  mm chamfer on the concrete in order to gain space, but this possibility would need the approval of the radioprotection authorities.

Another issue which needs attention is the trenches on the floor of existing tunnel. The position of these trenches, used for cabling and plumbing, has been optimized for the existing ring. Implementing the upgrade lattice V0313, we observe in some areas the girders are positioned on or close to the trench. In these cases, the trench will be filled by concrete or covered by a thick steel plate.

In four areas of the V0313 lattice layout, if the center of dipole number 4 on 7BA cell is used as a beamline source, the front-end beamline will pass within 190 mm of the radiation shield. Special design supports with half frames fixed on the wall must be used in this case in order to position all components inside the tunnel.

### RF cavity implementation

Several scenarios have been studied for the implementation of the RF cavities in the V0313 lattice. The most practical one from RF point of view would be to use SDM02 for the fundamental RF cavities and the SDC03 for the harmonic cavity. The advantage of this solution is that the cryogenic Helium liquefier is already installed near to SDC03 should a super conducting design be retained.

This solution would be certainly the most cost-effective layout for RF system, but in this case two straight sections will completely be occupied by the RF components, reducing the number of available ID beamlines. In order to maintain the number of available ID straights to that which already exists, it is proposed to keep the fundamental RF systems in SDM02 but the harmonic cavity will share SDL11 long straight section ( $L = 7355$  m) with an insertion device. In this configuration, the Helium liquefier needs to be moved to a new area near SDL11.

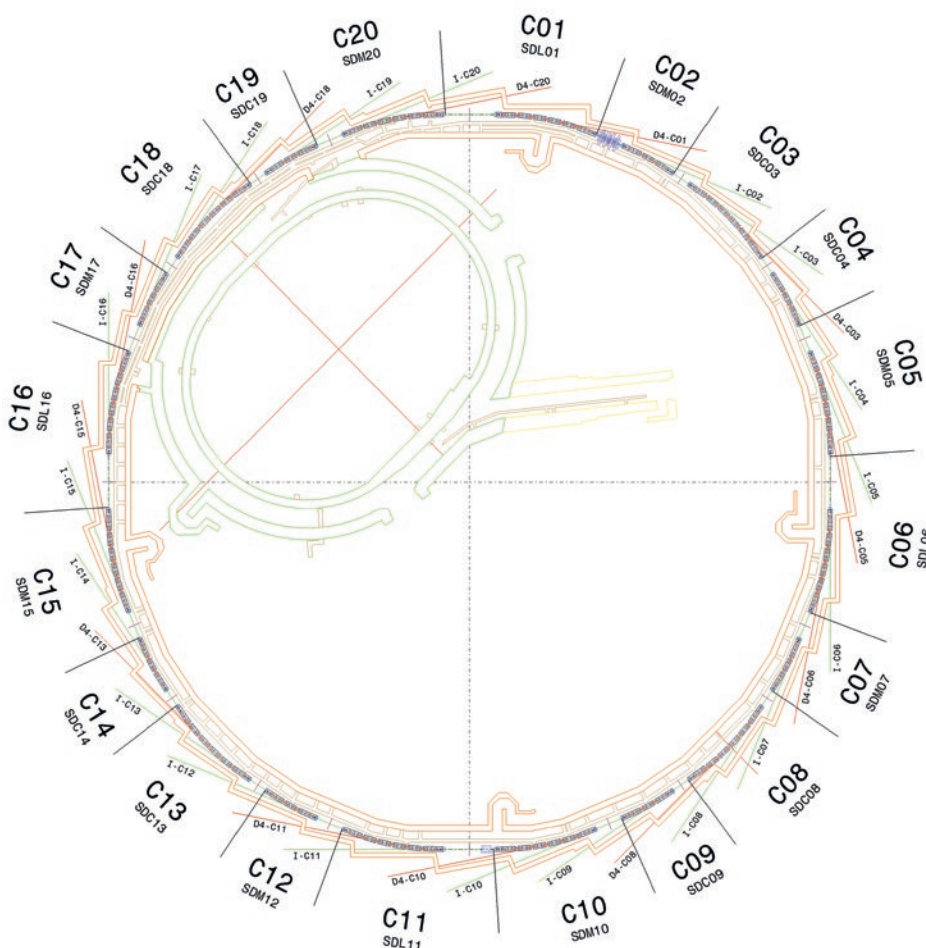


Figure 1: Cell breakdown definition

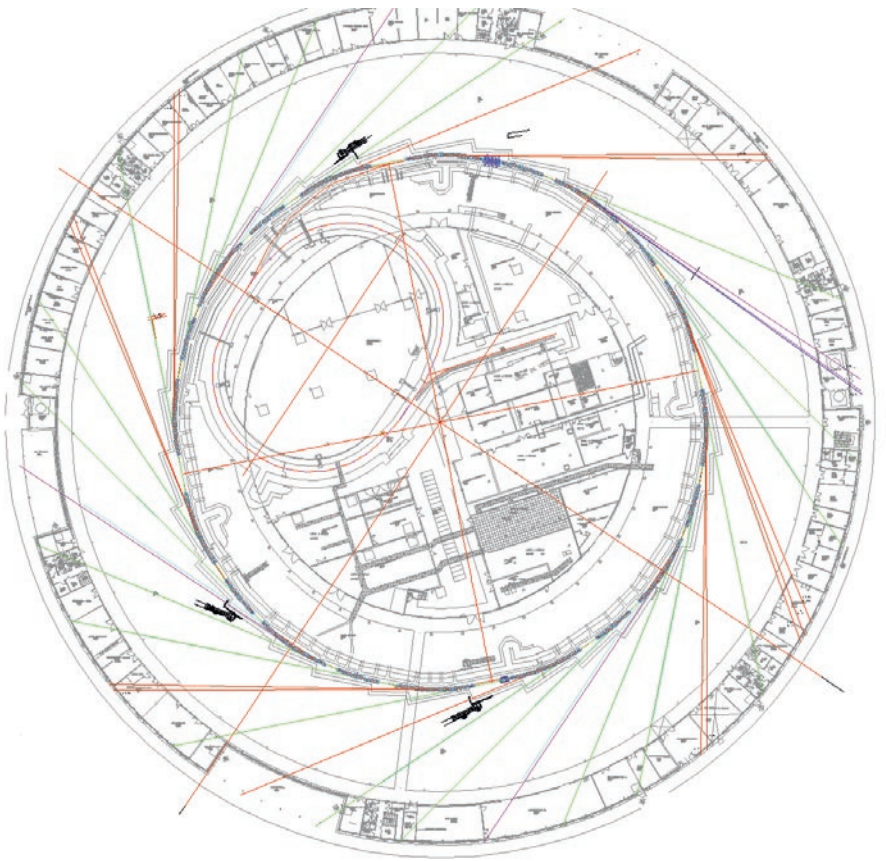


Figure 2: Lattice V0313 implementation in existing tunnel

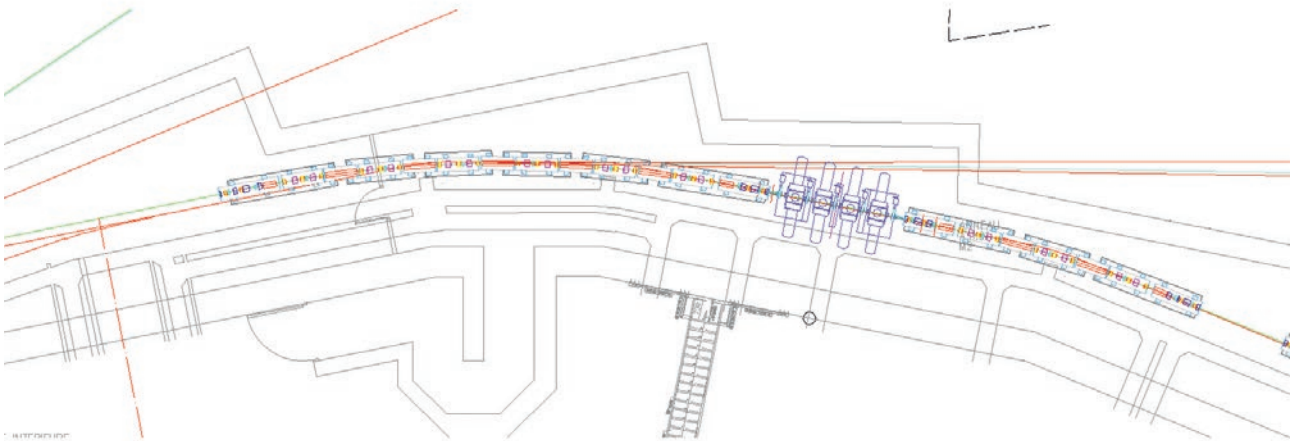


Figure 3: Lattice V0313 implementation in existing tunnel

## Support buildings and logistics

### Introduction

The disassembly of the booster and the storage ring, some beamlines, technical gallery equipment and part of the utilities, will require covered and enclosed safe storage areas. It is important to distinguish well ahead of time the logistic flows of equipment according to their usage. Equipment coming out of the tunnels will need a detailed radiological survey classification that can last several years. Other equipment will need to be preserved or refurbished under appropriate environmental conditions, whereas others will get disposed in the normal industrial waste.

Following the strategy developed in section Disassembly, Pre-staging and Installation, new equipment, its storage, and the pre-assembled and pre-staged accelerator and beamline components, will require adequate space, specific controlled measurement environments, workshops, handling and conveying. This will result in dedicated specifications starting with the quality of the slab, temperature control, sufficient crane capacity, etc. High-quality storage or assembly areas are needed for several years, since the construction of the new insertion devices and new beamlines will be realized over a (predicted) period of almost 10 years. As a consequence, the corresponding structures will have to be designed to last for the same period of time or even longer.

The space requirement has yet to be matured, in particular for the Experimental Division, but the minimum space requirement has already been estimated with a minimum area of:

- 2500 m<sup>2</sup> of long-term high-quality buildings for duration larger than 20 years.
- 3000 m<sup>2</sup> of temporary buildings for duration limited to 5 to 6 years.

### SOLEIL site

At SOLEIL, presently no space is available with the necessary surface area for assembly and testing work for the accelerators and the beamlines. In considering the crucial importance of space management for the upgrade and beyond, a reflection has already been started about the possibility of constructing new buildings with cost minimization as a major criterion.

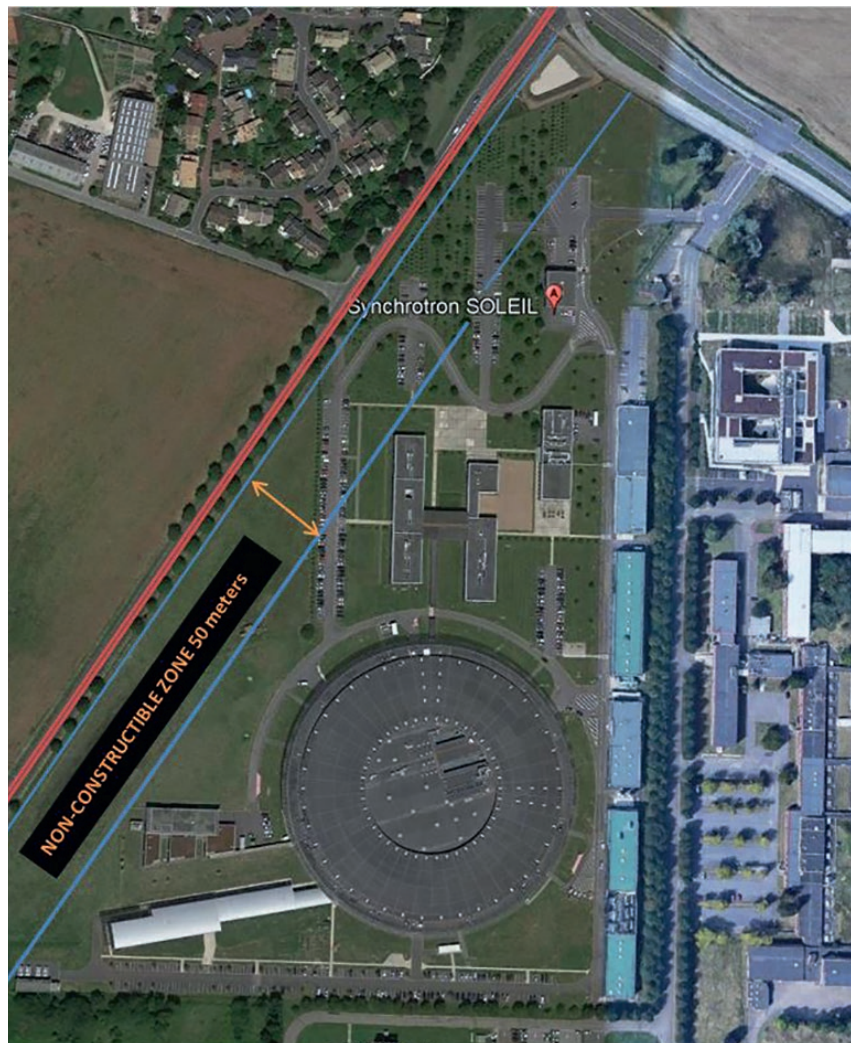


Figure 4: SOLEIL site top view

### Constructible areas

SOLEIL site surface area is of 135 000 m<sup>2</sup> of which 51 592 m<sup>2</sup> is already occupied. The PLU (Local Urbanization Plan) of Saint-Aubin imposes heavy constraints such as a maximum building height of 11.5 m, the prohibition to build in the zone parallel to the main road (D306) extending to a width of 50 m along the road (Figure 4), which reduces significantly the available constructible area to only 50 408 m<sup>2</sup>.

Nevertheless, the Departmental Direction for Urban Planning authorizes the construction of temporary buildings in the 50-meter zone for a maximum period of 5 years. The buildings and infrastructures must then be dismantled and the area regrassed.

### Study of the nature of the soils

In order to determine the nature of the ground, a study was conducted to determine the load-bearing capacity of

the soils, which is dependent on the geomechanical performance in kN/m<sup>2</sup> of the soil medium and the different geological layers. This study will allow us to dimension the foundations of the building infrastructures. The study showed that the soil is made up of 4 different layers (Figure 5). It is an agricultural type soil with a low load-bearing capacity. The use of concrete columns will be necessary for geomechanical loads larger than 500 daN/m<sup>2</sup>.

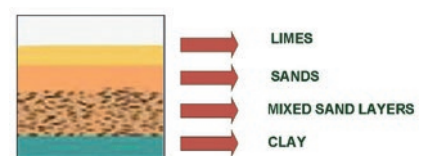


Figure 5: Soil nature



## Extensions buildings for assembly and pre-staging

The synchrotron building includes 3 available open spaces (called the “East ear”, “South ear” and “West ear”) along the external periphery of the building (the East and West ears are shown in Figure 6). It is proposed to use the East and West ears to build two extensions that fit with the Synchrotron building in terms of size and architectural style.

### East Extension

The current proposition is to dedicate the East extension (Figure 7) for the assembly and pre-staging of the new storage ring. The ground floor and the first floor of the extension (Figure 8) will be at the same levels respectively as the Synchrotron building ones to allow good circulation between the two buildings and the distribution of utilities and service networks such as:

- Energies (electrical, water, gas and compressed air networks, air extraction network, etc.).
- Secondary Networks (ethernet, WIFI, phone, fire safety, access control, etc.).

The East ear extension can have a ground surface of 715 m<sup>2</sup> and a first-floor area of 680 m<sup>2</sup> for a total of 1 395 m<sup>2</sup>. As reported in section Disassembly, Pre-staging and Installation, the plan is to use the ground floor area mainly for test equipment and girder assembly and the first floor for all vacuum system characterization activities. At the end of the assembly, the ground floor will be used partly for the new insertion devices construction. The first floor will be converted into laboratories, offices and meeting rooms.

### West Extension

In the line of the current reflection, the West extension (Figure 9) is dedicated to the modification of some beamlines and/or the construction of new ones. The possible surface area of the ground floor is of the order of 715 m<sup>2</sup> and that of the first floor is of the order of 408 m<sup>2</sup> which corresponds to a total of 1 123 m<sup>2</sup>.

This extension will be used over several years because the program of upgrading or building new beamlines will take several years to keep up with the new science. The activities in the ground floor will have very little impact on the activity of the Synchrotron.

## Temporary buildings

As mentioned above, the disassembly of equipment leaving the tunnels, experimental hall and technical galleries

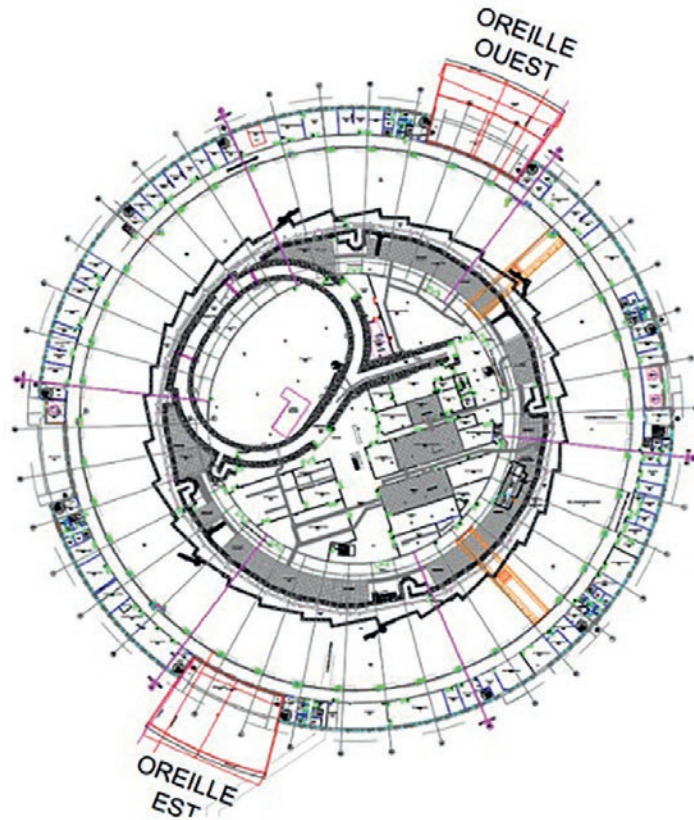


Figure 6: Synchrotron building with its East and West extensions (“Oreille Est” and “Oreille Ouest”)

will require large on-site storage areas. The existing duration of these areas is dictated by the time required to complete the mandatory radiation contamination safety measurements, which are currently estimated to last 5 years.

As in the case of the East ear extension, all necessary networks will be supplied and routed via existing or new gutters either from the Synchrotron building or from the central building.

### Temporary building topology

After some investigation, it seems that a solution would be to use industrial metallic-textile modular structures with galvanized lacquered sheet metal facades and insulating sidings. The roofing consists of a PVC-coated polyester membrane (Figure 10).

- Module of 1 000 m<sup>2</sup> (width 30 m x length 33.5 m).
- Module of 500 m<sup>2</sup> (width 20 m x length 25 m).

### Building foundations

An assessment in the initial phase has determined that the storage space required in the temporary buildings is about 3 000 m<sup>2</sup>. Two buildings of 1 000 m<sup>2</sup> and two others of 500 m<sup>2</sup> is the configuration proposed at this stage. The type of foundation will

be determined according to the desired bearing capacity. It should be noted that 43% (1 987 m<sup>2</sup>) of projected concrete slab will be built within the 50 m exclusion zone (Figure 4) and will therefore have to be dismantled at the end of the project.

In addition to these buildings, it will be necessary to find buildings outside the SOLEIL site with the characteristics listed in the introduction, for the storage of the 212 girders once assembled.

## Life base for external companies

### Buildings

Throughout the duration of the works, SOLEIL will be hosting a large number of all kinds of contractors, made up of large teams who will be working at SOLEIL over long periods of time. An initial estimate has shown that up to 80 additional people will be present during peak periods. A life base has been sized accordingly taking into account the so-called “CRAMIF” regulations, which impose minimum equipment and surface areas to be made available to companies depending on the number of people. This living base will be located next to the temporary buildings. It is likely that a structure employing mobile building modules will be used.

### Parking, accommodation and catering

SOLEIL will provide private parking spaces to accommodate the companies' professional vehicles. Similarly, the SOLEIL restaurant will be able to provide catering for 80 external employees. In the event that the teams of external companies are far from their home bases, SOLEIL will be able to accommodate them in its guest house, which has 80 rooms, according to terms and conditions that will remain to be defined and commensurate with any residual experimental program.

### Heavy vehicle infrastructure

Regarding the infrastructure, site will need to be accommodated in order to ensure the fluidity of logistics flows such as:

- A heavy vehicle parking area (for 2 trucks simultaneously). This area of 300 m<sup>2</sup> (5 m x 60 m) should be located in front of the temporary buildings in order to facilitate the loading and unloading operations. To optimize costs existing parking spaces will be reallocated for this purpose.
- An unloading area of 600 m<sup>2</sup> (6 m x 100 m) to allow forklift trucks (Fenwick type) to unload the trucks and transport their contents to the temporary buildings.
- Identifying the traffic lanes on the site to optimize the flow of trucks. A circular traffic flow is considered ideal if the incoming trucks do not interact with outgoing trucks. In order to develop this solution, several road improvements will be needed.
- A temporary waste storage area equipped with 6 m x 2.44 m containers should be made available.

### Utilities adaptation

As for the present facility, highly reliable and efficient utilities are needed for the operation of the Accelerators, Beamlines and Laboratories after the upgrade. This includes:

- Cooling circuits and HVAC (Heating, Ventilation, and Air Conditioning),
- Compressed Air,
- Special fluids (Liquid He [LHe], Liquid N<sub>2</sub> [LN2], Gaseous N<sub>2</sub> [GN2]),
- Electricity: High Voltage, Low Voltage distribution, secured.

The upgrade project will extend the use of the facility by a few decades, it is then important to make an exhaustive inventory of all utilities equipment, carry out a full



Figure 7: East ear



Figure 8: East ear extension



Figure 9: West ear

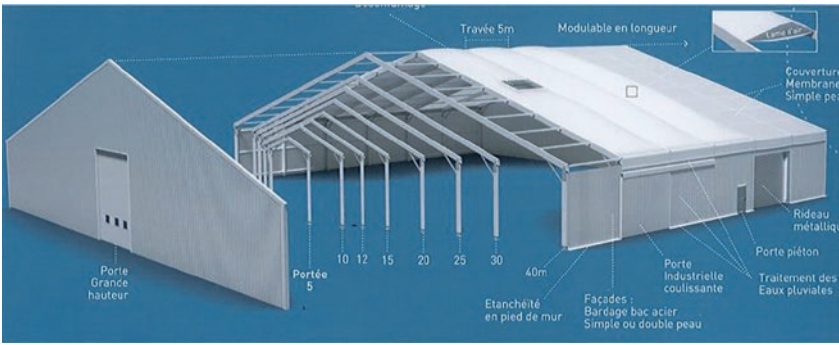


Figure 10: Temporary building structure

obsolescence review of all systems and propose upgrades or replacements where they are needed. Utility requirements and equipment specifications for the new accelerators, beamlines and new buildings (see section Support Buildings and Logistics) will also be recorded and integrated into the overall study.

## Cooling and HVAC systems

### Cooling circuits

The cooling water production station is presently composed of four cooling producer groups and six aero cooling towers. The regulation temperature of the chilled water circuits is 6 to 8°C. The infrastructure is aging (two cooling towers, recovered from the former laboratory LURE, are already refurbished), uses significant quantities of tap water and needs heavy and costly preventive and corrective maintenances. It is necessary to make a comparative study with different technical solutions in order to provide a reliable cooling water production station for the next 20 years.

The proposed solutions must allow managing the forthcoming obsolescence of the existing equipment, ensuring equipment redundancy for continued operation of the cooling system at any time, facilitating maintenance actions without stopping the system, while reducing energy consumption and complying with European regulations for environment.

Three technical solutions have been studied during the CDR phase:

- Preventive Maintenance optimization and upgrade of the existing system.
- New system based on the use of adiabatic dry coolers.
- New system based on the use of new generation aero cooling towers.

Criteria such as obsolescence, efficiency, redundancy, maintenance, electrical energy consumption, clean water, regulation and environment were used

in this study. The initial findings show a clear advantage for the adiabatic dry cooler system that can respond positively to all these criteria. One disadvantage of a solution using dry coolers instead of air cooling towers is the need for more exchange surfaces going beyond the present building capacity. The comparison study should continue including other aspects like budget, schedule, and resources. This will be an urgent goal in the Technical Design Report (TDR) phase.

Three cooling water circuits are currently derived from the chilled water system: a 30°C network feeding the booster, the RF rooms and the power supply rooms, a 21°C cooling low conducting water network (LCW) for the rest of the storage ring equipment and 17°C cooling water used for the beamlines. Discussions are underway to see if the number of different temperature set points can be reduced and their regulation temperatures made uniform and adjusted to optimize the efficiency of the cooling stations, contributing to energy efficiency and reducing SOLEIL's environmental footprint.

The cooling circuits for the booster and the storage ring tunnels will be completely re-constructed and adapted to their respective new lattice configuration. Special attention will be given to filtering and adequate diagnostics in order to ease up maintenance and interventions.

The 17°C PVC network circuit is rather fragile and does not allow any modification or extension which could be problematic as some beamlines will move and new ones constructed. Its replacement, by a more durable system, is under study.

### HVAC systems

HVAC systems are essential for maintaining the set point temperatures, guaranteeing very good stability of the components of the Accelerators and beamlines. The objectives for the new

storage ring tunnel are to maintain the current level of thermal stability ( $\pm 0.1^\circ\text{C}$ ) or even improve it ( $\pm 0.05^\circ\text{C}$ ), at the same time as reducing energy consumption, operating and maintenance costs.

Studies are underway to determine the optimal value of the cooling air temperature, in order, to reduce electricity consumption. For example, one can also choose to heat up rather than to cool down the air, as it is the case in the MAX-IV facility.

In the current situation, there is no air temperature control in the LINAC and the booster tunnels. In the ongoing stability studies, the benefit or even the need to add such a system in both tunnels will be discussed. Calculations will be made by dynamic thermal simulations for all the tunnels of the accelerators taking into account the new distribution, and in particular the specificities of the magnets and insertion devices in the storage ring tunnel. It is also planned to perform the same analysis for the technical gallery hosting the electronic racks.

For the experimental hall housing the beamlines, thermal simulations and a temperature measurement mapping of the hall will be carried out at the beginning of the TDR phase. These studies should help in identifying areas for improvement in order to limit temperature variations in the synchrotron building. Beamlines both with and without lead lined or experimental control hutches will be taken into account, as well as the ambient environment around the beamlines as far as possible. The performance of the building envelope, which provides very little protection against climatic variations such as heat waves, should be reviewed. Humidity is a parameter that is already significant for certain experiments, and its control will also be considered among the studies to be carried out.

## Special fluids

### Liquid nitrogen

In the frame of the upgrade, cryogenic undulators will likely become the preferred technology for high energy photon sources for the beamlines, requiring a third (new) liquid nitrogen network independent of the beamlines. Increased beam power will lead to an increased prevalence of cryogenic optical cooling implying extensions to the existing network. Consequently, a complementary storage area, or an increase of the capacity of the present storage tank from 10000 to 20000 liters, are being studied. In addition, improvements in the capacity

to maintain and purge the network locally are highly desirable.

Gaseous emissions, from cryogenic coolers, have consequences both for air quality and heat budget in the synchrotron building. Collecting nitrogen gas from the cryo-systems or other equipment will be carefully studied during the TDR phase including a solution for the release of the gas directly through the roof or the facade of the synchrotron building.

#### Nitrogen gas

There has been a fairly significant increase in the use of ultra-high purity nitrogen gas at low pressure (2 bars) by several beamlines in recent years. The construction of a clean GN<sub>2</sub> distribution network in the whole synchrotron building is proposed, improving safety by reducing still further the number of gas bottles inside the building. This network will be supplied from the collected nitrogen gas or from an external source.

#### Liquid helium

A project for improving the existing helium gas recovery system performance and reduce noise and vibration from the pumps is already underway. In any case, the collected amount is expected to decrease with an increasing use of closed-loop systems for beamline applications. The control system must be reviewed in order to be consistent with the centralized technical management system (GTC) or the SOLEIL Programmed Logic Controller (PLC) standard.

#### Compressed air

The current compressed air production is designed to serve needs according to their location (building) and not according to the type of use. The compressed air requirements and increased criticality for the beamlines, the machine, and the support units will have to be identified during the first phase of the TDR. The collection of this data will allow us to define the technical characteristics of the future production, and to determine the new distribution according to the usage in terms of pressure or flow rate, which will be dedicated to the machine, the beamlines, or other equipment. This production facility and these new networks should be better adapted to meet the future requirements.

#### Utilities for the special fluids

The production of LHe for the storage ring superconducting Radiofrequency system is sensitive to interruptions and disturbances in the flow of 17°C and

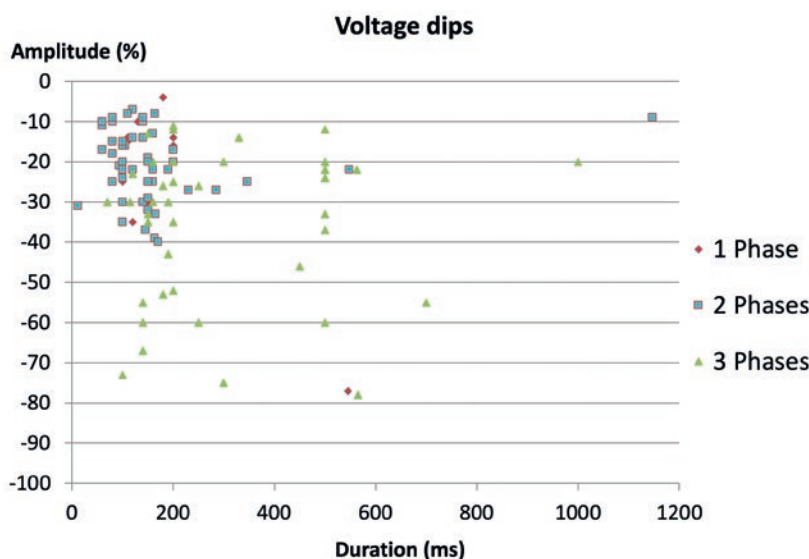


Figure 11 : Voltage dips record from 2007 to 2019 in terms of duration and amplitude in one of the 3 phases of the grid power.

21°C water cooling networks and the compressed air network. Any interruption of one of these networks for a few seconds causes 90 minutes to 6 hours of downtime for the beam in the storage ring. Increased robustness, protections, redundancies and backups should make it possible to eliminate these events and substantially gain in beam availability. In particular, the existing redundancy of the helium refrigerator cycle compressors is only very partially exploited, the two compressors being cooled by the same circuit. To secure and make them fully redundant, the cooling power will be increased by 50% and the cooling flow doubled with independent cooling ducts.

Finally, an upgrade of the positioners of the helium refrigeration control valves will significantly reduce the continuous consumption of compressed air by 16 N m<sup>3</sup> / h.

#### Electricity

Currently, SOLEIL is served, by one of the two 20 kV feeders (LUNE and EUROPA), with a power of 10 MW each supplying five 20 kV/400 V transformers distributed along the perimeter of the facility. An evaluation of the overall electricity needs of the new accelerators and beamlines is in progress. A significant decrease of the power consumption of the storage ring is foreseen (about 50% of the present value), whereas computational and experimental needs are increasing.

It is expected to keep the existing transformers mentioned above. On the other hand, the 50 Hz AC distribution to

the power supply cabinets of the storage ring (and most probably of the booster) will have to be changed entirely. This includes the low voltage general switchboards as well as all the ac cables. In fact, both the neutral regime (which will, a priori, have to be switched from IT to TN-S, as many power supply cabinets will require a single-phase supply) and the cable sections will be different.

Grid power quality will remain a major concern. At SOLEIL, voltage dips are the principal cause of power quality issues and result in many hours of stored beam (with an average value of around 19 hours per year over the period from 2007 to 2019 and a maximum of 44 hours in 2012) or experimental beamtime lost every year. Power loss results in early aging or even breakage of equipment for both the accelerators and the beamlines, and recovery from power loss is heavy in terms of human resources. As shown in Figure 11, most of the dips last less than 200 ms, with an amplitude drop lower than 40%. For the upgraded machine, it is therefore essential that equipment possess, by design, a certain immunity to correctly function in this environment. In this perspective, work has been started to define immunity levels for the equipment in order to ensure proper operation during the most common network disturbances without tripping the accelerator and to protect sensitive experimental equipment. The quality of the grid power will be monitored directly by the control system. A study was carried out to enable the entire electrical installation to be secured, but the corresponding solutions are prohibitively expensive. Consequently, the most sensitive storage ring devices (power



supply controllers, RF control systems, cryogenics controls and auxiliaries, IDs, BPMs and vacuum equipment...) will continue to be fed by Uninterruptible Power Supplies (UPS). Moreover, each beamline will be equipped with its own UPS (as will soon be the case on the existing facility). Finally, it is envisaged to be able to measure and monitor energy consumption by use point.

Special focus should be given to ElectroMagnetic Compatibility (EMC). For instance, it is expected that the beam feedback and feedforward systems will apply corrections at much higher rates on the new storage ring. Minimizing cross-talk and noise disturbances introduced by high bandwidth power supplies is of great importance. The EMC emission (and immunity) levels will have to be defined at early stage for all equipment. In particular, the design of the switched-mode power supplies will have to be coordinated with the design of the electricity mains distribution and grounding, and of the overall cabling (with appropriate choices for the connectors, for the related cable trays). As far as possible, the input AC/DC stage of these power supplies should use 'clean' rectifiers absorbing sinusoidal currents.

## Disassembly, pre-staging and installation

### Introduction

Limiting the beam downtime duration for the SOLEIL user scientific program to less than two years is a major constraint in the upgrade project. This duration can be affected by specific phases in accelerator construction: equipment disassembly, site preparation, installation of new equipment, equipment checkout, and accelerator commissioning. Moreover, during the same period of time concurrent activities with the Experimental Division work will happen: beamline reconfiguration, realignment but also installation of a few new beamlines will occur in parallel to accelerator construction.

The planning of all these sequences is aimed at minimizing the down time by including good methodology, anticipation, right resources and maximizing the amount of integration work including full equipment tests that can be done outside the tunnel.

The first thoughts and taking into

account the feedback from the ESRF-EBS upgrade (knowing that the scope of the SOLEIL upgrade is much wider), the implementation stage should be completed within 18 months for the accelerators part following the tentative planning:

- Disassembly of the present storage ring: 4 months (T0+4 mo)
- Site (tunnel and technical gallery) preparation: 3 months (T0+5 mo)
- Installation of the new storage ring: 8 months (T0+12 mo)
- Commissioning of the equipment: 6 months (T0+14 mo)
- Commissioning of the new storage ring with beam: 4 months (T0+18 mo)
- Commissioning of the beamlines: 3 months (T0+21 mo)
- Contingency: 3 months,

where in each task are indicated the duration in months (mo) and the end time of the execution from the starting time (T0) when the present installations are shut down.

It is important to note that an operation in an area can start only when the previous operation is completed.

The tasks related to the booster upgrade are very similar to those of the storage ring; they should be performed with less duration than these latter ones and happen in parallel. Adequate human resource allocation, well-organized plan to deal especially with the concurrent activities is one of the keys to complete the project in a timely manner.

### Disassembly

The present storage ring tunnel is divided into four zones (AS1 through AS4) composed of four cells. Removal and site preparation process will be developed with a focus on methods that allow activities to be conducted in parallel. The roof of the tunnel is removable and the two 7.7 tons overhead cranes will be used to remove the old storage ring components. The preventive maintenance of the cranes must be more sustained and the spare parts should be available to minimize shutdown period of the cranes. On the contrary, the booster has an immovable roof, only the two large shielding doors of the booster tunnel will be used to remove the old equipment and install new equipment. The teams involved in this part will be composed of SOLEIL staff that has the qualification and expertise together with subcontractors. All material to be removed from the two tunnels will be radiologically characterized using robotics systems. The large amounts of iron, copper, steel and

aluminum thus recuperated will be valued and proposed for sale once the radiological measurements have validated their integrity. A dedicated temporary building with a surface area of 1500 m<sup>2</sup> (see section Support Buildings and Logistics) is foreseen for housing equipment awaiting radiation tests. In addition it will require separate areas for the storage, reuse, or disposal of materials removed from the storage ring, booster and the technical gallery. It is important to mark and track components that will be re-used, so that careful handling is guaranteed. Prior to the disassembly operation in the tunnels and in the technical gallery, all electrical sources must be de-energized and locked out. They will be put back into service as required or as necessary. All operations that can or must be performed before the shutdown date will be identified ahead of time. Detailed plans, technical and human resources and timelines for the removal of the old storage ring, booster and equipment in the technical gallery will be finalized before the end of the first year of the TDR phase.

### Pre-staging

To avoid any risk of delays, the last girder of the storage ring must be assembled before the starting of the shutdown. To minimize the assembly effort inside the tunnel a rigorous workflow has to be developed to thoroughly test each component before it is accepted for installation. The construction of a dedicated new building is expected (see section Support Buildings and Logistics), where the ground floor will be used for the equipment testing and the complete assembly of the girders. This latter could be properly stored outside of the SOLEIL site. On the first floor of this new building, it is planned to assemble and store the vacuum chambers, to perform their quality tests and their baking out including their NEG activation. At the current stage, the ground floor will be used first to host and measure the magnets (starting in 2024 and ending in 2025) while the assembly of the girders will start beginning 2026. It is considered that the new building must then be ready beginning of 2024. In order to achieve that, and to allow for a reasonable time contingency, it may be necessary to start the design of the new building as early as January 2021. The area needed to the refurbishment of the in-vacuum insertion devices, the construction of the new ones and the storage and test of front-end equipment is still under discussion. It is proposed that the new booster will be procured from a single manufacturer who will provide complete girder assemblies

and will take care of the installation of the entire booster.

The other new building (see section Support Buildings and Logistics) will be dedicated to the assembly and pre-staging of the beamlines.

A lot of preparation work has to be done during the operation of SOLEIL, so special care has to be taken to minimize the impact on the beam quality and accelerator and beamlines reliability.

### **Tunnel preparation and installation**

The preparation work should include old cables, cable trays and pipes removal, floor and wall preparation including painting, air handling units' modification, geodesic alignment preparation, etc. The drilling of the new holes in the shielding wall to accommodate with the photon exit of the new beamlines will be carried out during this period.

Once the tunnel is empty and clean, either in totality or zone-wise, the appropriate installation activities will start. Similarly to the disassembly period, the circulation lanes will also have to be carefully studied, with suitable handling means, to transport equipment into the Synchrotron building without any risk and minimum impact of the experimental hall. The two main entry gates to the building will have to be kept open; therefore, it is not excluded that some parts of the beamlines in the vicinity may have to be temporarily dismantled to clear out the paths. In the storage ring tunnel, the support plinths of the girders will be positioned and anchored to the building foundation slab followed by the installation of the girders themselves, the magnets equipped with their vacuum chambers, in-vacuum undulators, front-ends, cooling pipes, cables and cable trays. booster and technical gallery installation of racks should occur in parallel

with the installation of the storage ring. In order to ensure a smooth installation a detailed and dedicated installation planning is necessary with adequate follow-up: it will allow installation works to run in parallel with *e.g.* alignment and cabling.

The preliminary target disassembly, pre-staging and installation schedule is given in [Figure 12](#).

The disassembly and installation operations will present a number of safety issues. The existing safety rules and procedures will be scrupulously reviewed to make sure that all actions are within the remit of normal SOLEIL operations.

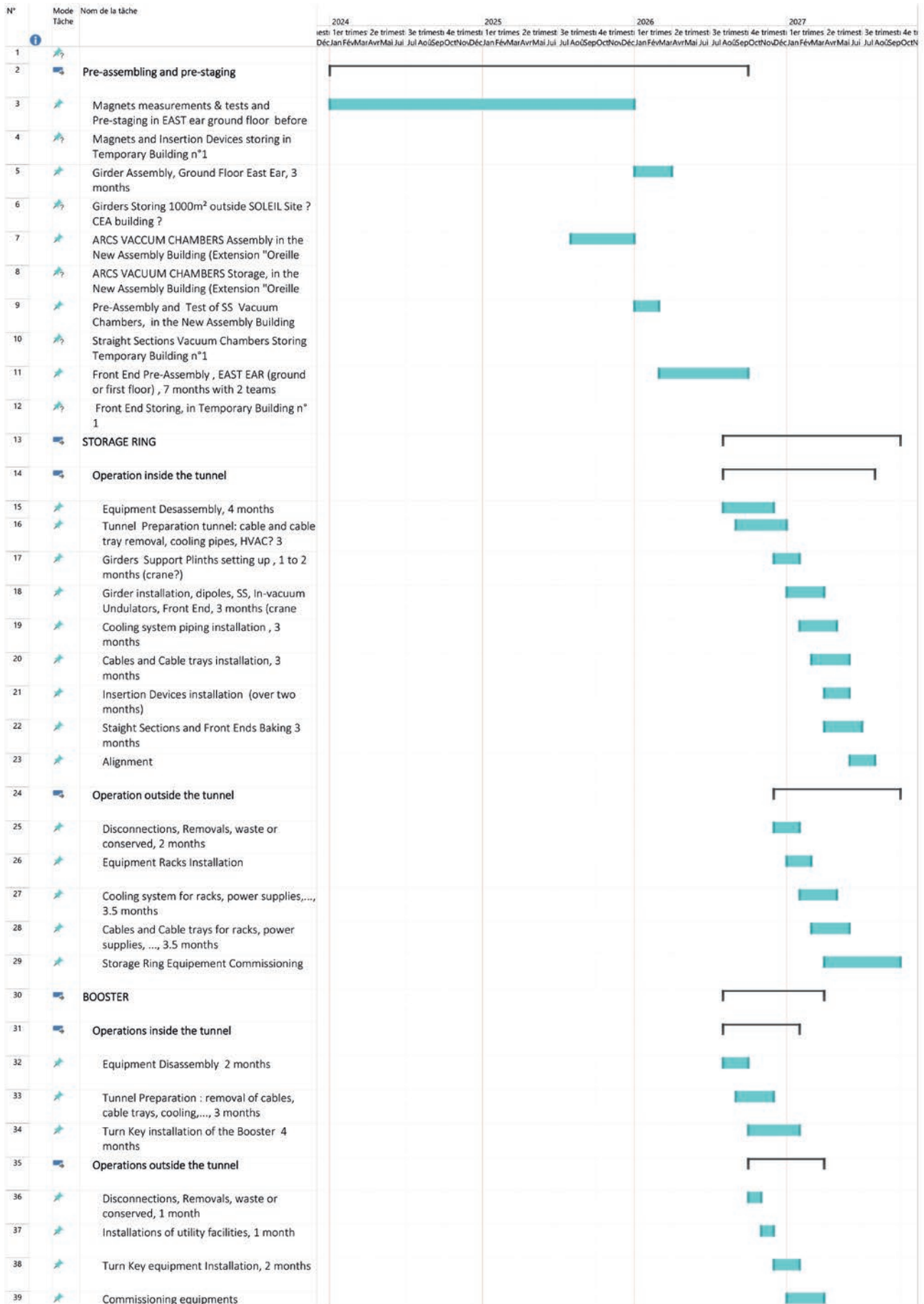
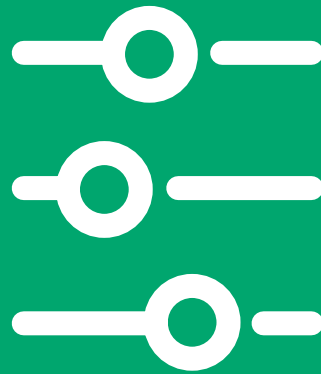


Figure 12: outline disassembly pre-staging and installation schedule



# 7 - Risk management



## Project risk analysis

Risk analysis involves identifying and managing any kind of event that could affect the ability of the project to achieve its objectives. It focuses on assessing the risks, estimating their causes and impacts on the progress of the project. Each risk is identified, ranked and prioritized according to risk "level" criteria. Actions, sometimes involving a decision-making and / or arbitration process, are then implemented to reduce the risks and are monitored in a "risk management plan".

Risk analysis started during the Conceptual Design Phase will be updated regularly, at dedicated meetings with the work package managers and presented at each key stage of the project. Risk analysis is a "living"

process: some risks are mitigated or even reduced as the project progresses, whilst new risks may appear.

Risk analysis is under the responsibility of the project manager. Assisted by the Quality Manager, he/she will ensure that the list of risks remains exhaustive and that actions are taken and / or proposed to reduce each risk level.

A common approach for all Work Packages (WP) has been put in place. Shared by all, this approach makes it possible to bring together all the stakeholders around the "Risks" issue.

We first determined rating models (from 1 to 4) for severity (Minor / Moderate / Critical / Very Critical) and for probability

(Unlikely / Unlikely / Likely / Frequent). The product of severity and probability defines the "level" of risk, which is ranked from 1 to 16. We then developed a "Risk matrix" grid in order to determine each risk: nature, severity, probability, level, as well as its causes, impacts and the solutions proposed to mitigate it. For each proposed workaround, a new risk level calculation is performed. Thus the matrix, with its color code, makes it possible to quickly visualize whether the major risks (beyond "8") can be reduced or not.

This risk analysis was conducted on each work package (44 in total) enabling us to identify the risks for each of the components of the Upgrade: scientific case, technological scheme (Lattice,

SM2 - Injection WP							
No	Type of risk	Equipment	Cause	Impact	Estimate		
					Severity	Probability	Level
Off-axis injection							
5	Technical	Feasibility demonstration of injection pulsed magnets	Complexity of equipment (MIK, Septum), technological limits	Off-axis injection impossible	4	3	12
6	Technical	Feasibility demonstration of injection pulsed magnets	Long time required for the design and development of such equipment (MIK, Septum)	Choice of the type of injection decided late	4	3	12
7	Organisational and technical	Injection into the storage ring upgrade	To carry out both the operation of the current machine and the particularly complex studies for the upgrade at the same time	Unsustainable TDR planning, demotivation of teams, departures of some colleagues	4	2	8
8	Human resources	Pulsed magnet expertise	A large part of the expertise relies on the group's two engineers. Several retirements of experienced Assistant Engineers to be anticipated	Lack of expertise to carry out the most complex injection pulsed magnets	4	2	8

Injection...), equipment (Magnets, Fluids, IT infrastructures...), management process (Purchasing, Finances, Human Resources, Security, Document management...).

Technical risks were identified (linked for example to the innovative nature of the design, requirements on the production of equipment, environmental constraints, prototype development, etc.), but also risks related to "human resources" (ie, to staff and their availability), or to "Safety", "Suppliers" and also "organizational" risks (related to interfaces, procedures, internal and external collaborations, etc.). Note that special attention must be paid to these latter risks: they are often as numerous as technical risks, but are more difficult to reduce because they are not

under the exclusive control of business experts.

Mitigation solutions have been proposed with actions intended to control the risk(s): R&D, partial or complete prototyping, tests, bid for external resources, improvement in communication... The validation of part of these proposals, for the machine, was introduced in the planning of the CDR phase. In addition, the analysis of the construction of SOLEIL carried out during the CDR phase was invaluable for the risk analysis as it highlighted a number of points of vigilance and made it possible to think immediately about solutions.

Finally, the risk analysis carried out for each WP was then consolidated at the

upper level (Machine, Infrastructures, IT, Experiences, Administration) in order to have a global view of the risks of the Upgrade Project. This work, which will be further developed in the Technical Design Phase, will make it possible to keep regular focus on major risks, ie those with a risk level greater than or equal to 8.

#### Example: risk analysis on the off-axis injection in the Injection WP

The risk analysis reveals two types of risk: a technical risk and a Human Resources risk, as shown in the extract below.

For technical risk, the preliminary risk analysis ranked this model at the critical level, "12", due to the technological

Comment on the nature of the severity (performance, cost, schedule)	Action to be implemented to mitigate risks	Result after mitigation	New estimate after mitigation			Comment on the nature of the severity (performance, cost, schedule)
			Severity	Probability	Level	
Impacts performance, planning, and final cost	Prototyping by pieces (CDR), close collaboration between SOLEIL's technical teams, technical reviews with international experts (CDR + TDR), releasing certain constraints (beam stay clear, transparency objectives for injection), studying the possibility of implementing a more classical injection with less complex pulsed magnets	OK	4	2	8	Impacts performance, planning, and final cost
Impacts performance, planning, and final cost	Human resources in adequacy with the issue of this macrotask, high priority on this project within the Division	OK	4	2	8	Impacts performance, planning, and final cost
Impacts performance, planning, and final cost	Recruitment of one pulsed magnet engineer. At the Division level: setting up a project team, organising tasks and responsibilities, planning, monitoring, etc.	OK	4	1	4	Impacts performance, planning, and final cost
Impacts performance, planning, and final cost	Recruitment of one pulsed magnet engineer, transmission of expertise within the group, drafting of technical notes by the group's experts, anticipation of retirements	OK	4	1	4	Impacts performance, planning, and final cost



difficulty of demonstrating the feasibility of pulsed off-axis injection devices. Indeed, this type of injection requires the development of an innovative Multipole Kicker (MIK). The WP manager proposed several solutions that lower the risk to level "8": implementation of human resources (teamwork of several SOLEIL groups, strengthening of resources); setting up of a Review (September 7 and 8, 2020) with international experts; work in parallel on a technologically less innovative but much more expensive swap out injection scheme.

In the preliminary risk analysis of this work package, the human resources risk was ranked at a quite high level, "8", as the pulsed magnet expertise is based on two engineers only. The proposed solution, which is to share skills within the teams and to hire a new engineer, makes it possible to lower the risk level to 4.

### Documentation

The number of documents issued is a source of several risks, including the dissemination of non-validated documents, the use of outdated versions, loss of confidentiality, registration gaps, etc. The reduction of these risks involves the implementation of an effective document management strategy in terms of traceability, reliability, conservation, accessibility and dissemination of information. The strategy adopted is based on two components:

- firstly, the rigorous application of the document control procedure that exists at SOLEIL in SOLEIL Management Plan;

- secondly, the Electronic Document Management tool used at SOLEIL, called "MERIDIAN Web". A dedicated "box" as well as an architecture adapted to the project have been defined and implemented in this software package. This tool allows the documents relating to the project to be identified by a specific grid and numbering. This archiving ensures that all stakeholders in the project have access to the latest version of the documents produced, thus guaranteeing them unique, validated and reliable information (working hypotheses).

### Feedback on SOLEIL construction

To move towards a successful Upgrade project, we build on the experience gained during SOLEIL's construction. This feedback is a very rich source of data, both on technical and organizational (methodology, resources, planning) aspects for designing the phases of the Upgrade project.

The methodology is based on an inventory of our working procedures, in parallel with analysis of causes of gaps, successes..., which took place during SOLEIL's construction, by comparing the initial planning to the "As constructed" one, in order to monitor vigilantly the Upgrade and improvements to be made.

Non-exhaustive examples are provided below.

First, we carried out a master planning with major macro-tasks and milestones representing the "As constructed" SOLEIL schedule, from the beginning of

the machine installation, going through the ring commissioning, and up to the first milestones of operating beamlines. This work has been based on the planning (study, design, manufacturing, and installation) of the machine, beamlines and infrastructures. The analysis of this planning and the associated resources (materials and human) during SOLEIL's construction helps us to build the SOLEIL upgrade project phases and resource needs.

Another example is the work on machine and beamlines installation plans. To assess the impacts of the the CDR reference lattice on the machine and beamlines implementation, in terms of technical feasibility, costs, resources, and planning, we need to have updated "As constructed" plans in our document management system. These plans already exist at SOLEIL, but some of them require an update and integration into general plans. The update of the plans with the nomenclature and implantations check-in with on-site measurements, is on progress for a number of beamlines and machine components.

To summarize, this feedback started in the CDR phase is very important to manage SOLEIL upgrade project. This work will continue during the TDR phase on other technical aspects and methods.



## 8 - **Radiation protection**



## Radiation protection issues in the storage ring upgrade

Synchrotron SOLEIL operation is submitted to an authorization by the French Nuclear Safety Authority (ASN). The upgrade of SOLEIL's storage ring (SR) will require at least a new ASN authorization for the operation of the new machine. Thus, prior to this demand, it will be mandatory that SOLEIL will have to submit another authorization request in order to proceed to the dismantling of the existing storage ring. Both files must include an impact study in terms of ionizing radiation hazards for the workers, the public and the environment.

These two studies will be led during the TDR phase and the authorization files will be submitted at the latest, 2.5 years before the shutdown for the dismantling authorization and 1.5 years before the first electron beam production for the operation authorization. At the CDR phase, the radiation study is mainly focused on the ability of the present storage ring bulk shielding to prevent ionizing radiation hazards from the new storage ring and photon beams.

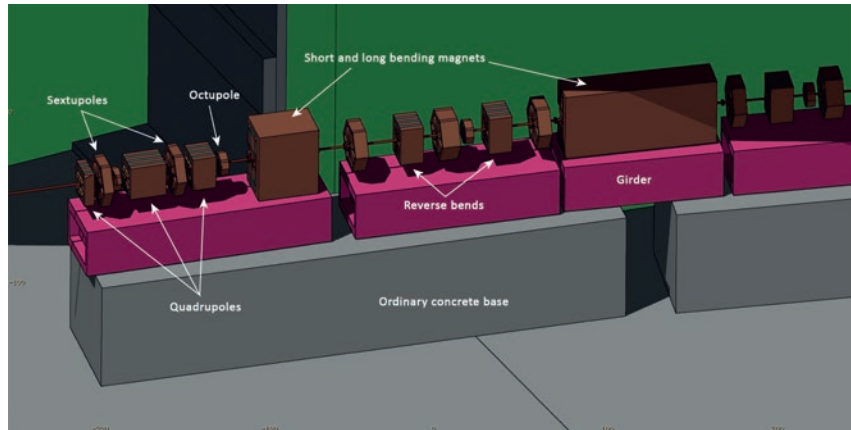


Figure 1: Magnet types along the arc



Figure 2: General display of V0313 7BA-4BA HOA lattice in SOLEIL storage ring tunnel

## Preliminary studies

### Main assumptions

Calculations have been made for the CDR reference lattice with a maximum of permanent magnets for dipoles, quadrupoles and reverse bends. The sextupoles and octupoles are considered as electromagnetic ones. Such a lattice will lead to 20 cells with room for 20 straight sections available for insertion devices (ID). The reference beam, with the most challenging performances and constraints, is the uniform filling pattern with a stored beam current of 500 mA and an emittance of about 80 pm.rad. For such a beam, we made pessimistic assumptions with a beam lifetime of 2 hours in top-up operation mode and an injection efficiency rate of 50%.

The injection is driven by a septum and a multipole injection kicker (MIK), both installed in the storage ring injection region of SDL01.

### Modelisation and Monte Carlo calculations

A 3D model is built as accurate as possible for the tunnel walls with some huge simplifications for equipment such

as girders, magnets, vacuum pipes and so on. At the CDR stage, IDs, front-ends, most of magnet coils, vacuum pumps, alignment windows, supports, fluid pipes and electrical cables are omitted.

Girders are designed as hybrid type with an ordinary concrete base and a steel frame. Magnet poles and yokes are reproduced with simplified shapes and made of iron with addition of permanent magnets in samarium-cobalt alloy. Beam pipes are represented as cylindrical with a 10 mm internal diameter for common straights and elliptical with a 28 mm outer width and 12 mm outer height. Both types of pipes are made of oxygen free copper.

Monte Carlo calculations are performed with FLUKA<sup>[1,2]</sup> code from CERN. At this CDR stage, the physical models of the V0313 lattice are not yet mature enough in order to predict the beam losses pattern and profile along the ring. So, beam losses are roughly modelled as uniformly spread along the inner edge of the vacuum beam pipe with a grazing incidence in the beam reference plan.

Figures 1 and 2 show the 3D geometry model developed with FLUKA code of the storage ring with its main components.

## Storage ring tunnel shielding

### Stored beam – Standard cell

#### Normal beam losses

Normal beam losses due to beam lifetime are dominated by vacuum interactions and Touschek effect and are supposed to lead to spread beam losses around the ring. For safety conservative reasons, we conservatively assumed that up to 30% of total normal beam losses will occur in one single cell. For a uniform 500 mA beam with a lifetime of 2 hours, it means a total power of 228 mW, which means 68.4 mW in a single cell.

Figure 3 presents the total (photons + neutrons) ambient equivalent dose rate for such beam losses rate spread along a single cell. One can see that the dose rates behind the concrete walls of the ring will remain below a  $0.50 \mu\text{Sv}\cdot\text{h}^{-1}$  goal limit with maximum value observed of  $0.47 \mu\text{Sv}\cdot\text{h}^{-1}$ . Dose rates on the roof surfaces (not shown here) are very similar to those observed on side walls. However, attention should be paid on the ratchet wall dose rates that may be able

to exceed  $0.5 \mu\text{Sv}\cdot\text{h}^{-1}$  in small location almost punctual in the very close vicinity of the ratchet walls with local dose rates that could reach  $0.9 \mu\text{Sv}\cdot\text{h}^{-1}$ .

#### Accidental beam losses

As it is requested by French Nuclear Authority, accidental beam losses have to be evaluated in a conservative way in order to estimate the impact on workers, public and environment in such a case. We assume a total beam loss in a standard cell for both a total beam loss spread in only one cell and a one-point beam loss at the beginning of the first arc of the cell. **Figure 4a** shows that, in case of a total beam loss of 500 mA stored beam, spread in only one standard cell, the resulting dose will be of about 45 to 62  $\mu\text{Sv}$  in the close vicinity of the tunnel walls and roof.

In case of an almost punctual total beam loss scheme, total ambient dose resulting could reach up to 86  $\mu\text{Sv}$  as shown on **figure 4b**.

These results are very close in terms of amplitude to those evaluated for present storage ring at former TDR stage in case of accidental beam losses.

### Beam injection – Injection region

#### Normal injection beam losses

As for the present storage ring, normal beam losses at injection are supposed to be mainly concentrated in injection region which benefits of reinforced shielding with heavy concrete walls and roof (hematite) and additional iron layer for both inner and outer walls.

The injection efficiency rate is assumed to be of 50% and most conservative case is for long pulse mode (LPM – 300 ns long bunch) injected beam of 10 nC at 3 Hz repetition rate considering a full transmission of the bunches from the linac, Transfer Line 1, booster and Transfer Line 2 up to the storage ring. Then beam losses are simulated to be located into the injection septum.

**Figure 5** shows the ambient equivalent dose resulting from such a case and able to be accumulated in case of top-up operation with 1 injection pulse every 2 minutes.

One can see that ambient equivalent dose accumulated in one hour will be at worst of the order of  $0.46 \mu\text{Sv}$ . Dose observed on roof surfaces are of the same amplitude order than on side walls. However, accumulated dose can reach punctually 1.2 or 1.3  $\mu\text{Sv}$  in the very close vicinity of both 1<sup>st</sup> and 2<sup>nd</sup> ratchet walls downstream of the septum.

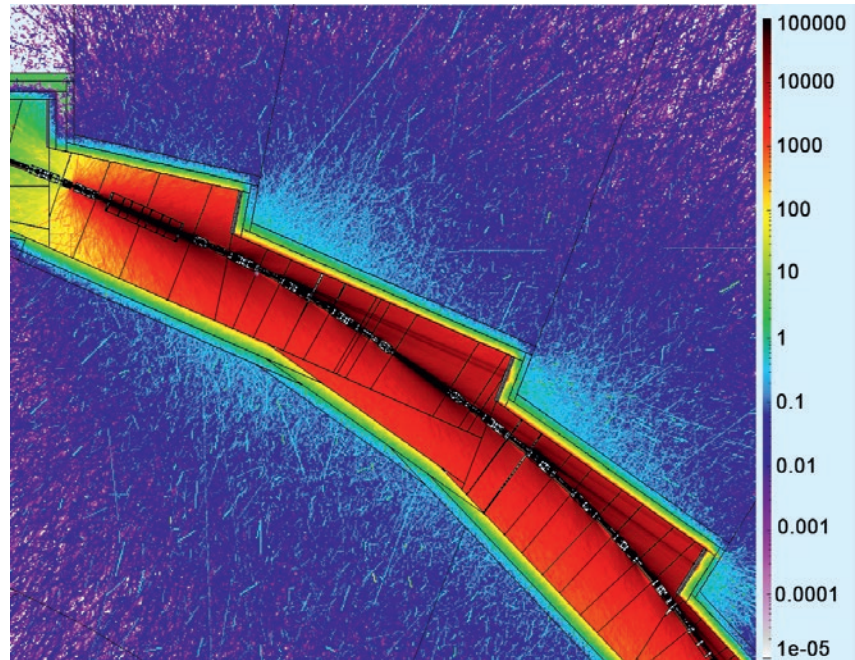


Figure 3: Total ambient equivalent dose rates ( $H^*(10)$  – color scale in  $\mu\text{Sv}\cdot\text{h}^{-1}$ ) for 30% of normal beam losses in one cell for a 500 mA beam with lifetime of 2 hours

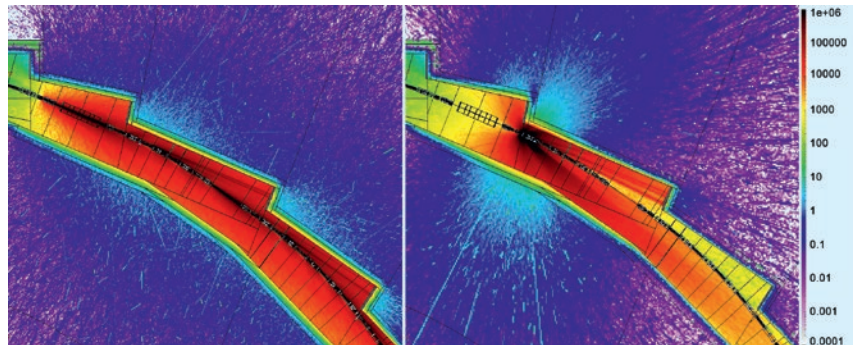


Figure 4a (left): Total ambient equivalent dose ( $H^*(10)$  in  $\mu\text{Sv}$ ) in case of a total 500 mA beam loss spread in one single cell

Figure 4b (right): Total ambient equivalent dose ( $H^*(10)$  in  $\mu\text{Sv}$ ) in case of a total 500 mA beam loss in first bending magnet of the upstream arc of the cell

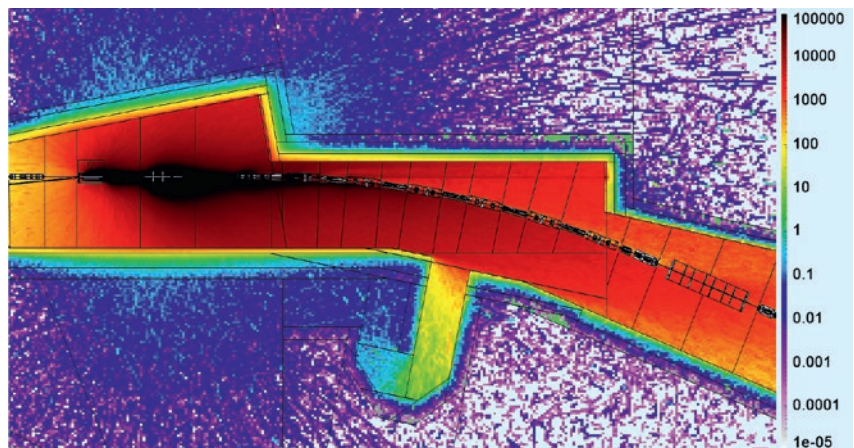


Figure 5: Total ambient equivalent dose ( $\mu\text{Sv}$  in one hour) for normal injection beam losses into the septum for a 10 nC pulse with 50% injection efficiency every 2 minutes.

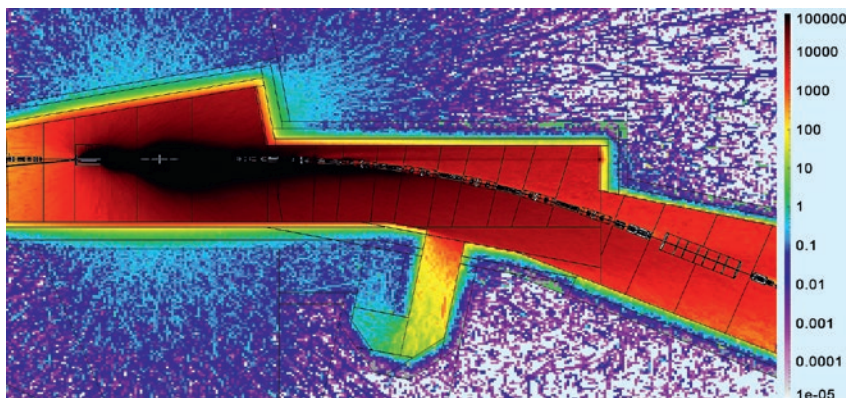


Figure 6: Total ambient equivalent dose rate ( $\mu\text{Sv}\cdot\text{h}^{-1}$ ) for full injection beam losses into the septum at 3 Hz and 10 nC - 0% efficiency.

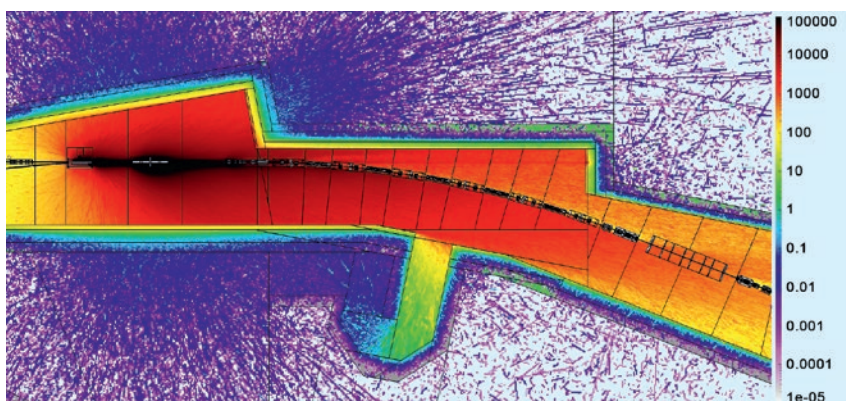


Figure 7: Total ambient equivalent dose ( $H^*(10) - \mu\text{Sv}$ ) in case of a full 500 mA stored beam loss in the injection region.

### Full injected beam loss

Full beam losses are considered as above concentrated in the injection region for a 0% injection efficiency rate of a 10 nC/LPM beam. One can see on Figure 6 that the total ambient dose rates can reach 30 up to 140  $\mu\text{Sv}\cdot\text{h}^{-1}$  for such a case.

### Full stored beam loss at injection region

In case of a full stored beam loss at injection region, the dose level reached in the vicinity of inner and outer walls and roof of the SR tunnel is evaluated.

The former SR of SOLEIL was initially designed to concentrate the main beam losses into the injection region which was therefore built with enhanced shielding. A similar approach is foreseen for the new SR. Figure 7 shows that, in case of a total beam loss of 500 mA stored beam, located in the septum, the resulting dose will be of about 5  $\mu\text{Sv}$  in most positions and up to 40  $\mu\text{Sv}$  only in the close vicinity of the tunnel walls and roof around the septum

(beam loss position). One can notice that these results are slightly lower than those obtained in the standard cell as expected. Again, these results are very similar and of the same order of magnitude than those obtained at TDR stage of the present storage ring.

### Storage ring shielding conclusion

Though these preliminary calculations were performed with very pessimistic assumptions, results show that present storage ring shielding may be able to support and be efficient enough for the upgraded storage ring in terms of radiation safety. Despite these promising results, attention will have to be paid to ratchet wall dose levels. Thus, beam behavior should be driven in such way that beam losses will be mainly concentrated into the injection region or in a specific enhanced shielded region of the storage ring in order to limit beam losses in standard cells. Injection efficiency rate issue for both storage ring

filling and top-up must be addressed too in order to be better than at least 75%-80% to avoid any radiation safety interlock. These points will be investigated in more accurate details during the TDR stage.

## Brief considerations about beamlines shielding

### Insertion device beamlines

The shielding requirements for the optics hutches of the insertion device (ID) beamlines are mainly dominated by scattered gas-Bremsstrahlung power. Considering first that straight sections will have a slightly shorter length than today. Second that, thanks to the drastically beam emittance reduction, the front-end opening will be reduced. And third, considering that the new storage ring will benefit from an almost entire NEG coating of the beam pipes, if pumping efficiency is good enough, the residual gas pressure in the vacuum SR vessels may be equal or similar to its present level. So shielding requirements for optics hutches should not increase.

Regarding experimental hutches, it will depend of the use of the ID itself and they may require some additional shielding if a new ID is used with shorter period and reduced gap and/or the same ID as now is used with smaller gap. These two cases should be investigated in detail at the TDR stage.

### Bending magnet beamlines

In the case of the bending magnet (BM) beamlines, shielding wall thicknesses of optics and experimental hutches are completely determined by scattered synchrotron radiation. For the new lattice, most of the BMs will have a magnetic field intensity of  $B_z = 1.71$  T as the present ones. So, no shielding reinforcement of the BM beamline hutches is foreseen. Meanwhile, some BM beamlines will benefit from the use of superbend with magnetic field of 3 T. In these cases, shielding reinforcements will be needed depending of the beamline characteristics and optical scheme. This point should be investigated in detail at the TDR stage.

## REFERENCE

[1] Overview of the FLUKA Code, G. Battistoni et al., Annals of Nuclear Energy 82, 10-18 (2015). [2] FLUKA, A multi-particle transport code, A. Ferrari, A. Fasso, P. Sala et al., CERN-INFN (2005).



9 – **Socio-economic  
impact**



## Introduction

An assessment of the facility's socio-economic impact was launched in 2019-2020. This assessment involves a comprehensive architecture of effects, the BETA-EvaRIO<sup>1</sup> framework, as shown in Figure 1 below.

The analysis differs from the standard Cost/Benefit Analysis (as part of the "Inputs-Outputs-Outcomes-Impacts" evaluation scheme<sup>2</sup>) by taking explicitly into consideration:

1• The different phases of the infrastructure life cycle going from conception to exploitation via maintenance and upgrade (cf. the blue arrows in Figure 1).

2• The Learning Processes, *i.e.* the creation of different types of knowledge triggered or boosted by the large scale Research Infrastructure –RI– (referred to as LP in Figure 1).

3• A meso-economic level of analysis *e.g.* the level of connected communities and knowledge networks (corresponding to the red areas of Figure 1).

More precisely, the BETA/EvaRIO architecture distinguishes two broad categories of socio-economic effects for a whole range of key actors (designers, standard and specialised suppliers, other RI operators, academic and industrial users, hosted students, visitors...):

(i) the learning effects linked to actors' activities at SOLEIL: practicing an activity with SOLEIL results in augmenting actors' capacity, and hence their performance at SOLEIL as well as in other activities; (ii) the multiplier economic effects due to SOLEIL's (and other agents') expenses as they pervade the whole macro-economic system. Such expenses are usually referred to as the Economic Footprint in the impact evaluation literature (hence the EF designation in Figure 1).

In line with this global framework, that differentiates Learning Process effects from Economic Footprint effects, a collaboration has been started with the

## Beta/EvaRIO evaluation Framework

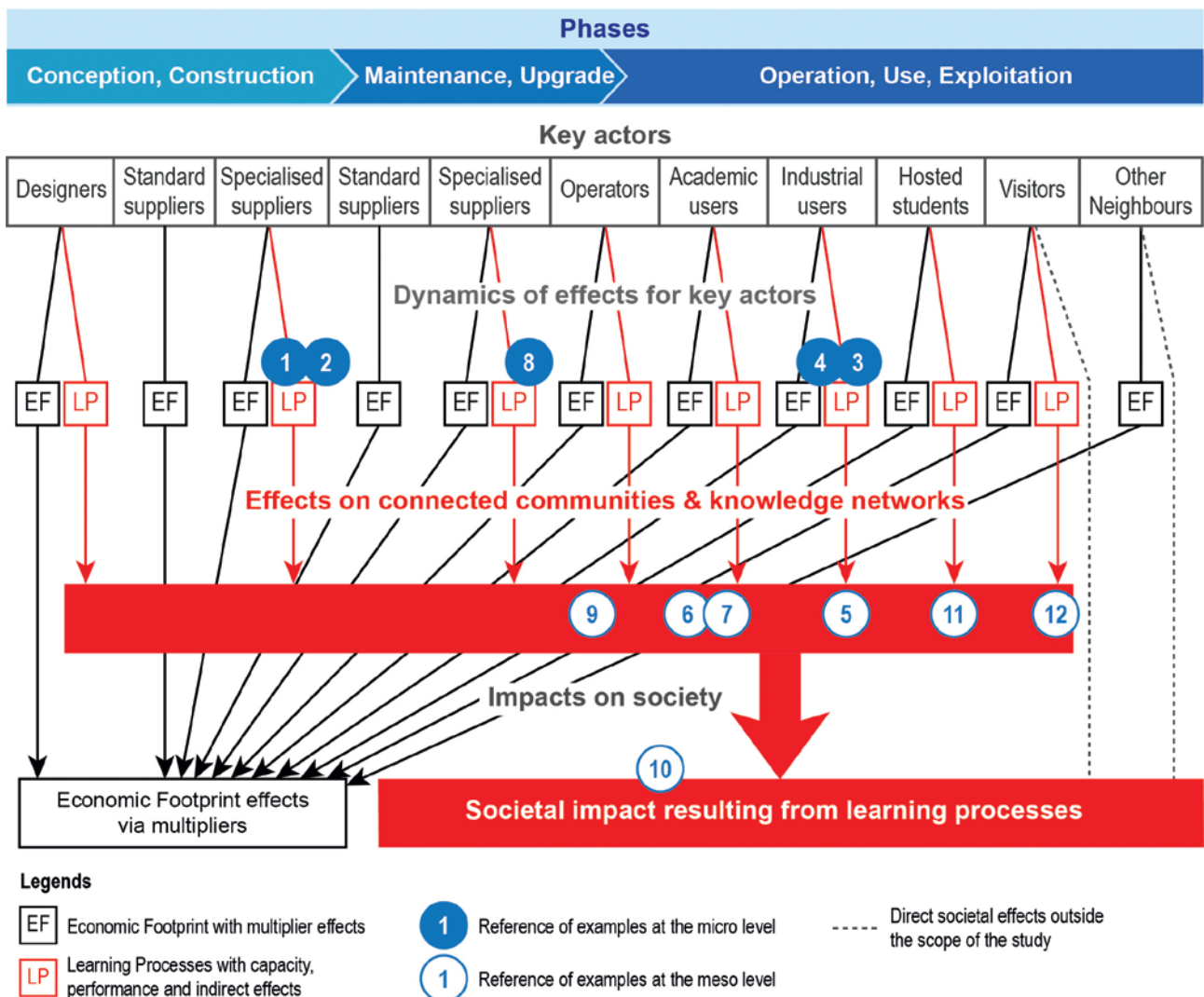


Figure 1

<sup>1</sup>The BETA (Bureau d'économie théorique et appliquée) is a research laboratory of Université de Strasbourg, CNRS, INRAE, and Université de Lorraine. EvaRIO (Evaluation of Research Infrastructures in Open innovation and research systems) is a Coordination and Support Action project funded by the European Commission under the 7th Framework Programme (grant N° 262281 - Research Infrastructures INFRA-2010-3.2). This 2-year project (2011-2013) aimed at developing an evaluation framework and a set of specific evaluation methods and tools well suited to research infrastructures (RIs) in the currently changing context towards an open innovation and research environment. EvaRIO was conducted by the BETA.

<sup>2</sup>Required by the Secrétariat Général pour l'Investissement, attached to the Prime Minister.

BETA in order to investigate the learning effects (the LP boxes in the [Figure 1](#) architecture), as synthesized below, while the company VERTIGO LAB handled the analysis of SOLEIL's expenses and their multiplier effects (the EF boxes in the architecture), as presented page 181. SOLEIL's proposed upgrade will undoubtedly have significant future societal and economic benefits in all areas in which both the above studies have demonstrated SOLEIL's impacts since its construction.

## Multiple impact studies by the bureau of theoretical and applied economy (BETA – Bureau d'économie théorique et appliquée, Strasbourg)

### Scope of the BETA studies

The BETA focuses particularly on the ex post effects of learning processes and on the structuring of R&D networks. Specific methods and indicators are developed in order to cover most of the LP boxes in the architecture of effects presented above ([Figure 1](#)). They are organized in ten Work Packages (WP), corresponding broadly to the following fields of research:

- SOLEIL's impact on "specialized suppliers" (WP1 & 2, each one using a different method) as well as on "industrial users" (WP3),
- the "creativity of academic users" (WP4) and the structure of "users' publication networks" (WP6),
- the "dynamics of surrounding communities and networks" (WP7) with a particular view on scientific user communities and public-private clusters such as *pôles de compétitivité*,
- the "INRAe – SOLEIL collaboration" (WP5) used as a transverse illustrative case of user learning effects,
- the "doctoral and postdoctoral training networks" (WP8),
- the "outreach actions of researchers" (WP9),
- the "opening of research data" (WP10).

### Methods of the BETA studies

Concerning methodological aspects of the BETA evaluation approach, extensive investigations have been conducted either from data collected from SOLEIL, or via online surveys addressed to representative samples, or through interviews with selected people reflecting diverse and exemplary cases.

The methods use quantitative as well as qualitative approaches, *i.e.* data analyses, econometrics and Social Network Analysis (SNA) based on graph theory on the one side, and case studies, observation and text analyses on the other side. Most studies gather data back to the beginning of the operation, or even to the building of SOLEIL as far as suppliers are concerned. The same methods could be reproduced after SOLEIL's Upgrade in order to assess its socio-economic impacts.

Some examples are provided to illustrate the kind of effects at stake. They appear in blue and white bubble in the architecture graphic - [Figure 1](#).

### Some examples

#### Examples of effects on specialised suppliers: micro level

Amongst others, recent examples of joint developments, co-patenting and transferred technology, are:

#### 1 Co-patenting and transfer of technology

- Transfer of technology is used when all developments were made at SOLEIL. A recent example is that of the "Corona" technology (3D nanometric metrology of rotations) with a transfer of know-how and a patent license to the German SME Attocube.
- When an SME has an industrial expertise allowing SOLEIL to consolidate the development of an innovation, SOLEIL can take the opportunity to co-file a joint ownership patent with this SME, as it happened with the French SME Sigmaphi for adjustable magnetic multipoles.
- Another international opportunity for co-development arose recently with the innovative design of the DHYANA detector which generated a commercial flow: after a very recent transfer of information and the publication of an article characterizing

the detector, the Canadian company AXIS Photonique have sold several DHYANA detectors, marketed under the name AXIS SXR, as part of an ongoing collaboration aiming at giving SOLEIL a strategic lead with highly innovative 2D soft X-ray streak cameras being developed by AXIS.

#### 2 Reputation / showroom effect

- Agilent, a specialized supplier, regularly provides SOLEIL's biology laboratory with prototypes for testing, and information about future products. As a result of this collaboration, additional instrumentation/devices were sold to new customers who discovered them at SOLEIL: the HPLC (high performance liquid chromatography) systems were taken up by the SOLEIL users.

#### Examples of effects on industrial user: micro & meso levels<sup>3</sup>

SOLEIL provides industry with beamtime access on a full cost basis, as well as support for innovation, techniques and expertise. About a 100 different companies have become customers of SOLEIL since 2008, which demonstrates the contribution of the facility to their business.

#### 3 Job creation in Contract Research Organizations (CROs)

A striking example of SOLEIL's impact on industrial users is the installation of LBS3 (a laboratory funded by SERVIER and operated by NovAliX) at SOLEIL. The LBS3 laboratory, established in 2016, contributes to the pharmaceutical industry, hence to drug development. The LBS3 installation has led to the creation of 5 jobs (high level of qualifications) at NovAliX. More generally, several CROs get developing and employ staff to work with SOLEIL (from apprentices to Post-doctoral fellows and scientists). In the future, further development of the industrial use, boosted by the upgrade, should lead to similar effects.

#### 4 Socio-economic benefits generated by new industrial applications made possible through research in connection with SOLEIL synchrotron

Research conducted at SOLEIL by several industrial users resulted in product innovations contributing to increasing competitiveness of the French economy.

<sup>3</sup> For reasons of confidentiality, mentioning concrete examples is hardly possible.



## 5 Participation in industrial networks

Cosmetic Valley is the World's leading perfumery cosmetics network. SOLEIL is a member, with a dozen partners, of the Cosmetic Valley R&D platform: SOLEIL works with three SMEs (two from Normandy, one from the Ile-de-France region) within the "safety of cosmetic products" branch based in Normandy; SOLEIL is also a partner of the "efficiency of cosmetic products" branch located in Ile de France, as well as other academic laboratories.

### Examples of effects on academic user communities: quantitative and qualitative analyses at meso level

With more than 12,000 scientists from all disciplines having used the infrastructure, SOLEIL plays an irreplaceable role for a number of scientific communities, both National and European.

## 6 Structuring of new user's communities

Through fine analysis of the publication network of two beamlines (PROXIMA-1 and SMIS), it has been possible to show the impact of SOLEIL on the structure of their respective users' communities. The emergence of a new user community (clinicians and surgeons) in the case of infrared spectroscopy (SMIS) was highlighted. The senior beamline leader played a crucial role.

## 7 Exploring new schemes to support clinicians

A network effect leading to a societal impact concerns medical research in which SOLEIL is pioneering modes of collaboration with hospitals. The DIAGOTRON concept is a remarkable example of collaboration to develop new techniques for the hospital, at the same time as investigating the capability of synchrotron radiation to provide clinical information by the examination of biopsies. It was started after a long and fruitful collaboration with hospitals which resulted in specific links between hospitals and SOLEIL around subjects of cooperative research (for example, brain cancer). A test phase of the DIAGOTRON project allowed hospitals to send samples of grafts / implantations to be characterized on beamlines through multi-line access for diagnosis (especially on the DISCO beamline, but also on the

tomography beamline, ANATOMIX). It is planned to develop an innovative sample changer suitable for several methods and compatible with biopsy samples, as well as to develop the necessary workflow (including biopsy security and result confidentiality).

### Examples of effects on operator(s): micro & meso levels

SOLEIL upgrade will require specific, high level equipment and therefore develop advanced instrumentation which has an impact on other operators, either via technology transfer & co-development or via collaboration within infrastructure networks.

A past success is the development of **8 solid state amplifiers**, launched at the storage ring of SOLEIL in 2006. These amplifiers proved to be very reliable; they led to technology transfers and are now in use at the ESRF and SESAME.

More recently, **8 SOLEIL expertise in magnetism contributed to "µPPI" technology** (miniaturization of electronic thrusters/engines for nanosatellites, including the magnetic modeling and design provided by SOLEIL). The start-up Exotrail which was created after a maturation process supported by the SATT Paris-Saclay is exploiting a license of know-how and patents jointly held by 4 academic partners (including SOLEIL)

## 8 Many more examples could be cited

SOLEIL shares three patents with the INRAé, which is both operator and SOLEIL user. ESRF and SOLEIL (with the recent addition of DIAMOND Light Source) are creating software for the examination and analysis of surface diffraction data.

The PandaBox **8** is an open hardware<sup>4</sup> electronic platform design to synchronize mechatronic systems and Detector in a real-time manner for simultaneous and multi-technique scanning experiments. This collaborative development with Diamond was done to address obsolescence of the existing systems at both institutes and implement new requirements such as support of multiple encoder, need for more processing power. Interestingly enough, this example entails also effects for specialized suppliers (Bubble **(1)** in Figure 1): for manufacturing, today the platform is supplied by two companies:

EEGI (France) and Quantum Detector (United Kingdom). The performances of the system are recognized and MAX IV purchased a set of rack to the French manufacturer this year.

## 9 The example of TANGO control system is emblematic of long-term international cooperation

The SOLEIL control system's core foundation named TANGO is a software framework developed by a community of large scientific instruments<sup>5</sup>. SOLEIL was a pioneer as the first collaborator of the ESRF, creator of TANGO, in 2002. SOLEIL was the first installation to deploy and operate TANGO in production on all its Accelerators and Beamlines. Over time, the SOLEIL control team has actively contributed to make TANGO a mature and stable product, which has been a key factor in attracting new members to the TANGO community. The TANGO framework is now a de-facto standard control system middleware, its community is continuously growing and is currently composed of eleven members, including SOLEIL, contributing to its kernel components; it is also installed on many other scientific facilities, in France and abroad; more and more private companies are providing TANGO-pluggable instruments or TANGO expertise consulting; some universities are using it as an introduction to distributed architectures. The international TANGO collaboration is growing and is successfully impacting the scientific community and the industry as it drives built-in quality, productivity, open-source and co-development practices.

## 9 European collaborations

SOLEIL is leading the LEAPS-INNOV<sup>6</sup> work package "insertion devices" and co-leading the work-packages "development of high throughput X-ray spectroscopy detector system" with Diamond Light Source, and "production of high-performance X-ray mirror and grating substrate" with ESRF. SOLEIL's part is funded through the LEAPS-INNOV project.

### Societal impacts: examples

## 10 Food safety

Research on the consumption (by the rat) of the food additive E171 (titanium dioxide, TiO<sub>2</sub>), found in sunscreens, toothpaste, candies etc., was carried out by scientists from INRA Toulouse in

<sup>4</sup> www.ohwr.org

<sup>5</sup> https://www.tango-controls.org/about-us/#mission

<sup>6</sup> LEAPS is the League of European Accelerator-based Photon Sources. LEAPS-INNOV is a European H2020 project involving all LEAPS partners starting in 2020.

collaboration with ANSES, CEA-Université Grenoble-Alpes, Luxembourg Institute of Science and Technology and SOLEIL. The research shows that TiO<sub>2</sub> can penetrate the intestinal wall and end up in the body. Disorders of the immune system and the development of pre-cancerous lesions in the colon have been observed in animals following prolonged ingestion of TiO<sub>2</sub>. These results have led the health authorities to take hold of this national public health issue, so that candy manufacturers in particular have changed the composition of their products in record time.

### 11 Training is a major aspect of SOLEIL societal impact

- 249 PhDs and postdoctoral contracts have been funded or co-funded since 2013 (116 post-doctoral contracts and 133 PhDs).

Many types of training can be identified, for example in the field of crystallography:

- SOLEIL organizes a school of "crystallography and synchrotron radiation" every two years.
- The NACRES<sup>7</sup> project aims to structure scientific relations between crystallographers (academics and industrial researchers) from the Nouvelle Aquitaine region, and SOLEIL. The NACRES project involves 5 research topics dealing with very different aspects of crystallography; it brings together biologists, chemists and condensed matter physicists. 4 PhD students and a post-doctorate will thus be funded equally by the Nouvelle Aquitaine Region and SOLEIL over a period of five years, representing a strong contribution to doctoral and post-doctoral training.
- A popular MOOC "journey to the heart of living things with X-rays" was designed in collaboration with local research laboratories and SOLEIL, and was followed by the recent publication of a book "Journey to the heart of life with X-rays". Whereas a number of similar training courses can be found on the internet, this particular course emphasized the role of the synchrotron in structural biology, and was prepared in French.

The training provided by SOLEIL is not directed only to academic actors; it is also

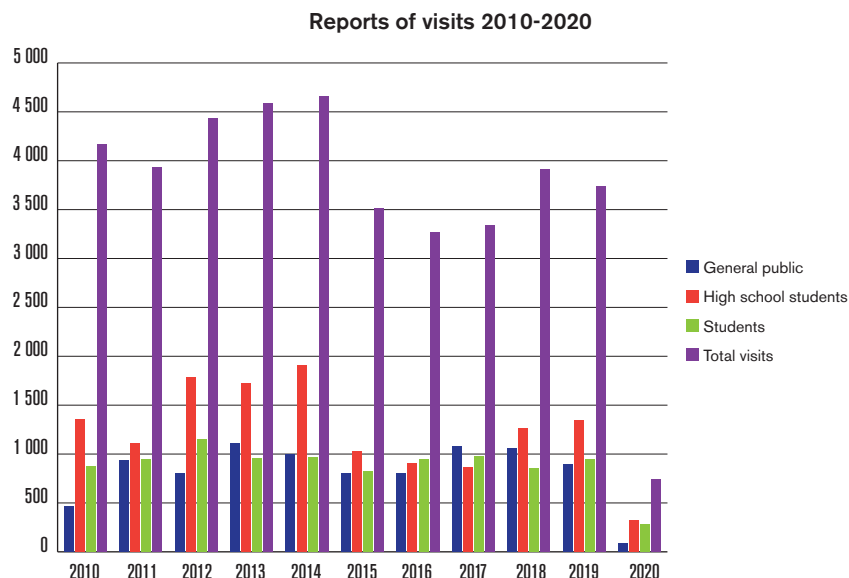


Figure 2

intended for industrial actors. SOLEIL is in the process of raising awareness among institutions and companies very early in the process of research. For example, a workshop on Digital Volume Correlation introducing synchrotron tomography methods in an industrial context took place at SOLEIL in 2018. This event was co-organised by SOLEIL, ThermoFisher, the startup EikoSim and 3Dmagination, a service provider of 3D imaging methods based in the UK.

### 12 Another strong impact is outreach towards the general public and school pupils with an average of 4000 visitors per year (Figure 2)

SOLEIL is a center for exchanges and for spreading scientific and technical knowledge. In particular, SOLEIL has built strong partnerships with the Rectorat de Versailles, Universities, and local actors<sup>8</sup>. SOLEIL is for example reaching out to primary schools thanks to the "primary lights" project born under the leadership of the rector in place in 2015, the World Year of Physics. The aim was to reach a young audience, who cannot come on site, through their teachers. Between 2015 and 2018, three educational kits<sup>9</sup>, containing equipment for pupils to realize their own experiments in class, were created on the subjects "shadow and light", "color" and "light and energy". They allow a multidisciplinary approach

to light, by integrating written and oral expression, visual arts and science. Over this period these kits were lent to between 7 and 10 classes per year, and 75 teachers attended, on SOLEIL's site, a training session explaining their use in class. Since then, 83 more teachers have been trained.

## The impact of SOLEIL's expenditure on the local, regional and international economy: a study by VERTIGO LAB

The study of socio-economic benefits carried out by VERTIGO LAB is focused on an "ex post" evaluation, namely the socio-economic impacts generated by the expenditure intended for the SOLEIL Synchrotron. This assessment considers the different impacts (*i.e.* direct, indirect, induced and catalytic impacts) of SOLEIL's expenditure on the economy through a model based on the multiplier method<sup>10</sup>.

### Mission objectives

The socio-economic impact of SOLEIL's activities is estimated at different geographic levels, by evaluating the multiplier effects (or spillover effects) of

<sup>7</sup> NACRES: Nouvelle Aquitaine, Cristallographie et Rayonnement Synchrotron.

<sup>8</sup> 28 training courses provided to secondary school teachers since 2004; 2,326 visits by middle school and high school students, students and teachers in 2019.

<sup>9</sup> These kits contain educational sheets, material allowing students to design and carry out experiments in small groups, and scientific complements.

<sup>10</sup> Input-output model developed by the Nobel Prize economist Wassily Leontief: Leontief, W., 1986, Input-Output Economics, 2nd edition, Oxford University Press, 436 pages.



its activities on the local (Essonne and Ile-de-France), national (France), European and global economy. At these different geographic levels, the economic and social contributions of SOLEIL are calculated, in terms of revenues for business (turnover), the creation of economic wealth (value added) and employment (number of jobs). A specific multiplier is also evaluated for SOLEIL Synchrotron, and compared to the multipliers of the other economic sectors at these different geographical scales.

### Scope of the study

SOLEIL synchrotron generates socio-economic benefits “ex post” through the expenditures which were necessary for the construction and operation of the facility (investment and operating expenses).

The scope of the study (Table 1) covers all expenditure made by SOLEIL over the period 2002-2019, for its purchases (80% of the expenditure) of supplies, services, and building works, those made by employees paid by SOLEIL, as well as expenditure made by the different categories of visitors (users, students, manufacturers, student teachers, etc.), doctoral and post-doctoral students working at SOLEIL and not funded by SOLEIL.

Investment	• Buildings and infrastructure
	• Computers
	• Accelerators
	• Beamlines and instrumentation
Operation (excluding payroll)	• Others
	• Buildings and infrastructure
	• Electricity
	• Fluids
	• Water
	• Computers
	• Accelerators
	• Beamlines and instrumentation
	• Others (support, CEO, Administration, Security...)
	Payroll
• Beamlines (and laboratories)	
• Sources (management of sources + technicians)	
• Technology transfer and valorization	
• Scientific outreach and reception of visitors	
• Training	
<b>(excluding investment and payroll)</b>	
Salary of doctoral / post-doctoral students not funded by SOLEIL	
Visitor and user spending	

Table 1: Nomenclature adopted for the evaluation of the socio-economic benefits of SOLEIL period 2002-2019



10 - **Innovation  
strategy**



During the facility construction and over more than 10 years of operation, SOLEIL has demonstrated its ability to manage and promote innovation, the cumulative balance mid-2020 giving 14 families of patents filed (in ownership or in co-ownership) and 12 knowledge transfers (patents, know-how, software) carried out to Very Small Enterprises and Small and Medium Enterprises (SMEs), mostly French.

The upgrade project represents an opportunity to further value the creativity of SOLEIL staff. In accordance with its position as a major player in the field of cutting-edge synchrotron radiation instrumentation, and with its mission of opening up to the industrial world, SOLEIL will identify and promote all kinds of innovation in its upgrade project, not only technological (material and digital technologies), but also organizational, relational, or services.

Good practice progressively built over two decades will be the basis for our strategy:

- Identify all potential inventions as early as possible to preserve their potential for innovation and business development, particularly in terms of non-disclosure of knowledge, differentiating own (exclusive) inventions, which are easier but a priori more risky, and inventions resulting from cooperation between SOLEIL and third parties, for which the risk is shared but the management is often more complex;
- Analyze each invention to assess its level of maturity (design, prototyping, validation) and the additional actions necessary for its development: identifying partners owning skills and/or resources lacking at SOLEIL, R&D or innovation co-funding, market study, intellectual property study, etc.;
- Based on this analysis, define a strategy for managing and promoting innovation: selection of the methods for maturing the innovative project, identification of suitable co-financing (readiness level, amount, duration, etc.), choice of the mechanism of knowledge protection (secrecy, patent or dissemination without protection), evaluation of potential markets, choice of the type of licensee operating company;
- Ask for advice the industrial representatives of the Strategic Orientation Committee for Industry at SOLEIL (COSIS) on planned service or product innovations either for beamlines or accelerators, in order to keep SOLEIL facilities durably attractive for industry.

### **Catalyze the emergence of inventions generated by the SOLEIL upgrade project**

A business development officer has been recruited early September 2020 on a fixed-term contract to work full-time on the SOLEIL upgrade in order to make an exhaustive survey and an analysis of all potential inventions related to the upgrade project.

For each invention, the main inventor and the business development officer establish, within a framework of strict confidentiality, an initial shared diagnosis on the invention, ensuring the co-construction and the monitoring of the innovative project throughout its life cycle (design, prototyping, validation, manufacture and operation). A systematic pre-assessment of the potential markets of the invention is jointly achieved, with identification of the fields of application of increasing size: SOLEIL alone, other synchrotron radiation centers, other particle accelerators, other Large Scale Facilities, scientific instrumentation for other sectors (industry, services, hospitals, etc.).

For technological innovations, a systematic and iterative analysis has been started for the concepts validated for the current machine design (proof of concept phase corresponding to a Technology Readiness Level (TRL) between 1 and 3) and for the prototypes and demonstrators already being manufactured (demonstration phase corresponding to a TRL between 4 and 6).

After validation of the technology, industrialization and manufacturing (industrialization phase corresponding to a TRL between 7 and 9) are entrusted to a company pre-qualified by SOLEIL to subcontract the technological device for its sole needs, and possibly to manufacture and market the device on a larger scale for third parties present in larger markets, under an operating license granted by SOLEIL.

### **Initiate and support the structuring and the maturation of innovations resulting from the SOLEIL upgrade project**

When SOLEIL lacks knowledge, experience or human resources for a specific innovative project, industrial and/or academic players (universities, research organizations, major research facilities) are searched, in a collaborative innovation approach with sharing of resources and risks, however limiting the

number of partners to the strict minimum and avoiding any nested collaborations (interdependence between new projects and already active projects) with the same partner.

When the innovation resulting from knowledge (know-how, patents, software) developed by SOLEIL, alone or with the assistance of third parties, addresses markets large enough to need industrial and commercial exploitation, it will be transferred to:

- Companies that participated in the co-development of the innovative project, as mentioned above;
- Young innovative companies created during or at the end of the innovation process, if possible with the help of SOLEIL employees and with its support;
- Industrial companies, primarily French SMEs, competent in the field of this specific innovation and interested by a new product or a new service to add to their offer.

When needed, the search for co-financing is carried out within the framework of Calls for Innovation projects launched by local, regional or national public funders, such as for example the LabEx PALM & Nanosacly and the Paris-Saclay University for the most upstream projects, or the SATT Paris-Saclay, the Ile-de-France Region or the Public Investment Bank for projects closest to markets.

### **Consolidate the initial innovation results of the SOLEIL upgrade**

Several strategic areas of innovation have already been identified by the business development officers of SOLEIL, such as for example, ultra-high vacuum, electron beam injection, nano-positioning, insertion devices and detectors.

A first SOLEAU envelope was filed at the INPI early September 2020 and a patent application is in preparation for imminent filing by the industrial property consulting company mandated by SOLEIL.

SOLEIL strategic objective is to strengthen support for innovative projects already identified and to continue to detect new emerging innovations, in agreement with the recommendations of the Strategic Orientation Committee for Industry in order to strengthen our competitiveness and ability to respond to the needs of industry in the coming decades.



11 – **Planning,  
Purchasing,  
Human Resources**

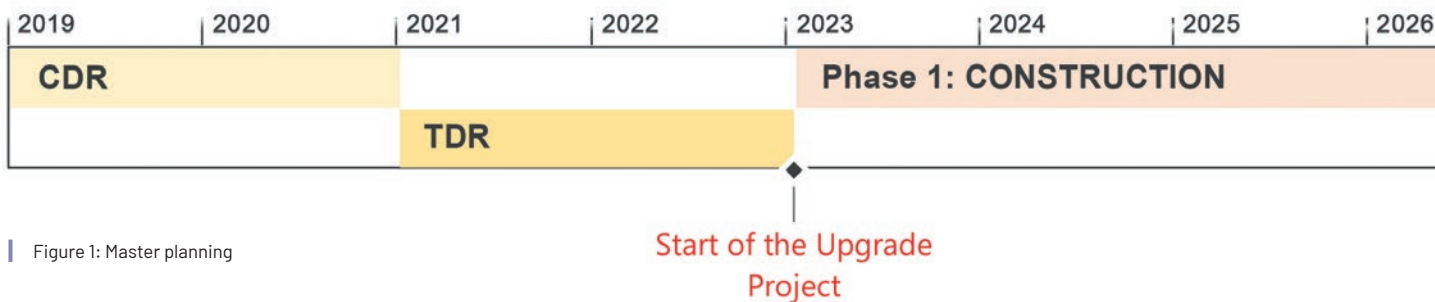


Figure 1: Master planning

## Planning

The master planning (Figure 1) has been prepared together with the project budget. This makes it possible to fully align the milestones entered in the schedule (acceptance, reception of a pre-series, commissioning) for an equipment with its respective purchasing procedure and costing. The risk-management strategies set up in the different Work Packages (WP) such as prototypes, models, feedbacks, etc. were integrated at this early stage. The high level schedule of the project is the result of this work.

## Phases

After two preliminary phases, Conceptual Design and Technical Design including preparatory work (prototyping, construction of building extensions for equipment assembly, infrastructure...), the planning is divided into two phases of five years each. Phase 1 "Construction" includes the realization of the accelerators, the modifications and the realignment of a group of beamlines. It also incorporates the machine shutdown and the beginning of the storage ring commissioning. Phase 2 "Towards full performance" starts with the continuation of the storage ring commissioning and the first beamlines commissioning; it then progresses towards the full performance of the beamlines thanks to the availability of the latest insertion devices.

## Detail planning

This planning work will continue during the Technical Design Phase in order to develop the detailed planning of the entire Upgrade project and to visualize the critical paths. The schedule will be built from detailed task sequences defined in

the work package, and will of course take into account the resources required; this is the only way to establish a consolidated, reliable schedule, and to know exactly all the resources needed for successful completion of the project.

## Purchases

The SOLEIL upgrade will allow the construction of a new facility (accelerators, beamlines and infrastructure) at the cutting edge of technology. Major purchases will then be made within a fixed schedule. These purchases will be numerous, diverse in terms of typology of equipment, and sometimes complex, pushing the state of the art of commercially available products.

The objective of this chapter is to clarify how SOLEIL is going to anticipate and manage these purchases, both in terms of volume and amount, within strict compliance with the applicable procedures and regulations.

## Complex purchases

To meet this challenge, SOLEIL will have to acquire state-of-the-art technological equipment and atypical tools that are, for some of them, not available on the market. To address this issue and improve, SOLEIL staff of purchasers will follow a long-term training "Expert public purchaser" in order to keep on improving their skills.

Besides, the use of the innovation partnership, provided for in Article L. 2172-3 of the Public Procurement Code, as a lever for more complex purchases, will aim to facilitate innovative public procurement and help purchasers make better strategic use of their

markets in order to promote innovation. The acquisition of innovative solutions plays a key role in improving efficiency and quality, and helps overcoming the structural difficulties of research and development (R&D) markets which require reopening competition at the end of the R&D phase to acquire the innovative products, services or works resulting from it.

This new procedure has never been implemented at SOLEIL, but will suit certain needs in the context of the SOLEIL upgrade, such as the purchase of optical components of sufficient quality to preserve beam coherence, for example. A benchmark has already been realized by the Purchasing Group on the use of this new procedure in the research sector.

## Respect of deadlines

The Purchasing Group's involvement at the early stages of product definition and procurement will provide the purchasers with an overview of the dossiers that will be processed in the coming years. It enables quantification of the volume of these future purchases on the one hand, but also to further refine the group's organization between upcoming and current purchases.

With this very complete view of purchases, the group will draw up a schedule with the prescribers, select the type of procedure to be implemented, identify the legal deadlines for procedures, and also SOLEIL internal deadlines (analysis, drafting of documents, validation, etc.), including payment terms. Furthermore, close involvement of the Purchasing group at all stages will make it possible to streamline internal purchase approval



mechanisms, particularly for purchases involving heavy financial investment.

In addition to the aspects related to the regulatory deadlines of the procedures, the group must be able to best anticipate future purchases by early optimization of framework agreements adapted for recurrent purchases and multi-year contracts, so as to benefit from a high responsiveness of the service providers when needs arise.

For the implementation of an optimized process control of our purchases, working closely with the Contracts and Purchasing Committee (CCA) of SOLEIL will be necessary. This committee is composed of representatives of the shareholders (CNRS and CEA). Its objective is to monitor the application of public expenditure rules by analyzing a posteriori our markets between €210,000 and €1,000,000 (both excluding VAT) and, any draft of an amount > €1,000,000 excluding VAT. Their analysis (whether favorable or not) on each dossier requires an additional delay of 15 days.

Eventually and in the purpose to best anticipate the upgrade, the group must work on updating reference documents (Procurement guide) and on the creation of standard documents such as technical specifications or consultation and draft contract rules.

### Supplier excellence

With SOLEIL Upgrade, the Purchasing Group must be able to access the most competent suppliers on the market. Supplier referencing is not allowed by the Public Procurement Code. However, in order to allow the prescriber to have

a panel of suppliers that meets the specifications and technical requirements of more specific purchases, two axes can be proposed to secure the markets, namely:

1) Sourcing is an action taken by the purchaser in order to identify the suppliers as well as the characteristics of the goods likely to meet a need. This is an active approach where, for a specific segment or area, potential supplier research and evaluation by purchasers is performed prior to the launch of the procurement procedure. Studies and prior exchanges cannot be interpreted as favoritism, since this prior analysis of supplier markets is done solely in order to listen and ask questions, but in no way to provide information to potential candidates.

This action can be carried out through the use of relays such as professional or economic organizations representative of the sector of activities, consular structures (chambers of trade crafts, chambers of commerce and industry...), contacts with purchasers from other organizations encountered during the "benchmarking", but also during the direct collection of information such as documentation received from potential suppliers, from publications or commercial exhibitions, from targeted visits to suppliers, etc.

2) Another means of selecting suppliers experienced in the field is the notice of a competitive public tender (AAPC) which is the qualification system that allows the pre-selection of candidates. It consists of qualifying the companies considered able to meet the requirements through prior electronic publication of segments of overall requirements in the Official Bulletin of Public Procurement Announcements,

Official Journal of the European Union or in a Journal of Legal Announcements. Once the administrative, economic and technical selection has been carried out, the qualified companies are entitled to receive detailed tender documents concerning the invitations to tender of the concerned segments (restricted procedure).

Finally, it is very interesting to point out that this search for the most competent suppliers for SOLEIL upgrade will also directly benefit the selected suppliers. These suppliers will potentially develop skills, via these markets which may be at the cutting edge of technology. This significant socio-economic impact should greatly benefit French suppliers, because of the necessary and numerous exchanges with the SOLEIL teams.

### Other aspects

Because of its statutes, SOLEIL complies with the advertising and competitive procedures provided for in the regulation of public procurement for all its purchases. As a contracting authority, SOLEIL complies with the Public Procurement Code (CCP).

By using the state purchasing platform (PLACE), SOLEIL fulfils its obligation to purchase on a dematerialized platform which allows SOLEIL not only to create quotation requests, but also to enter into consultations and make them available online to economic operators (potential suppliers). It must be stressed that PLACE is also used by our governing bodies (CNRS/CEA).

Besides, in the coming year, a discussion with SOLEIL's insurance broker will take



place to inform him about the Upgrade project with the aim of renegotiating all SOLEIL insurance policies. This should result in reducing or alleviating unforeseen effects that may be encountered.

## Human resources

Clarifying how SOLEIL is going to anticipate and provide the human resources (HR) required at all stages of its Upgrade is essential.

In order to get a broad and exhaustive vision of the requested human resources, a survey to inventory the needs will be conducted among the group managers.

Various levers are already identified, which will provide the human resources necessary for this upgrade project:

- Use of temporary staff;
- Anticipation of recruitment;
- Internal mobility;
- Provision of staff;
- Training and mentoring.

The strategy for the planned survey as well as for the various levers identified is described below.

### Collecting information from the teams

Each group manager will convey his-her vision of the changes and future HR needs within his group/beamline, by filling/completing a questionnaire.

Based on the collected information, a summary document will be issued in order to assess the anticipated/planned staff movements (retirements during the upgrade period, proposed replacements, potential resignations with or without replacement, etc.), the ad hoc needs (for the duration of the upgrade) together with the potential solutions (additional training for permanent staff, use of external resources, internal or external mobility, assistance from other synchrotrons or infrastructures...) as well as the consequences of the shutdown period on some groups (Mission Office, Users' Office, Machine Operation, Hall Coordinators, on-call groups...).

Progress and adjustment overviews will regularly be carried out with the group managers, evolving the working document as the project progresses and according to the priorities defined by the management.

A communication will be made to stakeholders at each important step.

### Use of temporary staff

The normal duration of fixed-term contracts (18 months) for temporary increase in activity will be inadequate in some situations. The "contrat de projet" would allow, when necessary, the recruitment of engineering and research staff for a maximum period of 36 months. In order to authorize the use of the "contrat de projet", a collective agreement is required and negotiations with the SOLEIL trade unions must be conducted.

### Anticipation of recruitments

Most of our staff are experienced and some of them have been involved in the construction of SOLEIL. Due to SOLEIL's current age pyramid, a significant turnover is expected during SOLEIL's upgrade. This has to be anticipated well in advance and will then create a very interesting opportunity to benefit from peak-loads.

More precisely, 62 permanent staff aged 55 and over (42 are under 60 and 20 are over 60) are likely to retire during the first ten years of the upgrade (2021-2030) as follows:

- Women: 15
- Men: 47
- Executives: 22
- Non executives: 40

24 group leaders are part of these staff, *i.e.* 40% of the group leaders.

The departures of these experienced staff will be anticipated and will allow present staff at SOLEIL to apply and develop their career.

Anticipating these departures will ensure the best possible knowledge transfer, while benefiting from "peak-load" through the recruitment of new employees on permanent contracts.

### Internal mobility

During the shutdown period, staff will have the opportunity to contribute to activities related to the upgrade of SOLEIL outside the scope of their usual position. Those will obviously be shift workers (machine operators and experimental hall coordinators), other support staff, as well as beamline scientists.

Depending on the needs, some of these staff may have to fulfill a different

mission to theirs. As a result, the collective agreements governing the conditions of these staff would have to be revised or amended, or amendments to the employment contract might be implemented for a limited period.

It will therefore be a real opportunity to ensure that each SOLEIL staff, whatever their occupation, can participate, according to his-her skills, in this collective SOLEIL upgrade project.

### Provision of staff

Besides, SOLEIL may benefit from the provision of personnel coming from other research organizations to strengthen its workforce and skills over either short or long periods.

Provision of staff from the CNRS and the CEA is a very interesting opportunity to consider, as some of their staff, particularly technical staff, would increase their skills and experience through their participation to some operations of SOLEIL upgrade. Such an approach would be positive for all the stakeholders.

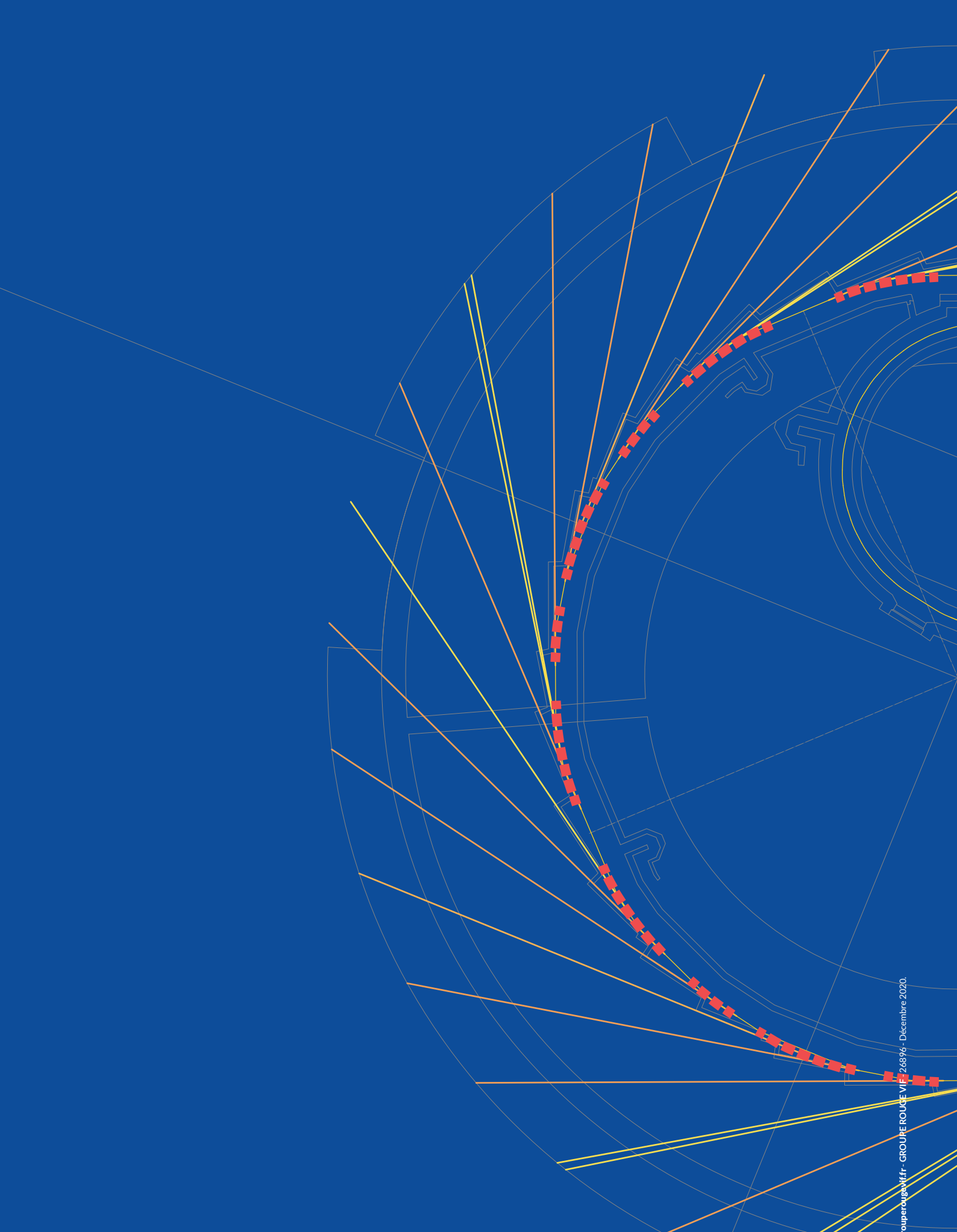
Concerning the other facilities, an identical scheme could be considered, with additionally the possibility of implementing temporary exchanges of staff, especially in the scientific and technical fields.

### Training & tutoring

SOLEIL's skills development plan already includes training in the purpose to prepare the upgrade. Some staff will need additional training that will be included in the skills development plan as needs arise and skills are upgraded.

Knowledge transfer actions can be implemented to anticipate changes. The introduction of tutoring is a means of transmitting knowledge used at SOLEIL (apprentices, young people's integration, etc...) and which could be developed in order to anticipate future changes such as: retirements, professional development, changes in missions, etc.





**SYNCHROTRON SOLEIL**  
L'ORME DES MERISIERS, 91190 SAINT-AUBIN